Idaho National Engineering and Environmental Laboratory

INEEL/EXT-98-00799
Rev. 1

January 1999

Fuel Summary Report: Shippingport Light Water Breeder Reactor

G. L. Olson
R. K. McCardell
D. B. Illum

LOCKHEED MARTIN

DISCLAIMER

DISCLAIMER

INEEL/EXT-98-00799
Rev. 1

January 1999

Fuel Summary Report: Shippingport Light Water Breeder Reactor

G. L. Olson
R. K. McCardell
D. B. Illum

INEEL/EXT-98-00799
Rev. 1

Fuel Summary Report: Shippingport Light Water Breeder Reactor

G. L. Olson
R. K. McCardell
D. B. Illum

Published January 1999

Idaho National Engineering and Environmental Laboratory
Department
Lockheed Martin Idaho Technologies Company
Idaho Falls, Idaho 83415

ACKNOWLEDGMENTS

Special appreciation goes out to Dr. Don Graczyk at Argonne National Laboratory-East, who made the destructive evaluation data available for our use, and to Steve McKinney at LMITCO, who evaluated and summarized that data.

CONTENTS

FIGURES

TABLES

ACRONYMS

ANL-E	Argonne National Laboratory-East
ANL-W	Argonne National Laboratory-West
APS	Atomic Power Station
AWBA	Advanced Water Breeder Applications
BTU	British Thermal Unit
COS	Cut Off System
DE	destructive examination
DOE	Department of Energy
ECF	Expended Core Facility
EFPH	effective full power hours
EOL	end of life
FIR	fissile inventory ratio
ICPP	Idaho Chemical Processing Plant
INEEL	Idaho National Engineering and Environmental Laboratory
INTEC	Idaho Nuclear Technology Engineering Center
LCS	Linear Closure Station
LWBR	Light Water Breeder Reactor
MDA	module disassembly apparatus
MWhr	megawatt hour
NDE	non-destructive examination
NPE	neutron poison equivalence
OD	outer diameter
PIFAG	Production Irradiation Fuel Assay Gauge
PSMT	planned shutdown for maintenance and testing
REX	Rod Examination

RRS	Rod Removal System
RXA	recrystallization annealed
SDA	stress-relief annealed
SRA	stress relief annealed
w/o	weight percent

Fuel Summary Report: Shippingport Light Water Breeder Reactor

1. INTRODUCTION

The Shippingport Light Water Breeder Reactor (LWBR) was a small water cooled, U-233/Th-232 cycle breeder reactor developed by the Pittsburgh Naval Reactors to improve utilization of the nation's nuclear fuel resources in light water reactors. The LWBR was operated at Shippingport Atomic Power Station (APS), which was a Department of Energy (DOE) (formerly Atomic Energy Commission)-owned reactor plant. Shippingport APS was the first large-scale, central-station nuclear power plant in the United States and the first plant of such size in the world operated solely to produce electric power.

Shippingport's program was started in 1953 to confirm the practical application of nuclear power for large-scale electric power generation. Subsequent to development and successful operation of the Pressurized Water Reactor, the Atomic Energy Commission in 1965 undertook a research and development program to design and build a Light Water Breeder Reactor core for operation in the Shippingport Station. In 1976, with fabrication of the Shippingport LWBR core nearing completion, the Energy Research and Development Administration, now DOE, established the Advanced Water Breeder Applications (AWBA) program to develop and disseminate technical information which would assist U.S. industry in evaluating the LWBR concept for commercial-scale applications. The AWBA program was conducted under the technical direction of the Office of the Deputy Assistant Secretary for Naval Reactors of DOE (WAPD-TM-1315, p. iii).

The Shippingport LWBR was operated successfully from 1977 to 1982 at the APS. During the five years of operation, the LWBR generated more than 29,000 effective full power hours (EFPH) of energy.

After final shutdown, the 39 core modules of the LWBR were shipped to the Expended Core Facility (ECF) at Naval Reactors Facility at the Idaho National Engineering and Environmental Laboratory (INEEL). At ECF, 12 of the 39 modules were dismantled and about 1000 of more than 17,000 rods were removed from the modules for proof-of-breeding and fuel performance testing. Some of the removed rods were kept at ECF, some were sent to Argonne National Laboratory-West (ANL-W) in Idaho and some to ANL-East in Chicago for a variety of physical, chemical and radiological examinations. All rods and rod sections remaining after the experiments were shipped back to ECF, where modules and loose rods were repackaged in liners for dry storage. In a series of shipments, the liners were transported from ECF to Idaho Nuclear Technology Engineering Center (INTEC), formerly the Idaho Chemical Processing Plant (ICPP). The 47 liners containing the fully-rodded and partially-derodded core modules, the loose rods, and the rod scraps, are now stored in underground dry wells at CPP-749.

2. REACTOR INFORMATION

2.1 Reactor

2.1.1 Name

The name of the reactor site is the Shippingport Atomic Power Station. Pressurized water reactors were originally operated at Shippingport, then the Light Water Breeder Reactor (LWBR) was designed and constructed to fit into the existing reactor core vessel. The LWBR is the only breeder reactor core to operate at Shippingport APS, and is distinguished from the other cores from the same location on that basis.

2.1.2 Reactor Type/Design

The LWBR was designed as a pressurized, light-water moderated and cooled thermal reactor that utilized the thorium/uranium-233 fuel cycle. Figure 2-1 presents a schematic of the breeding process showing Th-232 conversion to uranium. The LWBR core was developed for reactor operation within the constraints of the Shippingport plant. The interior modules were designed so that they could be used directly in a large LWBR core. The design provided a good simulation of a large LWBR core environment in the interior of the core, and permitted net breeding in the entire core (WAPD-TM-1600, p. 15).

Nuclear design of the LWBR core utilized a seed-blanket concept similar to that successfully applied to the first two PWR cores operated at Shippingport, but with reactivity control provided by core geometry changes (movable fuel) instead of poison rods (WAPD-TM-1387, p. 4). Figure 2-2 shows the arrangement of the core components in the Shippingport reactor vessel. Figure 2-3 shows a plan cross section of the LWBR core installed in the Shippingport pressurized water reactor vessel.

The LWBR core was designed to minimize parasitic neutron absorption in core and structural materials. Among the core design features, which contributed to improved neutron economy in the LWBR, were:

1. Use of movable fuel to control core reactivity, rather than conventional poison control rods, soluble poison, or burnable poison.

2. Use of peripheral radial and axial thoria reflector blanket regions to reduce neutron leakage from the core.

3. Use of Zircaloy with a low hafnium content (<40 ppm) for fuel rod cladding and for all structures in the active fuel region except the fuel rod support grids

4. Use of stainless steel (AM-350) rather than Iconel for fuel rod support grids (WAPD-TM-1326).

The four primary fuel regions (seed, standard blanket, power-flattening blanket, and reflector blanket) were each optimized to maximize neutron absorption in thorium and to minimize neutron loss (WAPD-TM-1387, p. 4). The three central fuel modules of the core are identical and symmetrical.

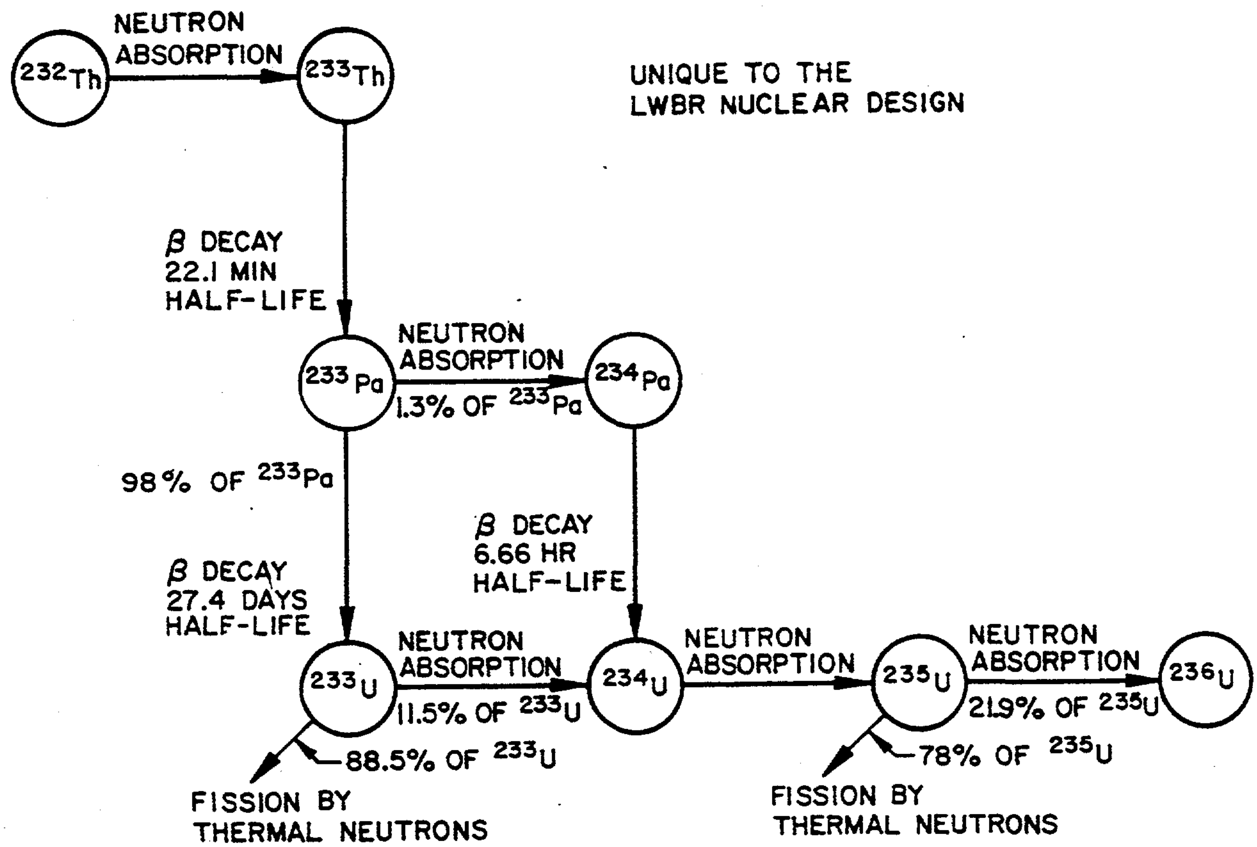

Figure 2-1. Conversion of Thorium-232 to Uranium by neutron absorption and radioactive decay in LWBR (WAPD-TM-1387).

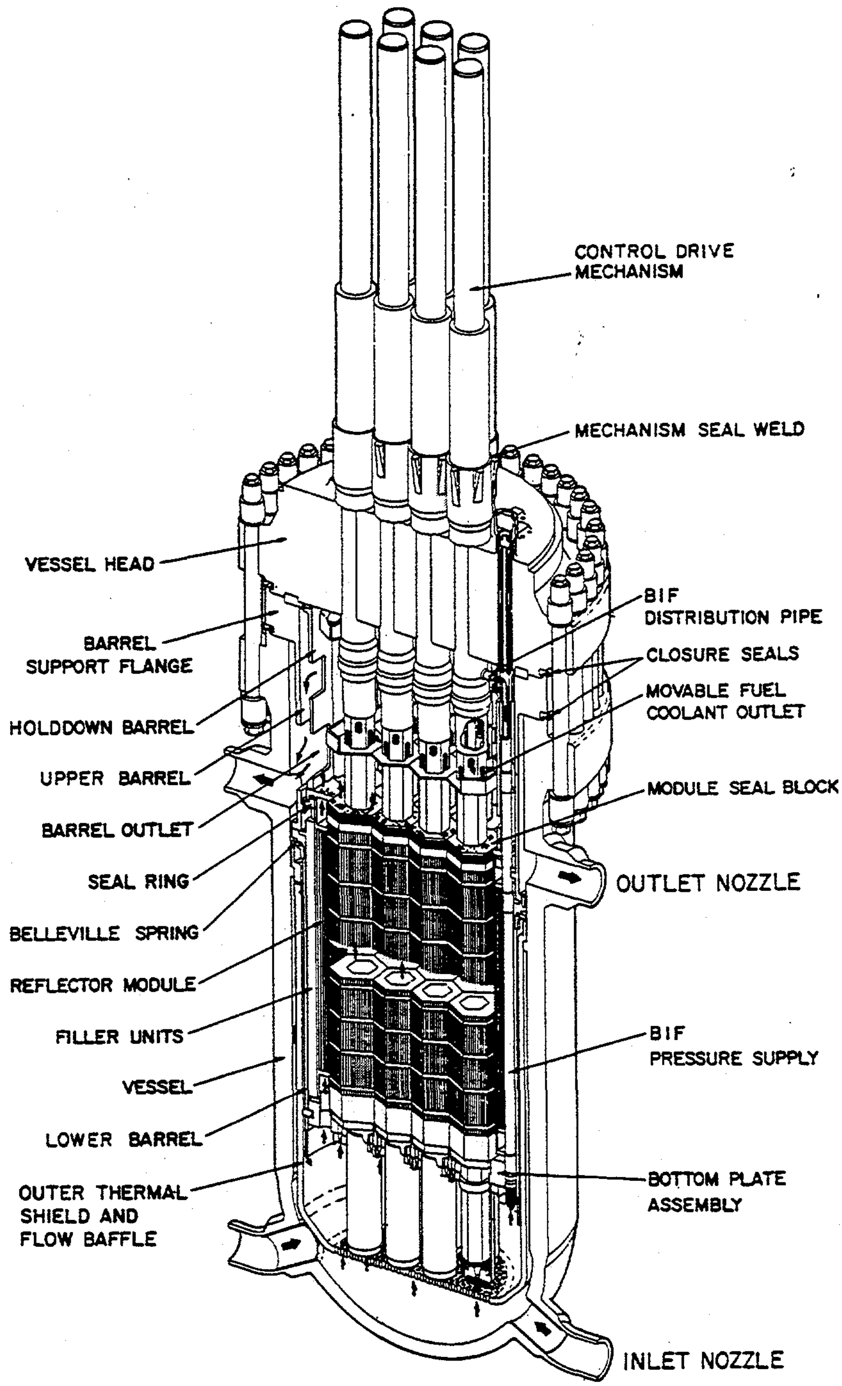

Figure 2-2. LWBR core in Shippingport Reactor Vessel (WAPD-TM-1208).

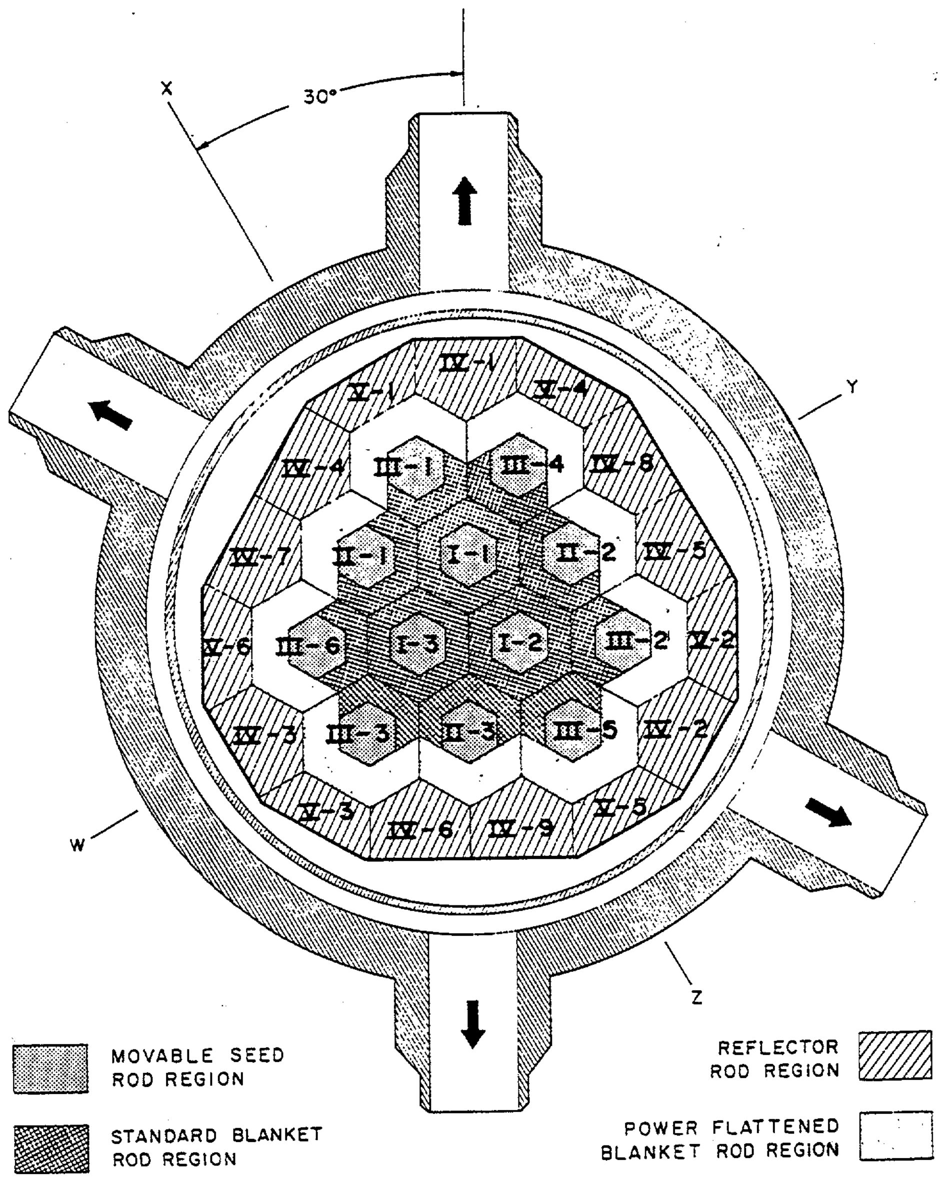

Figure 2-3. LWBR cross section module identification (WAPD-TM-1336).

They are designed as modules which could be used in a large central station reactor plant. The central seed and blanket modules were surrounded by nine module groups, each consisting of a seed, standard blanket, and a power-flattening blanket module. The power-flattening blankets were slightly thicker and contained slightly somewhat higher U-233 content than the standard blanket regions of the inner modules. Use of this more highly loaded power-flattening blanket region produced a relatively uniform power distribution within the interior of the core, thereby better simulating the environment of a typical large core. The power flattening increased the U-233 loading required for the small core used in Shippingport (WAPD-TM-1314, p. 4).

The seed, with highly enriched (>5% by weight) UO_2, about 98% of which was U-233, provided neutrons efficiently. The fertile fuel in the blanket absorbed excess neutrons efficiently and produced fissile fuel. Both the seed and blanket were optimized to maximize neutron production and minimize neutron loss (WAPD-TM-1409). Reactivity in a seed-blanket reactor is dominated by the seed; thus changes in seed geometry can cause reactivity variations. The central movable seed concept for fuel reactivity control eliminated the need for control poisons (WAPD-TM-1409, p. 3).

Water entered the vessel through four inlet nozzles at the bottom of the reactor vessel. The water was heated as it flowed upward through the modules past the fuel elements, and exited the vessel through the outlet nozzles after a single pass through the core (WAPD-TM-1600).

Because an objective of LWBR was to demonstrate breeding capability, the level of process control, quality assurance and documentation of manufacturing and inspection data during core fabrication was very rigorous (WAPD-TM-1278, p. I-3). All rods were individually identified and documentation was maintained to permit traceability of material, manufacturing history and inspection data for all components. The number of variations in rod and fuel pellet types required the implementation of controls during loading and overchecks of finished rods to assure that all rods were correctly loaded.

2.1.3 Reactor Location

Shippingport is located on the south bank of the Ohio River in Shippingport Borough, Beaver County, Pennsylvania, about 30 miles northwest of Pittsburgh.

2.1.4 Owner, Operator, Designer, and Builder

The LWBR was developed and designed by the Bettis Atomic Power Laboratory (operated by Westinghouse Electric Corporation). Design and development occurred under the technical direction of the Division of Naval Reactors of the U.S. Department of Energy (addendum to WAPD-TM-1455, p. 2). The Shippingport LWBR was installed in the Shippingport Atomic Power Station and was operated by Duquesne Light Company (WAPD-TM-1455, p. 2).

2.2 Reactor Parameters

2.2.1 Reactor Physical Dimensions

The reactor vessel at Shippingport was approximately 10 m (33 ft) high with an inner diameter of 2.7 m (9 ft) and a nominal wall thickness of 22.5 cm (8-7/8 in) (WAPD-TM-1342). Within the vessel was a core barrel, a long cylinder that locates fuel assemblies within the vessel. The core barrel was supported in the vessel by a large doughnut-shaped weldment, called the support flange, that rests on top of the vessel. The support flange also served as the entrance point of various types of core instrumentation and safety injection piping. The support flange was clamped in position by the 127 cm (50-inch) thick steel closure head using 15 cm (6–inch) diameter studs, which were installed in mating bolting flanges of the closure head and reactor vessel (WAPD-TM-1342, p. 2).

2.2.2 Core Grid Locations

There were nine grids in the seed assembly and eight in the blanket assembly (WAPD-TM-1326). The grid volume per fuel rod data are given in Table 2-1, and account for only the number of grids present over the fuel height and only the fraction per level actually present in the fuel lattice. Remaining grid volumes are contained in metal-water regions exterior to the fuel lattice regions. (**Note:** Table 2-1 lists 6, 6.5, or 7.5 for the number of grids in the fuel height. The table shows fewer grids in the fuel height because one grid is entirely above the fuel and half of a grid is below the fuel in each assembly (WAPD-TM-1326).)

2.2.3 Maximum Design Parameters

Data for peak local linear power rating, and fluence for each of the four LWBR fuel regions (seed, power-flattening and standard blanket, and reflector regions) are presented in Table 2-2.

Table 2-1. Average as-built LWBR fuel lattice characteristics (WAPD-TM-1326, Table II-1).

	Seed	Standard Blanket	Power Flattening Blanket	Reflector Blanket
Rod center - center spacing (in.)	0.3686	0.6304	0.6304	0.9005
Rod outer diameter (in.)	0.3063	0.5717	0.5274	0.8323
Rod surface-surface spacing (in.)	0.0623	0.0587	0.1030	0.0682
Clad thickness (in.)	0.02217	0.02808	0.02642	0.0419
Clad thickness/diameter ratio	0.072	0.049	0.050	0.050
Number of grid levels	9	8	8	6
Number of grids in fuel height	7.5	6.5	6.5	6
Grid fraction/level, in fuel lattice	0.846	0.79	0.79	0.80
Grid volume/fuel rod ($in.^3$)*	0.130	0.211	0.211	0.422
Metal/water volume ratio†	1.740	2.981	1.764	3.486
Total number of fuel rods	7428	3234	3581	3047
Number of flux-well rods	None	3	4	1
Total fissile loading (kg)	198.6	116.3	186.1	None
Total Th-232 loading (kg)	5206.5	9487.1	8788.3	18574.2

*Volume in fuel rod lattice based on number of grids in fuel height and the grid fraction per level in the fuel lattice.

†Under nominal hot conditions and with grid volume per fuel rod homogenized throughout the fuel regions.

Table 2-2. Peak local liner power rating burnup and fluence for each of LWBR fuel regions (WAPD-TM-1387 Table 1).

Parameter	Fuel Region: Seed	Fuel Region: Standard Blanket	Fuel Region: Power Flattening Blanket	Fuel Region: Reflector
Peak Linear Power (kw/ft)				
Best Estimate	6.7	8.9	8.7	3.6
Design	8.8	11.7	11.5	4.7
Peak Depletion (10^{20} f/cc)				
Best Estimate at 18,000 EFPH	8.3	3.4	3.9	0.5
Best Estimate at 29,047 EFPH	11.4	5.3	5.7	1.0
Design at 18,000 EFPH	9.7	4.3	4.6	0.6
Design at 29,047 EFPH	13.4	6.7	7.0	1.3
Peak Burnup (MWD/MTM)				
Best Estimate at 18,000 EFPH	38,900	15,200	17,000	2,400
Best Estimate at 29,047 EFPH	53,400	23,200	25,200	4,500
Design at 18,000 EFPH	45,300	19,000	20,500	2,800
Design at 29,047 EFPH	62,500	29,600	30,800	5,600
Maximum Rod - Average Depletion (10^{20} f/cc)				
Best Estimate at 18,000 EFPH	4.4	2.0	2.2	0.3
Best Estimate at 29,047 EFPH	6.4	3.0	3.3	0.5
Design at 18,000 EFPH	4.7	2.2	2.5	0.3
Design at 29,047 EFPH	7.0	3.5	3.8	0.6
Maximum Rod - Average Burnup (MWD/MTM)				
Best Estimate at 18,000 EFPH	20,500	8,700	9,800	1,200
Best Estimate at 29,047 EFPH	29,800	13,200	14,700	2,200
Design at 18,000 EFPH	22,100	9,700	10,900	1,300
Design at 29,047 EFPH	32,900	15,500	16,800	2,700
Peak Fluence (10^{20} n/cm^2, >1 Mev)				
Best Estimate at 18,000 EFPH	66.3	48.4	38.5	17.7
Best Estimate at 29,047 EFPH	96.5	73.8	58.6	27.8
Design at 18,000 EFPH	70.3	53.8	44.0	20.0
Design at 29,047 EFPH	104.7	84.0	69.0	32.1

3. FUEL INFORMATION

The fuel used in the LWBR was U-233, which is produced by neutron absorption in thorium. U-233 was observed to have a neutron regeneration factor (η) of 2.3 (WAPD-TM-1387, p. 27). The central portion of the core had a seed-blanket configuration consisting of 12 movable-fuel seed assemblies each surrounded by a stationary blanket assembly. The seed-blanket assemblies were designated as Types I, II, or III based on the nature of the blanket assemblies surrounding the seeds.

3.1 Assembly Information

3.1.1 General Description

Rods in the seed and blanket modules contained stacked binary fissile fuel in the form of ThO_2-UO_2 fuel pellets. Binary stack lengths and fuel loadings varied axially within seed and blanket modules. Figure 3-1 is a schematic axial cross-section of a seed/standard blanket configuration showing the highly-enriched fuel in the central seed surrounded by lower-enriched fuel of diminishing stack lengths toward the standard blanket. Figure 3-2 depicts how the rods are configured radially within the seed module, and Figure 3-3 depicts the rod cross-section for the standard blanket module. Figure 3-4 is a schematic of the axial cross-section of a seed/power-flattening blanket configuration of the Type II and Type III modules. Figure 3-5 and 3-6 depict the axial rod configuration for the Type II and III blanket modules, respectively.

The tops and bottoms of the fuel rods in the seed and blanket modules were stacked with fertile material in the form of ThO_2 fuel pellets. The three Type I modules, characterized by the equal-sided hexagonal standard blanket, were designed insofar as practical to represent modules that could be used in a large central station reactor plant.

Type II and III modules were characterized by the shape of the blanket modules, which contained both standard and power-flattening components. Type II modules contained hexagonal blankets that had two power flattening sides and four standard blanket sides; Type III blankets were hexagons with three power-flattening and three standard blanket sides. Power-flattening sides were wider than the standard sides, but the rods in the power-flattening blankets were smaller in diameter and higher in U-233 than rods in the standard blankets (WAPD-TM-1326).

The seed-blanket assemblies were surrounded by an outer reflector region designed to reduce neutron leakage. There were 15 reflector modules; Type IV reflectors were five-sided (Figure 3-7) and Type V reflectors were four-sided (Figure 3-8). Reflector modules contained rods with only ThO_2 pellets. Surrounding the reflector modules were 15 stainless steel, nonfuel filler units whose purpose was to limit core flow leakage by filling the space between the reflector modules and the core vessel (WAPD-TM-1326, p. 4).

In all, there were 17,288 rods in the 39 modules of the LWBR core. The number of rods in each fully-rodded module is listed in Table 3-1. Some of the rod locations were filled with flux wells instead of fuel rods, as shown in schematics for the modules.

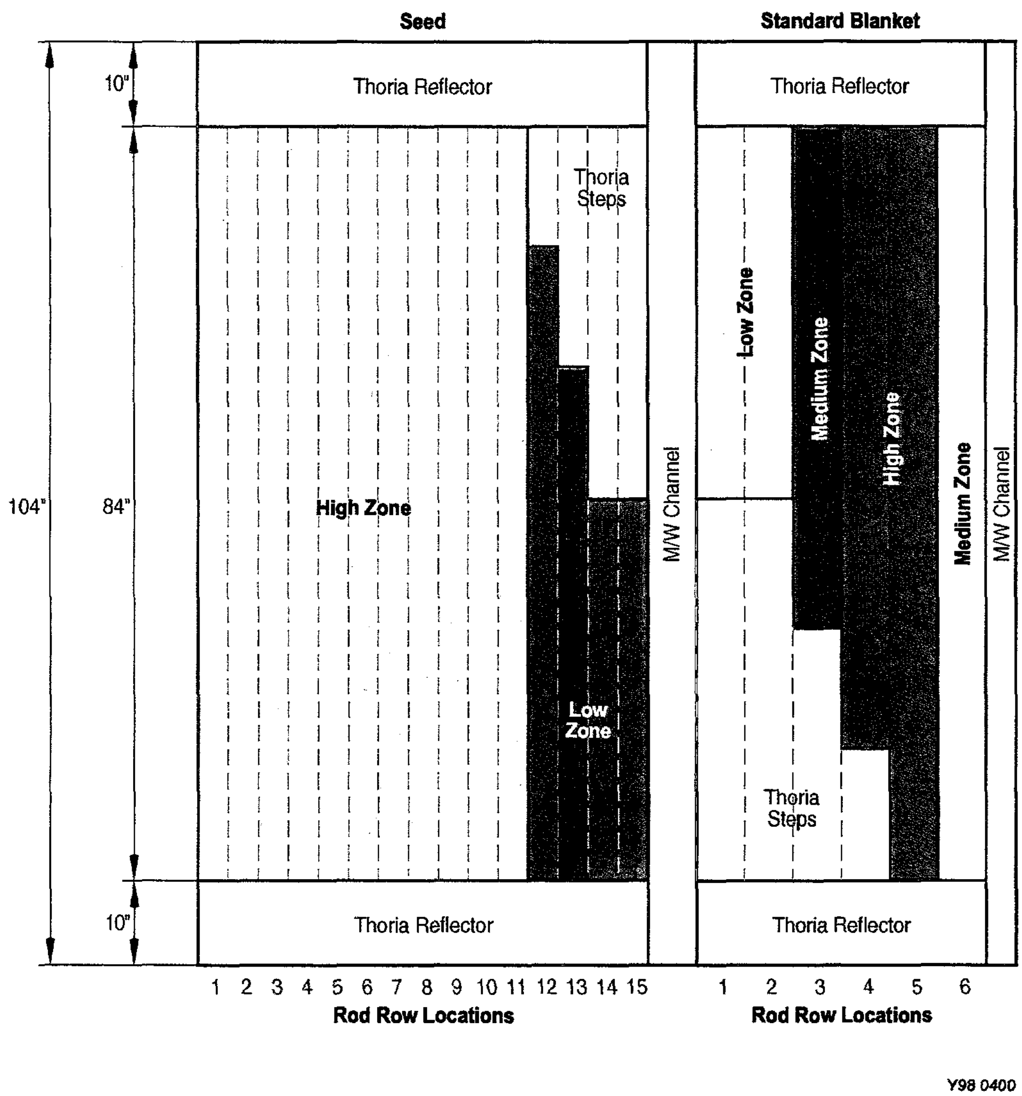

Figure 3-1. R-Z schematic of a Type I Module (modified from WAPD-TM-1326 Figure II-4).

Rod Type[1]	Binary Stack Length	Enrichment (U-fissile wt %)[2]	Theoretical Density (g/cm³)[2]	Mass Initial Fissile (g)/Rod[3]	Number of Rods/Core	Mass Initial Fissile (g)/Core
05, 06	84"	5.195	10.042	34.57	3,972	137,312
04	70"	4.327	10.035	23.92	792	18,945
03	56"	4.327	10.035	19.14	864	16,537
01, 02, 07, 08	42"	4.327	10.035	14.33	1,800	25,794
					7,428	198,586

619 Rods (306 top mounted)
.306" Diameter
.369" Pitch

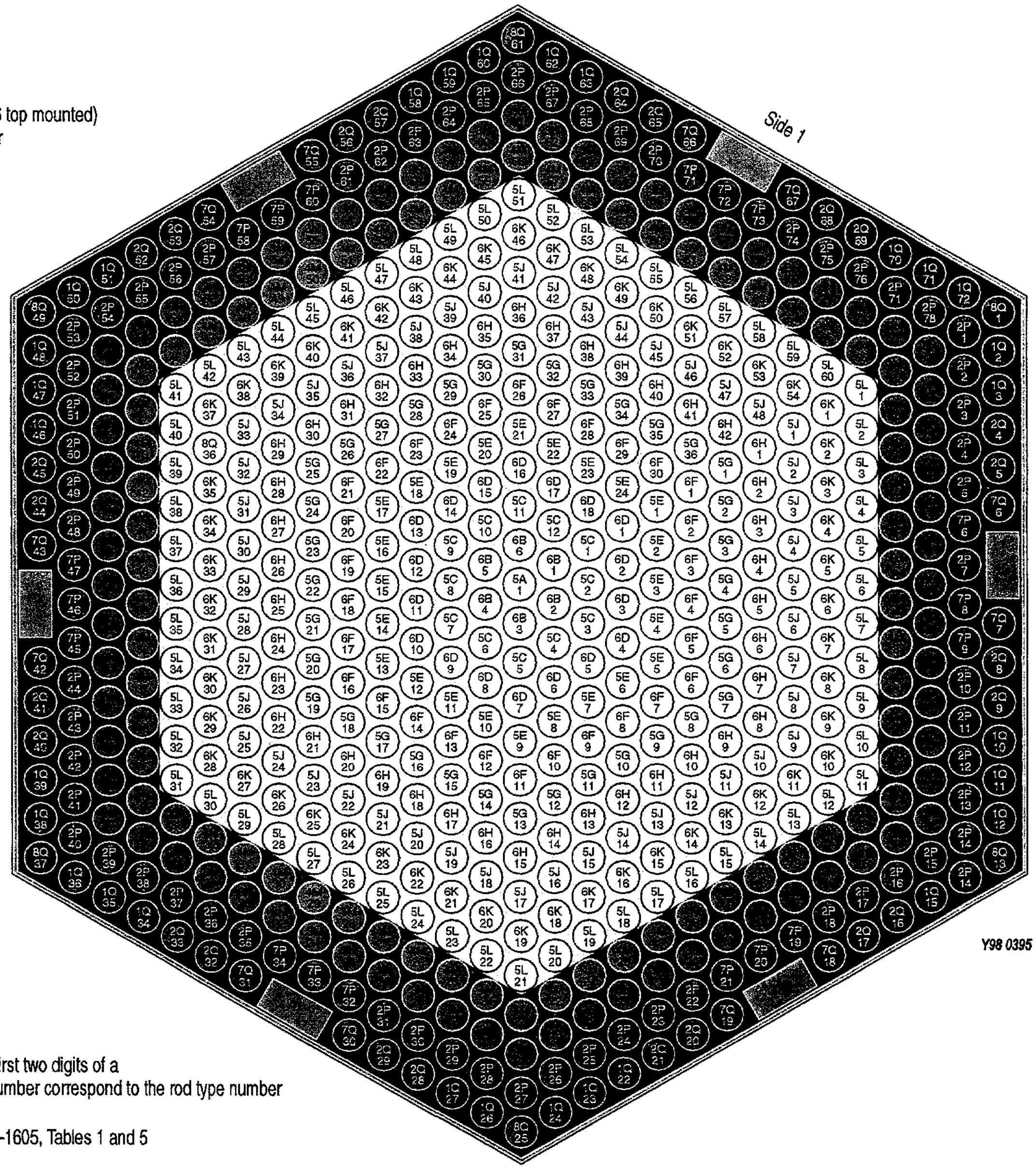

[1] Rod type: First two digits of a rod serial number correspond to the rod type number

[2] WAPD–TM–1605, Tables 1 and 5

[3] WAPD–TM–1612, Table V-2. WAPD–TM–1326, Table A-5

Figure 3-2. LWBR Movable Seed Module rod and cell identification (modified from WAPD-TM-1326 Figure II-4).

Rod Type[1]	Binary Stack Length	Enrichment (U-fissile wt %)[2]	Theoretical Density (g/cm^3)[2]	Mass Initial Fissile (g)/Rod[3]	Number of Rods/Core B1	B2	B3	Total	Mass Initial Fissile (g)/Core
11,12	42"	1.211	10.009	16.45	378 +	240 +	354 =	972	15,989.4
14	56"	1.662	10.013	30.34	216 +	129 +	186 =	531	16,110.5
13	70"	2.000	10.016	45.47	231 +	135 +	192 =	558	25,372.3
16	84"	2.000	10.016	54.66	252 +	141 +	198 =	591	32,304.1
15	84"	1.662	10.013	45.66	252 +	138 +	192 =	582	26,574.1
					1,329 +	783 +	1,122 =	3,234	116,350.4

443 Rods (222 top mounted)
.5715" Diameter
.630" Pitch

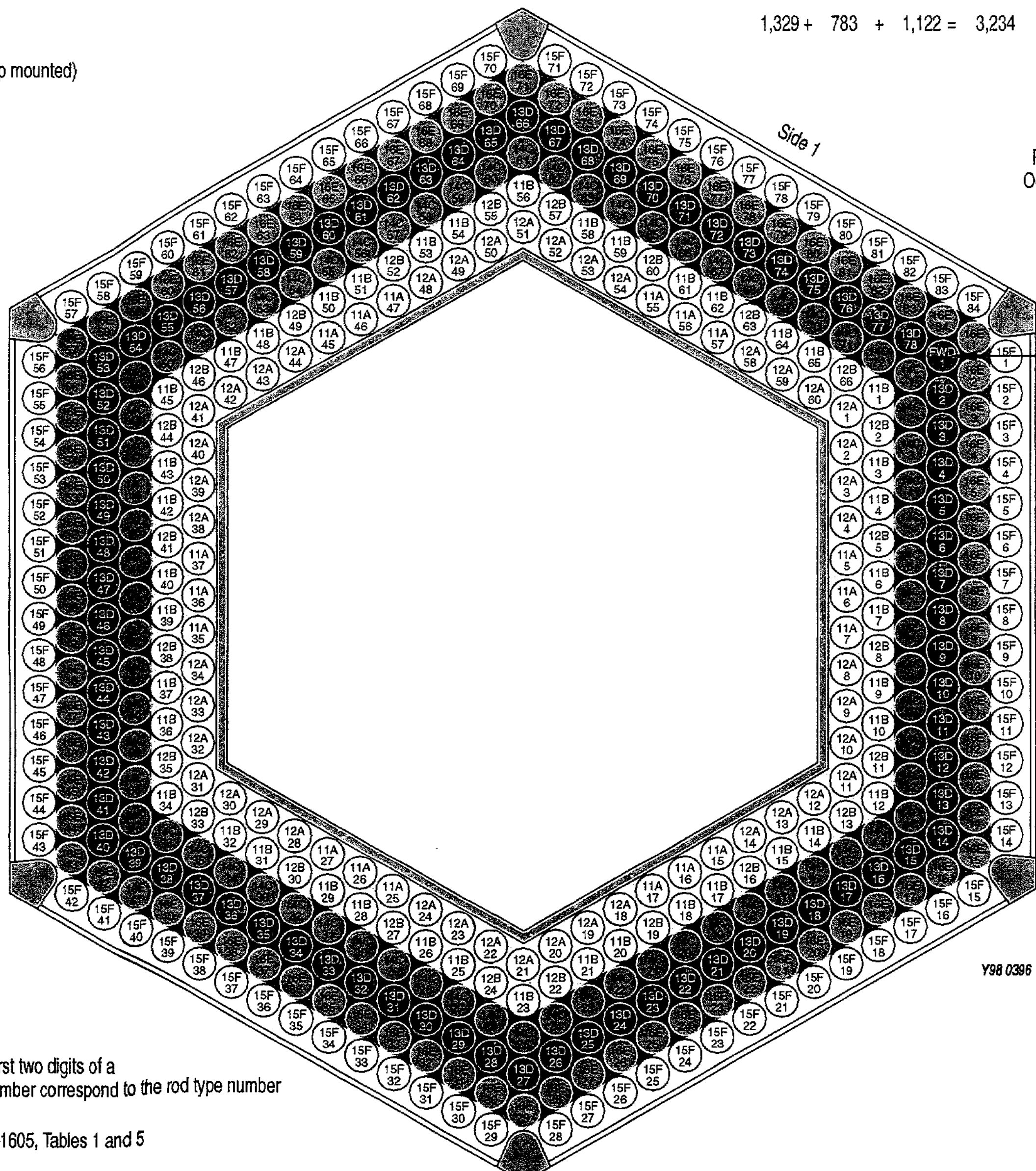

[1] Rod type: First two digits of a rod serial number correspond to the rod type number

[2] WAPD–TM–1605, Tables 1 and 5

[3] WAPD–TM–1612, Table V-2. WAPD–TM–1326, Table A-5

Figure 3-3. LWBR Type I Blanket Module rod and cell identification (modified from WAPD-TM-1605 Figure A1-1).

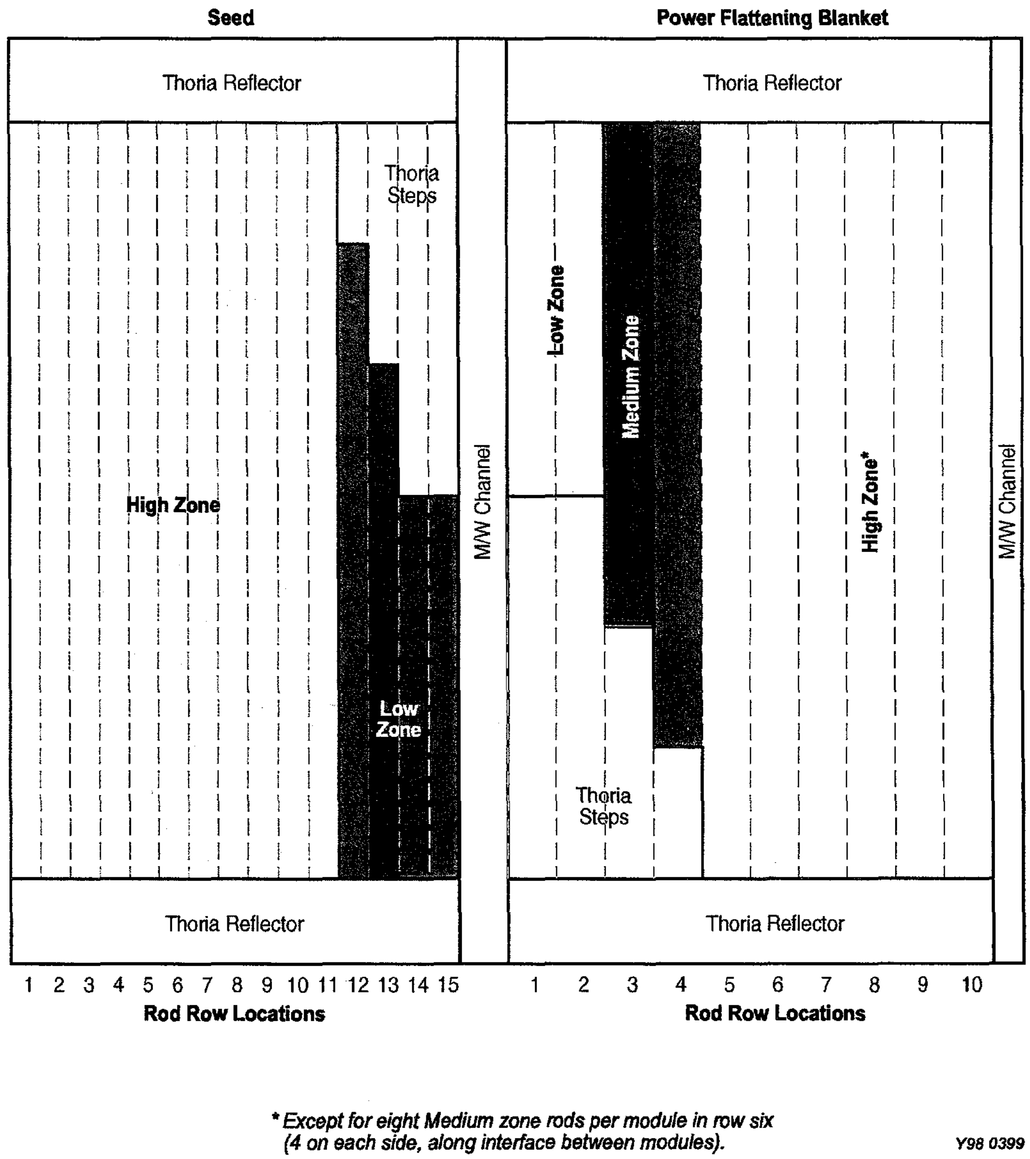

Figure 3-4. R-Z schematic of power flattening sides of Type II and Type III Blanket Modules (modified from WAPD-TM-1326).

Rod Type[1]	Binary Stack Length	Enrichment (U-fissile wt %)[2]	Theoretical Density (g/cm^3)[2]	Mass Initial Fissile (g)/Rod[3]	Number of Rods/Core	Mass Initial Fissile(g)/Core
21, 22	42"	1.649	10.013	18.96	180	3,412.8
24	56"	2.005	10.016	30.74	93	2,858.8
23	70"	2.733	10.022	52.56	93	4,888.1
25, 27	84"	2.733	10.022	63.06	517	32,602.0
26	84"	2.005	10.016	46.4	24	1,113.6
					907	44,875.3

Region 1
261 Standard Rods (131 top mounted)
.5712" Diameter
.630" Pitch

Region 2
303 Power Flattening Rods (151 top mounted)
302 for Types II-1 and Types II-3
.5265" Diameter
.630" Pitch

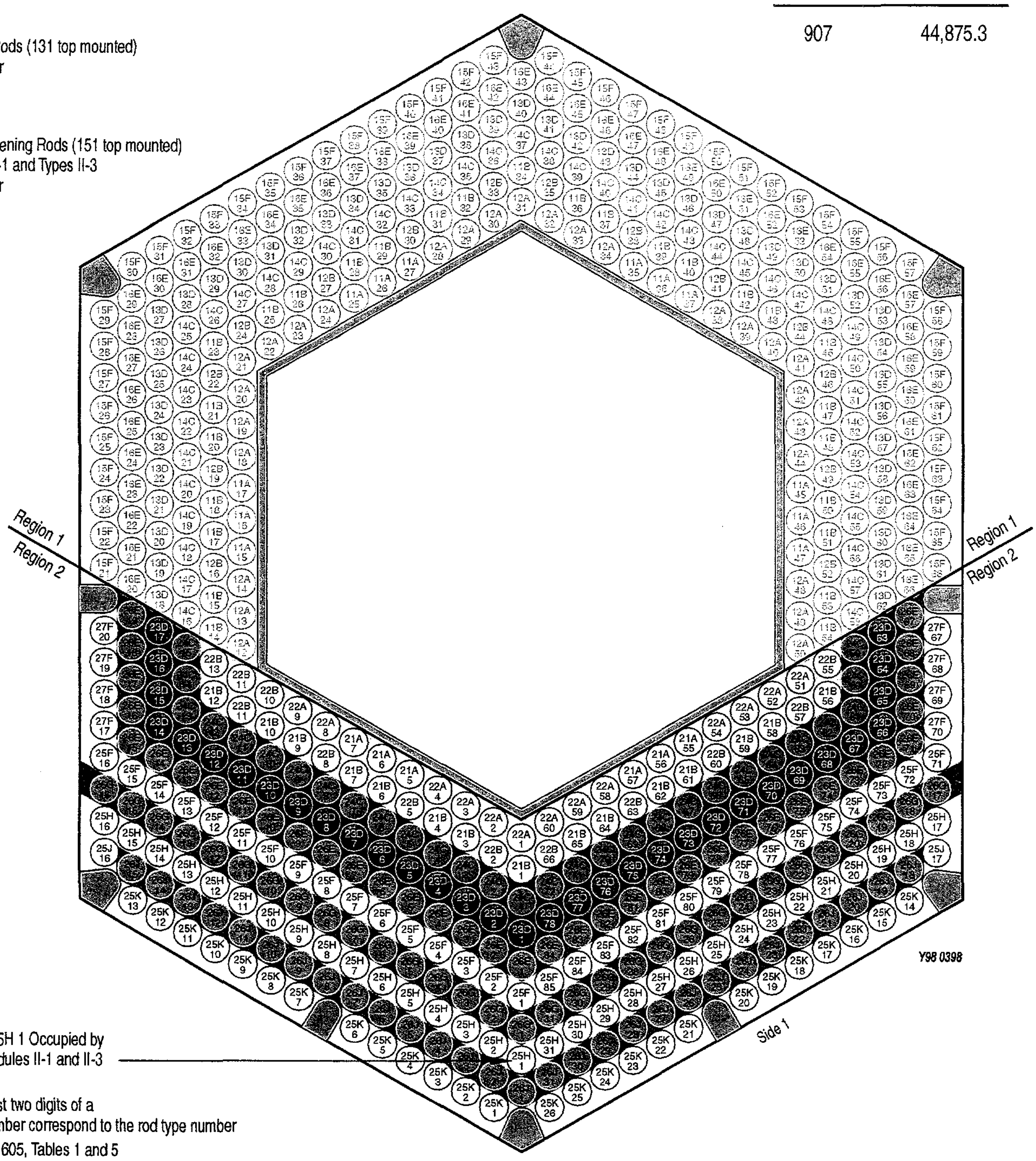

Rod Location 25H 1 Occupied by Flux Well in Modules II-1 and II-3

[1] Rod type: First two digits of a rod serial number correspond to the rod type number
[2] WAPD–TM–1605, Tables 1 and 5
[3] WAPD–TM–1612, Table V-2. WAPD–TM–1326, Table A-5

Figure 3-5. Type II Blanket Module rod and cell identification (modified from WAPD-TM-1605 Figure A1-3).

	Rod Type[1]	Binary Stack Length	Enrichment (U-fissile wt %)[2]	Theoretical Density (g/cm^3)[2]	Mass Initial Fissile (g)/Rod[3]	Number of Rods/Core	Mass Initial Fissile (g)/Core
	21,22	42"	1.649	10.013	18.96	486	9,214.6
	24	56"	2.005	10.016	30.74	258	7,930.9
	23	70"	2.733	10.022	52.56	264	13,875.8
	25, 27	84"	2.733	10.022	63.06	1,618	102,031.1
	26	84"	2.005	10.016	46.4	48	2,227.2
						2,674	135,279.6

Region 1
187 Standard Rods (94 top mounted)
.5715" Diameter
.630" Pitch

Region 2
446 Power Flattening Rods (94 top mounted)
445 for Types III-1 and Types III-2
.5265" Diameter
.630" Pitch

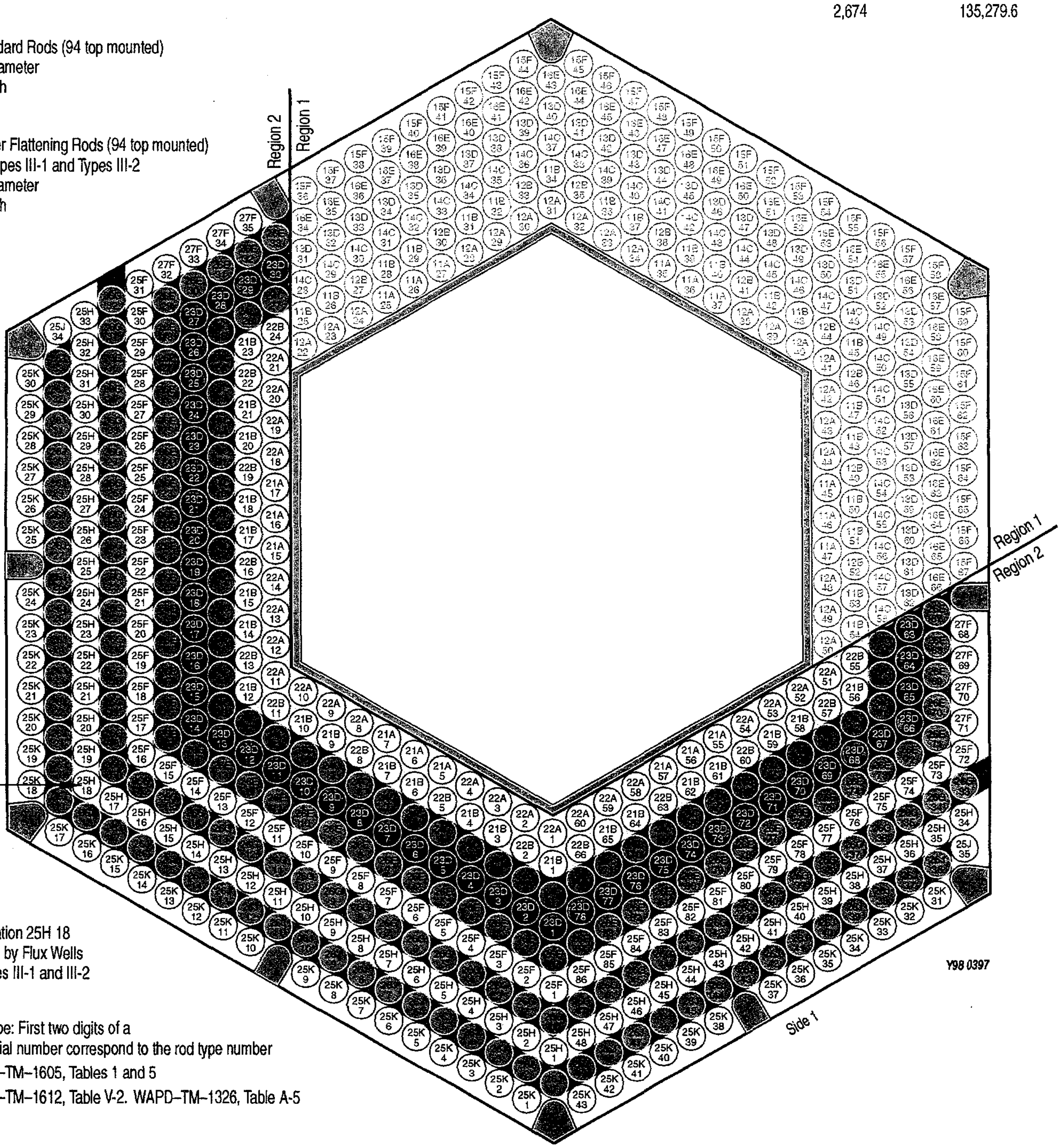

Rod Location 25H 18
Occupied by Flux Wells
in Modules III-1 and III-2

[1] Rod type: First two digits of a rod serial number correspond to the rod type number

[2] WAPD–TM–1605, Tables 1 and 5

[3] WAPD–TM–1612, Table V-2. WAPD–TM–1326, Table A-5

Figure 3-6. LWBR Type III Blanket Module rod and cell identification (modified from WAPD-TM-1605 Figure A1-4).

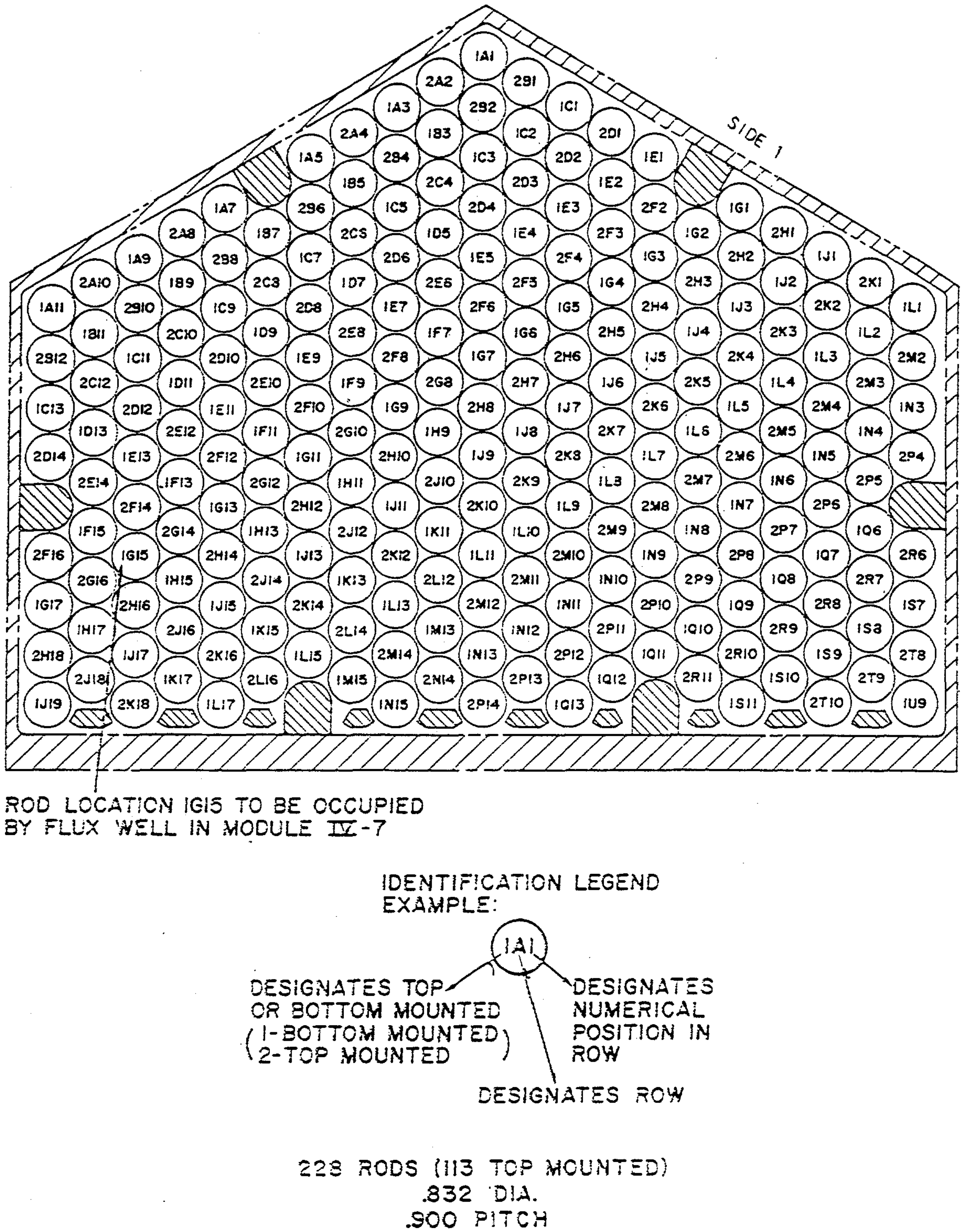

Figure 3-7. LWBR Type IV Reflector Module rod and cell identification (WAPD-TM-1605, Figure A1-5).

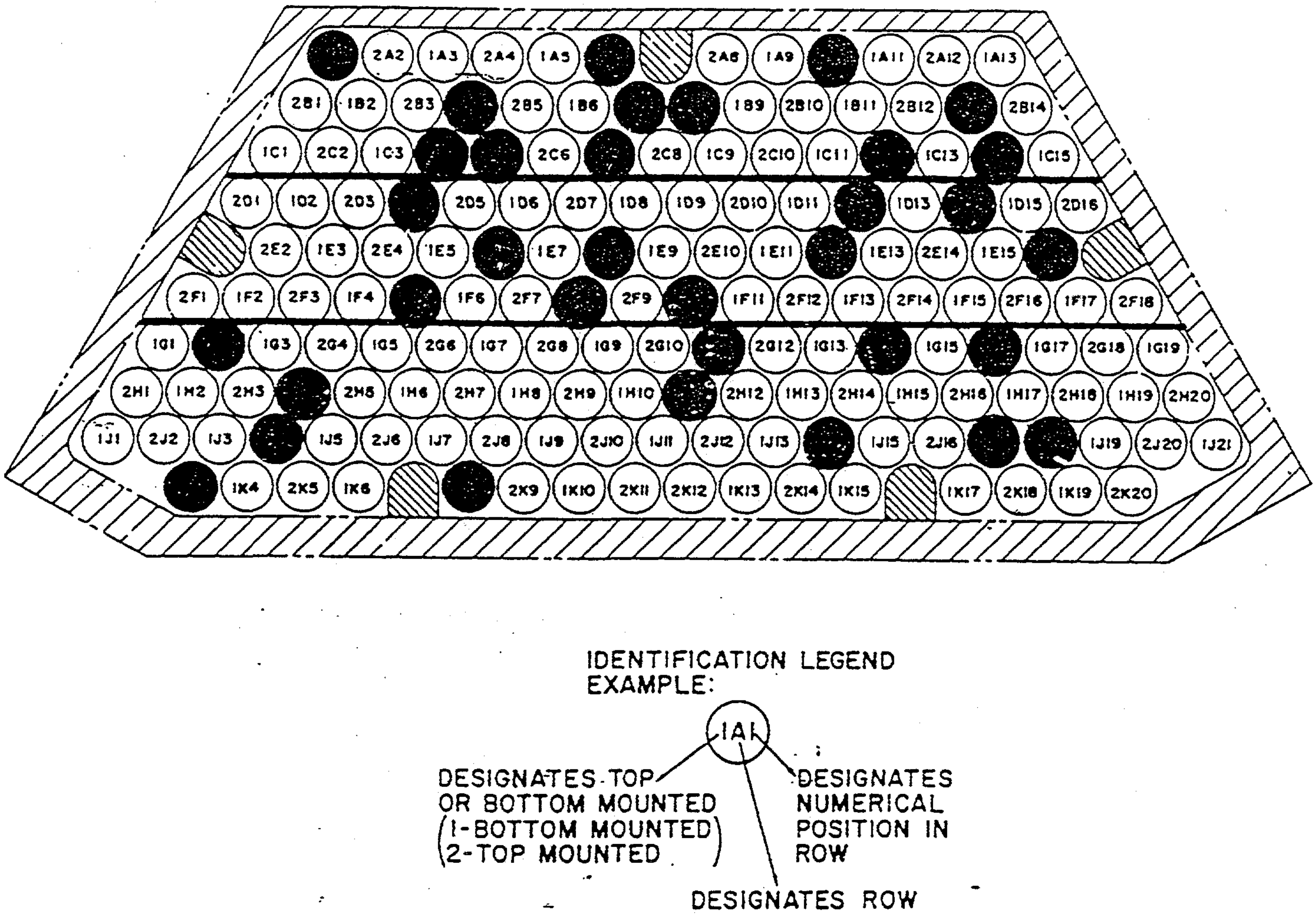

Figure 3-8. Type V Reflector Module (blackened dots represent the rods removed from RV-4 for proof-of-breeding tests, from WAPD-TM-1612 Figure V-13).

Table 3-1. Number of rods in each type of module (not including deductions for flux wells).

Seed	619 × 12
Type I Blanket	444 × 3
Type II Standard Blanket	261 × 3
Type II Power-Flattening Blanket	303 × 3
Type III Standard Blanket	187 × 6
Type III Power-Flattening Blanket	446 × 6
Type IV Reflector	228 × 9
Type V Reflector	167 × 6
Total	17,304 (including 16 flux wells)

3.1.2 Date of Fabrication

Fabrication was completed between 1976 and 1977, and the LWBR core began operating in the Fall of 1977 (WAPD-TM-1278, p. iii). Approximately 24,000 fuel rods were manufactured from which about 17,290 were assembled into the LWBR core (WAPD-TM-1278, p. I-1).

3.2 Fuel Information

3.2.1 General Description

The LWBR core was fueled with Th-232 and U-233, which was zoned axially and radially to maximize neutron economy (WAPD-TM-1326, p. 6+). Fuel rods were fabricated with many features that had never been used in fuel elements of commercial reactors. Uranium-233 was selected for the fissile fuel because it has the largest neutron regeneration factor ($\eta = 2.3$) in the thermal and epithermal region of any of the potential fissile fuels (Pu-239, Pu-241, U-235, and U-233). Neutron regeneration is the average number of neutrons produced in fission per neutron absorbed in fissile fuel. In addition, U-233 has a much lower total fission gas release at typical operating heat flux conditions. Assuming iodine release is proportional to total fission gas release, less iodine is released using U-233 in thoria, resulting in less iodine stress corrosion cracking in the cladding (WAPD-TM-1387, p. 27).

Pellets were loaded into Zircaloy-4 cladding tubes, which were welded at both ends to solid end plugs (WAPD-TM-1600, WAPD-TM-1244, p. IV-1, WAPD-TM-1326, p. 5). Within the tube and above the fuel stack, there was a plenum void to house the plenum spring, which allowed fuel stack expansion to accept fission gas released from the fuel. This design served to minimize internal gas pressure.

Several types of pellets were manufactured and loaded in the rods to permit variable loadings. The ceramic pellets were either thoria or binary (ThO_2 and UO_2). Hundreds of pellets were loaded in each rod; hundreds of rods were loaded in each of the core's 39 modules. Physical, chemical, and radiological properties of the pellets, rods, and modules are presented in the next sections.

The thoria-based fuel system had many operating advantages over the urania system, with some fabrication disadvantages. Fabrication difficulties of importance to design included uranium homogeneity, which is difficult to obtain in a single fire process, and attainment of high density because of thoria's high melting temperature and reduced diffusion coefficients at normal sintering temperature. Attainment of uranium homogeneity limits was achieved by comicronizing and by thoroughly *mixing* the binary compositions. High density was achieved by using micronized powder and a slightly higher than normal sintering temperature (WAPD-TM-1605, p. 20-21).

Best estimate melting point is about 5950° F for UO_2-ThO_2 fuel systems containing 2 to 6 weight percent UO_2. Thermal conductivity and corrosion resistance of the thoria based system was higher than the urania system (p. 21, WAPD-TM-1605).

3.2.1.1 Core Components. The LWBR core consists of seed, blanket, and reflector modules, which contain hundreds of fuel rods apiece. Table 3-2 shows the number of rods for the seed, standard blanket and power flattening blanket modules along with the initial loadings of thorium and uranium. Seed and blanket assemblies contained both fissile U-233 and fertile Th-232, while the reflector blanket fuel modules contained only thorium (as-built). The heavy metal content of the seed, blanket and power-flattening blanket modules is given Table 3-3.

To enhance breeding performance, the standard blanket region had a high metal-to-water ratio of 2.98. The power flattening blanket fuel region had a lower metal-to-water ratio of about 1.76 and a higher UO_2 concentration than the standard blanket. The power flattening blanket was located on the outer periphery of the nine seed-blanket assemblies surrounding the three center seed-blanket assemblies. As a result, the overall radia core power distribution was flattened (WAPD- TM-1605, p. 5).

3.2.1.1.1 Seed. At the beginning of life, the seed module contained the most highly enriched fuel within the core. There were two enrichments: the more highly-enriched fuel (wt%=5.195) occupied the central 11 rows, and fuel of lower enrichment (wt%=4.327) occupied the outer four rows (Figure 3-2). The binary stack length decreased from the center, with the central 11 rows having a binary stack length of 84" and the outer most rows having a binary stack length of 42" (Figures 3-1 and 3-2).

3.2.1.1.2 Standard Blanket. The standard blanket modules contained three enrichments (low=1.211 wt%; medium=1.662 wt%; high=2 wt%) and four binary stack lengths (Figure 3-3). Binary stack lengths increased with distance from the central seed, and so did the enrichments, with the exception of the most outer row, which had a medium enrichment of 1.662 wt% U-fissile. Average as-built fuel characteristics of the standard blanket are presented in Table 3-4.

3.2.1.1.3 Power-flattening Blanket. The power flattening blanket modules contained three fuel enrichments (1.649, 2.005 and 2.773 wt%) and four binary stack lengths (Figures 3-4 and 3-5). Enrichment and binary stack length increased with distance from the central seed, with the exception of the outer-most six rows, which had long binary stack lengths but only moderate (2.005 wt%) enrichment. Average as-built fuel characteristics are presented in Table 3-4.

3.2.1.1.4 Reflector. The reflector modules contained rods with only thoria pellets. Rod configurations for Type IV and V reflectors are shown in Figures 3-7 and 3-8.

Table 3-2. Seed and blanket module initial thorium and uranium loadings (WAPD-TM-1612, Table III-1).

Module	Rods	Thorium kgs	^{232}U Grams	^{233}U Grams	^{234}U Grams	^{235}U Grams	^{236}U Grams	^{238}U Grams	$U^{fissile}$ Grams
Seed I-1	619	433.61	0.12	16505.1	215.12	13.04	2.68	48.92	16518.1
I-2	619	433.60	0.11	16506.9	218.02	14.95	3.21	48.66	16521.8
I-3	619	433.91	0.10	16522.9	215.80	12.21	2.70	48.83	16535.1
II-1	619	433.88	0.10	16529.4	215.21	11.79	2.57	48.55	16541.2
II-2	619	433.66	0.10	16528.4	216.03	12.46	2.74	47.85	16540.8
II-3	619	434.09	0.10	16568.7	215.20	11.49	2.49	45.85	16580.2
III-1	619	433.57	0.11	16505.3	214.12	12.25	2.47	49.03	16517.5
III-2	619	433.87	0.11	16545.4	214.16	11.01	2.33	47.44	16556.5
III-3	619	434.07	0.11	16557.8	214.11	10.90	2.32	47.46	16568.7
III-4	619	434.08	0.11	16552.1	214.04	10.85	2.28	47.34	16563.0
III-5	619	434.11	0.10	16562.0	213.93	10.69	2.24	46.69	16572.7
III-6	619	434.04	0.11	16557.2	214.96	11.40	2.45	47.39	16568.6
Totals	7428	5206.55	1.34	198441.2	2580.75	143.10	30.53	574.04	198584.3
Std. I-1	443	1299.45	0.13	16166.5	220.01	15.69	4.41	42.11	16182.2
Blkt. I-2	443	1299.37	0.13	16163.9	218.54	14.85	4.07	42.19	16178.7
I-3	443	1299.30	0.13	16161.5	217.06	13.97	3.73	42.24	16175.4
II-1	261	765.65	0.07	9325.4	125.49	8.26	2.22	24.56	9333.6
II-2	261	765.91	0.07	9324.0	126.84	9.05	2.53	24,39	9333.0
II-3	261	765.71	0.07	9329.1	126.12	8.55	2.35	24.31	9337.6
III-1	187	548.50	0.05	6619.9	90.10	6.42	1.81	17.20	6626.4
III-2	187	548.69	0.05	6623.3	90.39	6.59	1.86	17.25	6629.9
III-3	187	548.62	0.05	6618.4	90.50	6.67	1.90	17.18	6625.1
III-4	187	548.69	0.05	6623.6	90.19	6.47	1.82	17.32	6630.1
III-5	187	548.72	0.05	6626.4	90.26	6.49	1.83	17.28	6632.9
III-6	187	548.46	0.05	6619.7	91.26	7.09	2.06	17.17	6626.7
Totals	3234	9487.14	0.97	116201.6	1576.82	110.17	30.63	303.26	116311.7
Pwr. II-1	302	741.39	0.11	15590.0	202.42	16.22	4.72	77.94	15606.3
Flat.II-2	303	743.51	0.11	15644.8	198.72	14.85	3.92	90.47	15659.7
Blkt.II-3	302	741.36	0.11	15588.4	192.90	13.25	3.44	95.46	15601.7
III-1	445	1092.25	0.17	23155.6	291.57	21.14	5.68	132.64	23176.7
III-2	445	1092.02	0.17	23131.0	305.97	26.29	7.57	117.14	23157.3
III-3	446	1094.47	0.17	23212.3	289.36	20.53	5.33	141.33	23232.9
III-4	446	1094.36	0.17	23197.7	310.19	27.32	7.93	112.01	23225.1
III-5	446	1094.55	0.17	23201.8	303.67	25.16	7.16	120.02	23227.0
III-6	446	1094.30	0.17	23210.8	295.43	22.61	6.00	136.16	23233.4
Totals	3581	8788.26	1.39	185932.6	2390.28	187.41	51.80	1023.23	186120.1
Core Totals (Excluding Reflector)	14243	23481.96	3.70	500575.4	6547.86	440.69	112.97	1900.53	501016.1

Table 3-3. Seed and blanket module as-built properties (WAPD-TM-1326, Table A-14).

	Module Type	Module S/N	Rods	U-232 Grams	U-233 Grams	U-234 Grams	U-235 Grams	U-236 Grams	U-238 Grams	U-Fiss Grams	Thorium KGS	Mean Clad OD Inches	Mean Clad Wall Inches	Mean Grid Pitch Inches	Mean Grid Wgt Grams
	I-1	L-BB01-04	619	0.1199	16512.0	215.2	13.0	2.7	48.9	16525.0	433.607	0.30626	0.02221	0.36851	1533.
	I-2	L-BB01-05	619	0.1182	16513.9	218.1	15.0	3.2	48.7	16528.8	433.601	0.30620	0.02218	0.36861	1533.
	I-3	L-BB01-06	619	0.1196	16522.5	215.8	12.2	2.7	48.8	16534.7	433.919	0.30630	0.02222	0.36850	1531
	II-1	L-BB01-09	619	0.1189	16528.6	215.2	11.8	2.6	48.6	16540.4	433.890	0.30636	0.02226	0.36857	1539.
S	II-2	L-BB01-10	619	0.1188	16528.7	216.0	12.5	2.7	47.9	16541.2	433.660	0.30636	0.02219	0.36852	1549.
E	II-3	L-BB01-13	619	0.1201	16567.1	215.2	11.5	2.5	45.9	16578.6	434.097	0.30626	0.02215	0.36863	1542.
E	III-1	L-BB01-07	619	0.1207	16511.4	214.2	12.3	2.5	49.1	16523.6	433.571	0.30616	0.02215	0.36862	1529.
D	III-2	L-BB01-08	619	0.1208	16543.6	214.1	11.0	2.3	47.4	16554.6	433.882	0.30621	0.02214	0.36857	1541.
	III-3	L-BB01-12	619	0.1212	16554.8	214.1	10.9	2.3	47.5	16565.7	434.082	0.30621	0.02212	0.36859	1542.
	III-4	L-BB01-11	619	0.1196	16550.2	214.0	10.9	2.3	47.3	16561.1	434.090	0.30627	0.02218	0.36850	1550.
	III-5	L-BB01-14	619	0.1197	16560.2	213.9	10.7	2.2	46.7	16570.9	434.114	0.30620	0.02213	0.36863	1552.
	III-6	L-BB01-16	619	0.1205	16554.4	214.9	11.4	2.5	47.4	16565.8	434.047	0.30621	0.02214	0.36857	1557.
	Seed Totals		7428	1.4380	198447.4	2580.7	143.2	30.5	574.2	198590.4	5206.560				
S	I-1	L-GU52-01	443	0.1353	16171.3	220.1	15.7	4.4	42.1	16187.0	1299.455	0.57171	0.02808	0.63049	2239.
T	I-2	L-GU52-02	443	0.1360	16169.1	218.6	14.9	4.1	42.2	16184.0	1299.371	0.57166	0.02806	0.63040	2230.
D	I-3	L-GU51-01	443	0.1365	16166.6	217.1	14.0	3.7	42.3	16180.5	1299.300	0.57168	0.02811	0.63044	2228.
	II-1	L-GV51-01	261	0.0784	9328.5	125.5	8.3	2.2	24.6	9336.8	765.649	0.57172	0.02809	0.63053	1314.
B	II-2	L-GS22-01	261	0.0778	9326.7	126.9	9.1	2.5	24.4	9335.8	765.910	0.57176	0.02817	0.63044	1313.
L	II-3	L-GV52-01	261	0.0785	9331.8	126.2	8.6	2.4	24.3	9340.3	765.716	0.57165	0.02806	0.63051	1310.
A	III-1	L-GW51-01	187	0.0554	6622.3	90.1	6.4	1.8	17.2	6628.8	548.505	0.57166	0.02807	0.63029	930.
N	III-2	L-GW52-01	187	0.0552	6625.5	90.4	6.6	1.9	17.3	6632.1	548.695	0.57156	0.02805	0.63020	935.
K	III-3	L-GW53-01	187	0.0551	6621.1	90.5	6.7	1.9	17.2	6627.8	548.624	0.57172	0.02806	0.63024	933.
E	III-4	L-GT22-01	187	0.0550	6626.2	90.2	6.5	1.8	17.3	6632.7	548.692	0.57172	0.02812	0.63021	935.
T	III-5	L-GT22-02	187	0.0554	6628.6	90.3	6.5	1.8	17.3	6635.1	548.720	0.57166	0.02811	0.63021	932.
	III-6	L-GT22-03	187	0.0547	6622.1	91.3	7.1	2.1	17.2	6629.2	548.463	0.57163	0.02800	0.63028	930.
	Blkt Totals		3234	0.9733	116239.8	1577.2	110.4	30.6	303.4	116350.1	9487.100				
P	II-1	L-GV51-01	302	0.1148	15588.5	202.4	16.2	4.7	77.9	15604.7	741.395	0.52755	0.02643	0.63053	1525.
F	II-2	L-GS22-01	303	0.1145	15643.5	198.7	14.8	3.9	90.5	15658.3	743.518	0.52745	0.02646	0.63044	1525.
	II-3	L-GS52-01	302	0.1137	15586.2	192.9	13.3	3.4	95.5	15599.5	741.370	0.52742	0.02644	0.63051	1521.
B	III-1	L-GW51-01	445	0.1696	23153.1	291.5	21.1	5.7	132.6	23174.2	1092.258	0.52743	0.02640	0.63029	2217.
A	III-2	L-GW52-01	445	0.1687	23129.3	306.0	26.3	7.6	117.1	23155.6	1092.029	0.52740	0.02638	0.63020	2230.
N	III-3	L-GW53-01	446	0.1688	23209.8	289.3	20.5	5.3	141.3	23230.3	1094.481	0.52744	0.02643	0.63024	2224.
K	III-4	L-GT22-01	446	0.1700	23195.6	310.2	27.3	7.9	112.0	23222.9	1094.364	0.52746	0.02641	0.63021	2229.
E	III-5	L-GT22-02	446	0.1698	23199.2	303.6	25.2	7.2	120.0	23224.4	1094.561	0.52741	0.02643	0.63021	2222.
T	III-6	L-GT22-03	446	0.1693	23208.2	295.4	22.6	6.0	136.1	23230.8	1094.307	0.52744	0.02640	0.63028	2218.
	PFBK Totals		3581	1.3592	185913.4	2390.0	187.3	51.7	1023.0	186100.7	8788.283				
	Core Totals		14243	3.7705	500600.6	6547.9	440.9	112.8	1900.6	501041.2	23481.943*				

* Excluding reflector blanket thorium

Table 3-4. Average as-built LWBR core fuel characteristics (WAPD-TM-1326, Table II-2).

	Pellet OD (in.)	Pellet Length (in.)	Percent of Theoretical Density	U-Fissile (w/o)*	U-Fissile (grams/in.)	Fissile Loading (kg)	Loading Th-232 (kg)
Seed							
Thoria	0.2556	0.530	98.01	None	None	None	1846.6
Low zoned	0.2520	0.444	97.71	4.337	0.3416	61.28	1179.5
High zoned	0.2520	0.615	97.55	5.202	0.4114	137.31	2180.4
Standard Blanket							
Thoria	0.5106	0.616	97.80	None	None	None	3670.0
Low zoned	0.5105	0.531	98.61	1.214	0.3920	15.99	1141.6
Medium zoned	0.5105	0.868	98.22	1.668	0.5421	42.68	2205.9
High zoned	0.5105	0.785	98.11	2.005	0.6498	57.67	2469.6
Power Flattening Blanket							
Thoria	0.4696	0.447	98.06	None	None	None	2632.4
Low zoned	0.4695	0.870	98.03	1.654	0.4537	10.24	533.5
Medium zoned	0.4695	0.786	98.04	2.009	0.5509	13.58	580.1
High zoned	0.4696	0.701	97.91	2.739	0.7492	162.29	5042.3
Radial Reflector Blanket	0.7417	0.741	97.28	None	None	None	18574.2
TOTAL						501.04	42056.1

$$\text{*U-Fissile (w/o)} = \frac{\text{U-233} + \text{U-235}}{UO_2 + ThO_2} \times 100$$

U Isotopic Composition

U-232	<0.001 w/o
U-233	98.23
U-234	1.29
U-235	0.09
U-236	0.02
U-238	0.37

3.2.1.2 Rods. There were a total of 23 different rod types in the LWBR core (WAPD-TM-1278, p. II-1). Each fuel rod was composed of a Zircaloy-4 seamless tube filled with oxide fuel pellets. The fuel rods in each of the seed, standard blanket, power-flattening blanket, and reflector regions of the core were of different diameter, physical length, binary stack length (length of the rod occupied by binary pellets), and initial uranium loadings. Radial and axial variations of fuel loading were employed in every region of the core except the reflector modules. Rod lengths ranged from about 279 to 300 cm (110 to 118 in.) and diameters ranged from 0.76 to 2.03 cm (0.3 to 0.8 in) (Table 3-5). A plenum region at the top of each rod provided void volume to accommodate released fission gas, and a helical coiled spring to exert pressure on the pellets to keep the stack together.

In each rod, there was only one type of binary fuel pellet, but multiple loading densities within modules. For example, in any blanket module, there were three binary loading densities, but each rod contained a single type of binary pellet. The combination of radial and axial fuel zones served the dual purpose of achieving an acceptable peak-to-average power ratio and providing adequate movable fuel reactivity worths. Average as-built core fuel characteristics for all 12 LWBR fuel compositions are presented in Table 3-4.

Tops and bottoms of the seed and blanket rods were packed with 25.4 cm (10 in.) stacks of thoria pellets (reflectors) for the 213 cm (84 in.) binary stacks (see Figures 3-1 and 3-4). Rods varied slightly in length, depending on their location and loading within the core. Seed rods were 296.21 cm (116.62 in) and blanket rods were 298.83 cm (117.65 in).

There were 9, 8, and 6 grids levels per each seed, blanket and reflector module, respectively. Approximately half of the fuel rods in each module were fixed to the top of the module and the other half to the bottom of the module (WAPD-TM-1605, p. 8).

Irradiation of the rods caused the rod diameters to shrink. Shrinkage for the various rod types ranged from: .03 to .06 mm (1.2 to 2.5 mils) for seed rods; .07 to .10 mm (2.9 to 3.8 mils) for standard blanket rods; .06 to .07 mm (2.4 to 2.8 mils) for power flattening blanket rods; and .07 to .13 mm (2.9 to 5.5 mils) for reflector rods (not including groove depths of .1 mm (.004 in) maximum in blanket rods and ridge heights of .03 mm (.001 in.) maximum in reflector rods) (WAPD-TM-1605, p. 119).

3.2.1.2.1 ***Seed rods***—LWBR seed modules had eight types of seed fuel rods designated as 01, 02, 03, 04, 05, 06, 07, and 08 (Figure 3-2). Rod types with odd designations were fixed to a baseplate at the bottom of the seed module, and rod types with even designations were fixed to a baseplate at the top end of the module (WAPD-TM-1605, p. 10). Nominal length of the rods (excluding the end stem) was 296 cm (116.6 in.). Outside diameter (OD) was nominally 0.777 cm (.306 in), and seed rods weighed about 2 pounds apiece (p. 37 of WAPD-TM-1605). Seed rods had a 25.4 cm (10 in.) plenum at the top of the fuel stack to accommodate fission gas release. The plenum included an Inconel compression spring at the top of the stack to minimize formation of axial gaps in the stack during handling, normal reactor operation, and shock loading (e.g., from scrams, check value slams, earthquakes, etc., p. 13 in WAPD-TM-1605).

The seed fuel rods had two different binary (UO_2-Th_2) loadings (4.327 or 5.195 wt.% U-fissile), and four different stack lengths (42, 56, 70, or 84 inches, Figure 3-1). Table 3-6 lists the fissile loading for each rod type. Figure 3-9 shows a seed fuel rod and identifies the varying dimensions of the eight different types of seed rods (identified as 01-08 in the imbedded table). The rod type identifiers correspond with the identifiers provided in Figure 3-2.

Table 3-5. LWBR fuel rod dimensions (WAPD-TM-1605, Table 4).

Attribute	Seed	Standard Blanket	Power Flattening Blanket	Reflector
Rod length	116.620 ±.065	117.650 ±.065	117.650 ±.065	110.85 ±0.065
Cladding Type**	RXA	SRA	SRA	SRA
Cladding Outside*** Diameter	0.306 ±.0015 +.003 -.002	0.5715 ±.0015 ±.0025	0.5275 ±.0015 ±.0025	0.832 ±.003
Cladding Inside*** Diameter	0.262 ±.001 ±.002	0.516 ±.001 ±.002	0.475 ±.001 ±.002	0.748 ±.001 ±.002
OD/t	13.9	20.6	20.1	19.8
Pellet Diameter	0.252 ±.0005	0.5105 ±.0005	0.4695 ±.0005	0.7415 ±.0005
Cladding-Pellet Radial Gap	0.0042-0.0057	0.002-0.0035	0.002-0.0035	0.002-0.0045
Plenum Length	10.0 ±.100	9.9 ±.055	9.9 ±.055	3.955 ±.040

*All dimensions in inches, except as noted

**RXA - Recrystallization Annealed
SRA - Stress Relief Annealed

***Average and local tolerance

Table 3-6. Initial loadings of blanket rods.

Rod Type	Module Type	U-fissile wt%[1]	Theoretical Density (g/cm^3)[1]	Binary stack length (in)	Thoria end length[2] (in)	# Rods per core	Initial loading per rod[3] (g-fissile)	Initial loading per core[4] (g-fissile)	Final loading per core[5] (g-fissile)	Fissile loss (Initial-Final) (g-fissile)	Cladding O.D.[6] (in)	Rod Length[5] (in)
05 or 06	Seed I	5.195	10.042	84	20	993	34.57	34328	24578	9750	0.31	116.62
04	Seed I	4.327	10.035	70	34	198	23.92	4736	3474	1262	0.31	116.62
03	Seed I	4.327	10.035	56	48	216	19.14	4134	3375	760	0.31	116.62
01, 02, 07, or 08	Seed I	4.327	10.035	42	62	450	14.33	6449	6289	159	0.31	116.62
05 or 06	Seed II	5.195	10.042	84	20	993	34.57	34328	25532	8796	0.31	116.62
04	Seed II	4.327	10.035	70	34	198	23.92	4736	3572	1165	0.31	116.62
03	Seed II	4.327	10.035	56	48	216	19.14	4134	3429	705	0.31	116.62
01, 02, 07, or 08	Seed II	4.327	10.035	42	62	450	14.33	6449	6294	155	0.31	116.62
05 or 06	Seed III	5.195	10.042	84	20	1986	34.57	68656	52764	15892	0.31	116.62
04	Seed III	4.327	10.035	70	34	396	23.92	9472	7327	2145	0.31	116.62
03	Seed III	4.327	10.035	56	48	432	19.14	8268	6962	1307	0.31	116.62
01, 02, 07, or 08	Seed III	4.327	10.035	42	62	900	14.33	12897	12609	289	0.31	116.62
11 or 12	Std B-1	1.211	10.009	42	62	378	16.45	6218	13583	-7365	0.57	117.65
14	Std B-1	1.662	10.013	56	48	216	30.34	6553	8930	-2376	0.57	117.65
13	Std B-1	2	10.016	70	34	234	45.47	10640	11217	-577	0.57	117.65
16	Std B-1	2	10.016	84	20	252	54.66	13774	13355	419	0.57	117.65
15	Std B-1	1.662	10.013	84	20	252	45.66	11506	12047	-541	0.57	117.65
11 or 12	Std B-II	1.211	10.009	42	62	240	16.45	3948	8345	-4397	0.57	117.65
14	Std B-II	1.662	10.013	56	48	129	30.34	3914	5238	-1324	0.57	117.65
13	Std B-II	2	10.016	70	34	135	45.47	6138	6420	-282	0.57	117.65
16	Std B-II	2	10.016	84	20	141	54.66	7707	7452	255	0.57	117.65
15	Std B-II	1.662	10.013	84	20	138	45.66	6301	6569	-268	0.57	117.65
11 or 12	Std B-III	1.211	10.009	42	62	354	16.45	5823	11936	-6113	0.57	117.65
14	Std B-III	1.662	10.013	56	48	186	30.34	5643	7421	-1778	0.57	117.65
13	Std B-III	2	10.016	70	34	192	45.47	8730	9066	-336	0.57	117.65
16	Std B-III	2	10.016	84	20	198	54.66	10823	10445	378	0.57	117.65
15	Std B-III	1.662	10.013	84	20	192	45.66	8767	9097	-330	0.57	117.65

Table 3-6. (continued).

Rod Type	Module Type	U-fissile wt%[1]	Theoretical Density (g/cm³)[1]	Binary stack length (in)	Thoria end length[2] (in)	# Rods per core	Initial loading per rod[3] (g-fissile)	Initial loading per core[4] (g-fissile)	Final loading per core[5] (g-fissile)	Fissile loss (Initial-Final) (g-fissile)	Cladding O.D.[6] (in)	Rod Length[5] (in)
21 or 22	PF B-II	1.649	10.013	42	62	138	18.96	2616	4207	-1590	0.53	117.65
24	PF B-II	2.005	10.016	56	48	87	30.74	2674	3056	-382	0.53	117.65
23	PF B-II	2.733	10.022	70	34	99	52.56	5203	4567	636	0.53	117.65
25 or 27	PF B-II	2.733	10.022	84	20	561	63.06	35377	30490	4887	0.53	117.65
26	PF B-II	2.005	10.016	84	20	24	46.4	1114	1017	97	0.53	117.65
21 or 22	PF B-III	1.649	10.013	42	62	402	18.96	7622	11775	-4153	0.53	117.65
24	PF B-III	2.005	10.016	56	48	246	30.74	7562	8481	-919	0.53	117.65
23	PF B-III	2.733	10.022	70	34	276	52.56	14507	12861	1646	0.53	117.65
25 or 27	PF B-III	2.733	10.022	84	20	1704	63.06	107454	94584	12870	0.53	117.65
26	PF B-III	2.005	10.016	84	20	48	46.4	2227	2035	192	0.53	117.65
Number per core						3585		501431	470395			

Footnotes

1. WAPD-TM-1605, Table 1 and Table 5. Note: wt% of U-fissile in binary ($UO_2 + ThO_2$) fuel
2. Total length of fuel is 104", which is equal to binary stack length plus 10" of thoria on one end of the rod and a variable length on the other end. From WAPD-TM-1605.
3. WAPD-TM-1612, Table V-2. WAPD-TM-1326, Table A-5.
4. Calculated=(Rods/Core)*(Initial Fissile Loading/Rod)
5. WAPD-TM-1612, Table V-2.
6. WAPD-TM-1605, p. 14, Table 4

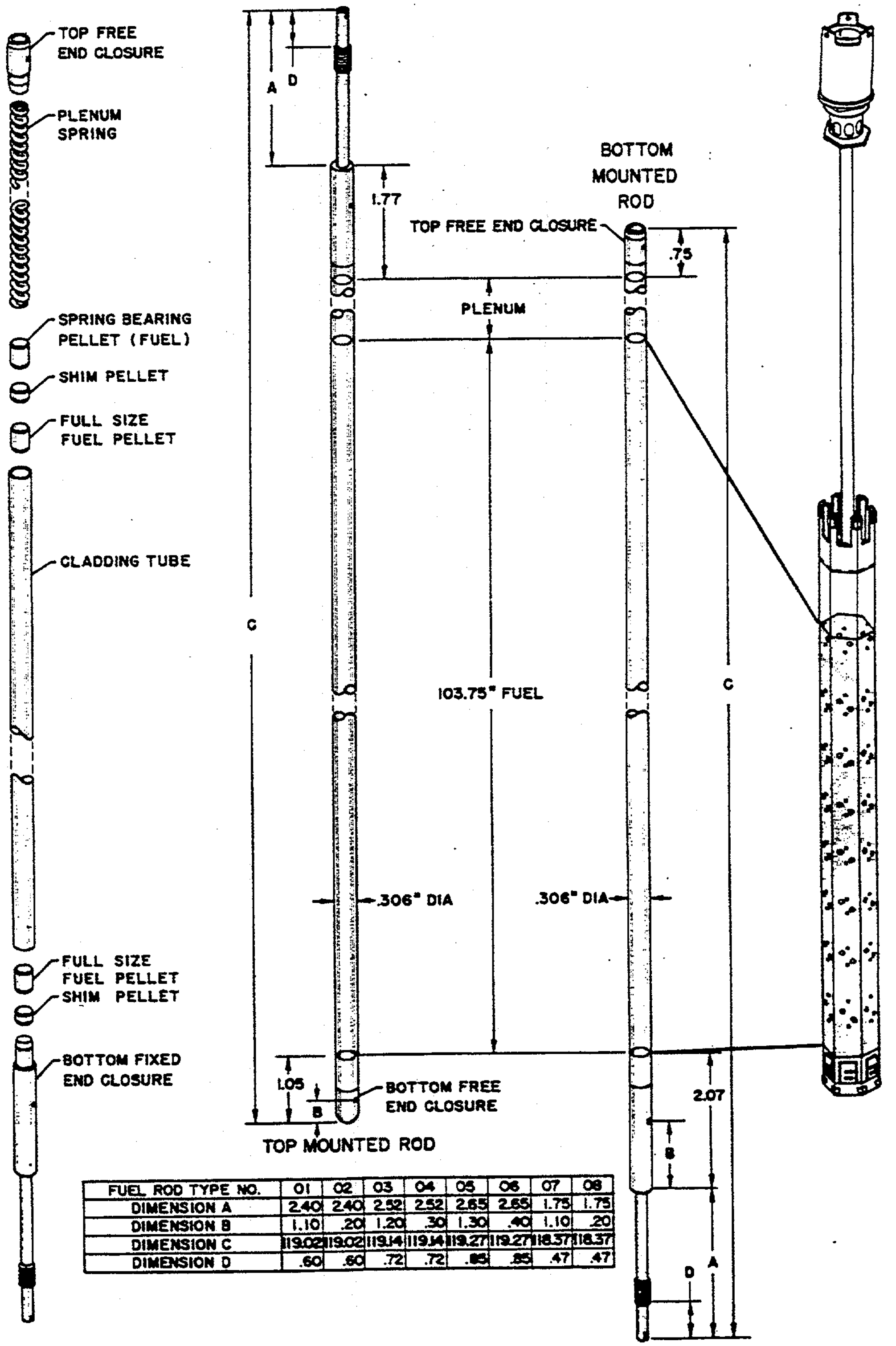

FUEL ROD TYPE NO.	01	02	03	04	05	06	07	08
DIMENSION A	2.40	2.40	2.52	2.52	2.65	2.65	1.75	1.75
DIMENSION B	1.10	.20	1.20	.30	1.30	.40	1.10	.20
DIMENSION C	119.02	119.02	119.14	119.14	119.27	119.27	118.37	118.37
DIMENSION D	.60	.60	.72	.72	.85	.85	.47	.47

Figure 3-9. LWBR Seed Fuel Rods (WAPD-TM-1605 Figure 3).

3.2.1.2.2 ***Blanket rods***—LWBR had six types of standard blanket fuel rods designated as 11, 12, 13, 14, 15, and 16 (corresponding to identifiers in Figure 3-3), and seven types of power flattening blanket fuel rods designated as 21, 22, 23, 24, 25, 26, and 27 (corresponding to identifiers in Figures 3-5 and 3-6). Figure 3-10 shows LWBR standard and power flattening blanket fuel rods. The standard blanket fuel rods had three binary loadings and four stack lengths. Loading and binary stack lengths for standard and power flattening blanket fuel rods are presented in Table 3-7. Rod types with odd designations were fixed to the bottom of the modules. Rod types with even designations were fixed to the top of the module (WAPD-TM-1605, p. 13). Standard blanket rods weighted about 8 pounds apiece, and power-flattening blanket rods weighed about 7 pounds (p. 37, WAPD-TM-1605).

3.2.1.2.3 ***Reflector rods***—Figure 3-11 shows a reflector rod. Reflector rods had only two rod types: 31 and 32. Both contained only thoria pellets. Rod type 31 was attached to the bottom of the module, and rod type 32 was attached to the top of the fuel module.

Reflector fuel rods had a 10 cm (4 in.) plenum with an Inconel support sleeve. The axial gap between the support sleeve and the top of its pellet stack was nominally 0.58 cm (0.23 in.). Each reflector rod had an Inconel compression spring at the top of the fuel stack to minimize the formation of in stack pellet-to-pellet gaps. Each top-mounted reflector fuel rod had a hemispherical free end. Each bottom-mounted fuel rod had a square free end. The rods were backfilled with helium at 1-atm pressure during welding. Dimensions for reflector fuel rods are also summarized in Table 3-5. Reflector rods weighed about 16 pounds apiece (p. 37 WAPD-TM-1605).

3.2.1.3 ***Pellets.*** The LWBR core contained about 3 million fuel pellets. Approximately 1.6 million of the pellets were binary (uranium oxide-thorium oxide) and the rest were thoria. There were several different sizes, shapes, and enrichments of pellets fabricated for the various rod types. All pellets were ceramic, more or less right circular cylinders, and either ThO_2 or binary (ThO_2 -$^{233}UO_2$). Binary pellets were used only in the seed and blanket modules of the reactor. There were eight sizes of binary pellets. Thoria pellets were fabricated in four different sizes: one for each type of rod (i.e., seed, standard blanket, power flattening blanket, and reflector rods)(Table 3-8).

Uranium in the UO_2 pellets was 98.23% enriched with fissile U-233 (WAPD-TM-1326, p. 11; WAPD-TM-1612, p. 5).

Each powder blend, either binary or thoria, received a unique blend designation. A representative sample of pellets from a blend was taken and used to determine the characteristics of the blend. The pellet properties that were measured and needed for the computational model of the core were length, diameter, and weight for all pellets in the sample, and weight percent of total uranium and uranium isotopic weight percents for binary pellets. These properties for binary pellets were stored in a computer file for each binary blend manufactured and used to compute uranium and thorium loadings of binary fuel rods (WAPD-TM-1314, pp. 27-28).

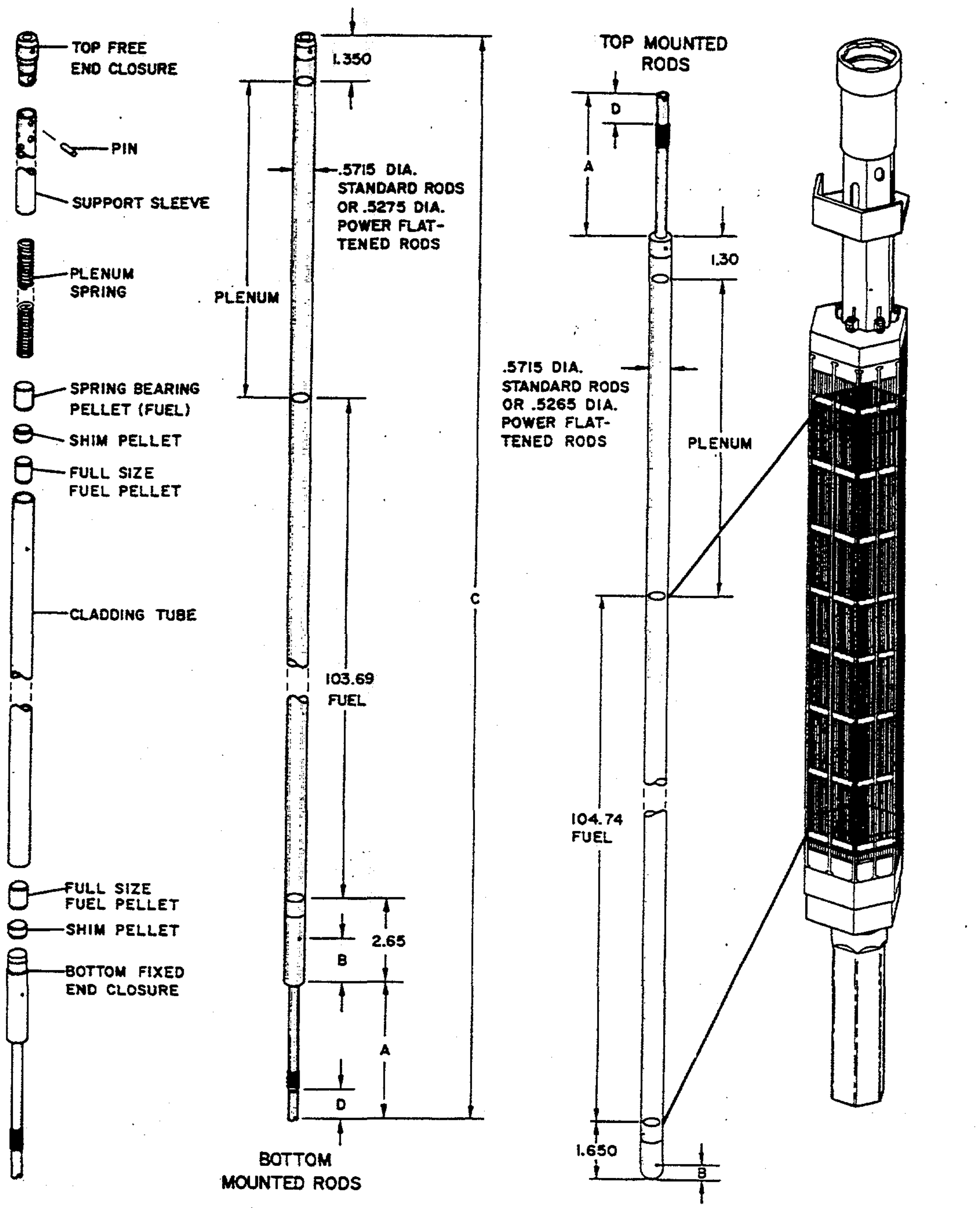

FUEL ROD TYPE NO.	11	12	13	14	15	16	21	22	23	24	25	26	27
DIMENSION-A	4.23	4.23	4.35	4.35	4.47	4.47	4.23	4.23	4.35	4.35	4.47	4.47	4.60
DIMENSION-B	1.40	.50	1.50	.60	1.60	.70	1.70	.80	1.80	.90	1.90	1.00	2.00
DIMENSION-C ± .07	121.9	121.9	122.0	122.0	122.1	122.1	121.9	121.9	122.0	122.0	122.1	122.1	122.3
DIMENSION-D	.78	.78	.90	.90	1.03	1.03	.78	.78	.90	.90	1.03	1.03	1.16

Figure 3-10. LWBR Blanket fuel rods (WAPD-TM-1605, Figure 4). Standard and Power-Flattening rods are depicted here. Standard rods have a Rod Type number <20.

Table 3-7. Standard and Power Flattening Blanket Rod binary fuel loadings (WAPD-TM-1605, Table 5).

Standard Blanket

Type	Composition w/o* U-fissile	Theoretical Density (gm/cc)	Binary Stack Length (in.)
11	1.211	10.009	42.0
12	1.211	10.009	42.0
13	2.000	10.016	70.0
14	1.662	10.013	56.0
15	1.662	10.013	84.0
16	2.000	10.016	84.0

Power Flattening Blanket

Type	Composition w/o* U-fissile	Theoretical Density (gm/cc)	Binary Stack Length (in.)
21	1.649	10.013	42.0
22	1.649	10.013	42.0
23	2.733	10.022	70.0
24	2.005	10.016	56.0
25	2.733	10.022	84.0
26	2.005	10.016	84.0
27	2.733	10.022	84.0

*w/o = weight percent

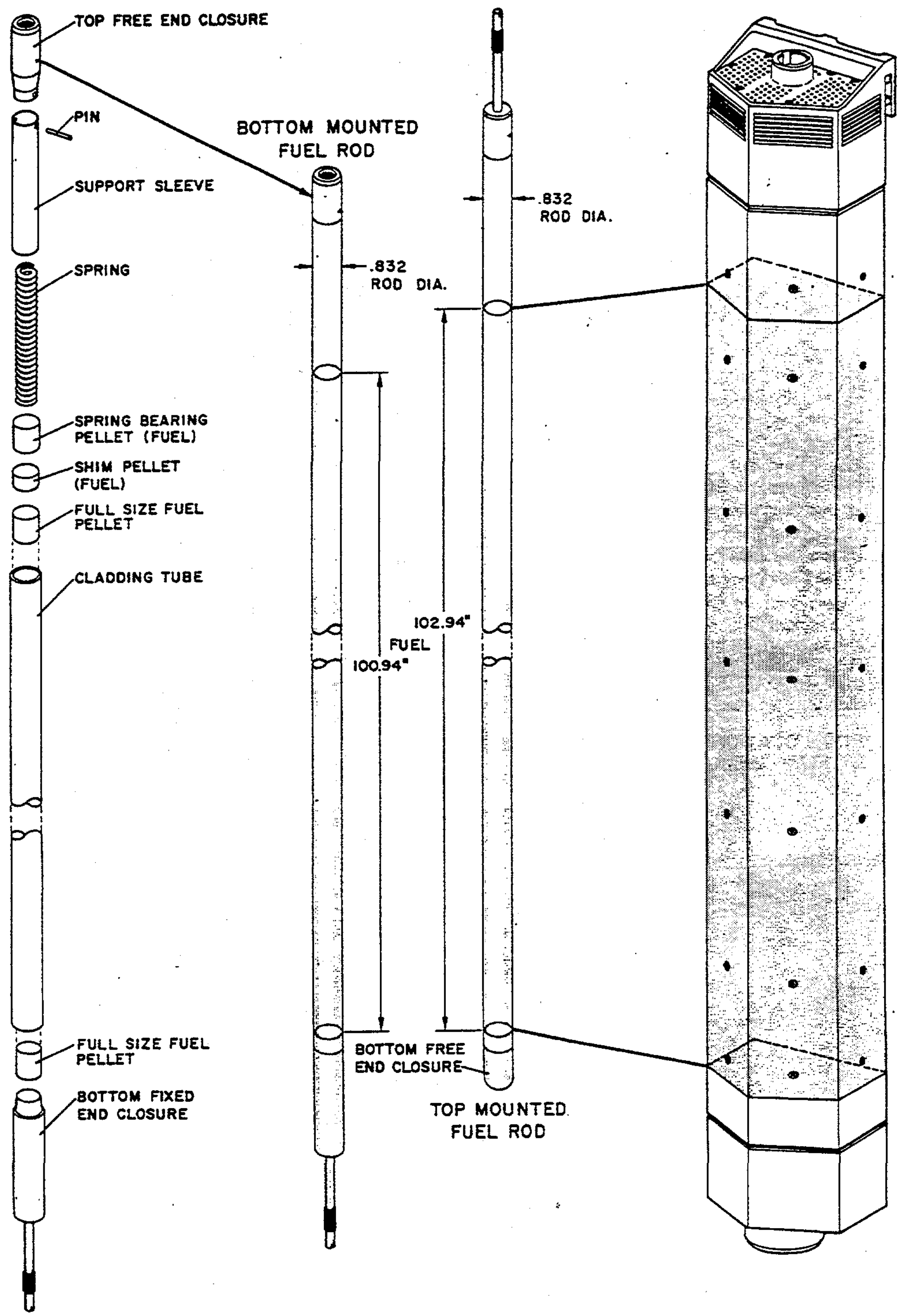

Figure 3-11. LWBR Reflector Fuel Rods (WAPD-TM-1605, Figure 5).

Table 3-8. LWBR Fuel Pellet dimensions (WAPD-TM-1387, Table 4).

Zircaloy-4 Cladding	Seed	Standard Blanket	Power Flattening Blanket	Reflector
Outside Diameter	0.306 ± .0015 avg +.003 / -.002 local	0.5715 ± .0015 avg ± .0025 local	0.5275 ± .0015 avg ± .0025 local	0.832 ± .003 avg ± .003 local
Inside Diameter	0.262 ± .002 local ± .001 avg	0.516 ± .002 local ± .001 avg	0.475 ± .002 local ± .001 avg	0.748 ± .001 avg ± .0025 local
Nominal Wall Thickness	0.022	0.02775	0.02625	0.042
Outside Diameter to Thickness Ratio	13.9	20.6	20.1	19.8
Cladding Heat Treatment**	RXA	SRA	SRA	SRA
UO_2-ThO_2 Fuel Pellets				
Diameter	0.252 ± .0005	0.5105 ± .0005	0.4695 ± .0005	-
Length	0.445 ± .020 0.615 ± .020	0.530 ± .020 0.870 ± .020 0.785 ± .020	0.870 ± .020 0.785 ± .020 0.700 ± .020	- - -
End Shoulder Width	0.046 ± .008	0.055 ± .015	0.055 ± .015	-
Endface Dish Depth	0.009 ± .003	0.014 ± .004	0.014 ± .004	-
Chamfer or Taper-				
Depth	0.015 ± .005	0.001 - 0.004	0.001 - 0.004	-
Length	0.015 ± .015	0.100 - 0.200	0.100 - 0.200	-
Range of Individual Pellet Densities, % of Theoretical	94.55 - 99.27	96.55 - 99.38	95.26 - 98.60	-
Fuel-Cladding Diametral Gap	0.0085 - 0.0115	0.004-0.007	0.004-0.007	-
ThO_2 Fuel Pellets				
Diameter	0.2555 ± .0005	0.5105 ± .0005	0.4695 ± .0005	0.7415 ± .0005
Length	0.530 ± .020	0.615 ± .020	0.445 ± .020	0.740 ± .060
End Shoulder Width	0.055 ± .010	0.055 ± .010	0.055 ± .010	0.074 ± .010
Endface Dish Depth	0.009 ± .003	0.014 ± .004	0.014 ± .004	0.014 ± .004
Edge Configuration	0.015 ± .005 Chamfer	0.006 ± .004 Chamfer	0.006 ± .004 Chamfer	Square Edge
Range of Individual Pellet Densities, % of Theoretical	95.14 - 99.75	93.10 - 99.36	95.37 - 99.95	93.08 - 99.08
Fuel-Cladding Diametral Gap	0.005 - 0.008	0.004 - 0.007	0.004 - 0.007	0.005 - 0.008

* All dimensions are in inches, except as noted.
** RXA = Recrystallization Annealed
SRA = Stress Relief Annealed

3.2.1.3.1 ***Seed pellets:*** Seed pellets were right circular cylinders with chamfers on both ends to ease loading into tubing, facilitate movement of the pellet stack in the tubing during power operation, and reduce pellet chipping during fabrication, rod handling, and power operation. The seed pellets had dished ends to reduce axial expansion of the stack (WAPD-TM-1244).

Binary pellets used in the seed rods were 0.64 cm (.252 in.) diameter, and either 1.13 or 1.56 cm (0.445 or 0.615 in.) long. The shorter pellets had enrichments of about 4.3 weight % U-fissile (Table 3-4). The longer (.615") pellets had identical diameters, but enrichments of 5.2 wt% U-fissile (Table 3-4). The pellets were sintered to 97 or 98 percent of their theoretical density of about 10 g/cm^3 to maximize pellet dimensional stability.

Shim pellets of thoria fuel were used near the top and bottom of the fuel stack to make up the desired fuel stack length. A spring-bearing fuel pellet with only one dished end was used at the top of the fuel stack. Dimensions for seed fuel pellets are presented in Table 3-8.

3.2.1.3.2 ***Blanket pellets:*** There were four types of pellets manufactured for the standard blanket rods, and four types manufactured for the power-flattening blanket rods. Standard and power flattening blanket binary fuel pellets were right circular cylinders with tapers on both ends to minimize ridging of cladding due to pellet hourglassing. The pellets had dished ends to reduce fuel stack axial expansion (WAPD-TM-1387, p. 25). Dimensions for blanket pellets are presented in Table 3-8, and theoretical density and fissile loading are presented in Table 3-7.

3.2.1.3.3 ***Reflector pellets***: All pellets in reflector rods were thoria (no binary pellets). Pellets were right circular cylinders with square edges and had dished ends to minimize axial expansion of the fuel stack (WAPD-TM-1387). Dimensions of reflector pellets are presented in Table 3-8.

3.2.2 Uranium Isotope Content

Isotopic weight percent content of the fuel is in Table 3-9. Isotopic mass loadings are provided in Tables 3-2 and 3-3.

3.2.3 Chemical Form

LWBR fuel is a ceramic based fuel in a thoria matrix.

3.2.4 Poisons, or Other Additives

Core reactivity control was achieved by moving the seed up and down within the stationary blanket assemblies using individual control drive mechanisms. Changing the axial position of the seed relative to the blankets changed the relative amounts of neutron absorptions in the fissile (U-233) and fertile (Th-232) fuel materials. To shut the reactor down, the seed assemblies were positioned 152.4 cm (60 in.) below the bottoms of the blanket assemblies as shown in Figure 3-12. To start up the reactor, the seed assemblies were raised, thus bringing the U-233 bearing parts of the fuel closer together. The control scheme was analogous in concept and operation to that of conventional poison rod control in that negative reactivity addition and core shutdown were achieved by lowering the control elements, and positive reactivity addition is achieved by raising the control elements (WAPD-TM-1336, p. 6).

Table 3-9. Uranium isotopic weight percent by fuel composition (WAPD-TM-1326, Table A-11).

	U-232	U-233	U-234	U-235	U-236	U-238
Seed						
Low zoned	0.00075	98.3088	1.2899	0.07947	0.01775	0.30333
High zoned	0.00070	98.3679	1.2742	0.06711	0.01397	0.27610
Standard Blanket						
Low zoned	0.00084	98.3037	1.3289	0.08805	0.02411	0.25442
Medium zoned	0.00082	98.3218	1.3144	0.08078	0.02102	0.26118
High zoned	0.00082	98.2597	1.3504	0.10466	0.03032	0.25412
Power-Flattening Blanket						
Low zoned	0.00082	98.3074	1.3193	0.08665	0.02258	0.26323
Medium zoned	0.00079	98.2260	1.3620	0.11257	0.03247	0.26613
High zoned	0.00070	98.0419	1.2433	0.09690	0.02648	0.59072

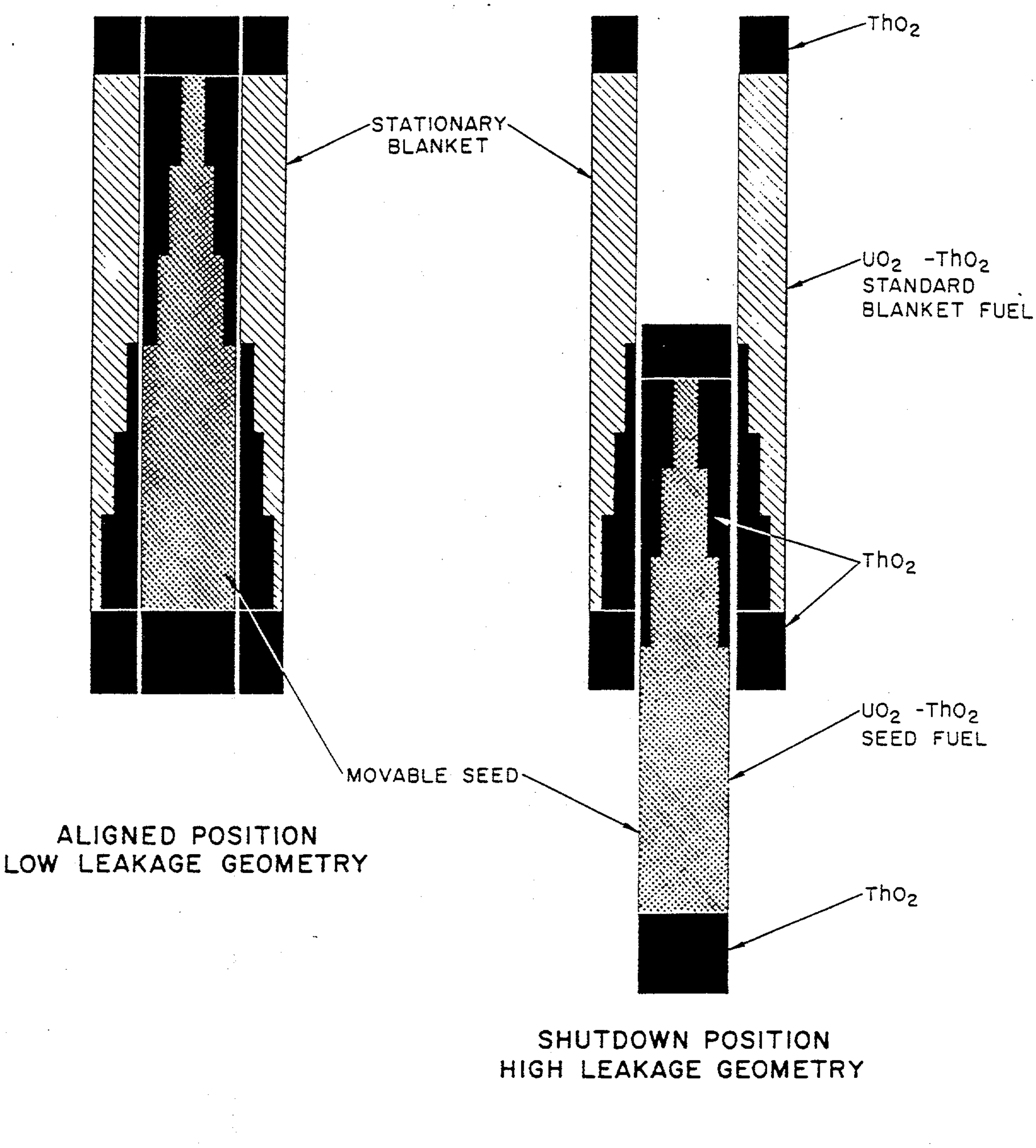

Figure 3-12. Movable fuel control (WAPD-TM-1336, Figure II-3).

Neutron poison equivalence (NPE) was determined on every tenth pellet blend using mass spectrometry to quantify fuel impurities, which interfered with breeding performance. NPE is discussed in WAPD-TM-1326, Appendix B, and NPE data are presented in Table 3-10.

3.2.5 Physical Dimensions

Dimensions of the modules are presented in Figure 3-13. The maximum height of the binary fuel ($^{233}UO_2 + ThO_2$) region of both seed and blanket is 213 cm (84 in.) with about 25 cm (10 in.) of ThO_2 added to each end for the purpose of reducing axial neutron leakage from the core. This makes the overall fuel height in each fuel rod approximately 264 cm (104 in).

Average as-built fuel lattice characteristics for the four regions are presented in Table 2-1. As shown, center-to-center spacings of the rods are 0.94, 1.60, and 2.9 cm (.37, .63, and .90 in.) for the seed, blanket and reflector rods, respectively. Rod outer diameters are 0.78, 1.45, 1.34, and 2.11 cm (.31, .57, .53 and .83 in.) for the seed, standard blanket, power-flattening blanket and reflector, respectively. The number of each type of rod is presented in Table 3-6.

3.2.6 Particle Size Distribution

Production specifications for the powder used in production of the fuel pellets are provided in Table 3-11. The levels of surface area and particle size shown are necessary for the production of high density, high integrity thoria and binary pellets. Surface areas were monitored using a gas absorption surface area analyzer, and statistical limits were imposed for postmicronized surface areas. Surface area measurement was an essential product control for micronized powders (WAPD-TM-1244, p. V.C-2). Grain size of LWBR fuel at end of life is shown in Table 3-12.

3.2.7 % Theoretical Density

Percent of theoretical densities for the pellets ranged from 97.28 to 98.61 % (Table 3-13).

3.2.8 Fuel Matrix Composition

The fuel pellets contained from 1-5 weight percent U-233 in a thoria matrix (WAPD-TM-1244, p. I-2).

3.2.9 BOL Linear Distribution of Fissile Material

Average as-built LWBR fissile loading by module type is presented in Table 3-14. Mass fissile loads were: 32.71, 41.55, and 46.41 kg for Types I, II, and III modules respectively (WAPD-TM-1326).

Table 3-10. Neutron Poison Equivalence (NPE) (WAPD-TM-1326, Table A-17)

Composition	Blends Sampled	Average NPE
Low seed	13	14.3
High seed	23	14.2
Low standard blanket	3	17.1
Medium standard blanket	21	13.2
High standard blanket	9	17.7
Low power flattening blanket	2	15.8
Medium power flattening blanket	2	14.3
High power flattening blanket	5	19.3
All binary	78	14.8
Seed thoria	5	15.2
Standard blanket thoria	18	14.7
Power flattening blanket thoria	4	6.8
Reflector blanket thoria	36	28.7
All thoria	63	22.2
All binary and thoria	141	18.2

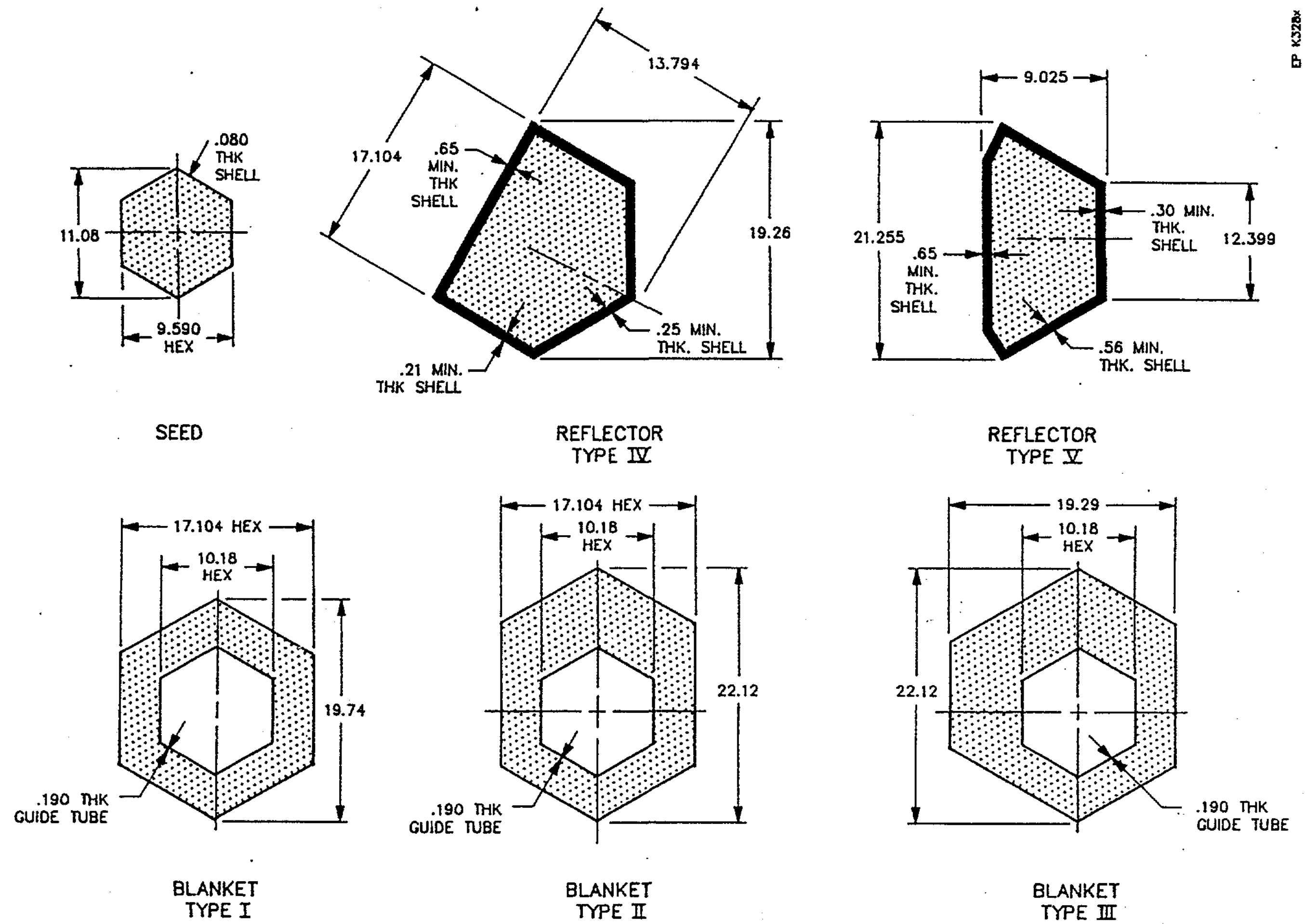

Figure 3-13. Cross-sectional dimensions of the LWBR modules (WAPD-TM-1608, Figure 24).

Table 3-11. Production specifications for pellets (WAPD-TM-1244, Table V.C-1).

Powder Type		Typical As-Received Characteristics	Typical As-Micronized Characteristics
ThO_2-UO_2	Surface area	4.5-6.0 m^2/g	8.0-9.0 m^2/g
	Average particle size	1.5-2.2 μ	0.5 μ
ThO_2	Surface area	6.5-7.5 m^2/g	9.0-9.5 m^2/g
	Average particle size	1.4-1.8 μ	0.5 μ

Table 3-12. Grain size of LWBR fuel at end-of-life (WAPD-TM-1606, Table 8).

Rod Type	Rod S/N	Fast Neutron Fluence 10^{20} n/cm^2	Burnup (MWD/MTM)	Grain Diameter, μm		ASTM Grain Size		Type Pellet
				Edge	Center	Edge	Center	
Seed	0400736	49	24,850	60	70	5.3	4.6	Binary
		54	36,990	40	40	6.3	6.4	Binary
	0606773	96	40,870	70	80	4.8	4.3	Binary
		33	17,300	65	80	5.0	4.5	Binary
	0205071	75	51,580	N/M	N/M	N/M	N/M	Binary
	0507672	86	46,900	95	125	3.8	3.0	Binary
Standard Blanket	1606710	73	22,350	150	80	2.6	4.3	Binary
		58	18,910	125	70	3.0	4.6	Binary
	1504272	64	19,130	115	105	3.3	3.6	Binary
	1105717	71	23,090	150	105	2.6	3.6	Binary
		71	13,750	65	50	5.0	5.6	Thoria
	1208823	51	10,180	75	N/M	4.6	N/M	Thoria
Power Flattening Blanket	2514164	39	22,320	70	45	4.6	6.0	Binary
	2607600	42	17,520	80	45	4.5	5.9	Binary
		59	24,290	150	85	2.6	4.2	Binary
	2610746	57	24,790	75	55	4.6	5.3	Binary
Reflector	3102657	4	280	45	N/M	6.0	N/M	Thoria

N/M = Not Measured
MWD/MTM = Megawatt days per metric ton of metal (uranium plus thorium)

Table 3-13. Average as-built pellet density and void fraction (WAPD-TM-1326, Table A-10).

	Percent Theoretical Density	Theoretical Density (gm/cm3)	Void Fraction
Seed			
Thoria	98.013	9.999	0.01253
Low zoned	97.712	10.035	0.01704
High zoned	97.554	10.042	0.01172
Standard Blanket			
Thoria	97.796	9.999	0.01399
Low zoned	98.608	10.009	0.02494
Medium zoned	98.224	10.013	0.01335
High zoned	98.115	10.016	0.01600
Power Flattening Blanket			
Thoria	98.057	9.999	0.01966
Low zoned	98.034	10.013	0.01998
Medium zoned	98.041	10.016	0.01753
High zoned	97.906	10.022	0.01578
Reflector Blanket	97.282	9.999	0.01317

Table 3-14. Average as-built LWBR loading by module type (WAPD-TM-1326, Table II-3).

	Fissile Loading (kg)		
Module Regions	Type I Module	Type II Module	Type III Module
Seed†	16.53	16.55	16.56
Standard blanket	16.18	9.34	6.63
Power flattening blanket	None	15.66*	23.22*
Total blanket	16.18	25.00*	29.85*
Module total	32.71	41.55*	46.41*

*Two Type II and two Type III modules have 0.06 kg less loading due to flux well locations.
†A 12-seed average of 16.55 kg was used for all seeds in the calculations.

3.3 Cladding

3.3.1 General Description of all Element Cladding Types used in the Reactor

All rods were clad with Zircaloy-4 cladding (WAPD-TM-1605, pp. 10 and 17). Data for the cladding are summarized in Tables 3-3 and 3-15. Dimensions for tubing are provided in Table 3-16.

Seed rod cladding: The seed cladding was freestanding (i.e., the cladding would not collapse onto the fuel pellets). Seed fuel rod cladding was recrystallization annealed (RXA) Zircaloy-4 (WAPD-TM-1605).

Blanket fuel cladding: For LWBR operating pressure and temperatures, cladding for both standard and power flattening fuel rods was nonfreestanding (i.e., the cladding would collapse onto the fuel pellets after exposure in the core). Blanket fuel rod cladding was highly cold-worked and stress relief annealed (SRA) Zircaloy-4 (WAPD-TM-1605).

Reflector fuel rod cladding: Reflector cladding was highly cold worked and stress relief annealed (SRA) Zircaloy-4. Cladding was nonfreestanding for LWBR operating pressure and temperature (WAPD-TM-1605).

3.3.2 Form

To improve neutron economy, blanket and reflector fuel rods were designed with nonfreestanding, thin-walled Zircaloy-4 tubing, highly cold worked and stress relief annealed. The seed fuel rods, because of their higher duty demands, were fabricated with freestanding recrystallization-annealed (RXA) Zircaloy-4 cladding. All cladding was fabricated from selected Zircaloy-4 ingots with less than 40 ppm hafnium content, which is lower than normal, to reduce parasitic absorption of neutrons (WAPD-TM-1387, p. 10).

3.3.3 Composition

Cladding consisted of Zircaloy-4 tubes with a low hafnium content (WAPD-TM-1326, p. 3). Neutron poisoning in zirconium was found to be attributed to the 2 to 3 percent of hafnium present in natural zirconium (WAPD-TM-1409, p. 6). Zircaloy used for cladding and all other structures in the active fuel region except the fuel rod support grids had a low hafnium content (<40 ppm)(WAPD-TM-1326, p.). Ingot requirements for LWBR low hafnium Ziorcaloy-4 tubing are presented in Table 3-17. Stress corrosion cracking in zircaloy tubing is caused by pressure as low as 20,000 psi in the presence of controlled amounts of iodine gas at typical fuel rod operating temperatures. Normal yield strength of irradiated zircaloy is 40000 to 60000 psi. (WAPD-TM-1387, p. 51). Cladding fabrication is discussed in WAPD-TM-1289.

3.3.4 Thickness

Wall thickness of each tube was measured over a spiral pattern as the tube rotated and advanced under the transducer station, which used a high frequency ultrasonic puls-echo measuring technique. Cladding wall thicknesses ranged from about .023" to .044", depending on the rod type (seed rods had the thinnest cladding)(Table 3-16).

Table 3-15. LWBR fuel rod cladding material properties (WAPD-TM-1605, Table 3).

Attribute	Seed	Standard Blanket	Power Flattening Blanket	Reflector
Final Heat Treatment Temperature, degrees F	1225 ±25	925 ±25	925 ±25	925 ±25
Final Heat Treatment Time (hrs)	2 - 5	2 - 5	2 - 5	2 - 5
70 F Yield Strength (ksi)*	54.66 49.74	79.77 73.55	80.71 76.13	77.79 72.36
700 F Yield Strength (ksi)*	18.57 17.37	51.14 47.89	53.13 50.67	49.49 46.56
70 F Yield/Ult. Ratio*	1.472 1.405	1.363 1.310	1.359 1.330	1.367 1.330
700 F Yield/Ult. Ratio*	1.951 1.872	1.259 1.212	1.254 1.226	1.288 1.261
70 F Elongation (%)*	29.2 27.04	21.87 20.41	19.63 18.49	23.57 22.16
700 F Elongation (%)*	35.75 32.19	20.61 18.83	18.17 16.90	21.87 20.33

*Average and lower 95/95 tolerance interval

Table 3-16. Requirements for LWBR tubing (WAPD-TM-1289, Table A-2).

A. Nondestructive Inspections

1. Inside Diameter

a. Local

Type	Nominal*	Tolerance
Seed	0.262	± 0.0015
PFB	0.475	± 0.0020
Std. B.	0.516	± 0.0020
Refl.	0.748	± 0.0025

b. Average (All) Nominal ± 0.0010

2. Outside Diameter-Local

Type	Nominal*	Tolerance*
Seed	0.3105	± 0.0020
PFB	0.5310	± 0.0020
Std. B.	0.5760	± 0.0020
Refl.	0.8350	± 0.0025

3. Wall Thickness

Type	Nominal*	Minimum*
Seed	0.0243	0.0225
PFB	0.0280	0.0260
Std.B.	0.0300	0.0280
Refl.	0.0435	0.0413

4. Wall Eccentricity-Maximum*

	Limits Per Purchase Order					Final LWBR Limit#	
	Initial Lots		Remaining Lots		Target		% of Nominal
Type	No.	Limits	No.	Limit	Limit	Max	Wall Thickness
Seed	8	.0024	18	.0016	.0010	.0013	5.36
PFB	3	.0028	18	.0021	.0015	.0017	6.07
Std.B.	8	.0030	15	.0022	.0015	.0017	5.67
Refl.	All	.0035	-	-	.0022	.0022	5.06

*All dimensions are stated in inches.
#Limits achieved by additional inspection and/or sorting performed at Bettis.

Table 3-16. (continued).

5. Wavelength of Helical Wall Eccentricity

Type	Minimum*
Seed	
PFB	80
Std. B.	
Refl.	70

6. Length

Type	Nominal*	Tolerance*
Seed	119	+0.5, -0.0
PFB	117	+0.5, -0.0
Std.B.	117	+0.5, -0.0
Refl.	110.5	+0.5, -0.0
At Bettis	Fuel Rod Nominal	±0.015

7. Perpendicularity of End Face (at Bettis only)

All — The deviation from perpendicularity to the OD surface of the end two inches shall be limited to 0.006 in/in.

8. Edge Squareness (at Bettis only)

All — The maximum deviation from square edges as chamfer or rounding of the ID or OD edge of the end face shall not reduce the local wall thickness at the end face by more than 0.003 inch.

9. Straightness

All — 0.010 inch maximum deflection (bow) of the tube from the center of a 15 inch chord (gage length).

---

* All dimensions are stated in inches.
# Limits achieved by additional inspection and/or sorting performed at Bettis.

Table 3-16. (continued).

10. Internal Free Path

A right cylindrical plug (stainless steel) with an OD surface finish of 16 micro-inch AA or finer must pass freely through the full length of each finished tube as a last inspection prior to packing for shipment. The following plug sizes apply:

Tube Type	Seed*	PFB*	Std.B.*	Refl.*
Nominal Tube ID	0.262	0.475	0.516	0.748
Plug OD				
Min	0.2585	0.4710	0.5120	0.7435
Max	0.2590	0.4715	0.5125	0.7440
Length of Plug (excluding end taper, tolerance is ± 0.005)				
Nominal	1.048	1.900	2.064	2.999
Nominal Fuel Pellet O.D. (tolerance is ±0.0005)				
UO_2 in ThO_2	0.2520	0.4695	0.5105	0.7415
ThO_2 only	0.2555	0.4695	0.5105	0.7415
Nominal Fuel Pellet Length (Reference)				
UO_2 in ThO_2	0.615	0.870	0.875	NA
ThO_2 only	0.530	0.445	0.615	0.740

11. Visual Surface Inspection

The tubing OD and ID surfaces must be free of unacceptable surface conditions as determined by visual inspection. These unacceptable conditions include, but are not limited to, scratches, abrasions, nicks, dents, pits, holes, foreign material, and material defects (cracks, laps, seams, lamination, etc.).

12. Surface Finish

CONDITION: BRIGHT PICKLED
MAXIMUM SURFACE ROUGHNESS (MICROINCH A.A)

Tube Type	O.D.	I.D.
Seed Power Flattening Blanket Standard Blanket	32	32
Reflector	32	125

*All dimensions are stated in inches.

Table 3-16. (continued).

13. Material Quality

The tubing must be free of material and fabrication defects which exhibit a stronger response to the ultrasonic search beam than 80% of the response exhibited by the standard notches contained in the test calibration tube. The dimensions of the standard notch are shown below. Test sensitivity notches, half the depth of the standard notches must be reproducibly detected. All dimensions are in inches.

Tube Type	Nom.Wall	Standard Defect Notch (Max) Depth	Length	Width
Seed	0.0242	0.0020	0.0200	0.003
PF Blanket	0.0280	0.0021	0.0210	0.003
Standard Blanket	0.0300	0.0022	0.0225	0.003
Reflector	0.0435	0.0032	0.0326	0.003

B. Destructive Testing

1. Chemistry

Compliance with the requirement for ingot composition (Table A-1) satisfies the basic chemistry requirements of the finished tubing. Samples from each lot of finished tubing must meet the limits noted for the five elements listed below.

Elements	ppm Max.	ppm Min.
Hydrogen	25	0
Nitrogen	80	0
Oxygen		
Individual Analysis	1800	900
Average from one ingot**		
Seed	1700	900
Blanket & Reflector	1600	900
Nickel	70	0
Hafnium	45	0

2. Surface Chemistry

Fluorine on ID surface in micrograms per square decimeter

Target 30 to 40
Alert 65

**Average of all finish tubing analyses from one ingot.

Table 3-16. (continued).

3. Corrosion Resistance

	Test Condition	Max. Weight Gain
a.	14 days in 750°F steam at 1500 psig	38 mg/dm^2
b.	14 days in 680°F water at 2705 psig	28 mg/dm^2 (preproduction only)

The corrosion tested tubing must exhibit a continuous lustrous, black, adherent, corrosion film consistent with established visual standards.

4. Longitudinal Uniaxial Tensile Properties

Tube Type	(U/Y Ratio) (Min)[(a)]	0.2% Offset Yield Strength (psi) Min.	Max.	% Total Elongation (b)
a. Room Temperature				
Seed	1.20	35,000	-	20.0
PF Blanket Standard Blanket Reflector	1.15	55,570	-	8.1
b. 700°F				
Seed	1.5	15,500	30,000	20.0
PF Blanket Standard Blanket Reflector	1.15	43,500	69,500	8.1

5. Circumferential Tensile Properties (Burst Test)

Tube Type	Minimum % Ductility at 700°F[(c)]
Seed	20
PF Blanket Standard Blanket Reflector	5

(a) Ratio of Ultimate Tensile Strength to 0.2% Offset Yield Strength
(b) Minimum in 2 inch gage length
(c) Percent increase in circumference of metallic portion of the bulge measured from fracture edge to fracture edge around the maximum circumference of the ruptured specimen.

Table 3-16. (continued).

6. Texture (Contractile Strain Ratio or CSR)

Tube Type	Limits Min.	Max.
Seed PF Blanket Std.Blanket	1.2	2.0
Reflector	1.2	2.3

7. Hydride Orientation

The orientation of the zirconium hydride platelets (needles) in the finished tubing must be such that no more than the specified percent of the classifiable hydride needles are aligned within 30° of the radial direction (i.e., parallel to the tube radius).

	Max. Individual Wall Segment Reading O.D., Middle, or I.D. Third of Wall Thickness	Max. Avg. of Three Segments For Each Sample
Seed	50%	45%
Blanket & Reflector	30%	Not Applicable

8. Post-Anneal Cold Work

Seed (RXA)	3.0% Maximum
Blanket & Reflector (SRA)	Not Applicable

9. Grain Size

Seed	ASTM 9-12.5 (in the finished tubing)
Blanket & Reflector	ASTM 8-12.0 (at completion of the alpha recrystallization anneal prior to the last reduction)

10. Metallographic Inspection for Equiaxed Grains

Seed (RXA)	No distorted or non-equiaxed (non-recrystallized) grains permitted.
Blanket & Reflector (SRA)	There must be no evidence of recrystallization; i.e., there must be no equiaxed grains.

Table 3-16. (continued).

11. Metallographic Defects

All Tube Types	All metallographic inspections for hydride orientation, post anneal cold work, grain size, and equiaxed grains shall include an inspection for the presence of any defects exceeding 0.0040 inch in any dimension. Defects in excess of 0.0040 inch are not permitted.

C. Cold Work in Final Reduction

The amount of cold work (CW)(*), or the reduction in cross-section area, in the last tube reduction shall be within the following ranges for the specified final heat treatment.

Tube Type	Final Reduction	Final Heat Treatment (d)
Seed	50 to 70%	RXA
PFB Std.B. Refl.	60 to 80%	SRA

D. Final Heat Treatment

All tubes shall have a final heat treatment within the specified limits for the tube type. The size and placement of the load within the furnace, the mass in the furance, and the furnace operating characteristics must be balanced such that the inntermost (slowest heating) tube in the load receives the minimum heat treatment while the outermost (fastest heating) tube does not receive an excessive heat treatment. The prescribed heat treatment parameters for all LWBR tubes are shown in the following table.

Final Heat Treatment(d)	Tube Type	Temperature (°F)		Hours Above Min. Temp.	
		Min.	Max.	Min.	Max.
RXA	Seed	1200	1250	2	4.5
SRA	PF Blanket Standard Blanket Reflector	900	950	1	5.5

(*) The calculation is

$$\% \; CW = \frac{A-a}{A} \times 100 \text{ where:}$$

A = cross-section area before reduction
a = cross-section area after reduction

(d) RXA is recrystallization anneal and SRA is stress relief anneal.

Table 3-17. Ingot requirements for LWBR Zircaloy-4 tubing (WAPD-TM-1289, Table A-1).

Zircaloy-4 Tubing

I. Alloy Chemistry#

Element	Symbol	% Min.	% Max.
Tin	Sn	1.20	1.70
Iron	Fe	0.18	0.24
Chromium	Cr	0.07	0.13
Oxygen	O	0.09	0.15
Iron + Chromium	-	0.28	0.37
Zirconium	Zr	Remainder	

II. Group A Impurity Limits

Element	Symbol	ppm Max.	ASTM B-353-1977 ppm Max.+
Aluminum	Al	75	
Boron	B	0.5	
Cadmium	Cd	0.5	
Carbon	C	270	
Cobalt	Co	20	
Copper	Cu	50	
Hafnium	Hf	35	100
Hydrogen	H	25	
Magnesium	Mg	15	20
Manganese	Mn	50	
Nickel	Ni	70	
Niobium	Nb	100	
Nitrogen	N	60	80
Silicon	Si	110	200
Tantalum	Ta	200	
Titanium	Ti	40	50
Tungsten	W	80	100
Uranium	U	3	3.5
Uranium Isotope	U-235	0.025	

Table 3-17. (continued).

III. Group B Impurity Limits†

Element	Symbol	ppm Max.	ASTM B-353-1977 ppm Max.+
Chlorine	Cl*	15*	
Fluorine	F*	50*	
Gadolinium	Gd	5	
Lead	Pb	100	
Molybdenum	Mo	50	50
Phosphorus	P	50	
Samarium	Sm	10	
Thorium	Th	7	
Vanadium	V	50	
Zinc	Zn	100	

IV. Ingot Composition - Materials Source and Limits

Source	Limits
Sponge	50% min.
Solid Scrap	40% max.
Ingot Turnings	15% max.

V. Ingot Hardness - Brinell Hardness Number (BHN)

Test	10 mm ball, 3000 kg load
Limits	200 BHN max. individual
	187 BHN max. average of 10 at room temperature

VI. Miscellaneous Tests

Ultrasonic Inspection
Surface Finish
Visual Inspection
Magnetic Inspection

---

* For information only.
\# Identical to ASTM B-353-1977 (Ref. (c)). except as noted.
† Only specified in ASTM B-353-1977 as noted.

4. OPERATING HISTORY

Originally designed for 18,000 EFPH of operation, LWBR was operated for 29,047 EFPH (1EFPH is the equivalent of operating the core for 1-hr at rated power, namely, 236.6 Mw (thermal)) from Sept. 1977 until Oct 1, 1982 (from WAPD-TM-1542, p. 1-9, and ICPP Fuel Receipt Criteria attached to WAPD-NRF(L)C-104, p.3). Average daily generator output as net electrical megawatts and reactor coolant temperature are presented in Figure 4-1 (from WAPD-TM-1542 Figure 1-1). The EFPH, number of hours the reactor was critical, and gross electrical output (in MWhr) are presented for the LWBR by quarter from 1977-1982 in Table 4-1.

During most of core life, the LWBR was operated as a base load station (WAPD-TM-1606, p. 35). During the first 3 years of operation (18,500 EFPH), the core was subjected to 204 planned swingload cycles to demonstrate the core transient capability and generating system load follow to simulate operation of a large commercial nuclear reactor (WAPD-TM-1606, p.35). A swing load cycle is defined as power reduction from about 90% to 35-60% for 4-8 hrs, then back to 90% or higher power. Despite shutdowns and swing, the reactor achieved a high capacity factor of 65% and high availability factor of 86% (WAPD-TM-1606, p. 35).

For its initial 18000 EFPH, the maximum allowable reactor power was established as 72 Mw gross (electric) and the average coolant temp was 531 degrees F. System pressure was initially 2000 psia, with subsequent reductions to 1940 psia at 4325 EFPH, to 1870 psia at 7132 EFPH, and to 1815 psia at 10,932 EFPH to reduce the probability of fuel rod cladding collapse (WAPD-TM-1600, p. 63-68: Also 88.7 GWD).

In the LWBR irradiation test program, two cladding defects occurred during planned power ramps. Both were hairline cracks attributed to stress corrosion cracking. SCC was shown in laboratory tests on unfueled tubing specimens to occur at stress levels as low as 20000 psi in the presence of controlled amounts of iodine gas at typical fuel rod operating temperatures (WAPD-TM-1387, p. 51.)

The timeline for the LWBR reactor is presented in Table 4-2.

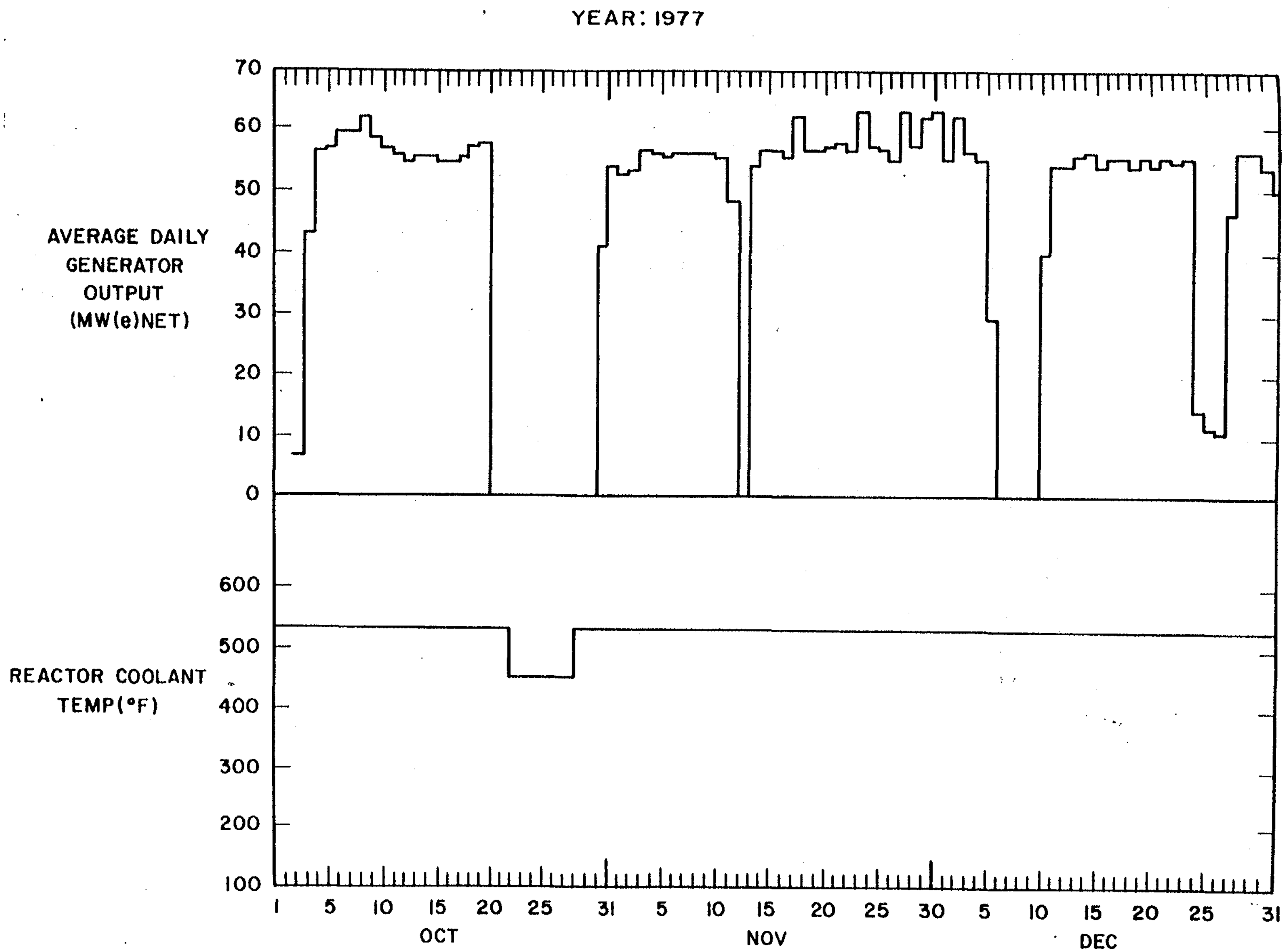

Figure 4-1. LWBR operational history - 1977 (WAPD-TM-1542, Figure 1-1).

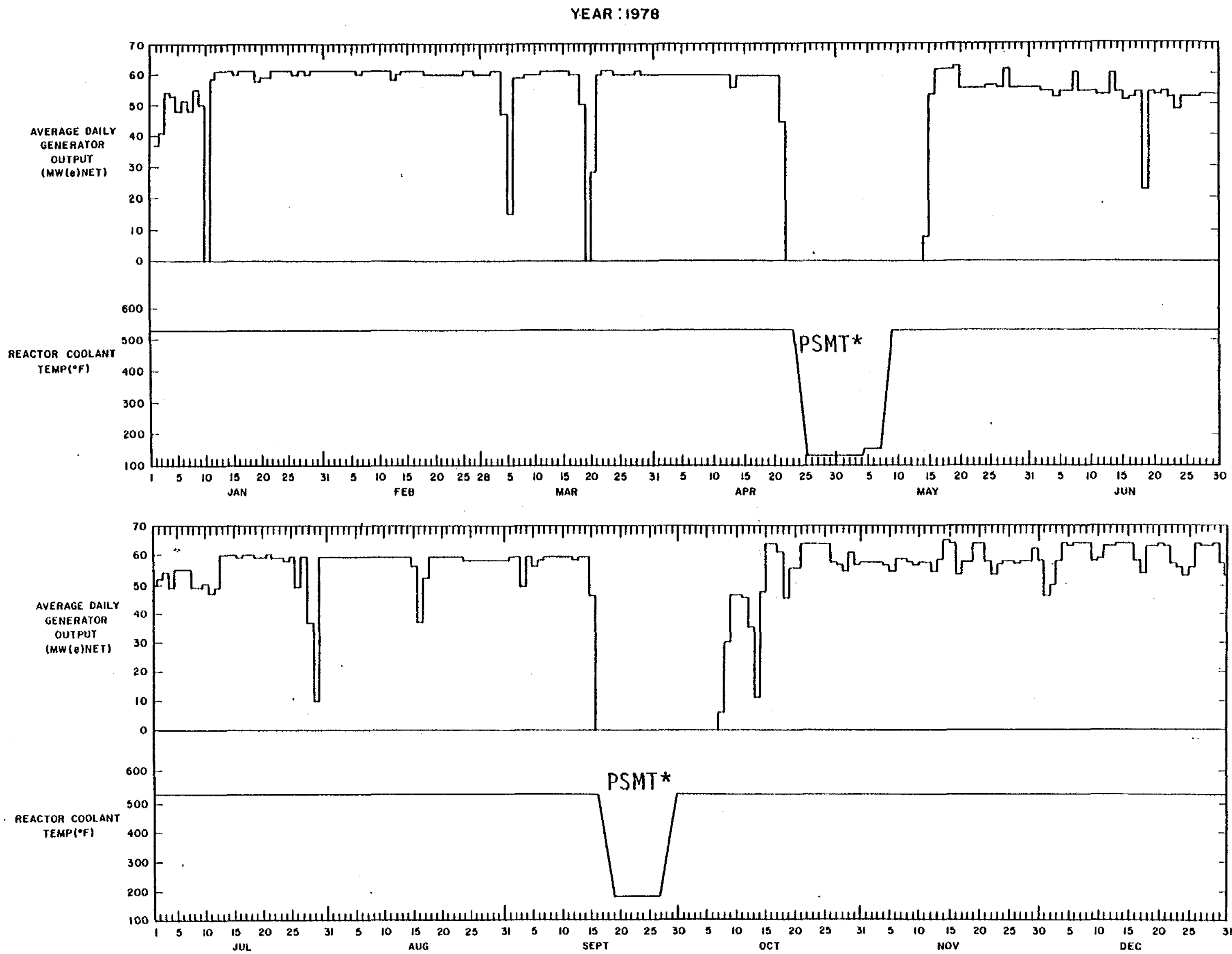

FIGURE I-1. LWBR OPERATIONAL HISTORY (SHEET 2 OF 6) - 1978

Figure 4-1. (Continued.)

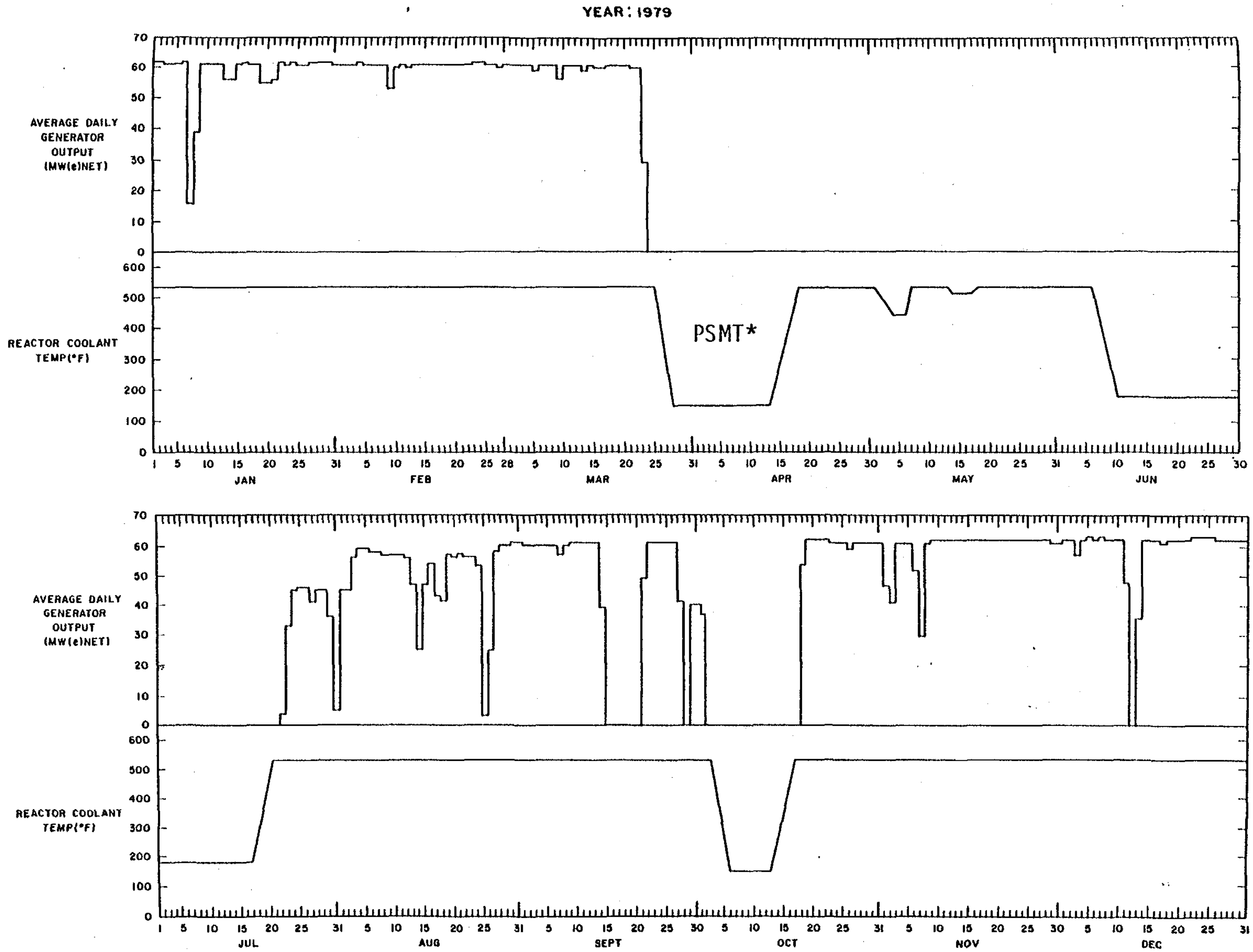

FIGURE 1-1. LWBR OPERATIONAL HISTORY (SHEET 3 OF 6) – 1979

Figure 4-1. (continued).

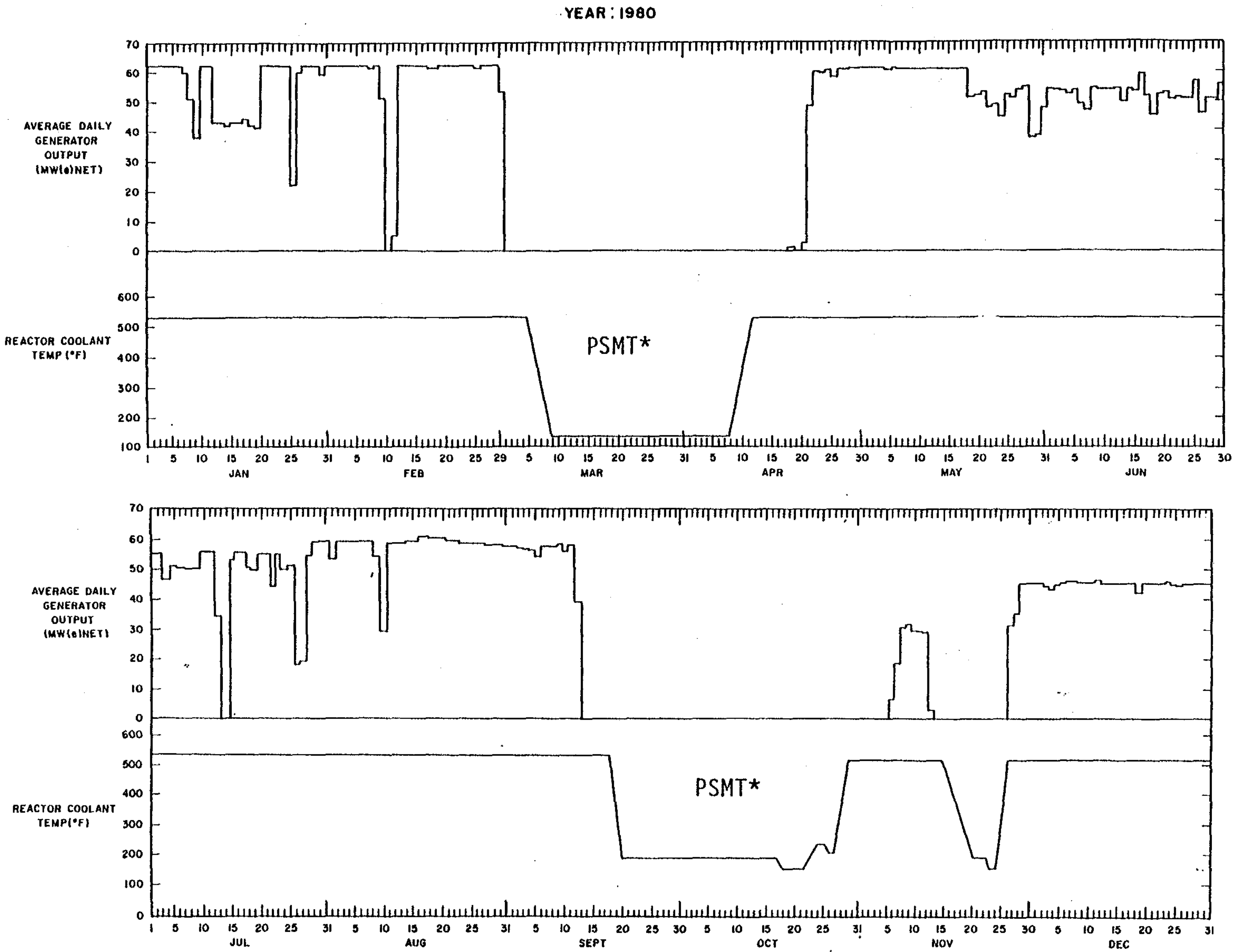

FIGURE 1-1. LWBR OPERATIONAL HISTORY (SHEET 4 OF 6) - 1980

Figure 4-1. (continued).

YEAR: 1981

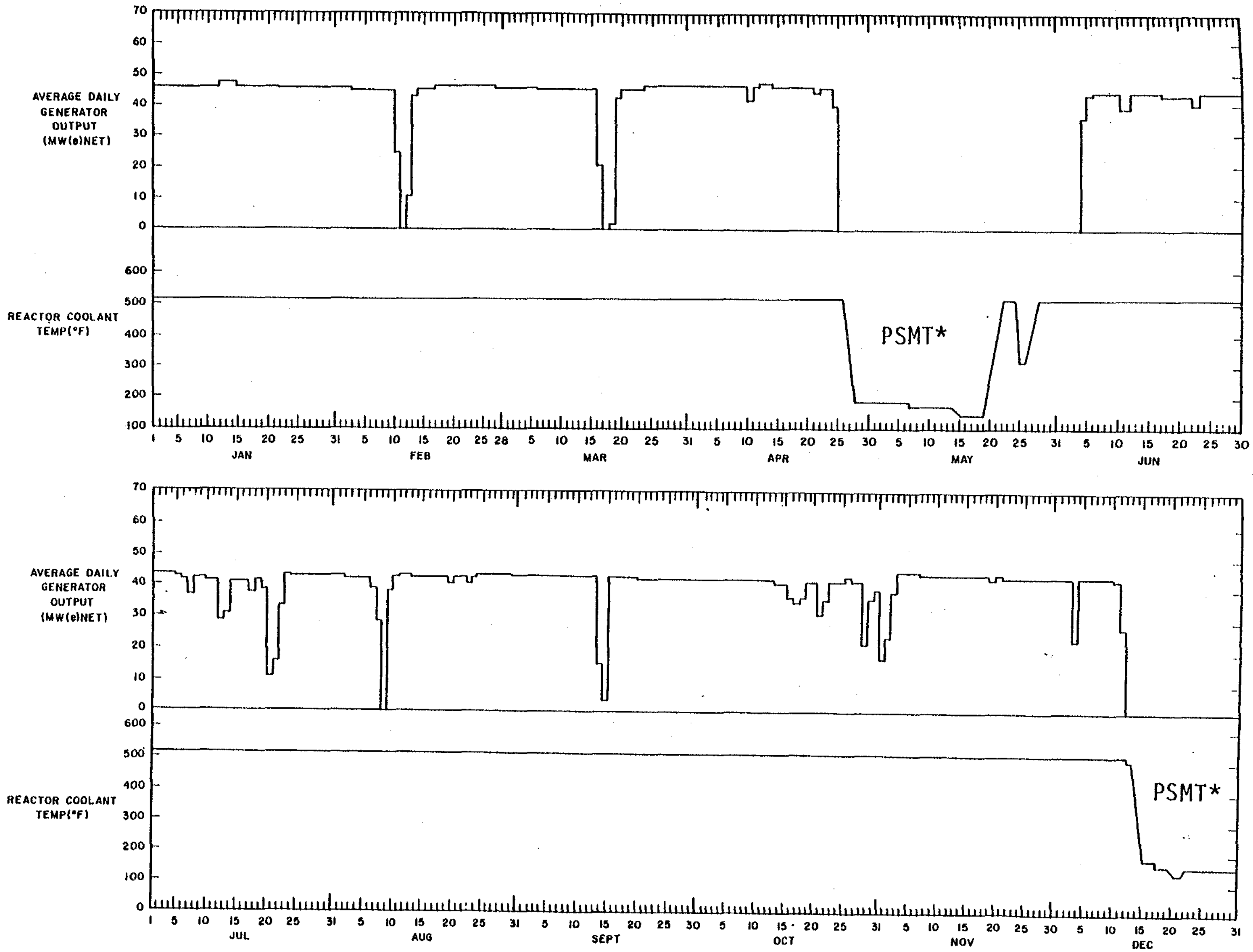

FIGURE I-1. LWBR OPERATIONAL HISTORY (SHEET 5 OF 6)-1981

Figure 4-1. (continued).

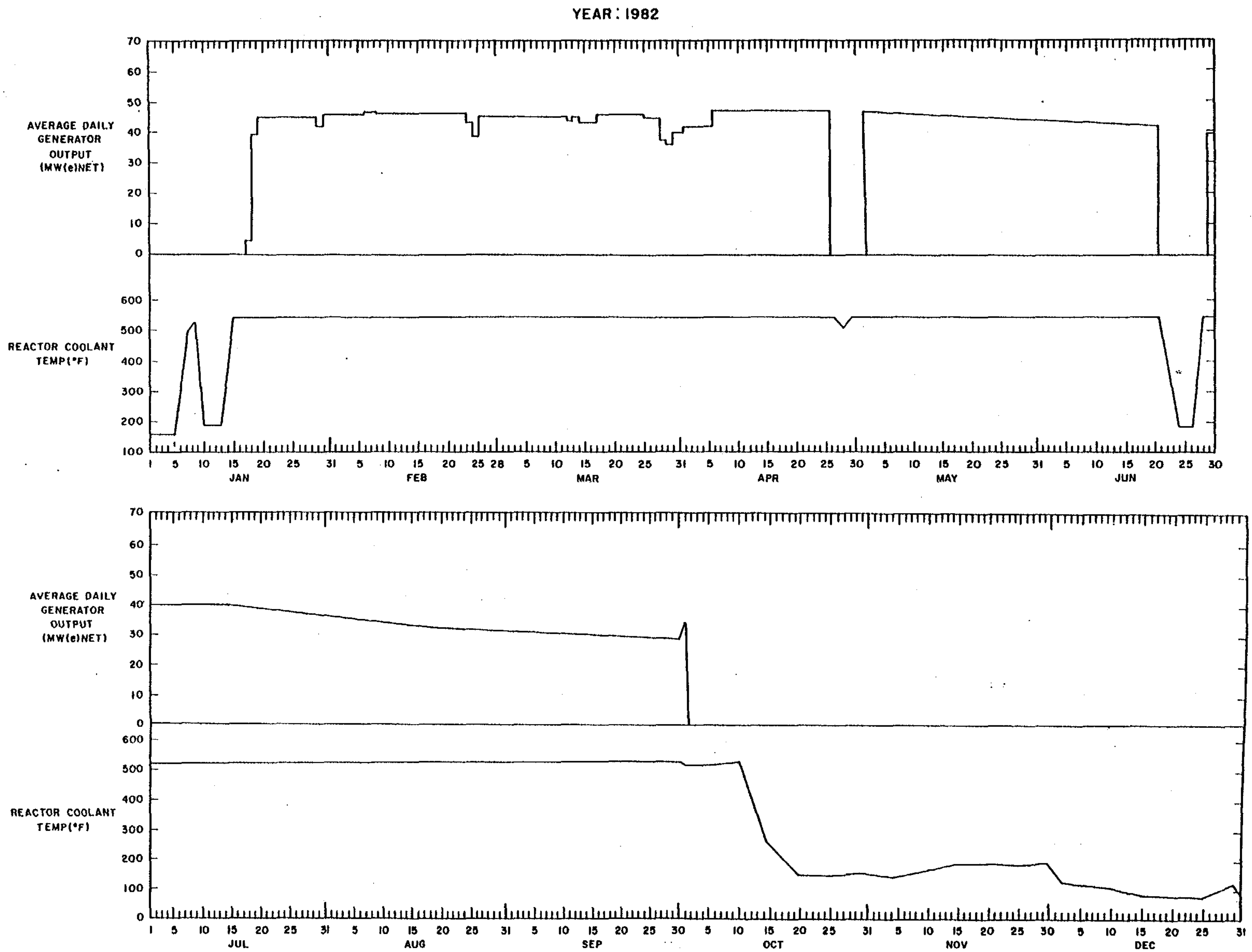

FIGURE I-I. LWBR OPERATIONAL HISTORY (SHEET 6 OF 6) -1982

*PSMT = planned shutdown for maintenance and testing.

Figure 4-1. (continued).

Table 4-1. Summary of LWBR station performance (WAPD-TM-1542, Table 1-1).

Year	Quarter	EFPH* This Quarter	EFPH* To Date	Hrs Reactor Critical This Quarter	Hrs Reactor Critical To Date	Gross Electrical Output Mwhr To Date
1977	3	270.4	270.4	641.9	641.9	17899
	4	1553.9	1824.3	1814.2	2456.1	134232
1978	1	2010.4	3834.7	2137.9	4594.0	283947
	2	1536.6	5371.3	1695.6	6289.6	396929
	3	1761.0	7132.3	1859.3	8148.9	523279
	4	1878.1	9010.4	2111.6	10260.5	662675
1979	1	1921.9	10932.3	1945.5	12206.0	805655
	2	0	10932.3	346.9	12552.9	805655
	3	1353.9	12286.2	1574.7	14127.6	903425
	4	1734.9	14021.1	1802.3	15929.9	1034503
1980	1	1304.6	15325.7	1415.4	17345.3	1133200
	2	1544.2	16869.9	1815.4	19160.7	1248104
	3	1636.8	18506.7	1782.1	20942.8	1366698
	4	757.7	19264.4	1213.3	22156.1	1423380
1981	1	1617.6	20882.0	2090.3	24246.4	1545038
	2	960.6	21842.6	1462.6	25713.0	1615465
	3	1649.5	23492.1	2151.9	27864.9	1731032
	4	1311.4	24803.5	1715.8	29580.7	1824592
1982	1	1355.7	26159.2	1807.6	31388.3	1923224
	2	1459.7	27618.9	1911.7	33300.0	2029313
	3	1422.8	29041.7	2208.0	35508.0	2128542
	4	5.7	29047.4	293.1	35801.1	2128943

*EFPH - Equivalent Full Power Hours [where full power is defined as 236.6 Megawatts thermal, Mw(t)]

Table 4-2. Timeline of events for the LWBR.

Fabrication completed	1976 or 1977
Reactor loading	1977
Initial criticality of core	Aug. 26, 1977 (WAPD-TM-1455 addendum, p. 3)
Full power operation	Sep. 21, 1977 (WAPD-TM-1455 addendum, p. 3)
Achieved depletion to 18,298 EFPH	Sep. 12, 1980 (WAPD-TM-1455 addendum, p. 3)
Operated at 80% of maximum, reduced temperature and pressure	Sep 12 1980 through Dec. 11, 1981 (18,298-24,451 EFPH) (WAPD-TM-1455 addendum, p. 3)
Maintenance and testing	21,094-24,541 EFPH
Reactor operation to 29,047 EFPH	1977-82
Reactor disassembly	Dec 1982-Aug1984 (WAPD-TM-1552, p. 7-9)
Shipping from Shippingport (10 shipments)	Sept. 1984 (WAPD-TM-1552, p. 9)
Water pits S4-39 and N4-43 at ECF for the majority of fuel disposal operations (WAPD-TM-1601, p. 1-4)	
Dismantling at ECF 17 rods to ANL-E 12 rods to ANL-W	1984
Testing: PIFAG Chronology of Assay operations are provided in Table 24 (from Table 4 of WAPD-TM-1614, p. 81)	June 1984-May 1987 (WAPD-TM-1614, p. 2).
Repackaging at ECF	
Shipping to INTEC	1986-1987
Dry Storage at INTEC	Current

5. REACTOR PERFORMANCE EVALUATION

5.1 The Calculational Model

A calculational model was developed to analyze the as-built core and predict core nuclear performance prior to core operation. The use of the U-233/Th fuel system led to the need for an extensive analysis of available cross section data and other basic nuclear data for U-233 and thorium which has previously been given less attention than U-235 and U-238. The U-233 cross section dependence on energy is particularly complex with broad resonances and strong multilevel effects. In addition, the U-233 cross section interferes with the thorium resonances and with the resonances of its own precursor Pa-233. A highly accurate Monte Carlo analytical standard was developed as a substitute for a full core mockup critical. Partial core mockup experiments were used to qualify this calculational standard (WAPD-TM-1314, p. 7).

End-of-life destructive and nondestructive examinations verified that the modeled inventories were accurate.

5.2 End-of-Life Destructive and Nondestructive Examinations

The LWBR modules and rods were examined destructively and non-destructively to assess reactor and breeding performance. Examinations started in 1982, when the core was being removed from the reactor. At Shippingport, the modules were visually examined using an underwater closed circuit television camera, which verified that no indications of rough handling or other unusual conditions were present (from p. 4 of WAPD-NRF(L)C-104 Fuel Receipt Criteria Part B April 30, 1987). Following initial examination and loading, the modules were sent to ECF.

At ECF, 12 of the 39 core fuel modules were prepared for fuel rod removal: 4 from the seed region, 4 from the standard blanket region, 3 from the power flattening blanket region, and one from the reflector region. From those 12 selected modules, more than 1000 rods were removed for testing and proof of breeding experiments. Of the 1000+ rods, 524 were non-destructively evaluated at ECF using the Production Irradiation Fuel Assay Gauge (PIFAG) to obtain fuel loading. To verify PIFAG and obtain accurate data for the proof of breeding, 17 of the 524 PIFAG-analyzed rods were completely dissolved and destructively assayed by ANL-E. Uranium isotopic data for each rod type are presented in Table 5-1, including destructive examination data (shaded), non-destructive examination data from the PIFAG (maximum assay results) and modified data. Information about the calculational model used to obtain the modeled data are presented in WAPD-TM-1314. Information about destructive and non-destructive testing follows. An additional 12 PIFAG rods were destructively examined at ANL-W for fission gases.

Table 5-1. Modeled and measured[1] end-of-life isotopic content of LWBR fuel rods.

Rod Type	Module Type	Th-232	U-232	U-233	U-234	U-235	U-236	U-238	Total U	U-233+ U-235	Initial Fissile (Modeled)	Max. Fissile from PIFAG NDE Assay
		(g)	(g)	(g)	(g)	(g)	(g)	(g)	(g)	(g)	(g)	(g)
1,2,7,8											14.33	
	S1-1	0.7	0.03	13.69	1.67	0.29	0.03	0.03	15.74	13.98		14.23
	S1-1 P39		0.02	13.57	1.69	0.29	0.03	0.04	15.64	13.86		13.99
	S2-3	0.71	0.02	13.75	1.48	0.23	0.02	0.03	15.53	13.98		14.27
	S3-1	0.71	0.02	13.82	1.32	0.19	0.02	0.03	15.4	14.01		14.32
	S3-2	0.71	0.02	13.82	1.32	0.19	0.02	0.03	15.4	14.01		14.38
3											19.14	
	S1-1	0.7	0.03	15.29	1.89	0.33	0.03	0.04	17.61	15.62		15.68
	S1-1 N63		0.02	15.3	1.88	0.34	0.04	0.05	17.63	15.64		15.68
	S2-3	0.7	0.03	15.6	1.7	0.28	0.02	0.04	17.67	15.88		15.77
	S3-1	0.7	0.02	15.88	1.53	0.23	0.02	0.04	17.72	16.11		15.98
	S3-2	0.7	0.02	15.88	1.53	0.23	0.02	0.04	17.72	16.11		16.44
4											23.92	
	S1-1	0.69	0.03	17.17	2.13	0.38	0.04	0.05	19.8	17.55		17.52
	S1-1 M49		0.02	17.06	2.12	0.37	0.03	0.07	19.67	17.43		17.52
	S2-3	0.69	0.03	17.72	1.93	0.31	0.03	0.05	20.07	18.03		18.06
	S3-1	0.69	0.02	18.24	1.76	0.26	0.02	0.05	20.35	18.5		18.77
	S3-2	0.69	0.02	18.24	1.76	0.26	0.02	0.05	20.35	18.5		18.92
5,6											34.57	
	S1-1	0.68	0.03	24.34	2.54	0.41	0.03	0.07	27.42	24.75		25.71
	S1-1 L29		0.02	22.33	2.73	0.46	0.04	0.08	25.66	22.79		22.96
	S1-1 C10		0.02	25.15	2.51	0.4	0.03	0.08	28.19	25.55		25.67
	S2-3	0.68	0.03	25.37	2.31	0.35	0.03	0.07	28.16	25.72		26.88
	S3-1	0.68	0.02	26.28	2.1	0.29	0.02	0.07	28.78	26.57		27.67
	S3-2	0.68	0.02	26.28	2.1	0.29	0.02	0.07	28.78	26.57		27.58
11,12											16.45	
	B1-3	2.9	0.1	35.4	3.25	0.54	0.05	0.03	39.37	35.94		36.83
	B1-3 A49		0.08	35.9	3.87	0.7	0.07	0.04	40.66	36.6		36.8
	B2-2	2.9	0.09	34.3	2.98	0.47	0.04	0.03	37.91	34.77		35.88
	B3-2	2.91	0.08	33.3	2.73	0.41	0.03	0.03	36.58	33.71		34.07
	B3-6	2.91	0.08	33.3	2.73	0.41	0.03	0.03	36.58	33.71		34.72
13											45.47	
	B1-3	2.87	0.1	47.2	4.42	0.74	0.06	0.08	52.6	47.94		47.65
	B1-3 D24		0.06	46.43	4.35	0.73	0.07	0.1	51.74	47.16		47.38
	B2-2	2.87	0.09	46.87	4.22	0.68	0.06	0.08	52	47.55		47.683
	B3-2	2.87	0.08	46.59	4.02	0.63	0.05	0.08	51.45	47.22		47.25
	B3-6	2.87	0.08	46.59	4.02	0.63	0.05	0.08	51.45	47.22		47.07
14											30.34	
	B1-3	2.92	0.09	40.74	3.63	0.61	0.05	0.06	45.18	41.35		40.9
	B1-3 C3		0.06	40.03	3.59	0.58	0.04	0.07	44.37	40.61		40.76
	B2-2	2.92	0.09	40.05	3.42	0.55	0.04	0.06	44.21	40.6		40.96
	B3-2	2.92	0.08	39.4	3.21	0.5	0.04	0.06	43.29	39.9		39.85
	B3-6	2.92	0.08	39.4	3.21	0.5	0.04	0.06	43.29	39.9		39.85

Table 5-1. (continued).

Rod	Module									U-233+	Initial	Max. Fissile
	Type	Th-232	U-232	U-233	U-234	U-235	U-236	U-238	Total U	U-235	Fissile	from PIFAG
Type											(Modeled)	NDE Assay
		(g)	(g)	(g)	(g)	(g)	(g)	(g)	(g)	(g)	(g)	(g)
15											45.66	
	B1-3	2.88	0.1	47.04	4.66	0.76	0.07	0.09	52.72	47.8		48.78
	B2-2	2.88	0.1	46.88	4.5	0.72	0.06	0.09	52.35	47.6		48.38
	B3-2	2.88	0.09	46.71	4.29	0.67	0.06	0.09	51.91	47.38		48.23
	B3-6	2.88	0.09	46.71	4.29	0.67	0.06	0.09	51.91	47.38		48.08
16											54.66	
	B1-3	2.89	0.1	52.19	4.92	0.8	0.07	0.1	58.18	52.99		52.81
	B1-3 E56		0.07	51.41	5.23	0.88	0.08	0.12	57.79	52.29		52.51
	B2-2	2.89	0.09	52.1	4.74	0.75	0.07	0.1	57.85	52.85		52.88
	B3-2	2.9	0.09	52.06	4.53	0.7	0.06	0.1	57.54	52.76		52.51
	B3-6	2.9	0.09	52.06	4.53	0.7	0.06	0.1	57.54	52.76		52.64
21,22											18.96	
	B2-2	2.45	0.06	30.09	2.67	0.4	0.03	0.04	33.29	30.49		31.05
	B3-2	2.45	0.05	28.98	2.29	0.31	0.02	0.04	31.69	29.29		30.5
	B3-6	2.45	0.05	28.98	2.29	0.31	0.02	0.04	31.69	29.29		30.26
	B3-6 B62		0.04	28.91	2.27	0.32	0.03	0.05	31.62	29.23		29.37
23											52.56	
	B2-2	2.42	0.06	45.57	3.95	0.57	0.05	0.22	50.42	46.14		46.03
	B3-2	2.42	0.05	46.13	3.53	0.47	0.04	0.22	50.44	46.6		46.86
	B3-6	2.42	0.05	46.13	3.53	0.47	0.04	0.22	50.44	46.6		46.71
	B3-6 D29		0.05	44.45	4.4	0.71	0.08	0.12	49.81	45.16		45.36
24											30.74	
	B2-2	2.46	0.06	34.68	2.98	0.45	0.04	0.06	38.27	35.13		35.23
	B3-2	2.46	0.05	34.11	2.62	0.37	0.03	0.06	37.24	34.48		34.49
	B3-6	2.46	0.05	34.11	2.62	0.37	0.03	0.06	37.24	34.48		34.89
	B3-6 C13		0.02	33.61	2.21	0.28	0.02	0.08	36.22	33.89		34.02
25,27											63.06	
	B2-2	2.43	0.05	53.87	3.78	0.47	0.04	0.26	58.47	54.34		55.86
	B3-2	2.43	0.03	55.13	3.3	0.38	0.03	0.26	59.13	55.51		57.41
	B3-6	2.43	0.03	55.13	3.3	0.38	0.03	0.26	59.13	55.51		57.53
	B-3-6 F73		0.04	53.07	4.27	0.62	0.07	0.15	58.22	53.69		53.75
	B3-6 H1		0.01	57.1	2.51	0.23	0.01	0.46	60.32	57.33		57.44
26											46.4	
	B2-2	2.43	0.05	53.87	3.78	0.47	0.04	0.26	58.47	54.34		42.75
	B3-2	2.43	0.03	55.13	3.3	0.38	0.03	0.26	59.13	55.51		43.14
	B3-6	2.43	0.03	55.13	3.3	0.38	0.03	0.26	59.13	55.51		42.85
	B3-6 E31		0.05	50.7	4.9	0.78	0.09	0.15	56.67	51.48		51.62
Reflector												
	Maximum		0.04	32.39	1.22	0.1	0	0	33.75	32.49		39.69
	Minimum	6.04										
	R4-3 B1		0.04	34.63	1.49	0.14	0.005	0.002	36.307	34.77		34.93
	R4-3 E3		0.01	23.68	0.68	0.04	0.001	0.002	24.413	23.72		23.87

NOTES: [1]Modeled results not shaded. Destructive evaluation data shaded. Assay data in last column.
(shaded) = results from destructive evaluation
= results from modeling (unless in Assay column)
Assay data for DE rods taken from WAPD-TM-1614

5.2.1 Nondestructive Examinations

Nondestructive examinations were performed to confirm breeding, assess support structure and fuel rod performance, and provide a database for evaluation of design procedures (Table 5-2). The end-of-life examination program included examinations of entire modules as well as individual components (rods, grids, bolts, etc.) and crud examination (Table 5-3).

PIFAG. The Production Irradiated Fuel Assay Gauge (PIFAG), discussed in WAPD-TM-1614, was used to non-destructively measure the fissile fuel content of 524 spent fuel rods from 12 LWBR modules. Cell locations of the 524 rods are shown in Figure 5-1 through 5-13. The 524 rods were selected using a statistical sampling plan, and the resulting data were used to estimate the end-of-life fissile inventory for the whole core. EOL fissile data from PIFAG were compared with data from extensive destructive evaluations to assess the accuracy of the PIFAG. EOL and BOL data were compared to determine if breeding had occurred (WAPD-TM-1614, p. 1). Results from PIFAG are presented in Appendix B.

PIFAG used the method of active neutron interrogation and delayed neutron counting (see WAPD--TM-1614) to determine the fissile uranium loading of each rod. PIFAG was assembled in a hot cell at Naval Reactors ECF. As-fabricated (unirradiated) rods were used to calibrate the PIFAG. Isotopic loadings for individual unirradiated seed, standard blanket, power flattening and reflector rods are presented in Table 5-4. Core rod testing was conducted from June 1984 to May 1987 (WAPD-TM-1614).

Rods were irradiated by neutrons from four Cf-252 sources, then delayed neutrons resulting from the fissions occurring from the source were counted as the rod passed through the detector region. The In-Cd liner in the PIFAG could be positioned to provide thermal or epithermal neutron interrogation spectrum. After an epithermal mode foreground pass, the rods were gamma scanned, and a cumulative gamma ray spectrum was recorded (WAPD-TM-1614, p. 19). PIFAG performance was closely monitored. The accuracy of the PIFAG was determined by comparing PIFAG results with destructive analysis results for 17 of the rods (p. 34, p. 50, p. 74 WAPD-TM-1614). PIFAG results were within 0.5% of the destructively examined results in all 17 cases. Table 5-1 shows the comparative results of PIFAG and the destructively evaluated rods.

REX. The REX gauge measured fuel rod length, diameter, oxide thickness, ovality, wear mark depth and volume, and provided a 5X visual examination and video recording capabilities. The gage also had the capability of ultrasonic screening of the fuel rod cladding for defects.

19 rods were removed for nondestructive examinations in the Rod Examination (REX) gauge (12 of those were also destructively examined at ANL-W). The 19 were selected to evaluate the effects of a broad range of parameters on fuel rod performance and included: 6 seed rods, 7 standard blanket rods, 3 power flattening rods, and 3 reflector rods. Their approximate locations are shown in Figure 5-14.

Table 5-2. Summary of NDE examinations.

Test	Purpose	No. Samples	Results	Location of Test
PIFAG (active neutron interrogation and delayed neutron counting)	Fissile fuel content, proof-of-breeding	524 rods from 12 modules (Figures 5-1 through 5-13)	See Appendix B	ECF hot cells
Gamma scan (PIFAG)	Measure in-stack gaps, binary fuel stack lengths, and axial profiles	24 rods: 9 seed 8 Standard blanket 4 Power flattening blanket 3 Reflector	No in-stack gaps between pellets noted with gamma scan (WAPD-TM-1605, p. 182). Resolution 0.2 in.. Maximum binary fuel elongation: Seed: 0.722 in. Blanket: 0.541 in. (WAPD-TM-1605, Table 27)	ECF hot cells
Rod pull force measurements (Rod Removal System, RRS)	Prevent overstressing a rod during disassembly, measure residual spring forces in support grids	1072 (test rods and rods for accessing test rods)	Upper 95% tolerance limit and maximum pull forces: Seed: 29 lbs/90 lbs Blanket: 52 lbs/96 lbs Reflector: 56 lbs/145 lbs (From WAPD-TM-1605, Figures 14-16, Table 9).	ECF
In-bundle bow and gap measurements (Vertical Inspection Gage Inspection Package, VIGIP) Underwater	For NRC core certification safety analysis, standard deviations of %gap closure required (p. 39 of 1605). Fuel rod performance	1 seed 5 blankets 1 reflector (see WAPD-TM-1605, Figure 7)	Module bowing: S2-3: 0.03 in. B3-2: 0.098 in. R4-4: 0.160 in. (from WAPD-TM-1605, p. 72). Other results in App. A4 and A5, Figs 21-30 in WAPD-TM-1605.	Bettis

Table 5-2. (continued).

Test	Purpose	No. Samples	Results	Location of Test
Rod length (Rod Examination Gage, REX)	Evaluate in-reactor length increases from thermal expansion, system pressure, irradiation growth of Zircaloy cladding, and pellet-cladding interaction.	6 seed 7 standard blanket 3 PF blanket 3 reflector	Elongation about 0.3-0.6 inches for all types (see WAPD-TM-1605 Table 10)	ECF
Visual inspections (REX, underwater camera)	Cladding cracking and collapse	Almost 1100 from 12 modules	Usual wear. No evidence of gross cladding deformation, cracked cladding, excessive wear or any other unusual conditions (WAPD-TM-1605 p. 98). Negligible post-transition oxide.	ECF
Free hanging bow (REX, 5X video recordings at 0, 45, 90, and 135 degree orientations)	Calculate seeding force and BOL bow of each rod	5 seed 4 StB 3 PFB 3 Refl (p. 103)	Calculated EOL in-bundle span bows from free hanging bow data were significantly smaller than worst case bow predictions except for span 7 of seed rod 1606710 (see WAPD-TM-1605 p. 110, data in Tables 13 and 14)	ECF
Cladding diameter and in-stack ovality measurements (REX axial profilometer; cladding outside diameters measured at 0, 45, 90 and 135 degree orientation)	Evaluate fuel rod ridging, grooving, ovality	19 rods	Diameter shrinkage and ovality less than predicted, (see WAPD-TM-1605 Figures 44-46 and Table 15). Shrinkage 1-6 mils.	ECF
Plenum ovality (REX)	To confirm stability of the freestanding RXA cladding in the seeds, and confirm predictions of cladding deformation for nonfreestanding SRA blanket cladding (p. 47)	14: 4 seed 7 StdBkt 3 PF Bkt (p. 47)	Ovalities < 2 mils for seed rods and < 4 mils for blanket rods (see WAPD-TM-1605, Table 17)	ECF

Table 5-2. (continued).

Test	Purpose	No. Samples	Results	Location of Test
Wear mark depth volume, and location (REX orbiting profilometer)	Confirm fuel rod design analysis procedure for rod wear; overall view of rod wear for grid support system	14: 4 seed 7 Std Bkt 3 PF Bkt	Wear marks virtually nonexistent (WAPD-TM-1605 p. 128)	ECF
Oxide thickness (Nortec 5 MHZ eddy current oxide thickness, EDCOT, gage in the axial profilometer)	Axial variations of oxide thickness	12 DE rods + 4 others	Oxide thickness less than 0.2 mil over the bottom 30 in. of each rod. Peak of 1.46 mils near the seventh grid level in rod 400736, which coincides with top of binary stack; peak of 1.56 mils between 6th and 7th levels in 606773 (see WAPD-TM-1605 Table 19)	ECF
Cladding defects (REX ultrasonic gage)	Determine if cracks formed as a result of core operation and to locate defect indications (WAPD-TM-1605 p. 54)	12 DE (WAPD-TM-1605 p. 147)	No indications of significant defects, through-cladding cracks, or other unusual conditions in 9/12 rods. 1 StBkt and 2 PFBkt rods had strong UT indications (>10 mils) which were not surface marks and not confirmable with metallographic analysis (WAPD-TM-1605 p. 147)	ECF
Crud measurements (de-crud with four solutions then quantitative analysis)	Characterize crud deposits on the external surface including elements and radioisotopes in crud.	Seed 0504502 Std. Blanket 1605629 Reflector 3220018	Characteristics of crud shown in Table 5-3. Local smudge-like areas of crud were frequently observed on the rods. Descaling was largely effective (WAPD-TM-1605 p. 152)	ANL-W

Table 5-2. (continued).

Test	Purpose	No. Samples	Results	Location of Test
Neutron radiography	For proper cutting of rods, examining fuel pellet integrity, and determining fuel stack and plenum dimensions in the intact fuel rods (p.57)	12 DE rods: 4 seed (2 with binary stack length of 84 in., 1 with 70 in. binary stack length, 1 with 42 in. binary stack length). 4 Standard blanket (2 with 42 in. binary stack length, 1 with 84 in. binary stack and high enrichment, and 1 with 84 in. binary stack length and medium enrichment) 3 Power Flattening blanket (84 in. with high enrichment) 1 Reflector	None of the radiographs gave an indication of defected cladding or massive hydriding. (WAPD-TM-1605 p. 164). Pellet stacks were generally stable and continuous. Most pellet cracks were hairline; few indicate fuel separation.	ANL-W NRAD facility

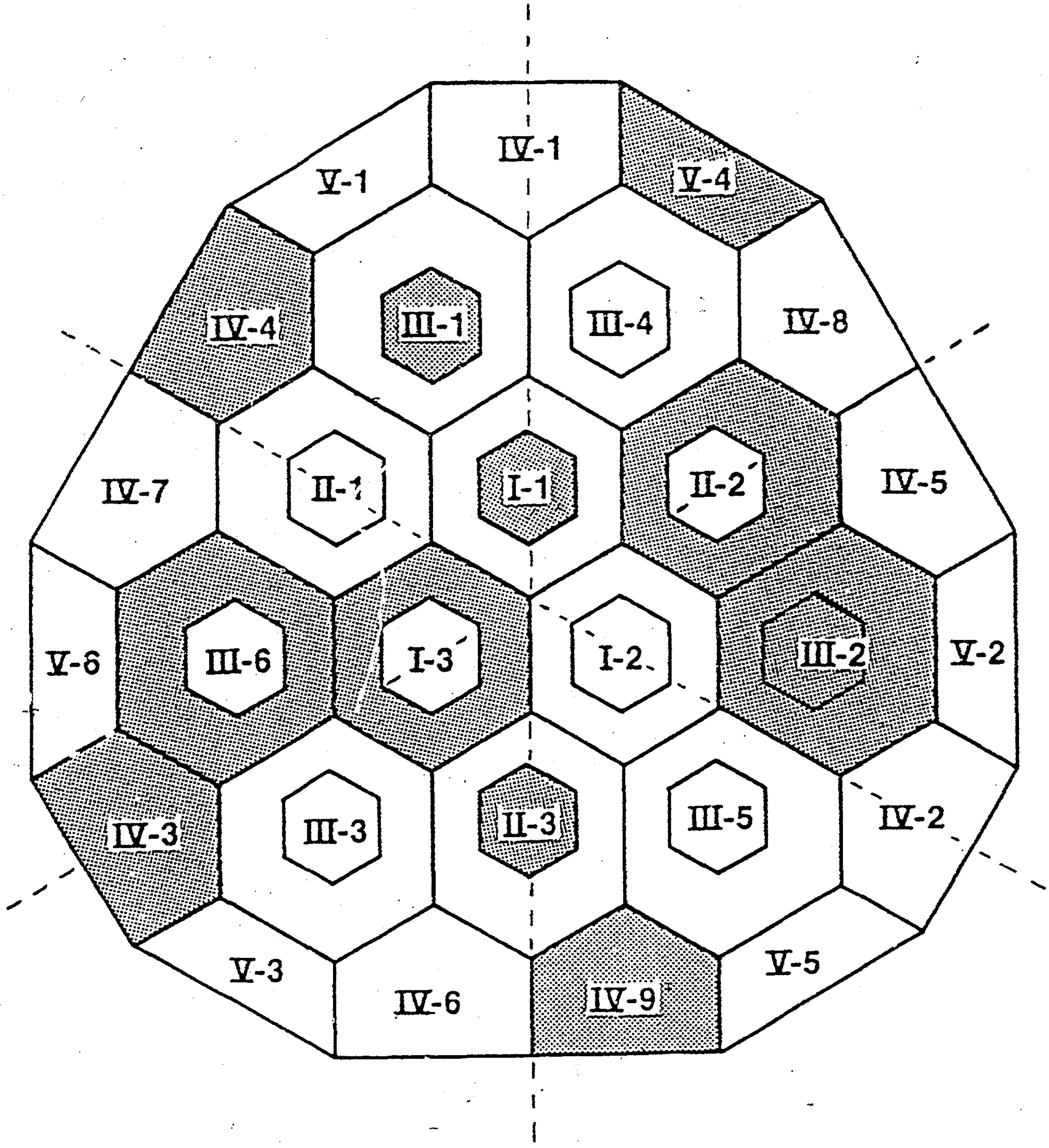

Figure 5-1. Diagram of LWBR core, showing locations of Proof-of-Breeding Modules (shaded) and boundaries of Sixth-Core Sectors (dashed) (WAPD-TM-1612, Figure V-1).

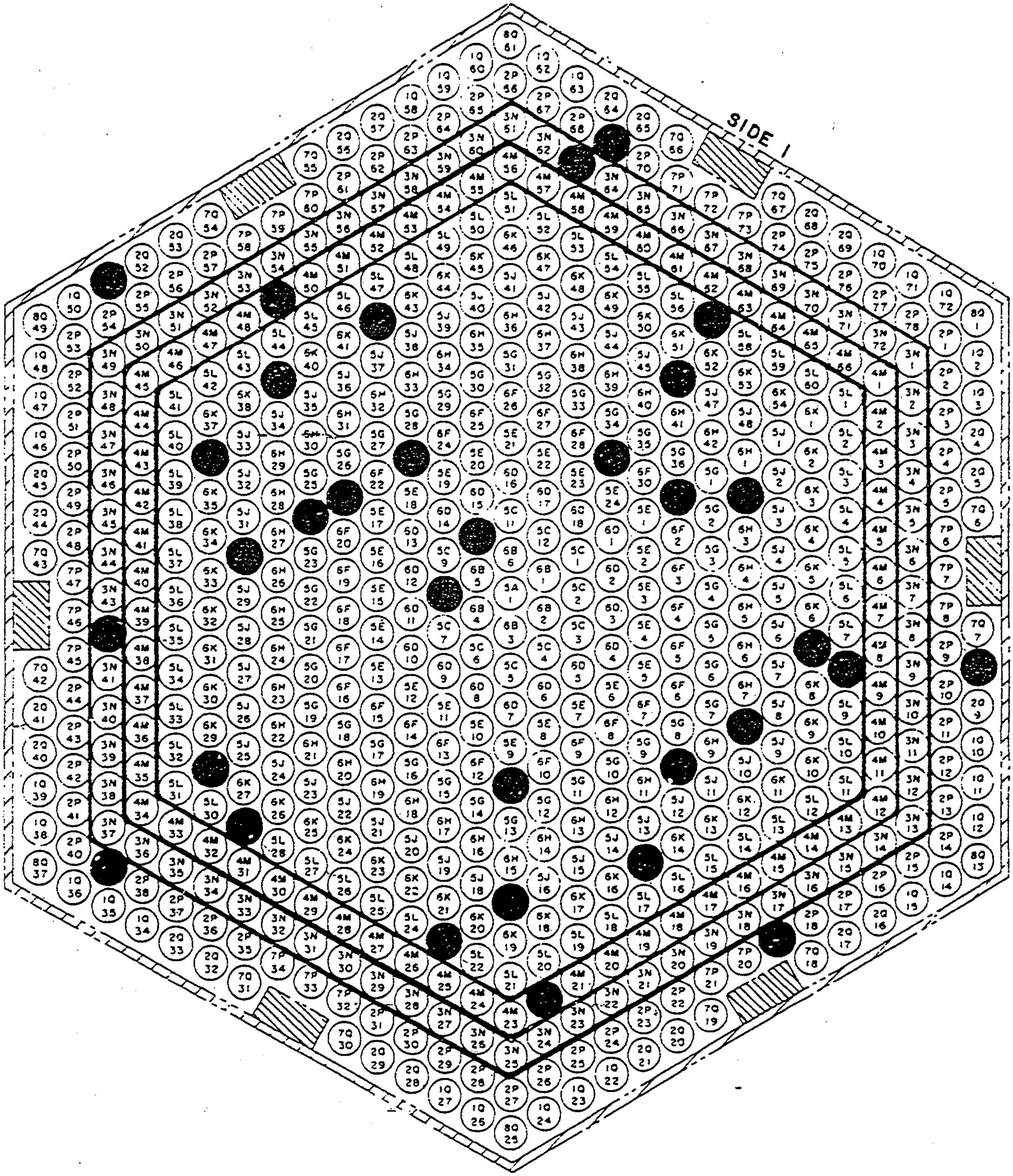

Figure 5-2. Location of Proof-of-Breeding Rods in Seed Module I-1 (WAPD-TM-1612, Figure V-2).

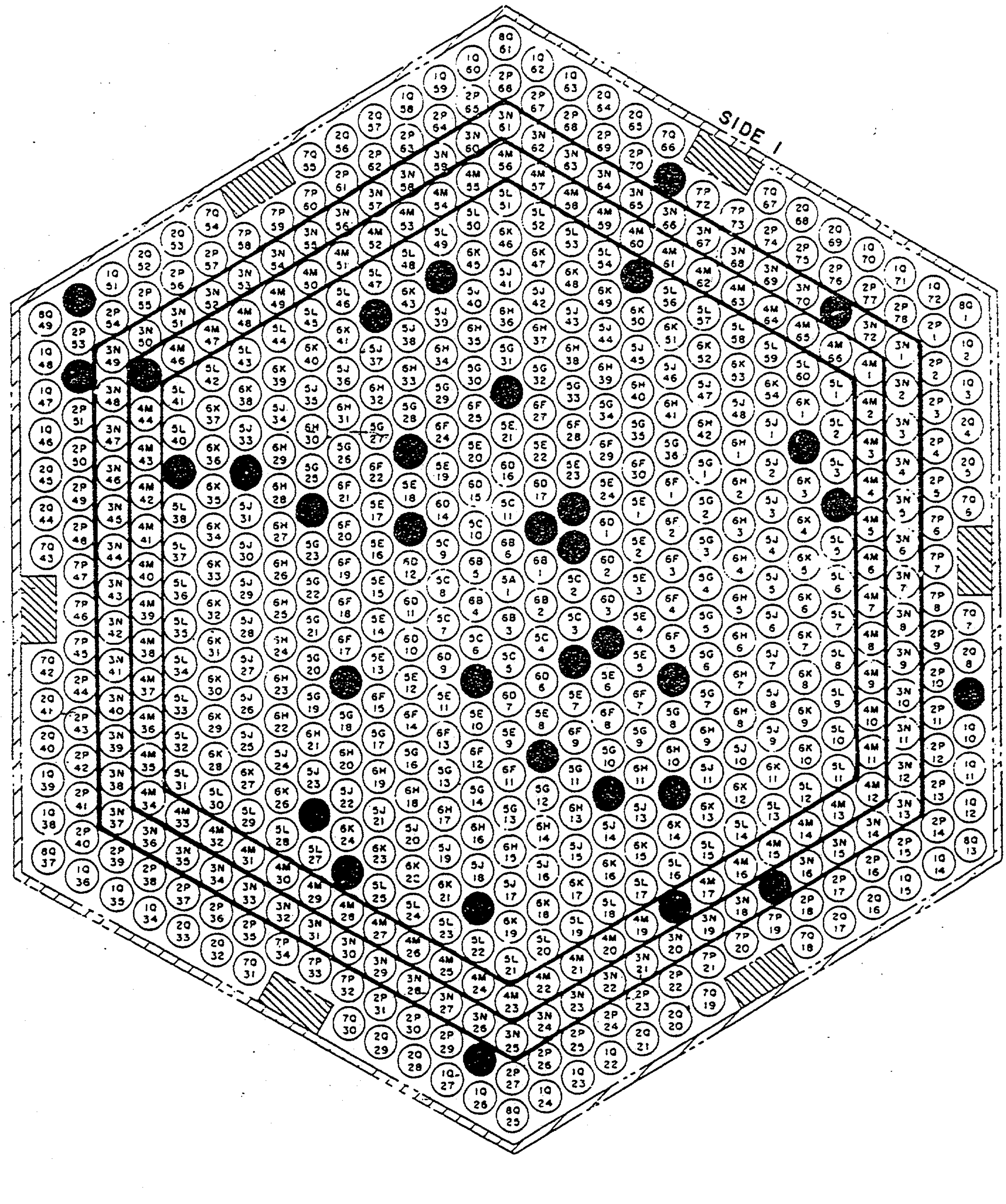

Figure 5-3. Location of Proof-of-Breeding Rods in Seed Module II-3. (WAPD-TM-1612, Figure V-3).

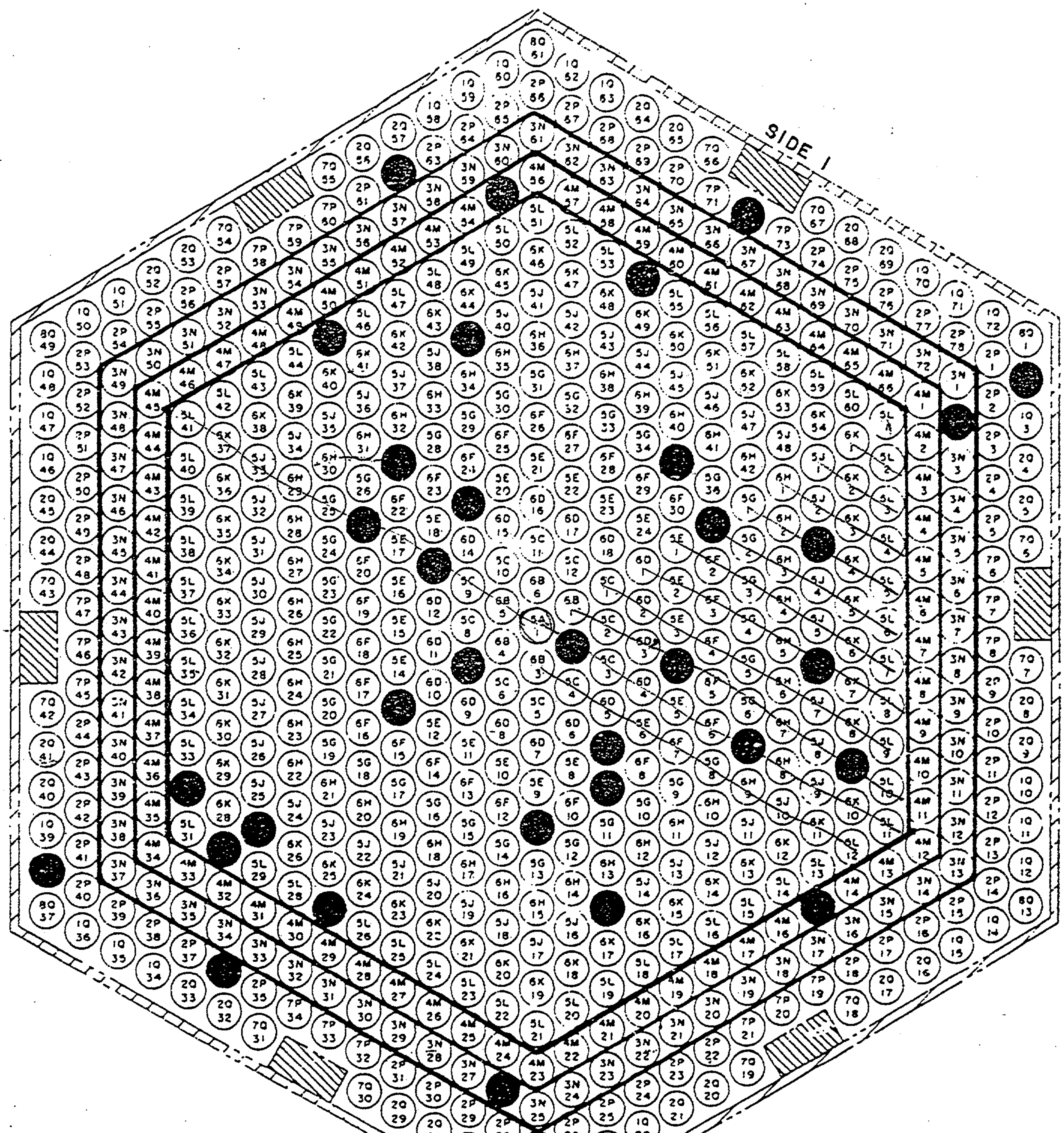

Figure 5-4. Location of Proof-of-Breeding Rods in Seed Module III-1 (WAPD-TM-1612, Figure V-4).

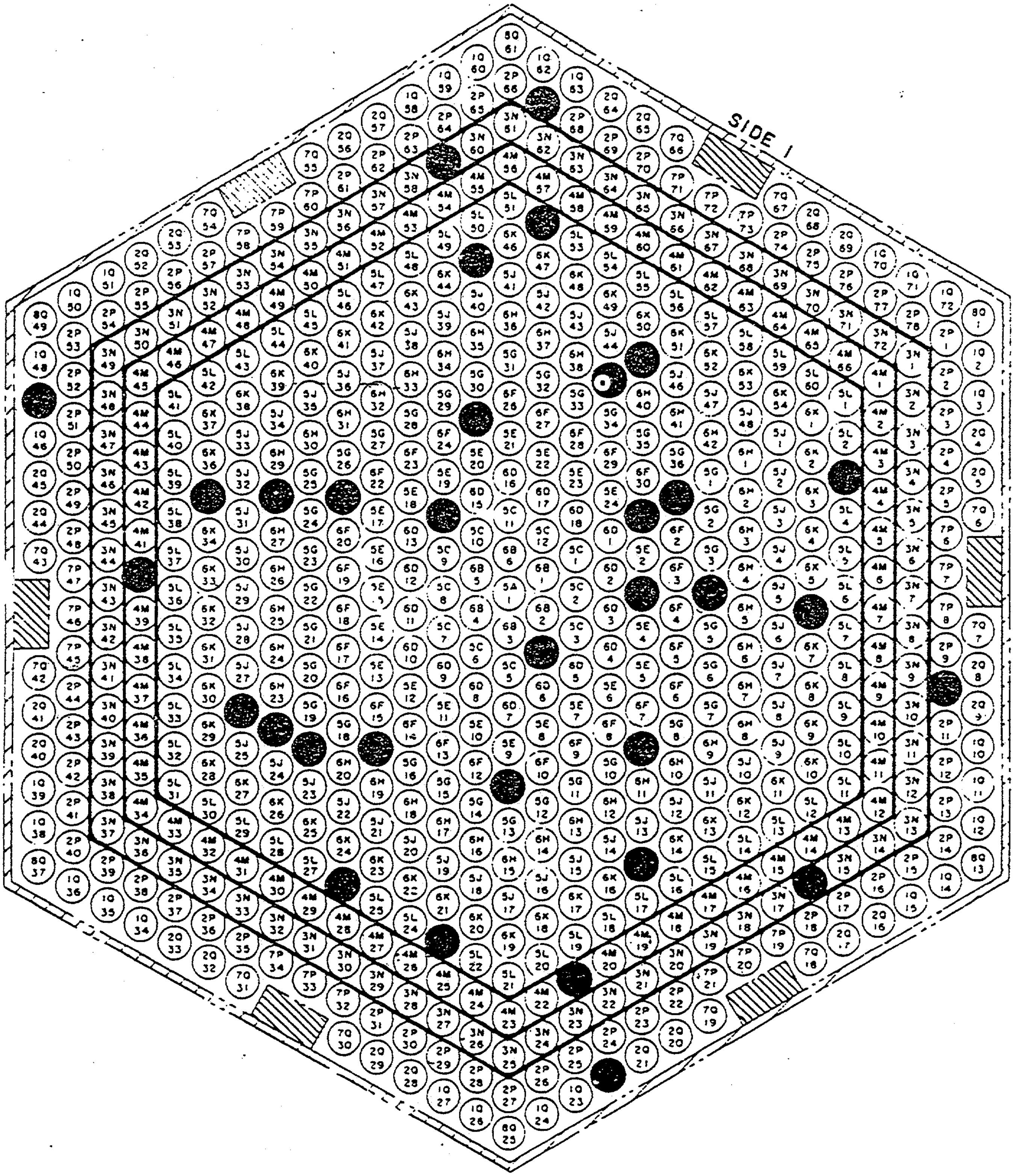

Figure 5-5. Location of Proof-of-Breeding Rods in Seed Module III-2 (WAPD-TM-1612, Figure V-5).

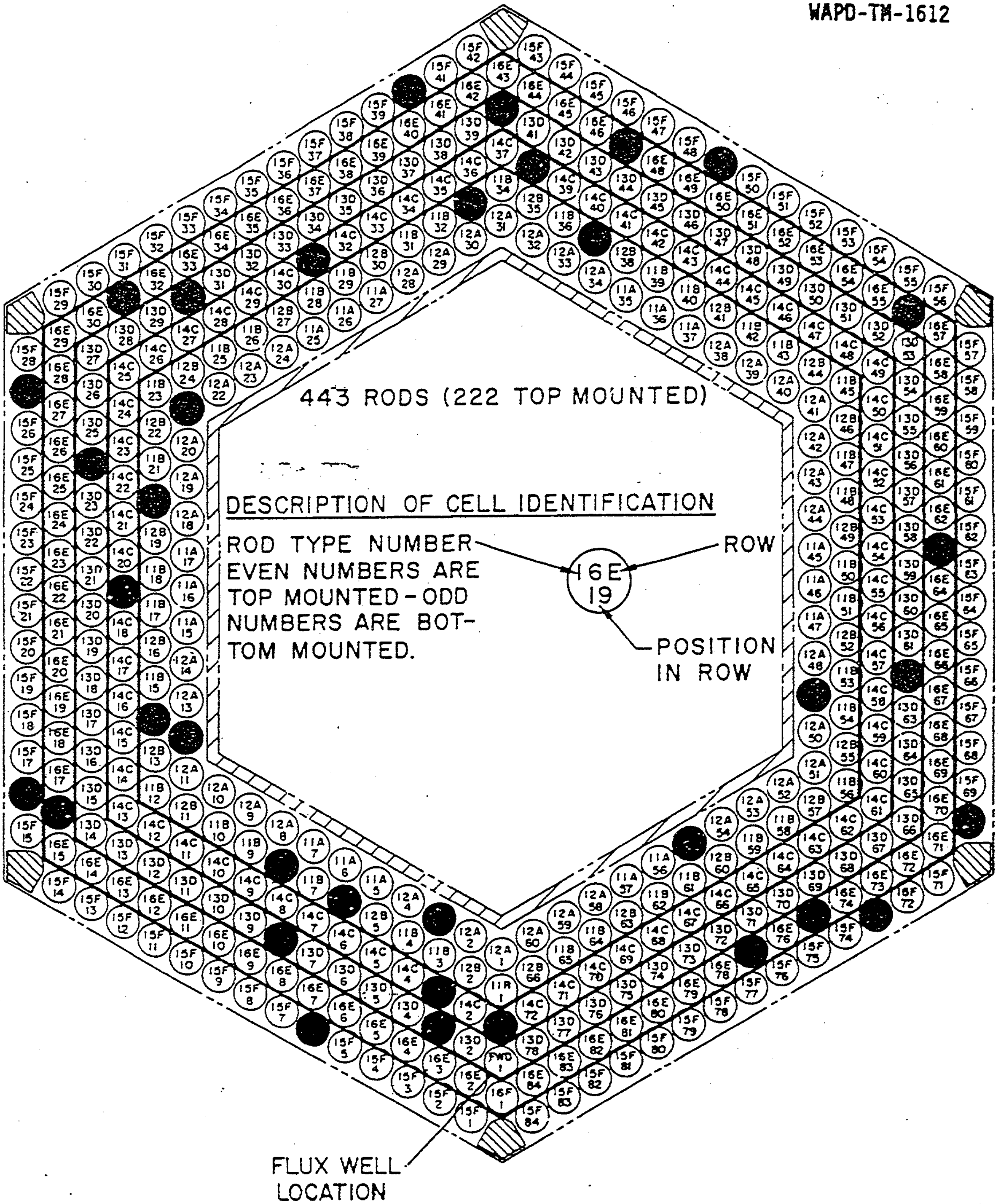

Figure 5-6. Location of Proof-of-Breeding Rods in Blanket Module I-3 (WAPD-TM-1612, Figure V-6).

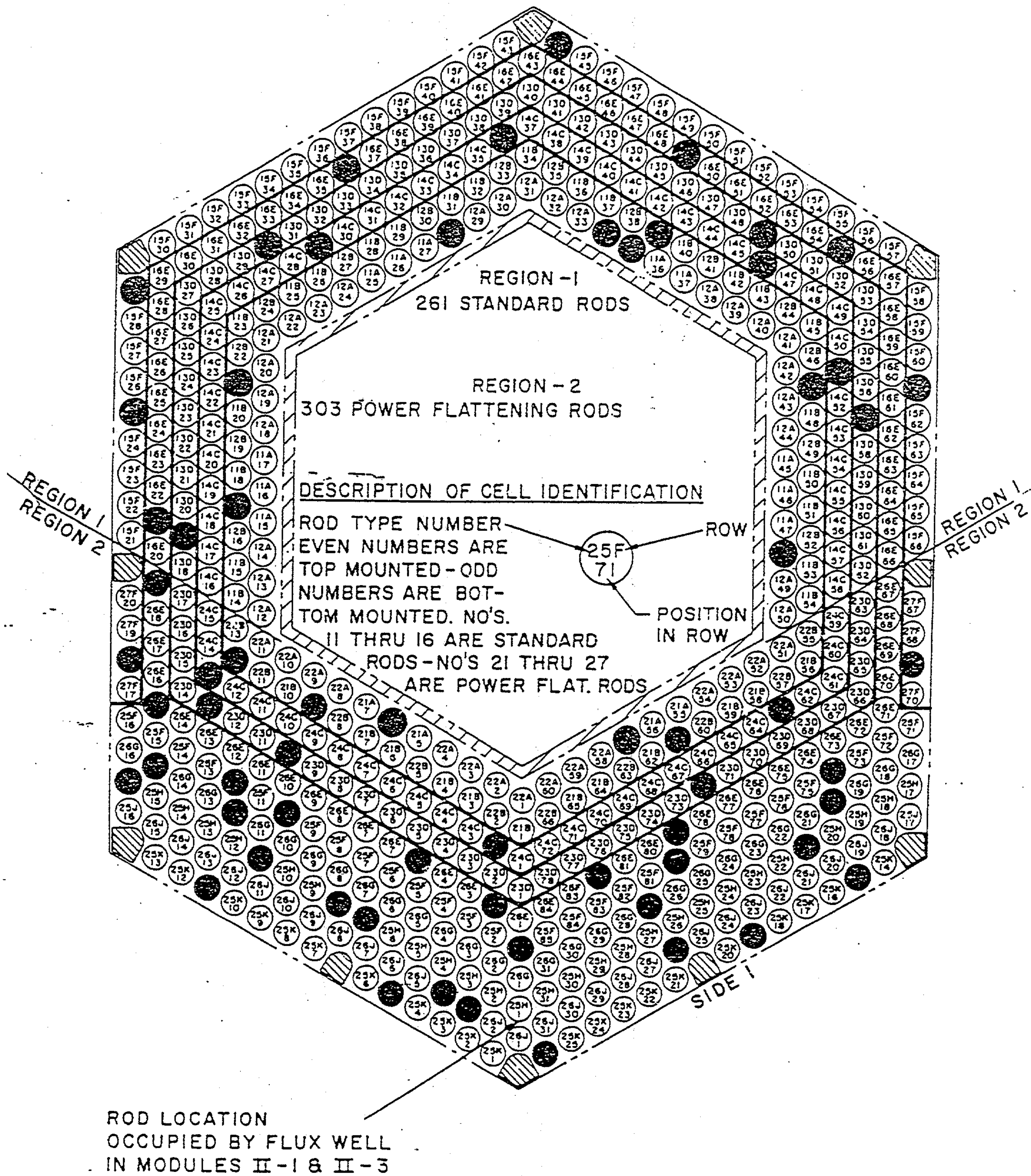

Figure 5-7. Location of Proof-of-Breeding Rods in Blanket Module II-2 (WAPD-TM-1612, Figure V-7).

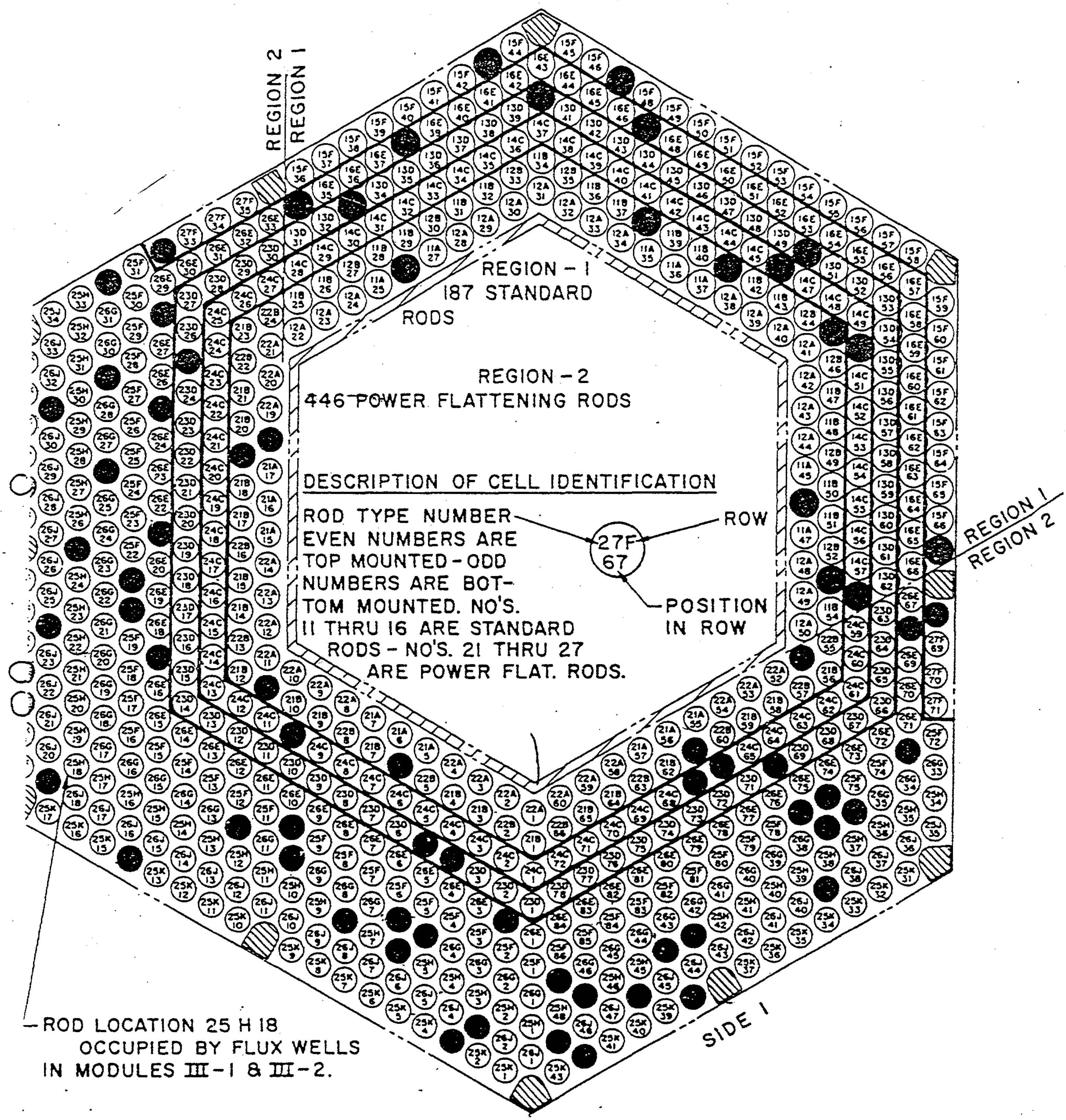

Figure 5-8. Location of Proof-of-Breeding Rods in Blanket Module III-2 (WAPD-TM-1612, Figure V-8).

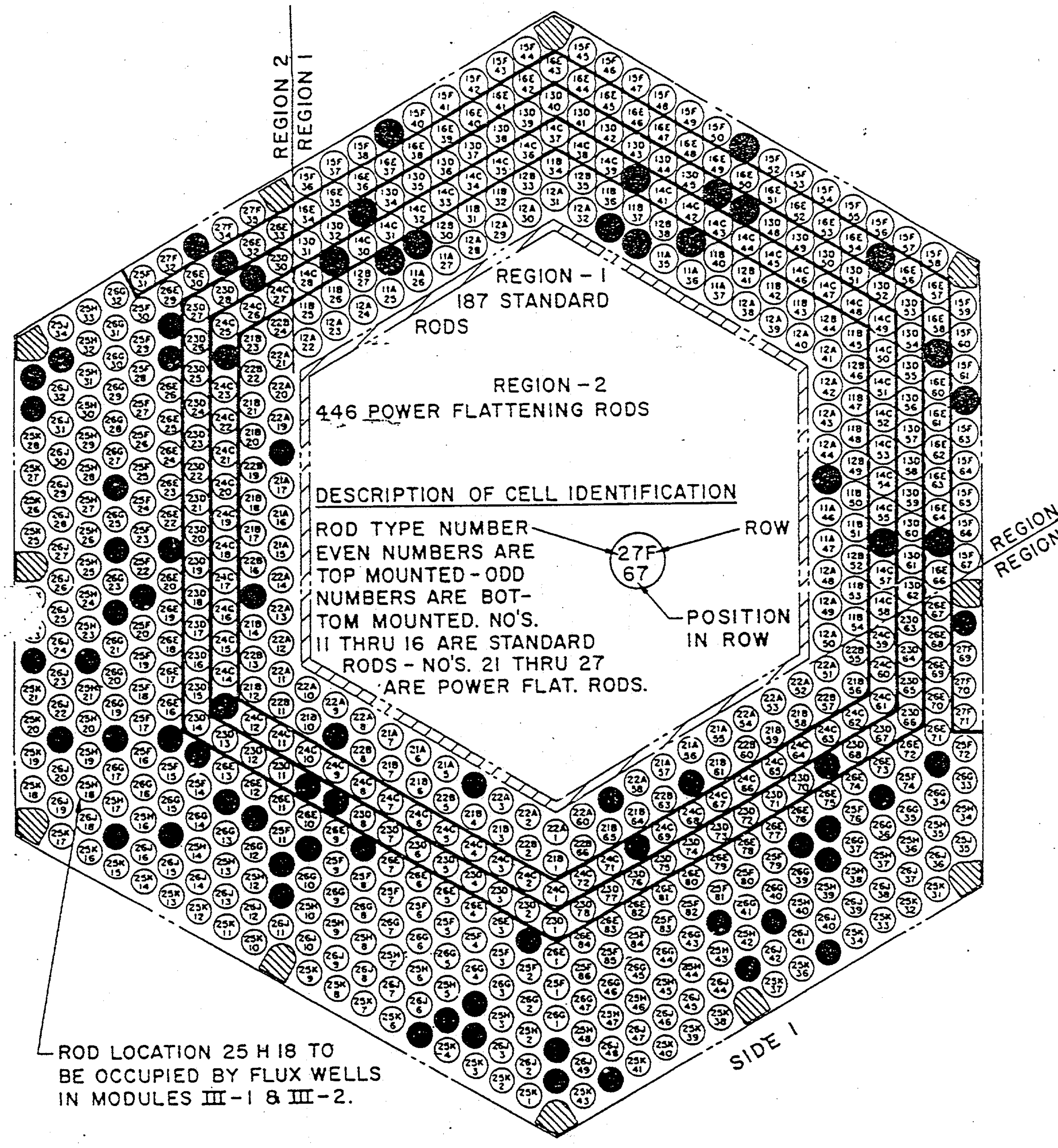

Figure 5-9. Location of Proof-of-Breeding Rods in Blanket Module III-6 (WAPD-TM-1612, Figure V-9).

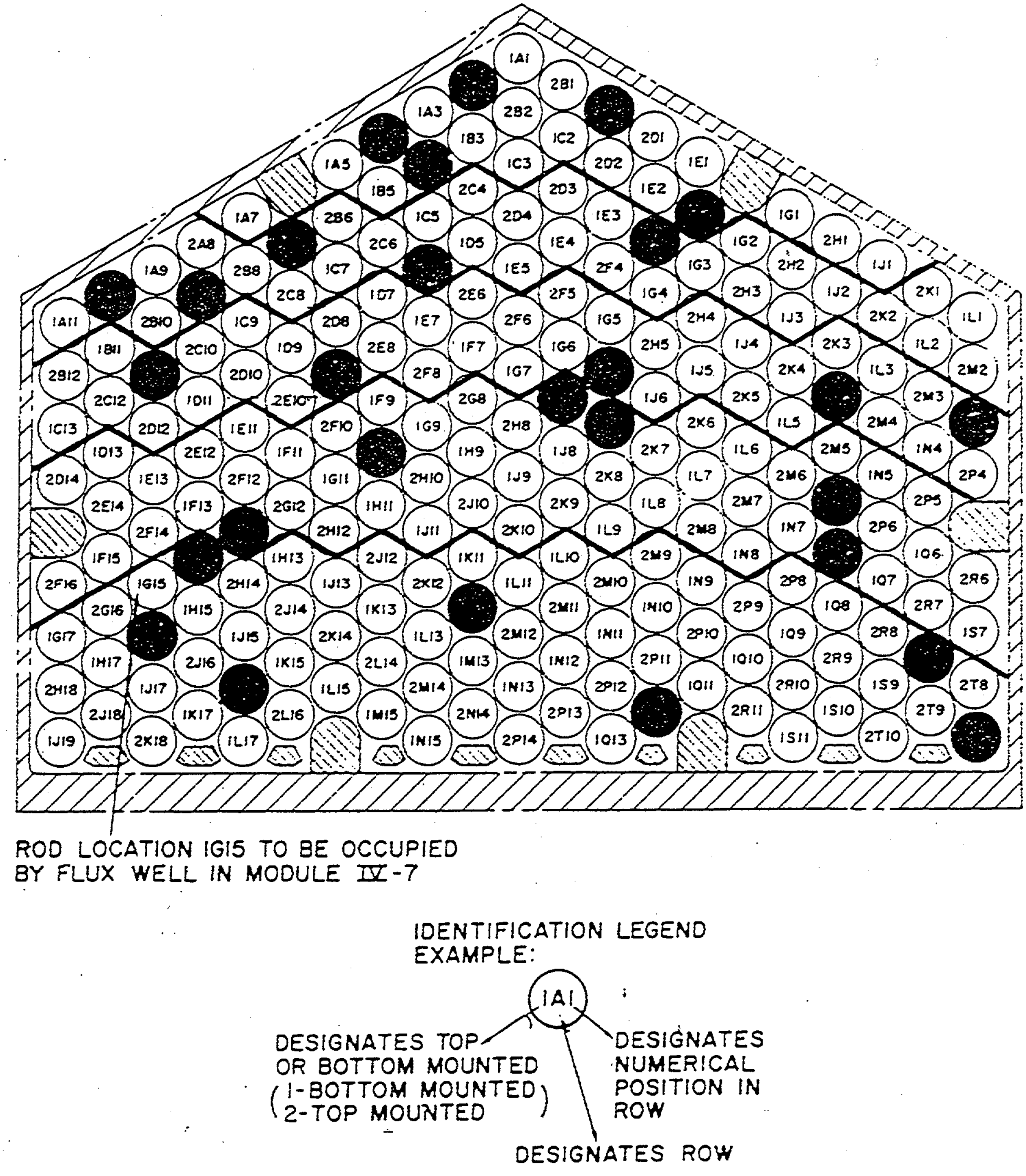

Figure 5-10. Location of Proof-of-Breeding Rods in Reflector Module IV-4 (WAPD-TM-1612, Figure V-10).

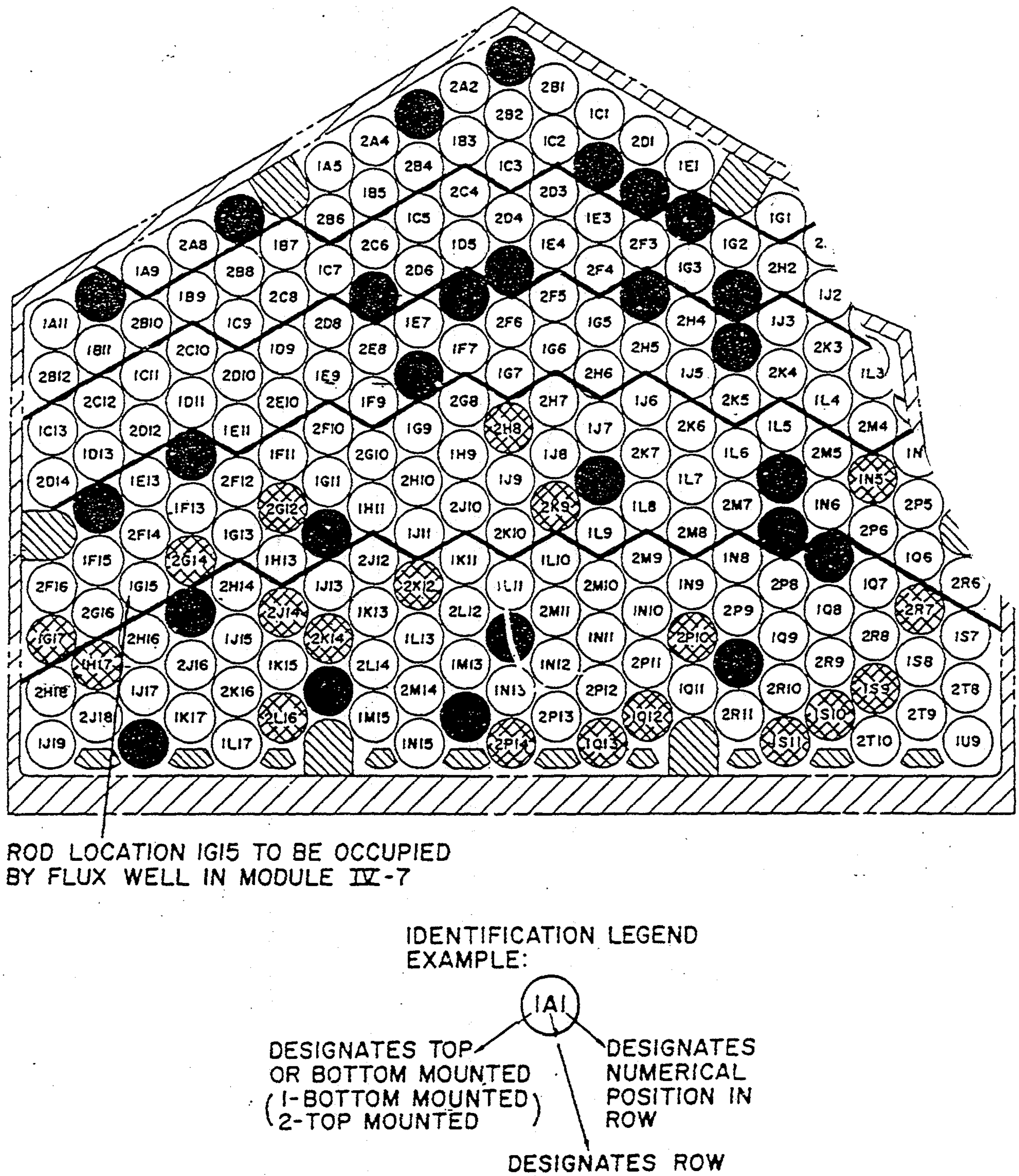

Figure 5-11. Location of Proof-of-Breeding Rods in Reflector Module IV-9. Twenty additional rods not part of original POB sample are indicated by cross hatching (WAPD-TM-1612, Figure V-11).

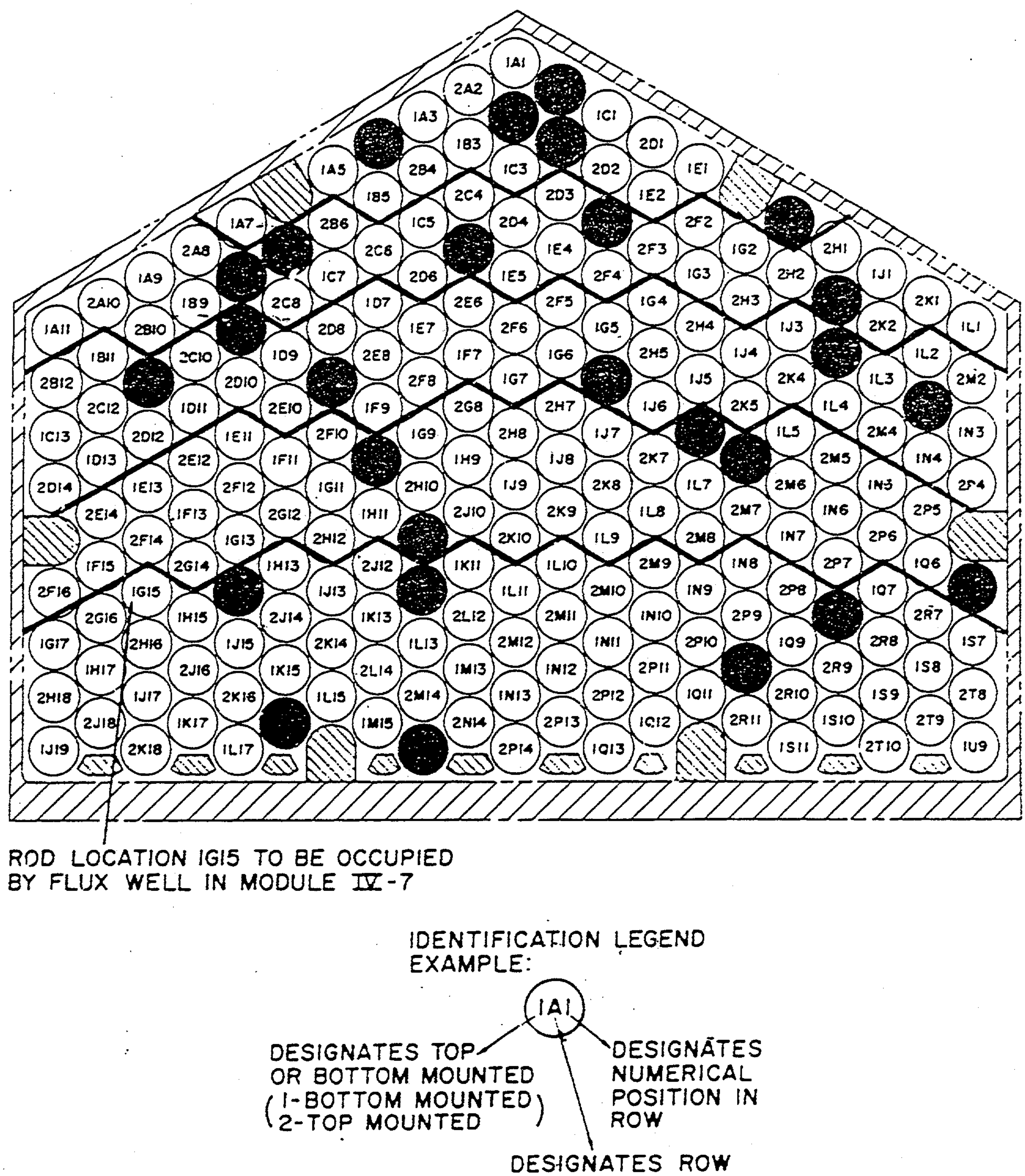

Figure 5-12. Location of Proof-of-Breeding Rods in Reflector Module IV-3 (WAPD-TM-1612, Figure V-12).

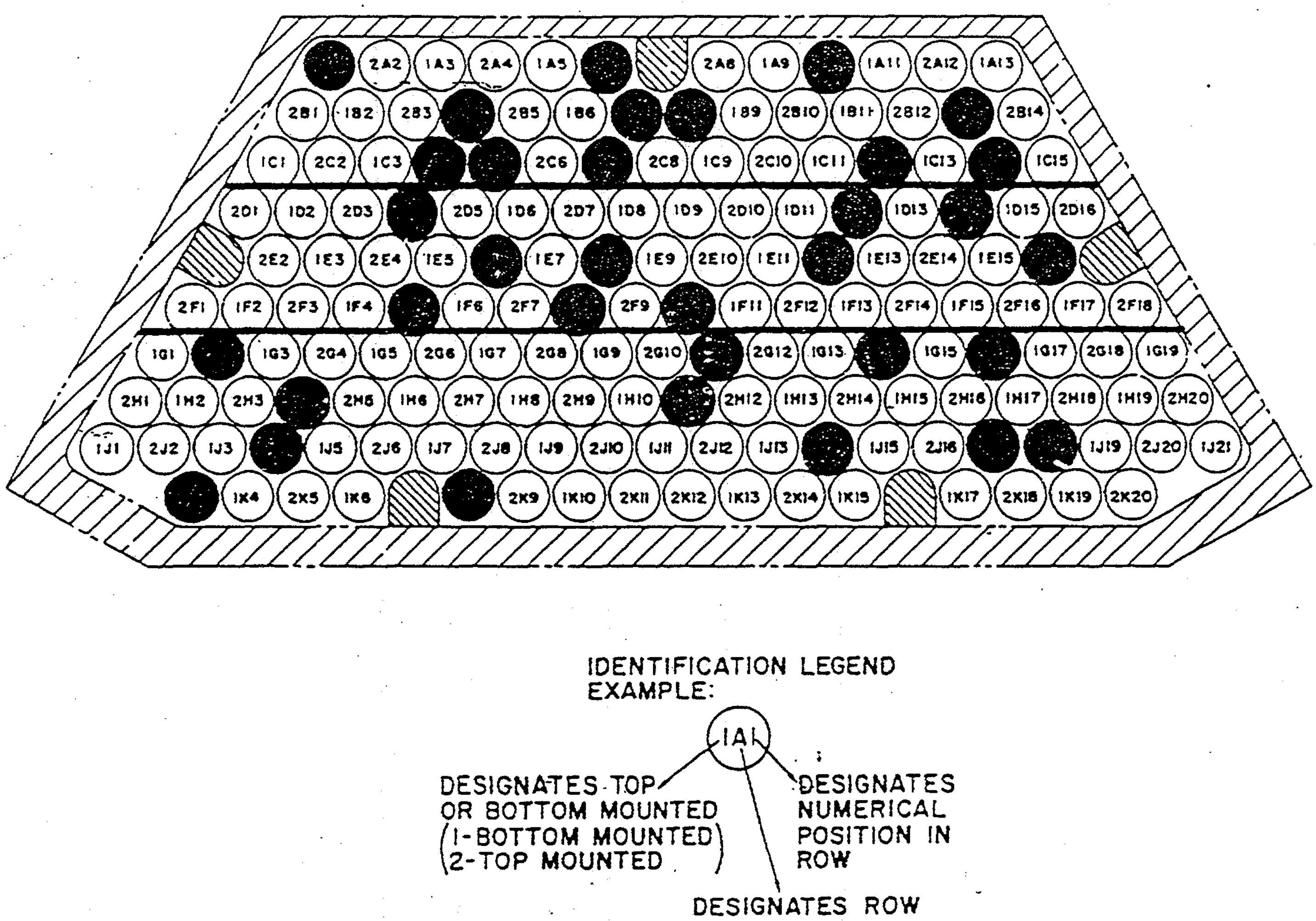

Figure 5-13. Location of Proof-of-Breeding Rods in Reflector Module V-4 (WAPD-TM-1612, Figure V-13).

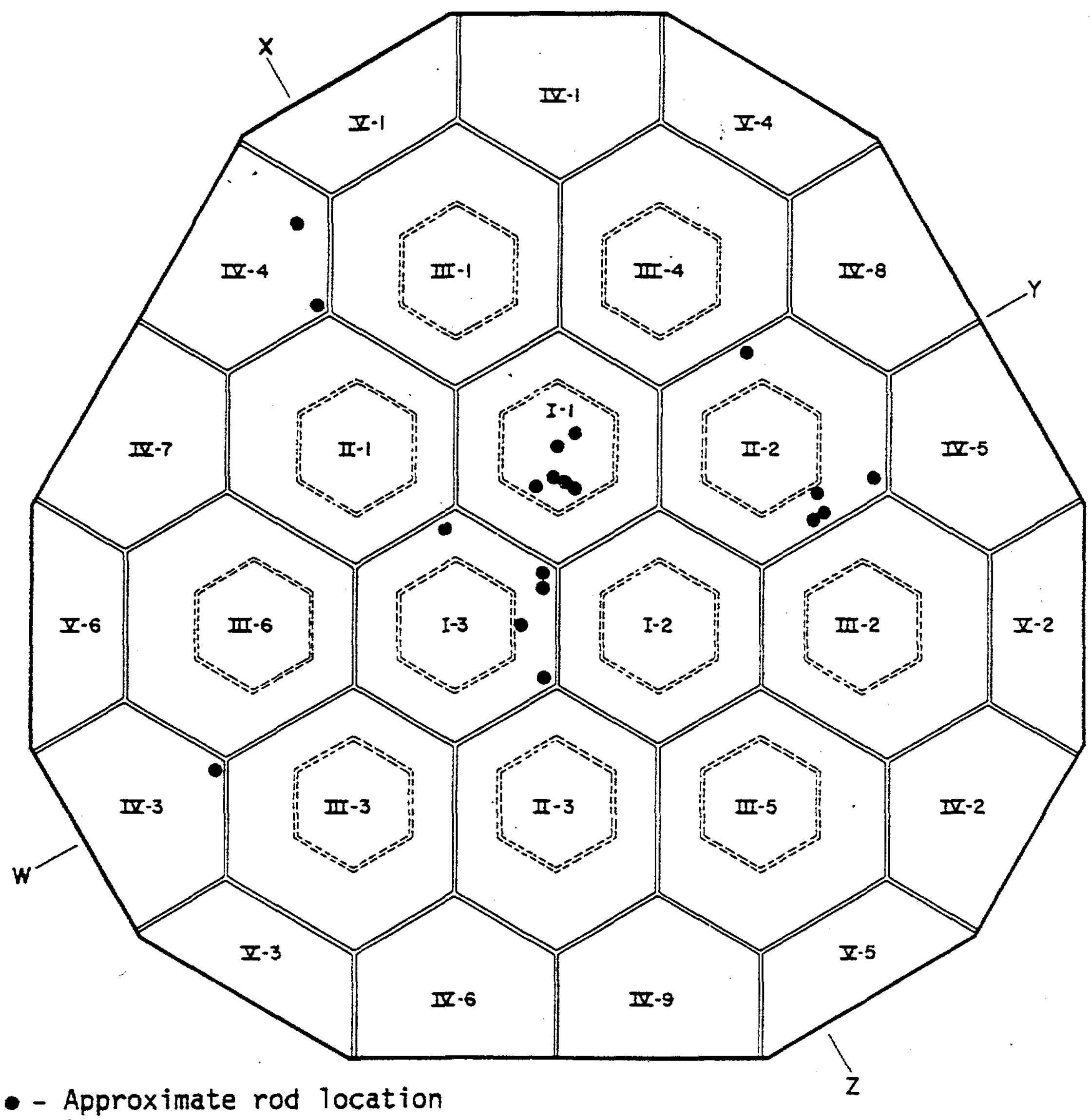

Figure 5-14. REX examination fuel rod locations (WAPD-TM-1605, Figure 9).

Table 5-3. Fuel rod crud characterization (WAPD-TM-1605, Table 21).

Seed Rod 0504502

Increment	Fe	Ni	Cr	Co	Cu
	Elements (mg/dm^2)				
First	0.38	0.45	0.10	nd*	nd*
Second	0.26	0.26	0.03	nd*	nd*
Third	0.54	0.88	0.08	nd*	nd*

Increment	^{55}Fe	^{63}Ni	^{60}Co	^{54}Mn	^{125}Sb
	Radioisotopes ($\mu Ci/dm^2$)				
First	3.87	3.45	10.21	7.74	nd*
Second	3.54	1.70	15.21	5.76	nd*
Third	5.23	1.95	26.87	6.54	trace

Blanket Rod 1605629

Increment	Fe	Ni	Cr	Co	Cu
	Elements (mg/dm^2)				
First	0.48	0.39	0.08	nd*	nd*
Second	0.73	0.56	0.04	nd*	nd*
Third	2.02	0.86	0.09	nd*	nd*

Increment	^{55}Fe	^{63}Ni	^{60}Co	^{54}Mn	^{125}Sb
	Radioisotopes ($\mu Ci/dm^2$)				
First	3.02	1.91	12.68	3.30	nd*
Second	8.52	5.57	42.61	7.10	nd*
Third	13.83	4.18	62.76	5.81	trace

Reflector Rod 3220018

Increment	Fe	Ni	Cr	Co	Cu
	Elements (mg/dm^2)				
First	0.49	0.47	0.04	nd*	nd*
Second	0.34	0.86	0.04	nd*	nd*
Third	0.40	0.04	0.04	nd*	nd*

Increment	^{55}Fe	^{63}Ni	^{60}Co	^{54}Mn	^{125}Sb
	Radioisotopes ($\mu Ci/dm^2$)				
First	2.03	1.48	2.61	3.47	nd*
Second	4.58	5.08	9.66	2.69	nd*
Third	2.16	0.73	5.13	nd*	nd*

*nd - not discernible

Table 5-4. Calibration rod isotopic loadings. All values are in grams (WAPD-TM-1614, Table 24).

a. Seed Rods

Rod ID	^{232}U *	^{233}U	^{234}U	^{235}U	^{236}U	^{238}U	^{232}Th
05001	0.0	0.0	0.0	0.0	0.0	0.0	745.5
05004	0.0	0.0	0.0	0.0	0.00	0.0	746.2
05061	2.05E-5	3.401	0.0400	2.92E-3	4.18E-4	0.0351	728.2
05062	2.05E-5	3.402	0.0400	2.92E-3	4.18E-4	0.0352	728.4
05121	4.91E-5	8.131	0.0957	6.99E-3	9.98E-4	0.0840	721.1
05122	4.91E-5	8.132	0.0957	6.99E-3	9.98E-4	0.0840	721.5
05273	1.11E-4	18.308	0.215	0.0157	2.25E-3	0.189	712.1
0100500	9.97E-5	14.196	0.194	0.0176	3.90E-3	0.0448	716.5
0301754	1.55E-4	19.110	0.233	4.47E-3	1.94E-4	0.0697	708.1
0401863	1.67E-4	23.698	0.323	0.0294	6.52E-3	0.0743	698.0
0414466	1.67E-4	24.077	0.321	0.0201	4.65E-3	0.0705	702.6
05431	2.25E-4	28.709	0.350	6.71E-3	2.92E-4	0.104	695.8
05432	2.25E-4	28.709	0.350	6.71E-3	2.92E-4	0.104	695.6
0511165	2.49E-4	34.548	0.431	0.0133	1.75E-3	0.0782	691.9
0527674	2.48E-4	34.797	0.457	0.0269	6.37E-3	0.1005	691.6

b. Regular Blanket Rods

Rod ID	^{232}U	^{233}U	^{234}U	^{235}U	^{236}U	^{238}U	^{232}Th
15002	0.0	0.0	0.0	0.0	0.0	0.0	2954.3
15004	0.0	0.0	0.0	0.0	0.0	0.0	2959.0
15061	8.35E-5	13.838	0.163	0.0119	1.70E-3	0.143	2949.5
15064	8.35E-5	13.828	0.163	0.0119	1.70E-3	0.143	2949.0
1103425	1.41E-4	16.445	0.221	0.0135	3.51E-3	0.0452	2931.2
1104780	1.40E-4	16.431	0.221	0.0135	3.51E-3	0.0451	2936.2
15122	2.57E-4	32.814	0.475	0.0478	0.0154	0.0823	2910.7
15124	2.58E-4	32.829	0.475	0.0478	0.0154	0.0823	2912.2
1412359	2.54E-4	30.094	0.392	0.0190	3.98E-3	0.0826	2953.6
1501827	3.89E-4	45.577	0.612	0.0380	9.74E-3	0.124	2915.2
1512019	3.89E-4	45.528	0.611	0.0380	9.73E-3	0.124	2914.9
1300545	3.83E-4	45.399	0.604	0.0362	9.15E-3	0.119	2904.0
1613659	4.59E-4	54.397	0.719	0.0431	0.0111	0.143	2923.6
1613834	4.59E-4	54.380	0.719	0.0431	0.0111	0.143	2922.3

c. Power Flattening Blanket Rods

Rod ID	^{232}U	^{233}U	^{234}U	^{235}U	^{236}U	^{238}U	^{232}Th
25001	0.0	0.0	0.0	0.0	0.0	0.0	2488.9
25004	0.0	0.0	0.0	0.0	0.0	0.0	2493.2
25063	7.04E-5	11.660	0.137	0.0100	1.43E-3	0.120	2489.8
25064	7.03E-5	11.646	0.137	0.0100	1.43E-3	0.120	2486.5
25122	1.69E-4	27.930	0.329	0.0240	3.43E-3	0.289	2473.8
25123	1.69E-4	27.940	0.329	0.0240	3.43E-3	0.289	2474.7
2100153	1.60E-4	18.910	0.250	0.0144	3.46E-3	0.0496	2477.8
2103140	1.58E-4	18.972	0.257	0.0180	4.83E-3	0.0521	2471.2
25161	3.19E-4	37.813	0.500	0.0292	6.92E-3	0.0984	2459.3
25163	3.22E-4	38.168	0.505	0.0295	6.99E-3	0.0993	2459.2
2402626	2.43E-4	30.601	0.424	0.0343	9.97E-3	0.0826	2472.6
2700468	3.82E-4	46.313	0.636	0.0519	0.0146	0.126	2452.6
2701624	3.56E-4	46.523	0.683	0.0749	0.0237	0.124	2455.7
2303222	3.76E-4	52.579	0.639	0.0440	8.59E-3	0.415	2433.6
2500452	4.43E-4	62.959	0.732	0.0398	7.71E-3	0.482	2427.1
2502616	4.51E-4	63.139	0.747	0.0464	0.0122	0.439	2431.0

d. Reflector Rods

Rod ID	^{232}U	^{233}U	^{234}U	^{235}U	^{236}U	^{238}U	^{232}Th
3106718	0.0	0.0	0.0	0.0	0.0	0.0	6089.4
3108707	0.0	0.0	0.0	0.0	0.0	0.0	6028.1
3102143	0.0	0.0	0.0	0.0	0.0	0.0	6036.7
31062	1.75E-4	29.048	0.342	0.0250	3.57E-3	0.300	6033.9
31063	1.75E-4	29.052	0.342	0.0250	3.57E-3	0.300	6037.6
31123	4.19E-4	69.363	0.816	0.0596	8.52E-3	0.717	5978.9
31124	4.19E-4	69.401	0.817	0.0596	8.52E-3	0.717	5976.9

* Notation n.nnE-n ≡ $n.nn \times 10^{-n}$

5.2.2 Destructive Examination

Twelve of the rods examined using the REX gauge were shipped to ANL-W for nondestructive neutron radiography, then were punctured to obtain fission gases. Seventeen of the 524 rods examined for fissile content with the PIFAG were shipped to ANL-E for destructive examination for the isotopic content. Destructive examinations conducted on both the 12 rods and the 17 rods are summarized in Table 5-5 and discussed briefly below.

5.2.2.1 Fission Gas Release at End-of-Life. Twenty nine rods were selected for fission gas (xenon and krypton) analysis: 12 were sent to ANL-W and 17 to ANL-E. Rods were chosen to represent a broad range of as-built and core operating characteristics and to cover a broad range of power density, fuel burnup, and rod neutron fluence. Operating characteristics of the 12 rods selected for analysis by ANL-W are presented in Table 5-6.

Only fission gas released from the plenum was measured at ANL-W. In contrast, ANL-E measured fission gas from the plenum, as well as fission gas released during rod shearing and rod dissolution. The method for fission gas sampling of the plenum involved puncturing the rod cladding with a laser, collecting the released gases in a sample collection tube, and analyzing by mass spectrometry for xenon and krypton (WAPD-TM-1606, pp. 39-40). Results from the plenum tap from both sets of samples are presented in Table 5-7. Results from the plenum puncture, shearing, and dissolution samples for the 17 rods are presented in Table 5-8.

Plenum gas analyses were only obtained for 11 of the 12 sampled rods at ANL-W (the twelfth sample was lost during plenum tap), and from 16 of the 17 rods from ANL-E (one sample was contaminated with nitrogen and oxygen from the room). Results from the 11 ANL-W samples and all 17 ANL-E samples are presented in Table 5-6[1]. Core locations of the 28 rods can be determined using the cell numbers presented in Table 5-7 along with the cell maps presented in Section 3. All rods were shown to have gas release levels below the low-temperature prediction line. Because fuel rods from peak temperature and peak depletion locations were included in the samples, all fuel was considered to have operated at temperatures below 2580° F (WAPD-TM-1606, pp. 49-50).

5.2.2.2 Isotopic Results. The 17 rods shipped to ANL-E were analyzed for isotopic inventory. Total uranium and uranium isotopic (U-233, U-234, U-235, U-236, U-238) analyses were performed by thermal ionization mass spectrometry. Due to the interference of Th-232, U-232 was determined by alpha spectrometry (ANL-E data reports). Fission products Cs-137, Ce-144, and Zr-95 were determined by gamma spectrometry (high purity germanium detector with associated automated multi-channel analyzer/data management system) on weighed aliquots of the samples. Cs-137 and Ce-144 were determined on a sample aliquot by direct counting. Zr-95 was obtained after processing the sample aliquot through a cleanup procedure to reduce interferences. The losses of Zr-95 were accounted for by using before and after values of the Ce-144. Error requirements for Zr-95 measurements made after 10/84 were waived, due to the short half life (64.02 days) (ANL-E data reports).

---

[1] According to the notes attached to the sample report for the contaminated sample (Rod "R"), ANL-E provided Bettis with sufficient data to calculate or compile fission data for Rod "R".

Table 5-5. Destructive examinations (from WAPD-TM-1606).

Test	Purpose	No. of Samples	Results	Testing facility
Fission gas release (mass spectrometry)	Quantify fission gases, which are an indication of fuel temperatures achieved during reactor operation.	12 rods by ANL-W 17 rods by ANL-E	Estimated operating temperature of reaction about 2580° F (WAPD-TM-1606, p. 49-50). Fission gas in the gap (plenum) comprises less than 1% of total fission gases measured from the rods (ANL-E data).	ANL-W did the 12 (1 lost gas sample) ANL-E did the 17
Metallographic Examination	Size and spatial distribution of pores, cracks, grain size, internal and external corrosion, fuel and cladding mechanical and chemical interaction, hydriding, hydrogen in cladding	12 rods (or pellets from the rods) selected by Bettis.	Low burnup thoria pellets were intact. Binary pellets often cracked but freestanding within the cladding. Fine porosity. No evidence of fuel bonding to Zirc cladding in seed, but some in blanket region rods. No massive hydriding. (WAPD-TM-1606, pp.50-123)	ANL-E
Cladding behavior	Detect cladding inadequacies	Cladding of 12 rods checked	No through-cladding defects detected	ECF
Cladding oxide			Thickness of the oxide ranged from .05 mil to 1.75 mils (Table 10 of WAPD-TM-1606)	ECF
Cladding hydride			Hydride size and distribution varied by rod type. Total H content: Seed: 50-100 ppm Blkt: 25 to 100 ppm Refl: 25-50 ppm (WAPD-TM-1606, pp. 87-88)	ECF

Table 5-5. (Continued).

Test	Purpose	No. of Samples	Results	Testing facility
Fuel depletion (fissions per cc of fuel). Isotopic dilution mass spec of HNO3-HF dissolved samples for total Th and U, isotopic U, and La-139 and Nd-148 . La-139 and Nd-148 were burnup monitors (p. 124). Gamma spec for Cs-137 and Ce-144	Compare DE to calculated burnup and qualify the calculational model (p. 44).	2 of the 12 DE rods were analyzed for fuel burnup (from a seed and standard blanket). For each rod, one sample pellet was taken from top thoria region and second sample from adjacent top binary pellet.	Measured depletion and burnup values were consistently lower (about 10% or less) than calculated values for both burnup (WAPD-TM-1606 Table 15). Calculated values based on a 3.5" rod segment vs. measured values based on pellet analysis.	ANL-E
Iodine and Cs analysis of fuel and cladding	I and Cs are possibly corrosive agents causing stress corrosion cracking. Tests to determine the fraction of these nuclides that migrate to the gap region and into the cladding.	2 sample locations per 2 seed rods 2 sample location in 2 standard blanket rods	Minute quantities of I-129 in rod or pellet. Iodine confirmed to be in fuel, none in cladding. Cs primarily dissolved in the fuel and small quantities in cladding.	ANL-E
Tensile testing of cladding		At room temperature: 2 seed 1 standard blanket 1 reflector At 500° F: 2 seed 1 reflector	Mechanical properties of LWBR fuel adequate throughout core life (WAPD-TM-1606 Tables 16 and 17 and p. 127)	

Table 5-6. Operating characteristics of the 12 LWBR DE fuel rods at end of life (WAPD-TM-1606, Table 6).

Module Type	Rod S/N	Peak Power (Kw/ft)	Peak Depletion (10^{20} f/cc)	Peak Burnup MWD/MTM*	Peak Fast Fluence (>1 Mev) (10^{20} n/cm^2)
Seed I-1	0400736	6.7	9.52	44,500	85.0
Seed I-1	0606773	4.4	8.81	41,200	96.5
Seed I-1	0205071	5.5	11.43	53,400	75.5
Seed I-1	0507672	4.2	10.12	47,300	87.9
Blanket I-3	1606710	8.7	5.07	22,300	73.0
Blanket I-3	1105717	8.6	5.18	22,800	71.4
Blanket I-3	1504272	7.4	4.37	19,200	64.2
Blanket II-2	1208823	6.9	4.25	18,700	55.4
Blanket II-2	2610746	8.7	5.70	25,200	57.7
Blanket II-2	2514164	8.3	5.05	22,300	38.6
Blanket II-2	2607600	8.4	5.53	24,400	58.6
Reflector IV-3	3102657	3.4	0.96	4,100	25.9

* MWD/MTM = Megawatt days per metric ton of metal (uranium plus thorium)

Table 5-7. LWBR fuel rod fission gas release at end of life (WAPD-TM-1606, Table 7).

Rod S/N	Cell	Module	Rod-average Depletion (10^{20} f/cc)	Fission Gas: Generated in Fuel* (mol)	Fission Gas: Measured in Plenum Tap (10^{-5} mol)	Fission Gas: Recovered Fraction**	Fission Gas: Released (%)***
0606773	6B4	SI-1	5.4	0.02683	1.22	0.803	0.06
0507672	5L31	SI-1	6.4	0.03198	2.51	0.725	0.11
0504042	5L29	SI-1	6.0	0.03007	2.37	0.734	0.11
0507057	5C10	SI-1	5.1	0.02575	1.30	0.744	0.07
0400736	4M33	SI-1	5.3	0.02631	1.51	0.912	0.06
0401744	4M49	SI-1	4.8	0.02398	3.76	0.849	0.18
0307602	3N63	SI-1	4.2	0.02120	1.36	0.767	0.08
0205071	2Q41	SI-1	4.5	0.02266	1.02	0.782	0.06
0201562	2P39	SI-1	3.8	0.01890	1.06	0.816	0.07
1606710	16E57	BI-3	2.9	0.05723	3.10	0.662	0.08
1605519	16E56	BI-3	2.9	0.05693	2.76	0.659	0.07
1504272	15F11	BI-3	2.5	0.04831	1.90	0.726	0.05
1400544	14C3	BI-3	1.9	0.03791	1.77	0.959	0.05
1302864	13D24	BI-3	2.4	0.04582	1.49	0.675	0.05
1200830	12A49	BI-3	2.1	0.04051	1.37	0.695	0.05
1208823	12A12	BII-2	1.8	0.03436	0.89	0.788	0.03
1105717	11A46	BI-3	2.2	0.04304	2.27	0.722	0.07
2610746	26E68	BII-2	3.3	0.05531	3.22	0.646	0.09
2606481	26E31	BIII-6	3.1	0.05424	3.43	0.743	0.09
2514164	25K13	BII-2	2.9	0.04741	1.63	0.629	0.06
2513854	25F73	BIII-6	2.6	0.04345	1.46	0.655	0.05
2502102	25H1	BIII-6	1.3	0.02209	0.22	0.770	0.01
2400408	24C13	BIII-6	1.4	0.02319	0.38	0.725	0.02
2300711	23D29	BIII-6	2.8	0.04622	2.54	0.633	0.09
2102187	21B62	BIII-6	1.5	0.02380	0.44	0.729	0.03
3102657	1A1	RIV-3	0.5	0.01856	0.17	0.983	0.01
3211456	2B1	RIV-3	0.4	0.01659	0.12	0.788	0.01
3110505	1E3	RIV-3	0.2	0.00687	0.04	0.999	0.01

* Calculated from rod-average depletion
** Ratio of helium recovered to calculated amount present from initial fill and {n,γ} reaction
*** Gas release = (Amount measured in plenum tap)/(Amount generated)/(Recovered fraction)

Table 5-8. Fission gases (Kr + Xe) released during processing of LWBR rods. (Source: Data packages from ANL-E).

Rod ID	Gas released in plenum puncture (g)	Gas released in shearing (g)	Gas released in dissolution (g)	Total gas released (g)	% plenum gas in total
2606481	.0037	.0140	5.3379	5.3556	.0691
2513854	.0017	.0138	4.9268	4.9423	.0344
2502102	.0003	.0065	2.3256	2.3324	.0129
2102187	.0005	.0065	2.8505	2.8575	.0175
2400408	.0005	.0044	2.5041	2.5091	.0199
2300711	.0030	.0192	4.9428	4.9650	.0604
3211456	.0001	.0032	1.8676	1.8709	.0053
1605519	.0033	.0151	6.6098	6.6283	.0498
1200830	.0016	.0158	5.0025	5.0198	.0319
1302864	.0018	.0091	5.3405	5.3514	.0336
1400544	.0022	.0078	4.2974	4.3074	.0511
0504042	.0029	.0183	3.6756	3.6968	.0784
0507057	.0016	.0131	3.0711	3.0859	.0518
0201562	.0013	.0161	2.4877	2.5051	.0519
0307602	.0012	.0134	2.7539	2.7685	.0433
0401744	.0046	.0181	3.0852	3.1079	.1480

Results from isotopic analyses were sent to LMITCO by the former project manager of the destructive evaluation at ANL-E (i.e., Don Graczyk in the Analytical Chemistry Laboratory, Chemical Technology Division at ANL-E). These results are summarized in Table 5-9 and in Appendix D.

Data from the NDE (PIFAG) and DE (ANL-E dissolution) for fuel loading were compared to assess the accuracy of the PIFAG and to demonstrate breeding; results showed the Fissile Inventory Ratio (FIR) (ratio of the fissile inventory at end-of-life versus beginning-of-life) was 1.0139., which included fissile inventory gains in the reflector rods.

5.3 Burnup and Fuel Depletion

Fuel depletion is defined in terms of fissions per cubic centimeter of fuel. Depletion, also known as burnup, is often given in terms of megawatt days per metric ton of metal (uranium plus thorium)(from WAPD-TM-1606, p. 44). Calculated burnup data are provided in several places in WAPD-TM-1606 (p. 37) for the 12 rod samples that were destructively examined at ECF.

Only two of the 12 rods destructively evaluated by ANL-W were selected for burnup evaluation and model verification: seed rod 0205071 and standard blanket rod 1606710 (WAPD-TM-1606, p. 44). Two fuel pellets from each of the two rods were analyzed and compared with calculated burnup values to qualify the calculational model. For each of the two fuel rods examined for burnup, one of the pellets was taken from the top thoria region and the second pellet was taken from the adjacent top binary pellet.

Table 5-9. Isotopic results in grams from ANL-E on 17 LWBR rods (ANL-E data).

Serial#	Type	Length (in)	U-232	U-233	U-234	U-235	U-236	U-238	Cs-137	Ce-144	Zr-95
2606481	PFB 3-6 E31	118.19	0.048833	50.697	4.9377	0.77915	0.086475	0.15378	1.3314	0.068311	0.00029782
2513854	PFB 3-6 F73	118.17	0.038269	53.065	4.2727	0.61827	0.069008	0.15432	1.0884	0.05748	0.00025527
2502102	PFB 3-6 H1	118.07	0.011363	57.097	2.5111	0.22817	0.014398	0.45712	0.55456	0.030255	0.00014121
2102187	PFB 3-6 B62	118.1	0.035986	28.912	2.2675	0.31601	0.025272	0.047159	0.62564	0.039853	0.00023205
2400408	PFB 3-6 C13	118.14	0.02448	33.612	2.2119	0.28089	0.022936	0.077994	0.56341	0.033364	0.0001649
2300711	PFB 3-6 D29	118.16	0.047229	44.4489	4.4039	0.71007	0.075831	0.12314	1.2045	0.062935	0.00029186
3211456	R 4-3 B1	111.17	0.03567	34.63	1.4876	0.1396	0.00497	0.002403	0.40327	0.031655	0.00016271
1605519	SB 1-3 E56	118.17	0.072399	51.405	5.2338	0.88411	0.075202	0.11883	1.444	0.074399	0.00033378
1200830	SB 1-3 A49	118.21	0.075275	35.902	3.8718	0.69573	0.065544	0.036364	1.124	0.070642	0.00034347
1302864	SB 1-3 D24	118.16	0.060678	46.432	4.3487	0.73112	0.069634	0.09946	1.169	0.06352	0.0002886
1400544	SB 1-3 C3	118.15	0.061431	40.025	3.5948	0.5826	0.044207	0.072962	0.98522	0.057713	0.00028351
504042	S 1-1 5L29	116.98	0.023971	22.331	2.7358	0.46199	0.040206	0.082102	0.78023	0.037911	0.00017893
507057	S 1-1 5C10	116.97	0.022944	25.151	2.5057	0.40467	0.030226	0.082867	0.66492	0.034177	0.00016321
201562	S 1-1 2P39	116.86	0.022106	13.568	1.689	0.29413	0.027545	0.044155	0.49799	0.031122	0.00017505
307602	S1-1 3N63	117	0.021506	15.303	1.881	0.33739	0.035724	0.050802	0.54545	0.031287	0.00015271
401744	S1-1 4M49	116.94	0.023016	17.058	2.124	0.37119	0.032009	0.072576	0.61732	0.032358	0.00016065
3110505	R4-3 E3	111.21	0.014029	23.68	0.6758	0.044932	0.001001	0.001645	0.17928	0.014956	0.000087136

Pellets were removed from the cladding and dissolved in acid solution (HNO_3-HF) without comminution (pulverization). After decontamination of the analytes from interferences and radioactive fission products, total thorium and uranium, isotopic uranium, and stable fission products La-139 and Nd-148 were measured by isotopic dilution mass spectroscopy. (Note from p. 124: La-139 and Nd-148 were burnup monitors.) The mass spectrometer was calibrated with istopically pure ThO_2 and an NBS uranium standard.

Calculated and measured burnup data for the two seed pellets (rod #0205071 from location Q41) and the two blanket pellets (rod #1606710 from location E57) are presented in Table 5-10. Calculated burnups for a larger variety of rods are presented in Table 5-6.

5.4 Iodine and Cesium Analysis of the Fuel Cladding

Stress corrosion cracking of metallic components, such as the Zircaloy-4 cladding, has historically been a problem concerning reactor safety and fuel performance. Iodine and cesium have been identified as possible corrosive agents causing stress corrosion cracking. Under reactor conditions, fission product iodine can react with Zircaloy. Measurement of fission product iodine and cesium inventories in the fuel rod samples was performed to determine the fraction of these nuclides that migrate to the gap region and into the cladding. (The gap region was defined as the fuel-cladding gap, fuel cracks, and the interconnected, open porosity in the fuel.) The quantity of fission products I-129 and Cs-137 in the fuel-cladding gap and, separately, dissolved in the fuel and cladding were determined for two seed fuel rods and two standard blanket fuel rods (WAPD-TM-1606).

Fission products I-129 and Cs-137 deposited in the gap were determined by immersing the fuel and cladding, separately, in 2N HCl for 30 minutes. Ultrasonic vibration was applied to aid in dissolving any iodine and cesium deposits from the cladding surface only. Fuel particles remaining in the cladding and fuel wash solution were analyzed for Cs-137 by gamma-ray spectroscopy. The I-129 was precipitated and the precipitate was counted for I-129 with a calibrated lithium-drifted germanium detector (WAPD-TM-1606 pp. 44-45).

The I-129 and Cs-137 inventory in fuel and cladding were determined using similar techniques described above. Results for the analyses are presented in Table 5-11 and 5-12. All analyses demonstrate that almost all the I-129 and Cs-137 stayed in the fuel rather than migrating to the gap where they could have induced accelerated corrosion and cracking. These results agree with the non-destructive examination findings with the REX that no gross cladding defects resulted from reactor operations (see Table 5-1).

Table 5-10. Comparison of measured and calculated fuel depletion and burnup (WAPD-TM-106, Table 15).

		Measured at End of Life		Calculated	
Rod S/N	Type Fuel	Depletion (10^{20} f/cc)	Burnup (MWD/MT)	Depletion (10^{20} f/cc)	Burnup (MWD/MT)
Based on ^{139}La					
0205071	Thoria	3.85	17,720	4.27	19,670
	Binary	10.39	48,630	11.56	54,090
1606710	Thoria	0.13	560	0.14	630
	Binary	0.83	3,670	0.86	3,780
Based on ^{148}Nd					
0205071	Thoria	4.04	18,610	4.27	19,670
	Binary	10.55	49,390	11.56	54,090
1606710	Thoria	0.13	580	0.14	630
	Binary	0.86	3,640	0.86	3,780

Table 5-11. Concentration of I-129 in LWBR fuel rod cladding and fuel pellets (µg/g) (WAPD-TM-1606 Table 16).

Rod S/N	Type Fuel	Sample No.*	Cladding Wash	Fuel Wash	In Cladding	In Fuel
Seed Region Fuel						
0205071	Thoria	1A	N.D.	N.D.	N.D.	123.2
		1B	N.D.	N.D.	N.D.	135.7
	Binary	2A	N.D.	0.1	N.D.	309.3
		2B	N.D.	0.2	N.D.	317.9
0507672	Binary	1	N.D.	N.D.	N.D.	261.9
	Binary	2	N.D.	N.D.	N.D.	335.4
Blanket Region Fuel						
1606710	Binary	1A	0.4	0.2	N.D.	130.4
		1B	N.D.	N.D.	N.D.	153.3
	Binary	2	N.D.	N.D.	N.D.	136.0
1105717	Thoria	1	N.D.	N.D.	N.D.	112.8
	Binary	2	N.D.	N.D.	N.D.	149.3

* A and B samples were obtained from adjacent fuel rod sections.
N.D. = Not Detected

Table 5-12. Concentration of ^{137}Cs in LWBR fuel rod cladding and fuel pellets (μg/g) (WAPD-TM-1606, Table 17).

Rod S/N	Type Fuel	Sample No.*	Cladding Wash	Fuel Wash	In Cladding	In Fuel
Seed Region Fuel						
0205071	Thoria	1A	0.1	1.8	2.8	1609.8
		1B	0.1	3.0	3.1	527.8
	Binary	2A	0.2	4.3	5.9	1261.5
		2B	0.2	4.4	6.5	294.0
0507672	Binary	1	0.2	2.4	5.8	1355.2
	Binary	2	**	**	6.2	1317.0
Blanket Region Fuel						
1606710	Binary	1A	0.6	0.4	2.8	622.1
		1B	0.1	0.6	N.M.	812.7
	Binary	2	0.1	0.4	2.9	571.6
1105717	Thoria	1	1.9	0.4	1.5	234.5
	Binary	2	0.1	0.7	1.8	622.0

* A and B samples were obtained from adjacent fuel rod sections.
** 0.2 μg/g was recorded for a combined cladding and fuel wash solution.
N.M. = Not Measured

6. SHIPPING AND STORAGE

6.1 Shipment from Shippingport to ECF

After the reactor was shut down, the fuel modules were loaded into modified M-130 casks and shipped to ECF in 10 shipments (4 shipments of blanket modules, 2 of seed modules, and 4 of reflector modules)(WAPD-TM-1553, p. 7). M-130 container modifications were reviewed by the NRC and a Certificate of Compliance was issued (WAPD-TM-1553, p. 7).

The M-130 container is an upright, right circular cylinder, with outside dimensions of 84 in diameter by 158 in. high. Inside dimensions are 55 in. diameter by 132 in. high (WAPD-TM-1553 Appendix A). An empty M-130 shipping container as modified for use for LWBR irradiated fuel shipments is shown in Figure 6-1. Each of the M-130 containers was fitted with module holders, which were designed to accommodate the largest of each module type within the respective containers. The M-130s modified for blankets used special inserts for the Type I and Type II blanket modules; the M-130s modified for reflectors used special inserts for the Type V reflectors (WAPD-TM-1553, p. A1-4). A recessed head was used for LWBR shipping because of module length and the need for specified holddown devices required in the event of a container accident. Module holders for seed, blanket, and reflector modules are shown in Figures 6-2 through 6-4.

An A-frame on the railcar served to suspend the M-130 slightly from the deck of the railcar and functioned as a shock absorber (Figure 6-5). Energy absorbers were also fastened to the top of each M-130 container. A baseplate provided additional shielding to reduce expected radiation levels at the top of the M-130 container (WAPD-TM-1553).

M-130 preparations for shipment were as follows:

1. Loaded containers were flushed with nonborated water to reduce boron residue. Surfactant was added to the water used to flush the seed module container to enhance drainage from horizontal surfaces which were not present in other containers.

2. Containers were filled with neon gas.

3. Decay heat generation values for the seed shipments and for the first blanket shipment were obtained by performing a calorimetric test.

Details for the shipping operations from Shippingport to ECF are provided in WAPD-TM-1553. All shipments were completed successfully, with no damage to fuel modules.

6.2 Storage and Handling at ECF

Figures 6-6 through 6-8 provide pictorial views of a seed, blanket and reflector module as received at ECF. The fuel modules contained fuel rods, fuel rod support grids, module support structures, and instrumentation. Upon receipt at ECF, the internal atmosphere of each M-130 shipping cask was sampled for fission gases to determine the integrity of the fuel rod cladding. These tests indicated that all shipments were completed without damage to the fuel cladding in any of the fuel modules (WAPD-TM-1601, p. 2-1).

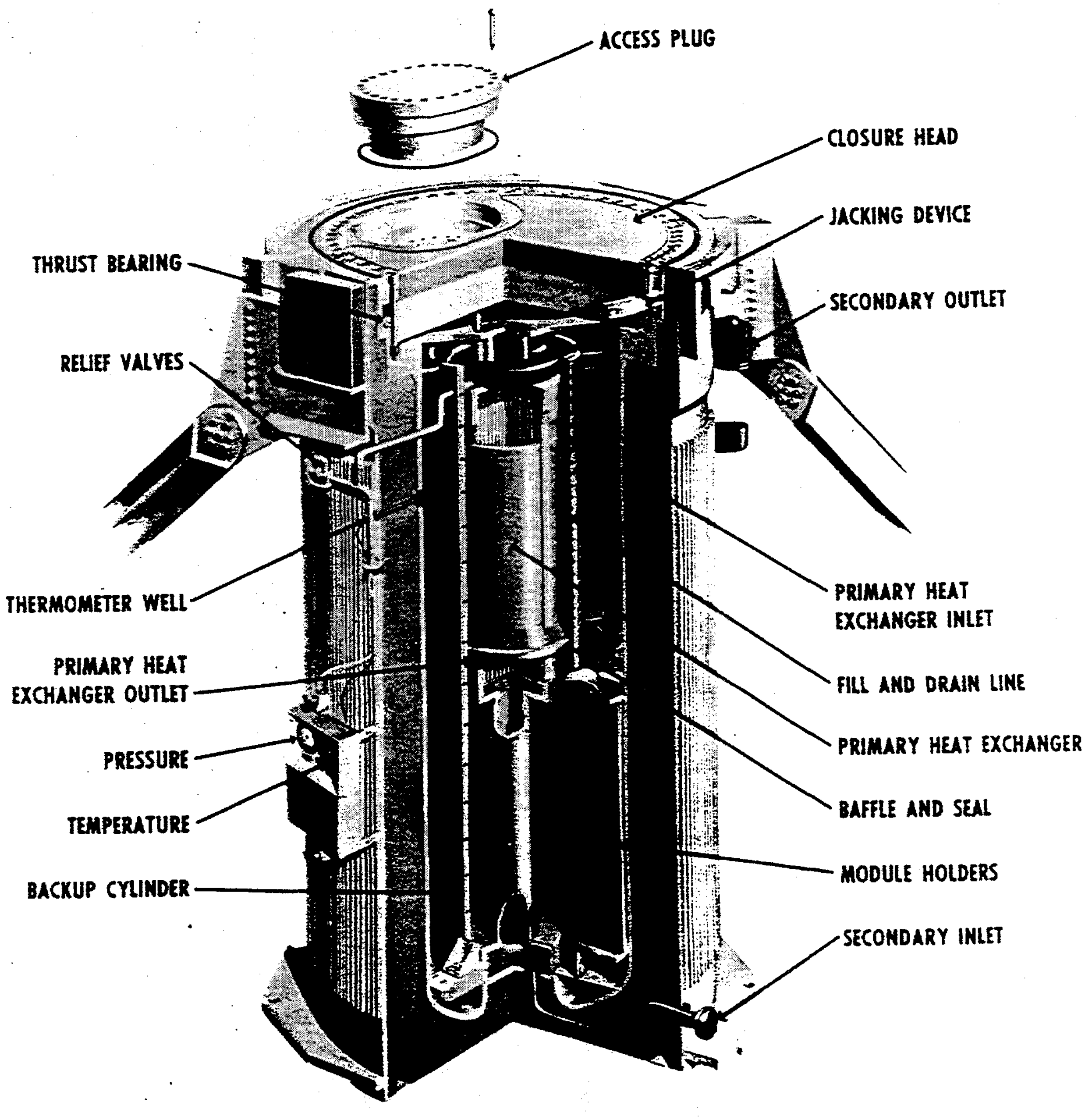

Figure 6-1. M-130 shipping container as modified for LWBR fuel shipments (WAPD-TM-1611, Figure 8).

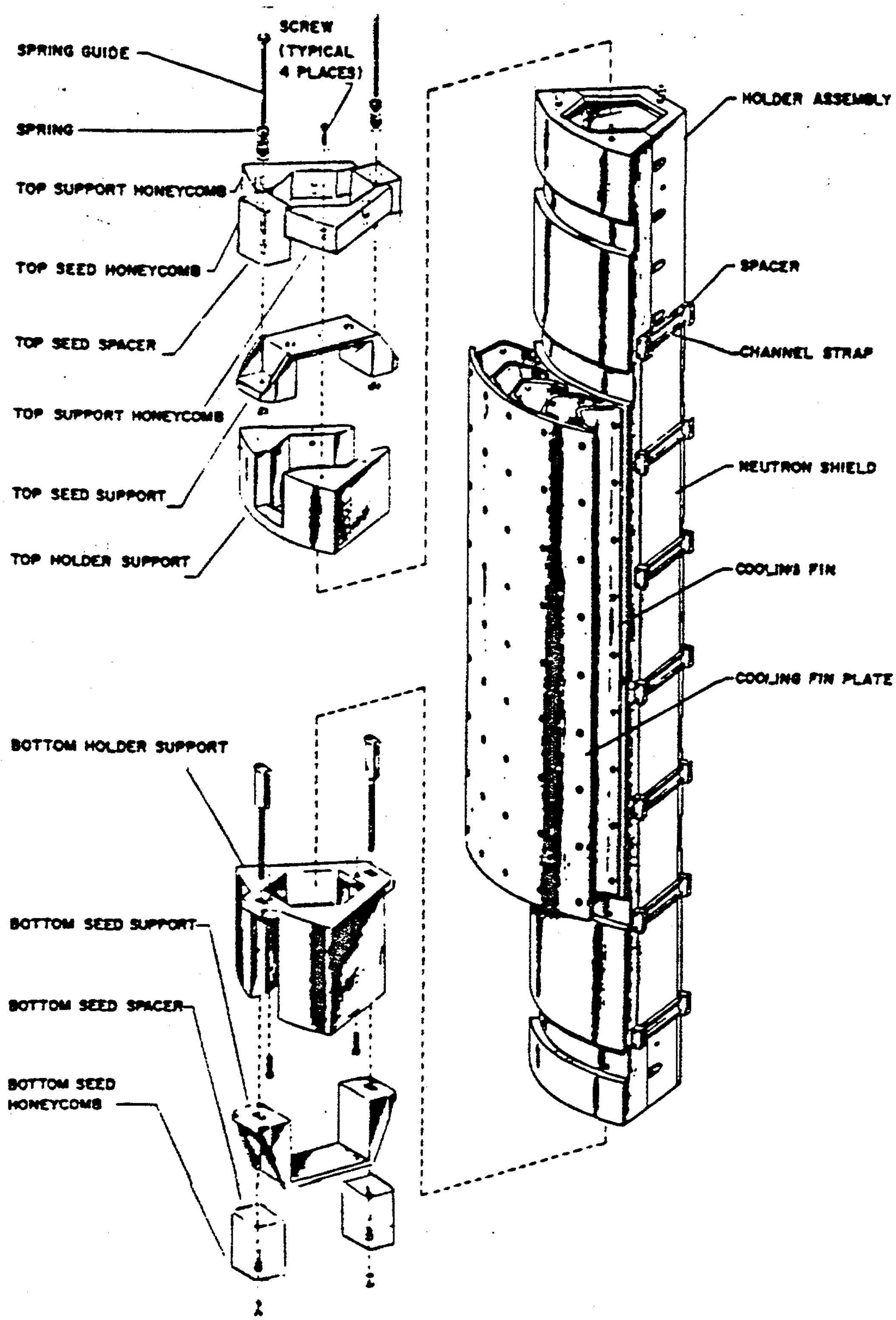

Figure 6-2. Module holder for seed modules (WAPD-TM-1553, Figure A1-3).

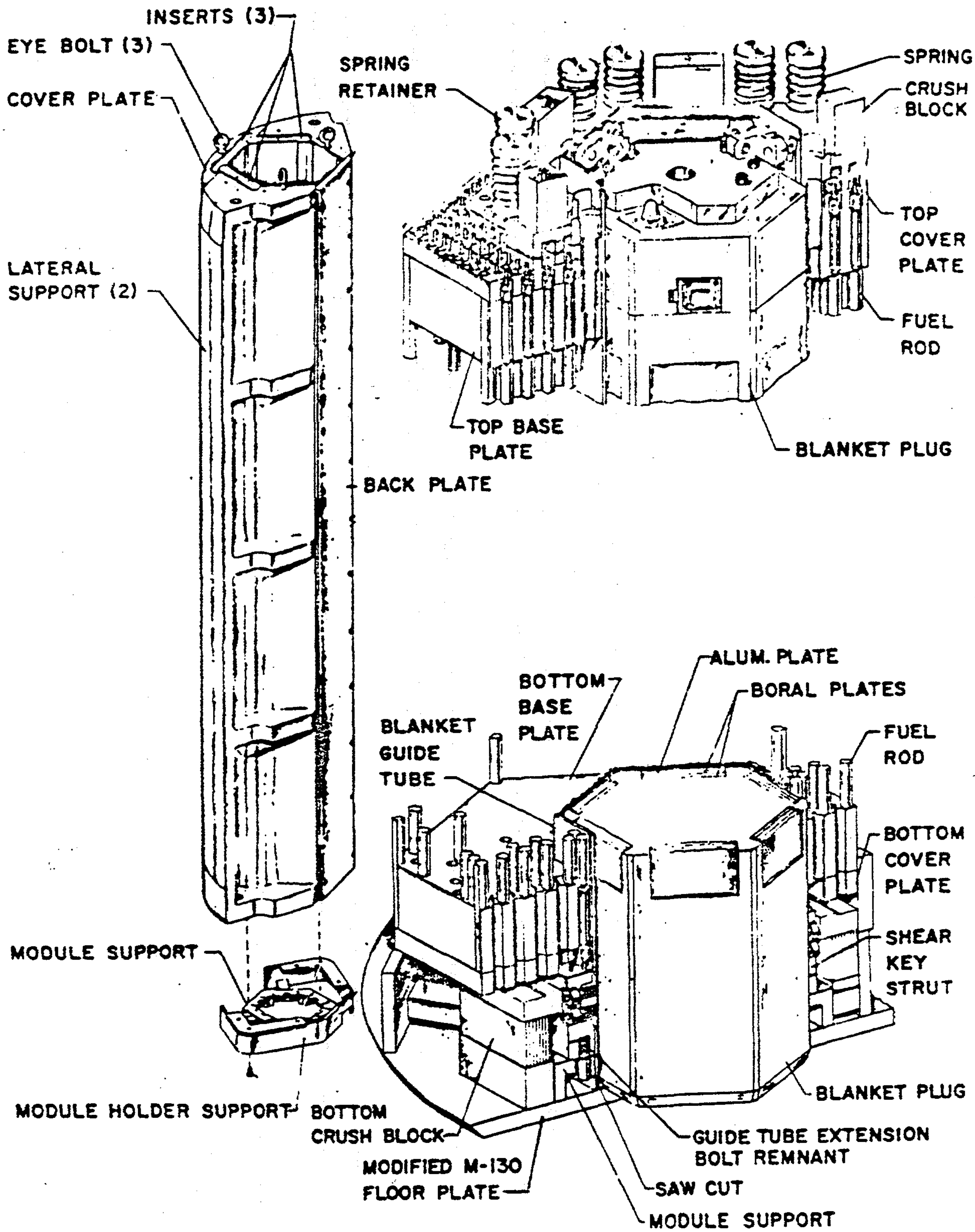

Figure 6-3. Module holder for blanket modules (WAPD-TM-1553, Figure A1-4).

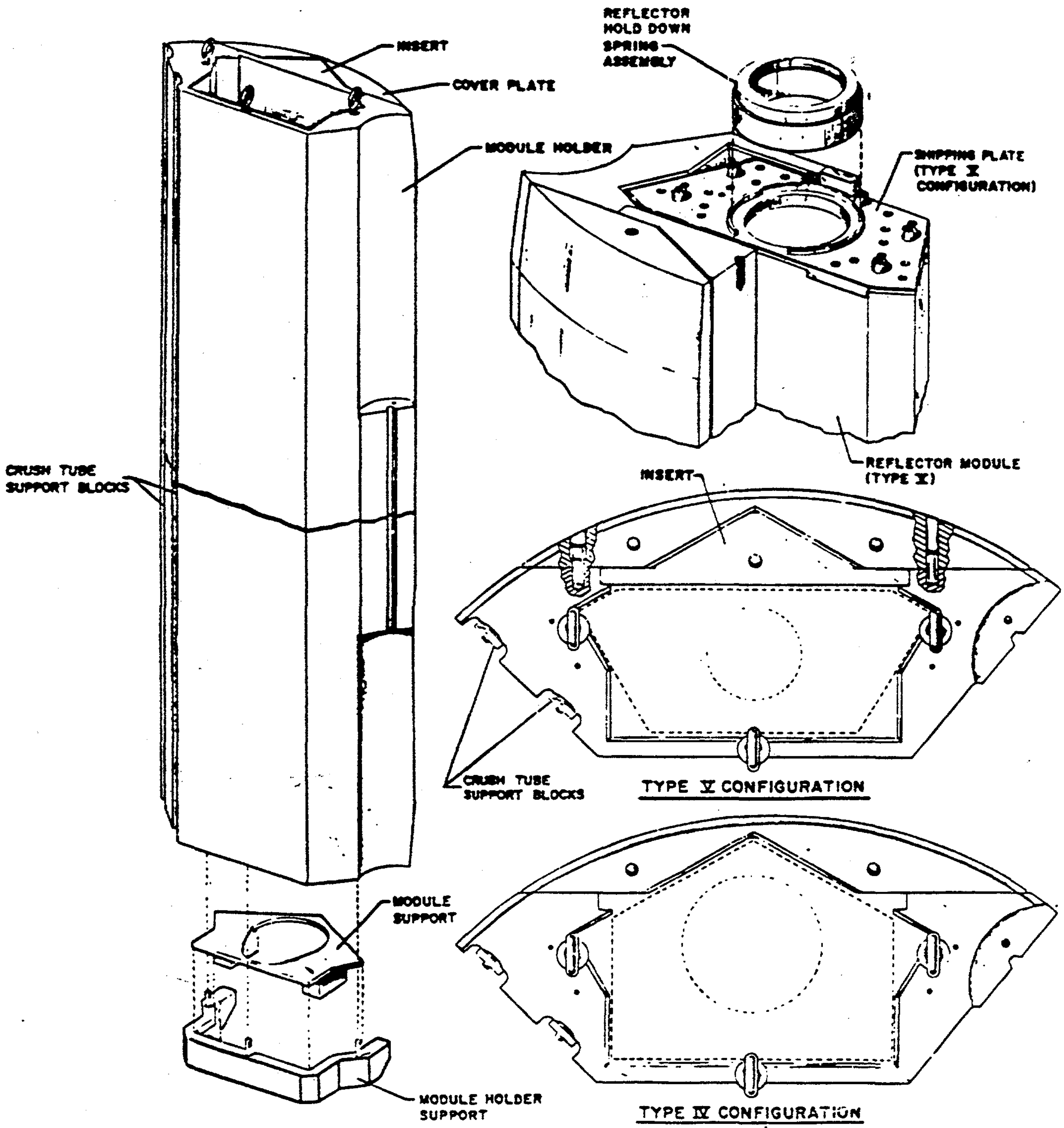

Figure 6-4. Module holder for reflector modules (WAPD-TM-1553, Figure A1-5).

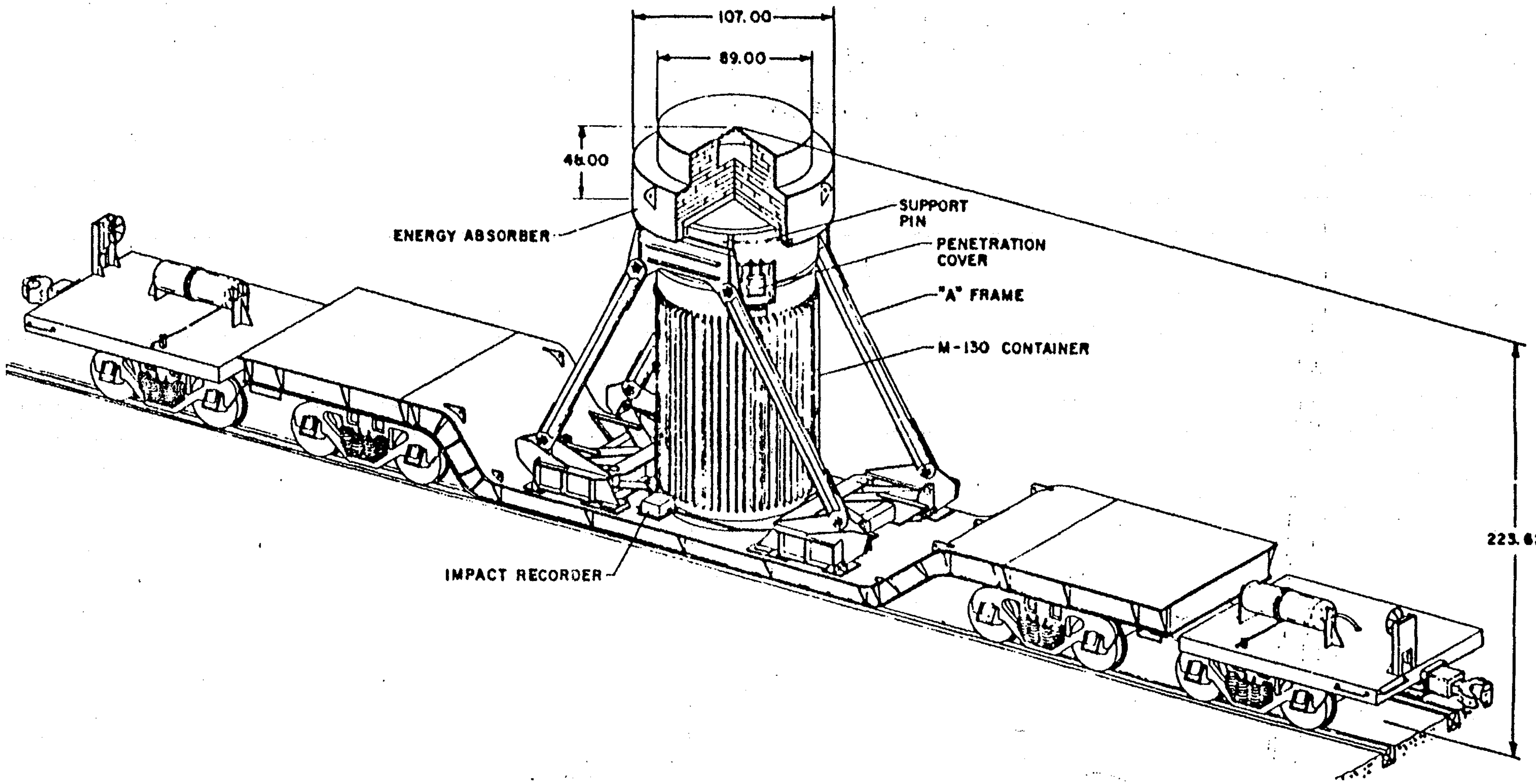

Figure 6-5. M-130 irradiated fuel shipping system (WAPD-TM-1553 figure A1-1).

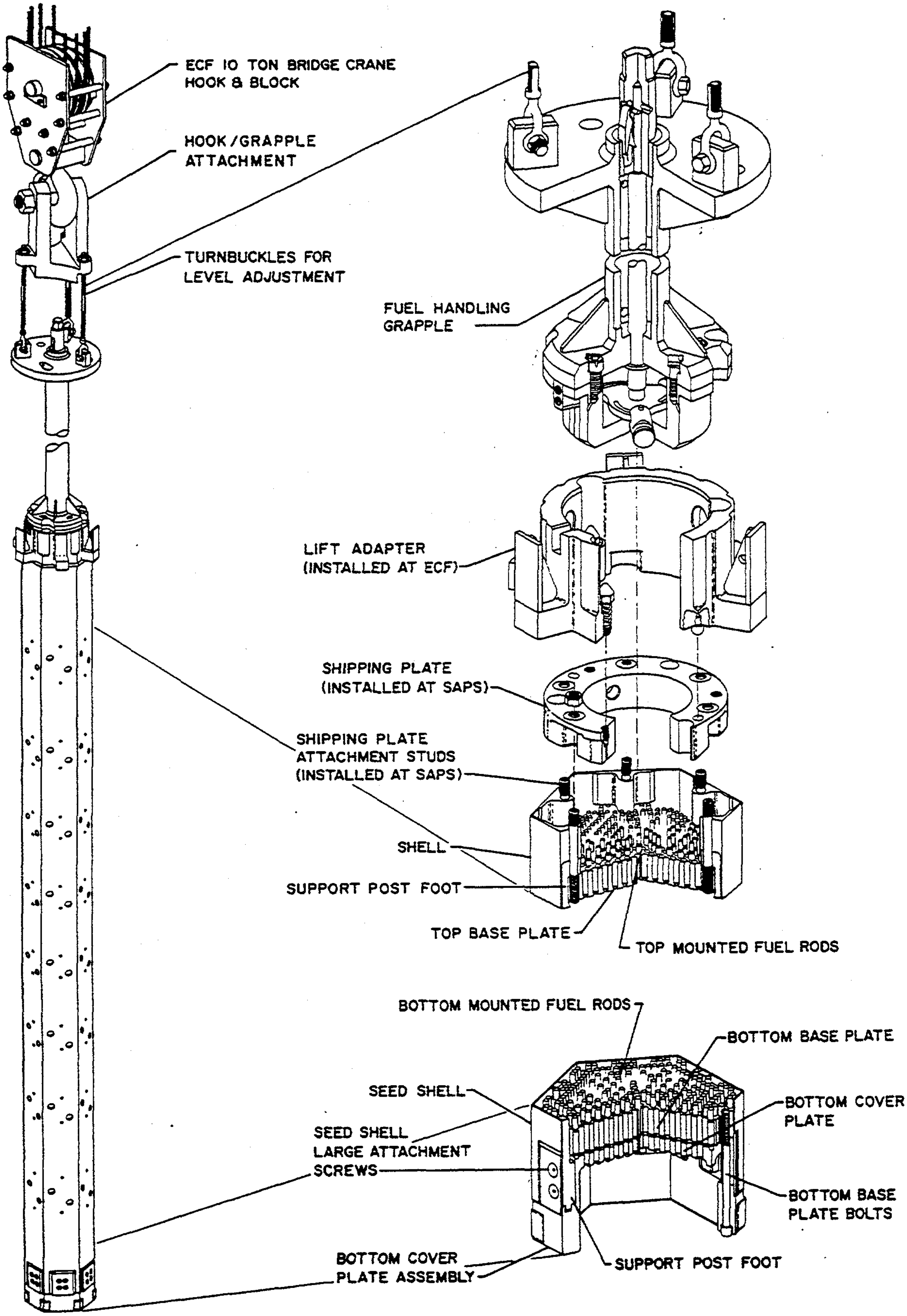

Figure 6-6. LWBR seed module as received at ECF (WAPD-TM-1601, Figure 1-1).

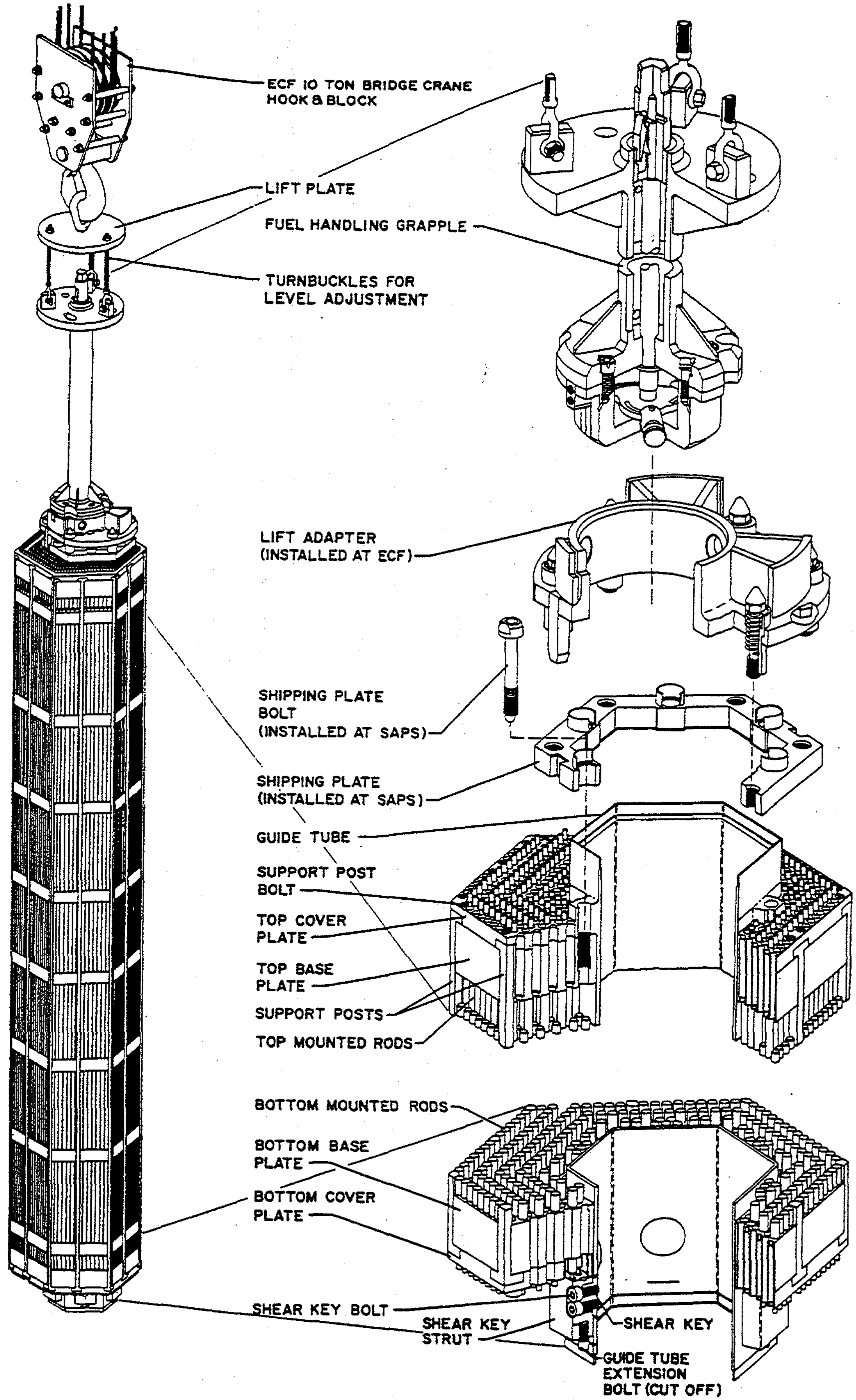

Figure 6-7. LWBR blanket module as received at ECF (WAPD-TM-1601, Figure 1-3).

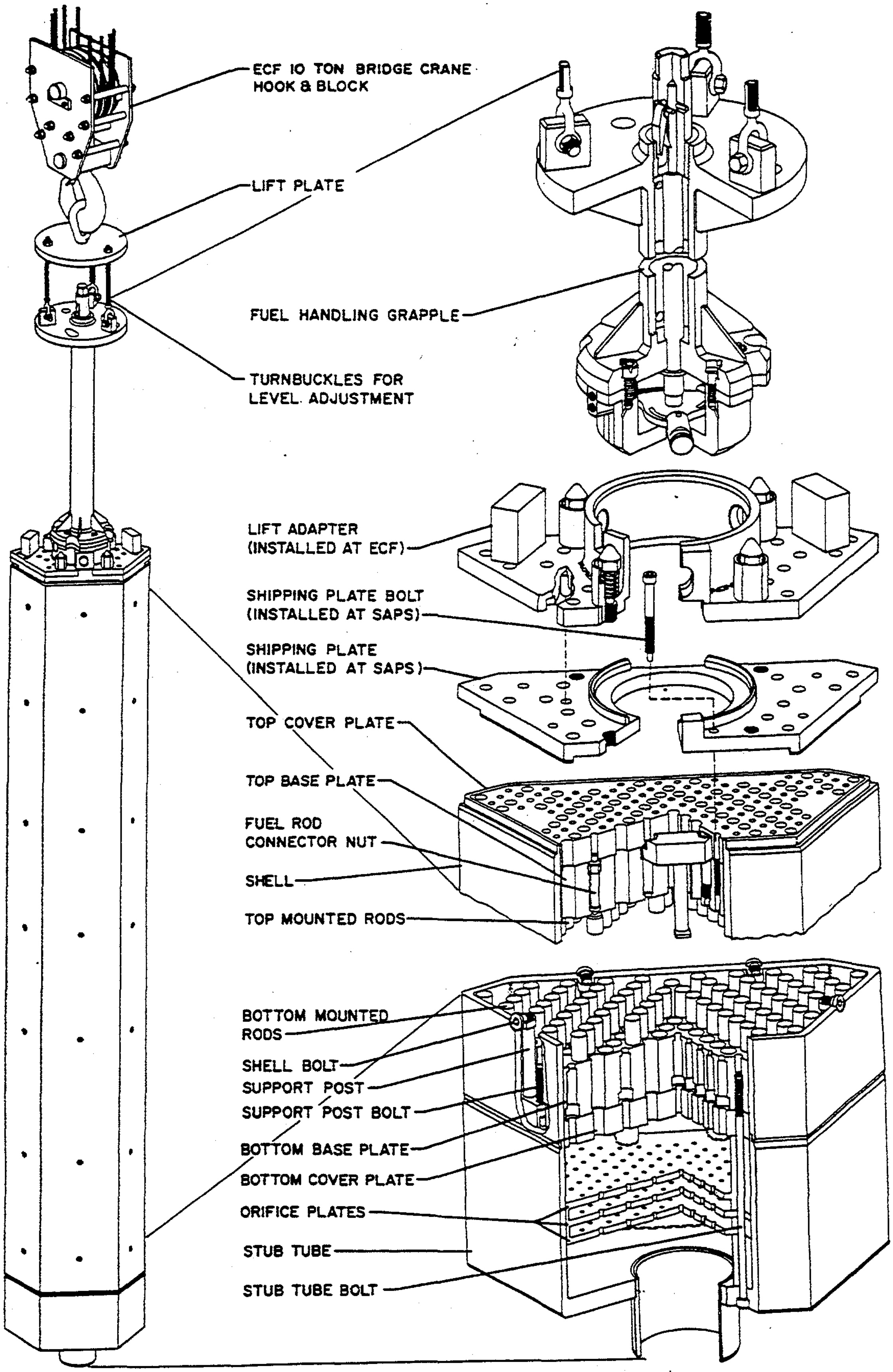

Figure 6-8. LWBR reflector module as received at ECF (WAPD-TM-1601, Page 1-15).

The shipping container was transferred from the railcar to the water pit, and lift adapter plates were installed on each fuel module, which provided a means to grapple and lift the fuel modules in the vertical orientation (WAPD-TM-1608, p. 17). The fuel module grapple is shown in Figure 6-9. The fuel modules were then transferred individually to one of two water pits for storage in the module storage racks. The ECF water pits are shown in Figure 6-10. All LWBR modules were individually installed into a liner for storage purposes at ECF. Liners were 64.77 cm (25.50 in) in diameter and a length, with the closure head installed, of 400.81 cm (157.80 in) (WAPD-TM-1601, p. 3-1).

Fourteen modules were remotely disassembled on either the cutoff system (COS) or module disassembly apparatus (MDA) to free core components and fuel rods (WAPD-TM-1608, p. 17). The MDA was used on two modules to machine module shell screws and slit module shells to permit external visual examination of the exposed fuel rods and to free module structural components for examination (including shells, grid sections, and grid fasteners). The COS was used on 12 modules (four of each module type) to cut off both ends of the module which severed the structural components to free all fuel rods. About 1000 select fuel rods were removed using the rod removal system (RRS) from these 12 modules for EOL testing and access to other rods. Fuel assemblies excluded from the EOL program were transported from ECF to ICPP while examinations of the selected LWBR fuel assemblies were in progress (WAPD-TM-1601, p. 1-2). After each module processing operation, the modules were returned to their designated storage liners. When all scheduled module examinations were completed, the storage liners were transferred to the Liner Closure Station (LCS) for final closure head installation and water removal.

The modules were visually examined in the Module Visual Station at ECF. No unusual conditions were noted (Attachment to WAPD-NRF(L)C-104 Fuel Receipt Criteria Part B April 30, 1987). For 3-5 years (depending on the liner) the fuel was stored in ECF water pits. The pits were about 32 m (105 ft) long, 12.2 m (40 ft) wide, and 10.7 m (35 ft) deep (WAPD-TM-1601, p. 1-4).

6.2.1 Water Removal at ECF

Fuel liner blowdown removed the bulk water from the liner. A schematic of the liner blowdown system is presented in Figure 6-11 in WAPD-TM-1601. The water blowdown process occurred under water. The liner head was bolted onto the storage liner. Compressed air was forced through the blowdown system until the flowmeter downstream of the blowdown tank registered 450 gallons, assuring the fuel storage liner was empty of bulk water.

Air circulation through the fuel storage liner was the second fluid process. A schematic of the liner air circulation system is presented in Figure 6-12. Dry compressed air was pumed for 20 minutes at about 17 cfm through the air dryer system, down through the fuel liner and filter system, and into the blowdown tank (WAPD-TM-1601). The forced air displaced the water out of the storage liner through the liner's standpipe, the drain fitting, and the drain umbilical tool, forcing the water out. Once the bulk amount of water was removed from the liner, only droplets of water remained on all of the fuel and liner surfaces.

Residual water was removed using a vacuum pump, then the liner was backfilled with neon gas. Leak testing with neon gas to 150% of the maximum postulated liner pressure was performed underwater for 20 minutes to ensure that the storage liners were adequately sealed for shipment and storage. The dried and sealed liner was then transferred to the Peach Bottom Cask shipping container for subsequent shipment to ICPP for underground (dry) storage.

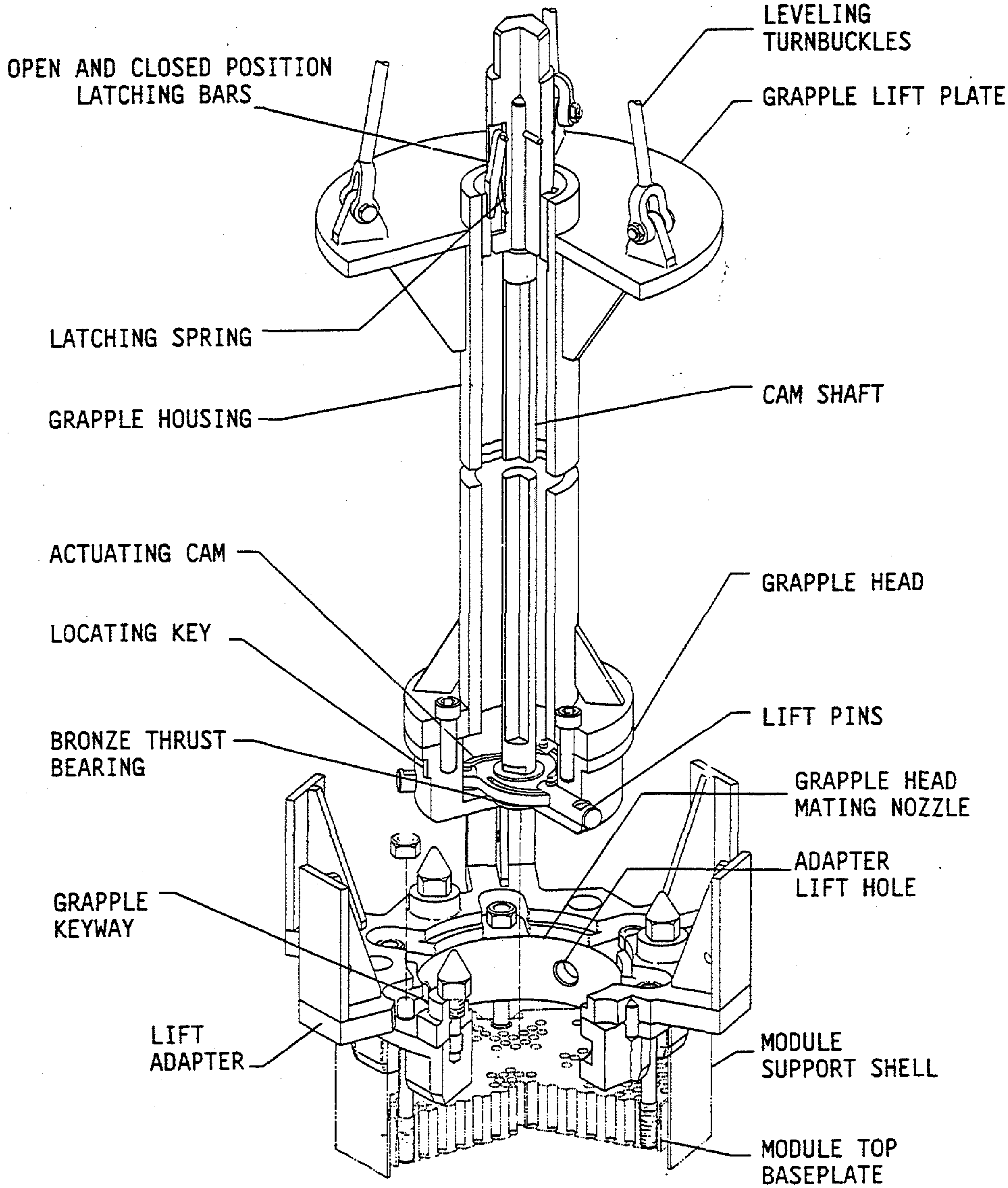

Figure 6-9. LWBR fuel module grapple shown with seed module (WAPD-TM-1608, figure 8).

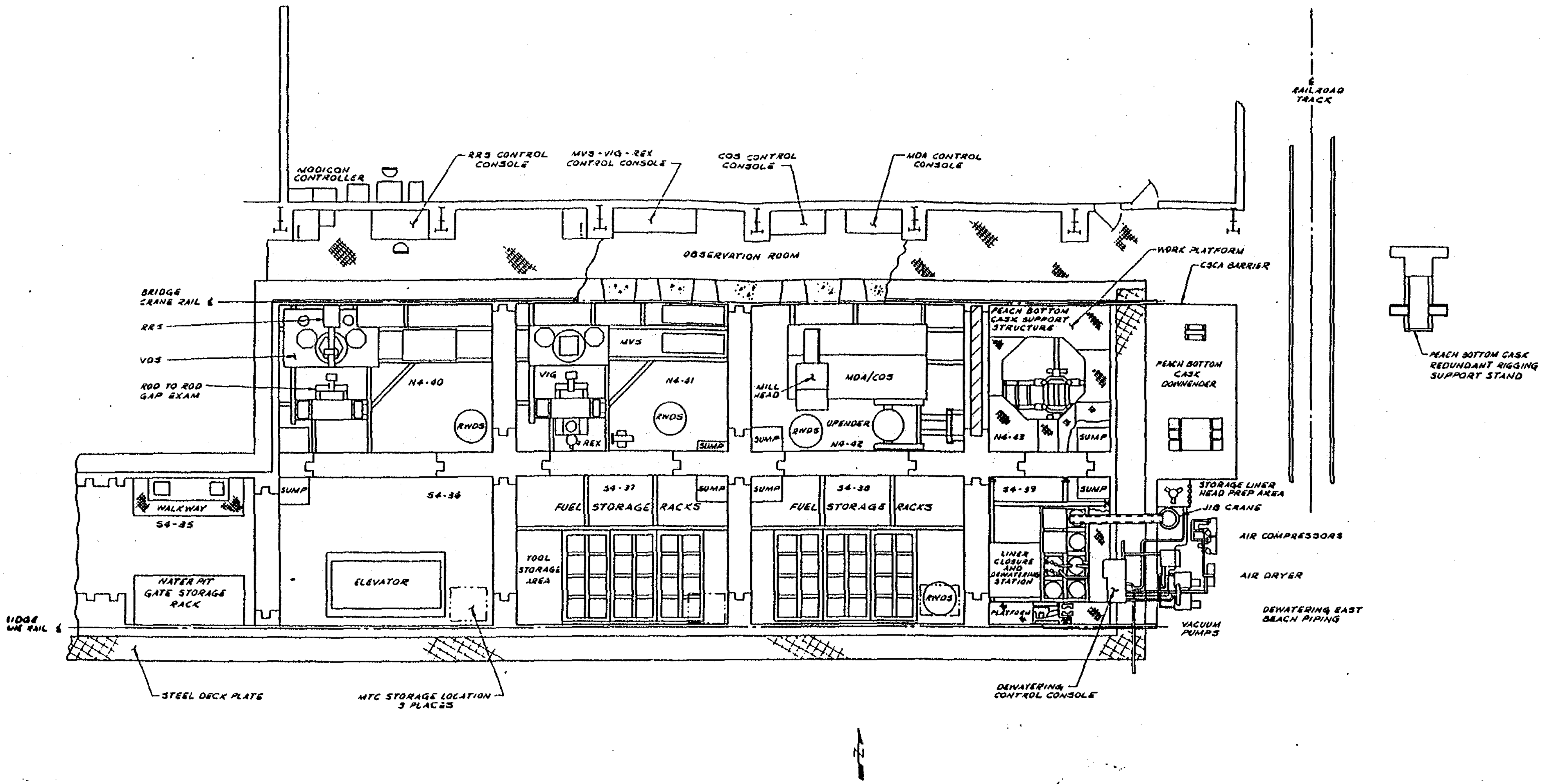

Figure 6-10. Area of ECF Water Pits used for LWBR program (WAPD-TM-1601, Figure 1-4).

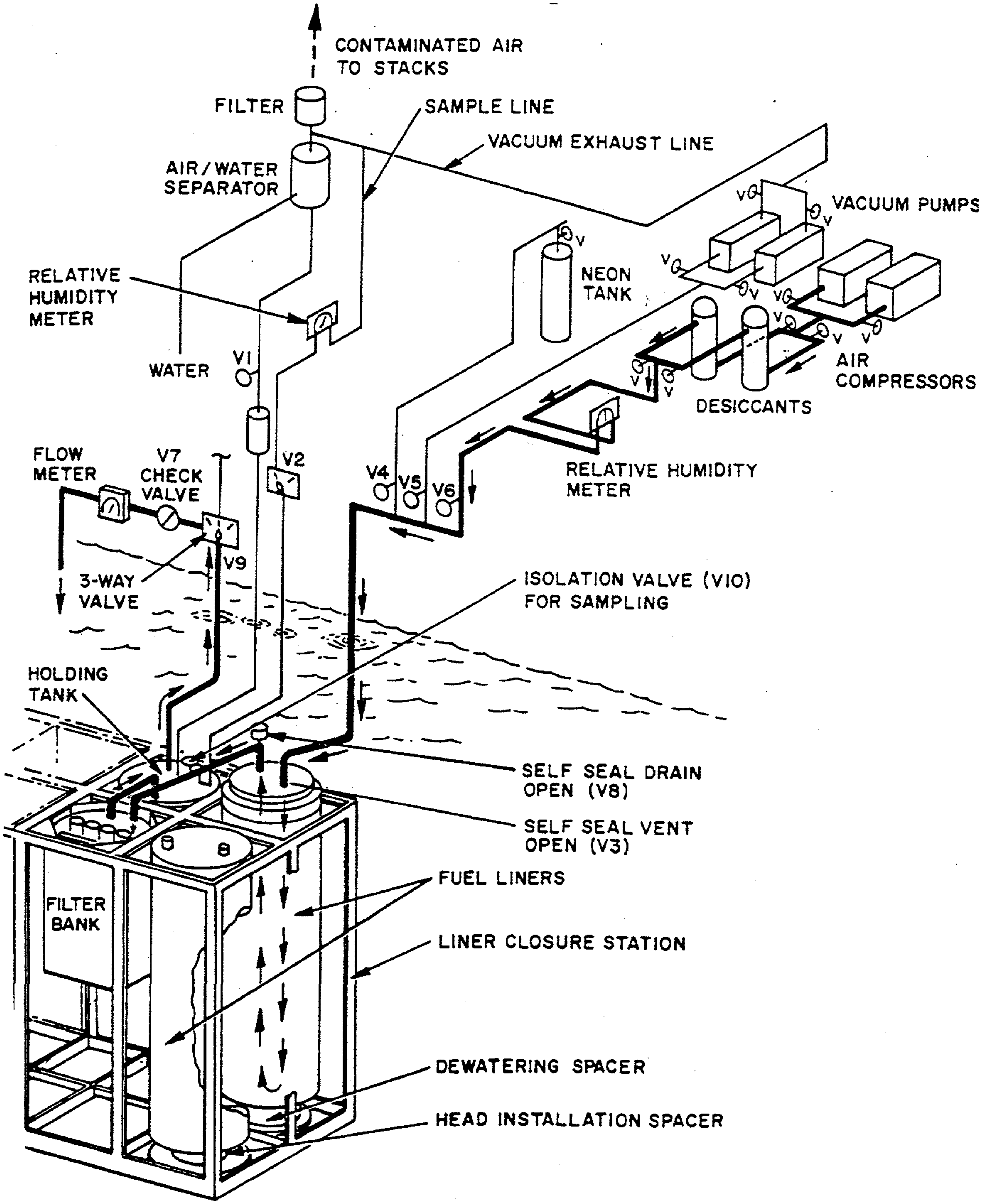

Figure 6-11. LWBR storage liner blowdown schematic (WAPD-TM-1601, Figure 3-11).

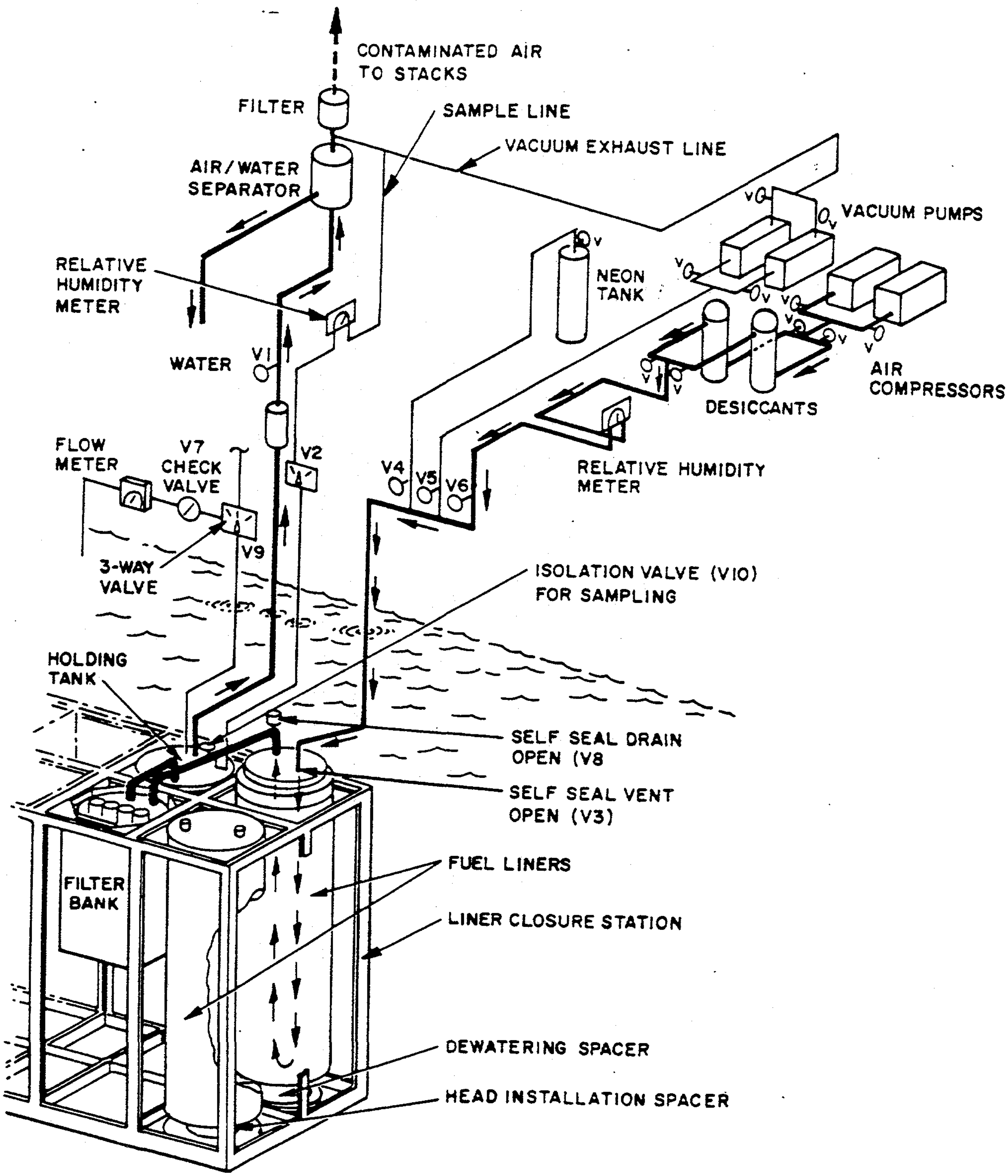

Figure 6-12. LWBR storage liner air circulation schematic (WAPD-TM-1601, Figure 3-15).

6.2.2 Shipment from ECF to ICPP

Two types of fuel storage liners (rod and module) were fabricated for the LWBR fuel disposal program. The exterior of all storage liners was a cylindrical shell with an outer diameter of 64.77 cm (25.50 in) in diameter and a length, with the closure head installed, of 400.81 cm (157.80 in) (WAPD-TM-1601, p. 3-1). The interior of the rod storage liners had tube bundle inserts to house the individual fuel rods. The interior of the module storage liners had features configured to the various module cross sections. A typical LWBR fuel module storage liner is shown in Figure 6-13. Each module type had a corresponding storage liner type because of the vastly different sizes and cross-sectional shapes of the LWBR fuel modules. Liner internals were fabricated to accept both as-received and cut modules. Liners containing LWBR assemblies and loose rods were shipped from ECF to ICPP in a Peach Bottom Cask from December of 1985 until the last of the test rods were packaged and shipped in 1987 (Fuel Receipt Criteria).

The storage liner preparation process included monitoring for fission products (Cs-137 and Cs-134) and fission gas (Kr-85) to indicate the possible existence of through-clad defects in fuel rods. No through-clad defects were indicated by fill water analysis for cesium when the modules arrived at ECF from Shippingport. However, positive indications were discovered during ECF liner preparations of two of the 12 LWBR seed modules (3-5 and 3-6) at initiation of the neon gas bleed cycle (WAPD-TM-1601, p. 3-37). After further testing, it was determined that the results suggested that there were fuel rod cladding defects in seed modules 3-5 and 3-6, although available data were insufficient to conclude that fuel rod defects actually existed in the modules (p. 3-38). The mechanism that may have led to a cladding defect while the modules were in storage at ECF was not identified (WAPD-TM-1601, p. 3-39). The presence of through-clad defects in seed modules 3-5 and 3-6 remains questionable (p. 3-39). Part C of the Fuel Receipt Criteria confirms the potential for cladding defects in the FRC Questionnaire:

For Seed 3-5: "An indication of radioactive gas was noted during initial bleedoff. A gas sample taken during neon bleedoff indicated 8×10^{-6} µCi/mL K-85...Further sampling indicated no presence of Krypton 85."

For Seed 3-6: "A gas sample taken during neon bleedoff indicated 1.2×10^{-4} uCi/mL Kr-85...Further sampling indicated 3.2×10^{-5} µCi/mL Kr-85 at the initiation of vacuuming. However, sampling one hour into vacuuming and at the initiation of neon bleedoff indicated no presence of Krypton 85."

6.3 Storage at ICPP

The 39 LWBR core modules, plus 7 containers of intact fuel rods and 1 container of cut fuel rods, are presently in underground dry storage at CPP-749 in the upright position, in the right circular liners described above (outside diameter of 25.50 in. and length of 157.80 in.) (WAPD-TM-1601, p. 3-1). The exteriors of all the liners are identical, except for the unique labels painted on the top of the liner closure heads. Video tapes showing the loading of the liners into the Peachbottom transport casks confirmed that all the labels were legible when the casks were loaded at ECF for shipment to ICPP for dry storage (Olson and McCardell viewed the tapes; tapes are in records storage with other LWBR records with Vicky Boyer at INTEC).

The Dry Well Design for irradiated LWBR Fuel Storage Dry Wells is shown in Figure 6-14. The plot plan of LWBR fuel storage facility at CPP-749 is shown in Figure 6-15.

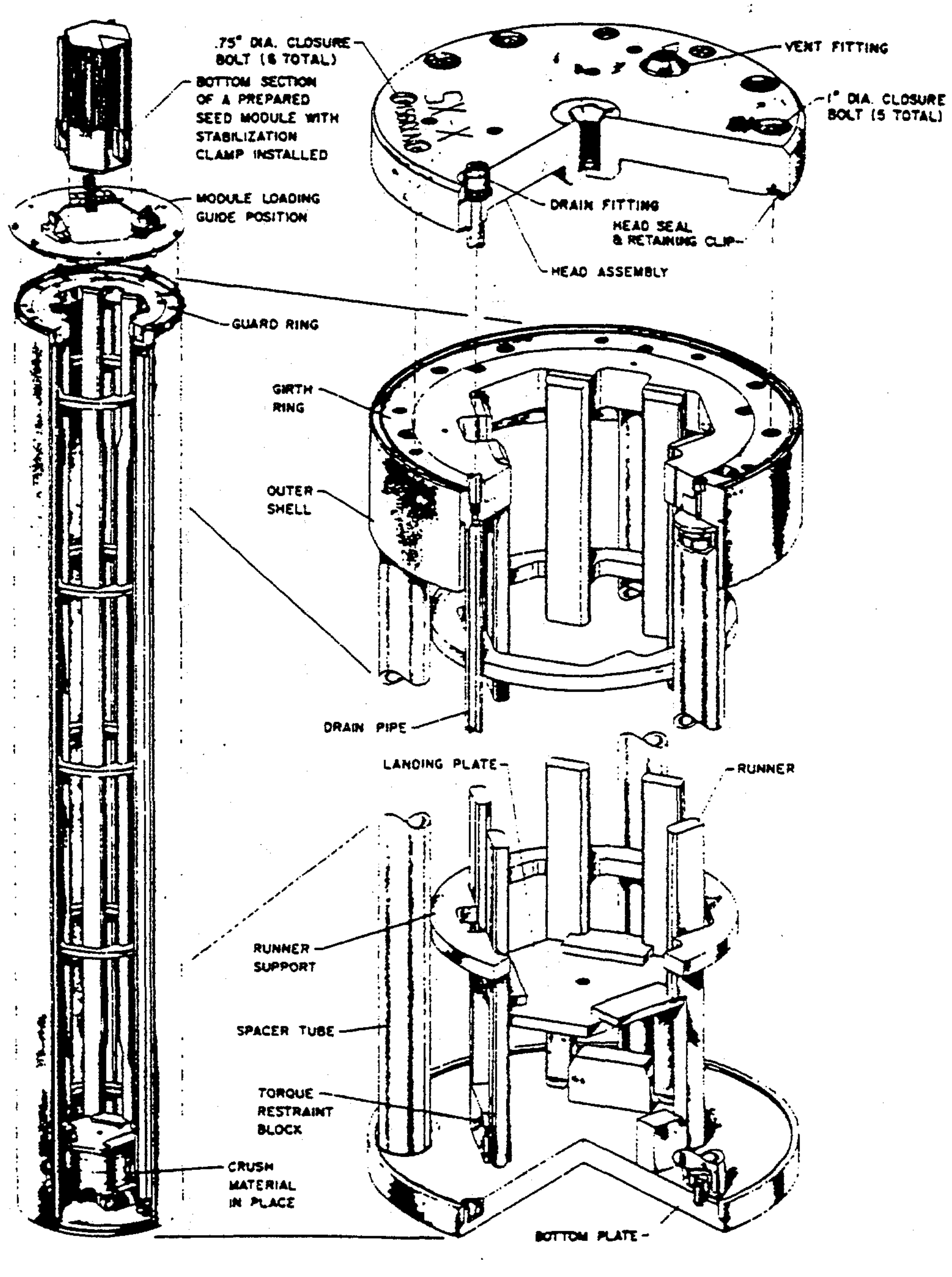

Figure 6-13. Typical LWBR fuel module storage liner (WAPD-TM-1601, Figure 3-1).

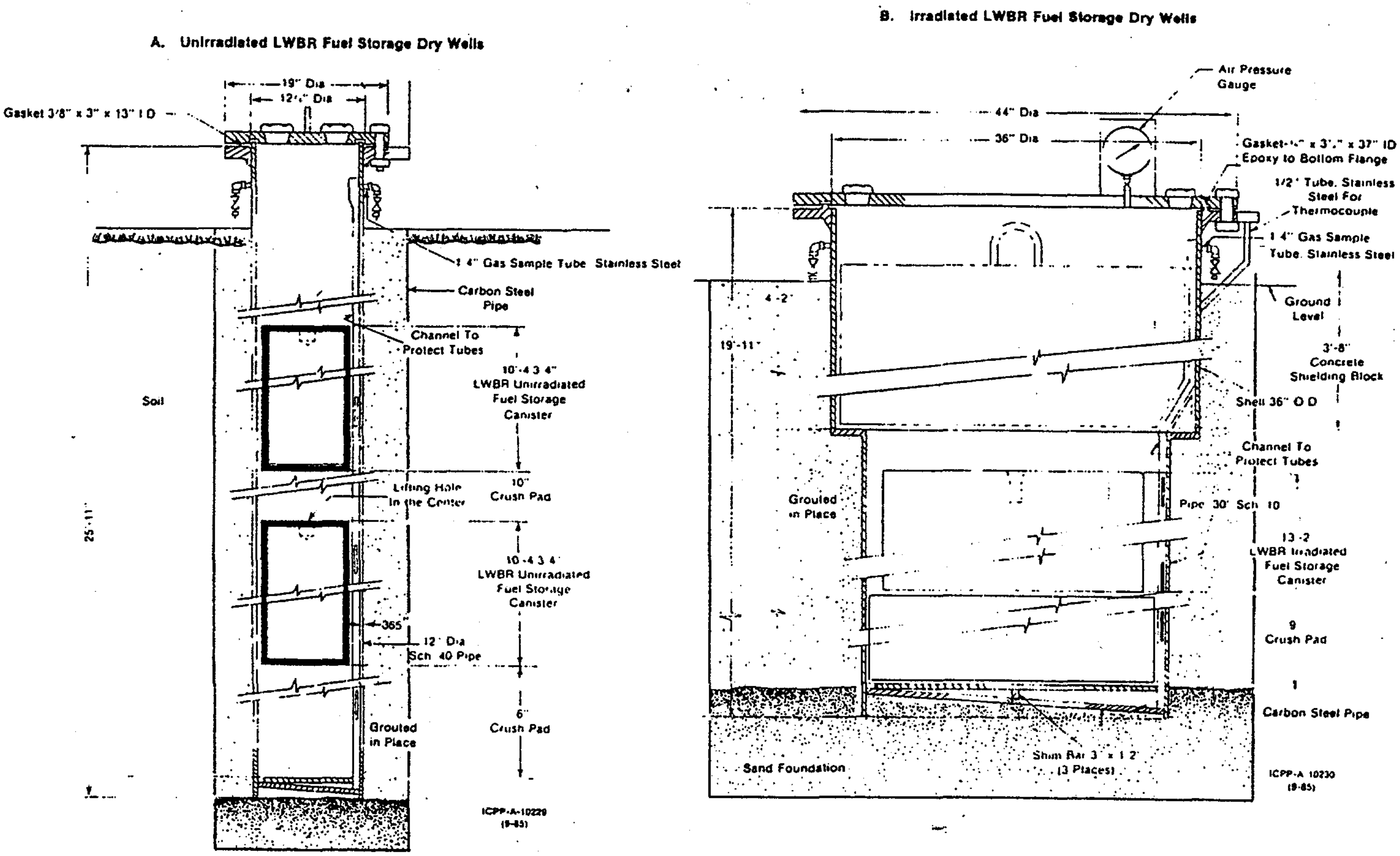

Figure 6-14. Section views of the dry well design for both unirradiated and irradiated LWBR fuel storage dry wells (WIN-107-4.7A Figure 19).

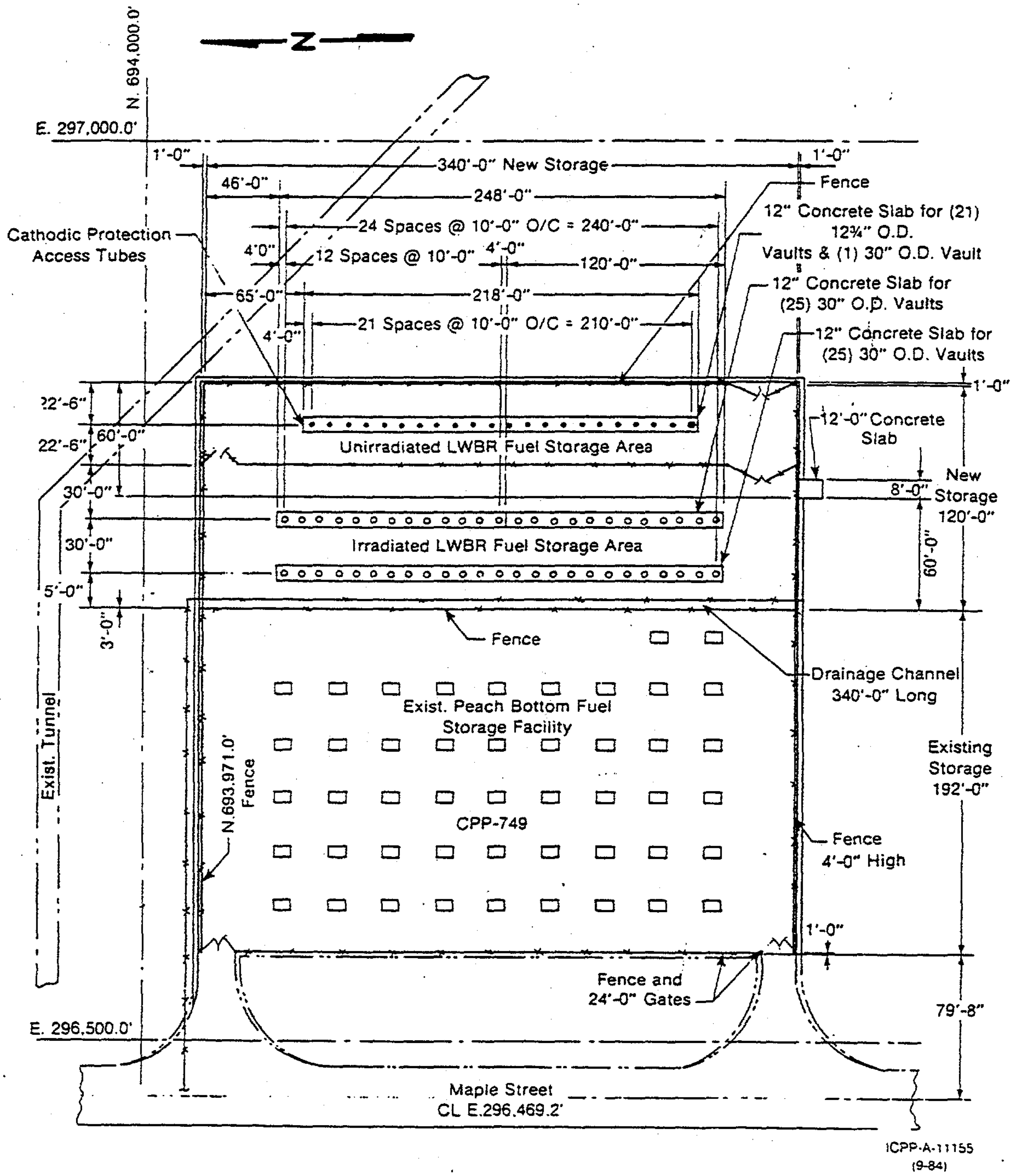

Figure 6-15. Plat plan of the LWBR fuel storage facility (WIN-107-4.7A, Figure 20).

There are 27 "Type A" liners, which contain intact LWBR modules (i.e., modules from which no rods have been removed). Type A liners are configured to fit seed, standard and power flattening blanket, and reflector modules. There are 12 "Type B" liners, which contain partially-derodded modules. Rods had been pulled from the various modules for testing and to access the rods chosen for testing. There are 7 "Type C" liners, which contain intact spent fuel rods (irradiated and unirradiated; unirradiated rods were used for calibration of instruments during post-irradiation testing). Type C liners contain cells that are appropriately sized for the various diameters of the seed, blanket and reflector rods. There is one "scrap can" liner (Liner 15718), which contains sections and pieces of unirradiated rods and irradiated rods that had been cut up or punctured for testing purposes, as well as unirradiated rods used for calibration.

Table 6-1 identifies the types of storage liners, how many rods are in each type of storage liner, the liner number, and the ICPP dry well number. Table 6-2 details the number and type of fuel rods for each Type C liner. Appendix C lists the rod serial numbers of each of the rods stored in the Type C liners. Figures 6-16 through 6-22 identify the location of the rods within the Type C liners. Liner numbers, module serial numbers, and module types were confirmed March 18, 1998, by viewing a video of the loading of the Peachbottom casks taken at Extended Core Facility (ECF). Post-irradiation isotopic data for the rods in the Type C liners are presented by rod in Part C of the Fuel Receipt Criteria.

In addition to the A, B, and C type liners, there is a "scrap can" of cut fuel rods which is also stored at CPP-749. There are at least 22 containers within the scrap can, and these containers contain irradiated, unirradiated, intact, and cut fuel rods. Many of the rods have been run through a variety of tests, which may have altered their physical, chemical and/or radiological status. The contents of the scrap can and information about the various tests that were conducted on the fuels inside the scrap can, are provided in Appendix A.

6.4 Condition of SNF

Fuel in "Type A" canisters is intact. Type B canisters contain partially derodded modules. Derodding involved sawing off the top of the core with the cut-off system described in WAPD-TM-1608. Type C canisters contain rods that have been removed from the modules that now occupy the Type B canisters.

The scrap can (liner #15718) contains fuel in various stages of disassembly/destruction due to destructive and non-destructive tests on the rods (see Appendix A). Some 260 to 275 test rods similar to the LWBR fuel rods are included in liner #15718. Most of the test rods were tested under normal LWBR pressure and temperature conditions but some operated at low system pressure and low coolant temperatures. With the exception of two of 271 rods described in WAPD-TM-1208, no breach of cladding integrity was observed in any test rod during normal operations. Intentionally severe-overtest conditions resulted in two rods damaged (WAPD-TM-1208 p. 30).

6.5 Thermal Output

Heat output data are provided for each of the storage liners in the Part C Fuel Receipt Criteria and are presented Table 6-3. Alternatively, estimated decay heat can be derived from the predicted decay heat curves developed for the LWBR. The LWBR curves (Figure 6-23) represent the best estimated decay heat generation rates as a function of cooling time for the hottest fully-rodded seed, blanket and reflector modules (i.e., upper limit rates). Assuming Time 0=October 1982, and Time@10 years=1992, the decay heats for the various modules in 1992 are approximately:

Table 6-1. Types and contents of LWBR storage lines.

					A	B	C	D	E	F	G
Dry Well#	Canister ID	Fuel Piece Serial #	Liner #	Liner Type[3]	#Rods Initially[4]	#Rods in "A" liner	#Rods in "C" liner[5]	# POB Rods[6]	# DE Samples[7]		#Should be in "B" liners A-(C+E+F)
									ANL-W	ANL-E	
I- 7	S-1-1	L-BB01-04	15601	B	619		42	33	4	5	568
I-34	S-1-2	L-BB01-05	15602	A	619	619					
I-37	S-1-3	L-BB01-06	15603	A	619	619					
I-44	S-2-1	L-BB01-09	15604	A	619	619					
I-12	S-2-2	L-BB01-10	15605	A	619	619					
I-46	S-2-3	L-BB01-13	15606	B	619		128	34			491
I- 6	S-3-1	L-BB01-07	15607	B	619		43	34			576
I- 5	S-3-2	L-BB01-08	15608	B	619		39	33			580
I-11	S-3-3	L-BB01-12	15609	A	619	619					
I-35	S-3-4	L-BB01-11	15610	A	619	619					
I-39	S-3-5	L-BB01-14	15611	A	619	619					
I-38	S-3-6	L-BB01-16	15612	A	619	619					
I-15	B-1-1	L-GR01-01	15613	A	442	442					
I-30	B-1-2	L-GR01-02	15614	A	442	442					
I-13	B-1-3	L-GU51-01	15615	B	443		45	36	3	4	391
I- 8	B-2-1	L-GS01-01	15616	A	563	563					
I-50	B-2-2	L-GS22-01[1]	15617	B	564		80	65	4		480
I-36	B-2-3	L-GS01-02	15618	A	563	563					
I- 3	B-3-1	L-GT01-01	15619	A	632	632					
I-18	B-3-2	L-GW52-01	15620	B	632		391	72			241
I-16	B-3-3	L-GT01-03	15621	A	633	633					
I- 9	B-3-4	L-GT01-04	15622	A	633	633					
I-28	B-3-5	L-GT01-05	15623	A	633	633					
I-14	B-3-6	L-GT22-03	15624	B	633		78	75		6	549
I- 2	R-4-1	L-RA01-06	15625	A	228	228					
I-27	R-4-2	L-RA01-02	15626	A	228	228					
I-41	R-4-3	L-RA01-10	15627	B	228		30	27	1	2	195
I-43	R-4-4	L-RA01-09	15628	B	228		76	29			152
I-40	R-4-5	L-RA01-07	15629	A	228	228					
I-31	R-4-6	L-RA01-04	15630	A	228	228					
I-10	R-4-7	L-RA01-05	15631	A	227	227					
I-32	R-4-8	L-RA01-08	15632	A	228	228					
I-42	R-4-9	L-RA01-03	15633	B	228		57	28			171
I- 1	R-5-1	L-RB01-07	15634	A	166	166					
I- 4	R-5-2	L-RB01-04	15635	A	166	166					
I-26	R-5-3	L-RB01-06	15636	A	166	166					
I-17	R-5-4	L-RB01-08	15637	B	166		37	34			129
I-33	R-5-5	LRB01-03[2]	15638	A	166	166					
I-29	R-5-6	L-RB01-05	15639	A	166	166					
				Total	17288	11690	1046	500	12	17	4523

Table 6-1. (continued).

					A	B	C	D	E	F	G
Dry Well#	Canister ID	Fuel Piece Serial #	Liner #	Liner Type[3]	#Rods Initially[4]	#Rods in "A" liner	#Rods in "C" liner[5]	# POB Rods[6]	# DE Samples[7]		#Should be in "B" liners A-(C+E+F)
									ANL-W	ANL-E	
I-19	FR-B-1	Blanket	15682	C			175				
I-20	FR-B2	Blanket	15684	C			144				
I-48	FR-B3	Blanket	15685	C			243				
I-21	FR-B4	Blanket	15687	C			62				
I-45	FR-R1	Reflector	15681	C			127				
I-47	FR-R2	Reflector	15683	C			80				
I-22	FR-S1	Seed	15686	C			270				
I-23		624sections	15718								
				Total			1101				

[1]The technician actually stated that the serial number was L-G522-01 (mistaking the S for a 5)

[2]The tape audio is the only documentation of the serial number. Serial number does not appear on the shipping forms.

[3]Reference: Bolton, Christensen and Hallinan (1989). Final Safety Analysis Report. March 1989. WIN-107-4.7A, Rev. 1.

[4]Reference: WAPD-TM-1326 Table A-17 for seed and blanket.WAPD-TM-1605 for reflector. One flux thimble in each of the following modules: B1-1, B1-2, B2-1, B2-3, R4-7.

[5]Part B of Fuel Receipt Criteria lists the serial numbers of each rod in Type C liners.

[6]Reference: WAPD-TM-1612 (Sep 1987) Figures V-2 through V-13. Note: number of rods shown in figures differs from the number of rods accounted for in Table V-1 of same report.

[7]Number of rods destructively evaluated. ANL-W performed DE on 12 rods. ANL-E+A32 performed DE on 17 rods.

Table 6-2. Number and type of fuel rods in each liner.

MODULE#	LINER#							
	15681[1]	15682[1]	15683[2,3]	15684[2]	15685[3,4]	15686[3,4]	15687[4,5]	TOTAL
S1-1						42		42
S2-3						128		128
S3-1						43		43
S3-2						39		39
B1-3		31			6		8	45
B2-2		7		39	23		12	81
B3-2		91		91	180		29	391
B3-6		46		14	4		14	78
R4-3	27		3					30
R4-4	37		39					76
R4-9	56		1					57
R5-4	7		30					37
Unirrad	0	0	7		30	18		55
TOTAL NUMBER OF RODS	127	175	80	144	243	270	63	1102
Liner mass (lb)[6]	2017	2365	2495	2365	2365	2696	2365	
Mass of contents (lb)[6]	4783	3435	3506	4802	3985	3524	4970	
Total Mass (lb)[6]	6800	5800	6001	7167	6350	6220	7335	

[1]Reference: Letter WAPD-NRF(L)-C-93
[2]Reference: Letter WAPD-NRF(L)-C-104
[3]Reference: Letter WAPD-NRF(L)-149
[4]Reference: Letter WAPD-NRF(L)-117
[5]Reference: Letter WAPD-NRF(L)-123
[6]Reference: Part C Fuel Receipt Criteria. Note: it is unknown why liners with fewer rods outweigh some liners with more rods.

Table 6-3. Data from Part C Fuel Receipt Criteria (by liner number).

Liner No.	Type	Conter	MFP (Ci)	U-233 (Ci)	Th-232 (Ci)	Total Ci (Ci)	Surface Rad. (mrem/hr)	Rad. at 3 ft (mrem/hr)	Mass (g) U before burnup	Mass (g) U after burnup	Fissile (g) before burnup	Fissile (g) after burnup	Decay heat (watts)	Module Mass (lb)	Liner Mass (lb)	Total Mass (lb)
15601	B	S-1-1	4.0 E05	1.46E+02	4.38E-02	4.0 E05	11.5	0.3	16785	12841	16505	11308	462.9	2013	2696	4709
15602	A	S-1-2	4.0 E05	1.59E+02		4.0 E05	6.5	3.5	16792	14014	16507	12343	586	1654	2696	4350
15603	A	S-1-3	4.0 E05	1.82E-03		4.0 E05	9.5	5.5	16803	14014	16523	12343	465.9	1654	2696	4350
15604	A	S-2-1	4.0 E05	1.60E+02	4.77E-01	4.0 E05	7.2	3	16808	14243	16529	12752	414	1654	2696	4350
15605	A	S-2-2	4.0 E05			4.0 E05	8.3	3	16808	14243	16528	12752	419.3	1654	2696	4350
15606	B	S-2-3	4.0 E05	1.30E+02	3.77E-04	4.0 E05	5.4	1.2	16844	11530	16569	10330	448.3	2013	2696	4709
15607	B	S-3-1	4.0 E05	1.46E+02	4.38E-02	4.0 E05	3.9	1.6	16783	13414	16505	12169	377	2013	2696	4709
15608	B	S-3-2	4.0 E05	1.46E+02	4.38E-02	4.0 E05	3.4	1.2	16821	13460	16545	12211	377	2013	2696	4709
15609	A	S-3-3	4.0 E05	1.50E+02		4.0 E05	4	0.2	16833	14457	16558	13118	379.6	1654	2696	4350
15610	A	S-3-4	4.0 E05	1.59E-02		4.0 E05	5.4	2.2	16827	14457	16552	13118	480.5	1654	2696	4350
15611	A	S-3-5	4.0 E05	1.60E+02	1.26E-01	4.0 E05	5.9	2	16836	14457	16562	13118	379.6	1654	2696	4350
15612	A	S-3-6	4.0 E05	1.38E+02	1.26E-01	4.0 E05	4.3	0.7	16834	14457	16557	13118	374.8	1654	2696	4350
15613	A	B-1-1	4.0 E05	1.55E+02	1.43E-01	4.0 E05	9	2.5	16834	14457	16166	19363	696.8	4212	2238	6450
15614	A	B-1-2	4.0 E05	1.54E+02	1.43E-02	4.0 E05	14.8	4.9	16444	21579	16164	19363	889.5	4212	2238	6450
15615	B	B-1-3	4.0 E05	1.38E+02	1.26E-01	4.0 E05	14	2.4	16439	19041	16161	17086	698	4718	2238	6956
15616	A	B-2-1	4.0 E05	2.80E+02		4.0 E05	20.5	3.5	25377	27954	24915	25427	879	4890	2210	7100
15617	B	B-2-2							25440	23795	24969	21641	755.9	5410	2210	7620
15618	A	B-2-3	4.0 E05	1.59E-02		4.0 E05	19	8	25384	27954	24917	25427	937.6	4890	2210	7100
15619	A	B-3-1	4.0 E05	2.78E+02		4.0 E05	35	9	30342	31784	29776	29285	994.7	6015	3300	9315
15620	B	B-3-2	4.0 E05	1.55E+02	1.43E-01	4.0 E05	3.6	2	30328	11999	29754	11075	732.2	5809	2647	8456
15621	A	B-3-3	4.0 E05	1.55E+02	1.43E-01	4.0 E05	13	3.1	30404	31844	29831	29343	740.8	5303	2647	7950
15622	A	B-3-4							30395	31844	29821	29343	890	5303	2647	7950
15623	A	B-3-5	4.0 E05	2.78E+02		4.0 E05	25	8								
15624	B	B-3-6	4.0 E05	1.38E+02	1.26E-01	4.0 E05	7	1.8	30409	27525	29830	25360	744	5809	2647	8456
15625	A	R-4-1	4.0 E05		1.10E-01	4.0 E05	2.7	1								
15626	A	R-4-2	4.0 E05		1.10E-01	4.0 E05	3.4	0.32	0	2975	0	2902	28.36	4933	2667	7600
15627	B	R-4-3							0	2413	0	2361	21.7	4933	2667	7600
15628	B	R-4-4	4.0 E05		1.31E-01	4.0 E05	0.6	0.3	0	1596	0	1569	21.1	5200	2667	7867
15629	A	R-4-5	4.0 E05		1.26E-01	4.0 E05	1.35	0.25	0	3255	0	3175	25.3	4933	2667	7600
15630	A	R-4-6	4.0 E05		1.43E-02	4.20E+05	1.15	0.25	0	3255	0	3175	29.3	4933	2667	7600
15631	A	R-4-7	4.0 E05		1.43E-02	4.0 E05	0.8	0.3	0	3246	0	3167	27	4933	2667	7600
15632	A	R-4-8	4.0 E05		1.43E-02	4.0 E05	1.4	0.7	0	3255	0	3175	29	4933	2667	7600
15633	B	R-4-9	4.0 E05		1.31E-01	4.0 E05	<.1	<.1	0	2516	0	2454	21.4	5200	2667	7867
15634	A	R-5-1	4.0 E05		1.10E-01	4.0 E05	1.2	0.2								
15635	A	R-5-2	4.0 E05		1.10E-01	4.0 E05	0.3	0.2	0	1689	0	1662	10.3	4028	2322	6350
15636	A	R-5-3	4.0 E05		1.10E-01	4.0 E05	0.45	0.2	0	1689	0	1662	41	4028	2322	6350

Table 6-3. (continued).

Liner No.	Type	Conter	MFP (Ci)	U-233 (Ci)	Th-232 (Ci)	Total Ci (Ci)	Surface Rad. (mrem/hr)	Rad. at 3 ft (mrem/hr)	Mass (g) U before burnup	Mass (g) U after burnup	Fissile (g) before burnup	Fissile (g) after burnup	Decay heat (watts)	Module Mass (lb)	Liner Mass (lb)	Total Mass (lb)
15637	B	R-5-4	4.0 E05		1.31E-01	4.0 E05	0.3	0.15	0	1255	0	1236	9.5	4204	2322	6526
15638	A	R-5-5							0	1689	0	1662	11.4	4028	2322	6350
15639	A	R-5-6	4.0 E05		1.10E-01	4.0 E05	0.5	<.1	0	1689	0	1662	12	4028	2322	6350
15681	C	FR-R1	1.20E+03		8.50E-02	1.20E+03	0.4	0.17	0	2207	0	2144	23.44	4783	2017	6800
15682	C	FR-B1	2.10E+04	8.50E+01	1.90E-01	2.10E+04	2.6	0.15	9040	9132	8865	8418	744.2	3435	2365	5800
15683[1]	C	FR-R2	4.00E+04	1.89	2.12E-01	4.00E+04	0.2	<.1	201	1313	197	1281	73.12	2494.5	3506	5800
15684[1]	C	FR-B2	1.20E+03	6.70E+01	4.20E+01	1.27E+03	5	1.3	7092	7391	6958	6765	753	2635	4802	7167
15685	C	FR-B3	2.40E+04	98.33	7.13E-01	2.40E+04	4.9	1.8	10530	11422	10332	10545	751.5	3985	2365	6350
15686	C	FR-S1	3.00E+05	67.8	2.08E-01	3.00E+05	2.3	0.8	7230	6121	7109	5516	446.8	3524	2696	6220
15687	C	FR-B4	1.20E+03	30	1.94E-01	1.23E+03	5.4	0.1	2464	2978	2421	2705	751.5	4970	2365	7335
15718	Scrap													7207.2	1036	8243

[1]It is likely that the weights of the liner and contents are switched, and that the mass of the 15683 and 15684 liners are similar to the mass of liners 15682, 15685, and 15687 (i.e., less than 3000 lbs.)

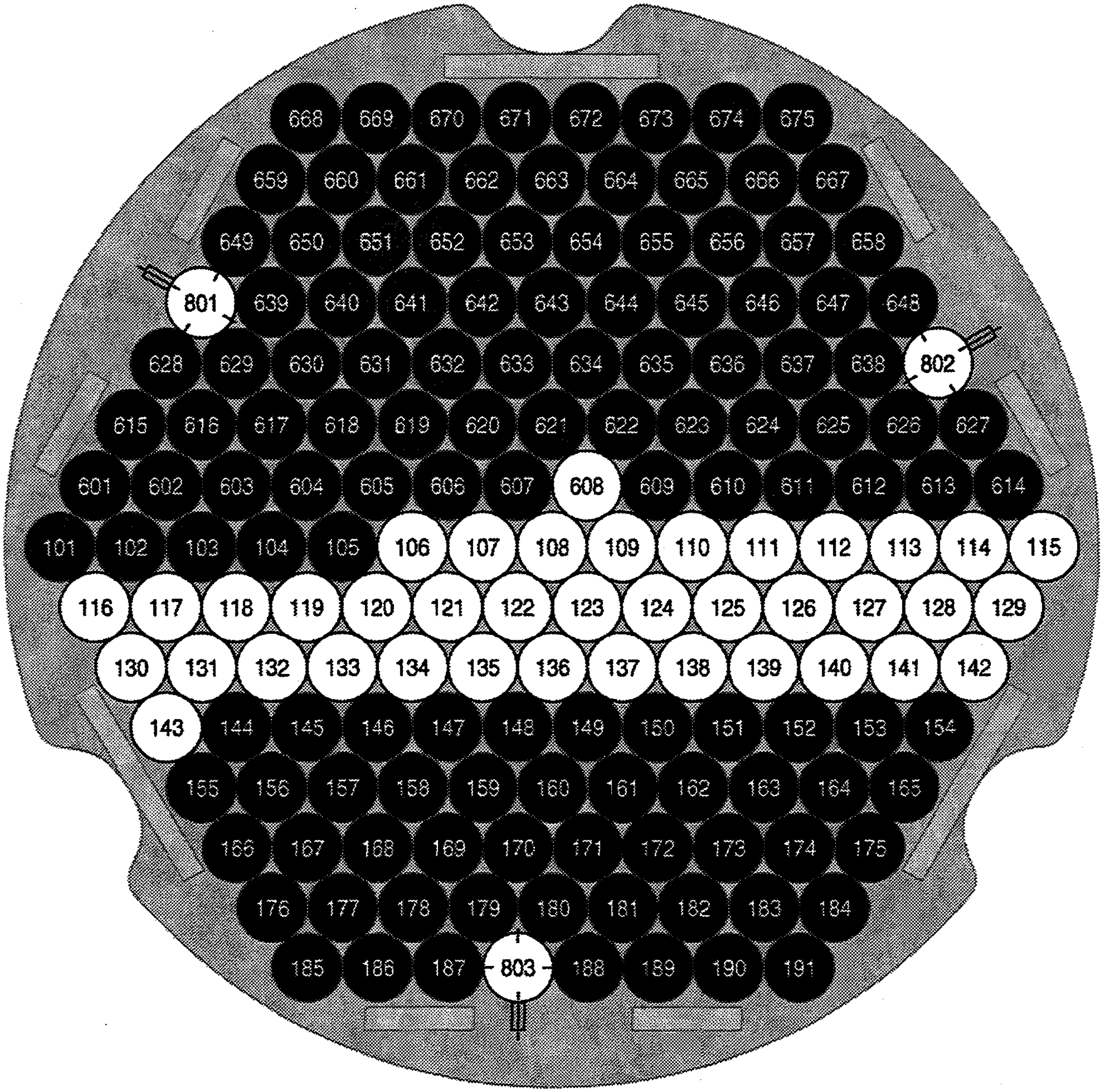

Figure 6-16. Occupied liner cells and cell serial numbers for reflector rod storage liner #15681 (see attachment to letter WAPD-NRC(L) C-93).

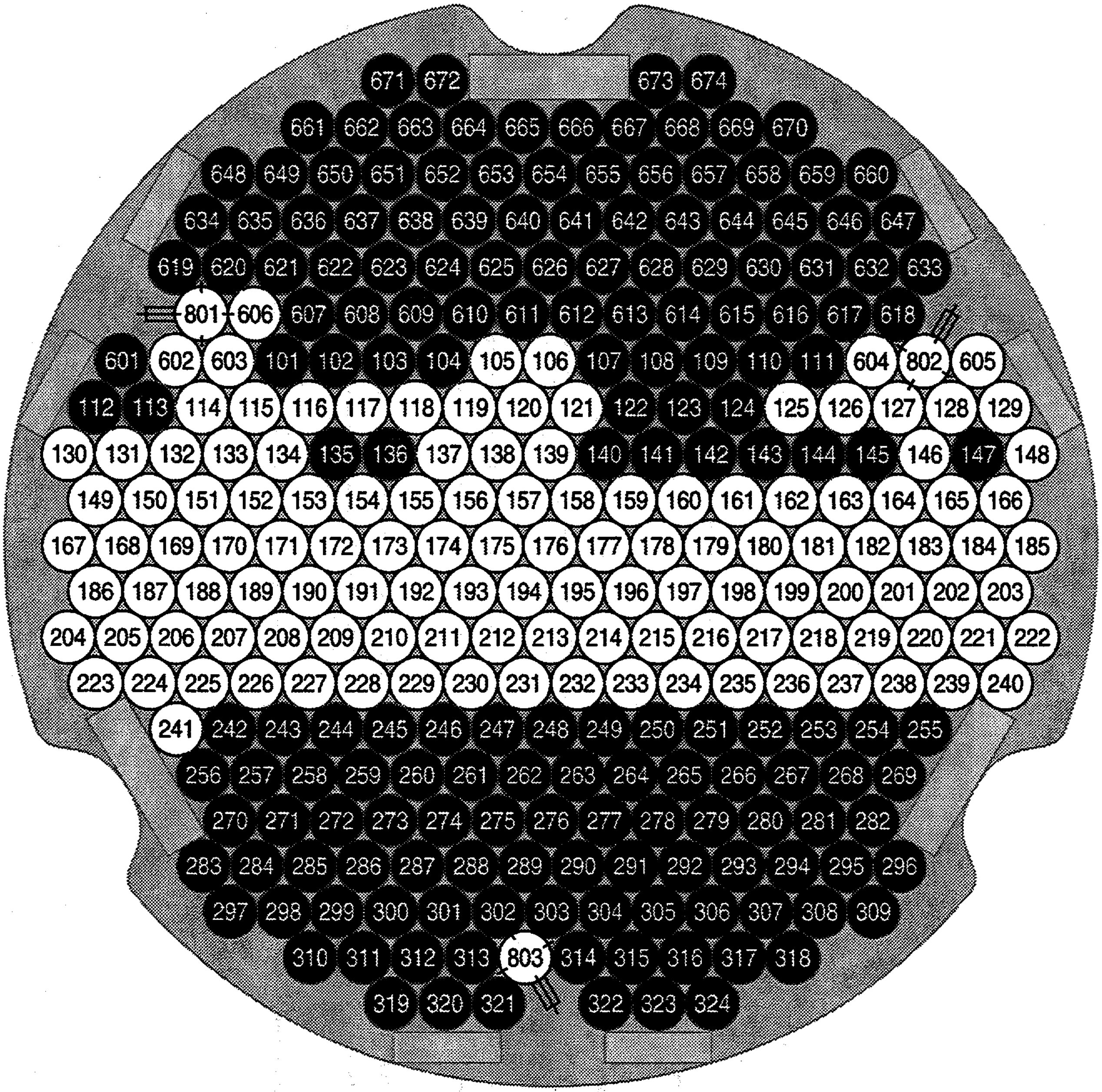

Figure 6-17. Occupied liner cells and cell serial numbers for blanket rod storage liner #15682 (see attachment to letter WAPD-NRC(L) C-93).

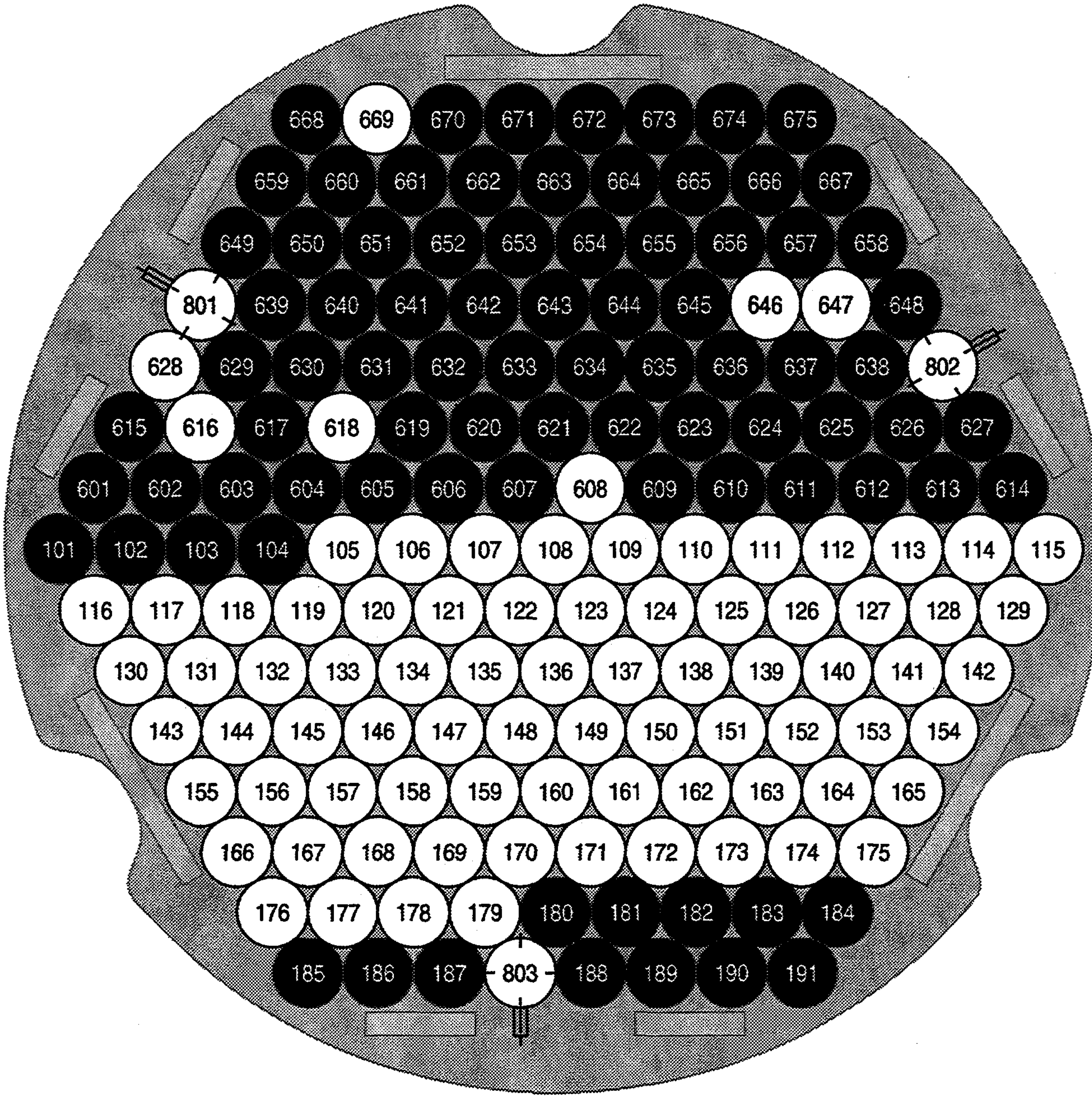

Figure 6-18. Occupied liner cells and cell serial numbers for reflector rod storage liner #15683 (see attachment to letter WAPD-NRC(L)104 and WAPD-NRF(L)C-149).

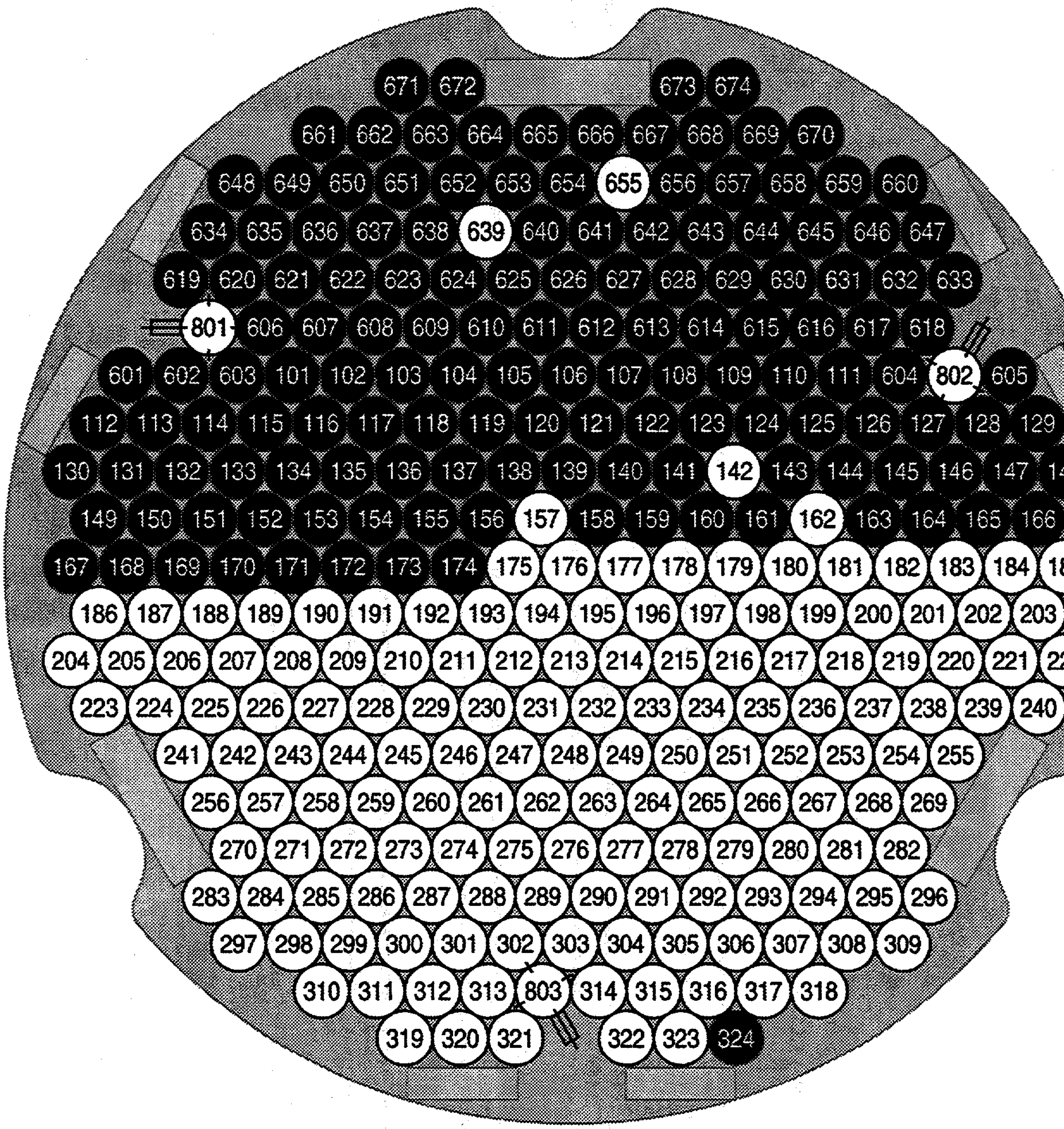

Figure 6-19. Occupied liner cells and cell serial numbers for blanket rod storage liner #15684 (see attachment to letter WAPD-NRC(L) C-104).

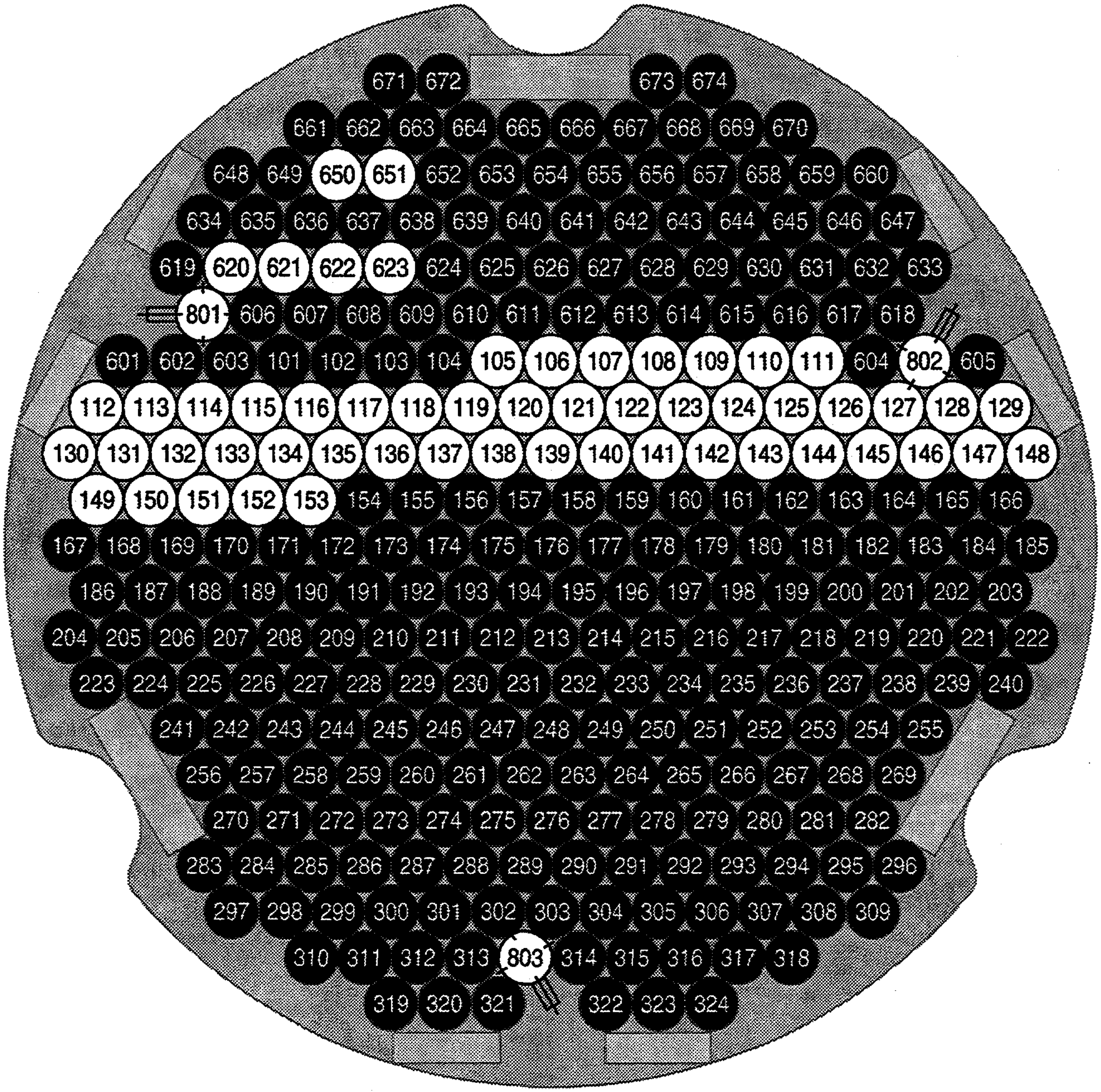

Figure 6-20. Occupied liner cells and cell serial numbers for blanket rod storage liner #15685 (see attachment to letter WAPD-NRC(L)149 and WAPD-NRF(L)C-117).

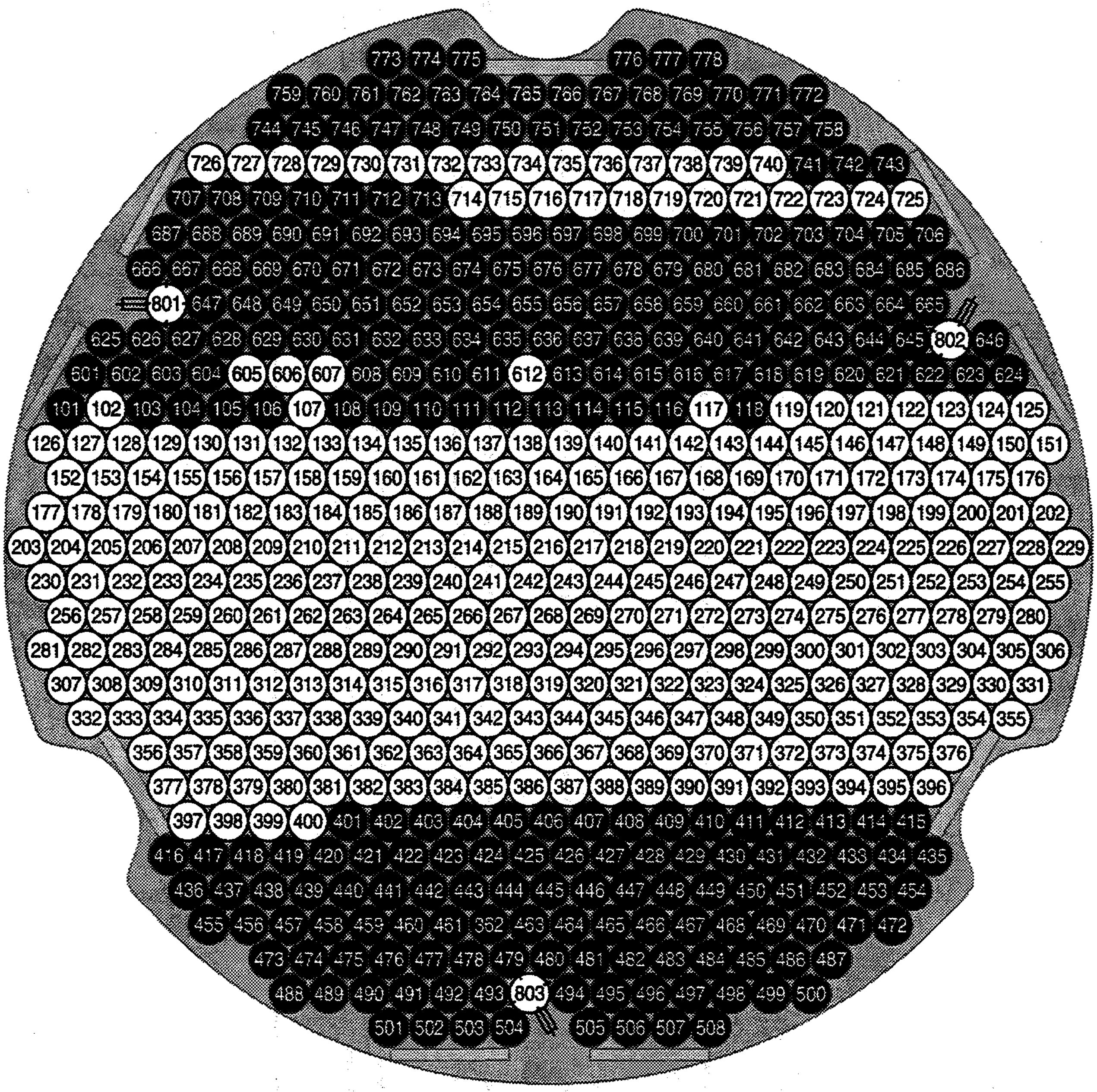

Figure 6-21. Occupied liner cells and cell serial numbers for seed rod storage liner #15686 (see attachment to letter WAPD-NRC(L)149 and WAPD-NRF(L)C-117).

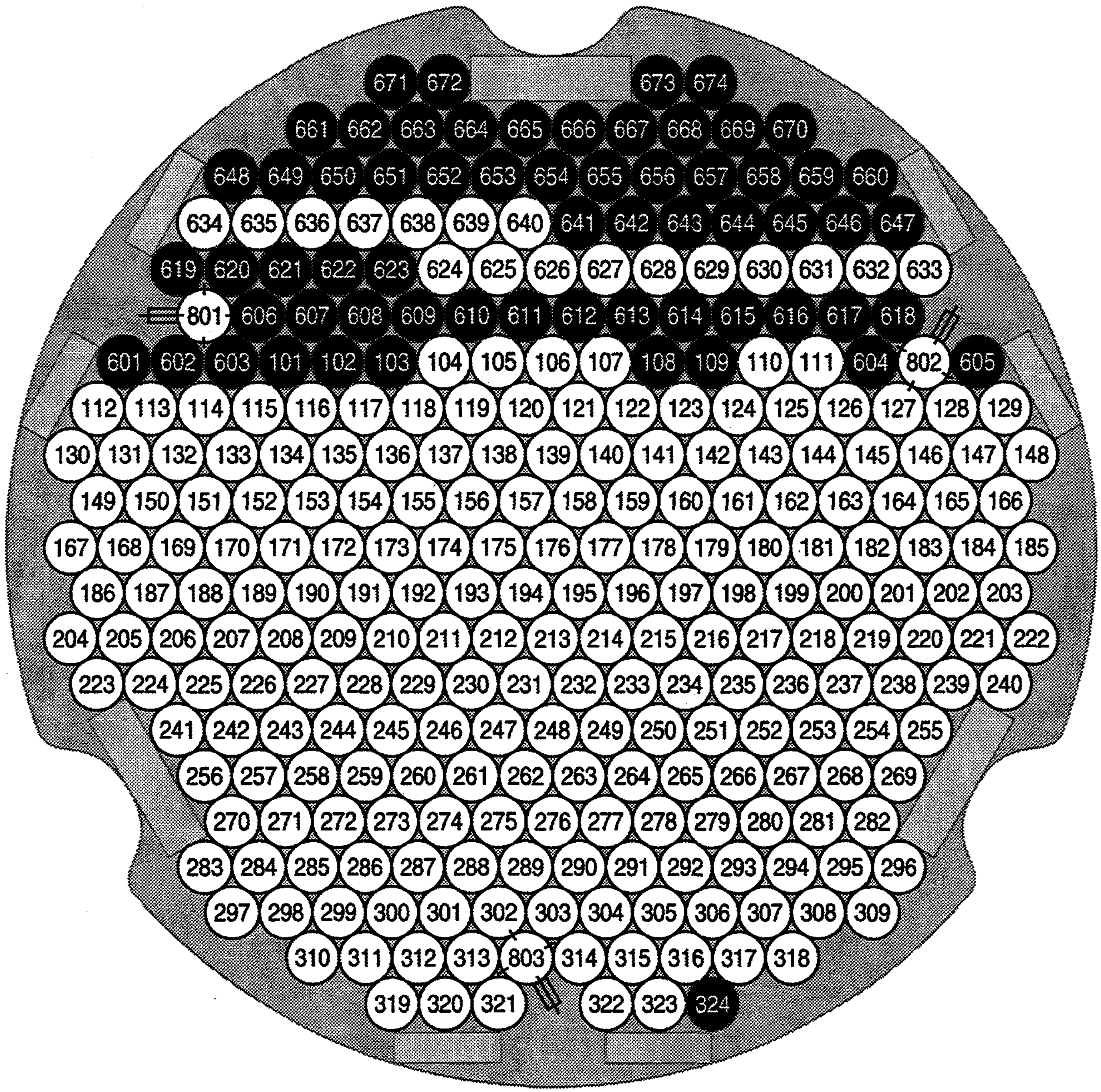

Figure 6-22. Occupied liner cells and cell serial numbers for blanket rod storage liner #15687 (see attachment to letter WAPD-NRC(L)123 and WAPD-NRF(L)C-117).

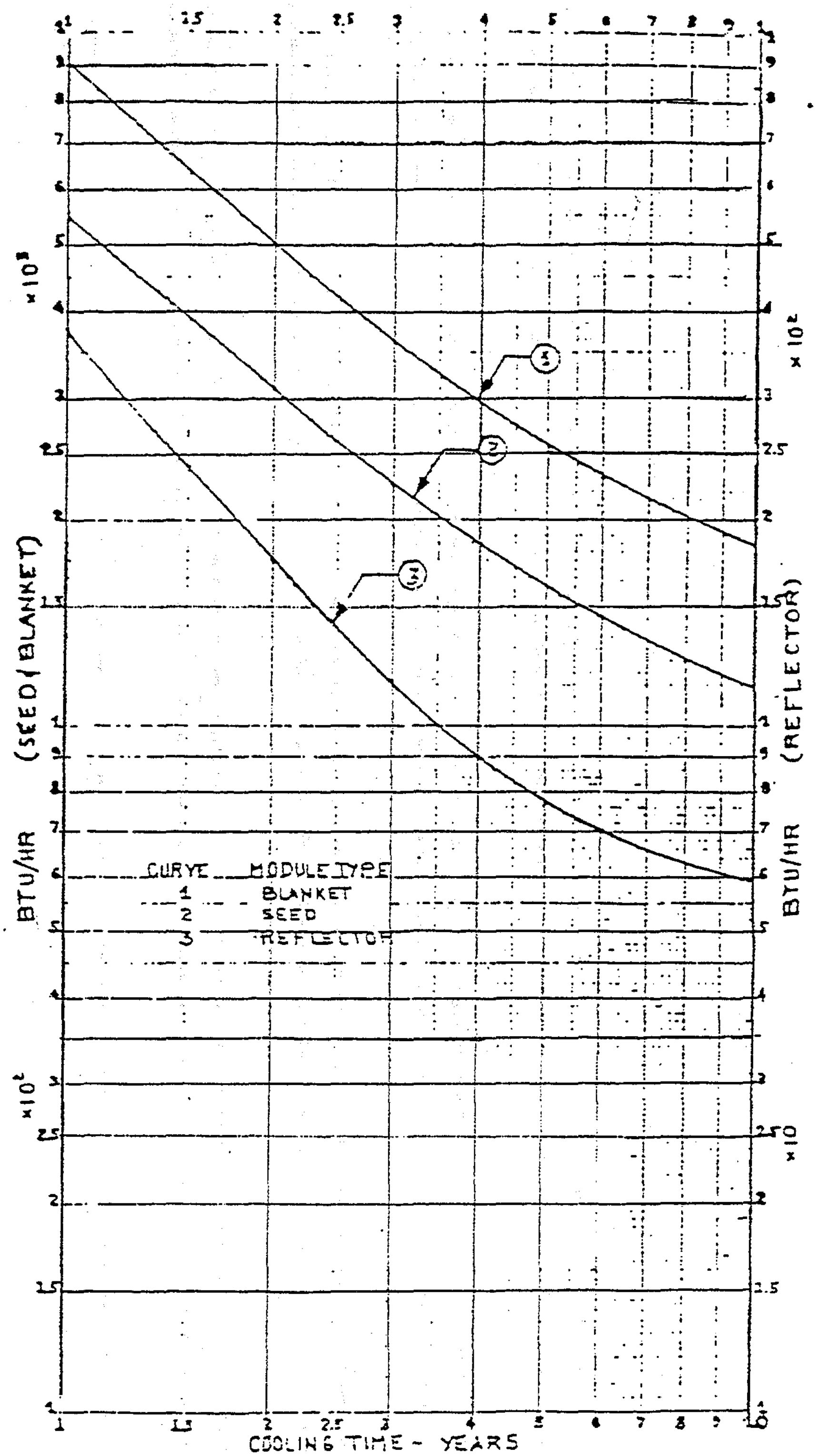

Figure 6-23. Decay heat as a function of cooling time for the hottest fully-rodded seed, blanket and reflector modules (attached to WAPD-NRF(L)C-104 (curve on p. 15, some discussion on p. 4-5), April 30, 1987, Fuel Receipt Criteria, Part B).

Seed: 2.15×10^3 BTU/Hr (assumes 619 rods)

Blanket: 1.8×10^3 BTU/Hr (assumes 564 rods)

Reflector: 6.0×10^2 BTU/Hr (assumes 228 rods)

For modules that are no longer intact (i.e., those stored in the Type B liners), and for the Type C liners, some other method of estimating thermal output must be developed.

Note: The predicted decay heat curve was verified against LWBR decay heat measurements taken on the core 16 to 20 days after shutdown, and on the M-130 shipments of modules 340 to 637 days after shutdown. The measurements support the use of the predicted decay heat curve (See p. 5 on Attachment to WAPD-NRF(L)C-104, April 30, 1987).

6.6 Liquid Content of Canister

While at ECF, the fuel handling unit was stored in the fuel storage liner in the ECF waterpit. Prior to shipment, the can was dried to the extent that no liquid water remained in the can (see p. 5 of the Attachment (Part B FRC) transmitted in WAPD-NRF(L)C-104, April 30, 1987). As stated in Part B FRC (p. 7 of Attachment to WAPD-NRF(L)C-104, April 30, 1987), "Prior to shipment, the LWBR fuel storage liner must be internally dry and contain an inert atmosphere. A liner is defined as dry when all liquid water has been removed. The drying process was confirmed by checkout and testing of the LWBR Liner Closure Station dewatering equipment used on an actual fuel storage liner both at a vendor shop and at ECF. ECF will certify that the liner for each FHU is dry and contains the inert atmosphere as required."

Pressure testing (hydrostatic test, neon and helium gas tests, and a hydraulic jack test) was conducted prior to shipment and results are included in the Part C Fuel Receipt Criteria.

7. SUMMARY

The LWBR core operated from 1977-82 without major incident. The fuel and fuel components suffered minimal damage during operation, and the reactor testing was deemed successful. Extensive destructive and non-destructive post irradiation examinations confirmed that the fuel was in good condition with minimal amounts of cladding deformities and fuel pellet cracks. Fuel was placed in wet storage upon arrival at ECF, then dried and sent to INTEC for underground dry storage. It is likely that the fuel remains in good condition at its current underground dry storage location at INTEC. Reports show no indication of damage to the core associated with shipping, loading, or storage.

8. REFERENCES

WAPD-TM-1208. D. R. Conners, et. al., *Design of the Shippingport Light Water Breeder Reactor*, January, 1979

WAPD-TM-1244. J. Belle, et. al., *ThO_2 and ThO_2-$^{233}UO_2$ High Density Fuel Pellet Manufacture for the Light Water Breeder Reactor*,WAPD-TM-1244(L), January, 1976.

WAPD-TM-1278. V. V. DeGeorge and I. Goldberg, eds., *The Fabrication and Loading of Fuel Rods for the Light Water Breeder Reactor (LWBR Development Program*, WAPD-TM-1278, March, 1986.

WAPD-TM-1289. J. H. Eyler, *Development and Control of the Process for the Manufacture of Zircaloy-4 Tubing for LWBR Fuel Rods (LWBR Development Program)*, WAPD-TM-1289, January, 1981.

WAPD-TM-1314. L. B. Freeman (editor). *The Calculational Model Used in the Analysis of Nuclear performance of the Light Water Breeder Reactor (LWBR).* August 1978.

WAPD-TM-1315. B. R. Beaudoin. *Loading Assurance Methods Used in the Manufacture of the Light Water Breeder Reactor (LWBR)*, WAPD-TM-1315, September, 1987.

WAPD-TM-1326. H. C. Hecker, *Summary of the Nuclear Design and Performance of the Light Water Breeder Reactor (LWBR)*, WAPD-TM-1326. June, 1979.

WAPD-TM-1336. W. K. Sarber, ed., *Results of the Initial Nuclear Tests on the LWBR (LWBR Development Program)*, WAPD-TM-1336, June 1976.

WAPD-TM-1342. R. J. Massimino and D. A. Williams, *The Installation of the Light Water Breeder Reactor at the Shippingport Atomic Power Station (LWBR Development Program)*, WAPD-TM-1342, May, 1983

WAPD-TM-1387. W. R. Cambell, et. al., *Light Water Breeder Reactor Fuel Rod Design and Performance Characteristics (LWBR Development Program)*, WAPD-TM-1387, October, 1987.

WAPD-TM-1409. H. C. Hecker and L. B. Freeman, *Design Features of the Light Water Breeder Reactor Which Improve Fuel Utilization in LWRs (LWBR Development Program)*, WAPD-TM-1409, August, 1981.

WAPD-TM-1455. W. K. Sarber, *Reactor Physics Test Program for the Light Water Breeder Reactor (LWBR) Core at Shippingport (LWBR Development Program)*, WAPD-TM-1455, Addendum, December 1983.

WAPD-TM-1542. W. A. Budd, ed., *Shippingport Operations With the LWBR Core (LWBR Development Program)*, WAPD-TM-1542, March, 1986.

WAPD-TM-1552. I. A. Selsey, et. al., *Light Water Breeder Reactor Fuel Module Disassembly at the Shippingport Atomic Power Station (LWBR Development Program)*, WAPD-TM-1552, October, 1987.

WAPD-TM-1553. I. A. Selsey, et. al., *Shipment of the Light Water Breeder Reactor Fuel Assemblies from the Shippingport Atomic Power Station to the Expended Core Facility (Idaho) (LWBR Development Program)*, WAPD-TM-1553, October, 1987.

WAPD-TM-1600. LWBR Staff, *Water Cooled Breeder Program Summary Report (LWBR Development Program),* WAPD-TM-1600, October, 1987.

WAPD-TM-1601. B. W. Hodgers, et. al., *Preparation of LWBR Spent Fuel for Shipment to ICPP for Long Term Storage (LWBR Development Program),* WAPD-TM-1601, October, 1987.

WAPD-TM-1605. D. A. Gorscak, et. al., *End-Of-Life Nondestructive Examination of Light Water Breeder Reactor Fuel Rods (LWBR Development Program),* WAPD-TM-1605, October, 1987.

WAPD-TM-1606. K. D. Richardson, et. al., *End of Life Destructive Examination of Light Water Breeder Reactor Fuel Rods,* WAPD-TM-1606, October, 1987.

WAPD-TM-1608. R. J. Greenberger and E. L. Miller, *Primary Disassembly of LWBR Modules for Core Evaluation (LWBR Development Program),* WAPD-TM-1608, October, 1987.

WAPD-TM-1612. W. C. Schick, Jr., et. al., *Proof of Breeding in the Light Water Breeder Reactor (LWBR Development Program),* WAPD-TM-1612, September, 1987.

WAPD-TM-1614. G. Tessler, et. al., *Nondestructive Assay of Spent Fuel Rods From the LWBR (LWBR Development Program),* WAPD-TM-1614, September, 1987.

Bibliography

Benton, Hugh, et al. (1997), Technical Strategy for the Management of Spent Nuclear Fuel , March, 1997.

BMI-X-1020. J. R. Springer, et. al., Fabrication, Characterization, and Thermal-Property Measurements of ThO_2-UO_2 Fuel Materials (LWBR Development Program), October 1967.

Duncombe, E., et. al., Comparisons With Experiment of Calculated Dimensional Changes and Failure Analysis of Irradiated Bulk Oxide Fuel Test Rods Using the CYGRO-1 Computer Program, September, 1966.

Technical Specifications/Standards : 4.7B4 "Integrity of Storage Canisters & Canister Lifting Tools for Dry Well Storage of LWBR Fuels". 4.7B6 "Spare Dry Well Requirement for LWBR Fuel Storage". 4.7B7 "Handling of LWBR Fuel Storage Canisters -- Peach Bottom Transfer Cask". 4.7C2 "Surveillance of the LWBR Fuel Storage Dry Wells".

WAPD-TM-466. S. J. Green, et. al., Critical Heat Flux Tests on a Coolant Channel Simulating a Closely Spaced Lattrice of Rods (LWBR Development Program), March, 1969.

WAPD-TM-520. R. C. Hoffman and J. F. Yerman, Further Experimental Results of the Irradiation of Long Duplex Pellet Screening Tests in the NRX Reactor (NLDR-2/3/4 Tests) (AWBA Development Program), October, 1982.

WAPD-TM-614. S. Milani and S. H. Weiss, Small Uranium-233 Fueled Seed-And-blanket Critical Experiments (LWBR-LSBR Development Program), November 1967.

WAPD-TM-628. B. A. Hersey and H. B. Meieran, Behavior of an Intentionally Defected Fuel Rod Which Ruptured During Irradiation (Rod BETT 79-64D) (LWBR Development Program), July, 1969.

WAPD-TM-629. R. M. Berman, et. al., Irradiation Behavior of Zircaloy-Clad Fuel Rods Containing Dished-End UO_2 Pellets (LWB-LSBR Development Program), July, 1967.

WAPD-TM-630. H. B. Meieran, et. al., Short Term Irradiation of Zircaloy-4 Clad Fuel Rods Containing Low Density or Annular ZrO_2-UO_2 Ceramic Fuel Pellets: X-1-t Test (LWBR-LSBR Development Program), June, 1968.

WAPD-TM-631. J. T. Engle and H. B. Meieran, Performance of Fuel Rods Having 97 Percent Theoretical Density UO_2 Pellets Sheathed in Zircaloy-4 and Irradiateds at Low Thermal Ratings (LSBR/LWBR Development Program), July, 1968.

WAPD-TM-664. J. E. McCauley, Observations on the Irradiation Behavior of a Zircaloy-4 Clad Rod Containing Low Density ThO_2-5.3 w/o UO_2 Pellets (LWBR Development Program), December 1969.

WAPD-TM-758. D. C. Jacobs, The In-Pile Thermoconductivity of Selected ThO_2-UO_2 Fuels at Low Depletions (LWBR Development Program), May, 1969.

WAPD-TM-782. S. Kass, Effects of Pressure Upon the Corrosion of Zircaloy-4 (LWBR Development Program), October 1968.

WAPD-TM-794. E. Duncombe, Analysis of Void Migration, Clad Collapse and Fuel Cracking in Bulk Oxide Fuel Rods (LWBR Development Program), July, 1968.

WAPD-TM-869. J. H. Eyler, The Characteristics of the Zircaloy-4 Tubing in LWBR Fuel Rods (LWBR Development Program), November, 1979.

WAPD-TM-900. C. C. Busby and K. B. Marsh, High Temperature Deformation and Burst Characteristics of Recrystallized Zircaloy-4 Tubing (LWBR Development Program), January 1970.

WAPD-TM-901. D. C. Jacobs, In-Pile and Unirradiated Thermal Conductivity of a Single-Fired ThO_2 + 10 w/o UO_2, (LWBR Development Program), February, 1970.

WAPD-TM-906. Stanley Kass, The Influence of Prior Corrosion History Upon the Hydrogen Pickup by Zircaloy During Subsequent Exposure in Hot Water (LWBR Development Program), December, 1970.

WAPD-TM-909. J. M. Markowitz and J. C. Clayton, Comparison of Oxide Nuclear Fuels in High Temperature Water (LWBR Development Program), February, 1970

WAPD-TM-940. E. Duncombe and I. Goldberg, Comparison of Dimensional Changes in Fuel Rods With Predictions Under Cyclic Conditions of Power and System Pressure (LWBR Development Program), March, 1940.

WAPD-TM-973. R. C. Daniel, In-Pile Dimensional Changes of Zircaloy-4 Tubing Having Low Hoop Stresses (LWBR Development Program), July, 1971.

WAPD-TM-986. J. F. Giovengo, In-Pile Dimensional Changes of ThO_2-UO_2 With Non-Free-Standing Cladding (LWBR Development Program), November, 1970.

WAPD-TM-1117. J. A. Mitchell, ed., BMU Series of ^{233}U Fuelled Critical Experiments (LWBR Development Program), January 1975.

WAPD-TM-1208, D. R. Conners, et. al., Design of Shippingport Light Water Breeder Reactor (LWBR Development Program), January, 1979.

WAPD-TM-1226. Kotula, J., LWBR Automated Fuel Rod Loading Verification Gage System (LWBR Development Program), February, 1979.WAPD-TM-1239. A. J. Caffarel, The Inspection of Assembled LWBR Fuel Rods for Internal Dimensions and Pellet Integrity Utilizing In-Motion Radiography (LWBR Development Program), February, 1979.

WAPD-TM-1256. R. W. Stooksberry, Conceptual Evaluation of Nondestructive Assay of $^{233}UO_2$-ThO_2 Fuel Rods (LWBR Development Program), January, 1979.

WAPD-TM-1285. Eyler, J. H. (1981), Development and Control of the Process for the Manufacture of Zircaloy-4 Tubing for LWBR Fuel Rods, January,1981.

WAPD-TM-1316. Beaudoin, B. R., et. al. (1979), A system of Datatran Modules which Process Core Fuel Loading for use in As-Built Calculations (LWBR Development Program), February, 1979.

WAPD-TM-1317. Gourley, B. R., et al.. (1981), Fabrication of Seed, Blanket and Reflector Fuel Assemblies for the Light Water Breeder Reactor (LWBR Development Program. May 1981.

WAPD-TM-1326. H. C. Hecker, Summary of the Nuclear Design and Performance of the Light Water Breeder Reactor (LWBR) (LWBR Development Program), June 1979.

WAPD-TM-1347. R. M. Stackhouse, ed., Fuel Rod Grid Interaction Wear: In-Reactor Tests (LWBR Development Program), November, 1979.

WAPD-TM-1348. C. S. Galtz, The Friction Grip Enclosure - A Means for Increasing the Fatigue Life of Fuel Rod End Welds (LWBR Development Program), March, 1983.

WAPD-TM-1350. I. Goldberg, et. al., Fission Gas Release From ThO_2 and ThO_2-UO_2 Fuels (LWBR Development Program), August, 1978.

WAPD-TM-1350, Addendum. I. Goldberg, et. al., Fission Gas Release and Grain Growth in ThO_2-UO_2 Fuel Irradiated at High Temperature (LWBR Development Program). July, 1979.

WAPD-TM-1350, Addendum 2. J. F. Giovengo, et. al., Fission Gas Release From High Burnup ThO_2 and ThO_2-UO_2 Fuels Irradiated at low Temperature (LWBR/AWBA Development Program), May, 1982.

WAPD-TM-1368. Emert, C. J., The Nondestructive Assay of UO_2-ThO_2 Fuel Pellets Using the Delayed Neutron Pellet Assay Gage(LWBR Development Program). June, 1979.

WAPD-TM-1376. R. C. Hoffman and J. Sherman, Irradiation Testing of Internally Pressurized and/or Graphite Coated Zircaloy-4 Clad Fuel Rods in the NRX Reactor (LWBR Development Program), November, 1978.WAPD-TM-1421. H. C. Hecker, Nuclear Analysis and Performance of the Light Water Breeder Reactor (LWBR) Core Power Operation at Shippingport (LWBR Development Program), April, 1984.

WAPD-TM-1378C. D. Sphar and J. Sherman, Early-In-Life Performance of Short Rod Duplex Pellet Screening (D-1) Test (AWBA Development Program), November, 1979.

WAPD-TM-1393. J. C. Clayton, Cladding Corrosion and Hydriding in Irradiated Defected Zircaloy Fuel Rods (LWBR Development Program), August, 1985.

WAPD-TM-1394. D. M. Ivak and L. A. Waldman, Iodine and Cesium in Oxide Fuel Pellets and Zircaloy-4 Cladding of Irradiated Fuel Rods (LWBR Development Program), March 1979.

WAPD-TM-1440. J. C. Clayton, Corrosion and Hydriding of Irradiated Zircaloy Fuel Rod Cladding (LWBR Development Program), September, 1982.

WAPD-TM-1460. C. D. Sphar, et. al., Irradiation Performance of Duplex Fuel Pellet Test Rods Depleted to 9×10^{20} Fissions/cm^3 of Compartment - D-1 Test (AWBA Development Program), January, 1982.

WAPD-TM-1481. L. A. Waldman, et. al., Irradiation Performance of Long Rod Duplex Fuel Pellet Bundle Test -LDR Test (LWBR Development Program), April, 1982.

WAPD-TM-1492. R. C. Hoffman, et. al., Experimental Results of the Irradiation of Long Duplex Pellet Screening Tests in the NRX Reactor (NLDR-1 Test) (AWBA Development Program), July, 1982.

WAPD-TM-1529. A. J. Smithnosky, In-Reactor Tests of Externally Pressurized, Short, Unsupported Lengths of Zircaloy Tubing (AWBA Development Program), October 1982.

WAPD-TM-1548. J. C. Clayton, In-Pile and Out-of-Pile Corrosion Behavior of Thoria-Urania Pellets (LWBR Development Program), January, 1987.

WAPD-TM-1602, J. E. Wargo and K. D. Richardson, Light Water Breeder Reactor End-Of-Life Component Examinations at Shippingport Atomic Power Station and Module Visual and Dimensional Examinations at the Expended Core Facility (LWBR Development Program), October, 1987.

WAPD-TM-1603, B. C. Smith and W. R. Campbell, LightWater Breeder Reactor Fuel Element Performance Characteristics for Extending Core Lifetime (LWBR Development Program), October, 1987.

WAPD-TM-1607. B. C. Smith, ed., End-Of-Life Examinations of Light Water Breeder Reactor Grids and Other Module Structural Components (LWBR Development Program), October, 1987.

WAPD-TM-1609. Fodor, G. (1987). Light Water Breeder Reactor Rod Removal System (LWBR Development Program), October, 1987.

WAPD-TM-1610. W. S. Bacvinskas, et. al., Light Water Breeder Reactor Module and Rod Examinations LWBR Development Program, October, 1987.

WAPD-LP(CE)FD-38 attachment. Hecker , H. C., and C. J. Simon (1984), Idaho Chemical Processing Plant Part A Fuel Receipt Criteria for the LWBR Core, October, 1984.

WAPD-NRF(E)FD-09 attachment. Hecker , H. C., and C. J. Simon (1985), ICPP Fuel Receipt Criteria (Part A) for the LWBR Core (Rev. 3), January, 1985.

WIN-107-4.7A-Rev 1, Bolton, S. R., et al., ICPP Final Safety Analysis (Section 4.7) "Storage of Unirradiated and Irradiated Light Water Breeder Reactor Fuel in Underground Dry Wells at ICPP", March, 1989.

Appendix A

SCRAP STORAGE LINER

August 11, 1998

Abstract

This report describes the storage canister and fuel from several irradiation tests that were conducted as part of the Light Water Breeder Reactor (LWBR) and Advanced Water Breeder Applications (AWBA) programs; also included are summaries of reports for several of the tests. Fuel from this testing has been shipped to the Idaho National Engineering and Environmental Laboratory (INEEL). The fuel was irradiated at several reactors and includes a large vary of fuel compositions. Some of the fuel was sectioned for examination but the majority is intact. A small amount of the fuel is unirradiated. Most of the fuel rods used for this testing are contained in one basic fuel handling unit (FHU) scrap storage liner or canister at the Idaho Nuclear Technology and Engineering Center (INTEC). The intact fuel is stored in unsealed or sealed containers in the canister while the sectioned fuel is all stored in sealed containers.

Table of Contents

Figures

Tables

Acronyms and Abbreviations

ACT-LPR	Advanced Concept Test, Long Pressurized Rods
AECL	Atomic Energy of Canada, Limited
ALT1	Alternate Short Rod Screening Test
ALT2	Alternate Short Rod Screening Test
ATR	Advanced Test Reactor
AWBA	Advanced Water Breeder Applications
B1	Blanket Rod Screening Test
B1M	Blanket Rod Screening Test
B1R	Blanket Rod Screening Test
B3	Six-Rod Assembly Test
B3A	Six-Rod Assembly Test
BBT	Blanket Bundle Test
BOL	beginning of life
C7-LSBR	Large Seed Blanket Reactor Development
cc	cubic centimeter
CFSF	Cut Fuel Storage Containers
CHORT	Corrosion and Hydriding of Reactor Tubing computerized corrosion analysis program
cm	centimeter
D1	Duplex Short Rod Screening Test
dpm	disintegrations per minute
EFPH	effective-full-power hours – the quotient of megawatt hours of operation and megawatt capability at 100% power
f	fission/s
FHU	Fuel Handling Unit
ft	foot/feet
g	gram
GRIP-I	Grid Rod In-Pile Test
GRIP-II	Grid Rod In-Pile Test
GRIP-IIIA	Grid Rod In-Pile Test
GRIP-IIIB	Grid Rod In-Pile Test
GRIP-IIIC	Grid Rod In-Pile Test
He	helium
INEEL	Idaho National Engineering and Environmental Laboratory
INTEC	Idaho Nuclear Technology and Engineering Center
K_{eff}	The effective multiplication factor is a numerical value indicating how near a particular geometric configuration of nuclear material may be to sustaining a nuclear chain reactor ($K_{eff} = 1.0$ is a critical mass).
kW	kilowatt
KWO	Kernkraftwerk Obrigheim
L12-LSBR	Large Seed Blanket Reactor Development
LBR	Long Blanket Rod Test
LDR	Long Duplex Rod
LDR	Long Duplex Rod Screening Test
LOCA	loss of coolant accident
LSR	Long Seed Rod Test
LWBR	Light Water Breeder Reactor
M13-S2	Seed Rod Screening Test
M13-S2A	Seed Rod Screening Test

M13-S3	Seed Rod Screening Test
M13-S5	Seed Rod Touching Test
MEL	metallographic
MELBA	Multipurpose Extended Life Blanket Assembly
Mev	million electron volts
mil	one thousandth of an inch
ml	milliliter
MOSC	metal O-ring sealed containers
MT	metric ton
MTM	metric ton of metal (uranium + thorium)
MTR	Material Test Reactor
MTU	metric ton uranium
MWD	megawatt day
n	neutrons
NA	not applicable
NLBR	New Long Blanket Rod Test
NLDR	New Long Duplex Rod
NLDR-1	NRX Long Duplex Rod Test
NLDR-2	NRX Long Duplex Rod Test
NLDR-3	NRX Long Duplex Rod Test
NLDR-4	NRX Long Duplex Rod Test
NLSR	New Long Seed Rod Test
OD	outside diameter
OD/t	outside diameter/thickness (cladding)
PBIT	Pre-Breeder Bundle Irradiation Test
PCI	pellet-cladding interaction
PM	Power Monitor-instrumented alloy rod
RAC	Rod Alpha Containers
RXA	re-crystallization annealed
SABRE	Special Assembly Blanket Rod Elements
sec	second
SIDR	Short Intentionally Defected Rod Test
SP	Special Physics Tests
SPIRE	Seed Prototype Irradiation Rod Experiment
SRA	stress relief annealed
ST	Sealed Tube
StT	Storage Tube
SWLD	Blanket Swing-load Test
TD	theoretical density
TIPPETT II	Thoria Performance Test
U^D	depleted uranium
U^E	enriched uranium
U^N	natural uranium
UT	Unsealed Tubes
w/o	weight percent
^{235}U	uranium-235 isotope
^{233}U	uranium-233 isotope

1. INTRODUCTION

Several irradiation tests were conducted as part of the Light Water Breeder Reactor (LWBR) and Advanced Water Breeder Applications (AWBA) programs. Most of the fuel rods used for this testing are contained in one basic fuel handling unit (FHU) scrap storage liner or canister at the Idaho Nuclear Technology and Engineering Center (INTEC).

2. REACTOR INFORMATION

2.1 Reactors Used

The test reactor cores used for the tests served primarily to provide the neutron environment for the LWBR irradiation tests. Test fuel rods in the development program were from the following reactors: 1) the Advanced Test Reactor (ATR), 2) the Engineering Test Reactor (ETR), 3) the Light Water Breeder Reactor (LWBR), 4) Pressured Water Reactor (PWR), and 5) the National Research Experimental (NRX) Reactor.

2.1.1 The ATR

The ATR, which is located at the Idaho National Engineering and Environmental Laboratory (INEEL), is a light-water-moderated and -cooled four-lobe reactor using 93% enriched uranium and beryllium refection owned by United States Department of Energy (DOE) and currently operated by Lockheed Marten Idaho Technologies Company (LMITCO). It provides a thermal flux (1 x 10^{15} n/cc-sec) environment for a multiplicity of high-pressure loops. The cylindrical symmetry of the experimental loops, their diameter (averaging about 3 inches), and the large number of samples to be irradiated at one time strongly influence the choice of the reactor type. ATR was originally designed to study the effects of intense radiation on reactor materials for space and commercial power programs, especially fuels; it was used in developing advanced naval reactor cores and advanced fuel systems. The ATR test reactor core served primarily to provide the neutron environment for the irradiation tests.

2.1.2 The ETR

The ETR located at the INEEL began operation in 1957 and operated until 1981 with a thermal operating level of 175 megawatts. The ETR was owned by DOE and operated by EG&G; it was operated in support of the LWBR fuels and materials development until May 1, 1973, after which it was converted to support the Liquid Metal Fast Breeder Reactor safety program. The ETR test reactor core served primarily to provide the neutron environment for the irradiation tests.

2.1.3 The LWBR and PWR

The Shippingport Atomic Power Station located on the south bank of the Ohio River in Shippingport Borough, Beaver County Pennsylvania was the first large-scale, central station application of nuclear power for civilian use in the United States. DOE and the Duquesne Light Company jointly owned the station. The Duquesne Light Company operated it since its initial startup in December 1957 and shut it down in 1983. During its operating period two pressured water reactor (PWR) cores and one Light Water Breeder Reactor (LWBR) core were used. PWR Core I operated until February 1964, having been partially refueled three times (4 different Seed cores used). Following plant modifications, Core 2 was installed and began power operation in May 1965. Core 2 underwent one partial refueling in 1969 (2 different Seed cores used), and continued in operation until February 1974 when the plant was shut down for repair of the turbine generator. At that time preparations began for refueling with the LWBR core, which began power operation in calendar year 1978 and operated until 1983.

2.1.4 The NRX Reactor

The NRX reactor at the Chalk River Nuclear Laboratory (CRNL) in Chalk River, Ontario, Canada is owned and operated by Atomic Energy of Canada, Ltd. (AECL). The NRX is a natural uranium, heavy water-moderated, light water-cooled reactor. It is equipped with several test loops that provide pressure, flow, and heat removal systems independent of the reactor for the irradiation of test specimens. The major advantage of the NRX reactor is that full length fuel assemblies can be irradiated in the test loops.

2.2 Irradiation Tests

The irradiation test abbreviations, test descriptions, and the reactor used for the testing are given in Table 1[1].

TABLE 1 - IRRADIATION TESTS

Test	Description	Reactor
ACT-LPR	Advanced Concept Test, Long Pressurized Rods	NRX
ALT1	Alternate Short Rod Screening Test	ATR
ALT2	Alternate Short Rod Screening Test	ATR
B1	Blanket Rod Screening Test	ETR
B1R	Blanket Rod Screening Test	ETR
B1M	Blanket Rod Screening Test	ETR
B3	Six-Rod Assembly Test	ETR
B3A	Six-Rod Assembly Test	ETR
BBT	Blanket Bundle Test	ETR
C7-LSBR	Large Seed Blanket Reactor Development	ETR
D1	Duplex Short Rod Screening Test	ATR
GRIP-I	Grid Rod In-Pile Test	ETR
GRIP-II	Grid Rod In-Pile Test	ETR
GRIP-IIIA	Grid Rod In-Pile Test	ETR
GRIP-IIIB	Grid Rod In-Pile Test	ETR
GRIP-IIIC	Grid Rod In-Pile Test	ETR & ATR
LBR	Long Blanket Rod Test	NRX
LDR	Long Duplex Rod Screening Test	ETR
LSR	Long Seed Rod Test	ETR
L12-LSBR	Large Seed Blanket Reactor Development	ETR
M13-S2	Seed Rod Screening Test	ETR
M13-S2A	Seed Rod Screening Test	ETR
M13-S3	Seed Rod Screening Test	ETR
M13-S5	Seed Rod Touching Test	ETR
NLBR	New Long Blanket Rod Test	NRX
NLDR-1	NRX Long Duplex Rod Test	NRX
NLDR-2	NRX Long Duplex Rod Test	NRX
NLDR-3	NRX Long Duplex Rod Test	NRX
NLDR-4	NRX Long Duplex Rod Test	NRX
NLSR	New Long Seed Rod Test	NRX
PBIT	Pre-Breeder Bundle Irradiation Test	ATR
SABRE	Special Assembly Blanket Rod Elements	PWR C-1 S-4
SPIRE	Seed Prototype Irradiation Rod Experiment	ETR
SWLD	Blanket Swing-load Test	ETR
TIPPETT II	Thoria Performance Test	ETR
SIDR	Short Intentionally Defected Rod Test	NRX
PM	Power Monitor-instrumented alloy rod	?
SP	Special Physics Tests	?

3. FUEL INFORMATION

3.1 Fuel Rod Properties

The irradiation test fuel rod properties and compositions are given in Tables 2 and 3[1]. Cladding heat treatment was either recrystallization anneal (RXA) or stress-relief anneal (SRA) with a cladding thickness range of 0.018 to 0.039 inches. For all test fuels the plenum region above the fuel stack contained an Inconel-X-750 plenum spring that placed an axial load on the fuel stack. All rods used helium (He) internal gas at the beginning of life (BOL) pressure given in Table 2.

TABLE 2 - IRRADIATION TEST FUEL ROD PROPERTIES

Test	BOL Rod Length, inch	BOL Nominal Rod OD, inch	Clad thickness, inch	Clad type	BOL He, psi	Max Exposure of Cladding nvt x 10^{-20}	Peak Depletion x 10^{-20} f/cc	BOL enrich. %
ACT-LPR	115.6	0.613	0.030	SRA	14.7	4.0	4.7	93.2
	105.1				500.0			
ALT1	11.0	0.300	0.018	SRA, RXA	300.0	31.5	14.0	-
			0.022					
ALT2	11.0	0.300	0.018	SRA, RXA	100.0	32.1	13.6	93.1
			0.022		300.0			
					500.0			
B1	93.0	0.613	0.024	SRA, RXA	14.7	8.2	1.2	93.2
B1R	93.0	0.613	0.030	SRA	14.7	11.5	1.2	93.2
B1M	93.0	0.568	0.024	SRA	14.7	32.4	3.9	93.2
B3 & B3A	44.8	0.716	0.025	SRA, RXA	14.7	13.0	2.9	93.2
			0.030					
BBT	86.3	0.526	0.028	SRA	14.7	21.0	5.3	93.2
		0.572	0.030					
C7-LSBR				SRA, RXA	14.7		<1.0	-
D1	11.0	0.300	0.019	RXA	100.0	43.0	14.0	
			0.022		500.0		29.0	
GRIP-I	96.0	0.250	0.020	SRA	14.7	25.0	7.0	93.1
			0.021					
GRIP-II	95.3	0.255	0.020	RXA	14.7	66.0	10.8	98.2
	94.3							
GRIP-IIIA	92.5	0.300	0.022	RXA	14.7	32.0	4.9	93.2
	89.8							
GRIP-IIIB	95.2	0.300	0.021	RXA	14.7	101.0	10.0	93.2
	91.9							
GRIP-IIIC	92.5	0.300	0.022	RXA	14.7	25.0	2.8	93.2
	89.8							
LBR	16.9	0.600	0.024	SRA, RXA	14.7	6.3	5.7	93.2
LDR	95.2	0.250	0.018	SRA, RXA	100.0	41.7	15.4	93.1
	91.9		0.022		500.0			
LSR	118.0	0.250	0.018	RXA	14.7	6.4	11.1	93.2
L12-LSBR	6.0	0.252	0.018	SRA	14.7	57.2	19.0	93.1
M13-S2	6.0	0.250	0.018	SRA	14.7	21.0	5.0	93.1

			0.022					
M13-S2A	6.0	0.250	0.019	SRA, RXA	14.7	21.0	9.1	93.1
M13-S3	6.0	0.250	0.018	SRA, RXA	14.7	23.0	9.4	93.1
			0.022					
NLBR	116.9	0.613	0.030	SRA	14.7	6.1	5.9	93.2
NLDR-1	110.0	0.300	0.021	SRA	100.0	8.1	16.8	93.1
NLDR-2	110.0	0.300	0.021	SRA	100.0	8.6	17.8	93.1
NLDR-4	110.0	0.300	0.021	SRA	100.0	3.5	7.2	93.1
PBIT	94.0	0.365	0.024	SRA	400.0	33.4	6.4	93.1
SABRE	84.0	0.563	0.033	SRA		5.1	2.0	N/A
SPIRE	96.0	0.280	0.018	SRA	14.7		7.0	
SWLD	11.3	0.551	0.027	RXA	14.7		0.2	93.2
SIDR	22.0	0.516	0.029	SRA	14.7	1.3	0.7	93.2
LWBR-Seed	116.6	0.306	0.019	RXA	14.7	109.0	10.0	97.5
LWBR-PFB	117.7	0.527	0.023	SRA	14.7	84.0	5.4	97.5
LWBR-SB	117.7	0.572	0.025	SRA	14.7	84.0	5.1	97.5
LWBR-R	113.8	0.832	0.039	SRA	14.7	55.0	1.0	

TABLE 3 - IRRADIATION TEST FUEL ROD FUEL COMPOSITIONS

ID	**Bottom 48.2 inches**	**Type**	**Top 38.2 inches**
SPIRE Test			
79-243	ZrO_2 21.2 w/o U^EO_2 + 4.12 w/o U^NO_2	Annular	ZrO_2 28 w/o U^NO_2 Solid, 96% TD
79-243	ZrO_2 39.6 w/o U^EO_2	Annular	ZrO_2 28 w/o U^NO_2 Solid, 96% TD
79-229	ZrO_2 40.1 w/o U^EO_2	Annular	ZrO_2 28 w/o U^NO_2 Solid, 96% TD
79-213	ZrO_2 32.9 w/o U^EO_2	Annular	ZrO_2 28 w/o U^NO_2 Solid, 86% TD
79-216	ZrO_2 28.5 w/o U^EO_2 + 4.6 w/o U^NO_2	Annular	ZrO_2 28 w/o U^NO_2 Solid, 98% TD
79-220	ZrO_2 18.2 w/o U^EO_2 + 6.6 w/o U^NO_2	Solid	ZrO_2 36 w/o U^NO_2 Solid, 73% TD
79-221	ZrO_2 18.2 w/o U^EO_2 + 6.6 w/o U^NO_2	Solid	ZrO_2 36 w/o U^NO_2 Solid, 73% TD
79-222	ZrO_2 18.2 w/o U^EO_2 + 6.6 w/o U^NO_2	Solid	ZrO_2 36 w/o U^NO_2 Solid, 73% TD
79-215	ZrO_2 28.5 w/o U^EO_2 + 4.6 w/o U^NO_2	Annular	ZrO_2 28 w/o U^NO_2 Solid, 98% TD
79-217	ZrO_2 28.5 w/o U^EO_2 + 4.6 w/o U^NO_2	Annular	ZrO_2 28 w/o U^NO_2 Solid, 98% TD

ID	**Annulus Pellet**	**Cylindrical Central Pellet**
D1 Test		
97-12,23,40,&42	23.1 w/o U^EO_2 + in U^DO_2	100 % ThO_2
97-26 & 36D	22.8 w/o U^EO_2 + in U^DO_2	100 % ThO_2
97-2,3,4,8,9,&10	16.4 w/o U^EO_2 + in U^DO_2	100 % ThO_2
97-11,27,32,&49	33.8 w/o U^EO_2 + in ThO_2	100 % ThO_2
97-45	30.3 w/o U^EO_2 + in ThO_2	100 % ThO_2
97-29,30,32&34	36.9 w/o U^EO_2 + in ZrO_2 + 5 w/o CaO	100 % ThO_2
97-47	25.7 w/o U^EO_2 + in ZrO_2 + 5 w/o CaO	100 % ThO_2
97-15,16,19,20,21,22,&25	34.0 w/o U^EO_2 + in ZrO_2	100 % ThO_2
ALT1 Test		
97-67,74,&75	U^EO_2	N/A
97-69,70,&76	U^EO_2	100 % ThO_2
97-91&112	5.3 w/o U^EO_2 + ThO_2	N/A
97-86,87,89,&101	11.4 w/o U^EO_2 + ThO_2	N/A
97-73,80,99D,107,&120	27.3 w/o U^EO_2 + ThO_2	100 % ThO_2

97-72,77,&115	36.3 w/o U^EO_2 + 58.7 w/o ZrO_2 + 5 w/o CaO	100 % ThO_2
ALT2 Test		
97-83,95D,&109	U^EO_2	N/A
97-113&127	5.3 w/o U^EO_2 + ThO_2	N/A
97-43,93,103,110,116D,&122	11.4 w/o U^EO_2 + ThO_2	N/A
97-96D	ThO_2	N/A
97-92	U^EO_2	100 % ThO_2
97-84	27.3 w/o U^EO_2 + ThO_2	100 % ThO_2
97-51D&108	36.3 w/o U^EO_2 + 58.7 w/o ZrO_2 + 5 w/o CaO	100 % ThO_2
LDR Test		
	22.8 w/o U^EO_2 + 77.2 w/o U^DO_2	100 % ThO_2
	33.8 w/o U^EO_2 + 66.2 w/o ThO_2	100 % ThO_2
97-57	35.8 w/o U^EO_2 + 59.2 w/o ZrO_2 + 5 w/o CaO	100 % ThO_2
NLDR Test		
	22.8 w/o U^EO_2 - U^DO_2	100 % ThO_2
	35.5 w/o U^EO_2 - ThO_2	100 % ThO_2
97-61	35.8 w/o U^EO_2 + 59.2 w/o ZrO_2 + 5 w/o CaO	100 % ThO_2

BOL Binary Fuel Composition

Test	Composition	Test	Composition	Test	Composition
ACT-LPR	2.6 w/o $^{235}UO_2$-ThO_2	L12-LSBR	20.5 w/o U^EO_2 + ThO_2	M13-S2A	20.3 w/o $^{235}UO_2$-ThO_2
B1	2.0 w/o $^{235}UO_2$-ThO_2	L12-LSBR	29 w/o U^EO_2 + U^DO_2	M13-S2A	8.9 w/o $^{235}UO_2$-ThO_2
B1M	2.8 w/o $^{235}UO_2$-ThO_2	LBR	3.4 w/o $^{235}UO_2$-ThO_2	M13-S3	12 w/o $^{233}UO_2$-ThO_2
B1R	2.0 w/o $^{235}UO_2$-ThO_2	LSR	22.6 w/o $^{235}UO_2$-ThO_2	M13-S3	16.3 w/o $^{235}UO_2$-ThO_2
B3 & B3A	13 w/o $^{235}UO_2$-ThO_2	LWBR-PFB	2.73 w/o $^{233}UO_2$-ThO_2	M13-S3A	3.06 w/o $^{235}UO_2$-ThO_2
B3 & B3A	20 w/o $^{235}UO_2$-ThO_2	LWBR-SB	1.21 w/o $^{233}UO_2$-ThO_2	M13-S3A	8.36 w/o $^{233}UO_2$-ThO_2
B3 & B3A	30 w/o $^{235}UO_2$-ThO_2	LWBR-SB	1.66 w/o $^{233}UO_2$-ThO_2	NLBR	3.1 w/o $^{235}UO_2$-ThO_2
B3 & B3A	6 w/o $^{235}UO_2$-ThO_2	LWBR-SB	2.00 w/o $^{233}UO_2$-ThO_2	NLSR	19.2 w/o $^{235}UO_2$-ThO_2
BBT	17.1 w/o $^{235}UO_2$-ThO_2	LWBR-S	4.33 w/o $^{233}UO_2$-ThO_2	PBIT	100 % ThO_2
GRIP-I	24.7 w/o $^{235}UO_2$-ThO_2	LWBR-S	5.20 w/o $^{233}UO_2$-ThO_2	PBIT	5.9 w/o U^EO_2 + U^DO_2
GRIP-I	7.7 w/o $^{235}UO_2$-ThO_2	M13-S2	4.9w/o $^{235}UO_2$-ThO_2	PBIT	7.7 w/o U^EO_2 + ThO_2
GRIP-II	6.6 w/o $^{233}UO_2$-ThO_2	M13-S2	7.7 w/o $^{235}UO_2$-ThO_2	SABRE	U^NO_2
GRIP-IIIA	4.5 w/o $^{235}UO_2$-ThO_2	M13-S2	9 w/o $^{235}UO_2$-ThO_2	SIDR	3.06 w/o $^{235}UO_2$-ThO_2
GRIP-IIIB	3.6 w/o $^{235}UO_2$-ThO_2	M13-S2A	12.6 w/o $^{235}UO_2$-ThO_2	SIDR	8.36 w/o $^{235}UO_2$-ThO_2
GRIP-IIIC	4.5 w/o $^{235}UO_2$-ThO_2	M13-S2A	16.2 w/o $^{235}UO_2$-ThO_2	SWLD	1.92 w/o $^{235}UO_2$-ThO_2

The theoretical densities of binary UO_2-ThO_2 fuel for various mole percentages of UO_2 are given below in Table 4[2].

TABLE 4 – THEORETICAL DENSITIES OF UO_2-ThO_2 FUEL

Composition (mole % UO2)	Theoretical Density (g/cc)
100	10.96
90.1	10.85
80.1	10.75
69.9	10.65
60.1	10.55
50.1	10.46
40.3	10.37
30.1	10.28
20.2	10.18
10.1	10.09
0	10.00

3.2 General cladding description[3,4]

Both recrystallized annealed (RXA) and stress relief annealed (SRA) conditions were used for the Zircaloy-4 cladding; the properties (before pickling to final dimensions) are given below in Table 5. The outside diameter of the RXA tubing was decreased by about 4 mils to produce an outside diameter-to-thickness ratio (OD/t) of 13.9 which is representative of the LWBR seed rod design. The SRA tubing diameter was decreased by about 11 mils to produce an OD/t of 16.0, which is typical of commercial reactor practice.[3] The outside diameters reductions were achieved by pickling in a mixture of hydrofluoric and nitric acids following fuel rod assembly.

TABLE 5 – CLADDING PROPERTIES FOR D1 AND LDR TESTS

Property	RXA	SRA
As Fabricated outside Diameter (mil)	308±1	308±1
Inside Diameter (mil)	259±1	259±1
Wall Thickness (mil)	24.5	24.5
Final Heat Treatment (°F/hr)	1225/4	925/4
Cold-work, last of 3 Passes (%)	51	51
ASTM Grain Size	10	NA
Longitudinal Tensile Properties at 700°F		
0.2% Yield Stress (psi)	19,000	44,000
Ultimate-to-Yield Ratio	1.73	1.27
Total Elongation (%)	34	13
Contractile Strain Ratio	1.44	1.35
Chemistry (Billet Analysis)		
Hafnium (ppm)	23	23
Hydrogen (ppm)	4	4
Nickel (ppm)	30	30
Nitrogen (ppm)	30	30
Oxygen (ppm)	1300	1300

3.3 Destructive Examination[5]

3.3.1 Metallographic Samples

After collection of internal atmosphere gases, LWBR irradiation test fuel rods were sectioned to provide samples for measuring depletion, fluence, and hydrogen content and for metallographic evaluation. The metallographic samples were carefully mounted to preserve the corrosion oxide. Each piece was pressure-mounted by immersion in an epoxy resin (Hysol pressurized to 1000 psi) to lock fuel pieces in place. A silicone rubber sleeve was used to isolate the outside cladding surface from the Hysol while it was immersed in Hysol for 24 hours at room temperature. The Hysol was cured for two hours at 200°F. The pressure-mounted pieces were sectioned with a diamond cutoff wheel to provide both transverse and longitudinal metallographic samples. Transverse samples were mounted on end in metallographic rings so that grinding exposed a plane perpendicular to the axis of the rod. Longitudinal samples were mounted on their side; when ground, they revealed a plane parallel to the axis.

Metallographic planes of transverse and longitudinal rod sections were evaluated first in the as-polished state at magnifications from 5-1000X to observe the microscopic condition of cladding and fuel and corrosion of the cladding surface. Oxide thickness measurements were obtained from the metallographic cross section at random locations of each cladding sample. After the corrosion thickness measurements were made, cladding was etched with an H_2O_2-HNO_3 solution with HF additive to reveal the degree and distribution of hydride precipitates. An image-analyzing computer was used to determine the total porosity and porosity-size distributions in the duplex pellet annuli. The dimensions of the duplex pellet components in the transverse metallographic samples were measured and, along with the fuel length changes derived from neutron radiography, were used to determine the effects of porosity changes and swelling effects on the fuel volume.

3.3.2 Hydrogen Measurements

A manometer vacuum extraction method was used to measure hydrogen contents of the irradiated Zircaloy-4 cladding samples. This procedure uses induction heating of the cladding sections in a vacuum system. Gases evolved by vacuum extraction at 1000°C are collected, and hydrogen gas is isolated by diffusion through a palladium membrane permeable only to hydrogen. The amount of hydrogen is determined from the pressure, volume, and temperature. The overall accuracy of this method is ±10 ppm at the 2-sigma level based on measurements with standard samples obtained from the National Bureau of Standards. The hydrogen content of unirradiated companion cladding samples was subtracted from the irradiated Zircaloy-4 hydrogen values to estimate the increase in hydrogen (hydrogen pickup) due to corrosion.

3.3.3 Dissolution for analysis

Chemical analysis was used to determine the total amount of iodine and cesium present on the cladding inside surface and inside the cladding material.

For depletion analysis, aliquots of the dissolved fuel solution were separated and treated prior to using mass spectrographic determination of the uranium isotopes. The activities of ^{137}Cs, ^{144}Ce, and ^{95}Zr were measured by gamma-ray spectrometry. To determine the depletion in terms of fissions/cc, calculations of post-irradiation nuclide inventory were performed based on the pre-irradiation characteristics and the irradiation history.

For fluence (fast neutron flux exposure) determination, ^{54}Mn is measured by gamma-ray spectrometry and Fe is determined by atomic absorption analysis using NBS Zircaloy-2 360a Standard Reference Material. Fluence is determined from the transmutation of ^{54}Fe, present as an alloying agent in the Zircaloy cladding, to ^{54}Mn by means of an n,p reaction. Accounting for the irradiation history of the test rod and the decay of ^{54}Mn, the number of ^{54}Mn atoms produced per milligram of ^{54}Fe in the sample is derived; this quantity is proportional to the time integrated nuclear reaction rate, and when divided by the appropriate energy averaged nuclear cross section, yields the fluence.

3.4 Non-Destructive Examinations

Non-destructive examinations of the rods consisted of visual examinations, dimensional measurements, gamma ray scanning, and neutron radiography; dimensional measurements consisted of measuring the overall length and diameter of the cladding; gamma ray scanning and neutron radiography were used to determine the condition of the internal rod components. Non-destructive examinations of rods with intentional cladding penetrations consisted of the above plus examining the flow patterns downstream from the intentional defect holes.

4. STORAGE

4.1 Storage Canister

The Light Water Breeder Reactor (LWBR) and irradiation test fuel is contained in one basic fuel handling unit (FHU) scrap Type D storage liner or canister. The FHU identification number is engraved on the liner closure head. The canister contains 1) irradiated and unirradiated intact rods, 2) intact rods with intentional defects, 3) intact rod bundles, 4) and rod sections.

The fuel is stored in several containers inside the canister: metal O-ring sealed containers (MOSC), rubber O-ring sealed Cut Fuel Storage Container (CFSC), Rod Alpha Container (RAC), rubber O-ring sealed metallographic container (MEL), Sealed Tube (ST), Unsealed Tubes (UT) and rubber O-ring sealed LWBR Storage Tube (StT). Figures 1 through 9 illustrate the containers and loading in the canister[1].

The intact rods and rod bundles are housed in 22 UT and a special storage compartment. Intact defected rods, unirradiated intact rods, and rod sections are contained in nine MOSC. Further details of the storage canister is summarized as follows:

22 UT containing
- 20 of the tubes contain 225 intact rods
- 2 of the tubes contain intact rod bundles (LDR & GRIP-I bundles)

A special storage 3" square compartment of a metal spider containing
- Intact rods
- The intact rod bundle from the PBIT Test

8 MOSC (6" OD) containing:
- 89 RACs containing:
  - ✓ Rod sections
  - ✓ 3 intact rods
  - ✓ 6 intact defected rods

A MOSC (8" OD) containing:
- A MEL canister and 6 CFSCs containing short intact rods and rod sections
- 8 LWBR StT containing LWBR rod sections
- A ST containing:
  - ✓ 2 intact defected rods
  - ✓ 9 short intact rods
  - ✓ 6 Special Physics Test fuel rods

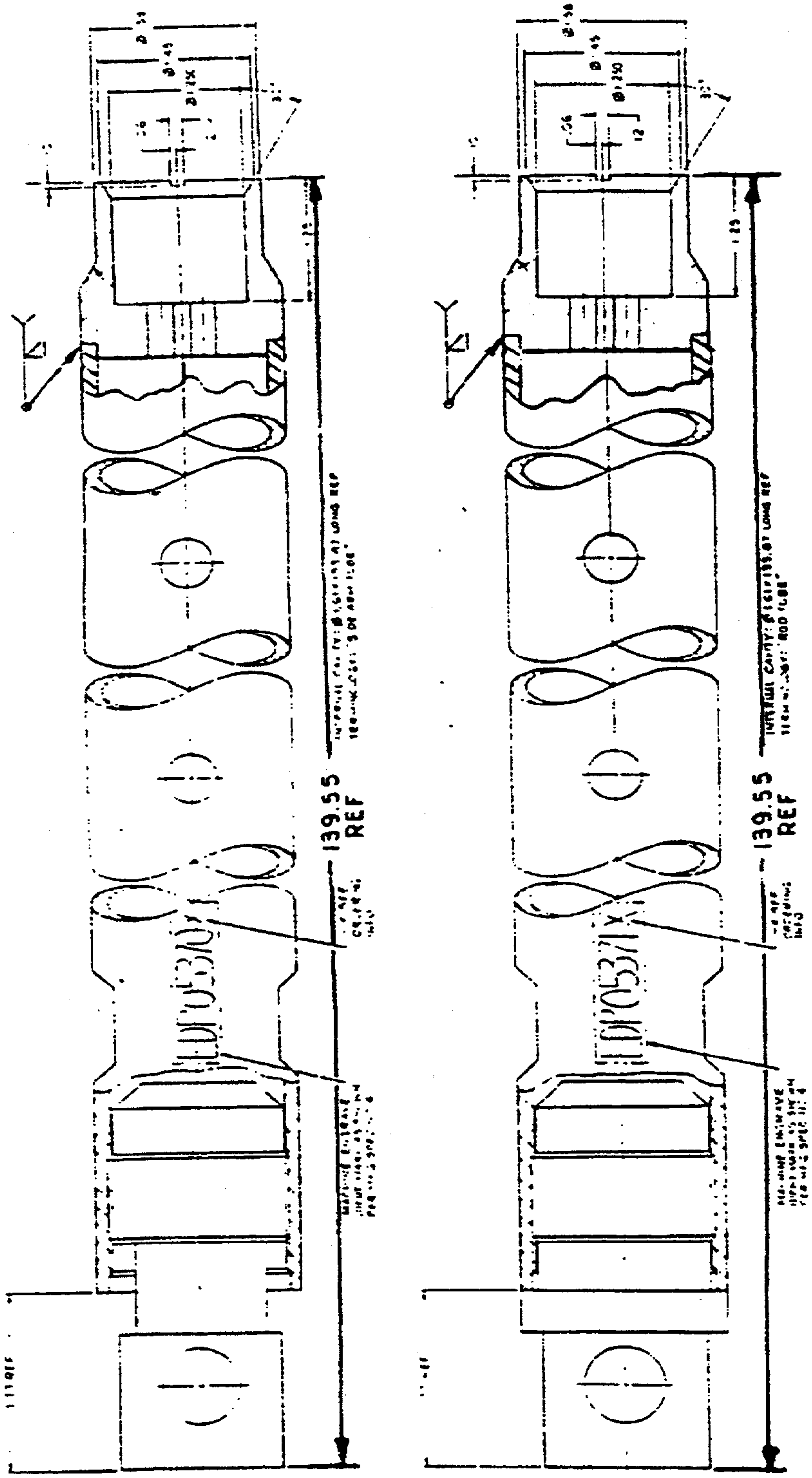

Figure 1 – Unsealed Storage Tube

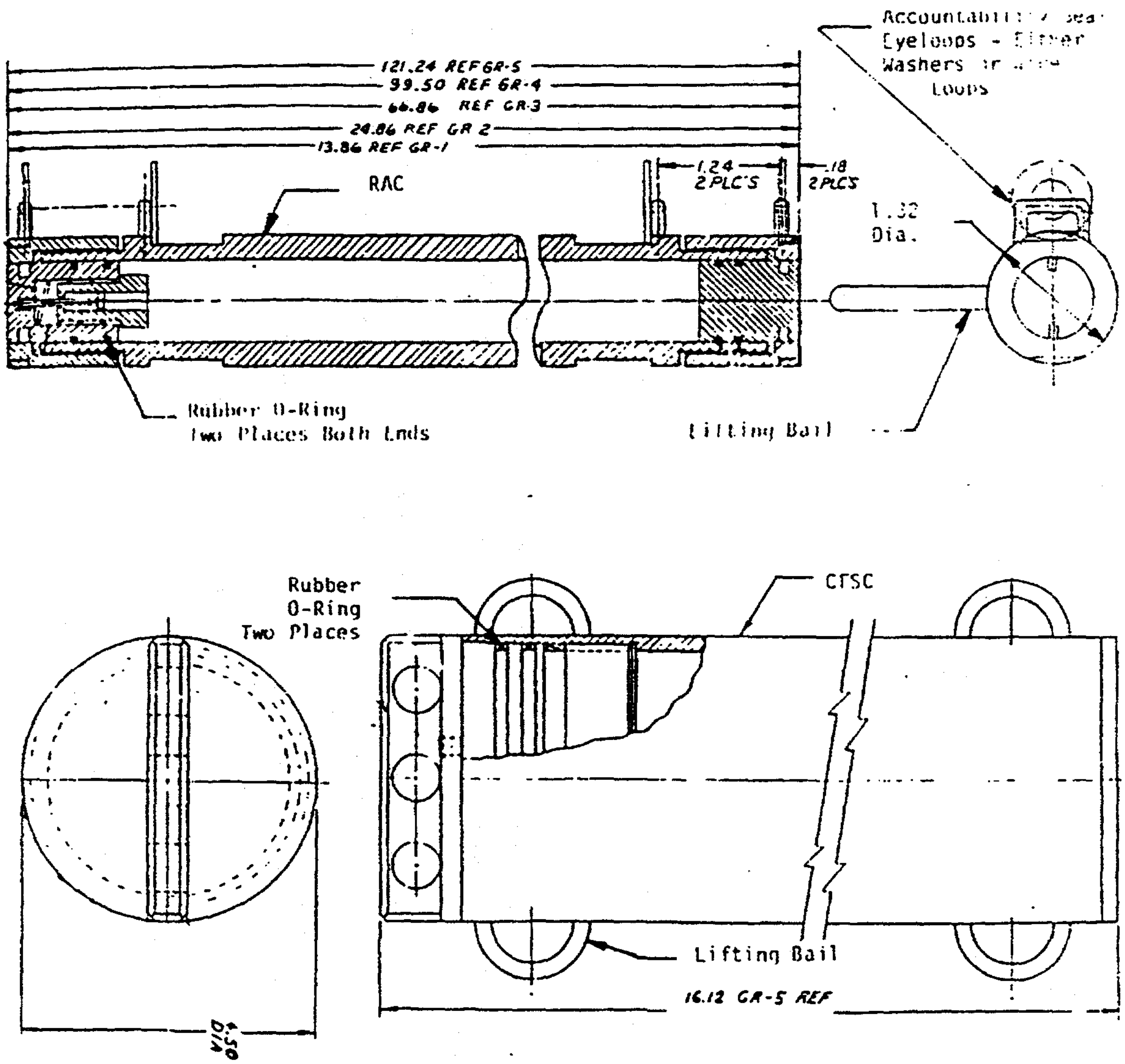

Figure 2 – Rod Alpha Containers and Cut Fuel Storage Containers

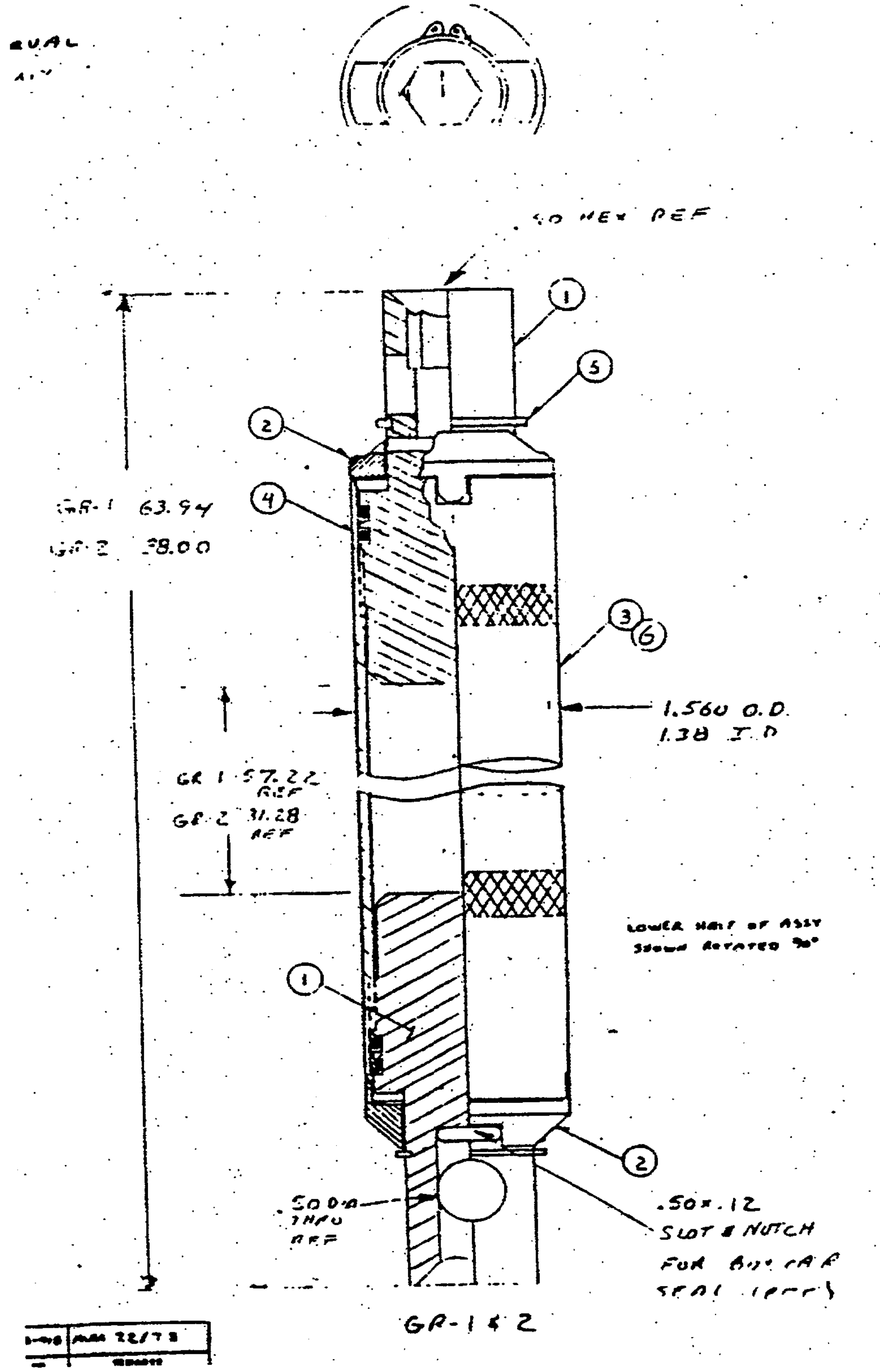

Figure 3 – Cut LWBR Fuel Rod Storage Tube

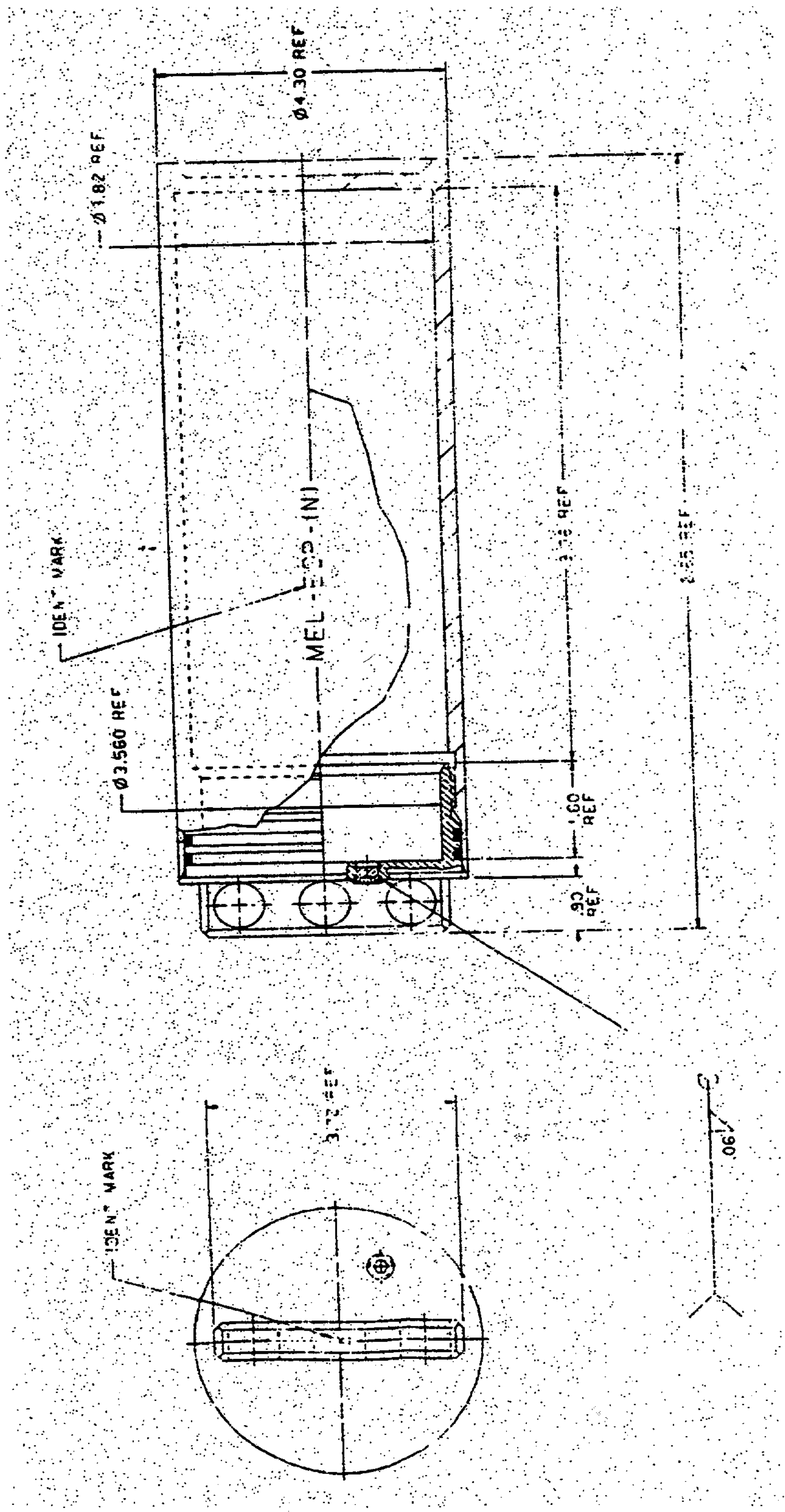

Figure 4 – Sealed MEL Container

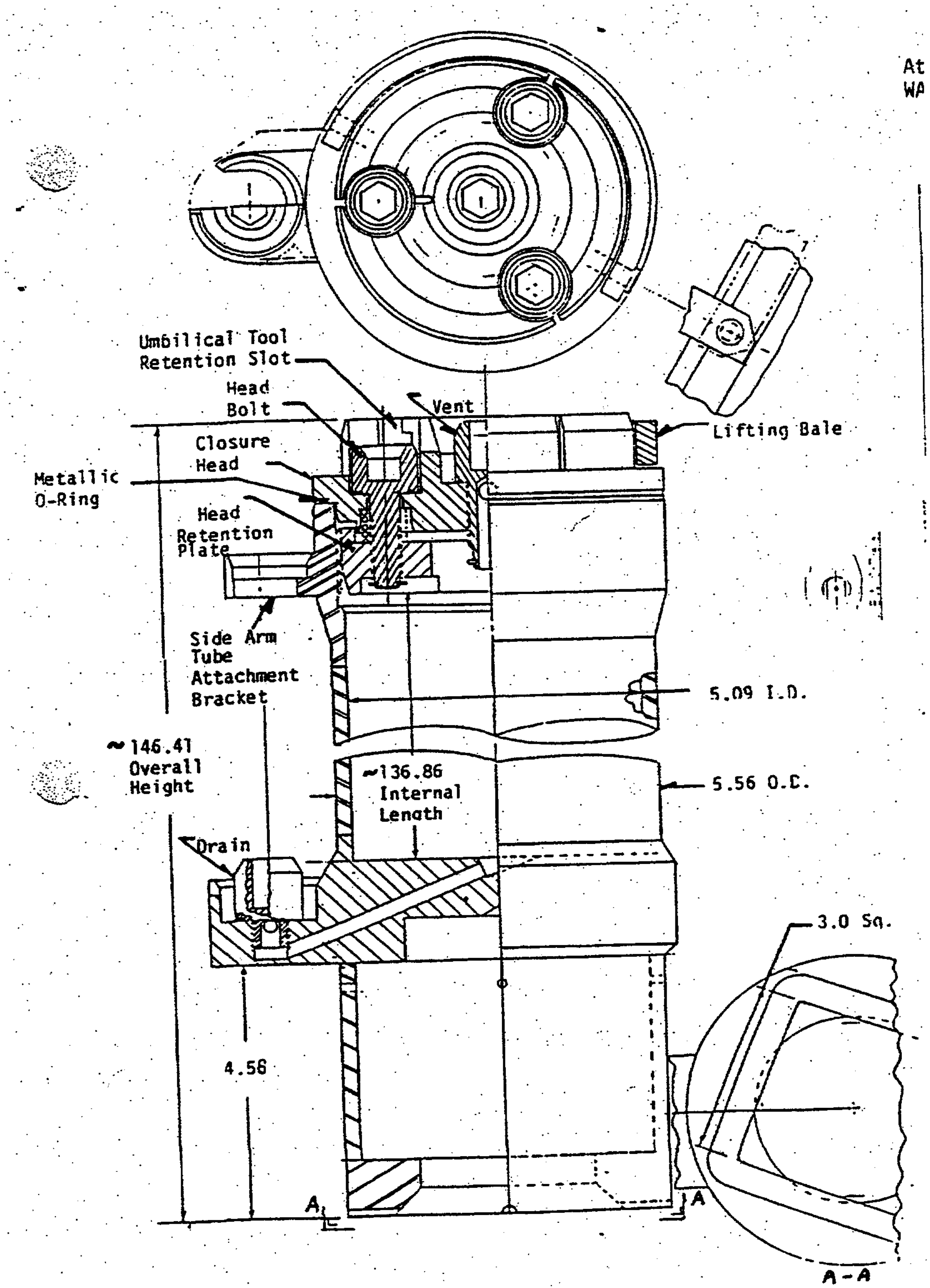

Figure 5 – 6" OD Metal O-Ring Sealed Containers

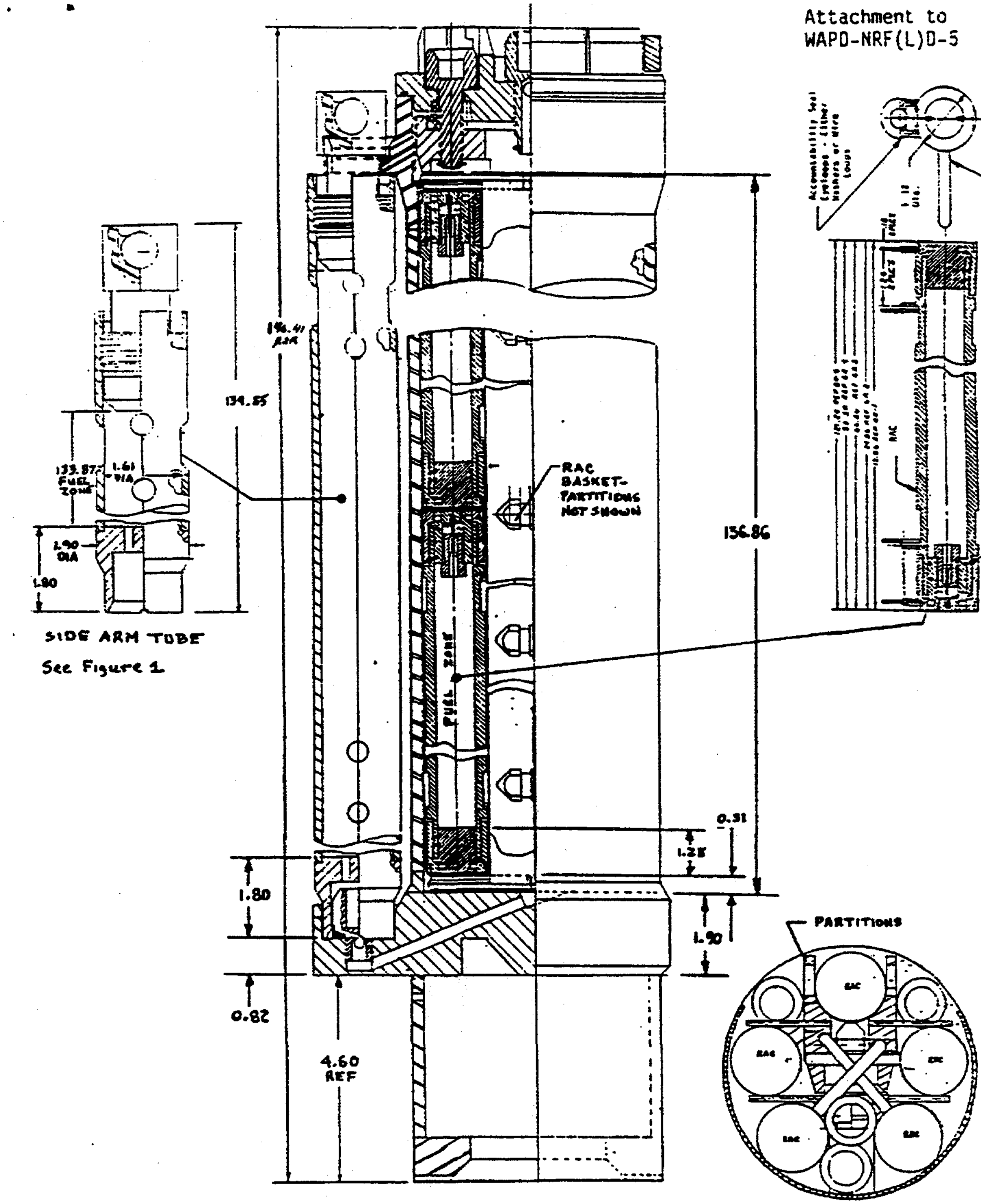

Figure 6 – Axial Loading of 6" Sealed Container

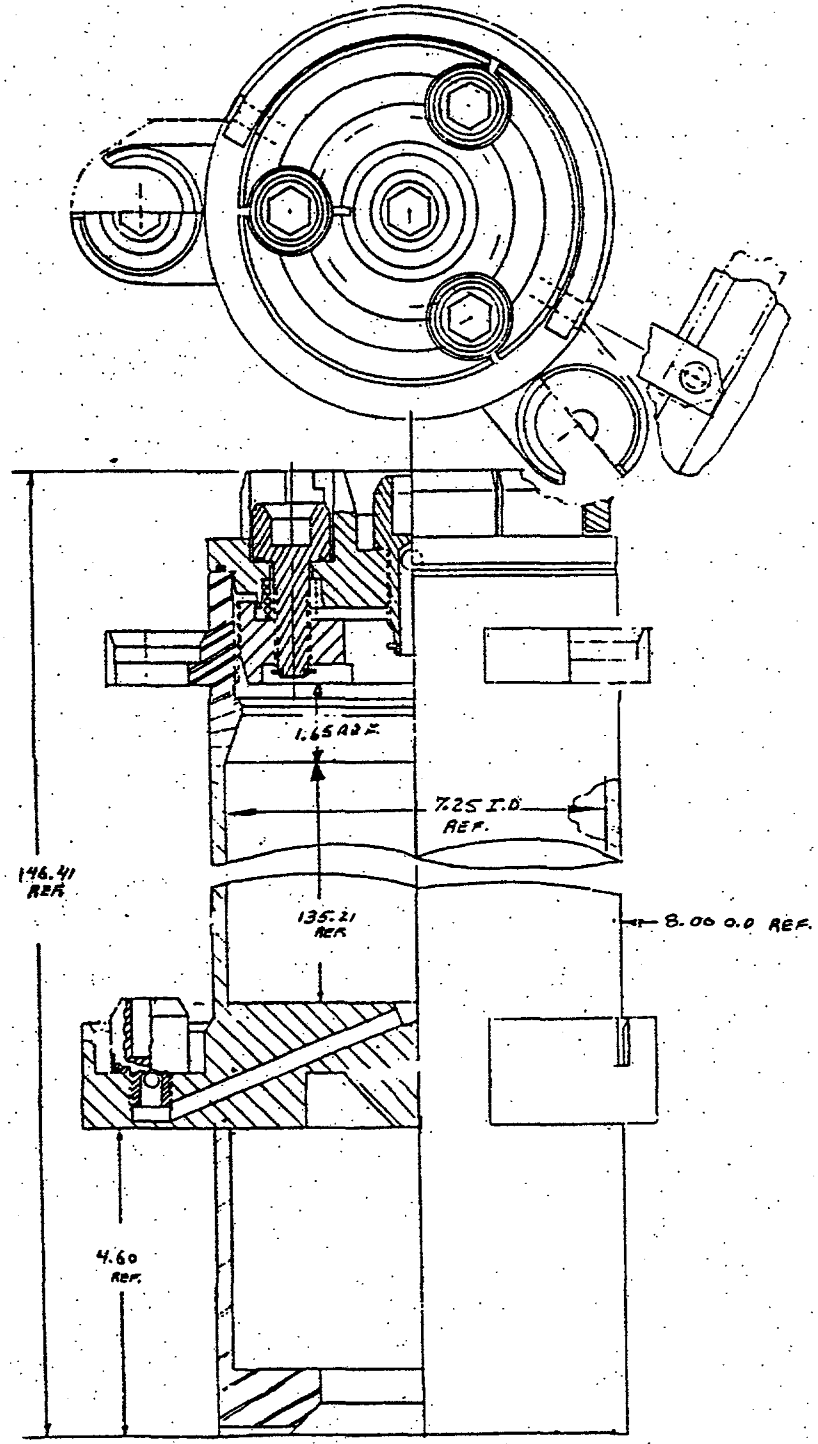

Figure 5 – 8" OD Metal O-Ring Sealed Container

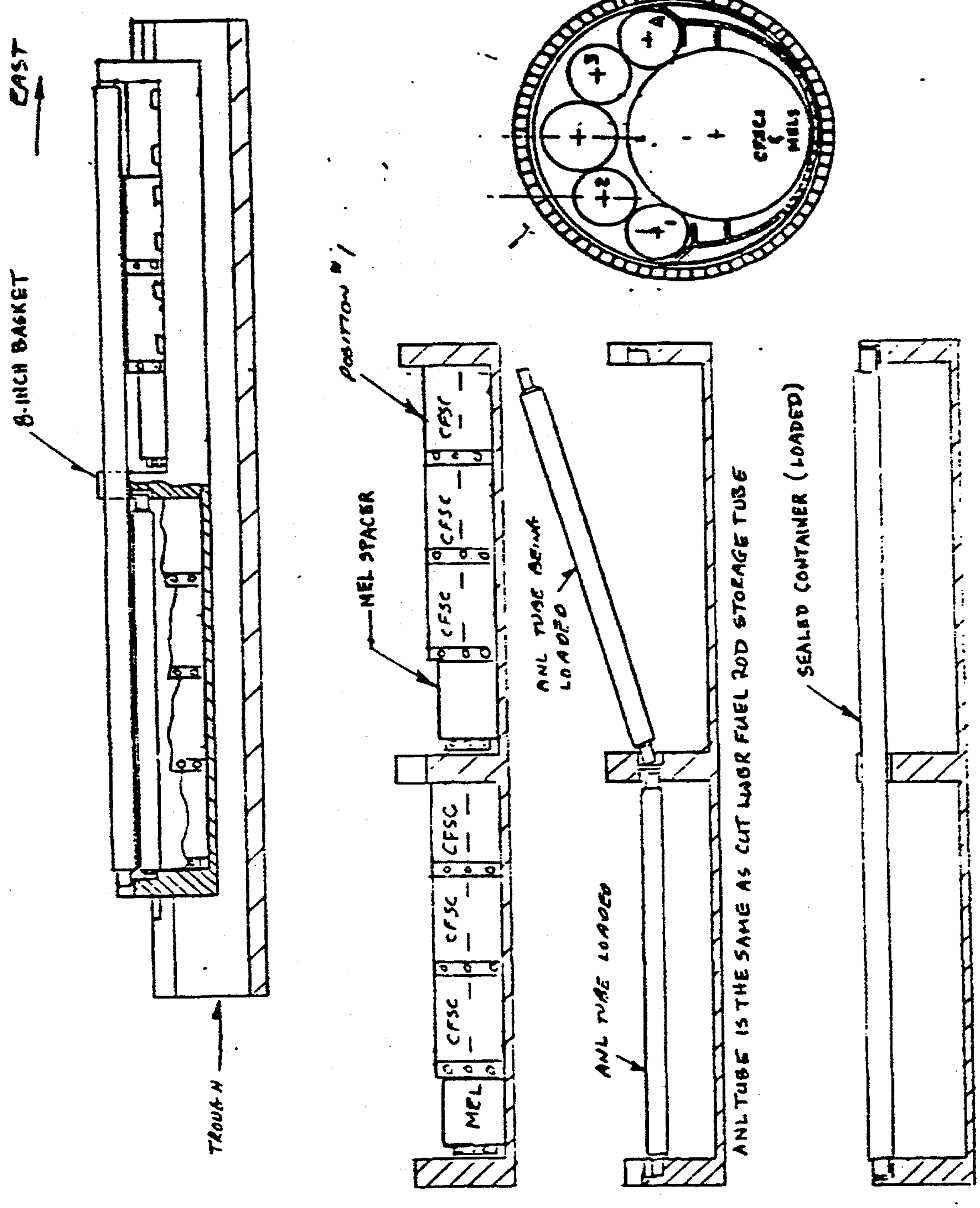

Figure 6 – Loading of the 8" OD Container

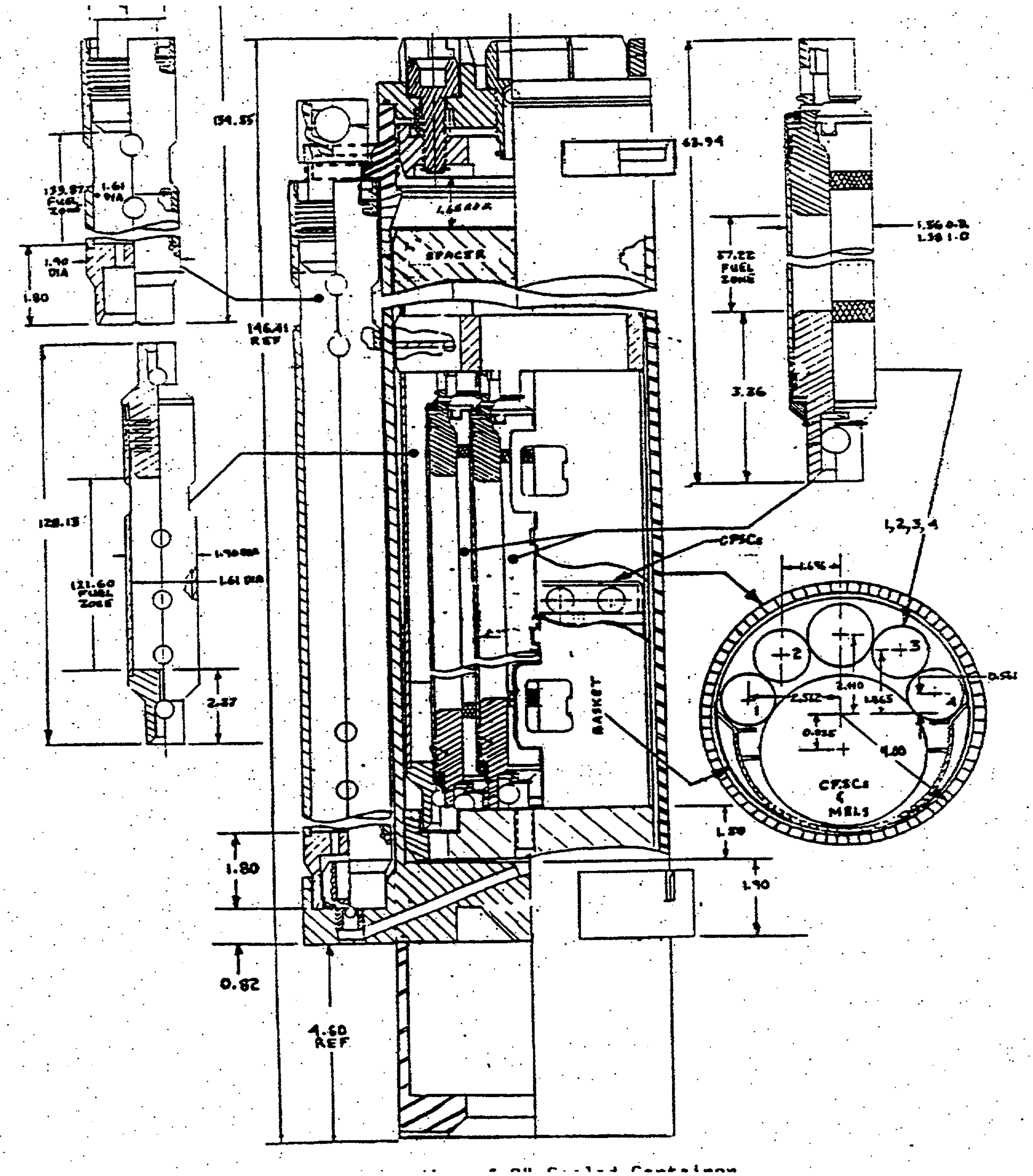

Figure 7 – Axial Loading of 8" OD Sealed Container

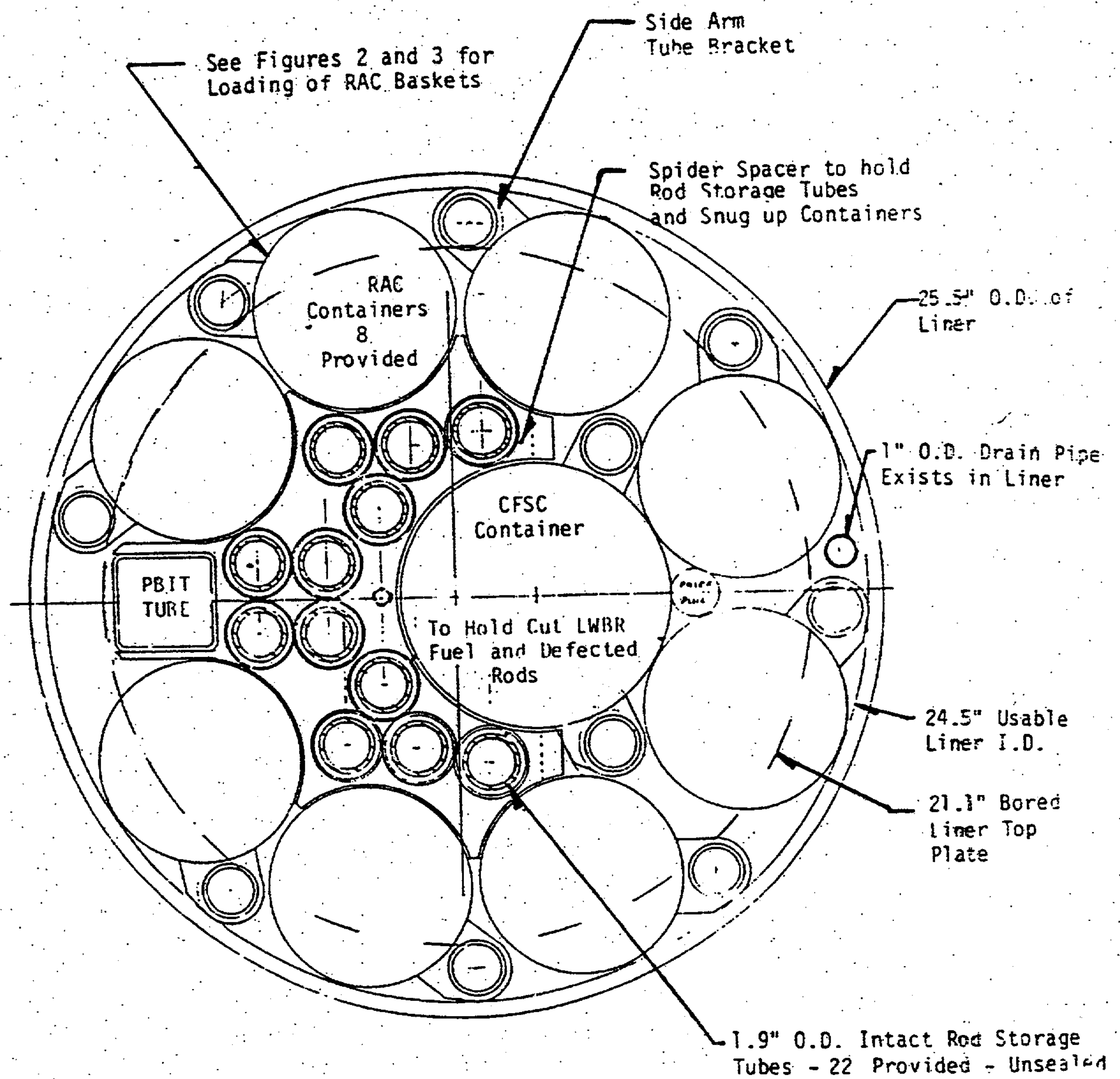

Figure 8 – Internal Loading Arrangement of the Scrap Canister

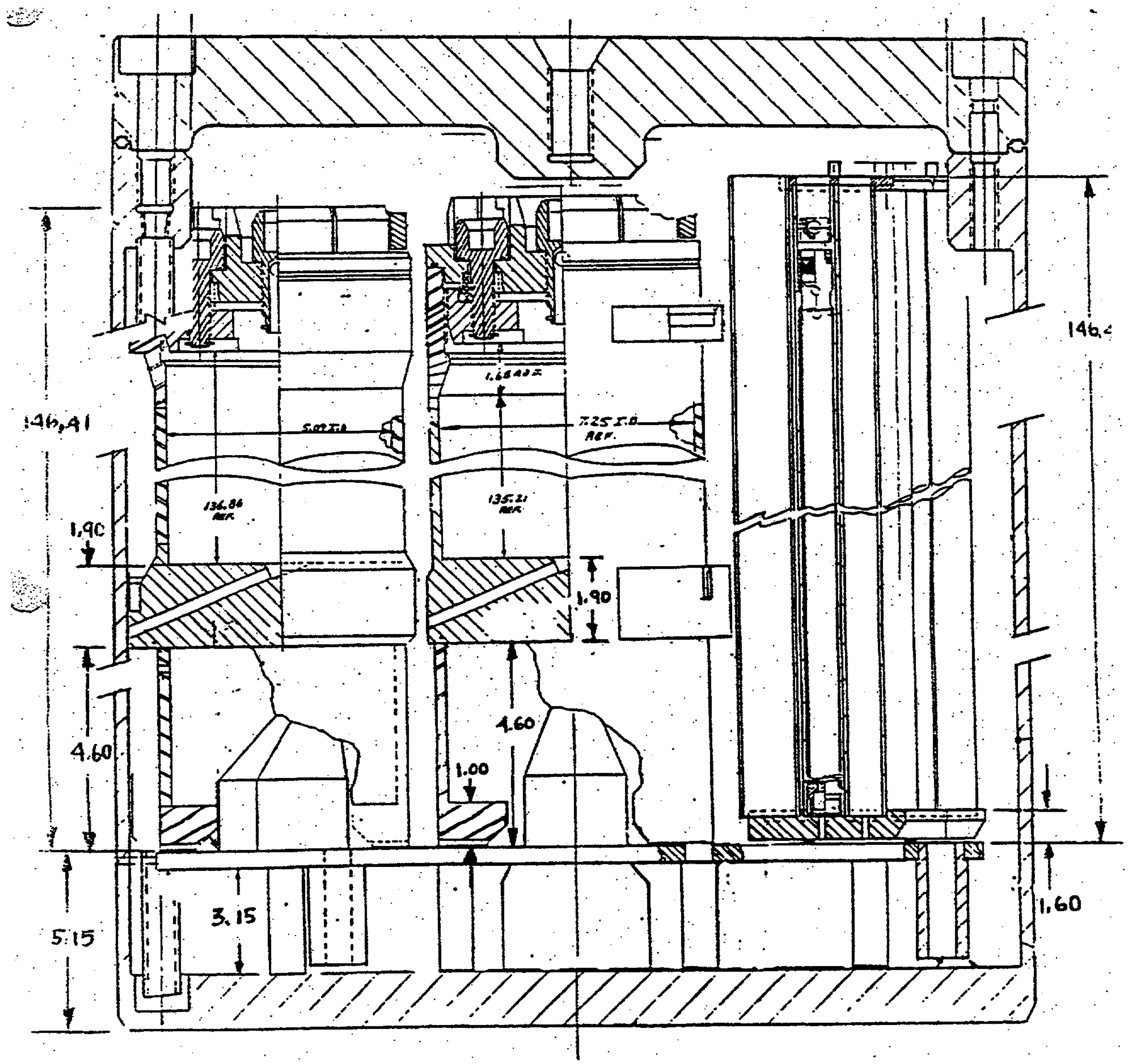

Figure 9 – Axial Loading of the Scrap Canister

The container serial numbers are given in the following Table[1].

TABLE 6 – CONTAINER SERIAL NUMBERS

Container	Serial #	Container	Serial #	Container	Serial #
Scrap canister	15718	RAC	26	RAC	75
6" OD MOSC	EDP 05373A	RAC	27	RAC	76
6" OD MOSC	EDP 05373B	RAC	28	RAC	78
6" OD MOSC	EDP 05373C	RAC	29	RAC	79
6" OD MOSC	EDP 05373D	RAC	30	RAC	80
6" OD MOSC	EDP 05373E	RAC	31	RAC	81
6" OD MOSC	EDP 05373F	RAC	32	RAC	82
6" OD MOSC	EDP 05373G	RAC	33	RAC	83
6" OD MOSC	EDP 05373H	RAC	34	RAC	89
8" OD MOSC	EDP 05374	RAC	35	RAC	90
CFSC	1	RAC	36	RAC	91
CFSC	2	RAC	37	RAC	92
CFSC	11	RAC	38	RAC	93
CFSC	14	RAC	39	RAC	94
CFSC	73	RAC	40	RAC	96
CFSC	115	RAC	41	RAC	97
LWBR StT	EDP 05376A	RAC	42	RAC	97-85
LWBR StT	EDP 05376B	RAC	43	RAC	98
LWBR StT	EDP 05376C	RAC	44	RAC	99
LWBR StT	EDP 05376D	RAC	45	RAC	100
LWBR StT	EDP 05376E	RAC	47	RAC	101
LWBR StT	EDP 05376F	RAC	48	RAC(deleted)	97-87
LWBR StT	EDP 05376G	RAC	49	ST	EDP 05395
LWBR StT	EDP 05376H	RAC	51	UT	EDP 05370A
MEL	EDP 05388A	RAC	52	UT	EDP 05370B
RAC	1	RAC	53	UT	EDP 05370C
RAC	2	RAC	54	UT	EDP 05370D
RAC	3	RAC	55	UT	EDP 05370E
RAC	4	RAC	56	UT	EDP 05370F
RAC	5	RAC	57	UT	EDP 05370G
RAC	7	RAC	58	UT	EDP 05370H
RAC	8	RAC	59	UT	EDP 05370J
RAC	9	RAC	60	UT	EDP 05370K
RAC	10	RAC	61	UT	EDP 05371A
RAC	12	RAC	62	UT	EDP 05371B
RAC	13	RAC	63	UT	EDP 05371C
RAC	14	RAC	64	UT	EDP 05371D
RAC	17	RAC	65	UT	EDP 05371E
RAC	18	RAC	66	UT	EDP 05371F
RAC	19	RAC	67	UT	EDP 05371G
RAC	20	RAC	68	UT	EDP 05371H
RAC	21	RAC	69	UT	EDP 05371J
RAC	22	RAC	70	UT	EDP 05371K
RAC	23	RAC	72	UT	EDP 05371L
RAC	24	RAC	73	UT	EDP 05371M
RAC	25	RAC	74		

A listing of the 624 pieces with the uranium and thorium content of the scrap canister is given in the following Table below[1]. The EDP# is the assigned ECF reference number. The following abbreviations are used: TR – Test Rod, TRS – Test Rod Section, FRS – Fuel Rod Section, U – Unirradiated Intact Rods, I – Irradiated Intact Rods, D – Irradiated Defected Intact Rods, P – Parent of Irradiated Rod Sections IB – Irradiated Rod Bundle and Conf. – configuration. ID numbers started with a "M" are from sectioned rods. The Table is sorted by Core and then ID.

TABLE 7 – SCRAP CANISTER URANIUM AND THORIUM CONTENT (BOL) BY PIECE

Ref#	EDP#	Core	Conf.	ID	Type	U, g	U^{235}, g	Th, g	U^{233}, g	U^N, kg	U^D, kg
394	44445	ALT1	TR	97-101		5.27	4.91	0.05			
421	44571	ALT1	TR	97-107		5.09	4.74	0.05			
396	44441	ALT1	TR	97-112		2.52	2.35	0.05			
423	45064	ALT1	TR	97-115		4.74	4.41	0.04			
424	44656	ALT1	TR	97-120	U	5.51	5.13	0.05			
398	44699	ALT1	TR	97-67	I	46	5	0.01			
431	44706	ALT1	TR	97-70	I	20	5	0.04			
399	44654	ALT1	TR	97-73	I	5.52	5.14	0.05			
367	44701	ALT1	TR	97-75	I	23	3	0.04			
400	44707	ALT1	TR	97-76	I	20	5	0.04			
570	44442	ALT1	TR	97-85		5.2	4.84	0.05			
402	44443	ALT1	TR	97-86	I	5.26	4.9	0.05			
369	44569	ALT1	TR	97-87	I	5.22	4.86	0.05			
403	44444	ALT1	TR	97-89	I	5.22	4.86	0.05			
404	44440	ALT1	TR	97-91	I	2.67	2.49	0.05			
382	45062	ALT2	TR	97-103		5.39	5	0.05			
363	45063	ALT2	TR	97-108		4.69	4.36	0.04			
422	44703	ALT2	TR	97-109		30	3	0.03			
395	44899	ALT2	TR	97-110		4.43	4.11	0.05			
384	45222	ALT2	TR	97-113		3	3	0.05			
385	44902	ALT2	TR	97-122	U	5.36	4.98	0.05			
386	45223	ALT2	TR	97-127	U	3	3	0.05			
533	44900	ALT2	TR	97-166D		5.3	4.92	0.05			
389	44897	ALT2	TR	97-43	I	5.36	4.97	0.05			
535	45055	ALT2	TR	97-51D	D	4.58	4.26	0.04			
392	45058	ALT2	TR	97-83	I	23.32	2.92	0.03			
435	44710	ALT2	TR	97-84	I	5	5	0.05			
393	44709	ALT2	TR	97-92	I	20	4	0.04			
405	44898	ALT2	TR	97-93	I	5.3	4.92	0.05			
571	45060	ALT2	TR	97-95D	D	46.99	5.52	0.01			
572	44658	ALT2	TR	97-96D	D			0.06			
536	53962	ALT2 ECFBARL	CHPS	97-121 CHIPS	P	0.45	0.42	0.01			
464	19782	B1	TR	79-427	I	19.79	18.4	2.06			
465	19781	B1	TR	79-430	I	19.62	18.3	2.05			
472	35391	B1	TR	79-577	I	18	16.8	2.1			
377	37882	B1M	TRS	79-573 Top Sec	P			1.15			
609	26774	B1M	TR	87-104I	I	0.65	0.61				
540	26775	B1M	TR	87-105	I	0.66	0.61				
541	26776	B1M	TR	87-106	I	0.65	0.61				
542	26777	B1M	TR	87-107	I	0.65	0.61				
543	24281	B1M	TR	87-111I	I	0.97	0.91				

TABLE 7. CONTINUED.

Ref#	EDP#	Core	Conf.	ID	Type	U, g	U^{235}, g	Th, g	U^{233}, g	U^N, kg	U^D, kg
544	24282	B1M	TR	87-112I	I	0.98	0.91				
545	24283	B1M	TR	87-113I	I	0.98	0.91				
546	24284	B1M	TR	87-114I	I	0.96	0.9				
547	26781	B1M	TR	87-115	I	0.97	0.9				
586	16443	B1M	TR	87-35 (B1M-369-3-ZR)	I	0.95	0.88				
9	37278	B1M	TRS	M2131		0.86	0.7	0.15			
525	43258	B1M	TRS	M2134		0.59	0.56	0.02			
10	37292	B1M	TRS	M2136		3.01	2.82	0.1			
11	37296	B1M	TRS	M2138		4.22	3.95	0.15			
12	37311	B1M	TRS	M2143		3.36	3.15	0.13			
13	37487	B1M	TRS	M2146				1.18			
207	37400	B1M	TRS	M2198		0.37	0.35	0.01			
208	37402	B1M	TRS	M2200		0.2	0.17	0.01			
209	37405	B1M	TRS	M2202		0.37	0.35	0.01			
210	37407	B1M	TRS	M2204		0.2	0.17	0.01			
21	37970	B1M	TRS	M2501		13.02	12.1	0.56			
22	38009	B1M	TRS	M2506		1.71	1.59	0.06			
23	38011	B1M	TRS	M2508		0.58	0.54	0.03			
24	38022	B1M	TRS	M2510		0.43	0.4	0.13			
25	38024	B1M	TRS	M2512		11.48	10.7	0.4			
26	38029	B1M	TRS	M2517		4.02	3.74	0.15			
27	38032	B1M	TRS	M2518				0.62			
28	38036	B1M	TRS	M2520				0.51			
227	39475	B1M	TRS	M2886		0.19	0.18	0.01			
228	39477	B1M	TRS	M2888		0.23	0.21	0.01			
229	39479	B1M	TRS	M2889		0.46	0.43	0.02			
230	39481	B1M	TRS	M2891		0.39	0.36	0.01			
231	39484	B1M	TRS	M2892		0.17	0.16	0.01			
16	40725	B1M	TRS	M3456		0.61	0.57	0.02			
528	43259	B1MA	TRS	M2503		0.57	0.53	0.02			
473	35291	B1RB	TR	79-581	I	19.05	17.8	2.05			
100	42426	B1RB	TRS	M4075		5.77	5.37	0.29			
101	42417	B1RB	TRS	M4079		7.38	6.88	0.36			
102	42415	B1RB	TRS	M4081		0.56	0.53	0.03			
53	42798	B1RB	TRS	M4157		0.24	0.22	0.01			
54	42602	B1RB	TRS	M4159		0.31	0.29	0.02			
55	42805	B1RB	TRS	M4161		0.42	0.39	0.02			
56	42884	B1RB	TRS	M4162		0.24	0.22	0.01			
57	42872	B1RB	TRS	M4164		0.31	0.29	0.02			
58	42865	B1RB	TRS	M4166		0.42	0.39	0.02			
96	42316	B1RB	TRS	Top Sct				1.09			
607	25453	BETT	TCAP	84-20	I	51.09	16.9	0.46			
444	08408	C7B3A	TR	79-299	I	216.3	202	1.45			
445	08409	C7B3A	TR	79-300	I	214.9	200	1.44			
539	08410	C7B3A	TR	79-301	D	338.8	316	1.36			
446	08411	C7B3A	TR	79-302	I	510.3	476	1.19			
447	08412	C7B3A	TR	79-304	I	99.61	92.9	1.56			
448	08413	C7B3A	TR	79-308	I	100.2	93.4	1.57			
449	24220	C7B3A	TR	79-350	I	217.7	203	1.46			
450	14339	C7B3A	TR	79-352	I	213.6	199	1.43			
451	20652	C7B3A	TR	79-356	I	504.4	470	1.18			
452	18946	C7B3A	TR	79-376	I	330	307	1.4			

TABLE 7. CONTINUED.

Ref#	EDP#	Core	Conf.	ID	Type	U, g	U^{235}, g	Th, g	U^{233}, g	U^N, kg	U^D, kg
34	38723	C7B3A	TRS	M2596		18.83	17.6	0.04			
35	38722	C7B3A	TRS	M2597		179.1	167	0.45			
36	38914	C7B3A	TRS	M2644		56.57	52.7	0.14			
37	38909	C7B3A	TRS	M2646		18.9	17.6	0.04			
61	40288	C7B3A	TRS	M3320		154.8	144	0.62			
62	40315	C7B3A	TRS	M3325		125.1	117	0.5			
38	40707	C7B3A	TRS	M3452		9.42	8.79	0.02			
256	40925	C7B3A	TRS	M3563		4.73	4.41	0.02			
97	42317	C7B3A	TRS	M4053		300.2	280	0.71			
98	42338	C7B3A	TRS	M4054		28.34	26.4	0.7			
99	42347	C7B3A	TRS	M4056		36.8	34.3	0.09			
78	42384	C7B3A	TRS	M4059		9.44	8.81	0.02			
79	42385	C7B3A	TRS	M4060		18.84	17.6	0.04			
80	42387	C7B3A	TRS	M4062		75.61	70.5	0.18			
103	42448	C7B3A	TRS	M4099		115.9	108	0.53			
106	42817	C7B3A	TRS	M4167		0.02	0.02	0			
107	42822	C7B3A	TRS	M4169		7.52	7.02	0.03			
285	43046	C7B3A	TRS	M4381		2.86	2.67	0.01			
117	43445	C7B3A	TRS	M4714		25.6	23.9	0.13			
128	43920	C7B3A	TRS	M5002		218.8	204	0.54			
129	43966	C7B3A	TRS	M5007		37.53	35	0.12			
130	44057	C7B3A	TRS	M5011		8.14	7.72	0.02			
471	23542	C7BBT	TR	79-516	I	169.5	158	1.8			
453	35139	C7BBT	TR	79-517	I	169.3	158	1.8			
167	35552	C7BBT	TRS	M1740		54.08	50.4	0.88			
168	35579	C7BBT	TRS	M1748		3.72	3.46	0.02			
169	35584	C7BBT	TRS	M1750		22.37	20.9	0.11			
170	35587	C7BBT	TRS	M1752				0.17			
2	37081	C7BBT	TRS	M2080		42.87	39.9	0.94			
3	37101	C7BBT	TRS	M2085		4.13	3.85	0.02			
4	37116	C7BBT	TRS	M2087				0.05			
524	43257	C7BBT	TRS	M2089				0.01			
5	37125	C7BBT	TRS	M2093				0.59			
6	37139	C7BBT	TRS	M2096				0.59			
7	37141	C7BBT	TRS	M2098		62.82	58.5	0.31			
8	37163	C7BBT	TRS	M2103		49.73	46.3	0.45			
190	37341	C7BBT	TRS	M2163		2.2	2.05	0.01			
191	37343	C7BBT	TRS	M2164		3	2.79	0.02			
192	37345	C7BBT	TRS	M2166		2.25	2.1	0.01			
193	37352	C7BBT	TRS	M2167		2.1	1.95	0.01			
194	37354	C7BBT	TRS	M2169		2.08	1.93	0.01			
195	37354	C7BBT	TRS	M2170		1.45	1.35	0			
196	37361	C7BBT	TRS	M2172		2.74	2.55	0.02			
197	37359	C7BBT	TRS	M2176				0.02			
201	27390	C7BBT	TRS	M2195		0.77	0.71	0			
206	37394	C7BBT	TRS	M2195		2.53	2.36	0.01			
211	37409	C7BBT	TRS	M2205		0.52	0.48	0			
212	37412	C7BBT	TRS	M2207				0			
213	37414	C7BBT	TRS	M2209		1.57	1.47	0.01			
214	37421	C7BBT	TRS	M2212				0			
32	38091	C7BBT	TRS	M2513				0.04			
29	38073	C7BBT	TRS	M2523				0.41			
30	38078	C7BBT	TRS	M2525		38.77	36.1	0.39			

TABLE 7. CONTINUED.

Ref#	EDP#	Core	Conf.	ID	Type	U, g	U^{235}, g	Th, g	U^{233}, g	U^N, kg	U^D, kg
247	43260	C7BBT	TRS	M2529		3.52	3.28	0.02			
31	38088	C7BBT	TRS	M2531		3.53	3.28	0.02			
270	43261	C7BBT	TRS	M2535				0.02			
33	38108	C7BBT	TRS	M2539				0.56			
232	39496	C7BBT	TRS	M2894				0.01			
233	39498	C7BBT	TRS	M2896		1.67	1.56	0.01			
234	39502	C7BBT	TRS	M2899				0			
59	40129	C7BBT	TRS	M3199		81.73	76.1	1			
272	43264	C7BBT	TRS	M3203		3.5	3.26	0.01			
273	40203	C7BBT	TRS	M3204		9.5	8.85	0.05			
60	40204	C7BBT	TRS	M3205		34.59	32.2	0.38			
257	40928	C7BBT	TRS	M3570		1.15	1.1	0			
258	40930	C7BBT	TRS	M3572		1.27	1.21	0.01			
90	42311	C7BBT	TRS	M3897		2.05	1.91	0.23			
91	42287	C7BBT	TRS	M3899		99.33	92.5	1.08			
92	42318	C7BBT	TRS	M3906		102.2	95.3	1.22			
284	42327	C7BBT	TRS	M4082				0.05			
39	42567	C7BBT	TRS	M4156		68.03	63.4	0.55			
517	00514	C7-LSBR	TR	79-174	D	136	69.4				
518	00512	C7-LSBR	TR	79-177	D	136.6	69.7				
519	00513	C7-LSBR	TR	79-187	D	137.2	70				
378	40435	D1	TR	97-10	I	22.05	3.91	0.03			
361	44446	D1	TR	97-102	U	5.21	4.85	0.05			
362	41702	D1	TR	97-104		30	3	0.03			
335	45061	D1	TR	97-105	U	4.69	4.36	0.04			
383	42301	D1	TR	97-11	I	5.96	5.7	0.05			
364	44901	D1	TR	97-117	U	5.31	4.93	0.05			
365	44902	D1	TR	97-118	U	5.36	4.97	0.05			
379	40546	D1	TR	97-12	I	21.8	5.21	0.03			
406	40584	D1	TR	97-15	I	4.77	4.64	0.03			
418	40585	D1	TR	97-16	I	4.82	4.69	0.04			
407	40586	D1	TR	97-19	I	3.96	3.84	0.04			
408	40430	D1	TR	97-2	I	22	3.9	0.03			
409	40587	D1	TR	97-20	I	4.39	4.26	0.04			
380	40588	D1	TR	97-21	I	4.83	4.69	0.03			
410	40590	D1	TR	97-25	I	5.06	4.9	0.04			
397	42307	D1	TR	97-26	I	22.28	5.12	0.03			
387	42304	D1	TR	97-27	I	7.3	6.99	0.05			
419	40577	D1	TR	97-29	I	4.9	4.75	0.03			
411	40431	D1	TR	97-3	I	17.69	3.21	0.04			
412	40578	D1	TR	97-30	I	4.54	4.4	0.04			
413	40579	D1	TR	97-31	I	3.72	3.6	0.04			
388	42305	D1	TR	97-32	I	7.4	7.09	0.05			
381	40530	D1	TR	97-34	I	3.72	3.6	0.04			
534	42308	D1	TR	97-36D	D	22.03	5.07	0.03			
347	40432	D1	TR	97-4	U	19.04	3.43	0.04			
420	40550	D1	TR	97-40	I	18.05	4.42	0.04			
414	40551	D1	TR	97-42	I	21.18	5.09	0.04			
390	43738	D1	TR	97-45	I	6.83	6.63	0.05			
391	43439	D1	TR	97-47	I	3.77	3.65	0.03			
343	42816	D1	TR	97-49	U	7.25	7.05	0.05			
366	45054	D1	TR	97-50	U	4.69	4.36	0.04			
430	44705	D1	TR	97-69	I	19	4	0.04			

TABLE 7. CONTINUED.

Ref#	EDP#	Core	Conf.	ID	Type	U, g	U^{235}, g	Th, g	U^{233}, g	U^N, kg	U^D, kg
432	45056	D1	TR	97-72	I	4.61	4.29	0.04			
433	44700	D1	TR	97-74	I	29	3	0.03			
401	45057	D1	TR	97-77	I	4.71	4.38	0.04			
344	44708	D1	TR	97-78	U	20	5	0.04			
348	40433	D1	TR	97-8	U	23.1	4.07	0.03			
434	44563	D1	TR	97-80	I	5.15	4.8	0.05			
368	44657	D1	TR	97-82	U			0.06			
370	44570	D1	TR	97-88	U	5.25	4.89	0.05			
349	40434	D1	TR	97-9	U	22	3.9	0.03			
345	45059	D1	TR	97-90	U	46.75	5.51	0.01			
346	44711	D1	TR	97-94	U	5	5	0.05			
573	44655	D1	TR	97-99D	D	5.15	4.8	0.05			
549	37072	D1	TRS	M2079		0.04	0.04	0.01			
224	39466	D1	TRS	M2880		0.03	0.03	0			
75	40679	D1	TRS	M3440		0.65	0.61	0.02			
253	43267	D1	TRS	M3443		0.22	0.2	0			
276	40683	D1	TRS	M3445		0.03	0.03	0			
277	40685	D1	TRS	M3447		0.1	0.09	0			
550	40735	D1	TRS	M3460		0.05	0.04	0			
161	41424	D1	TRS	M3794		2.3	0.55	0.01			
280	41451	D1	TRS	M3795				0			
51	41437	D1	TRS	M3803		2.42	2.35	0.02			
52	41433	D1	TRS	M3806		0.65	0.63	0.01			
268	41443	D1	TRS	M3807		0.16	0.15	0			
180	41658	D1	TRS	M3810		2.25	2.18	0.02			
181	41655	D1	TRS	M3813		0.63	0.61	0.01			
281	41714	D1	TRS	M3814		0.16	0.15	0			
282	41448	D1	TRS	M3824		4.16	1.01	0			
18	41455	D1	TRS	M3826		6.22	1.5	0.01			
283	41538	D1	TRS	M3827		1.37	0.33	0			
555	01353	GRIPI	TR	79-361	IB	66.95	62.4	0.25			
574	01354	GRIPI	TR	79-362	IB	69.77	65	0.26			
556	01356	GRIPI	TR	79-364	IB	66.67	62.1	0.25			
557	01358	GRIPI	TR	79-366	IB	64.44	60	0.24			
555	01359	GRIPI	TR	79-367	IB	68.62	63.9	0.25			
559	01360	GRIPI	TR	79-368	IB	68.36	63.7	0.25			
560	01361	GRIPI	TR	79-369	IB	67.99	63.3	0.25			
561	01362	GRIPI	TR	79-370	IB	69.25	64.5	0.26			
562	05359	GRIPI	TR	79-372	IB	63.48	59.1	0.24			
563	01364	GRIPI	TR	79-373	IB	71.22	66.3	0.26			
468	22882	GRIPII	TR	79-454	I	9.13		0.36	8.97		
469	53074	GRIPII	TR	79-459	I	7.53		0.36	7.36		
548	35696	GRIPII	TRS	M1756		0.71		0.01	0.7		
171	35636	GRIPII	TRS	M1763		5.83		0.31	5.71		
40	35998	GRIPII	TRS	M1923		0.91		0.01	0.89		
41	35888	GRIPII	TRS	M1930		5.74		0.08	5.64		
42	35877	GRIPII	TRS	M1931				0.22			
523	35879	GRIPII	TRS	M1932				0			
249	39173	GRIPII	TRS	M2820				0.01			
175	39266	GRIPII	TRS	M2826				0.02			
176	39242	GRIPII	TRS	M2828		4.46		0.23	4.39		
177	19247	GRIPII	TRS	M2830		1.45		0.02	1.42		
174	39262	GRIPII	TRS	M2924				0.02			

TABLE 7. CONTINUED.

Ref#	EDP#	Core	Conf.	ID	Type	U, g	U^{235}, g	Th, g	U^{233}, g	U^N, kg	U^D, kg
239	39740	GRIPII	TRS	M2994		0.1		0	0.09		
240	39743	GRIPII	TRS	M2996		0.11		0	0.1		
76	40751	GRIPII	TRS	M3462		1.83		0.03	1.8		
254	43255	GRIPII	TRS	M3464		0.13		0	0.13		
77	40747	GRIPII	TRS	M3466		6.33		0.31	6.22		
82	42223	GRIPII	TRS	M3697		0.26		0.01	0.25		
83	42218	GRIPII	TRS	M3699		0.9		0.01	0.88		
279	42208	GRIPII	TRS	M3701		0.13		0	0.13		
85	42211	GRIPII	TRS	M3703		0.13		0	0.13		
86	42216	GRIPII	TRS	M3704		0.51		0.01	0.5		
87	42214	GRIPII	TRS	M3706		5.09		0.3	4.99		
105	42550	GRIPII	TRS	M4126		0.5		0.01	0.49		
104	42533	GRIPII	TRS	M4122		0.2		0.23	0.2		
137	44751	GRIPII	TRS	M5137				0.17			
179	40710	GRIPII	TRS	M5454		0.13		0	0.13		
84	42205	GRIPII	TRS	M5702		0.51		0.01	0.5		
95	42186	GRIPIII	TRS	M2916		4.67	4.33	0.19			
93	42199	GRIPIII	TRS	M3911		1.35	1.26	0.04			
94	42196	GRIPIII	TRS	M3913				0.02			
475	29284	GRIPIIIA	TR	79-622	I	20.47	19.1				
172	36074	GRIPIIIA	TRS	M1978				0.02			
173	36051	GRIPIIIA	TRS	M1988		14.78	13.8	0.32			
183	36506	GRIPIIIA	TRS	M1997		0.19	0.18	0.01			
184	36554	GRIPIIIA	TRS	M2000		6.86	6.38	0.15			
185	36553	GRIPIIIA	TRS	M2001		9.91	9.22	0.24			
198	37364	GRIPIIIA	TRS	M2190				0.01			
199	37365	GRIPIIIA	TRS	M2191				0.01			
200	37366	GRIPIIIA	TRS	M2192				0.01			
217	57431	GRIPIIIA	TRS	M2220		0.14	0.13	0			
218	37440	GRIPIIIA	TRS	M2223		0.04	0.04	0			
219	37448	GRIPIIIA	TRS	M2225		0.07	0.07	0			
220	37444	GRIPIIIA	TRS	M2228				0.01			
221	37450	GRIPIIIA	TRS	M2229		0.07	0.07	0			
222	37453	GRIPIIIA	TRS	M2232		0.04	0.04	0			
223	37456	GRIPIIIA	TRS	M2234		0.16	0.15	0			
225	39468	GRIPIIIA	TRS	M2881		0.1	0.09	0			
67	40430	GRIPIIIA	TRS	M3238		3.19	2.98	0.07			
63	40377	GRIPIIIA	TRS	M3327		15.85	14.7	0.29			
64	40386	GRIPIIIA	TRS	M3329		5.92	5.5	0.12			
274	43265	GRIPIIIA	TRS	M3331		0.22	0.22	0			
65	40410	GRIPIIIA	TRS	M3334		1.14	1.06	0.03			
66	40473	GRIPIIIA	TRS	M3336		18.55	17.3	0.34			
275	40481	GRIPIIIA	TRS	M3339		0.69	0.64	0.01			
251	43266	GRIPIIIA	TRS	M3340		0.23	0.21	0.01			
261	40939	GRIPIIIA	TRS	M3578		0.04	0.04	0			
262	40944	GRIPIIIA	TRS	M3581		0.12	0.11	0			
263	40946	GRIPIIIA	TRS	M3582		0.04	0.04	0			
264	40949	GRIPIIIA	TRS	M3585		0.12	0.1	0			
250	40390	GRIPIIIA	TRS	M5330		0.68	0.63	0.02			
454	29549	GRIPIIIB	TR	79-630	I	19.49	18.2	0.48			
88	41615	GRIPIIIB	TRS	M3829		4.11	3.83	0.12			
89	41613	GRIPIIIB	TRS	M3831		0.44	0.41	0.01			
19	42466	GRIPIIIB	TRS	M4087		0.06	0.06	0			

TABLE 7. CONTINUED.

Ref#	EDP#	Core	Conf.	ID	Type	U, g	U^{235}, g	Th, g	U^{233}, g	U^N, kg	U^D, kg
20	42468	GRIPIIIB	TRS	M4089		0.11	0.1	0.01			
119	42614	GRIPIIIB	TRS	M4209		1.44	1.34	0.04			
108	42618	GRIPIIIB	TRS	M4210		0.15	0.14	0			
109	42621	GRIPIIIB	TRS	M4213		0.45	0.42	0.02			
110	42628	GRIPIIIB	TRS	M4216		3.1	2.89	0.06			
111	42808	GRIPIIIB	TRS	M4218		0.08	0.07	0			
112	42813	GRIPIIIB	TRS	M4221		0.03	0.03	0			
116	42665	GRIPIIIB	TRS	M4234		3.3	3.08	0.12			
113	42643	GRIPIIIB	TRS	M4279		1.21	1.13	0.04			
115	42659	GRIPIIIB	TRS	M4282		5.1	4.74	0.1			
120	42699	GRIPIIIB	TRS	M4289		0.44	0.41	0.01			
114	42651	GRIPIIIB	TRS	M4281		2.55	2.37	0.07			
121	42703	GRIPIIIB	TRS	M4291		2.06	1.92	0.06			
122	42706	GRIPIIIB	TRS	M4293		0.74	0.69	0.03			
123	42711	GRIPIIIB	TRS	M4297		2.54	2.36	0.05			
124	42715	GRIPIIIB	TRS	M4299		2.79	2.59	0.08			
125	42711	GRIPIIIB	TRS	M4301		1.18	1.1	0.03			
126	44075	GRIPIIIB	TRS	M4939		0.7	0.65				
127	44071	GRIPIIIB	TRS	M4941		0.74	0.69				
131	44257	GRIPIIIB	TRS	M5102		11.57	10.8	0.26			
132	44278	GRIPIIIB	TRS	M5108		1.21	1.13	0.04			
133	44280	GRIPIIIB	TRS	M5110		4.03	3.75	0.12			
134	44298	GRIPIIIB	TRS	M5111		0.1	0.09	0			
135	44304	GRIPIIIB	TRS	M5113		0.11	0.1	0			
136	44299	GRIPIIIB	TRS	M5115		0.1	0.09	0			
138	46707	GRIPIIIB	TRS	M6007		1.55	1.44	0.04			
118	46704	GRIPIIIB	TRS	M6009		0.05	0.04	0			
455	29750	GRIPIIIC	TR	79-634	I	25.16	23.4	0.48			
456	29751	GRIPIIIC	TR	79-635	I	24.96	23.2	0.48			
14	37900	GRIPIIIC	TRS	M2471		15.12	14.1	0.25			
15	37142	GRIPIIIC	TRS	M2473		4.97	4.64	0.11			
526	37959	GRIPIIIC	TRS	M2498		0.23	0.21	0.01			
527	37940	GRIPIIIC	TRS	M2499		0.22	0.2				
564	39019	GRIPIIIC	TRS	M2647		1.26	1.19	0.03			
248	43262	GRIPIIIC	TRS	M2649		0.22	0.21	0			
43	38989	GRIPIIIC	TRS	M2652		22.74	21.2	0.41			
44	39197	GRIPIIIC	TRS	M2728		0.46	0.43	0.01			
271	41263	GRIPIIIC	TRS	M2730		0.23	0.21	0.01			
45	39191	GRIPIIIC	TRS	M2733		6.69	6.23	0.14			
46	39189	GRIPIIIC	TRS	M2735		16.2	15.1	0.29			
226	39470	GRIPIIIC	TRS	M2883		0.08	0.07	0			
235	39513	GRIPIIIC	TRS	M2908		0.12	0.11	0			
241	39745	GRIPIIIC	TRS	M2987		0.09	0.08	0			
242	39747	GRIPIIIC	TRS	M2989		0.09	0.08	0			
243	39750	GRIPIIIC	TRS	M2991		0.06	0.06	0			
244	39752	GRIPIIIC	TRS	M2993		0.09	0.08	0			
245	39754	GRIPIIIC	TRS	M2994		0.08	0.08	0			
246	03975	GRIPIIIC	TRS	M2996		0.09	0.09	0			
17	40739	GRIPIIIC	TRS	M3458		0.23	0.21	0			
255	40737	GRIPIIIC	TRS	M3487		0.23	0.21	0.01			
470	31827	LBR	TR	79-468	I	92.91	86.6	3.24			
416	57236	LBR	TR	79-584	I	81	76	3			
417	57731	LBR	TR	79-707	I	79.3	73.9	2.8			

TABLE 7. CONTINUED.

Ref#	EDP#	Core	Conf.	ID	Type	U, g	U^{235}, g	Th, g	U^{233}, g	U^N, kg	U^D, kg
47	39534	LBR	TRS	M2911		28.15	26.2	1.2			
48	39630	LBR	TRS	M2918		2.11	1.97	0.07			
49	39633	LBR	TRS	M2921		9.84	9.17	0.31			
50	39637	LBR	TRS	M2925		17.73	16.5	0.85			
236	39731	LBR	TRS	M2976		0.3	0.28	0.01			
237	35133	LBR	TRS	M2978		0.44	0.41	0.01			
238	39736	LBR	TRS	M2981		0.24	0.22	0.01			
68	40527	LBR	TRS	M3393		37.61	35	1.49			
69	40544	LBR	TRS	M3398		26.46	24.6	0.84			
70	40553	LBR	TRS	M3400		4.12	3.84	0.13			
71	40555	LBR	TRS	M3402		6.59	6.15	0.51			
72	40642	LBR	TRS	M3421		40.33	37.6	1.39			
73	40654	LBR	TRS	M3426		12.32	11.5	0.41			
74	40657	LBR	TRS	M3429		18.21	17	0.58			
178	40460	LBR	TRS	M3432		0.8	0.75	0.08			
252	40639	LBR	TRS	M3435		0.81	0.75	0.02			
259	40932	LBR	TRS	M3573		0.65	0.61	0.02			
260	40937	LBR	TRS	M3577		0.22	0.2	0			
265	40951	LBR	TRS	M3586		0.63	0.6	0.02			
529	40954	LBR	TRS	M3589		0.63	0.59	0.02			
266	40955	LBR	TRS	M3590		0.19	0.17	0.01			
530	57332	LBR	TRS	M7030		0.83	0.77	0.02			
531	57328	LBR	TRS	M7OZ3		0.87	0.81	0.03			
426	57720	LDR	TR	97-162		224	49.5	0.46			
565	42670	LDR	TR	97-52	IB	257.2	57.4	0.28			
566	42671	LDR	TR	97-53	IB	244.9	54.6	0.32			
567	42672	LDR	TR	97-54	IB	183.6	41	0.36			
568	42760	LDR	TR	97-57	IB	52.83	51.6	0.33			
569	42814	LDR	TR	97-58	IB	75.48	73.7	0.45			
156	35240	LDR	TRS	M1658		3.03	2.82	0.39			
157	35231	LDR	TRS	M1664		24.38	22.7	0.79			
158	35257	LDR	TRS	M1671		18.75	17.5	0.59			
159	35269	LDR	TRS	M1677		9.75	9.08	0.31			
160	25270	LDR	TRS	M1679		0.42	0.39	0.31			
164	35384	LDR	TRS	M1681		54.92	51.2	0.3			
165	35416	LDR	TRS	M1682		6.24	5.81	0.09			
166	35407	LDR	TRS	M1686		28.81	26.8	0.12			
162	57313	LDR	TRS	M7020		33.39	31	1.2			
163	57327	LDR	TRS	M7027		33.59	31.2	1.29			
149	57256	LDR	TRS	M7929		97.75	21.8	0.15			
151	57285	LDR	TRS	M7929		13.33	2.97	0.02			
143	57277	LDR	TRS	M7932		17.78	3.97	0.02			
150	57278	LDR	TRS	M7935		51.09	11.4	0.05			
144	57282	LDR	TRS	M7937		33.33	7.43	0.03			
152	57291	LDR	TRS	M7940		2.4	0.54	0			
153	57308	LDR	TRS	M7943		1.54	0.34	0			
154	57310	LDR	TRS	M7945		1.63	0.37	0			
427	58207	LDR1	TR	97-61		72.73	71	0.34			
428	58208	LDR1	TR	97-62		331.6	74	0.34			
425	57237	LDR2	TR	97-123	U	248	57	0.36			
429	58209	LDR2	TR	97-64		98.37	91.6	0.55			
476	57558	LDR2	TR	97-65		256.3	59	0.43			
466	31895	LSR	TR	79-432	I	84.96	79.1	0.38			

TABLE 7. CONTINUED.

Ref#	EDP#	Core	Conf.	ID	Type	U, g	U^{235}, g	Th, g	U^{233}, g	U^N, kg	U^D, kg
467	46993	LSR	TR	79-434	I	92	86	0.4			
182	37063	LSR	TRS	79-608 (M2068)	P	46.05	42.9	0.26			
269	40256	LSR	TRS	M2071		0.98	0.91	0			
1	37050	LSR	TRS	M2073		58.61	54.6	0.31			
202	37269	LSR	TRS	M2147		0.66	0.61	0			
203	37275	LSR	TRS	M2150		0.38	0.35	0			
204	37323	LSR	TRS	M2151		0.58	0.54	0.02			
205	37329	LSR	TRS	M2154		0.42	0.39	0.02			
186	37331	LSR	TRS	M2155		0.58	0.54	0.02			
187	37334	LSR	TRS	M2158		0.42	0.39	0.02			
188	37336	LSR	TRS	M2159		0.57	0.54	0.02			
189	37339	LSR	TRS	M2162		0.42	0.39	0.02			
215	37424	LSR	TRS	M2215		0.44	0.41	0			
216	37428	LSR	TRS	M2218		0.44	0.41	0			
551	40835	LSR	TRS	M3471		1.31	1.22	0.02			
552	40852	LSR	TRS	M3474		20.33	18.9	0.07			
553	40821	LSR	TRS	M3477		15.1	14.1	0.05			
278	43268	LSR	TRS	M3479		0.66	0.61	0			
554	46637	LSR	TRS	M3482		22.96	21.4	0.08			
81	40839	LSR	TRS	M3494		17.35	16.2	0.07			
267	40959	LSR	TRS	M3593		0.41	0.38	0			
372	69947	LWBR	11 FRS	1/2 3102657	P	29.9		3.59	29.37		
588	70031	LWBR	11 FRS	1/2 3102657	P	90.04		3.7	88.39		
371	69946	LWBR	8 FRS	1105717 & 0507672	P	78.96		3.59	77.67		
606	70015	LWBR	13 FRS	1208823 & 0400736	P	47.06		3.28	46.27		
587	70030	LWBR	13 FRS	1504272 & 0205071	P	98.7		3.5	96.81		
605	70014	LWBR	9 FRS	1606710 & 0606773	P	72.2		3.25	70.92		
327	69912	LWBR	5 FRS	2514164& 1/2 2607600	P	0		2.48	0		
326	69911	LWBR	6 FRS	2610746 1/2 2607600	P	0		3.56	0		
457	02058	M13	TR	79-105	I	17.86	3.16				
458	21968	M13	TR	79-115	I	3.2	2.98				
459	12505	M13	TR	79-189	I	3.34	3.1	0.01			
350	12506	M13	TR	79-191	I	3.25	3.03	0.01			
461	01165	M13	TR	79-194	I	8.9	3.81	0			
460	12507	M13	TR	79-195	I	3.5	3.26				
351	12508	M13	TR	79-197	I	3.49	3.25				
474	01459	M13	TR	79-59	I	6.83	6.37	0.5			
495	00689	M13	TR	79-68	I	6.79	6.33				
496	12500	M13	TR	79-91	I	3.36	3.13	0.01			
497	12501	M13	TR	79-95	I	3.38	3.15				
357	12502	M13	TR	79-98	I	3.22	3				
575	24278	M13	TR	87-100I	I	0.66	0.62				
577	24280	M13	TR	87-102I	I	0.66	0.62				
578	26778	M13	TR	87-108	I	0.64	0.6				
579	10237	M13	TR	87-11	I	0.55	0.51				
580	15472	M13	TR	87-13	I	0.55	0.51				

TABLE 7. CONTINUED.

Ref#	EDP#	Core	Conf.	ID	Type	U, g	U^{235}, g	Th, g	U^{233}, g	U^N, kg	U^D, kg
581	11400	M13	TR	87-14	I	0.55	0.51				
582	17525	M13	TR	87-26	I	1.29	1.2				
583	10236	M13	TR	87-3	I	1.24	1.16				
584	11399	M13	TR	87-4	I	1.27	1.18				
585	15471	M13	TR	87-6	I	1.27	1.18				
499	30806	M13 ES5	TR	79-647	I	2.17	2.02	0.05			
506	31062	M13 ES5	TR	79-678	I	2.17	2.02	0.05			
507	31063	M13 ES5	TR	79-679	I	2.17	2.02	0.06			
509	30969	M13 ES5	TR	79-688	I	2.18	2.03	0.05			
511	30972	M13 ES5	TR	79-700	I	2.17	2.02	0.05			
503	30796	M13 F10S5	TR	79-660	I	2.16	2.01	0.05			
508	30967	M13 F10S5	TR	79-686	I	2.18	2.03	0.05			
510	30971	M13 F10S5	TR	79-690	I	2.18	2.03	0.05			
502	30801	M13 S5	TR	79-657	I	2.13	1.98	0.05			
504	30803	M13 S5	TR	79-665		2.13	1.98	0.05			
505	30792	M13 S5	TR	79-672	I	2.17	2.02	0.05			
352	17132	M13S2	TR	79-316	I	0.81	0.75	0.01			
353	17133	M13S2	TR	79-317	I	0.76	0.71	0.01			
373	17135	M13S2	TR	79-319	I	1.14	1.06	0.01			
489	08403	M13S2	TR	79-397	I	0.68	0.63	0.01			
374	17136	M13S2	TR	79-399	I	1.21	1.13	0.01			
375	17137	M13S2	TR	79-400	I	1.17	1.09	0.01			
376	17138	M13S2	TR	79-401	I	1.38	1.29	0.01			
480	29035	M13S2A	TR	79-377	I	1.58	1.47	0.01			
481	09796	M13S2A	TR	79-378	I	1.78	1.66	0.01			
482	29036	M13S2A	TR	79-379	I	1.72	1.61	0.01			
483	29037	M13S2A	TR	79-381	I	1.71	1.6	0.01			
484	29038	M13S2A	TR	79-383	I	2.7	2.46	0.01			
485	29040	M13S2A	TR	79-385	I	2.65	2.46	0.01			
486	29041	M13S2A	TR	79-386	I	1.98	1.84	0.01			
487	29042	M13S2A	TR	79-390	I	1.58	1.47	0.01			
488	29041	M13S2A	TR	79-394	I	1.6	1.49	0.01			
498	22087	M13S2A	TR	79-493	I	1.25		0.01	1.23		
477	11669	M13S3	TR	79-322	I	1.25	1.17	0.01			
478	29049	M13S3	TR	79-332	I	1.18		0.01	1.16		
354	11523	M13S3	TR	79-337	I	1.82	1.69	0.01			
479	29050	M13S3	TR	79-340	I	1.15		0.01	1.13		
355	11524	M13S3	TR	79-344	I	1.81	1.68	0.01			
490	29044	M13S3	TR	79-435	I	2.07	1.93	0.01			
356	11525	M13S3	TR	79-436	I	1.88	1.75	0.01			
491	29045	M13S3	TR	79-437.	I	1.96	1.83	0.01			
492	29046	M13S3	TR	79-438	I	2.09	1.95	0.01			
493	22085	M13S3	TR	79-485	I	1.24		0.01	1.22		
494	22086	M13S3	TR	79-491	I	1.25		0.01	1.23		
500	30799	M13-S5	TR	79-649	I	2.13	1.98	0.05			
501	30806	M13-S5	TR	79-650	I	2.17	2.02	0.05			
328	68977	MISC	MC	MEL-EDP-05388-A		298	167	2	2		
358	52579	PBIT	TR	87-222		1.19	1.11				
522	52580	PBIT	TR	87-223	I	1.19	1.11				
359	50116	PBIT	TR	87-224		1.19	1.11				
360	50127	PBIT	TR	87-225		1.19	1.11				
589	47889	PBIT	TR	97-132	IB	58.03	54	0.86			
590	48248	PBIT	TR	97-133	IB	58.37	54.4	0.86			

TABLE 7. CONTINUED.

Ref#	EDP#	Core	Conf.	ID	Type	U, g	U^{235}, g	Th, g	U^{233}, g	U^{N}, kg	U^{D}, kg
591	47890	PBIT	TR	97-134	IB	57.78	53.8	0.86			
592	48767	PBIT	TR	97-135	IB	58.36	54.4	0.86			
593	47891	PBIT	TR	97-136	IB	57.62	53.7	0.86			
594	48249	PBIT	TR	97-137	IB	58.3	54.3	0.87			
595	43250	PBIT	TR	97-138	IB	57.88	53.9	0.86			
596	47929	PBIT	TR	97-139	IB	58.06	54.1	0.86			
597	47892	PBIT	TR	97-140	IB	57.95	53.9	0.86			
598	47924	PBIT	TR	97-141	IB	829.4	49.6	0.15			
599	47893	PBIT	TR	97-142	IB	57.92	53.9	0.86			
600	48768	PBIT	TR	97-143	IB	58.28	54.3	0.87			
601	47930	PBIT	TR	97-144	IB	58.43	54.4	0.86			
602	47689	PBIT	TR	97-145	IB	57.54	53.6	0.86			
603	47931	PBIT	TR	97-146	IB	57.5	53.6	0.85			
604	47925	PBIT	TR	97-147	IB	830.8	49.7	0.15			
616	47794	PBIT	TR	97-148	IB	57.55	53.6	0.86			
617	47894	PBIT	TR	97-149	IB	58.03	54	0.86			
618	47926	PBIT	TR	97-150	IB	842.4	49.4	0.15			
619	47927	PBIT	TR	97-151	IB	841.1	49.3	0.15			
336	47932	PBIT	TR	97-152	U	57.69	53.7	0.86			
337	47928	PBIT	TR	97-153	U	843.1	49.4	0.15			
338	47795	PBIT	TR	97-154	U	58.42	54.4	0.87			
339	48251	PBIT	TR	97-155	U	57.57	53.6	0.86			
340	48766	PBIT	TR	97-156	U	830.3	49.7	0.15			
341	51900	PBIT	TR	97-157	U	27.17	25.3	0.88			
342	51901	PBIT	TR	97-158	U	27.23	25.3	0.88			
139	56405	PBIT	TRS	M7891		0.53	0.5				
140	56403	PBIT	TRS	M7893		0.53	0.5				
141	56456	PBIT	TRS	M7905		0.53	0.49				
532	56455	PBIT	TRS	M7906		0.12	0.11				
142	56446	PBIT	TRS	M7907		0.52	0.48				
615	30788	PM E10S5	TR	87-204	I	1.62	1.51				
520	30786	PM E18	TR	87-202	I	1.61	1.5				
614	30785	PM EAST	TR	87-200	I	1.61	1.5				
521	30787	PM EAST	TR	87-203	I	1.62	1.51				
576	24271	PM S10	TR	87-101I	I	0.66	0.62				
608	26773	PM S10	TR	87-103I	I	0.66	0.61				
610	26782	PM SE11	TR	87-116	I	0.97	0.9				
611	26783	PM SE11	TR	87-117	I	0.99	0.92				
612	26784	PM SE11	TR	87-118	I	0.99	0.92				
613	26785	PM SE11	TR	87-119	I	0.96	0.89				
537	02934	PWR1	FR	10 (K10)	I		0	0			130
286	00556	SABRE	FR	152	I						1820
287	00569	SABRE	FR	153	I						1820
288	00602	SABRE	FR	157	I						1820
289	00594	SABRE	FR	160	I						1820
290	00560	SABRE	FR	167	I						1820
306	00585	SABRE	FR	168	I						1820
307	00557	SABRE	FR	169	I						1820
308	00581	SABRE	FR	171	I						1820
309	00568	SABRE	FR	174	I						1820
310	00582	SABRE	FR	175	I						1820
311	00562	SABRE	FR	185	I						1820
292	00604	SABRE	FR	186	I						1820

TABLE 7. CONTINUED.

Ref#	EDP#	Core	Conf.	ID	Type	U, g	U^{235}, g	Th, g	U^{233}, g	U^{N}, kg	U^{D}, kg
293	00599	SABRE	FR	189	I						1820
312	00558	SABRE	FR	192	I						1820
313	00605	SABRE	FR	193	I						1820
314	00561	SABRE	FR	203	I						1820
315	00577	SABRE	FR	209	I						1820
294	00603	SABRE	FR	211	I						1820
295	00595	SABRE	FR	213	I						1820
296	00593	SABRE	FR	217	I						1820
316	00583	SABRE	FR	221	I						1820
317	00584	SABRE	FR	232	I						1820
318	00566	SABRE	FR	234	I						1820
329	00588	SABRE	FR	235	I						1820
297	00607	SABRE	FR	237	I						1820
330	00586	SABRE	FR	240	I						1820
319	00565	SABRE	FR	241	I						1820
298	00600	SABRE	FR	255	I						1820
299	00592	SABRE	FR	258	I						1810
331	00587	SABRE	FR	259	I						1810
332	00578	SABRE	FR	261	I						1810
320	00564	SABRE	FR	262	I						1810
321	00563	SABRE	FR	267	I						1810
333	00576	SABRE	FR	271	I						1810
300	00601	SABRE	FR	277	I						1810
301	00606	SABRE	FR	278	I						1810
322	00567	SABRE	FR	281	I						1810
302	00597	SABRE	FR	285	I						1810
334	00589	SABRE	FR	290	I						1810
303	00596	SABRE	FR	298	I						1810
323	00571	SABRE	FR	305	I						1810
324	00559	SABRE	FR	307	I						1810
325	00570	SABRE	FR	310	I						1810
291	00598	SABRE	FR	184	I						1820
304	00694	SABRE	TR	79-11	D					1000	
305	00695	SABRE	TR	79-24	D					900	
620	57551	SIDR	TR	97-168D		9.62	8.95	0.34			
621	57554	SIDR	TR	97-169		9.55	8.9	0.34			
622	57555	SIDR	TR	97-170D		9.57	8.92	0.34			
623	57556	SIDR	TR	97-171D		23.7	22.1	0.34			
624	57557	SIDR	TR	97-172		23.64	22	0.34			
538	61490	SP IFAG	ICR	0-1	U			0.2			
145	61494	SP IFAG	ICR	12-1	U	5.8		0.1	5.7		
146	61491	SP IFAG	ICR	2-1	U	1.8		0.1	1.8		
147	61492	SP IFAG	ICR	5-1	U	4.5		0.1	4.4		
155	61495	SP IFAG	TRS	6-1	U	5.3		0.1	5.2		
148	61493	SP IFAG	ICR	9-1	U	8.1		0	8		
436	01660	SPIRE	TR	79-213	I	56.65	52.8			40	
462	02006	SPIRE	TR	79-215	I	56.19	45.3			50	
437	01661	SPIRE	TR	79-216	I	56.13	45.3			50	
463	01662	SPIRE	TR	79-217	I	56.16	45.3			50	
438	02007	SPIRE	TR	79-220	I	29.96	28			50	
439	01663	SPIRE	TR	79-221	I	30.08	28.1			50	
440	15885	SPIRE	TR	79-222	I	30.1	28.1			50	
441	01196	SPIRE	TR	79-229	I	60.03	56			40	

TABLE 7. CONTINUED.

Ref#	EDP#	Core	Conf.	ID	Type	U, g	U^{235}, g	Th, g	U^{233}, g	U^N, kg	U^D, kg
442	15884	SPIRE	TR	79-242	I	60.62	56.6			40	
443	01187	SPIRE	TR	79-243	I	34.42	26.8			50	
415	19047	SWLD	TR	79-472	I	3.07	2.86	0.17			
512	11037	TIPPETT II	TR	81-45	I			0.02			
513	11039	TIPPETT II	TR	81-47	I			0.02			
514	11254	TIPPETT II	TR	81-48	I			0.02			
515	11251	TIPPETT II	TR	81-51	I			0.02			
516	11040	TIPPETT II	TR	81-52	I			0.02			

Given below are the tests and fuel rod IDs of the fuel that have been sectioned[1].

TABLE 8 – SECTIONED FUEL ID AND TEST INFORMATION

Test	ID	Test	ID	Test	ID	Test	ID
C7-B3A	79-307D	C7-B3A	79-375	GRIP-II	79-454	LWBR	2607600
C7-BBT	79-504D	C7-B3A	79-405	GRIP-II	79-459	LWBR	2610746
GRIP-II	79-441D	C7-BBT	79-502	GRIP-IIIA	79-613	LWBR	3102657
GRIP-IIIA	79-614D	C7-BBT	79-509	GRIP-IIIA	79-617	LWBR	0205071
GRIP-IIIB	79-609D	C7-BBT	79-513	GRIP-IIIA	79-623	LWBR	0400736
LDR	97-55D	C7-BBT	79-514	GRIP-IIIB	79-619	LWBR	0507672
LSR	79-433D	C7-BBT	79-522	GRIP-IIIB	79-621	LWBR	0606773
NLBR	79-583D	C7-BBT	79-524	GRIP-IIIB	79-624	LWBR	0702161
ACT-LPR	79-706	D1	97-22	GRIP-IIIB	87-215	M13-S5	79-656
ALT1	97-85	D1	97-23	GRIP-IIIC	79-610	M13-S5	79-671
ALT2	97-121	D1	97-37	GRIP-IIIC	79-631	NLBR	79-575
B1M	79-572	GRIP-II	79-442	GRIP-IIIC	79-632	NLBR	79-576
B1MA	79-570	GRIP-II	79-444	LWBR	1105717	NLBR	79-587
B1MA	79-573	GRIP-II	79-445	LWBR	1208823	NLSR	79-605
B1R	79-579	GRIP-II	79-449	LWBR	1504272	NLSR	79-608
C7-B3A	79-349	GRIP-II	79-450	LWBR	1606710	PM	87-221
C7-B3A	79-353	GRIP-II	79-453	LWBR	2514164	SP	87-220

The estimated Zircaloy-4 cladding weight of the irradiation test rods is given below[1].

TABLE 9 - ESTIMATED ZR-4 CLADDING WEIGHT OF IRRADIATION TEST RODS

Test I.D	Wt. Clad g/Rod	No. of Intact Rods	Total Clad Wt, g	No. of Sect. & Defect. Rods	Total Clad Wt, g
ACT-LPR	678.4	2	1356.8	1	678.4
ALT 1	20.8	23	478.4	1	20.8
ALT 2	20.8	18	374.4	4	83.2
B1	443.4	2	886.8	0	0
B1R	548.7	2	1097.4	1	548.7
B1M	409.6	0	0	3	1228.8
B3	261	5	1305	1	261
B3A	311	4	1244	5	1555
BBT	439	2	878	7	3073
D1	20.8	27	561.6	3	62.4
GRIP-I	149	10	1490	0	0
GRIP-II	150.6	2	301.2	8	1204.8
GRIP-IIIA	188	1	188	4	752
GRIP-IIIB	184.8	1	184.8	4	739.2
GRIP-IIIC	188.1	2	376.2	3	564.3
LBR	544.6	1	544.6	0	0
LDR	176.6	5	883	1	176.6
LSR	166.2	2	332.4	1	166.2
M13-S2,S2A	9.3	17	158.1	0	0
M13-S3,S3A	9.3	11	102.3	0	0
NLBR	689.1	4	2756.4	0	0
L12-LSBR	8.5	12	102	0	0
M13-S5	17.1	13	222.3	0	0
TIPPET II	8.6	5	43	0	0
NLDR-1	217.4	2	434.8	0	0
NLDR-2	217.4	2	434.8	0	0
NLDR-3	217.4	1	217.4	0	0
NLDR-4	217.4	1	217.4	0	0
MLSR	222.9	0	0	2	445.8
PBIT	259.5	27	7006.5	0	0
SABRE	495.6	44	21,806.40	2	991.2
SPIRE	152.7	10	1527	0	0
SWLD	53	1	53	0	0
SIDR	104.8	5	524	0	0
LWBR Seed	214.5	0	0	5	1072.5
LWBR SB	542.7	0	0	4	2170.8
LWBR PFB	460	0	0	2	920
LWBR R	1187.1	0	0	1	1187.1
Total Clad Weight*		**264**	**48088**	**63**	**17901.8**

*The estimate of clad weight does not account for end closures or internal hardware; multiply by 1.16 to account for end closure weight and 1.14 to account for rod internal hardware.

The weights of the fuel and FHU components are given in the following Table[1].

TABLE 10 – FUEL AND FHU COMPONENT WEIGHTS

Category of Fuel	UO_2, kg	ThO_2, kg
1. Rod Alpha Containers (RAC)	3.7	47.9
2. Cut Fuel Storage Containers (CFSC) & MEL	0.4	11.0
3. Cut LWBR Fuel	0.4	29.8
4. Intact Defected Rods	2.8	1.8
5. Intact SABRE Rods	90.7	0.0
6. Intact Rods	10.0	58.6
7. Intact Rod Bundles	6.5	21.2
Total	114.7	170.3

Canister Weight Breakdown	kg
Oxide Fuel UO_2	114.7
Oxide Fuel ThO_2	170.3
Oxide Diluent CaO	0.1
Oxide Diluent ZrO_2	3
Intact Rods and Bundles Cladding	64
Sectioned and Defected Rods Cladding	24
Storage Liner	913
Bottom Plate	69
Filler Plate	29
Spider	129
6"-Containers - 8	769
8"-Container - 1	198
RAC - 89	556
CFSC - 6	53
Rod Tubes - 22	332
LWBR Tubes - 8	33
LWBR Tube - 1	3
Defected Rod Tube	14
6"-Baskets - 8	151
8"-Basket - 1	35
MEL Container - 1	6
Miscellaneous Spacers	100
FHU Total	**3766**

The estimated ^{85}Kr content of representative irradiation test rods is given in following Table[1].

TABLE 11 – ESTIMATED ^{85}KR CONTENT OF REPRESENTATIVE IRRADIATION TEST RODS

Irradiation Test	Rod ID	Estimated ^{85}Kr Content, Ci	Cooling Time Since Est., Yr.
B3A	79-349	4.8	-13
	79-3/75	6	
	79-405	6.5	
B1	79-429	1.7	-14
B1R	79-579	1	-14
BIM	79-572	3.9	-13
	79-586	4.1	
BIMA	79-570	2	-13
	79-573	2	
BBT	79-502	5.3	-12
	79-509	5.9	
	79-522	3.9	
	79-513	1.1	
	79-514	1	
D1	97-22	0.1	-6
	97-23	0.1	
GRIP-I	79-363	1.3	-15
GRIP-II	79-440	2.6	-3
GRIP-IIIB	79-619	6.8	-12
	79-624	5.2	
LBR	79-467	19	-13
M13-S3	79-342	0.24	-13
NLBR	79-575	18.3	-11
	79-576	16.3	
	79-587	7.2	
NLSR	79-605	8.7	-12
	79-608	9	

The reactivity calculation results for various conditions as described are given below[1].

Condition	K_{eff} 95% CI
1. Flooded liner; fuel shifted toward PBIT side of liner; all RAC fuel in 2 RAC containers.	0.55
2. Flooded liner; PBIT lowered; extra fuel in calculation, 0.66 in RAC and CFSC.	0.66
3. Water removed from liner regions outside all containers; fuel as in calculation 2.	0.63
4. Water removed from liner and appears only as a reflector; fuel as in calculation 2.	0.14
5. Flooded liner; steel reduced by 15%; fuel as in calculation 2.	0.7
6. Liner in Peach Bottom (lead reflection); flooded liner; fuel and steel as in calculation 5.	0.71
7. Liner in Peach Bottom; water removed from storage liner except from RAC containers and CFSC container; fuel and steel as in calculation 5.	0.6
8. Additional fuel added to flooded liner (see text); liner loading increased from 11.4 to 11.9 kg fissile; steel as in. calculation 5.	0.7
9. Extra fuel in the form of slurry added to calculation of flooded liner; steel as in calculation 5.	0.89
10. Seed at 2 inches from the flooded liner; extra rod storage tube in liner; steel as in calculation 5.	0.83

5. IRRADIATED TEST REPORT SUMMARIES FOR SELECTED TESTS

5.1 Comparison of Dimensional Changes in Fuel Rods with Predictions under Cyclic conditions of Power and System Pressure[6]

The report describes various additions to the CYGRO model for calculating ratcheting effects; the effects include fuel cracking, clad collapse, friction between fuel and clad, clad anisotropy, and effects of neutron flux on clad creep. Physical, environmental, and operating characteristics of eight test rods were used to confirm the model. Three of the test rods (79-427, 79-430, and 79-468) are contained in the scrap canister. Physical characteristics of these rods is given below

Rod No.	Clad OD – in	Clad Thickness – mil	Clad Type[a]	Fuel-Clad Diametric Gap – mil	Fuel[b]	Fuel Density (% of theoretical)	Fuel Stack Length – in
79-427	0.600	24	SRA	4	ThO_2+1.98 w/o U^EO_2	98	29.8
79-430	0.600	24	RXA	10	ThO_2+1.98 w/o U^EO_2	98	29.8
79-468	0.600	24	SRA	11	ThO_2+3.42 w/o U^EO_2	98	84
a	Zircaloy-4 cladding, tube reduced, nominally 70% cold worked. SRA designates a stress relief at 950°F for four hours. RXA designates a re-crystallization anneal at 1250°F for four hours.						
b	Pressed and sintered pellets of length to diameter ratio between 1 and 2, with a 13-mil end-dish of 1.6 in. spherical radius.						

Environmental and operating characteristics of scrap canister rods are given below.

Rod No.	Peak Heat Flux – 10^3 Btu/hr-ft^2	Peak Fuel Temp. – °F[a]	Peak Fast Flux > 1 Mev – 10^{14} n/cm^2-sec	Peak Depletion[b] – 10^{20} f/cc	#. of Depressurizations - 10 f/cc
79-427	305	3075	1.21	0.37	2
79-430	301	3000	0.61	0.78	7
79-468	375	4525	0.15	1.94	15
a	Temperatures calculated using a computer program				
b	Calculated peak depletion at time of most recent examinations				

The results of the testing are as follows:

a. Mechanisms important to ratcheting were incorporated into the CYGRO model.
b. The observed progressive length increase of fuel rods having non-free-standing clad compared satisfactorily with the model.
c. When gross axial wrinkling is observed, the model is less exact; this may be expected since the size and nature of the fuel-clad contact forces are inherently less well known.
d. The choice of parameters which lead to correct axial elongation prediction often do not lead to good prediction of diameter shrinkage; this is believed to be associated with observed clad non-uniformity such as ridging, ovalness and wrinkling which invalidate the model to an extent depending on their severity.
e. Further progress may result from improved analysis of axial and circumferential non-uniformity, more accurate representation of clad collapse characteristics, and improved knowledge of the in-pile creep properties of fuel and clad.

5.2 In-Pile Dimensional Changes of Zircaloy-4 Tubing Having Low Hoop Stresses[7]

Short screening rods were irradiated in the M13 test loop of the Engineering Test Reactor (ETR). The Long Small Rod (LSR) full-length rods were irradiated in the E25 test loop of the National Research Experimental Reactor (NRX). The test name and the fuel rods used are given below.

Test	# of Rods	# of Rods in the Scrap Canister & Rod IDs
M13-S2	14	7 – (79-316, 79-317, 79-319, 79-322D, 79-399, 79-400, and 79-401)
M13-S2A	11	9 – (79-377, 79-378, 79-379, 79-381, 79-383, 79-385, 79-386, 79-390, and 79-394)
M13-S3	14	7 – (79-332, 79-337, 79-340, 79-435, 79-436, 79-437, and 79-438)
M13-S3A	10	3 – (79-485, 79-491, and 79-493)
M13-S4	7	0
LSR	6	3 – (79-432, 79-433D, and 79-434)

Several of the test rods were intentionally defected before irradiation by drilling a 5-mil diameter hole through the cladding after pre-irradiation corrosion testing. These rods are identified by the letter "D" following the rod number. Summary irradiation histories of the fuel rods are given.

The results of the testing are as follows:

a. Comparison of length and diameter changes indicates that the diametric shrinkage of the short 0.25-inch OD rods were due entirely to the external pressure, reaching a maximum of about 1-mil (0.4%) at $17x10^{20}$ fast nvt.
b. Diametric shrinkage in the bottom and middle regions of the long 0.25-inch OD rods was influenced by axial tensile stresses, imposed on the cladding by the fuel. This fuel-clad interaction increased the generalized stress over that imposed by the external pressure. Near $2x10^{20}$ fast nvt, shrinkage was about 6-mil (0.2%) in the absence of fuel-clad interactions but increased to about 2-mil (0.8%) in the presence of such interactions. A model using a modified version of CYGRO was proposed for simulating the performance of these rods.
c. The component of the length increase caused by Zircaloy growth was about 0.075% at $17x10^{20}$ fast nvt.

5.3 In-Pile Dimensional Changes of ThO_2-UO_2 Fuel Rods with Non-Free-Standing Cladding[8]

Axial ratcheting is the progressive extension or elongation of fuel rods in-pile under cyclic conditions of power and system pressure resulting from irradiation. Axial ratcheting is made up of three components: 1) stress-free Zircaloy growth, 2) diameter shrinkage due to system pressure, and 3) fuel-clad interaction. Data were presented for three series of irradiation testing of fuel rods with non-free-standing cladding: the C7, NRX and B1 series of tests. A physical description of the fuel rods along with a summary of the operational and measurement data is given.

Test	# of Rods	# of Rods in the Scrap Canister & Rod IDs
C7-B3	5	5 – (79-299, 79-300, 79-302, 79-304, and 79-308)
C7-B3A	9	9 – (79-349, 79-350, 79-352, 79-353, 79-356, 79-374, 79-375, 79-376, and 79-405)
NRX	6	3 – (79-468, 79-337, 79-575, and 79-576)
B1	4	2 – (79-427, and 79-430)
B1RA	1	1 – (79-577)
B1RB	2	2 – (79-579 and 79-581)
B1M	2	1 – (79-572)

The results of the testing are as follows:

a. Annealed cladding and low fast-flux environment resulted in the maximum amount of elongation.
b. Cold-worked cladding and low fast-flux environment resulted in the least amount of elongation.
c. Both cold-worked and annealed cladding resulted in elongation in the midrange of the data.
d. Flat-ended pellets resulted in elongation substantially greater than with dished-end pellets.
e. For flat-ended pellets high center temperature (>2500°F) resulted in elongation 2-3 times greater than rods operated at lower temperature (<2000°F).
f. Fuel clad diametric gap and clad diameter-to-thickness ratio had a significant but less pronounced effect on ratcheting.
g. Accelerated power cycling and fuel loading had no observed effect on ratcheting.
h. Pressure cycling appears to be the predominant mechanism inducing elongation from fuel-clad interaction; a correlation could not be determined between the number of pressure cycles or cladding texture and the extent of ratcheting.

5.4 Fuel Rod-Grid Interaction Wear: In-Reactor Tests[9]

Wear of the Zircaloy cladding of LWBR irradiation test fuel rods, resulting from relative motion between rod and rod support contacts, is reported. Measured wear depths were small, 0.0-2.7 mils, but are important in fuel element behavior assessment because of the local loss of cladding thickness, as well as the effect on grid spring forces that laterally restrain the rods. An empirical wear analysis model, based on out-of-pile tests, is presented. The model was used to calculate the wear on the irradiation test fuel rods attributed to a combination of up-and-down motions resulting from power and pressure/temperature cycling of the test reactor, flow-induced vibrations, and assembly handling scratches. The calculated depths are generally deeper than the measured depths.

The LWBR core employs ordered arrays of long (10 feet), small diameter (0.3-0.8 inch), Zircaloy clad, cylindrical fuel elements. The fuel rods are supported axially by threaded end connectors on the rods attached to either the top or the bottom base plate of a module assembly. Each rod is thus fixed at one end and free at the other end. Lateral support for the rods is provided by a series of supports, called grids, at several axial locations along the length of the rods. Each grid contains, for each rod, a hexagonal-shaped cell with a spring and opposing fixed reaction dimples set at 120 degrees circumferential from the spring. The spring applies lateral force on the fuel rod in the cell to hold it firmly against the dimples, while allowing relative axial movement between the rod and grid support points during reactor operation. Interaction between the fuel rod and the supporting springs and dimples caused by fuel rod length changes and vibration can result in wear on the Zircaloy cladding of the fuel rods. Wear of the AM-350 stainless steel grid contact points has been found by test experience to be negligible relative to the fuel rod cladding wear.

Cladding wear may be caused by the combined effects of three types of interaction between fuel rods and support grids: 1) handling scratches, often along the full rod length, that occur when fuel rods are initially pulled into the grid supports; 2) axial motion of the rod relative to the grid supports due to fuel rod axial expansion and contraction during reactor power cycles and pressure/temperature cycles; and 3) flow-induced vibratory wear.

Cladding wear is of concern 1) because the thinning of the cladding increases stresses in the thinned section with a consequent reduction in margin-to-failure stress limits, and 2) because of its contribution to a reduction in the grid spring fuel rod support force with potential for reduced rod-to-rod and rod-to-structure clearances. In addition, a complete loss of grid contact force may result in excessive fuel rod vibration, creating a potential wear/fretting condition, as demonstrated in out-of-pile wear tests.

The report presents fuel rod cladding wear data obtained from in- reactor rod bundles tested in the LWBR fuel element development program and compares these data to wear estimates predicted using a model developed from out-of-pile wear tests. The LWBR fuel rods were composed of high density ThO_2-UO_2 and ThO_2 fuel pellets contained within Zircaloy-4 tubes having outside diameters of about 0.30 or 0.57 inches, and lengths of about eight feet. The rods were pre-corrosion filmed before insertion into the grid supports prior to irradiation.

Wear measurements were obtained on 34 fuel rods; all but one of the fuel rods is in the scrap canister. The rods were supported laterally by AM-350 stainless steel grids using hexagonal-shaped grid cells that contain a spring and two dimples, or two pairs of circumferentially dimples, set at 120° circumferentially from each other. Altogether 1298 support contact points are represented by the 34 fuel rods examined. (The number of support contact points for each rod was determined by multiplying the number of spring and dimple reaction points at each grid level by the number of grid levels supporting the rod. Multiple sets of wear marks on several rods are also included in the total.) Only 176 contact points were directly measured. The remaining 1122 support contact points that were not measured because they were undetectable or obviously shallow are assumed to have wear depths of 0.0-0.5 mils. Ninety-five percent of the wear spot depths are 1.0 mil or less, 4 % are 1.1-2.0 mils, and 1 % are 2.1-2.7 mils deep.

During examination of the irradiated fuel rods, wear depths were measured at the free end grid levels and at other levels where visual examination indicated that significant cladding wear had occurred. Other cladding wear spots that appeared to be smaller than 0.5 mil in depth were usually not measured. For all but six of the 34 rods included in this report, maximum rod wear occurred at the free-end grid support location. The occurrence of maximum wear at the rod free ends is attributed to the fact that this location is where the longest rod axial movement relative to grids occurs during power and pressure/temperature cycling, with resulting higher reciprocating wear. Flow-induced vibration wear also is expected to be a maximum at the free end of top mounted rods because of rod excitation by coolant flow impingement on the ends of the rods.

Wear mark depth was measured nondestructively with a profilometry instrument considered to have an accuracy of ±0.2 mils. In addition, destructive examination of wear depth was performed metallographically on some rods by polishing transverse rod sections through the wear mark in successive planes about 20-30 mils apart. Photomicrographs taken at each plane were measured to obtain wear depth. The profilometry measurements agreed well with metallographic measurements.

All wear measurements, and their location with respect to individual grids and to grid springs and dimple reaction points, are given in the report. Also given are test reactor exposure times, numbers of actual power and pressure/temperature cycles, stroke lengths, and measured overall rod length increases. The rod identification numbers are given below for 33 of the rods in the scrap canister that were used for the wear measurements tests.

79-610	79-621	79-630	79-440	79-444	79-455	79-509	79-517
79-613	79-622	79-631	79-441D	79-445	79-459	79-513	79-522
79-614D	79-623	79-632	79-442	79-449	79-502	79-514	79-524
79-617	79-624	79-439	79-443D	79-450	79-504D	79-516	79-572
79-619							

The conclusions drawn from the testing are as follows:

a. Maximum measured wear depth on the irradiation tested fuel rods supported in grids having geometry similar to the LWBR design was 2.7 mils, and was located at the free-end grid support of a top-mounted fuel rod.
b. Fuel rod wear was deepest at the rod free-end grid support on 28 of 34 rods.
c. Top mounted rods had greater wear depth at the free-end grid support than bottom mounted rods. This condition is attributed to greater vibratory wear experienced by the top mounted rods due to impingement of the coolant flow on the bottom free-ends of these rods.
d. Wear depth on fuel rods that accumulated a high number of EFPH or power and pressure/temperature cycles was not significantly greater than that on rods with shorter test lives. This behavior is in accordance with the basis for the wear analysis model and is a result of rod axial growth during reactor operation.

e. Maximum-measured-wear depths were generally less than the total amount of wear predicted by a wear analysis model developed from out-of-pile reciprocating wear tests. The predicted values included reciprocating wear, plus an allowance for vibratory wear and assembly and handling scratches.
f. A high proportion, about 95%, of the rod-grid contact points examined had low wear of less than one mil depth.
g. High wear is sometimes found at contact points associated with off-nominal conditions such as high rod bowing or contacts between the rod and grid at other than the spring and dimples.

5.5 Fission Gas Release From ThO_2 and ThO_2-UO_2 Fuels[10]

Fission gas release data are presented from 51 fuel rods irradiated as part of the LWBR irradiation test program (23 of the fuel rods are contained in the scrap canister). The fuel rods were Zircaloy-4 clad and contained ThO_2 or ThO_2-UO_2 fuel pellets, with UO_2 compositions ranging from 2.0-24.7 w/o and fuel densities ranging from 77.8-98.7% of theoretical. Rod diameters ranged from 0.25-0.71 inches and fuel active lengths ranged from 3-84 inches. Peak linear power outputs ranged from 2-22 kW/ft for peak fuel burn-ups up to 56,000 MWD/MTM. Measured fission gas release was quite low ranging from 0.1-5.2%. Fission gas release was higher at higher temperature and burnup and was lower at higher initial fuel density. No sensitivity to UO_2 composition was evidenced. A calculational model is described which includes terms to represent fission gas release as a function of temperature, using a diffusion model, and as a function of density to account for release due to knockout and recoil at free surfaces. The model was developed on both a best estimate and bounding basis.

The amount of fission gases released from oxide fuel pellets during irradiation in power reactors is important to reactor design primarily in two design areas. First, release of fission gases from the fuel to the internal rod compartment results in an increase in rod internal pressure with increasing burnup. The higher internal pressure increases proximity to material property limits for a postulated loss of coolant accident (LOCA), during which fuel rod cladding can potentially experience high temperatures, resulting in loss of strength and more susceptibility to swelling and rupture. Second, since fission gases (primarily xenon and krypton) have much lower thermal conductivity than the initial fill gas (typically helium or argon) used in light water reactor fuel rods, more fission gas release can result in higher operating fuel temperatures due to the degraded heat transfer in the fuel-cladding gap.

The report contains (1) data on fission gas release from ThO_2 or ThO_2-UO_2 fuels obtained from 51 fuel rods from the LWBR test program, and (2) comparisons of the measurements to a calculational model used in performance assessments. Dimensional, material characteristics, and environmental history of the test fuel rods are described. The fission gas release measurements are given along with a description of the measurement procedures and an assessment of measurement uncertainty. The calculational model is described and the results of application of the model are compared with the measurements.

Measured fission gas release (measurement uncertainty of plus or minus 8% of nominal) was generally low, ranging from <0.1-5.2% of the fission gases theoretically produced by fissioning. Gas release was predominantly below 2% for high-density (95% theoretical or greater) fuels. Fission gas release was higher at higher temperatures, higher burnup and lower density. No sensitivity to UO_2 composition was observed.

A calculation model was presented which includes terms to represent fission gas release at both high temperatures (assuming a gas bubble diffusion model) and low temperatures (based on a recoil plus knockout mechanism). The high temperature term accounts for migrating gas bubbles that are released from the fuel due to intersection with a surface (e.g., cracks or open pores). Depending on specific fuel properties and burnup, critical temperatures for release of bubbles from dislocations and grain boundaries are calculated.

The low temperature term is adapted from a model that assumes that fission gas is released by recoil and knockout at free surfaces. Pellet density initially serves as a measure of free surface area, which increases with burnup (presumably due to fuel cracking). The model is developed on both a best estimate and bounding basis.

Gas release for long rods, which experience non-uniform power profiles, is calculated in several axial segments (using average power generation for each segment) and integrated along rod length. The best-estimate model fits through the middle of the scattered data. All data are conservatively bounded by the bounding model.

Rod Characteristics

Test fuel rods from the LWBR development program were Zircaloy-4 clad, non-pressurized (one atmosphere of helium, initial fill) and contained ThO_2 or ThO_2-UO_2 fuel pellets. Rod characteristics are summarized in the report for the 51 rods for which fission gas release data was obtained (23 of the fuel rods are contained in the scrap canister). The fuel rods are grouped by fuel type (100% ThO_2, ThO_2 + $^{233}UO_2$ and ThO_2 + $^{235}UO_2$). The identification numbers of the 23 rods contained in the scrap canister are given below (In the scrap canister there are no 100% ThO_2 fuel rods, three ThO_2 + $^{233}UO_2$ fuel rods [the first three below], and the rest are ThO_2 + $^{235}UO_2$ fuel rods).

79-442	79-509	79-570	79-576	79-613	79-632
79-445	79-513	79-572	79-605	79-617	79-656
79-449	79-514	79-573	79-608	79-623	79-671
79-349	79-522	79-575	79-610	79-631	

Fuel characteristics given for each rod are composition, pellet density, pellet dimensions, and in-core fuel pellet stack length. Fuel compositions ranged from pure thoria to about 25 w/o UO_2. Fuel densities were generally 95-98% theoretical oxide density (10.0 g/cc-ThO_2 and 10.24 g/cc-ThO_2 + 25 w/o UO_2). Nominal fuel pellet dimensions are given, including end-face geometry (flat or dished, with 4-22 mil dish depth). Fuel pellet diameters were 0.21-0.65 inch, with length/diameter ratios of 1.0-3.0. In-core fuel pellet stack length ranged from about 3-7 inches in short rods and from 30-84 inches in long rods.

Cladding heat treatment (RXA-recrystallization anneal or SRA-stress relief anneal), outside diameter, and diameter to wall thickness ratio are given for each rod. Rod diameters ranged from about 0.25-0.71 inch, with cladding OD/t ratios of 12-25. As-fabricated fuel-cladding diametric gaps were 2-10 mils. Fuel-cladding diametric gaps (no direct contact) are a source of thermal impedance and lead to higher fuel temperatures and greater gas release. Cladding OD/t and heat treatment affect the rate of creep down of the cladding diameter (under external pressure) and thereby the fuel-cladding diametric gap and gas release.

Rod Operating Parameters

The test rods were from three different test reactors: (1) the engineering Test Reactor (ETR), (2) the advanced Test Reactor (ATR), and (3) the National Test Reactor-Experimental (NRX). In-pile operating times ranged from <1000 to ~20,000 hours under nominal coolant conditions of 2000 psi and 550°F. Individual rod operating parameters are summarized in the report.

Peak and average axial linear power and fuel burnup are reported for each rod. Axial average values are equal to peak values for short rods, but are about 0.6-0.9 times the peak values for long rods. Peak linear power of most rods ranged from 2-15 kW/ft; four of the 51 rods were higher than 15 kW/ft up to a maximum of 22 kW/ft. Peak burnup ranged from about 1,000-56,000 MWD/MTM.

Peak values (axial position and operating history) of fuel temperatures at the rod centerline and pellet surface were calculated using the CYGRO[11]/FIGRO[12] computer programs. (Time averaged temperatures are about 80% of peak temperatures.) Centerline fuel temperatures at the peak axial power locations ranged from <2000 to over 4000°F and fuel pellet surface temperatures ranged from about 800-1800°F. These temperatures are low relative to the thoria-base oxide melting temperatures (about 5900°F) so that no significant fuel redistributions due to pellet coring or melting were expected.

The ThO_2 dislocation release temperature (for release of gas bubbles from dislocations) was also calculated for each rod, assuming peak conditions and using the model by Warner[13]. This temperature provides a measure of fractional fuel pellet volume for intermediate-high-temperature fission gas release. The ThO_2 dislocation release temperatures range from about 2630-2930°F.

The conclusions drawn from the testing within the range of parameters tested for 51 fuel rods are as follows:

a. Fission gas release is greater at higher fuel temperatures and burn-ups. These effects can be satisfactorily predicted by a model that accounts for gas bubble-coalescence, release from grain boundaries, and dislocations.
b. Higher initial fuel density results in significantly less fission gas release. This effect can be satisfactorily predicted by a model that accounts for release due to recoil and knockout of gas bubbles at free surfaces.
c. No sensitivity to UO_2 composition or rod diameter was observed.

Additional testing[14] was conducted on three fuel rods (79-349, 79-375, and 79-405). All three rods are contained in the scrap canister; 79-349 was included in the first gas testing. These rods experienced relatively high-constant-peak power (18-22 kW/ft). The data indicate that at these high powers (and thus high fuel temperatures), ThO_2-UO_2, 92-95% of theoretical density, experiences equiaxed grain growth and relatively high fission gas release (up to 15%). These data supplement the data on the 51 fuel rods from above, which indicated low fission gas release (from 0.1-5.2%) for operation predominately below 14 kW/ft.

Another test[15] was conducted using five fuel rods (none of the rods is in the scrap canister). The rods were operated to much higher burnups (up to 90,000 MWD/MTM) than the above rods. The data indicate that the low temperature component of fission gas release significantly increases at burnups exceeding about $20x20^{20}$ f/cc (80,000 MWD/MTM). It was postulated that the increase is caused by fuel microstructure changes at high burnup that result in large increase in surfaces where gas bubbles collect and eventually are released. Based on these data the low temperature term in the ThO_2-UO_2 gas release analysis procedure for both the best estimate and the bounding calculation procedures were modified to account for accelerated fission gas release at high burnup; this resulted in good best estimate and conservative bounding fits.

5.6 Irradiation Testing of Internally Pressurized and/or Graphite Coated Zircaloy-4 clad Fuel Rods in the NRX Reactor[16]

Alternate fuel rod design concepts were explored to improve performance capability for commercial scale light water pre-breeder cores to efficiently produce ^{233}U from thoria. The initial screening tests used three fuel rods and two previously tested rods. The three rods (79-584, 79-706, and 79-707) were assembled from spare components previously fabricated for an LWBR blanket irradiation test to provide a basis for comparison with two previously irradiated, non-coated, non-pressurized rods (79-583D and 79-587), one of which was intentionally defected. All five rods are contained in the scrap canister. The rod identification and basic feature of the rods follows:

a. pre-pressurized with helium to 500 psi at room temperature
b. graphite barrier coating on the cladding inside surface
c. combined pre-pressurization and graphite coating
d. previously irradiated, non-coated, non-pressurized rod, and intentionally defected (79-583D)
e. previously irradiated, non-coated, and non-pressurized rod

The helium pressurization, which is standard commercial practice, prevents collapse into unsupported gaps, delays fuel-cladding interaction due to reduced cladding pressure differential, and mitigates the reduction of the thermal conductivity of the gas mixture in the fuel-cladding gap with depletion. The graphite coating provides lubrication of the fuel-cladding interface thereby reducing fuel-cladding interaction, and may provide a barrier to fission product stress corrosion attack of the cladding. The tests of pressurized rods were directed at investigation of fuel rod performance, and were not focussed on thermal-hydraulic considerations.

The fuel was ThO_2-3.06 w/o UO_2 at a density of 95-98% of theoretical density. The fuel stack contained 84 inches of ThO_2-UO_2 pellets with thoria pellets above and below the ThO_2-UO_2 fuel stack. A 10-inch plenum incorporating a Fe-Ni-Cr alloy hold-down spring was present at the top of the stack.

The three test rods (79-584, 79-706, and 79-707) were irradiated, one rod at a time, in the NRX Reactor. The coolant was 2000-psi water at an average temperature of 560°F with a pH of 10.1-10.3 maintained by NH_4OH. Flow velocity was 19.6 ft/sec. Each rod was irradiated for about 100 full power days at peak linear power output of 13-14 kW/ft. Power was then increased by 30% to 17-18 kW/ft to simulate the increased power in an up-power maneuver. The power was maintained at the 30% higher level for about 40 full power days, and the rods reached a peak depletion of $1.5x10^{20}$ f/cc (5800 MWD/MT) and a peak, fast fluence (> 1 Mev) of $1.9x10^{20}$ n/cm^2. Rods 79-583D and 79-587 experienced similar histories except that 79-583D the intentionally defected rod (79-583D) did not experience the up-power maneuver. All rods were periodically removed from testing during reactor shutdowns and examined at Chalk River; these measurements included both rod length and diameter.

Based on comparisons between the non-pressurized, non-coated rod (79-587) and the pre-pressurized and graphite coated rod (79-707), initial pre-pressurization with helium plus graphite coating the inside cladding surface reduce both overall axial cladding strains and peak axial cladding strains. Diameter changes have also been significantly reduced. These reductions are attributed to reduced fuel-cladding interaction and possible enhanced fuel densification due to the relatively higher gas pressure on the fuel pellets. Either pre-pressurization or graphite coating by itself resulted in an intermediate level of improvement from the non-pressurized, non-coated rod, but these comparisons are not as direct due to differences in fuel-cladding gap size.

5.7 Early-In-Life Performance of Short Rod Duplex Pellet Screening (D-1) Test[3]

To support the development of the duplex pellet fuel element, a screening irradiation test was designed, fabricated, and irradiated in the Advanced Test Reactor (ATR) at the Idaho National Engineering Laboratory (INEL). The test consisted of 21 rods irradiated in three holders of seven rods each in a single ATR test loop. The length of the rods was restricted to 11 inches to allow a greater number of rods and thus a greater number of variables to be tested. Duplex pellet annuli of three different compositions was included. The seven rods of the first holder contained UO_2 annuli; the second holder contained UO_2- ZrO_2 annuli; and the third contained UO_2-ZrO_2-CaO annuli. Other test parameters were:

a. Two levels of rod internal pre-pressurization (100 and 500 psig at room temperature).
b. Two types of Zircaloy cladding heat treatment and diameter to thickness ratio (stress relief annealed with OD/t = 16.0 and recrystallized annealed with OD/t = 13.9).
c. Thoria spacers of three different thickness for separating duplex pellets axially to maintain axial alignment of the annulus and central core (0.05 inch, 0.1 inch and 0.5 inch).
d. Varying initial diametric clearance gap between the annulus and cladding (45-85 mils) and between the annulus and central pellet (21-102 mils).

The D-1 duplex pellet-screening test used 21 fuel elements (16 are in the scrap canister) 11 inches in length and 0.3 inch in diameter. The rods consisted of top and bottom Zircaloy-4 end-closures welded into seamless Zircaloy-4 cladding. Contained within the cladding was an 8-inch stack of fuel pellets and a 0.785-inch long plenum region containing an Inconel-X hold-down spring. All 21-test rods were irradiated simultaneously for 32.6 days in the Advanced Test Reactor at the INEEL. The rods operated at 13-15 kW/ft reaching depletion of $1.2\text{-}1.3\times10^{20}$ f/cc averaged over the total duplex pellet volume and ~ $2.4\text{-}2.6\times10^{20}$ f/cc in the annulus. The fast neutron fluence (E > 1 Mev) exposure of the rods ranged from $2.8\text{-}3.9\times10^{20}$ n/cm^2. The coolant was water pressurized to 2000 psi at an average temperature of 520°F. Coolant velocity past the rods was 18 ft/sec. Following irradiation, the 21 rods were subjected to nondestructive examination. In addition, one rod of each annulus composition type was subjected to destructive examination. Nondestructive examinations consisted of:

a. Visual inspections
b. Dimensional measurements
c. Neutron radiography
d. Gamma ray scanning.

Destructive examinations consisted of:

a. Collection and analysis of the rod internal atmosphere to determine fission gas release
b. Depletion analysis
c. Cladding fluence determination
d. Metallographic evaluation of fuel components and cladding.

Visual examinations of the rods as removed from the reactor revealed a thin gray layer of crud that was readily removed by wiping with alcohol soaked cloths. Removal of the crud layer revealed lustrous black oxide surfaces not noticeably different from the pre-irradiation condition. Rod average diameter changes were small, the greatest being a decrease of 0.52 mil. The changes correlated with cladding properties, fast fluence, and rod internal pressure as was expected in the absence of fuel-cladding interaction. Averaged diameter changes for rods in each cladding type-internal pressurization category agreed with calculations to within 0.24 mil.

Rod lengths increased by as much as 0.061% and, as in the case of diameter, correlated with cladding properties, fluence and rod internal pressure. Predicted length increases by stress-free Zircaloy growth, and elongation caused by the diameter change and anisotropy of the cladding material, were larger than the measured changes by factors of 1.5-2.9. However, the length changes were small and the over-prediction represented only 0.02-0.05% strain.

Neutron radiography revealed no evidence of fuel redistribution and/or melting. Cracking of the annuli of all three compositions was observed with the maximum degree of cracking noted in the UO_2-ZrO_2 annuli. Fuel stack lengths in the UO_2 annulus rods and in the UO_2-ZrO_2-CaO annulus rods decreased on the average by 0.22 and 0.40% respectively. The fuel stacks in the UO_2-ZrO_2 annulus rods showed an average length increase of 0.41%. There is no basis for expecting expansion of the fuel stacks in the UO_2-ZrO_2 rods and the length increase is believed to be associated with the significantly greater cracking observed for this fuel material and small separations of fuel pieces.

Gamma scans, performed primarily to determine the axial power shape in the rods, indicated that peak to minimum duplex pellet power in the rods was less than 1.25. This indicates that the differential neutron shrouding employed during irradiation to offset the basic neutron flux profile of the test reactor was effective.

Destructive analysis for depletion and fluence was completed for the UO_2 annulus rod. The measured depletion was 1.27×10^{20} f/cc of compartment (compartment is defined as: the volume inside the cladding per unit length of duplex pellet). The depletion implies a time-averaged rod power level of 14.4 kW/ft, in good agreement with the desired power level. The measured fast neutron fluence experienced by the cladding was 3.9×10^{20} n/cm^2, which corresponds to a time-averaged neutron flux of 1.4×10^{14} n/cm^2-sec.

The percentage of fission gas released from the fuel was measured on one rod of each fuel type with the following results:

Rod Type	Rod ID	Fission Gas Release
UO_2	97-23	0.06%
UO_2-ZrO_2	97-22	0.21%
UO_2-ZrO_2-CaO	97-37	0.39%

These low values indicate that the annulus temperatures were below the temperatures at which substantial migration of gas from dislocation and grain boundaries occurs.

Hydrogen concentration in the cladding of all three rods was about 25 ppm, which is consistent with the as-received content plus the expected hydrogen pickup in the pre-irradiation corrosion test and 32.6 days of in-pile operation. No change in cladding grain size was observed.

Oxide formation on the outside surface of the cladding for all three rods was observed to be one micron or less. About 0.5 micron was present in the pre-irradiation condition based on the rod weight gain during pre-irradiation corrosion testing. On the clad inside surfaces, oxide formation was irregular, varying from no discernible thickness over most of the surface to isolated patches with maximum thickness of 7 microns. The oxide formation was presumably caused by oxygen, produced during fission and released from the fuel, collecting at the cladding.

Metallographic evaluation of the microstructure of the Tho2 central pellets and spacers from all three rods indicated little change, if any, from the pre-irradiation condition. Porosity did not appear to have changed during irradiation. Grain size after irradiation varied in the range ASTM 6-10 (13-50 microns) compared to a pre-irradiation size range of ASTM 5-11 (9-70 microns) with no evidence of equiaxed or columnar grain growth.

Comparison of pre- and post-irradiation annulus porosity was made by means of a Quantimet Television Microscope analysis of pore volume. For the UO_2 rod, total porosity volume in the annulus decreased to about 70% of the pre-irradiation value near the outer surface and to 40-50% in the inner regions. The average diameter of the remaining pores was not appreciably different from the average pre-irradiation pore diameter. The post-irradiation grain size (12 microns average) was uniform and there was no evidence of change in grain size with irradiation. It was also observed that the porosity in the irradiated fuel was located primarily at the grain boundaries whereas both intra-granular and inter-granular pores existed in the pre-irradiation condition.

In the UO_2-ZrO_2-CaO annulus rod, Quantimet analysis showed an overall porosity decrease to about one-third of the pre-irradiation value, essentially equal to the decrease observed in the UO_2 annulus. The porosity change was not uniform across the annulus wall thickness; it varied from a decrease to one-half at the outside surface to one-fifth near the inside surface. The grain in the UO_2-ZrO_2-CaO fuel in the post-irradiation condition was ~40 microns (on the average) and there was no evidence of grain growth.

In the UO_2-ZrO_2 annulus rod, the pre-irradiation porosity was uniform across the annulus thickness but the pore size was significantly larger than the pore sizes in the UO_2 and UO_2-ZrO_2-CaO fuels. After irradiation, porosity appears to have been essentially eliminated. In addition, the lateral surfaces of the UO_2-ZrO_2 annulus show an irregular shape distinctly different from the other annulus materials. This may be due to non-uniform shrinkage associated with the greater UO_2-ZrO_2 densification and lower in-pile creep strength as compared to the UO_2 and UO_2-ZrO_2-CaO fuels. The average pre-irradiation grain size of the UO_2-ZrO_2 material was about 11 microns. After irradiation, etching of the fuel failed to reveal grain structure. The lack of UO_2-ZrO_2 post-irradiation grain structure is consistent with prior experience and may be associated with the phase transformation.

Based on the densification implied by the Quantimet analysis of metallo-graphic samples, and the assumed isotropic volume change and fuel swelling component of 0.7-percent $\Delta v/v$ per 10 f/cc, expected fuel stack length changes were derived and compared to the measured length changes with results as given below.

Fuel Stack Length Change			
Rod Type	**Rod ID**	**Derived From Densification Measurements**	**Measured From Neutron Radiographs**
UO_2	97-23	-0.5	-0.22
UO_2-ZrO_2	97-22	-1.7	+0.41
UO_2-ZrO_2-CaO	97-37	-0.7	-0.40

For the UO_2 and UO_2-ZrO_2-CaO rods, the measured stack shrinkage is 0.3% less than that implied by the net effect of densification and swelling. For the UO_2-ZrO_2 rods, the discrepancy is 2.1%. However, the measurements from the radiographs include the effects of annulus cracks and associated small separations. The large discrepancy for the UO_2-ZrO_2 fuel is probably because it was more extensively cracked than the other fuels.

In summary, examination of the 21 rods of the D-1 test after irradiation at 13-15 kW/ft for 32.6 days to peak depletions of $1.2\text{-}1.3\times10^{20}$ f/cc and fast neutron fluences of $2.8\text{-}3.9\times10^{20}$ n/cm^2 revealed no deficiencies in the early-in-life performance of rods with duplex pellets. The UO_2-ZrO_2 annuli duplex pellets had greater densification than the other two fuel types; however, this did not result in detrimental performance such as excessive operating temperatures or enhanced fission gas release.

The rod identification numbers of the 16 rods of this test contained in the scrap canister are given below.

97-1	97-19	97-23	97-36D
97-12	97-20	97-25	97-37
97-16	97-21	97-31	97-40
97-16	97-22	97-34	97-42

5.8 Cladding Corrosion and Hydriding in Irradiated Defected Zircaloy Fuel Rods[17]

Twenty-one LWBR irradiation test rods containing ThO_2-UO_2 fuel and Zircaloy cladding with holes or cracks operated successfully. Zircaloy cladding corrosion on the inside and outside diameter surfaces and hydrogen pickup in the cladding were measured. The observed outer surface Zircaloy cladding corrosion oxide thickness of the test rods were similar to thickness measured for non- defected irradiation test rods. An analysis model, which was developed to calculate outer surface oxide thickness of non-defected rods, gave results which were in reasonable agreement with the outer surface oxide thickness of defected rods. When the analysis procedure was modified to account for additional corrosion proportional to fission rate and to time, the calculated values agreed well with measured inner-oxide corrosion film values. Hydrogen pickup in the defected rods was not directly proportional to local corrosion oxide weight gain as was the case for non-defected rods.

The rod identification of the rods in the scrap canister is given below.

79-301D	79-353	79-504D	79-609D
79-307D	79-441D	79-583D	79-614D
79-322D	79-433D	79-587	

Note: Rods 79-353 and 79-587 defected in-service

Nuclear power reactors are designed, manufactured, and operated to avoid conditions known to cause in-pile fuel rod cladding defects. Stringent controls on manufacturing and inspection minimize the probability of cladding fabrication defects. However, defected fuel rods (i.e., where the cladding has a through-thickness hole or crack) have occasionally occurred in both test reactors and commercial power reactors. In the event of a cladding defect, coolant can enter the rod interior and hence the cladding internal surface is subject to oxide corrosion and hydrogen pickup. Most defected Zircaloy fuel rods operated satisfactorily until removal during a normal refueling. However, under certain conditions Zircaloy cladding may be degraded over time and pose a threat to continued operation. Therefore, the operational behavior of defected fuel rods is an important engineering consideration for a reactor core.

The report summarizes the cladding corrosion and hydriding results of the LWBR irradiation test program on defected ThO_2-UO_2- fueled Zircaloy-4 clad rods. Two major consequences of defected rod operation, internal surface cladding corrosion and cladding hydrogen pickup, were examined to determine if defected fuel rod corrosion rates and hydrogen pickup behave similarly to those of non-defected Zircaloy-4 rods; the non-defected rods are exposed to coolant on their outer diameter surfaces only. Cladding corrosion film thickness and hydrogen content measurement on intentionally defected Zircaloy-clad fuel rods from the LWBR irradiation test program are compared with values calculated by a computerized corrosion analysis procedure designated as CHORT (Corrosion and Hydriding of Reactor Tubing). The CHORT procedure was based on corrosion and hydriding data from non-defected irradiation test rods with only the outer cladding surface exposed to coolant. Predictions of corrosion oxide thickness are in reasonable agreement with measured data. However, hydrogen pickup in defected fuel rods was observed to behave differently than in non-defected rods. Unexpectedly high hydrogen concentration in cladding at low power segments of certain defected Zircaloy-4 fuel rods was observed and is attributed to gaseous hydrogen transport along the fuel rod cladding gap.

Defected Fuel Rod Corrosion and Hydriding

A defect is defined as a breach of cladding integrity, i.e., a perforation, slit, or pinhole, that usually leaks fission products to the coolant and coolant to the rod internals. A defected Zircaloy-clad fuel rod experiences greater cladding corrosion and hydriding than a normal non-defected rod since both inside and outside cladding surfaces are exposed to coolant. The amount of corrosion and hydriding on the outside surface of a defected fuel rod should be about the same as on a non-defected rod since the conditions are the same. If a defect occurs in the cladding, coolant may enter the fuel rod and reach high temperature when the core is taken to power. Corrosion and hydriding on the inside surface of the cladding will then occur at a faster rate than on the outside cladding surface; this is due to higher temperatures at the inner surface because of fissions on or very near the corroding surface.

The Shippingport LWBR core contained 12 hexagonal-shaped modules, which were arranged in a symmetric array, surrounded by 15 reflector modules. Each of the hexagonal modules contained a central movable fuel assembly (seed) surrounded by a stationary blanket assembly. The fuel was in the form of ceramic pellets that were sealed within Zircaloy-4 tubes. In the seed and blanket regions, the fuel pellets were composed of the mixed oxides of ^{233}U and ^{232}Th in solid solution. In the reflector region and in short sections at the tops and bottoms of the seed and blanket fuel rods, the pellets were ThO_2. The seed-blanket-reflector configuration of the LWBR core had 17,287 fuel rods. LWBR fuel rod cladding was used in two metallurgical conditions, re-crystallization annealed (RXA) seed rod tubing and stress-relief annealed (SRA) blanket and reflector rod tubing. Fuel rods were maintained in close-packed hexagonal arrays by AM-350 stainless steel grids. The LWBR core operated for 28,730 EFPH. The absence of high coolant activity indicated that there were no fuel rod cladding defects.

Hydrogen transport through the fuel-cladding gap can also occur in irradiated defected fuel rods by the following sequence of events. First coolant enters the rod through the defect and oxidizes the inner Zircaloy cladding surface through the reaction:

$$Zr + 2H_2O \rightarrow ZrO_2 + 2H_2$$

The hydrogen that is not absorbed by the Zircaloy (about 75%) is released to the fuel-cladding gap, thus enriching the atmosphere in hydrogen. In addition, some of the coolant entering the defect is decomposed to hydrogen and peroxide by radiolysis, $2H_2O \rightarrow H_2O_2 + H_2$. Thus the oxidant partial pressure is reduced both by corrosion of the internal surface of the Zircaloy cladding and by peroxide oxidation of the fuel. High levels of free hydrogen generated by the radiolysis of the coolant and fuel and cladding oxidation can migrate through the fuel-cladding gap to the end regions of the defected rod where the hydrogen is absorbed.

Experimental Details

Irradiation testing of defected fuel rods played an important role in development of fuel elements for the LWBR Core. The LWBR irradiation test program encompassed 30 individual tests of 271 fuel rods. The test rods were irradiated either in standard specimen holders or in bundles resembling portions of LWBR fuel rod modules. The coolant for these irradiation tests was pressurized water maintained at pH 10 by NH_4OH additions. Nineteen fuel rods (14 seed and 5 blanket) were intentionally defected with drilled holes prior to testing. A larger (~35 mil diameter) spotting hole was first drilled halfway through the cladding wall from the outside surface and then continued through the wall to the inside surface with a smaller (~5 mil diameter) defect hole. The fuel stacks of some of the defected rods were short (6-11 inches in length). However, five seed rods and four blanket rods were of LWBR length, i.e., up to 118 inches long. Holes were located about halfway up the fuel stack on short rods and within 24 inches of the bottom on long rods, except on seed rod 79-443D where the hole was located at the bottom end plug-pellet stack interface.. In addition, two blanket rods, which were irradiated at higher heat ratings than LWBR core rods, developed small cladding defects during planned in-service transient testing.

All 21 defected rods successfully operated with limited radioactivity release to the coolant. Startup activities, i.e., the values measured immediately after a defected test rod reached full power following a shutdown, were 5-10 times greater than the steady state activities due to release of fission products to the coolant. These high activities declined over a period of one to three days to the steady state level. The steady state coolant activity values of irradiation tests with defected rods were higher than similar tests containing only non-defected rods. For example, the ^{138}Cs activity in the GRIP IIIA test with defected rod 79-614D was $1x10^5$ dpm/ml compared to an activity value of $5x10^4$ dpm/ml for the GRIP IIIC test with no defected rods. Irradiation histories of the 21 LWBR defected rods, including the two which defected in-pile, are given in the report. The fuel rods with intentionally fabricated defects are identified by the letter "D" after the rod number. The seed-size irradiation test rods with RXA cladding were irradiated to peak depletions up to $12x10^{20}$ f/cc and peak fast neutron (>l Mev) fluences up to $101x10^{20}$ n/cm^2. The peak depletion and fluence for the LWBR core seed rods were $11x10^{20}$ f/cc and $97x10^{21}$ n/cm^2, respectively. The blanket-size test rods with SRA cladding were irradiated to peak depletions up to $4x10^{20}$ f/cc and fluences up to $12x10^{20}$ n/cm2. The peak depletion and fluence for the LWBR core blanket rods were $5x10^{20}$ f/cc and $74x10^{20}$ n/cm^2.

The objectives of the LWBR irradiation test program were:

a. to test fuel rods under heat fluxes, fast neutron fluxes, and fuel depletions expected in the LWBR core,
b. to confirm satisfactory performance for design lifetime,
c. and to support development of performance analyses for LWBR fuel rods.

The program for measuring corrosion and hydriding in Zircaloy-4 cladding of defected fuel rods consisted of rods from the 14 tests given below.

LWBR Defected Irradiation Tests Containing Fuel Rods Examined for Cladding Corrosion and Hydriding

Designation	Test Name	Rod Type	Heat Treat Cladding	Test Reactor
M-13-S2	Seed Rod Screening	Seed	RXA	ETR
M-13-S3	Seed Rod Screening	Seed	RXA	ETR
M-13-S3A	Seed Rod Screening	Seed	RXA	ETR
M-13-S4	Seed Rod Screening	Seed	RXA	ETR
GRIP II	Grid Rod In-Pile	Seed	RXA	ETR
GRIP IIIA	Grid Rod In-Pile	Seed	RXA	ETR
GRIP IIIB	Grid Rod In-Pile	Seed	RXA	ATR
LSR	Long Seed Rod	Seed	RXA	NRX
---	Production Thoria	Seed	RXA, SRA	ETR
C-7B3	Blanket Screening Test	Blanket	SRA	ETR
C7-B3A	Blanket 6-Rod Assembly	Blanket	SRA	ETR
C7-BBT	Blanket Bundle Test	Blanket	SRA	ETR
SBR	Short Blanket Rod	Blanket	SRA	NRX
NLBR	New Long Blanket Rod	Blanket	SRA	NRX

Post-Irradiation Examination Results

All of the defected rods were visually examined. The inside and outside corrosion cladding-surface oxide thickness were measured for 16 of the defected rods on at or near the fuel rod peak power position. The same 16 rods were analyzed for hydrogen content and distribution. Summaries of internal and external cladding-corrosion data for the 16 LWBR irradiated defected test fuel rods that were destructively examined are presented for RXA and SRA Zircaloy-4 cladding. External corrosion-oxide thickness measured on the defected fuel rods was about the same as those of non-defected rods with similar irradiation histories. Nine of the intentionally fabricated defected rods had a white or gray streak downstream from the defect hole (streamers). The defect hole streamer of GRIP IIIB Rod 79-609D was observed at the first interim examination (1330 EFPH). At 2360 hours the streamer consisted of a bright white area and a darker phase extending downstream from the defect hole and increasing in width as the distance from the hole increased. With continued irradiation the white portion increased in area and covered the darker phase. Post-irradiation examination confirmed the streamer to be ZrO_2. The nine oxide streamers were local and had no noticeable effect on general cladding integrity. It is thought that either eroded ThO_2 fuel or fission products emanating from the defect hole caused the accelerated corrosion of the Zircaloy cladding. Internal cladding surface oxide films in the defected rods were usually more variable in thickness and several times thicker than the external oxide films. The thicker inner-surface corrosion films are due to several factors: higher internal cladding surface temperatures (up to 780°F), fission-induced corrosion acceleration at the internal surface and exposure to a steam environment. The internal film on Rod 79- 587, however, was thinner than the external film because the rod was removed from test about 8.5 hours following the planned up-power transient test that produced the defect. Four of the intentionally fabricated defected rods experienced cladding swelling. Rod 79-504D swelled along the primary fuel stack. Three rods (79-433D, 79-307D, and 79-583D) had periods of normal dimensional changes during irradiation before any significant swelling, mainly in the plenum region, was detected. Blockage or partial blockage of the defect hole occurred in all four rods. The combination of hole blockage and swelling is indicative of water logging, i.e., excessive internal pressure built up by trapped coolant which deforms the cladding.

Zircaloy-4 Cladding Hydriding

Measured hydrogen pickups in irradiated LWBR non-defected test rods and autoclaved Zircaloy-4 tubing specimens were proportional to measured outside diameter corrosion thickness. The hydriding in defected Zircaloy fuel rods falls into three categories: expected due to corrosion, accelerated, and massive. Expected hydrogen pickup in defected rods results from the additional hydrogen which enters the cladding through the inside diameter ZrO_2 film during corrosion. Twelve of the 16 destructively-examined defected LWBR test rods exhibited normal behavior of this type (~100-1000 ppm H_2). Accelerated hydriding is defined as hydrogen absorption from the coolant far in excess of the nominal 25% pickup fraction of free H_2 produced by the $Zr-H_2O$ corrosion reaction for Zircaloy-4 (~several thousand ppm). Massive hydriding is the formation of regions of delta phase zirconium hydride in the cladding due to grossly accelerated hydrogen pickup (16,300 ppm).

The hydrogen contents of Zircaloy-4 cladding samples from the LWBR intentionally defected test rods are summarized in the report. Measurements were made with a vacuum extraction technique and by visual comparison with known metallographic standards. Due to the greater internal surface corrosion, the total hydrogen contents in the defected rod cladding were several times those in non-defected rod cladding with similar irradiation histories. For example, in the GRIP- IIIA test, defected rod 79-614D had 174 ppm hydrogen in the peak power region, whereas companion non-defected rod 79-617 had only 40 ppm hydrogen. Hydrogen pickup in non-defected fuel rods is proportional to corrosion oxide thickness and, therefore, is greater in peak power positions than in cooler, low power regions. In contrast, several defected test rods (79-433D, 79-443D, 79-609D, and 79-614D), that were examined at several power positions, had higher hydrogen contents in cooler, low power cladding regions where the corrosion was less. Also, due to the steep temperature and higher hydrogen concentration radial gradients in defected rods, hydrogen tends to diffuse from the hotter inside cladding surface to the cooler outside surface; this results in higher hydrogen concentrations at the outside cladding surface.

Several instances of localized accelerated and massive hydriding were observed. Two intentionally fabricated defected fuel rods (GRIP-II rod 79-443D and GRIP-IIIB rod 79-609D) had areas of accelerated hydriding with several thousand ppm of hydrogen. Localized areas of massive hydriding were found in C7-B3A rod 79-353, GRIP-II rod 79-441D, and GRIP-IIIB rod 79- 609D. These localized areas were converted to solid zirconium delta hydride (~16,300 ppm H_2). Massive hydriding was also accompanied by dimensional changes in these three rods due to the lower density of zirconium delta hydride compared with Zircaloy-4. However, none of these incidents interfered with the operation of the irradiation tests. For example, C7-B3A rod 79-353, which defected in-pile due to iodine stress-corrosion cracking, operated successfully for about 12,000 EFPH even though during post-irradiation examination the cladding was observed to be massively hydrided near the bottom end of the rod. None of these hydrided rods lost additional structural integrity during operation, which attests to their ability to function under localized accelerated and massive hydriding conditions.

Summary of Corrosion and Hydriding Behavior

Oxide films on internal surfaces of defected Zircaloy-4 fuel rods were several times as thick as films on external surfaces. This can be explained both by higher temperatures at the internal surface and by the effect of surface fissile enhancement.

Total hydrogen contents in defected fuel rod cladding were several times those in non-defected rod cladding. Further, evidence of hydrogen migration to cooler regions of the rods remote from the defect hole was observed, indicating that hydrogen pickup is not proportional to corrosion oxide thickness.

Hydrogen levels in the cladding of the defected fuel rods were generally higher at the external surface than at the internal surface because, in a sufficiently high thermal gradient, hydrogen diffuses toward the cooler region.

Defected rods with areas of accelerated or massive hydride continued to operate satisfactorily.

Conclusions

a. The measured outer surface Zircaloy cladding corrosion oxide thickness of both defected and non-defected LWBR irradiation test rods were similar and can be calculated using a model based on non-defected outer surface corrosion experience.
b. There is a significant corrosion enhancement on the inside-cladding surface in defected Zircaloy fuel rods that can be attributed to radiation damage caused by fission product recoil.
c. When modified to account for the additional corrosion caused by fission activity on the inner Zircaloy cladding surface, a model qualified to the corrosion of non-defected rods provided calculated values which agree well with measured inner oxide corrosion film values.
d. Hydrogen concentrations are higher than predicted in the lower power segments of defected Zircaloy fuel rods and are not proportional to oxide thickness. This phenomenon is attributed to gaseous hydrogen transport through the fuel-cladding gap; this results in high hydrogen concentrations in the gap at the top and bottom ends of the defected rod.
e. Hydrogen absorption models in which hydrogen pickup is calculated to be directly proportional to local corrosion oxide weight gain, while adequate for the prediction of external hydriding in non-defected rods, are unsuitable for prediction of axial hydrogen distribution in defected Zircaloy rods.

5.9 Iodine and Cesium in Oxide Fuel Pellets and Zircaloy-4 cladding of Irradiated Fuel Rods[18]

Measurements of fission product iodine and cesium are reported for thoria and binary (ThO_2-UO_2) fuels with various irradiation histories. These volatile fission products were measured on the cladding surface or in the fuel by using specially developed radiochemical techniques. The radiochemical iodine measurements are in agreement with a theoretical iodine release model for irradiated fuel. Microprobe examinations of irradiated fuel rod cladding sections show fission product cesium to be located preferentially at the pellet to pellet interface region. Fission product iodine was detected in the interface microprobe-limit region of one sample but generally remained below the limit of detection.

Twenty-two fuel rods were analyzed for this report; ten of these rods with their identification numbers given below are contained in the scrap canister.

79-353	79-449	79-576	79-605	79-617
79-442	79-572	79-587	79-610	79-671

Rod 79-587 failed in-pile during up-power transient.

The iodine and cesium concentrations obtained from radiochemical analysis of the twenty-two test-rods are given along with a summary of the irradiation history of each test rod. Electron microprobe examination of cladding segments from four irradiation test rods was also conducted to determine iodine and cesium distribution on the inside diameter surface of cladding. A brief summary of the results for two of the rods that are contained in the scrap canister is presented below.

Rod 79-442 – One of the two locations, corresponding to a pellet interface location on the clad surface had only barely detectable amounts of cesium. The second interface location displayed only background levels. No iodine, cadmium, tellurium or mercury was detected above the background levels anywhere on the sample.

Rod 79-576 – One of the two pellet-to-pellet interfaces on the cladding surface showed a relatively strong indication of cesium. No iodine, mercury, cadmium, or tellurium was detected above the sample background levels.

The conclusions of the report were as follows:

a. There is essential agreement of microprobe evaluation with the low-level of iodine found by radiochemical analysis. Results of both radiochemical and microprobe examinations suggested less iodine than calculated using the iodine release upper-bound calculation model. In one case, the radiochemical iodine measurement was greater than the upper bound model. Remeasurement of this rod, 79-617, showed a decrease in the iodine concentration to a level well below the upper-bound calculation. The upper-bound iodine calculation method presented in the report is therefore corroborated by the radiochemical data.

b. The presence of other volatile fission products on the cladding, cesium and tellurium were confirmed by electron microprobe evaluation. The cesium concentration obtained from radiochemical data was on the cladding in greater concentration than iodine, as might be expected due to its higher fission product yield. Similarly, the failure to detect cadmium on the cladding during microprobe examination was probably due to its extremely small fission product yield.

5.10 Corrosion and Hydriding of Irradiated Zircaloy Fuel Rod Cladding[19]

Irradiation histories of 47 LWBR test fuel rods 29 with RXA cladding and 18 with SRA cladding are given. The rod identification numbers of 25 of these rods, which are contained in the scrap canister, are given below

79-349	79-513	79-575	79-610	79-623
79-405	79-514	79-576	79-613	79-624
79-442	79-570	79-579	79-617	79-631
79-449	79-572	79-605	79-619	79-632
79-509	79-573	79-608	79-621	79-656

The results of the study are summarized below.

a. CHORT predictions compare well with measured corrosion data from out-of-pile autoclave tests on LWBR Zircaloy-4 tubing.
b. Corrosion thickness and hydrogen uptakes in LWBR irradiation test program fuel rod Zircaloy-4 cladding are less accurately accounted for by the CHORT program due in part to measurement scatter and material variability.
c. Both out-of-pile and in-pile test data indicate that SRA Zircaloy-4 corrodes faster than RXA Zircaloy-4 does.
d. Measured corrosion thickness of Maine Yankee, KWO, Turkey Point, and MELBA fuel rods are in reasonable agreement with CHORT predictions.

Destructive examination of LWBR irradiation test fuel rods for corrosion and hydriding determinations are described below.

A. Metallographic Sample Preparation

After collection of internal atmosphere gases, LWBR irradiation test fuel rods were sectioned to provide samples for measuring depletion, fluence, and hydrogen content and for metallographic evaluation. The metallographic samples were carefully mounted to preserve the corrosion oxide. Each piece was pressure-mounted by immersion in an epoxy resin (Hysol pressurized to 1000 psi) to lock fuel pieces in place. A silicone rubber sleeve was used to isolate the outside cladding surface from the Hysol while it was immersed in Hysol for 24 hours at room temperature. The Hysol was cured for two hours at 200°F. The pressure-mounted pieces were sectioned with a diamond cutoff wheel to provide both transverse and longitudinal metallographic samples. Transverse samples were mounted on end in metallographic rings so that grinding exposed a plane perpendicular to the axis of the rod. Longitudinal samples were mounted on their side; when ground, they revealed a plane parallel to the axis.

B. Metallography

Metallographic planes of transverse and longitudinal rod sections were evaluated first in the as-polished state at magnifications from 5-1000X to observe the microscopic condition of cladding and fuel and corrosion of the cladding surface. Oxide thickness measurements were obtained from the metallographic cross section at random locations of each cladding sample. After the corrosion thickness measurements were made, cladding was etched with an H_2O_2-HNO_3 solution with HF additive to reveal the degree and distribution of hydride precipitates.

C. Hydrogen Measurements

A manometric vacuum extraction method was used to measure hydrogen contents of the irradiated Zircaloy-4 cladding samples. This procedure uses induction heating of the cladding sections in a vacuum system. Gases evolved by vacuum extraction at 1000°C are collected, and hydrogen gas is isolated by diffusion through a palladium membrane permeable only to hydrogen. The amount of hydrogen is determined manometrically from the pressure, volume, and temperature. The overall accuracy of this method is ±10 ppm at the 2-sigma level based on measurements with standard samples obtained from the National Bureau of Standards. The hydrogen content of unirradiated companion cladding samples was subtracted from the irradiated Zircaloy-4 hydrogen values to estimate the increase in hydrogen (hydrogen pickup) due to corrosion.

5.11 Irradiation Performance of Duplex Fuel Pellet Test rods Depleted to $9x10^{20}$ Fissions/cm^3 of Compartment – D-1 Test[20]

The prime characteristics and variables of the 31 rods used in the test follows; the rod identification numbers of the 20 rods contained in the scrap canister are given below:

97-11	97-19	97-23	97-30	97-36D
97-12	97-20	97-25	97-31	97-37
97-15	97-21	97-27	97-32	97-40
97-16	97-22	97-29	97-34	97-42

The D-1 Test rods are 11 inches in length by 0.3 inch in diameter and consist of top and bottom Zircaloy-4 end- closures welded into seamless Zircaloy-4 cladding tubes. Cladding tube heat treatment is incorporated as a test variable. Rods were fabricated with recrystallization-annealed tubing or highly cold-worked stress-relief annealed tubes. Contained within the cladding tube are an 8-inch stack of fuel pellets and a 0.8-inch long plenum region containing an Inconel-X spring. Five different fuel stack arrangements were used for each of the duplex-annulus material type. These arrangements are designed to test various sizes and configurations of solid thoria spacers that maintain alignment of the duplex pellet components in the fuel stack. Each rod contains a solid cylindrical pellet, with about half the fuel loading of the duplex pellets, at each end of the duplex pellet stack. The purpose of these pellets is to reduce power peaking at the ends of the pellet stack. Thoria pellets are incorporated on the outboard side of the power peaking suppressor pellets, against the bottom end closure and against the plenum spring; this is done to limit operating temperatures of the bottom end closures and the plenum spring. The four-annulus compositions tested in the D-1 rods are:

Annulus	UO_2 w/o	ZrO_2 w/o	CaO w/o	ThO_2 w/o	^{235}U Enrichment (%)
UO_2	22.3				22.3
ZrO_2-UO_2	34.0	66.0			97.7
ZrO_2-UO_2-CaO	36.9	58.1	5.0		97.7
ThO_2-UO_2	33.8			66.2	93.1

The UO_2 fuel was included since it is the fuel most commonly employed in commercial reactors. The ZrO_2 based fuels were included because they contain essentially no ^{238}U. Absence of ^{238}U results in a significant neutron economy advantage. Inclusion of the thoria based binary fuel extends the technology developed in the LWBR program for solid pellets with this fuel system to include the duplex pellet geometry.

Other D-1 test variables are: (1) magnitude of initial diametric clearance gap between the annuli and cladding and between the annuli and central pellets, (2) levels of rod internal pre-pressurization and (3) defect operation.

Diametric clearance gaps between the annuli and cladding ranged from 45-84 mils which is in the range of current commercial design practice. The gaps between annuli and the thoria central pellets were varied from 24-102 mils to investigate the effect of a wide range of this parameter on rod performance.

The principal advantages of pre-pressurization are: 1) increased margin to cladding collapse in the presence of an axial gap between fuel pellets and 2) decreased degradation of the thermal conductivity of the rod's internal atmosphere as fission gases are released from the fuel. Degradation in gap thermal conductivity is lessened by the increased concentration of higher conductivity helium as compared with released fission gases. In addition, there is reduced cladding "creep-down" due to the reduced pressure differential across the cladding which delays fuel-cladding interaction, reduces cladding strain, and reduces the potential for formation of fuel stack gaps. On the other hand, higher internal pressure reduces the loss-of-coolant accident performance capability with respect to an unpressurized rod. Therefore, it is desirable to optimize the initial pressure level within the rods. To study these effects, initial helium pressures of 100 and 500 psig at room temperature were selected.

Although not included in the original test, rods containing intentional defects in the cladding were introduced as replacement rods for the UO_2 and ThO_2-UO_2 rods terminated for destructive examination at an early stage. The intentional defects, included to investigate the behavior of rods with breached cladding, were in the form of 5-mil diameter holes drilled through the cladding at the approximate axial midplane of the rods.

The prime characteristics and variables of the individual D-1 test rods are given in the report.

Fuel Components

Annuli - The outside chamfers at the pellet ends and the perpendicularity control were specified to minimize frictional forces between the fuel pellets and the cladding as the fuel stack lengthens and shortens with power changes. The chamfer eliminates sharp corners on the pellet while the limits on end face non-perpendicularity reduce pellet tilting tendencies and resulting radial forces of the pellet against the cladding. The chamfers also minimize the potential for creation of chips during rod loading. Chips, if present in the rod, may increase local strains in the cladding. The length-to-diameter ratio of the duplex-pellet annulus (2.1) is consistent with that of the LWBR seed pellets. The annulus wall thickness provides a nominal-annulus-to-central core cross sectional area ratio of unity that was considered acceptable with respect to manufacturing limitations and integrity during irradiation. With this 50/50 split the volumetric heat generation rate and depletion of the annulus is about twice that of solid pellets producing equal power.

The annulus outside-diameters are sized to provide clearance gaps in the range of present commercial practice, which avoids premature fuel-cladding contact. Large radial gaps reduce heat transfer capability and increase fuel temperatures. Increases in fuel temperatures must be limited to avoid fuel structural changes or melting which can lead to cladding failure. The UO_2 rods and the ThO_2-UO_2 rods contain fuel-to-cladding diametric gaps in the range 49-85 mils. Because of poorer heat conduction properties, the Zirconia-based fuels have fuel-to-cladding gaps in the 45-58 mil range.

High density (>96% TD) was desired for all fuel materials to maximize thermal conductivity, thereby resulting in higher power production at the maximum allowable temperature of the fuel. In addition, high density minimizes fuel dimensional changes in service and consequent axial shrinkage of the fuel stack. Axial shrinkage in rods of commercial length might lead to collapse of unsupported cladding if axial gaps were to form between pellets.

The densities (derived from pellet dimensions and weights) of the annular fuel materials are as follows:

	Density (Percent TD)		
Fuel Material	Average	Maximum	Minimum
UO_2	95.1	96.5	93.1
ZrO_2-UO_2	92.4	93.1	91.6
ZrO_2-UO_2-CaO	94.0	95.0	93.3
ThO_2-UO_2	96.7	96.0	97.2

The fuel-to-cladding gap for the ZrO_2-UO_2 annular pellets was set about 1 mil below the gap sizes for the other fuel compositions to compensate for the lower density.

Thoria Central Pellets - The thoria central pellets were prepared from available LWBR seed thoria pellets. The LWBR pellets, of about 98.8-percent TD, were nominally 0.256 inch OD and 0.530 inch long. The end dish depth and corner chamfers were 9 and 15 mils, respectively. Outside diameters of the thoria central pellets, were ground to different sizes to obtain a range of annulus-to-central pellet diametric gaps. This was done as a test variable, to evaluate the effect of central pellet eccentricity in the annulus on pellet temperatures and the effect of total clearance gap on fuel-cladding interaction. The length of the central cores was made less than that of the annuli to ensure that the annular pellets are longer than the central pellets at the highest predicted operating temperature and thus avoid axial gaps between the annuli.

Thoria Spacers - Thoria spacers separating the duplex pellets may be necessary to maintain the axial alignment of the fuel stack. The effect of these spacers was investigated in the seven test rods of each fuel material by varying the length of the spacers (0.050, 0.100, and 0.530 inch) and the number of duplex pellets between spacers. The rods ranged from no spacers in the duplex pellet stack to having a spacer at each duplex pellet interface. These were prepared by slicing long pellets transversely and breaking the corners by tumbling in silicon carbide grit. The outside diameter of these thin spacers was about the same as the duplex pellets of the particular rod in which the spacers were located. The design of the 0.530-inch long spacer was the same as for the LWBR seed thoria pellets. The concave dish in each end of 0.530-inch spacer reduced the convex shape that would exist at power in a flat ended pellet. Reduction of the convex contour minimizes axial expansion fuel-cladding interaction. The outside diameter of the long thoria spacers matched the outside diameter of the duplex pellets of the rod in which they were located.

Thoria End Pellets - One long spacer was used at the bottom of the fuel stack in each rod to reduce operating temperatures at the end closure insert. The thin thoria spacers were used as required at the top of the fuel stacks to reduce operating temperature of the plenum spring and to achieve the desired overall fuel stack and plenum lengths in the rods.

End Peak Suppressor Pellets - Power peaking was significant at the ends of the fuel stack of these short rods, which were in the high flux region of ends of the ATR. To limit this end peaking to acceptable values, ThO_2-UO_2 pellets with fissile loading of about 40% of the annular pellets were positioned at the top and bottom of the fuel stack of each rod. The design of these flux suppressor pellets was the same as the long thoria pellets except that they were 0.58 inch long.

Non-Fuel Components

End closures - The end closures, which were tungsten inert gas welded into the cladding tube, were machined from Zircaloy-4 bar stock. The bottom end closure was designed to provide lateral, axial, and rotational restraint of the rod in the test holder while the top end closure provided lateral restraint but permitted limited axial motion.

Plenum Springs - The 0.785-inch long plenum region above the fuel stack contains an Inconel-X spring that provides a pre-irradiation axial load of 1.82 pounds on the fuel stack. This force is about 12 times the fuel pellet stack weight and restrains the pellet stack from shifting during handling and shipment of the rods.

Cladding - The Zircaloy-4 cladding for the D-1 test rods was fabricated by the Wolverine Tube Division of Universal Oil Products. Both recrystallized annealed (RXA) and stress relief annealed (SRA) conditions were used; the properties are given below. The outside diameter of the RXA tubing was decreased by about 4 mils to produce an outside diameter-to- thickness ratio (OD/t) of 13.9 which is representative of the LWBR seed rod design. The SRA tubing diameter was decreased by about 11 mils to produce an OD/t of 16.0, which is typical of commercial reactor practice. The outside diameters reductions were achieved by pickling in a mixture of hydrofluoric and nitric acids following fuel rod assembly.

Properties Of Tubing For D-1 Test Rods

	RXA	SRA
As Fabricated outside Diameter (mil)	308±1	308±1
Inside Diameter (mil)	259±1	259±1
Wall Thickness (mil)	24.5	24.5
Final Heat Treatment (°F/hr)	1225/4	925/4
Cold-work, last of 3 Passes (%)	51	51
ASTM Grain Size	10	na
Longitudinal Tensile Properties at 700°F		
0.2% Yield Stress (psi)	19,000	44,000
Ultimate-to-Yield Ratio	1.73	1.27
Total Elongation (%)	34	13
Contractile Strain Ratio	1.44	1.35
Chemistry (Billet Analysis)		
Hafnium (ppm)	23	23
Hydrogen (ppm)	4	4
Nickel (ppm)	30	30
Nitrogen (ppm)	30	30
Oxygen (ppm)	1300	1300

Test Train Design

The in-pile hardware design used for the AWBA D-1 test was available from short rod tests in the LWBR Irradiation Testing Program. The D-1 rods are supported in the in-pile hardware by means of the end stems. The bottom, spade shaped end stems of the rods are inserted through the bottom base plate. Flats on the portion of the end stem engaged by the base plate prevent rotation of the rods. A locking plate goes over the spade ends and slides laterally engaging the spade ends to prevent axial movement of the rods. The round, cone-tipped end stems at the top of the rods are inserted through mating holes in the upper locator plate. The distance between the bottom base plate and the top locator plate is 0.2 inch larger than the shoulder to shoulder length of the rods. This allows for free elongation of the rods by thermal expansion and axial clad strain. In the holder internals, the rods have the cross-sectional array. The rods are arranged on a square pitch of 0.355 inch with rod spacing of 0.052 inch. The internal surface of the holder half shells are sculpted to represent the shape of additional rods, thus giving a flow pattern representative of a larger rod array.

The results of the study are summarized below.

<u>Non-Destructive Examinations</u>

Rods without Intentional Cladding Defects

Visual examinations of rods without intentional cladding defects resulted in no observations of irradiation induced effects that raise concern over rod performance. Early stage corrosion, in the form of isolated small white spots, was observed on some rods at an early state of irradiation but did not appreciably worsen with irradiation.

Rod cladding dimensional measurements, overall length and diameters, in general indicate that fuel-cladding interaction has not yet become significant in the D-1 test rods.

At a fast neutron fluence of $25x10^{20}$ n/cm^2, the maximum reached by any of the rods, overall length strains were at most 0.24% for rods with SRA cladding and 0.12% for rods with RXA cladding; the strains are principally the result of stress-free Zircaloy growth. The expected effects of rod internal pre-pressurization are evident in those rods with higher internal pressure that exhibit smaller length changes than rods with lower internal pressure.

Because of the lack of fuel-cladding interaction during the first half of test life, the diameter changes continued the trend of diameter shrinkage. Cladding heat treatment and thickness, level of rod internal BOL pressurization and fast neutron fluence are the determining effects. The stress relief annealed (SRA) clad rods with their thinner wall show greater diametric shrinkage than the recrystallized annealed (RXA) clad rods. Rods with higher fast neutron fluence show greater shrinkage. Furthermore, within the cladding material categories, the rods with lower BOL pressure show greater shrinkage due to the higher-pressure differential across the cladding.

Only one rod clearly shows onset of fuel-cladding interaction. Diameter traces for this rod reveal irregularities that correlate with the fuel stack components. Fuel-cladding contact was expected to occur first in this rod because of the unfavorable combination of characteristics, which included stress relief annealed cladding, low internal prepressurization, small-fuel-cladding clearance-gap, and high power rating.

Non-destructive examinations aimed at determining the condition of the internal rod components were gamma ray scanning and neutron radiography. The internal components of the rods did not have any abnormalities of intentional defects. Fuel stacks were shown to be in good condition with no evidence of pellet crushing or development of gaps between pellets. The various sizes and configurations of ThO2 spacers performed satisfactorily.

The lengths of the fuel stacks in the D-1 rods were measured from the neutron radiographs and compared with the pre-irradiation fuel stack length changes. Observed changes ranged from -1.3 to +1.5%. Although data at depletions beyond $\sim 1 \times 10^{20}$ f/cc-compartment are limited, tentative trends in fuel stack behavior were observed which correlate with duplex-pellet annulus material. The UO_2 annulus rods showed small increases or decreases in stack length (-0.40 to +0.15%) at depletions $<1.5 \times 10^{20}$ f/cc-compartment. However, the one rod radiographed a second time, at depletion of $\sim 6 \times 10^{20}$ f/cc-compartment had stack elongation of 0.39% following early-in-life shrinkage of 0.20%. This implies that following some early-in-life densification, fuel swelling becomes dominant.

Early-in-life fuel stack shrinkage was observed in the rods with ZrO_2-UO_2- CaO duplex pellets (ranging from 0.29%-0.45%) with no change during subsequent irradiation for the one rod radiographed again at depletion of $\sim 6 \times 10^{20}$ f/cc-compartment. Thus, it may be that in the ternary fuel, swelling is less than for UO_2 and/or that densification is greater. It is noted that the initial density, in terms of percent of theoretical, was lower for the ternary fuel (93.2% TD) than for the UO_2 fuel (95.5% TD).

Three rods with ThO_2-UO_2 duplex pellet annuli were subjected to neutron t radiography. Fuel stacks in all three elongated with a nearly linear growth rate of about 0.14% per 10^{20} f/cc-compartment.

The ThO_2-UO_2 rods had substantial shrinkage (up to 1.3%) at depletions above 2×10^{20} f/cc-compartment after initial increases; the increases are attributed to accumulation of small separations associated with the more extensive early-in-life cracking of the ZrO_2-UO_2 annuli as compared to the others. The subsequent shrinkage may be associated with lower in-pile creep-strength of the ZrO_2-UO_2 material. Evidence of dimensional instability of the ZrO_2-UO_2 annuli was revealed by destructive examination of rod 97-22.

Based on these non-destructive examination results it was concluded that performance of the duplex-pellet fuel system is quite good. Cladding and fuel pellet integrity was maintained and dimensional changes compared favorably with results of solid pellet tests previously conducted as part of the LWBR development program.

Rods with Intentional Cladding Defects

Non-destructive examinations of rods with intentional cladding penetrations revealed several features of interest not observed on non-defected rods.

On the external cladding surfaces of rods with intentional cladding defects, flow patterns downstream from the intentional defect holes were observed. The most extensive flow pattern was observed on the rod that contained duplex pellets with UO_2 annuli. The one other defected rod irradiated for a long time contained ThO_2-UO_2 annulus duplex pellets and evidenced a flow pattern that was much less extensive than for the UO_2 rod. This indicates that the ThO_2 based fuel may be less susceptible to erosion and/or corrosion than the UO_2 fuel.

Circumferential white corrosion rings were observed on the cladding of the defected rod with ThO_2-UO_2 fuel at the locations of 50-mil thick thoria spacers separating duplex pellets in the fuel stack. Neutron radiography and preliminary metallographic examination of the cladding from this rod demonstrated that the white corrosion rings are associated with substantial non-uniform concentrations of hydrogen in the cladding; the regions affected by the corrosion rings coincided with the regions of heaviest hydrogen concentration. Preliminary destructive examination results also indicate that the primary source of the hydrogen was accelerated corrosion of the cladding inner surface during irradiation in the defected state. It is believed that the fuel stack arrangement in this rod, consisting of pellets containing the fissile material (with high heat generation) interspersed with the ThO_2 spacers (with lower heat output), generated hydrogen "cold traps" in the cladding.

The circumferential white corrosion rings on the cladding external surface, coincident with the regions of high hydrogen concentrations, are thought to be a result of the hydriding. Diameter measurements revealed ridging of the cladding at the locations of the corrosion rings; the average diametric ridge height was 0.8 mils with a maximum of 1.2 mils. This ridging was probably caused by the cladding-material volume increases associated with the extensive hydriding from internal cladding corrosion. Subsequent development of the external accelerated corrosion rings resulted from disturbances in the protective corrosion film due to local straining and/or perhaps reduced corrosion resistance of zirconium hydride. In the intentionally defected rod with UO_2 duplex pellets, irregularities in gamma ray intensity from a pellet near the defect hole were observed. Neutron radiography of this rod revealed the abnormality to be a fractured pellet with some rearrangement of the pellet fragments. The damage to the duplex pellet is believed to be the result of forces generated by the pressure buildup release through the defect hole during rod startup. The damage occurred during the first 30 days of irradiation and did not noticeably worsen during 118 days of additional irradiation.

These abnormalities are the result of defect operation and are not specifically related to the duplex pellet fuel design. The local high concentration of hydrogen in the cladding was caused by variations in cladding temperature associated with the alternating arrangement of fissile and fertile fuel pellets in the fuel stack. This problem can be solved by eliminating the thoria spacers and using other methods to maintain axial registry of the duplex pellet components. Fractured pellets near intentional defect holes have also been observed in previous LWBR tests with solid pellets.

Destructive Examinations

Destructive examinations were not completed for non-defected rods and were only started on the ThO_2-UO_2 rod with intentionally defected cladding.

Over the depletion ranges covered, fission gas release percentages were for all four fuel systems being investigated in the D-1 test, and appeared to depend on fuel depletion more than on fuel material. The highest release measured is 1.75% for a ThO_2-UO_2 rod with depletion in the annulus material of 18.9×10^{20} f/cc. UO_2 and ZrO_2-UO_2-CaO rods with depletions of ~12×10^{20} f/cc had lower gas release, roughly in proportion to the annulus depletion.

Metallographic evaluations of the fuel components demonstrated that, macroscopically, all components appeared to be in good condition. Cracking of the duplex pellet components and the thoria spacers was observed but geometrical integrity was maintained with no evidence of crushing or crumbling. No evidence was found, for any of the fuel types, of mass transport by evaporation of material from the high temperature (inside) surface of the duplex pellet annuli and condensation in colder regions of the rod.

The metallographic samples were analyzed using a Quantimet 720 Image Analyzing Computer to determine the total porosity and porosity-size distributions in the duplex pellet annuli. For all fuel material types, total porosity decreased during early irradiation. For the UO_2 fuel, continued irradiation to 13.0×10^{20} f/cc of annulus material resulted in continued reduction of porosity. For the ZrO_2-UO_2-CaO fuel, the existence of non-uniformly distributed large pores resulted in high variability of the Quantimet results and larger uncertainties in the porosity volume percents. However, disappearance of small-fabricated porosity early in life and emergence of very fine porosity believed to be fission gas bubbles, with continued irradiation to 13.0×10^{20} f/cc of annulus material was evident. The ThO_2-UO_2 fuel, irradiated to the highest depletion (18.9×10^{20} f/cc of annulus material), also showed emergence of very small fission gas bubbles after initial disappearance of small pores; the translucency of the fuel and visibility of pores below the surface viewed complicated the pore volume analysis.

The dimensions of the duplex pellet components in the transverse metallographic samples were measured and, along with the fuel length changes derived from neutron radiography, were used to determine the effects of porosity changes and swelling effects on the fuel volume. For the UO_2 and ZrO_2-UO_2-CaO fuels, both at compartment depletions of ~6×10^{20} f/cc, decrease in the annulus volume is observed; whereas an increase in annulus volume is indicated for the ThO_2-UO_2 fuel at compartment depletion of 9.3×10^{20} f/cc. These volume changes correlate with the pre-irradiation densities of the pellets as shown in the following summary.

Fuel Material	Pre-irradiation Density (%TD)	Volume Change (%).
UO_2	95.5	-1.4
ZrO_2-UO_2-CaO	93.7	-4.7
ThO_2-UO_2	96.6	+1.2

For the UO_2 and ZrO_2-UO_2-CaO materials, no appreciable change in grain size, from that of the unirradiated fuel was noted. For the ThO_2-UO_2 material, considerable difficulty was experienced in developing grain structure by chemical etching. Indistinct grain boundaries were revealed near the pellet outside diameter with size unchanged from the unirradiated size. Throughout the inner regions of the annuli, a finer microstructure, without the angular shape characteristic of grains, was observed. At the high depletion of this material, ($18.9,x10^{20}$ f/cc of fuel material) it appears that subdivision of grains, perhaps associated with high concentration of fission products, may be occurring. This phenomenon does not appear to have had any deleterious effects on fuel performance, however.

The microstructure of the ThO_2 components, (central cores and spacer pellets) with maximum depletion of $\sim 0.5x10^{20}$ f/cc-compartment, was similar to that of the unirradiated material. Although there appeared to be a decrease in the population of very small pores, larger pores, which constitute the bulk of the porosity, were essentially unchanged in number or size. Grain size also was unchanged from the pre-irradiation condition.

Investigations of the rod cladding to develop data relative to stress- corrosion cracking included:

a. Metallography to assess cladding internal corrosion and fuel-cladding mechanical and chemical interaction.
b. Visual examination of the inside surface of cladding.
c. Examination of the inside surface of the cladding on the Scanning Electron Microscope. The cladding surface morphology of the irradiated cladding and of unirradiated cladding was studied.
d. Electron Microprobe analysis of the irradiated cladding inside surface to determine the elements present and the local distribution of each.
e. Chemical analysis to determine the total amount of iodine and cesium present on the cladding inside surface and inside the cladding material.
f. Macroscopically, the metallographic evaluation of the cladding revealed no evidence of cracking or other defects.

Corrosion of the external cladding surface resulted in an oxide layer typically 0.04-0.08 mils (1-2 microns) thick. About ½ of this corrosion was present following pre-irradiation corrosion testing. On the internal surface of the cladding from the higher depletion rods with UO_2 and ThO_2-UO_2 fuel, localized patches (nodules) of corrosion, typically several microns thick and with maximum thickness of about 0.3 mil (10 microns), were observed. Visual examination of the cladding surfaces indicated these to be evenly distributed over the surface except at pellet interfaces where none were found. Electron Microprobe analyses of the cladding from the UO_2 and ThO_2-UO_2

fueled rods indicate the corrosion nodules to be sites of concentration of uranium, thorium (if present in the fuel) and fission products. The coincidence of cladding corrosion nodules and fuel material/fission products implies a fuel transfer and fission enhancement mechanism for the formation of the corrosion. Simple rubbing of the fuel material on the cladding could be the cause.

This explanation is reinforced by observed differences in patterns of corrosion nodules on the cladding which correlate with different methods of fuel pellet grinding. The UO_2 fuel was centerless ground to diameter with the pellet simultaneously rotating and moving axially during the grinding. Corrosion nodules in the rod with UO_2 fuel were randomly distributed. The ThO_2-UO_2 fuel was plunge ground to diameter. In plunge grinding, the pellets do not move axially resulting in a series of minute ridges and grooves on the pellet surface. In the rod with ThO_2-UO_2, the corrosion nodules tended to be aligned in circumferential rows. Thus, it appears that fuel material transfer to the cladding occurred at points of fuel-cladding contact.

The cladding inner surface for the rod with ZrO_2-UO_2-CaO fuel was observed metallographically to have a continuous corrosion film about 0.3 mil rather than the patchy corrosion noted in the rods with the other fuel types. Visual examination of the interior cladding surface confirmed that the corrosion film covered essentially the entire surface; in addition the examination showed a mosaic-like appearance with individual parts of the mosaic roughly equal to the size of the fragments of the cracked annulus. Electron microprobe analysis of the cladding surface indicated spatially uniform concentrations of uranium, calcium and fission products. The causes of the differing appearance of the cladding associated with the ZrO_2-UO_2-CaO fuel as compared to the cladding associated with the UO_2 and ThO_2-UO_2 fuels is not well understood.

Corrosion nodules in the UO_2 and ThO_2-UO_2 fueled rods using replicas of the cladding surfaces observed visually with a Scanning Electron Microscopy ranged from <1 mil to ~3 mils in diameter. In areas not affected by the corrosion nodules, the surface appeared very similar to the unirradiated tubing. For the ZrO_2-UO_2-CaO rod, Electron microscopy shows a structure of very closely spaced corrosion patches.

Measurements were made of the quantities of iodine and cesium on the inside surface of cladding samples from rods of the different fuel types. The UO_2 and ZrO_2-UO_2-CaO fuel rods were at depletions of $\sim 6 \times 10^{20}$ f/cc-compartment and the ThO_2- UO_2 rod was at depletion of 9.3×10^{20} f/cc-compartment. Iodine and cesium on the surface were collected by means of a rinse with dilute nitric acid. The cladding sample was then dissolved to obtain iodine and cesium that had penetrated below the surface. Concentrations of these fission products found on and in the cladding, assuming uniform distribution, are as follows:

	Concentration (mg/dm2	
	Iodine	Cesium
UO_2 fueled rod 97-24	0.05	1.50
ZrO_2-UO_2-CaO fueled rod 97-39	0.05	0.85
ThO_2- UO_2 fueled rod 97-17	0.08	1.10

Microprobing of the cladding surfaces indicated that in the UO_2 and ThO_2- UO_2 rods, fission products were concentrated in corrosion nodules covering about ½ of the surface. Thus, local concentrations of iodine and cesium for the UO_2 and ThO_2-UO_2 rods might be about twice the values given in the above summary. In the ZrO_2-UO_2-CaO fueled rod, microprobing indicated uniform distribution of fission products.

The amounts of iodine found on or in the cladding of the three rods represent 0.26-0.31% of the amount of iodine calculated to have been generated in the fuel. These releases are a factor of 4-6 below the measured release of noble fission gases from the fuel. For cesium, the release percentages range from 0.16-0.34% and are a factor of 4-11 less than the percentage release of noble fission gases.

Based on the destructive examination results for non-intentionally defected D-1 test rods, it is concluded that performance capability of the duplex fuel system is excellent. For the range of depletion covered, fission gas release was low and fuel pellet integrity was maintained with minimal dimensional changes. No effects of irradiation beyond expectations were observed.

5.12 Irradiation Performance of Long Rod Duplex Fuel Pellet Bundle Test – LDR Test[3]

This test was conducted to investigate the performance characteristics of a long column of duplex fuel, interacting with the cladding, as distinguished from earlier tests of very short lengths of duplex fuel. The test was designated The Long Duplex Rod (LDR) Test. Six rods were used for the test (97-52, 97-53, 97-54, 97-55D, 97-57, and 97-58), all are contained in the scrap canister. The rods contained duplex-fuel stacks about 67 inches in length and were operated in a test reactor with a 48-inch fuel height; this resulted in an irradiated fuel length of about 63 inches. The LDR Bundle Test was irradiated in the north and southeast test loops of the Advanced Test Reactor (ATR); these loops provided separate pressure, flow, and heat removal systems, independent of those of the ATR facility; the ATR provided the neutron environment.

Individual fuel rod characteristics are listed in the report. All of the fuel rods had fuel cladding diametric gaps in the range 4.4-8.8 mils; they were operated at relatively high power levels, characterized near beginning of life (BOL) in the range 14-16.9 kW/ft, and to high depletions, the highest being 14.2×10^{20} f/cc of compartment (28.0×10^{20} f/cc of fuel annulus volume) during normal testing. At the end of normal testing, five rods were irradiated at a power level higher than in the preceding cycle, for a period of about 27 days. Four rods experienced an increase in power in the range 40-49% and one rod 19%. None of the rods failed. All dimensional data given in the report were obtained prior to the end of life (EOL) high power cycle. Properties of the cladding are the same as those given for the D-1 tests given above.

Significant variables included in the test were the following:

a. Three different fuel compositions were tested as the annular portion of the duplex fuel. These compositions were UO_2, ZrO_2-UO_2-CaO, and ThO_2-UO_2 respectively. In all cases, the central core pellet was ThO_2.
b. The duplex fuel was stacked with and without periodic full-diameter ThO_2 spacer pellets. Spacer pellets were intended to maintain axial registry between the annulus and the core.
c. Both stress relief annealed (SRA) and recrystallization annealed (RXA) Zircaloy cladding was used.
d. Rod internal pre-pressurization levels of 100 and 500 psig at room temperature were established.
e. In addition, one intentionally defected rod was tested.

Based on the resulting data, the following summary observations have been made:

a. Fuel rods with SRA cladding experienced greater elongation, and more cladding diametric shrinkage in regions where pellet-cladding interaction (PCI) was absent, than fuel rods with RXA cladding, as expected
b. Fuel rods prepressurized to 500 psig experienced less cladding elongation and less cladding shrinkage than fuel rods prepressurized to 100 psig, within each group of the two cladding types.
c. No differences in performance characteristics could be assigned to any of the three fuel compositions. As evidenced by rod diameter change, the largest amount of PCI occurred with the rod having ThO_2-UO_2 fuel. This observation has no special significance, however, since this rod operated at the highest power and to the highest depletion.
d. No appreciable PCI occurred in rods with RXA cladding at intermediate peak depletions of 6.0×10^{20} and 7.9×10^{20} f/cc of compartment, or at a high depletion of 11×10^{20} f/cc of compartment. This determination was made from axial diameter profiles.
e. Measurable PCI occurred in fuel rods with SRA cladding at high-peak compartment depletions of 11.7×10^{20} and 14.2×10^{20} f/cc compartment.
f. Of the two fuel rods which experienced the largest length change (rods with SRA cladding), the rod with the most pellet-cladding interaction, as indicated by axial diameter traces, did not show the largest length increase. The reason for this behavior may be related to two possible mechanisms acting separately or in concert; namely, (1) radial expansion of cladding would be expected to be reflected in a corresponding axial shrinkage and (2) a decrease in axial ratcheting could occur due to local locking and compartmentalization of fuel within the cladding. The latter mechanism may be enhanced by the presence of spacer pellets.
g. Neutron radiography showed a fuel stack length increase of 0.18% at a low peak compartment depletion of 1.1×10^{20} f/cc, indicating little or no densification in the high density, high fission rate UO_2 annular fuel.
h. Neutron radiographs of one fuel rod at a peak compartment depletion of 7.9×10^{20} f/cc, and a second rod at a peak compartment depletion of 11.7×10^{20} f/cc indicate no loss in the mechanical integrity of the annular fuel column; i.e., no fragmentation of the annuli. Fuel stack growth of about 0.5% was observed for these rods.

i. The neutron radiograph of one fuel rod identified a 0.14-inch gap in the central-core thoria-pellet stack in the upper portion of the rod, and a gap of 0.52 inch between the top of the central-core thoria-pellet stack and the top of the annular fuel stack. Based on these observations, the annular fuel stack was 0.66 inch longer than an uninterrupted central core stack. This rod was fabricated with no thoria spacer pellets and a central thoria core length 0.2 inch less than the annular fuel length to form an intentional axial gap. Comparison with an X-ray of the as-built rod revealed that the annular fuel stack had grown 0.37 inch and the central-core thoria-stack had contracted 0.09 inch.

j. A comparison was made of cladding elongation between two groups of rods, both had SRA cladding and one operated with solid ThO_2-UO_2 pellets; the other was the LDR test with UO_2 and ThO_2-UO_2 duplex pellets. These rods all operated with similar power and fuel cladding gaps. Based on the data, less PCI-induced length change occurs with duplex fuel.

k. Based on fuel rod-to-fuel rod gap measurements, no significant fuel rod bowing occurred over the life of the test.

l. The intentionally defected rod was fabricated with a 5-mil diameter hole but experienced a water logging event that increased the diameter of the unirradiated portion of the rod; this reached a stress level near yield and caused an apparent flux-induced creep bulging in the power region.

m. The intentionally defected rod, which had ThO_2 spacer pellets between adjacent duplex pellets, developed hydride rims and subsequent accelerated corrosion on the external surface of the cladding at the locations of the spacer pellets. These hydride rims were revealed in axial diameter traces and in neutron radiographs showing a typical hydride color contrast in cladding over thoria spacers. These hydride rims could result in cladding embrittlement and reduced load carrying capacity.

n. It is concluded that this program demonstrated satisfactory performance of the test bundle and of fuel rods containing duplex fuel pellets, which were irradiated to high fuel-annulus depletion and through a severe transient.

5.13 Experimental Results of the Irradiation of Long Rod Duplex Pellet Screening Test in the NRX Reactor, New Long Duplex Rod (NLDR) Test[21,22]

One of the designs developed by the Advanced Water Breeder Applications (AWBA) program for a commercial-scale, prebreeder reactor core was based upon the use of fuel rods containing duplex pellets. A duplex pellet consists of a cylindrical thoria central pellet within an oxide annulus that contains fissile material. During irradiation, ^{232}Th in the central pellet is converted to ^{233}U for subsequent use in a breeder reactor core. If a UO_2 annulus is used, it can be chemically separated from the thoria central pellet following irradiation so that the ^{233}U in the central pellet is kept free of contamination by other uranium isotopes. Freedom from contamination could also be achieved by use of separate fissile and fertile fuel rods. However, reactor core power densities comparable to those of commercial cores cannot be achieved when the thorium fraction in a separate fuel rod core is high enough for efficient production of ^{233}U.

The NLDR test series was accomplished in the National Research Experimental Reactor at the Chalk River Nuclear Laboratory in Chalk River, Ontario, Canada, which is owned and operated by Atomic Energy of Canada, Ltd. The reactor is a natural uranium, heavy water-moderated, light water-cooled reactor. It is equipped with several test loops, which provide pressure, flow, and heat removal system independent of the reactor for the irradiation of test specimens. The reactor core serves primarily to provide the neutron environment for the irradiation tests.

There are also a number of advantages of duplex pellets over solid pellets in both breeders and commercial reactor core applications. These advantages result mainly from the low operating fuel temperature. An irradiation test program was undertaken at Bettis to support development of duplex-pellet fuel rods. The New Long Duplex Rod (NLDR) test series (designated NLDR-1, NLDR-2, NLDR-3, and NLDR-4) was one part of this irradiation test program. The NLDR tests used six 110-inch-long, 0.3-inch-diameter Zircaloy-4 clad rods containing duplex pellets. The principal design variables are given below.

Principal Design Variables					
Rod ID	**Test**	**Annular Pellet Composition**	**Fuel Cladding Gap, mils**	**Special Features**	**Total Irradiation Time, EFPH**
97-61	NLBR-1	UO_2-ZrO_2-CaO	55	None	11,149
97-62	NLBR-1	UO_2	55	None	11,149
97-64	NLBR-2	ThO_2-UO_2	55	None	10,281
97-65	NLBR-2	UO_2	36	None	6,340
97-123	NLBR-3	UO_2	36	2 plenum springs	8,056
97-162	NLBR-4	UO_2	43	Longer central pellets	4,115

The test series was conducted to:

a. evaluate the behavior of duplex fuel pellets in long rods with pellet-cladding interaction axial loads similar to those which would be experienced by fuel rods in commercial service,
b. compare the performance of UO_2 and UO_2-ZrO_2-CaO duplex pellet fuel systems at power levels adjusted to reflect relative melting points,
c. compare the performance UO_2 duplex fuel with a smaller cladding gap,
d. compare the performance of fuel rod containing two plenum springs with fuel that has one spring, and
e. assess the effect of longer central thoria pellets on rod behavior.

The conclusions drawn from the testing are as follows:

a. All fuel rods experienced relatively small overall external dimensional changes with irradiation up to 17.8×10^{20} f/cc compartment (about 35.6×10^{20} f/cc annulus).
b. The UO_2 rod (97-64) experienced earlier fuel-cladding interaction and greater cladding length increases than the UO_2-ZrO_2-CaO rod (97-61) irradiated under the same conditions.

c. Beyond about 12-13x10^{20} f/cc peak depletion, both rods experienced cladding length decreases. This phenomenon had not been previously observed in Bettis long rod tests of solid ThO_2- UO_2 fuel pellets irradiated in the LWBR program.
d. Large gap ThO_2- UO_2 rod (97-64) exhibited overall length increase less than those of the large gap UO_2 rod (97-62) but greater than those noted for the large gap UO_2-ZrO_2-CaO rod (97-61).
e. Small gap UO_2 rod (97-65) experienced greater length increases and an earlier "turn around" in length change than large gap UO_2 rod (97-62).
f. At comparable depletions, small gap UO_2 rod (97-123) with two plenum springs experienced less length increase than any other UO_2 rod in the test; some of this difference is attributed to operation at only 75-80% of design power for about 1/3 of the lifetime.
g. UO_2 rod (97-162) with long central pellets experienced a greater initial length increase than any other NLDR test rod but its behavior at intermediate depletions was typical of the other UO_2 rods in the test.
h. Closure of both the fuel-to-cladding and annulus-to-central pellet gaps resulted in significant cladding diameter increases due to continued radial swelling of the fuel. This phenomenon was observed in all three fuel systems.

5.14 In-Pile and Out-of-Pile Corrosion Behavior of Thoria-Urania Pellets[23]

A total of 19 LWBR irradiation test rods from 14 irradiation tests (summarized in the report) composed the database for the in-pile portion of the fuel stability study. Nine of the rods are contained in the scrap canister (79-301D, 79-307D, 79-322D, 79-433D, 79-441D, 79-504D, 79-583D, 79-609D, and 79-614D). The 19 fuel rods contained ThO2, ThO_2-$^{235}UO_2$, and ThO_2-$^{233}UO_2$ fuel pellets. The rods (14 seed and 5 blanket) were intentionally defected with drilled holes prior to testing. A larger (~0.089-cm diameter) spotting hole was first drilled halfway through the Zircaloy-4 cladding from the outside surface and then continued through the wall to the inside surface with a smaller 5-mil diameter (~0.013-cm diameter) defect hole. Irradiation histories of the 19 defected rods are given; irradiation exposures were up to 19,970 EFPH with peak fluences (>l Mev) of up to 98 x 10^{20} n/cm^2. The coolant for these irradiation tests was pressurized water maintained at pH 10 by NH_4OH addition. Coolant oxygen, hydrogen, and chlorine concentrations were <0.14 ppm, 40-70 cc/kg, and <0.1 ppm, respectively. The irradiation tests were performed in the ETR, the ATR and the NRX. A summary of the in-pile testing results follows.

a. Satisfactory fuel performance was demonstrated in the ThO_2 and ThO_2-UO_2 fueled defected LWBR test rods irradiated to peak depletions up to 12x10^{20} f/cc and peak fast neutron (>l Mev) fluences up to 98x10^{20} neutron/cm^2.
b. Excellent fuel chemical, mechanical, and thermal behavior was shown for operating conditions up to peak linear power levels of 518 w/cm, peak heat fluxes up to 189 w/cm^2, and peak center temperatures up to 2366°K.
c. No evidence of significant corrosion or erosion of the fuel pellets was observed. Nine of the 19 intentionally defected rods displayed some minor indications of corrosion-erosion; white or gray streaks or spots manifested this just around or downstream from the defect hole openings. These effects were very local and were

most likely the result of a limited amount of fuel, fission product, or contaminated Zircaloy corrosion locally downstream of the hole.

d. No other indications of fuel corrosion-erosion were detected. The ThO_2 and ThO_2-UO_2 fuel pellets, when compared with previous in-pile tests on UO_2 and ZrO_2-UO_2 fuels, had lower levels of released activity, slower fission product leaching, and minimal fuel solution and attrition by the coolant.

e. No fuel grain growth was detected but there was some migration of porosity to the grain boundaries. Fuel cracking occurred as would be expected for long term operation of both defected and non-defected fuel rods. No evidence of fuel waterlogging was observed. (Waterlogging is deformation of the cladding caused by excessive internal fuel rod pressure of entrapped coolant as it flashes to steam during a power increase).

The conclusions drawn from the testing are as follows:

a. Both ThO_2 and homogeneous ThO_2-UO_2 (2-30 w/o UO_2) fuel pellets have excellent corrosion resistance - even in oxygenated, high temperature, pressurized water.

b. Thoria-urania is one of the most corrosion resistant of all UO_2 solid solution oxide fuels. Even when oxidative attack does occur, the mode of oxidation, growth of a second cubic phase permits the ThO_2-UO_2 samples to maintain their integrity.

c. Maintenance of fuel integrity in defected irradiation test rods was consistent with the favorable stability of out-of-pile corrosion tests on thoria-base fuel pellets.

d. Under the defect condition of exposure to high temperature water containing an oxidant (H_2O_2 or O_2 from fission fragment radiolysis of the water coolant), thoria-base fuels exhibit: 1) slower fission product leaching, 2) lower levels of released activity, and 3) slower fuel solution and attrition by the coolant than is the case for UO_2 and ZrO_2-UO_2 fuel systems.

e. Both the in-pile and out-of-pile test results support the conclusion that LWBR-type fuel rods containing ThO_2 and ThO_2-UO_2 pellets can successfully operate in the defect condition with limited radioactivity release to the coolant.

5.15 Internal Hydriding in Irradiated Defected Zircaloy Fuel Rods – a Review [24]

The purpose of the review was to summarize the test data, causes, mechanism, and methods of minimizing internal hydriding failures in defected Zircaloy-clad fuel rods. A defect is defined as a breach of cladding integrity, i.e., a perforation (slit. crock. or pinhole) that leaks fission products to the coolant and coolant to the rod internals. Many defected Zircaloy-clad fuel rods operated satisfactorily without diminishing core performance. A fuel rod failure is defined as loss of cladding integrity, high coolant activity level, and contamination of the coolant by particulate fuel.

Two types of hydriding, external hydriding produced by hydrogen outside the fuel rod and internal hydriding due to causes inside the fuel rod, were identified in Zircaloy-clad fuel rods. Internal hydriding is further classified as primary or secondary hydriding. Primary hydriding is generated internally in an initially non-defected Zircaloy fuel rod. Its sources are hydrogenous contaminants (moisture, oil, grease, etc.) introduced into the fuel rod during fabrication as well as any residual hydrogen in the oxide fuel resulting from the hydrogen sintering operation. In secondary hydriding the initial breach of the Zircaloy cladding is caused either by primary hydriding itself or by a non-hydride-related incident which allows coolant to enter and hydride the rod. Examples of a non-hydriding incident include stress-corrosion cracking induced by pellet-cladding interaction, power ramp, aggressive fission product attack, rod-to-rod contact causing high cladding temperatures, cladding wear at support grid contact points, etc. The report reviewed the problem of secondary hydriding, mainly in pressurized water reactors where the coolant contains some dissolved hydrogen.

Hydrogen pickup in Zircaloy fuel rods falls into three categories: expected due to corrosion, accelerated, and massive. Expected hydrogen pickup results from the additional hydrogen that enters the Zircaloy cladding through the ZrO_2 corrosion film (about 50-500 ppm). Accelerated hydriding is defined as hydrogen absorption from the coolant far in excess of the nominal 25% pickup fraction of free H_2 produced by the Zr-H_2O corrosion reaction for Zircaloy-4 (several thousand ppm). Massive hydriding is the formation of regions of delta phase zirconium hydride in the cladding due to grossly accelerated hydrogen pickup (16,300 ppm). At operating temperatures for PWRS, zirconium is thermodynamically unstable with respect to hydrogen and should completely hydride. The protective corrosion oxide surface film prevents the gaseous hydrogen in the coolant from reacting with the bare Zircaloy.

As part of the review intentionally defected rods from pre-LWBR tests, the LWBR (19 fuel rods - identification numbers of the rods in the scrap canister are given above), and the AWBA programs (3 fuel rods - 97-36D is in the scrap canister) were analyzed.

Pre-LWBR Tests

The Bettis Laboratory was one of the first to study the behavior of defected Zircaloy-clad UO_2 fuel rods in-pile and the factors affecting the limit of their performance. The initial work was carried out in the 1950s in support of the Shippingport PWR Core I blanket rods. Excessive cladding hydriding was observed in both intentionally defected rods and in rods that operationally defected in-pile (unintentionally defected). Hydrogen contents of 100-200 ppm were found in cladding near defects and 1400 ppm at the ends of the rods. It was concluded either that the intentionally fabricated defect holes of some rods became plugged or that areas of the rod away from the defect hole became effectively, isolated and behaved as though the rods were not defected. In any case, the cladding of these rods became stressed and ruptured during irradiation with resultant hydriding.

Since 1960 massive internal hydriding was found only in rods that operationally defected in-pile. Sixteen such in-pile defected rods were observed. Fuel compositions were mainly UO_2, ZrO_2-UO_2 and UO_2-ZrO_2-CaO. Irradiation periods in the defected state after cladding rupture varied from about five minutes to approximately 200 days. Cladding cracking, both ductile and brittle, was attributed to bad welds, burnout caused by molten fuel, cladding instability due to fuel swelling, and water logging. All 16 rods were destructively examined, and extensive areas of massive internal hydride were detected in 13 of them. Both accelerated and massive hydriding occurred at remote locations from the defect. Two of the remaining rods were found to have brittle cladding fractures. Hydride-was observed mainly in the cladding near the end caps. The cladding over the fuel stacks was relatively free of hydride. The last rod waterlogged and displayed only an overall high hydrogen content in the cladding (about 300 ppm) but did not exhibit massive hydriding.

Thirty intentionally fabricated defected rods were also tested during this period (1960-1970). These rods were fabricated with various pellet geometries (annular, dished-end, solid), pellet densities (84-98% theoretical), and fuel materials (UO_2, ZrO_2-UO_2, ThO_2-UO_2). The irradiation performance of these intentionally defected rods was satisfactory. Post irradiated fuel structures ranged from that of the pre-irradiated structures to almost total fuel melting.

Three cases of water logging occurred in these intentionally fabricated defected rods. Cladding diameter swelling was measured in a UO_2-fuel and a ZrO_2-UO_2 fuel rod. Another ZrO_2-UO_2 fuel rod ruptured resulting in cladding hydrogen concentrations of about 500 ppm, but massive internal hydriding was not found. This failure was attributed to excessive plastic straining caused by repeated water logging incidents during irradiation. With the exception of the ruptured rod, there were no detectable fuel losses associated with the irradiation of these 30 intentionally defected fuel rods.

Six of these intentionally defected rods contained ThO_2-UO_2 fuel. There were no unusual incidents during the irradiation of these rods indicating satisfactory performance.

The pre-LWBR test data can be summarized as follows:

a. Fuel rods with intentionally fabricated defects generally did not excessively hydride.

b. Fuel rods which defected in-pile generally had areas of accelerated or massive hydriding.

LWBR Tests

The Shippingport LWBR core contained 12 hexagonal-shaped modules which were arranged in a symmetric array surrounded by 15 reflector modules. Each of the hexagonal fuel modules contained a central movable seed assembly surrounded by a stationary blanket assembly. The fuel was ThO_2 and ThO_2-UO_2 pellets which were sealed in Zircaloy-4 tubes. The absence of higher-than-expected coolant activity during operation indicated that there was no detectable breach of the cladding in any of the LWBR rods.

As part of the LWBR irradiation test program, 19 fuel rods (14 seed and 5 blanket) were intentionally defected with drilled holes (0.005-inch diameter) prior to testing. In addition, two blanket test rods developed small cladding defects during planned in-service transient testing. The transient testing was at higher heating rates than occurred during LWBR reactor operations.

All 21 defected test rods operated successfully with limited radioactivity release to the coolant. No significant ThO_2 or ThO_2-UO_2 fuel erosion was detected. Due to the greater internal surface corrosion, the total hydrogen content in the defected rod cladding was several times those in non-defected rod cladding with similar irradiation histories 100-500 ppm compared to 30-70 ppm hydrogen). A pronounced variation in hydride concentration was observed through the cladding wall thickness of the defected rods. Hydrogen levels in the cladding were higher--at the external surface than at the internal surface because hydrogen diffuses toward the cooler region in a sufficiently high thermal gradient. The hydride concentrations for non defected rod cladding were relatively uniform.

Hydrides in the vicinity of the defect hole were generally low in concentration with typical uniform levels of about 100 ppm. This might occur from hydrogen escaping through the defect hole resulting in a low H_2/H_2O ratio or hydrogen diffusion to adjacent cooler cladding areas. Evidence of hydrogen migration to cooler regions of the rods remote from the defect hole was observed, indicating that local hydrogen levels are not always proportional to corrosion oxide thickness in defected rods.

Instances of localized accelerated and massive hydriding were detected in three intentionally defected and one operationally defected fuel rod. None of these incidents interfered with the operation of the irradiation tests. For example, one rod that defected, in service due to iodine stress corrosion cracking operated successfully for about 12,000 effective full power hours (EFPH). This rod was operational even though during post irradiation examination the cladding was observed to be massively hydrided near the bottom end of the rod. None of these hydrided rods lost structural integrity during operation, which attests to their ability to function under localized and massive hydriding conditions.

AWBA Tests

The Advanced Water Breeder Applications (AWBA) program used a duplex pellet concept. The duplex pellet design consisted of a cylindrical thoria central core inside an oxide annulus that contained the initial fissile material. Transmutation of the thorium in the duplex pellet to ^{233}U provides fuel for use in subsequent breeders. The irradiation test program supporting development of the duplex fuel pellet included three intentionally fabricated defected rods, two with UO_2 and one with ThO_2-UO_2 annuli.

Some slight erosion was noted in the UO_2 fueled defected rod. The irradiation performance of the ThO_2-UO_2 fueled defected rod compared favorably with that of the LWBR solid ThO_2-UO_2 pellet irradiation tests. Circumferential white corrosion rings were observed on the outside cladding surface of the defected rod with the ThO_2-UO_2 annulus at the locations of 50-mil thick ThO_2 spacers separating the duplex pellets in the fuel stack. Neutron radiography and metallographic examination of the cladding showed that the white corrosion rings were associated with substantial non-uniform concentrations of hydrogen in the cladding, with the regions affected by the corrosion rings coinciding with the regions of heaviest hydrogen concentration. In regions of cladding adjacent to the ThO_2-UO_2 annulus, hydrogen concentrations ranged from <100 ppm near the inner surface to several hundred ppm or more near the outer surface. In the cooler cladding adjacent to ThO_2 spacer pellets, much higher concentrations of hydrogen were observed. These concentrations varied from about 500 ppm near the inner surface to approximately 12,000 ppm in a rim about 3 to 5 mils thick at the outer surface. The fuel stack arrangement in this rod, consisting of pellets containing the fissile material (with high power and heat generation) interspersed with the ThO_2 spacers (with lower power and heat output), generated hydrogen cold traps in the cladding.

Diameter measurements revealed ridging of the cladding at the locations of the white corrosion rings. The average diametric ridge height was 0.8 mil with a maximum of 1.2 mils. This ridging could be caused by the volumetric increases associated with the extensive hydriding. Subsequent development of the accelerated white corrosion rings then resulted from disturbances in the protective corrosion film due to local straining and/or reduced corrosion resistance of zirconium hydride.

A summary of the review follows:

a. Intentionally defected Zircaloy test rods usually do not excessively hydride.
b. Zircaloy fuel rods that defect in service generally acquire localized areas of accelerated or massive hydride.
c. Both intentionally and operationally defected fuel rods with local areas of accelerated and massive zirconium hydride can operate without failure for extended periods of time under restricted power conditions.
d. Out-of-pile zirconium hydriding test data in H_2/H_2O gas mixtures shows that specimen characteristics (geometry and surface conditions) as well as environmental factors (hydrogen pressure, test temperature. and test time) affect the amount of hydrogen pickup in Zircaloy. In addition, the type of Zircaloy (2 or 4), the heat treatment, and minor variations in the alloying conditions were also found to influence hydrogen absorption.
e. The significant factors affecting internal hydriding in defected Zircaloy rods are defect size, sources of hydrogen, Zircaloy cladding inside surface properties, aggressive fission product attack on inner oxide film, nickel alloy contamination of Zircaloy, and the effects of heat flux and fluence.
f. Pertinent in-pile and out-of-pile test data and the significant factors affecting internal hydriding in defected Zircaloy fuel rods are used as a data base in constructing a descriptive model which explains hydrogen distribution in Zircaloy cladding of defected water-cooled reactor fuel rods.

g. Methods for minimizing secondary hydride failures in defected Zircaloy fuel rods include control of hydride orientation, protective coatings, hydrogen getters, and power operating restrictions.

References

1 C. A. Pruss, *ICPP Fuel Receipt Criteria for LWBR Core and Irradiation Test Fuel*, WAPD-NRF(L)D-96, August 10, 1987 and W. J. Babyak, *Revised Response to ICPP Fuel Receipt Criteria, Parts A and B, for the LWBR Irradiation Test Fuel*, WAPD-NRF(L)D-110, September 23, 1987

2 J. Belle & R. M. Berman, *Properties of Thora and Thora-Urania : A Review*, (LWBR Development Program), WAPD-TM-1340, June 1978

3 C. D. Sphar and J. Sherman, *Early-in-life Performance of Short Rod Duplex Pellet Screening (D-1) Test*, WAPD-TM-1378, November 1979

4 L. A. Waldman, C. D. Sphar, and T. H. Alff, *Irradiation Performance of Long Rod Duplex Fuel Pellet Bundle Test – LDR Test*, (AWBA Development Program), WAPD-TM-1481, April 1982

5 J. C. Clayton, *Corrosion and Hydriding of Irradiated Zircaloy Fuel Rod Cladding* (LWBR Development Program), WAPD-TM-1440, September 1982

6 E. Duncombe and I. Goldberg, *Comparison of Dimensional Changes in Fuel Rods with Predictions under Cyclic conditions of Power and System Pressure*, (LWBR Development Program), WAPD-TM-940, March 1970

7 R. C. Daniel, *In-Pile Dimensional Changes of Zircaloy-4 Tubing Having Low Hoop Stresses*, (LWBR Development Program), WAPD-TM-973, July 1970

8 J. F. Giovengo, *In-Pile Dimensional Changes of ThO_2-UO_2 Fuel Rods with Non-Free-Standing Cladding*, (LWBR Development Program), WAPD-TM-986, November 1970

9 R. M. Stackhouse, ed., *Fuel Rod-Grid Interaction Wear: In-Reactor Tests*, (LWBR Development Program), WAPD-TM-1347, November 1979

10 I. Goldberg et al., *Fission Gas Release From ThO_2 and ThO_2-UO_2 Fuels*, (LWBR Development Program), WAPD-TM-1350, May 1982

11 J. B. Newman, J. F. Giovengo, and L. P. Comden, *The CYGRO-4 Fuel Rod Analysis Computer Program*, WAPD-TM-1300, July 1977

12 I. Goldberg, *A Procedure for Calculation of Steady-State Temperature in Zircaloy-Clad Bulk Oxide Fuel Elements Using the FIGRO Computer Program*, WAPD-TM-757, November 1969

13 H. R. Warner, *Release of Fission Gases from Oxide Fuels*, (LWBR Development Program), WAPD-TM-805, July 1969

14 I. Goldberg, et al., *Fission Gas Release and Grain Growth in ThO_2 and ThO_2-UO_2 Fuel Irradiated at High Temperature*, (LWBR Development Program), WAPD-TM-1350ADD, July 1979

15 J. F. Giovengo, I. Goldberg, and C. D. Sphar, *Fission Gas Release From High burnup ThO_2 and ThO_2-UO_2 Fuels Irradiated at Low Temperature*, (LWBR Development Program), WAPD-TM-1350ADD2, August 1978

16 R. C. Hoffman and J. Sherman, *Irradiation Testing of Internally Pressurized and/or Graphite Coated Zircaloy-4 clad Fuel Rods in the NRX Reactor*, (AWBA Development Program), WAPD-TM-1376, November 1978

17 J. C. Clayton, *Cladding Corrosion and Hydriding in Irradiated Defected Zircaloy Fuel Rods*, (LWBR Development Program), WAPD-TM-1393, August 1985

18 D. M. Ivak and L. A. Waldman, *Iodine and Cesium in Oxide Fuel Pellets and Zircaloy-4 cladding of Irradiated Fuel Rods*, (LWBR Development Program), WAPD-TM-1394, March 1979

19 J. C. Clayton, *Corrosion and Hydriding of Irradiated Zircaloy Fuel Rod Cladding* (LWBR Development Program), WAPD-TM-1440, September 1982

20 C. D. Sphar, D. A. Mertz, and W. S. Roesener, *Irradiation Performance of Duplex Fuel Pellet Test rods Depleted to $9x10^{20}$ Fissions/cm^3 of Compartment – D-1 Test*, (AWBA Development Program), WAPD-TM-1460, January 1982

21 R. C. Hoffman, J. F. Yerman and T. H. Alff, *Experimental Results of the Irradiation of Long Rod Duplex Pellet Screening Test in the NRX Reactor (NLDR-1 Test)*, (AWBA Development Program), WAPD-TM-1492, July 1982

22 R. C. Hoffman and J. F. Yerman, *Further Experimental Results of the Irradiation of Long Rod Duplex Pellets Screening Tests in the NRX Reactor (NLDR-2/3/4 Tests)*, (AWBA Development Program), WAPD-TM-1520, October 1982

23 J. C. Clayton, *In-Pile and Out-of-Pile Corrosion Behavior of Thoria-Urania Pellets*, (LWBR Development Program), WAPD-TM-1548, January 1987

24 J. C. Clayton, *Internal Hydriding in Irradiated Defected Zircaloy Fuel Rods – a Review*, (LWBR Development Program), WAPD-TM-1604, October 1987

Appendix B

Fissile Fuel Loading Data from Non-destructive Examinations

Table 26

Seed Module I-1 Fissile Fuel Loadings in Grams

Rod No.	As-Built Loading	PIFAG Thermal Loading	PIFAG Thermal Standard Deviation Grams	PIFAG Thermal Standard Deviation %	PIFAG Epithermal Loading	PIFAG Epithermal Standard Deviation Grams	PIFAG Epithermal Standard Deviation %	Epithermal - Thermal Percent Difference
0502228	34.668	25.682	0.075	0.29	25.712	0.095	0.37	+0.11
0507057	34.682	25.598	0.071	0.28	25.665	0.045	0.18	+0.26
0603327	34.551	25.481	0.072	0.28	25.372	0.065	0.26	-0.43
0605269	34.494	25.224	0.073	0.29	25.245	0.070	0.28	+0.08
0603464	34.566	25.202	0.075	0.30	25.336	0.070	0.27	+0.53
0604519	34.164	25.133	0.074	0.29	25.182	0.069	0.27	+0.19
0603289	34.440	25.353	0.074	0.29	25.317	0.064	0.25	-0.14
0501128	34.646	25.153	0.080	0.32	25.296	0.070	0.28	+0.57
0600577	34.149	24.741	0.073	0.29	24.787	0.068	0.28	+0.18
0607184	34.446	24.830	0.074	0.30	24.827	0.072	0.29	-0.01
0601504	34.222	24.837	0.072	0.29	24.813	0.069	0.28	-0.10
0501779	34.740	24.240	0.075	0.31	24.291	0.071	0.29	+0.21
0501265	34.373	24.476	0.075	0.31	24.494	0.070	0.28	+0.07
0504648	34.702	24.802	0.072	0.29	24.871	0.065	0.26	+0.28
0606681	34.248	24.069	0.080	0.33	24.141	0.072	0.30	+0.30
0608165	34.648	24.115	0.075	0.31	24.245	0.079	0.32	+0.54
0608313	34.420	23.389	0.077	0.33	23.387	0.065	0.28	-0.01
0605572	34.468	23.720	0.077	0.32	23.825	0.065	0.27	+0.44
0606378	34.407	23.883	0.087	0.36	23.902	0.069	0.29	+0.08
0606461	34.542	24.098	0.076	0.32	24.120	0.082	0.34	+0.09
0500082	34.594	23.426	0.078	0.33	23.431	0.072	0.31	+0.02
0507333	34.679	23.042	0.083	0.36	23.106	0.070	0.30	+0.28
0504042	34.604	22.949	0.078	0.34	22.964	0.050	0.22	+0.07
0507782	34.710	23.510	0.078	0.33	23.668	0.080	0.34	+0.67
0404355	23.903	17.282	0.066	0.38	17.346	0.069	0.40	+0.37
0401744	23.697	17.449	0.065	0.37	17.523	0.043	0.24	+0.42
0302578	19.055	15.498	0.061	0.39	15.556	0.069	0.45	+0.38
0307602	19.179	15.635	0.057	0.36	15.684	0.039	0.25	+0.32
0700219	14.255	14.166	0.049	0.35	14.225	0.059	0.41	+0.42
0201562	14.219	13.910	0.050	0.36	13.993	0.037	0.26	+0.60
0200343	14.347	14.219	0.048	0.34	14.231	0.062	0.44	+0.09
0211224	14.253	14.012	0.055	0.39	13.995	0.054	0.39	-0.12
0100821	14.310	13.969	0.055	0.39	13.927	0.054	0.39	-0.30

Table 27

Seed Module II-3 Fissile Fuel Loadings in Grams

Rod No.	As-Built Loading	PIFAG Thermal Loading	PIFAG Thermal Standard Deviation Grams	PIFAG Thermal Standard Deviation %	PIFAG Epithermal Loading	PIFAG Epithermal Standard Deviation Grams	PIFAG Epithermal Standard Deviation %	Epithermal - Thermal Percent Difference
0518387	34.602	26.377	0.071	0.27	26.468	0.103	0.39	+0.34
0524623	34.688	26.544	0.061	0.23	26.584	0.079	0.30	+0.15
0626528	34.694	26.357	0.069	0.26	26.514	0.087	0.33	+0.59
0626573	34.865	26.488	0.068	0.26	26.687	0.099	0.37	+0.75
0610818	34.536	26.381	0.067	0.26	26.557	0.086	0.32	+0.67
0631800	34.836	26.779	0.075	0.28	26.880	0.086	0.32	+0.38
0623860	34.871	26.545	0.068	0.26	26.555	0.087	0.33	+0.04
0615739	34.623	25.999	0.075	0.29	26.182	0.084	0.32	+0.70
0624465	34.705	26.159	0.069	0.26	26.182	0.091	0.35	+0.09
0615409	34.582	26.406	0.077	0.29	26.393	0.088	0.33	-0.05
0623724	34.321	26.371	0.064	0.24	26.283	0.082	0.31	-0.33
0614648	34.634	26.420	0.076	0.29	26.464	0.090	0.34	+0.17
0531737	34.536	26.428	0.059	0.22	26.549	0.084	0.32	+0.46
0628315	34.763	25.744	0.077	0.30	25.728	0.121	0.47	-0.06
0532763	34.540	25.120	0.070	0.28	25.277	0.111	0.44	+0.62
0535466	34.602	25.919	0.060	0.23	26.092	0.084	0.32	+0.67
0622532	34.793	24.651	0.070	0.28	24.680	0.085	0.34	+0.12
0610607	34.336	24.535	0.069	0.28	24.502	0.096	0.39	-0.13
0610239	34.573	25.092	0.071	0.28	25.226	0.084	0.33	+0.54
0624382	34.819	25.597	0.064	0.25	25.804	0.084	0.33	+0.81
0618516	34.821	25.528	0.062	0.24	25.566	0.084	0.33	+0.15
0528325	34.187	23.616	0.076	0.32	23.599	0.085	0.36	-0.07
0536622	34.637	24.279	0.071	0.29	24.419	0.102	0.42	+0.58
0527703	34.446	24.693	0.065	0.26	24.744	0.083	0.34	+0.20
0535154	34.553	24.321	0.065	0.27	24.345	0.084	0.35	+0.10
0411534	23.967	17.829	0.070	0.39	17.860	0.071	0.40	+0.18
0411056	24.033	17.980	0.052	0.29	18.057	0.067	0.37	+0.43
0315310	19.120	15.670	0.070	0.45	15.773	0.080	0.51	+0.66
0312083	19.151	15.734	0.057	0.36	15.748	0.078	0.50	+0.09
0217061	14.350	14.065	0.046	0.33	14.181	0.067	0.47	+0.83
0202635	14.342	14.056	0.045	0.32	14.174	0.078	0.55	+0.84
0705084	14.225	14.208	0.044	0.31	14.267	0.105	0.74	+0.41
0216356	14.371	14.023	0.051	0.36	14.099	0.069	0.49	+0.54
0106614	14.268	13.762	0.042	0.30	13.805	0.062	0.45	+0.31

Table 28

Seed Module III-1 Fissile Fuel Loadings in Grams

Rod No.	As-Built Loading	PIFAG Thermal Loading	PIFAG Thermal Standard Deviation Grams	PIFAG Thermal Standard Deviation %	PIFAG Epithermal Loading	PIFAG Epithermal Standard Deviation Grams	PIFAG Epithermal Standard Deviation %	Epithermal - Thermal Percent Difference
0600633	34.439	27.188	0.076	0.28	27.182	0.083	0.31	-0.02
0505362	34.610	27.191	0.072	0.26	27.298	0.077	0.28	+0.40
0608349	34.699	27.617	0.063	0.23	27.667	0.071	0.26	+0.18
0506388	34.128	26.741	0.059	0.22	26.776	0.067	0.25	+0.13
0507039	34.636	26.978	0.061	0.23	27.026	0.067	0.25	+0.18
0510139	34.726	27.241	0.074	0.27	27.382	0.067	0.25	+0.52
0502200	34.596	27.444	0.058	0.21	27.603	0.068	0.25	+0.58
0602108	34.555	27.024	0.055	0.20	26.982	0.067	0.25	-0.16
0604876	34.524	26.729	0.057	0.21	26.714	0.067	0.25	-0.06
0603684	34.529	26.672	0.058	0.22	26.615	0.110	0.41	-0.21
0604472	34.544	27.316	0.057	0.21	27.487	0.067	0.24	+0.63
0506206	34.442	26.329	0.070	0.27	26.314	0.070	0.27	-0.06
0504363	34.596	27.309	0.063	0.23	27.542	0.066	0.24	+0.85
0508617	34.622	27.157	0.056	0.21	27.302	0.066	0.24	+0.54
0500385	34.463	26.270	0.060	0.23	26.288	0.067	0.25	+0.07
0501808	34.735	26.275	0.068	0.26	26.325	0.068	0.26	+0.19
0506453	34.341	25.703	0.061	0.24	25.825	0.078	0.30	+0.47
0502585	34.242	26.928	0.058	0.22	27.020	0.066	0.24	+0.34
0600430	34.518	25.321	0.064	0.25	25.360	0.063	0.25	+0.15
0602878	34.292	25.451	0.065	0.26	25.666	0.103	0.40	+0.85
0503622	34.390	24.827	0.064	0.26	24.860	0.067	0.27	+0.13
0504556	34.426	24.681	0.068	0.27	24.784	0.079	0.32	+0.41
0508451	34.726	25.104	0.062	0.25	25.078	0.067	0.27	-0.10
0508671	34.674	26.276	0.057	0.22	26.391	0.081	0.31	+0.44
0508516	34.736	25.975	0.059	0.23	26.012	0.061	0.23	+0.14
0407702	23.897	18.124	0.056	0.31	18.102	0.060	0.33	-0.12
0400083	23.813	18.763	0.047	0.25	18.774	0.057	0.30	+0.06
0302845	19.141	15.917	0.049	0.31	15.983	0.054	0.34	+0.42
0302203	19.132	15.778	0.050	0.32	15.785	0.055	0.35	+0.04
0203652	14.232	14.196	0.037	0.26	14.224	0.039	0.27	+0.20
0201342	14.300	14.276	0.031	0.22	14.316	0.052	0.36	+0.28
0701153	14.250	14.208	0.039	0.27	14.076	0.050	0.35	-0.93
0100683	14.332	13.835	0.041	0.29	13.982	0.051	0.36	+1.06
0102609	14.240	13.765	0.039	0.29	13.681	0.052	0.38	-0.62

Table 29

Seed Module III-2 Fissile Fuel Loadings in Grams

Rod No.	As-Built Loading	PIFAG Thermal Loading	PIFAG Thermal Standard Deviation Grams	PIFAG Thermal Standard Deviation %	PIFAG Epithermal Loading	PIFAG Epithermal Standard Deviation Grams	PIFAG Epithermal Standard Deviation %	Epithermal - Thermal Percent Difference
0537510	34.843	27.282	0.057	0.21	27.455	0.066	0.24	+0.63
0627076	34.534	27.507	0.063	0.23	27.579	0.066	0.24	+0.26
0537069	34.828	27.287	0.063	0.23	27.462	0.061	0.22	+0.64
0518333	34.501	27.086	0.060	0.22	27.065	0.057	0.21	-0.08
0606874	34.529	27.055	0.086	0.32	27.146	0.067	0.25	+0.34
0607561	34.466	26.585	0.075	0.28	26.785	0.067	0.25	+0.75
0601558	34.513	27.347	0.055	0.20	27.430	0.065	0.24	+0.30
0615216	34.483	27.465	0.054	0.20	27.576	0.083	0.30	+0.40
0516133	34.378	26.706	0.062	0.23	26.820	0.057	0.21	+0.43
0532120	34.815	26.747	0.062	0.23	26.881	0.061	0.23	+0.50
0536272	34.582	26.832	0.095	0.35	27.093	0.061	0.23	+0.97
0622889	34.474	26.632	0.057	0.21	26.666	0.061	0.23	+0.13
0618543	34.474	26.526	0.057	0.22	26.671	0.076	0.29	+0.54
0610275	34.438	27.157	0.055	0.20	27.244	0.065	0.24	+0.32
0608753	34.655	27.225	0.058	0.21	27.423	0.069	0.25	+0.73
0511625	34.596	26.484	0.061	0.23	26.552	0.053	0.20	+0.25
0517269	34.696	26.925	0.055	0.21	26.960	0.066	0.25	+0.13
0613676	34.686	25.860	0.061	0.23	25.774	0.072	0.28	-0.34
0630680	34.478	25.312	0.062	0.25	25.410	0.066	0.26	+0.39
0617865	34.321	26.257	0.056	0.21	26.464	0.089	0.34	+0.79
0624824	34.702	26.671	0.052	0.19	26.735	0.064	0.24	+0.24
0524302	34.636	25.012	0.067	0.27	25.121	0.060	0.24	+0.43
0526336	34.626	24.567	0.073	0.30	24.543	0.067	0.27	-0.10
0531728	34.516	24.768	0.065	0.26	24.758	0.078	0.31	-0.04
0523779	34.542	25.727	0.075	0.29	25.775	0.064	0.25	+0.19
0412652	23.966	18.064	0.056	0.31	18.072	0.049	0.27	+0.04
0408755	23.981	18.835	0.050	0.27	18.915	0.053	0.28	+0.42
0314384	19.179	15.842	0.051	0.32	15.879	0.054	0.34	+0.23
0315127	19.187	16.359	0.041	0.25	16.442	0.076	0.46	+0.50
0207428	14.292	14.220	0.042	0.29	14.379	0.051	0.35	+1.12
0202525	14.154	14.255	0.032	0.23	14.199	0.049	0.34	-0.39
0105624	14.445	14.087	0.046	0.32	14.081	0.051	0.36	-0.04
0106089	14.435	14.000	0.040	0.28	14.018	0.045	0.32	+0.13

Table 30

Blanket Module I-3 RB Rod Fissile Fuel Loadings in Grams

		PIFAG Thermal			PIFAG Epithermal			Epithermal - Thermal
			Standard Deviation			Standard Deviation		
Rod No.	As-Built Loading	Loading	Grams	%	Loading	Grams	%	Percent Difference
1208078	16.473	36.219	0.091	0.25	36.221	0.110	0.30	+0.00
1200665	16.442	36.058	0.090	0.25	35.997	0.103	0.29	-0.17
1200500	16.458	35.899	0.088	0.25	35.847	0.104	0.29	-0.14
1200830	16.454	36.884	0.097	0.26	36.796	0.081	0.22	-0.24
1107750	16.488	36.848	0.098	0.27	36.829	0.112	0.30	-0.05
1105477	16.502	35.122	0.081	0.23	35.387	0.101	0.29	+0.76
1208042	16.440	34.852	0.078	0.22	34.910	0.086	0.25	+0.16
1107623	16.469	34.967	0.082	0.23	34.787	0.092	0.27	-0.51
1103700	16.493	34.980	0.081	0.23	35.239	0.083	0.24	+0.74
1206347	16.461	35.341	0.083	0.23	35.469	0.094	0.27	+0.36
1106844	16.471	35.875	0.087	0.24	35.874	0.096	0.27	-0.00
1401166	30.494	40.877	0.091	0.22	40.902	0.128	0.31	+0.06
1400544	30.673	40.711	0.091	0.22	40.756	0.072	0.18	+0.11
1404356	30.051	40.043	0.099	0.25	40.404	0.133	0.33	+0.90
1411479	30.006	40.477	0.105	0.26	40.538	0.122	0.30	+0.15
1407187	30.515	41.183	0.106	0.26	41.345	0.109	0.26	+0.39
1306584	45.527	47.179	0.121	0.26	47.226	0.136	0.29	+0.10
1311738	45.432	47.107	0.118	0.25	47.177	0.140	0.30	+0.15
1302864	45.461	47.355	0.128	0.27	47.384	0.113	0.24	+0.06
1302873	45.443	47.397	0.128	0.27	47.430	0.132	0.28	+0.07
1311811	45.433	47.463	0.121	0.26	47.648	0.142	0.30	+0.39
1307152	45.427	47.749	0.149	0.31	47.709	0.166	0.35	-0.08
1510589	45.798	48.379	0.121	0.25	48.446	0.123	0.25	+0.14
1507058	45.808	47.928	0.117	0.24	47.957	0.118	0.25	+0.06
1506683	45.836	48.188	0.116	0.24	48.155	0.142	0.29	-0.07
1500386	45.752	48.422	0.142	0.29	48.437	0.126	0.26	+0.03
1500846	45.779	48.682	0.133	0.27	48.779	0.144	0.30	+0.20
1500157	45.808	48.491	0.129	0.27	48.279	0.127	0.26	-0.44
1503742	45.653	48.463	0.152	0.31	48.439	0.126	0.26	-0.05
1605876	54.491	52.386	0.123	0.23	52.576	0.148	0.28	+0.36
1612357	54.471	52.526	0.178	0.34	52.704	0.148	0.28	+0.34
1606278	54.452	52.512	0.152	0.29	52.636	0.159	0.30	+0.24
1605519	54.553	52.514	0.154	0.29	52.471	0.146	0.28	-0.08
1604318	54.748	52.542	0.138	0.26	52.705	0.158	0.30	+0.31
1604758	54.540	52.576	0.136	0.26	52.812	0.150	0.28	+0.45
1610157	54.503	52.579	0.133	0.25	52.602	0.180	0.34	+0.04

Table 31

Blanket Module II-2 RB Rod Fissile Fuel Loadings in Grams

Rod No.	As-Built Loading	PIFAG Thermal Loading	PIFAG Thermal Standard Deviation Grams	PIFAG Thermal Standard Deviation %	PIFAG Epithermal Loading	PIFAG Epithermal Standard Deviation Grams	PIFAG Epithermal Standard Deviation %	Epithermal - Thermal Percent Difference
1210125	16.463	36.098	0.089	0.25	35.880	0.094	0.26	-0.60
1210226	16.484	35.977	0.091	0.25	35.804	0.086	0.24	-0.48
1103672	16.379	35.854	0.095	0.27	35.784	0.108	0.30	-0.19
1208657	16.475	34.293	0.076	0.22	34.260	0.100	0.29	-0.10
1106137	16.480	33.513	0.070	0.21	33.608	0.116	0.35	+0.28
1106586	16.457	34.134	0.078	0.23	33.948	0.109	0.32	-0.54
1104525	16.403	34.882	0.081	0.23	34.959	0.121	0.35	+0.22
1102470	16.404	33.962	0.075	0.22	33.954	0.109	0.32	-0.02
1404668	30.083	39.917	0.099	0.25	39.980	0.120	0.30	+0.16
1412846	30.607	40.829	0.105	0.26	40.960	0.159	0.39	+0.32
1407748	30.248	40.012	0.098	0.25	40.032	0.145	0.36	+0.05
1402660	30.038	39.462	0.092	0.23	39.319	0.117	0.30	-0.36
1303248	45.523	46.165	0.110	0.24	46.457	0.179	0.39	+0.63
1302579	45.273	46.937	0.121	0.26	47.344	0.160	0.34	+0.87
1311334	45.511	47.133	0.140	0.30	47.683	0.192	0.40	+1.17
1305787	45.408	46.736	0.108	0.23	46.968	0.163	0.35	+0.50
1505363	45.489	47.766	0.112	0.23	47.806	0.112	0.23	+0.09
1504658	45.754	48.090	0.122	0.25	47.943	0.140	0.29	-0.31
1507619	45.679	48.454	0.133	0.27	48.376	0.176	0.36	-0.16
1504667	45.638	47.729	0.116	0.24	47.829	0.135	0.28	+0.21
1608083	54.657	51.750	0.112	0.22	52.121	0.136	0.26	+0.72
1603676	54.855	52.624	0.133	0.25	52.883	0.157	0.30	+0.49
1607479	54.600	52.492	0.132	0.25	52.784	0.182	0.35	+0.56
1602181	54.636	52.628	0.131	0.25	52.831	0.166	0.31	+0.39

Table 32

Blanket Module III-2 RB Rod Fissile Fuel Loadings in Grams

Rod No.	As-Built Loading	PIFAG Thermal Loading	PIFAG Thermal Standard Deviation Grams	PIFAG Thermal Standard Deviation %	PIFAG Epithermal Loading	PIFAG Epithermal Standard Deviation Grams	PIFAG Epithermal Standard Deviation %	Epithermal - Thermal Percent Difference
1105102	16.460	33.860	0.076	0.23	33.778	0.103	0.30	-0.24
1103012	16.425	34.105	0.076	0.22	34.072	0.104	0.30	-0.10
1207520	16.437	33.727	0.070	0.21	33.774	0.103	0.30	+0.14
1203709	16.389	33.824	0.113	0.33	33.868	0.103	0.30	+0.13
1100767	16.477	33.741	0.090	0.27	33.527	0.101	0.30	-0.63
1103460	16.394	32.532	0.075	0.23	32.497	0.100	0.31	-0.11
1402542	30.639	39.894	0.091	0.23	39.849	0.112	0.28	-0.11
1401828	30.192	39.566	0.091	0.23	39.716	0.103	0.26	+0.38
1410316	30.029	38.283	0.078	0.20	38.356	0.107	0.28	+0.19
1310187	45.413	46.101	0.109	0.24	46.110	0.125	0.27	+0.02
1310472	45.393	46.852	0.110	0.23	46.775	0.132	0.28	-0.16
1303872	45.563	47.082	0.115	0.24	47.246	0.163	0.34	+0.35
1514365	45.736	47.829	0.125	0.26	47.660	0.172	0.36	-0.35
1513339	45.714	48.186	0.117	0.24	48.227	0.148	0.31	+0.08
1511469	45.735	47.058	0.106	0.23	47.190	0.122	0.26	+0.28
1607416	54.562	51.499	0.110	0.21	51.608	0.133	0.26	+0.21
1607075	54.546	52.264	0.116	0.22	52.389	0.138	0.26	+0.24
1615502	54.667	52.743	0.125	0.24	52.512	0.142	0.27	-0.44

Table 33

Blanket Module III-6 RB Rod Fissile Fuel Loadings in Grams

Rod No.	As-Built Loading	PIFAG Thermal Loading	PIFAG Thermal Standard Deviation Grams	PIFAG Thermal Standard Deviation %	PIFAG Epithermal Loading	PIFAG Epithermal Standard Deviation Grams	PIFAG Epithermal Standard Deviation %	Epithermal - Thermal Percent Difference
1204542	16.457	34.555	0.084	0.24	34.721	0.108	0.31	+0.48
1200344	16.439	34.673	0.086	0.25	34.612	0.119	0.34	-0.18
1103443	16.450	34.117	0.079	0.23	34.134	0.127	0.37	+0.05
1101059	16.487	32.896	0.070	0.21	32.999	0.092	0.28	+0.31
1103315	16.399	33.108	0.076	0.23	32.994	0.094	0.29	-0.34
1104800	16.508	33.843	0.077	0.23	33.829	0.104	0.31	-0.04
1401882	30.705	38.748	0.085	0.22	38.943	0.110	0.28	+0.50
1404448	30.475	39.888	0.092	0.23	39.845	0.130	0.33	-0.11
1410646	30.523	38.704	0.082	0.21	38.891	0.129	0.33	+0.48
1306117	45.353	46.296	0.108	0.23	46.276	0.129	0.28	-0.04
1308564	45.529	46.917	0.118	0.25	47.065	0.169	0.36	+0.32
1305724	45.584	46.880	0.118	0.25	46.912	0.172	0.37	+0.07
1507545	45.760	47.751	0.109	0.23	47.770	0.117	0.25	+0.04
1513265	45.581	48.214	0.120	0.25	48.080	0.159	0.33	-0.28
1512486	45.619	47.736	0.111	0.23	47.815	0.125	0.26	+0.17
1603483	54.704	52.461	0.127	0.24	52.625	0.147	0.28	+0.31
1613457	54.482	52.333	0.135	0.26	52.640	0.178	0.34	+0.59
1601164	54.671	51.791	0.113	0.22	52.031	0.138	0.27	+0.46

Table 34

Blanket Module II-2 PFB Rod Fissile Fuel Loadings in Grams

Rod No.	As-Built Loading	PIFAG Thermal Loading	PIFAG Thermal Standard Deviation Grams	PIFAG Thermal Standard Deviation %	PIFAG Epithermal Loading	PIFAG Epithermal Standard Deviation Grams	PIFAG Epithermal Standard Deviation %	Epithermal - Thermal Percent Difference
2104416	18.977	31.138	0.086	0.28	31.054	0.131	0.42	-0.27
2103352	18.997	31.004	0.085	0.28	30.808	0.150	0.49	-0.63
2102225	18.985	30.632	0.086	0.28	30.606	0.096	0.31	-0.08
2102077	18.894	30.799	0.085	0.28	30.723	0.106	0.35	-0.25
2100245	18.925	30.416	0.079	0.26	30.415	0.087	0.29	-0.01
2405522	30.723	34.446	0.076	0.22	34.588	0.104	0.30	+0.41
2400287	30.771	35.286	0.109	0.31	35.228	0.101	0.29	-0.16
2406153	30.751	34.955	0.094	0.27	34.785	0.094	0.27	-0.49
2304138	52.563	45.815	0.129	0.28	45.864	0.147	0.32	+0.11
2303552	52.787	46.012	0.116	0.25	45.904	0.117	0.25	-0.23
2303560	52.787	45.919	0.110	0.24	46.031	0.128	0.28	+0.24
2610223	62.732	54.709	0.111	0.20	54.921	0.118	0.21	+0.39
2613505	63.183	54.060	0.115	0.21	54.309	0.128	0.24	+0.46
2610205	63.037	52.424	0.127	0.24	52.433	0.132	0.25	+0.02
2607600	63.042	51.687	0.135	0.26	51.714	0.128	0.25	+0.05
2620655	63.103	53.790	0.112	0.21	53.901	0.162	0.30	+0.21
2606389	62.571	53.904	0.107	0.20	53.962	0.118	0.22	+0.11
2504834	63.032	56.303	0.111	0.20	56.602	0.122	0.22	+0.53
2516759	63.108	54.553	0.121	0.22	54.547	0.121	0.22	-0.01
2517289	62.944	54.104	0.120	0.22	54.521	0.129	0.24	+0.77
2505025	63.122	53.928	0.124	0.23	54.027	0.137	0.25	+0.18
2518371	63.061	54.772	0.111	0.20	54.851	0.126	0.23	+0.14
2614769	63.115	54.475	0.113	0.21	54.791	0.113	0.21	+0.58
2610883	63.105	53.451	0.123	0.23	53.416	0.103	0.19	-0.07
2618866	63.394	54.400	0.120	0.22	54.706	0.122	0.22	+0.56
2608003	63.226	55.501	0.118	0.21	55.697	0.122	0.22	+0.35
2511663	63.033	55.335	0.138	0.25	55.206	0.133	0.24	-0.23
2504585	62.926	54.896	0.110	0.20	55.166	0.141	0.26	+0.49
2504347	62.838	54.750	0.121	0.22	54.721	0.111	0.20	-0.05
2516061	63.183	52.554	0.144	0.27	52.529	0.121	0.23	-0.05
2518142	62.980	54.576	0.114	0.21	54.554	0.129	0.24	-0.04
2617106	63.369	55.858	0.113	0.20	56.096	0.116	0.21	+0.42
2605583	62.732	55.354	0.106	0.19	55.359	0.123	0.22	+0.01
2616776	63.361	54.594	0.107	0.20	54.851	0.175	0.32	+0.47
2520288	62.914	53.976	0.105	0.20	54.223	0.115	0.21	+0.46
2513717	63.054	52.891	0.120	0.23	52.853	0.145	0.27	-0.07
2517823	62.702	52.225	0.125	0.24	52.152	0.118	0.23	-0.14
2504706	62.510	52.704	0.105	0.20	52.600	0.143	0.27	-0.20
2506814	63.221	54.818	0.102	0.19	54.822	0.116	0.21	+0.01
2701357	46.528	42.750	0.121	0.28	42.695	0.144	0.34	-0.13
2700055	46.187	42.474	0.120	0.28	42.392	0.116	0.27	-0.19

Table 35

Blanket Module III-2 PFB Rod Fissile Fuel Loadings in Grams

Rod No.	As-Built Loading	PIFAG Thermal Loading	PIFAG Thermal Standard Deviation Grams	PIFAG Thermal Standard Deviation %	PIFAG Epithermal Loading	PIFAG Epithermal Standard Deviation Grams	PIFAG Epithermal Standard Deviation %	Epithermal - Thermal Percent Difference
2202278	18.912	30.067	0.080	0.27	29.982	0.094	0.31	-0.28
2200805	18.907	30.548	0.079	0.26	30.503	0.117	0.38	-0.15
2100759	18.990	28.529	0.059	0.21	28.627	0.095	0.33	+0.34
2201178	18.913	28.105	0.059	0.21	28.079	0.085	0.30	-0.09
2202518	18.894	29.381	0.069	0.23	29.419	0.090	0.30	+0.13
2101758	18.894	29.609	0.070	0.23	29.338	0.090	0.31	-0.92
2402314	30.763	33.718	0.072	0.21	33.824	0.145	0.43	+0.32
2401048	30.769	34.312	0.078	0.23	34.432	0.111	0.32	+0.35
2401636	30.876	34.402	0.075	0.22	34.488	0.123	0.36	+0.25
2300601	52.531	46.680	0.092	0.20	46.821	0.110	0.24	+0.30
2300279	52.669	46.507	0.088	0.19	46.857	0.142	0.30	+0.75
2304652	52.765	45.950	0.105	0.23	46.003	0.118	0.26	+0.12
2302378	52.514	45.692	0.104	0.23	45.736	0.105	0.23	+0.10
2620509	63.028	55.998	0.097	0.17	56.247	0.114	0.20	+0.44
2603383	63.177	55.581	0.127	0.23	55.758	0.118	0.21	+0.32
2606775	63.024	54.587	0.107	0.20	54.585	0.150	0.28	-0.00
2600653	63.039	53.799	0.111	0.21	53.862	0.118	0.22	+0.12
2611002	63.067	53.403	0.117	0.22	53.741	0.143	0.27	+0.63
2608755	62.826	51.301	0.162	0.32	51.570	0.125	0.24	+0.53
2515513	62.860	56.244	0.100	0.18	56.122	0.142	0.25	-0.22
2517363	62.964	55.952	0.106	0.19	56.040	0.172	0.31	+0.16
2516777	62.965	55.740	0.101	0.18	56.166	0.116	0.21	+0.76
2511810	63.128	53.149	0.121	0.23	53.258	0.113	0.21	+0.20
2520656	63.103	54.400	0.130	0.24	54.738	0.131	0.24	+0.62
2516850	63.083	54.651	0.111	0.20	54.895	0.187	0.34	+0.45
2615016	62.991	56.980	0.126	0.22	57.207	0.157	0.27	+0.40
2601147	62.998	57.018	0.100	0.18	57.018	0.113	0.20	-0.00
2607031	62.956	56.721	0.103	0.18	57.033	0.114	0.20	+0.55
2602375	63.137	56.947	0.100	0.17	57.369	0.120	0.21	+0.74
2621407	62.964	55.324	0.106	0.19	55.636	0.108	0.19	+0.56
2608434	62.901	54.431	0.110	0.20	54.882	0.118	0.21	+0.83
2607325	63.161	52.721	0.112	0.21	52.865	0.088	0.17	+0.27
2605455	62.956	54.487	0.113	0.21	54.784	0.118	0.22	+0.54
2622433	63.145	54.942	0.110	0.20	55.158	0.110	0.20	+0.39
2622478	62.916	5[illegible].100	0.134	0.23	57.408	0.129	0.22	+0.54
2517704	62.780	56.768	0.098	0.17	57.185	0.113	0.20	+0.73
2511350	62.971	57.030	0.096	0.17	57.153	0.114	0.20	+0.22
2516281	63.138	55.888	0.099	0.18	55.743	0.108	0.19	-0.26
2512754	62.975	55.733	0.101	0.18	56.028	0.126	0.22	+0.53

Table 35 (Continued)

Blanket Module III-2 PFB Rod Fissile Fuel Loadings in Grams

Rod No.	As-Built Loading	PIFAG Thermal			PIFAG Epithermal			Epithermal - Thermal Percent Difference
		Loading	Standard Deviation Grams	Standard Deviation %	Loading	Standard Deviation Grams	Standard Deviation %	
2517244	62.948	56.010	0.100	0.18	56.290	0.114	0.20	+0.50
2517179	63.154	57.001	0.093	0.16	56.995	0.113	0.20	-0.01
2607563	63.014	57.091	0.098	0.17	57.314	0.126	0.22	+0.39
2603044	63.137	56.345	0.109	0.19	56.311	0.111	0.20	-0.06
2607471	62.989	56.077	0.119	0.21	56.214	0.104	0.19	+0.25
2611157	62.879	54.302	0.106	0.20	54.530	0.132	0.24	+0.42
2614640	63.134	54.418	0.103	0.19	54.699	0.116	0.21	+0.52
2610240	62.777	55.818	0.101	0.18	56.172	0.104	0.19	+0.63
2605152	62.950	57.039	0.094	0.17	57.217	0.113	0.20	+0.31
2502082	63.030	56.423	0.092	0.16	56.449	0.192	0.34	+0.04
2521022	63.033	56.277	0.097	0.17	56.379	0.112	0.20	+0.18
2518041	63.129	55.722	0.095	0.17	55.710	0.096	0.17	-0.02
2515585	63.070	55.428	0.119	0.22	55.488	0.112	0.20	+0.11
2516503	62.960	53.904	0.115	0.21	53.670	0.106	0.20	-0.43
2514128	63.172	54.478	0.156	0.29	54.417	0.112	0.21	-0.11
2516319	63.066	55.902	0.098	0.17	55.869	0.111	0.20	-0.06
2700643	46.374	42.939	0.110	0.26	43.143	0.112	0.26	+0.47
2701274	46.300	43.035	0.138	0.32	42.845	0.117	0.27	-0.44

Table 36

Blanket Module III-6 PFB Rod Fissile Fuel Loadings in Grams

		PIFAG Thermal			PIFAG Epithermal			Epithermal - Thermal
			Standard Deviation			Standard Deviation		
Rod No.	As-Built Loading	Loading	Grams	%	Loading	Grams	%	Percent Difference
2204855	18.997	29.110	0.063	0.22	29.154	0.088	0.30	+0.15
2204846	18.998	30.389	0.087	0.28	30.264	0.088	0.29	-0.41
2200840	18.977	29.275	0.071	0.24	29.282	0.090	0.31	+0.02
2101363	18.993	28.354	0.062	0.22	28.304	0.087	0.31	-0.18
2101464	18.980	28.964	0.092	0.32	28.820	0.094	0.32	-0.50
2102187	18.997	29.367	0.056	0.19	29.318	0.049	0.17	-0.17
2400408	30.780	33.914	0.054	0.16	34.018	0.053	0.16	+0.31
2406355	30.720	34.791	0.082	0.23	34.891	0.096	0.28	+0.29
2404018	30.802	33.952	0.078	0.23	34.003	0.093	0.27	+0.15
2305853	52.402	46.515	0.086	0.18	46.712	0.102	0.22	+0.42
2305449	52.385	46.629	0.093	0.20	46.415	0.108	0.23	-0.46
2300711	52.511	45.364	0.104	0.23	45.350	0.077	0.17	-0.03
2305312	52.551	45.734	0.106	0.23	45.975	0.114	0.25	+0.53
2612735	63.218	56.216	0.128	0.23	56.189	0.120	0.21	-0.05
2600314	63.295	55.488	0.118	0.21	55.482	0.119	0.21	-0.01
2622083	62.976	55.995	0.108	0.19	55.896	0.187	0.33	-0.18
2617005	63.090	56.536	0.109	0.19	56.587	0.121	0.21	+0.09
2612827	62.967	54.296	0.111	0.21	54.418	0.123	0.23	+0.23
2600745	63.053	53.214	0.124	0.23	53.525	0.125	0.23	+0.58
2604887	63.264	53.165	0.115	0.22	53.424	0.112	0.21	+0.49
2606481	63.116	51.575	0.115	0.22	51.624	0.082	0.16	+0.09
2503808	63.193	56.424	0.108	0.19	56.650	0.112	0.20	+0.40
2514045	63.138	56.710	0.120	0.21	56.610	0.151	0.27	-0.18
2512579	63.142	56.679	0.108	0.19	56.744	0.146	0.26	+0.11
2517226	62.858	55.472	0.119	0.22	55.650	0.120	0.22	+0.32
2513854	63.272	53.670	0.101	0.19	53.752	0.076	0.14	+0.15
2502578	63.238	54.631	0.115	0.21	54.650	0.113	0.21	+0.04
2510738	62.935	54.755	0.129	0.24	54.876	0.121	0.22	+0.22
2517208	63.451	54.944	0.110	0.20	55.122	0.122	0.22	+0.32
2616684	62.794	56.311	0.137	0.24	56.632	0.163	0.29	+0.57
2600377	62.449	56.691	0.105	0.19	56.722	0.153	0.27	+0.06
2606876	62.938	55.919	0.136	0.24	56.187	0.187	0.33	+0.48
2601367	63.052	55.776	0.150	0.27	55.753	0.122	0.22	-0.04
2620747	62.967	55.066	0.112	0.20	55.312	0.128	0.23	+0.45
2612625	63.108	55.213	0.113	0.20	55.442	0.124	0.22	+0.41
2613413	63.193	56.010	0.109	0.20	56.179	0.113	0.20	+0.30
2502102	62.999	57.295	0.073	0.13	57.440	0.070	0.12	+0.25
2505236	63.207	57.413	0.104	0.18	57.527	0.149	0.26	+0.20
2516824	62.952	56.808	0.104	0.18	57.021	0.119	0.21	+0.38

Table 36 (Continued)

Blanket Module III-6 PFB Rod Fissile Fuel Loadings in Grams

Rod No.	As-Built Loading	PIFAG Thermal Loading	PIFAG Thermal Standard Deviation Grams	PIFAG Thermal Standard Deviation %	PIFAG Epithermal Loading	PIFAG Epithermal Standard Deviation Grams	PIFAG Epithermal Standard Deviation %	Epithermal - Thermal Percent Difference
2500618	63.204	57.485	0.125	0.22	57.519	0.113	0.20	+0.06
2500589	63.127	56.389	0.119	0.21	56.655	0.125	0.22	+0.47
2503018	62.711	55.376	0.108	0.20	55.429	0.120	0.22	+0.10
2622175	63.162	56.680	0.104	0.18	57.041	0.110	0.19	+0.64
2610167	62.934	56.988	0.142	0.25	57.173	0.121	0.21	+0.32
2615512	63.205	57.207	0.102	0.18	57.224	0.152	0.27	+0.03
2622617	63.366	57.336	0.117	0.20	57.287	0.134	0.23	-0.08
2607509	63.011	56.533	0.186	0.33	56.878	0.132	0.23	+0.61
2605502	63.280	53.224	0.116	0.22	53.606	0.124	0.23	+0.72
2622507	63.002	55.019	0.107	0.19	55.047	0.145	0.26	+0.05
2513880	63.239	56.656	0.140	0.25	56.308	0.129	0.23	-0.61
2518169	63.144	54.956	0.100	0.18	55.134	0.158	0.29	+0.32
2507720	63.226	52.943	0.116	0.22	52.874	0.120	0.23	-0.13
2501670	63.187	52.467	0.115	0.22	52.478	0.120	0.23	+0.02
2513634	63.122	54.042	0.110	0.20	53.700	0.133	0.25	-0.63
2501157	63.199	56.730	0.116	0.20	56.300	0.167	0.30	-0.76
2700414	46.562	42.732	0.125	0.29	42.852	0.117	0.27	+0.28
2701430	46.217	42.883	0.119	0.28	42.726	0.116	0.27	-0.37

Table 37

Reflector Module IV-3 Fissile Fuel Loadings in Grams

Rod No.	As-Built Loading	PIFAG Thermal Loading	PIFAG Thermal Standard Deviation Grams	PIFAG Thermal Standard Deviation %	PIFAG Epithermal Loading	PIFAG Epithermal Standard Deviation Grams	PIFAG Epithermal Standard Deviation %	Epithermal - Thermal Percent Difference
3222566	0.000	6.904	0.024	0.35	6.785	0.099	1.46	-1.72
3224023	0.000	6.566	0.020	0.31	6.380	0.105	1.64	-2.83
3214250	0.000	4.513	0.021	0.46	4.405	0.118	2.69	-2.39
3126159	0.000	4.088	0.021	0.50	3.999	0.133	3.33	-2.18
3117560	0.000	6.260	0.018	0.29	6.117	0.120	1.97	-2.28
3102583	0.000	5.013	0.020	0.40	4.765	0.124	2.61	-4.95
3225085	0.000	11.024	0.026	0.24	10.711	0.111	1.04	-2.85
3115580	0.000	8.131	0.035	0.43	8.034	0.103	1.28	-1.18
3223188	0.000	12.298	0.033	0.27	12.402	0.131	1.06	+0.85
3117709	0.000	11.386	0.024	0.21	11.173	0.131	1.17	-1.87
3213858	0.000	9.089	0.027	0.30	8.719	0.119	1.36	-4.07
3111504	0.000	18.418	0.031	0.17	18.428	0.126	0.68	+0.05
3112815	0.000	15.912	0.038	0.24	15.749	0.114	0.73	-1.03
3120156	0.000	14.928	0.028	0.19	14.651	0.113	0.77	-1.86
3201776	0.000	14.452	0.031	0.22	14.261	0.103	0.72	-1.32
3211429	0.000	17.014	0.040	0.23	16.886	0.127	0.75	-0.75
3211034	0.000	15.086	0.022	0.15	15.002	0.115	0.77	-0.56
3114804	0.000	24.718	0.037	0.15	24.696	0.139	0.56	-0.09
3208834	0.000	22.434	0.038	0.17	22.296	0.147	0.66	-0.61
3110624	0.000	21.798	0.046	0.21	21.509	0.156	0.73	-1.32
3110505	0.000	23.874	0.031	0.13	23.687	0.102	0.43	-0.78
3122879	0.000	20.452	0.077	0.37	20.283	0.119	0.59	-0.82
3102657	0.000	37.346	0.059	0.16	37.163	0.135	0.36	-0.49
3220357	0.000	31.984	0.048	0.15	31.939	0.143	0.45	-0.14
3211456	0.000	34.845	0.052	0.15	34.934	0.111	0.32	+0.26
3207716	0.000	31.203	0.075	0.24	31.172	0.129	0.41	-0.10
3114326	0.000	29.237	0.069	0.23	29.396	0.119	0.40	+0.54
3126022	0.000	28.490	0.034	0.12	28.380	0.124	0.44	-0.39

Table 38

Reflector Module IV-4 Fissile Fuel Loadings in Grams

		PIFAG Thermal			PIFAG Epithermal			Epithermal - Thermal
			Standard Deviation			Standard Deviation		Percent
Rod No.	As-Built Loading	Loading	Grams	%	Loading	Grams	%	Difference
3216258	0.000	8.124	0.026	0.32	8.093	0.120	1.48	-0.39
3203774	0.000	6.148	0.024	0.39	6.225	0.131	2.11	+1.25
3222474	0.000	4.920	0.018	0.36	4.925	0.127	2.57	+0.11
3216139	0.000	6.385	0.025	0.39	6.398	0.112	1.75	+0.19
3120744	0.000	5.239	0.024	0.45	5.242	0.115	2.20	+0.07
3113006	0.000	6.905	0.033	0.48	6.893	0.119	1.73	-0.17
3118019	0.000	6.206	0.026	0.43	6.051	0.117	1.93	-2.49
3218669	0.000	11.718	0.029	0.25	11.544	0.124	1.07	-1.49
3122163	0.000	8.855	0.027	0.30	8.798	0.139	1.58	-0.64
3218413	0.000	14.517	0.027	0.19	14.286	0.133	0.93	-1.59
3123245	0.000	13.375	0.054	0.40	12.999	0.123	0.95	-2.81
3122605	0.000	11.319	0.030	0.27	11.100	0.115	1.03	-1.94
3222833	0.000	9.260	0.024	0.26	9.204	0.121	1.32	-0.60
3104664	0.000	16.343	0.055	0.34	16.177	0.143	0.89	-1.01
3127075	0.000	15.663	0.028	0.18	15.612	0.122	0.78	-0.33
3217506	0.000	16.087	0.069	0.43	15.999	0.215	1.34	-0.55
3105488	0.000	16.326	0.024	0.15	16.181	0.178	1.10	-0.89
3126470	0.000	18.584	0.035	0.19	18.640	0.226	1.21	+0.30
3208127	0.000	22.792	0.039	0.17	22.544	0.135	0.60	-1.09
3118708	0.000	25.674	0.049	0.19	25.442	0.158	0.62	-0.90
3103555	0.000	21.224	0.033	0.16	21.144	0.133	0.63	-0.38
3203379	0.000	21.800	0.062	0.29	21.662	0.135	0.62	-0.63
3203545	0.000	24.727	0.046	0.19	24.703	0.175	0.71	-0.09
3107082	0.000	39.323	0.063	0.16	39.343	0.175	0.45	+0.05
3217266	0.000	36.574	0.057	0.16	36.275	0.173	0.48	-0.82
3211236	0.000	33.092	0.059	0.18	32.948	0.170	0.52	-0.44
3214875	0.000	29.115	0.050	0.17	28.943	0.142	0.49	-0.59
3116167	0.000	35.794	0.055	0.15	36.000	0.140	0.39	+0.58
3220751	0.000	28.963	0.057	0.20	29.081	0.164	0.56	+0.41

Table 39

Reflector Module IV-9 Fissile Fuel Loadings in Grams

Rod No.	As-Built Loading	PIFAG Thermal Loading	PIFAG Thermal Standard Deviation Grams	PIFAG Thermal Standard Deviation %	PIFAG Epithermal Loading	PIFAG Epithermal Standard Deviation Grams	PIFAG Epithermal Standard Deviation %	Epithermal - Thermal Percent Difference
3124805	0.000	7.593	0.026	0.34	7.334	0.148	2.02	-3.41
3124556	0.000	6.937	0.019	0.28	6.730	0.116	1.72	-2.98
3222815	0.000	7.104	0.026	0.36	7.174	0.135	1.89	+0.99
3218540	0.000	7.359	0.021	0.28	7.383	0.120	1.62	+0.33
3226176	0.000	6.344	0.020	0.32	6.440	0.135	2.10	+1.51
3223529	0.000	5.490	0.017	0.32	5.584	0.136	2.43	+1.69
3111448	0.000	5.590	0.028	0.50	5.423	0.114	2.10	-2.98
3224683	0.000	5.464	0.027	0.50	5.208	0.120	2.30	-4.67
3221530	0.000	5.890	0.018	0.30	5.547	0.126	2.27	-5.82
3222667	0.000	4.827	0.022	0.45	4.878	0.139	2.84	+1.05
3223050	0.000	8.088	0.027	0.33	7.948	0.117	1.48	-1.73
3215048	0.000	5.819	0.021	0.37	5.757	0.158	2.75	-1.07
3220229	0.000	4.648	0.022	0.48	4.616	0.114	2.48	-0.68
3125005	0.000	5.425	0.023	0.43	5.219	0.116	2.22	-3.80
3121265	0.000	4.955	0.023	0.46	4.782	0.135	2.83	-3.50
3124886	0.000	4.713	0.017	0.37	4.574	0.114	2.48	-2.94
3207256	0.000	7.305	0.026	0.35	7.198	0.117	1.63	-1.47
3121476	0.000	5.140	0.031	0.60	5.136	0.170	3.31	-0.08
3121173	0.000	4.736	0.030	0.63	4.613	0.114	2.47	-2.60
3104417	0.000	4.647	0.022	0.47	4.688	0.114	2.44	+0.88
3223152	0.000	13.737	0.031	0.23	13.600	0.129	0.95	-0.99
3224564	0.000	13.188	0.028	0.21	12.958	0.190	1.46	-1.74
3218743	0.000	10.658	0.042	0.39	10.599	0.123	1.16	-0.56
3202757	0.000	9.222	0.029	0.32	9.013	0.163	1.81	-2.27
3126140	0.000	8.692	0.025	0.29	8.662	0.119	1.37	-0.33
3211135	0.000	13.133	0.047	0.35	12.926	0.136	1.05	-1.58
3225783	0.000	9.390	0.028	0.30	9.234	0.136	1.48	-1.65
3222135	0.000	10.652	0.026	0.24	10.701	0.119	1.12	+0.46
3224748	0.000	9.696	0.024	0.25	9.651	0.151	1.56	-0.47
3218844	0.000	10.854	0.029	0.27	10.688	0.113	1.06	-1.53
3121586	0.000	11.361	0.030	0.27	11.151	0.119	1.07	-1.85
3125389	0.000	8.823	0.027	0.31	8.577	0.116	1.36	-2.78
3224739	0.000	13.716	0.033	0.24	13.562	0.129	0.95	-1.13
3221448	0.000	20.296	0.035	0.17	20.313	0.128	0.63	+0.08
3221659	0.000	16.077	0.054	0.34	15.821	0.117	0.74	-1.59
3123474	0.000	20.216	0.044	0.22	19.939	0.127	0.64	-1.37
3123135	0.000	17.233	0.038	0.22	17.126	0.190	1.11	-0.62
3122513	0.000	15.744	0.032	0.20	15.768	0.116	0.73	+0.15
3220404	0.000	26.358	0.046	0.17	26.405	0.134	0.51	+0.18
3123263	0.000	21.170	0.031	0.15	21.113	0.179	0.85	-0.27
3120165	0.000	21.654	0.040	0.19	21.668	0.120	0.56	+0.06
3218577	0.000	27.276	0.050	0.18	27.068	0.134	0.49	-0.76
3221062	0.000	20.679	0.046	0.22	20.643	0.136	0.66	-0.18
3100282	0.000	39.550	0.074	0.19	39.687	0.147	0.37	+0.35
3123236	0.000	35.777	0.060	0.17	35.766	0.158	0.44	-0.03
3118836	0.000	31.837	0.061	0.19	31.806	0.168	0.53	-0.10
3206542	0.000	29.191	0.053	0.18	29.033	0.135	0.47	-0.54
3120376	0.000	27.846	0.050	0.18	28.005	0.179	0.64	+0.57

Table 40

Reflector Module V-4 Fissile Fuel Loadings in Grams

Rod No.	As-Built Loading	PIFAG Thermal Loading	PIFAG Thermal Standard Deviation Grams	PIFAG Thermal Standard Deviation %	PIFAG Epithermal Loading	PIFAG Epithermal Standard Deviation Grams	PIFAG Epithermal Standard Deviation %	Epitherma - Th: ·mal Percent Differenc
3200815	0.000	6.947	0.021	0.30	6.994	0.168	2.40	+0.68
3106846	0.000	7.723	0.025	0.33	7.581	0.118	1.56	-1.84
3201464	0.000	7.309	0.025	0.35	7.279	0.113	1.55	-0.42
3204810	0.000	6.958	0.033	0.48	6.932	0.119	1.71	-0.37
3106635	0.000	5.663	0.018	0.32	5.681	0.116	2.05	+0.32
3102620	0.000	6.436	0.020	0.32	6.294	0.120	1.90	-2.22
3208852	0.000	4.763	0.019	0.40	4.742	0.126	2.65	-0.43
3223675	0.000	5.372	0.024	0.45	5.353	0.117	2.19	-0.35
3111513	0.000	4.888	0.022	0.46	4.796	0.173	3.61	-1.89
3201160	0.000	4.683	0.020	0.42	4.672	0.117	2.51	-0.23
3210136	0.000	4.241	0.019	0.45	4.133	0.145	3.52	-2.53
3113336	0.000	4.998	0.023	0.46	4.838	0.116	2.39	-3.20
3105167	0.000	12.657	0.031	0.25	12.656	0.152	1.20	-0.01
3204663	0.000	12.730	0.030	0.24	12.667	0.164	1.30	-0.49
3203030	0.000	12.152	0.022	0.18	12.133	0.123	1.02	-0.16
3206423	0.000	10.825	0.036	0.34	10.201	0.135	1.32	-5.76
3220182	0.000	11.359	0.041	0.36	11.581	0.190	1.64	+1.95
3204609	0.000	10.806	0.029	0.26	10.819	0.123	1.14	+0.13
3217275	0.000	10.487	0.029	0.27	10.517	0.123	1.17	+0.28
3200705	0.000	8.724	0.027	0.31	8.657	0.121	1.40	-0.77
3105315	0.000	9.330	0.029	0.32	9.030	0.120	1.33	-3.21
3204636	0.000	9.403	0.027	0.29	9.201	0.166	1.80	-2.15
3102015	0.000	21.094	0.038	0.18	21.027	0.134	0.64	-0.32
3225453	0.000	24.197	0.044	0.18	24.192	0.138	0.57	-0.02
3213629	0.000	21.984	0.040	0.18	22.044	0.166	0.75	+0.27
3102318	0.000	18.093	0.035	0.20	17.828	0.131	0.73	-1.46
3226636	0.000	20.238	0.027	0.13	20.090	0.126	0.63	-0.73
3201380	0.000	20.200	0.040	0.20	20.184	0.134	0.67	-0.08
3100228	0.000	17.077	0.048	0.28	16.754	0.164	0.98	-1.89
3206762	0.000	15.186	0.028	0.18	15.116	0.129	0.85	-0.46
3106819	0.000	15.451	0.044	0.29	14.926	0.164	1.10	-3.39
3111228	0.000	16.225	0.035	0.21	15.850	0.133	0.84	-2.31
3204654	0.000	14.973	0.035	0.23	14.998	0.128	0.85	+0.17
3207458	0.000	14.459	0.028	0.20	14.319	0.121	0.84	-0.97

Appendix C

Serial Numbers of the Rods in the Type C Storage Liners

Liner Cell	Serial #	ModType	LinerType	Liner#
101	3120818	4-3	R	15681
102	3116829	4-3	R	15681
103	3225352	4-3	R	15681
104	3214013	4-3	R	15681
105	3206266	4-3	R	15681
144	3116443	4-4	R	15681
145	3122403	4-4	R	15681
146	3116508	4-4	R	15681
147	3116755	4-4	R	15681
148	3124547	4-4	R	15681
149	3121009	4-4	R	15681
150	3215104	4-4	R	15681
151	3224665	4-4	R	15681
152	3202216	4-4	R	15681
153	3203233	4-4	R	15681
154	3202243	4-4	R	15681
155	3200346	4-4	R	15681
156	3207568	4-4	R	15681
157	3207357	4-4	R	15681
158	3116553	4-4	R	15681
159	3118000	4-4	R	15681
160	3107486	4-4	R	15681
161	3117377	4-4	R	15681
162	3116865	4-4	R	15681
163	3123401	4-4	R	15681
164	3104572	4-4	R	15681
165	3207027	4-4	R	15681
166	3204680	4-4	R	15681
167	3204764	4-4	R	15681
168	3205507	4-4	R	15681
169	3220265	4-4	R	15681
170	3206578	4-4	R	15681
171	3206367	4-4	R	15681
172	3214884	4-4	R	15681
173	3216873	4-4	R	15681
174	3108779	4-4	R	15681
175	3107203	4-4	R	15681
176	3102419	4-4	R	15681
177	3122834	4-4	R	15681
178	3118880	4-4	R	15681
179	3122356	4-4	R	15681
180	3217322	4-4	R	15681
181	3101815	5-4	R	15681
182	3102354	5-4	R	15681
183	3210127	5-4	R	15681
184	3125500	4-9	R	15681
185	3121615	4-9	R	15681
186	3222768	4-9	R	15681
187	3220650	4-9	R	15681
188	3202032	4-9	R	15681
189	3126177	4-9	R	15681
190	3122521	4-9	R	15681
191	3126186	4-9	R	15681
601	3224203	4-3	R	15681
602	3214250	4-3	R	15681

603	3225085	4-3	R	15681
604	3222566	4-3	R	15681
605	3102015	5-4	R	15681
606	3105315	5-4	R	15681
607	3105167	5-4	R	15681
609	3113336	5-4	R	15681
610	3122879	4-3	R	15681
611	3114326	4-3	R	15681
612	3114804	4-3	R	15681
613	3111504	4-3	R	15681
614	3112815	4-3	R	15681
615	3120156	4-3	R	15681
616	3223188	4-3	R	15681
617	3213858	4-3	R	15681
618	3201776	4-3	R	15681
619	3211429	4-3	R	15681
620	3126022	4-3	R	15681
621	3126159	4-3	R	15681
622	3211034	4-3	R	15681
623	3206834	4-3	R	15681
624	3117709	4-3	R	15681
625	3115580	4-3	R	15681
626	3117560	4-3	R	15681
627	3102583	4-3	R	15681
628	3122513	4-9	R	15681
629	3120165	4-9	R	15681
630	3104417	4-9	R	15681
631	3121173	4-9	R	15681
632	3121476	4-9	R	15681
633	3124886	4-9	R	15681
634	3224683	4-9	R	15681
635	3226176	4-9	R	15681
636	3218540	4-9	R	15681
637	3224748	4-9	R	15681
638	3222815	4-9	R	15681
639	3211135	4-9	R	15681
640	3202757	4-9	R	15681
641	3218743	4-9	R	15681
642	3222667	4-9	R	15681
643	3221530	4-9	R	15681
644	3223529	4-9	R	15681
645	3120376	4-9	R	15681
646	3123474	4-9	R	15681
647	3123263	4-9	R	15681
648	3125389	4-9	R	15681
649	3125005	4-9	R	15681
650	3111448	4-9	R	15681
651	3124805	4-9	R	15681
652	3100282	4-9	R	15681
653	3118836	4-9	R	15681
654	3123135	4-9	R	15681
655	3123296	4-9	R	15681
656	3220404	4-9	R	15681
657	3221659	4-9	R	15681
658	3221448	4-9	R	15681
659	3218844	4-9	R	15681

660	3124556	4-9	R	15681
661	3121586	4-9	R	15681
662	3121265	4-9	R	15681
663	3126140	4-9	R	15681
664	3224739	4-9	R	15681
665	3215048	4-9	R	15681
666	3220229	4-9	R	15681
667	3207256	4-9	R	15681
668	3222135	4-9	R	15681
669	3225783	4-9	R	15681
670	3223152	4-9	R	15681
671	3223050	4-9	R	15681
672	3224564	4-9	R	15681
673	3206542	4-9	R	15681
674	3221062	4-9	R	15681
675	3218577	4-9	R	15681
101	1406785	1-3	B	15682
102	1607084	1-3	B	15682
103	1310849	1-3	B	15682
104	1103407	1-3	B	15682
107	1200225	1-3	B	15682
108	1411064	1-3	B	15682
109	1607066	1-3	B	15682
110	2701476	3-6	B	15682
111	2301756	3-6	B	15682
112	2401746	3-6	B	15682
113	2202655	3-6	B	15682
122	1604179	3-6	B	15682
123	1413275	3-6	B	15682
124	1200766	3-6	B	15682
135	1512524	3-6	B	15682
136	1310813	3-6	B	15682
140	2701265	2-2	B	15682
141	2302443	2-2	B	15682
142	2100170	2-2	B	15682
143	2304459	2-2	B	15682
144	2512103	2-2	B	15682
145	2406088	2-2	B	15682
147	2401012	2-2	B	15682
242	2517087	3-2	B	15682
243	2503467	3-2	B	15682
244	2520784	3-2	B	15682
245	2511240	3-2	B	15682
246	2520766	3-2	B	15682
247	2511039	3-2	B	15682
248	2505079	3-2	B	15682
249	2517657	3-2	B	15682
250	2512780	3-2	B	15682
251	2518656	3-2	B	15682
252	2505584	3-2	B	15682
253	2511452	3-2	B	15682
254	2510536	3-2	B	15682
255	2504420	3-2	B	15682
256	2516438	3-2	B	15682
257	2516402	3-2	B	15682

258	2506345	3-2	B	15682
259	2502248	3-2	B	15682
260	2520573	3-2	B	15682
261	2518243	3-2	B	15682
262	2513809	3-2	B	15682
263	2511149	3-2	B	15682
264	2516162	3-2	B	15682
265	2302268	3-2	B	15682
266	2101666	3-2	B	15682
267	2608378	3-2	B	15682
268	2611359	3-2	B	15682
269	2606317	3-2	B	15682
270	2620646	3-2	B	15682
271	2604245	3-2	B	15682
272	2612587	3-2	B	15682
273	2618765	3-2	B	15682
274	2612028	3-2	B	15682
275	2600010	3-2	B	15682
276	2602202	3-2	B	15682
277	2616730	3-2	B	15682
278	2613485	3-2	B	15682
279	2603412	3-2	B	15682
280	2402175	3-2	B	15682
281	2616327	3-2	B	15682
282	2602036	3-2	B	15682
283	2402276	3-2	B	15682
284	2621829	3-2	B	15682
285	2620884	3-2	B	15682
286	2403073	3-2	B	15682
287	2200134	3-2	B	15682
288	2205055	3-2	B	15682
289	2620049	3-2	B	15682
290	2608517	3-2	B	15682
291	2402340	3-2	B	15682
292	2204763	3-2	B	15682
293	2520867	3-2	B	15682
294	2503072	3-2	B	15682
295	2510076	3-2	B	15682
296	2303112	3-2	B	15682
297	2520463	3-2	B	15682
298	2304046	3-2	B	15682
299	2103417	3-2	B	15682
300	2501433	3-2	B	15682
301	2517161	3-2	B	15682
302	2512010	3-2	B	15682
303	2305808	3-2	B	15682
304	2517217	3-2	B	15682
305	2303305	3-2	B	15682
306	2101877	3-2	B	15682
307	2515329	3-2	B	15682
308	2517482	3-2	B	15682
309	2302874	3-2	B	15682
310	2100337	3-2	B	15682
311	2604135	3-2	B	15682
312	2404606	3-2	B	15682
313	2200116	3-2	B	15682

314	2200704	3-2	B	15682
315	2620637	3-2	B	15682
316	2604254	3-2	B	15682
317	2600819	3-2	B	15682
318	2406373	3-2	B	15682
319	2202334	3-2	B	15682
320	2612634	3-2	B	15682
321	2614879	3-2	B	15682
322	2602650	3-2	B	15682
323	2403046	3-2	B	15682
324	2200501	3-2	B	15682
601	2200840	3-6	B	15682
607	2513880	3-6	B	15682
608	2518169	3-6	B	15682
609	2507720	3-6	B	15682
610	2700643	3-2	B	15682
611	2300601	3-2	B	15682
612	2300279	3-2	B	15682
613	2304652	3-2	B	15682
614	1612357	1-3	B	15682
615	1606278	1-3	B	15682
616	2517179	3-2	B	15682
617	1604758	1-3	B	15682
618	1404356	1-3	B	15682
619	1411479	1-3	B	15682
620	2502082	3-2	B	15682
621	2521022	3-2	B	15682
622	1200500	1-3	B	15682
623	1208042	1-3	B	15682
624	1206347	1-3	B	15682
625	1510589	1-3	B	15682
626	1311811	1-3	B	15682
627	1307152	1-3	B	15682
628	1107750	1-3	B	15682
629	1105477	1-3	B	15682
630	1507058	1-3	B	15682
631	1506683	1-3	B	15682
632	1500386	1-3	B	15682
633	1500846	1-3	B	15682
634	1107623	1-3	B	15682
635	1103700	1-3	B	15682
636	1106844	1-3	B	15682
637	1610157	1-3	B	15682
638	1503742	1-3	B	15682
639	2518041	3-2	B	15682
640	1302873	1-3	B	15682
641	1500157	1-3	B	15682
642	2610167	3-6	B	15682
643	2615512	3-6	B	15682
644	2622617	3-6	B	15682
645	2507509	3-6	B	15682
646	2605502	3-6	B	15682
647	2622507	3-6	B	15682
648	2404018	3-6	B	15682
649	2204846	3-6	B	15682
650	2616684	3-6	B	15682

651	2600377	3-6	B	15682
652	2606876	3-6	B	15682
653	2601367	3-6	B	15682
654	2101464	3-6	B	15682
655	2612735	3-6	B	15682
656	2600314	3-6	B	15682
657	2501670	3-6	B	15682
658	2513634	3-6	B	15682
659	2501157	3-6	B	15682
660	2700414	3-6	B	15682
661	2503808	3-6	B	15682
662	2514045	3-6	B	15682
663	2512579	3-6	B	15682
664	2517226	3-6	B	15682
665	2516824	3-6	B	15682
666	2500618	3-6	B	15682
667	2500589	3-6	B	15682
668	2503018	3-6	B	15682
669	2622083	3-6	B	15682
670	2617005	3-6	B	15682
671	2612827	3-6	B	15682
672	2600745	3-6	B	15682
673	2502578	3-6	B	15682
674	2510738	3-6	B	15682
180	3107082	4-4	R	15683
181	3206304	4-4	R	15683
182	3220018	4-9	R	15683
183	3116856	4-4	R	15683
184	3217578	4-4	R	15683
185	3101885	4-4	R	15683
186	3123373	4-4	R	15683
187	3116223	4-4	R	15683
188	3107102	4-4	R	15683
189	3201069	4-4	R	15683
190	3218505	4-4	R	15683
191	3202674	4-4	R	15683
601	3102143	CALIB	R	15683
602	31124	CALIB	R	15683
603	31063	CALIB	R	15683
604	31123	CALIB	R	15683
605	3106718	CALIB	R	15683
606	31062	CALIB	R	15683
607	3108707	CALIB	R	15683
609	3203545	4-4	R	15683
610	3220751	4-4	R	15683
611	3127075	4-4	R	15683
612	3216258	4-4	R	15683
613	3214875	4-4	R	15683
614	3103555	4-4	R	15683
615	3118708	4-4	R	15683
617	3203379	4-4	R	15683
619	3104664	4-4	R	15683
620	3122163	4-4	R	15683
621	3222833	4-4	R	15683
622	3216139	4-4	R	15683

623	3217506	4-4	R	15683
624	3116167	4-4	R	15683
625	3118019	4-4	R	15683
626	3113006	4-4	R	15683
627	3120744	4-4	R	15683
629	3208127	4-4	R	15683
630	3211236	4-4	R	15683
631	3217266	4-4	R	15683
632	3218413	4-4	R	15683
633	3218669	4-4	R	15683
634	3222474	4-4	R	15683
635	3203774	4-4	R	15683
636	3207458	5-4	R	15683
637	3204654	5-4	R	15683
638	3206762	5-4	R	15683
639	3201380	5-4	R	15683
640	3226636	5-4	R	15683
641	3213629	5-4	R	15683
642	3122605	4-4	R	15683
643	3126470	4-4	R	15683
644	3105488	4-4	R	15683
645	3123245	4-4	R	15683
648	3111228	5-4	R	15683
649	3106819	5-4	R	15683
650	3100228	5-4	R	15683
651	3102318	5-4	R	15683
652	3111513	5-4	R	15683
653	3102620	5-4	R	15683
654	3106635	5-4	R	15683
655	3106846	5-4	R	15683
656	3204663	5-4	R	15683
657	3210136	5-4	R	15683
658	3201160	5-4	R	15683
659	3223675	5-4	R	15683
660	3208852	5-4	R	15683
661	3204810	5-4	R	15683
662	3201464	5-4	R	15683
663	3200815	5-4	R	15683
664	3204609	5-4	R	15683
665	3220182	5-4	R	15683
666	3206423	5-4	R	15683
667	3203030	5-4	R	15683
668	3110624	4-3	R	15683
670	3207716	4-3	R	15683
671	3220357	4-3	R	15683
672	3225453	5-4	R	15683
673	3204636	5-4	R	15683
674	3200705	5-4	R	15683
675	3217275	5-4	R	15683
101*	3107082	4-4	R	15683
102*	3206304	4-4	R	15683
103*	3116856	4-4	R	15683
104*	3220018	4-9	R	15683
101	1612210	3-2	B	15684
102	1614824	3-2	B	15684

103	1606884	3-2	B	15684
104	1600330	3-2	B	15684
105	1611275	3-2	B	15684
106	1602071	3-2	B	15684
107	1607571	3-2	B	15684
108	1514513	3-2	B	15684
109	1510874	3-2	B	15684
110	1500184	3-2	B	15684
111	1504144	3-2	B	15684
112	1500727	3-2	B	15684
113	1514329	3-2	B	15684
114	1510883	3-2	B	15684
115	1508865	3-2	B	15684
116	1405714	3-2	B	15684
117	1312764	3-2	B	15684
118	1303652	3-2	B	15684
119	1301387	3-2	B	15684
120	1302670	3-2	B	15684
121	1101555	3-2	B	15684
122	1110230	3-2	B	15684
123	1311215	3-2	B	15684
124	1408518	3-2	B	15684
125	1408554	3-2	B	15684
126	1206677	3-2	B	15684
127	1205788	3-2	B	15684
128	1208161	3-2	B	15684
129	1207447	3-2	B	15684
130	1401608	3-2	B	15684
131	1607048	3-2	B	15684
132	1304889	3-2	B	15684
133	1506288	3-2	B	15684
134	1502862	3-2	B	15684
135	1514614	3-2	B	15684
136	1514585	3-2	B	15684
137	1502009	3-2	B	15684
138	1514374	3-2	B	15684
139	1511543	3-2	B	15684
140	1312856	3-2	B	15684
141	1302038	3-2	B	15684
143	1308032	3-2	B	15684
144	1308537	3-2	B	15684
145	1110060	3-2	B	15684
146	1104837	3-2	B	15684
147	1205430	3-2	B	15684
148	1202214	3-2	B	15684
149	1205210	3-2	B	15684
150	1615042	3-2	B	15684
151	1608561	3-2	B	15684
152	1612413	3-2	B	15684
153	1614777	3-2	B	15684
154	1612274	3-2	B	15684
155	1606114	3-2	B	15684
156	1408509	3-2	B	15684
158	1408177	3-2	B	15684
159	1413468	3-2	B	15684
160	1602724	3-2	B	15684

161	1606756	3-2	B	15684
163	2621728	3-2	B	15684
164	2404615	3-2	B	15684
165	2202352	3-2	B	15684
166	1401754	3-2	B	15684
167	1201307	3-2	B	15684
168	2515860	3-2	B	15684
169	2700660	3-2	B	15684
170	2302130	3-2	B	15684
171	2505272	3-2	B	15684
172	2501588	3-2	B	15684
173	2516878	3-2	B	15684
174	2513827	3-2	B	15684
324	1103167	3-2	B	15684
601	2517208	3-6	B	15684
602	2505236	3-6	B	15684
603	2701430	3-6	B	15684
604	2305449	3-6	B	15684
605	2305312	3-6	B	15684
606	2101363	3-6	B	15684
607	2620747	3-6	B	15684
608	2612625	3-6	B	15684
609	2613413	3-6	B	15684
610	2622175	3-6	B	15684
611	2604877	3-6	B	15684
612	2305853	3-6	B	15684
613	2406355	3-6	B	15684
614	2204855	3-6	B	15684
615	2610223	2-2	B	15684
616	2613505	2-2	B	15684
617	2610205	2-2	B	15684
618	2620655	2-2	B	15684
619	2606389	2-2	B	15684
620	2614769	2-2	B	15684
621	2610883	2-2	B	15684
622	2618866	2-2	B	15684
623	2617106	2-2	B	15684
624	2605583	2-2	B	15684
625	2616776	2-2	B	15684
626	2405522	2-2	B	15684
627	2505025	2-2	B	15684
628	2518371	2-2	B	15684
629	2511663	2-2	B	15684
630	2504585	2-2	B	15684
631	2513717	2-2	B	15684
632	2517823	2-2	B	15684
633	2504706	2-2	B	15684
634	2506814	2-2	B	15684
635	2516759	2-2	B	15684
636	2400287	2-2	B	15684
637	2406153	2-2	B	15684
638	2608003	2-2	B	15684
640	2701357	2-2	B	15684
641	2700055	2-2	B	15684
642	2304138	2-2	B	15684
643	2303552	2-2	B	15684

644	2303560	2-2	B	15684
645	2103352	2-2	B	15684
646	2102225	2-2	B	15684
647	2102077	2-2	B	15684
648	2504347	2-2	B	15684
649	2516061	2-2	B	15684
650	2518142	2-2	B	15684
651	2520288	2-2	B	15684
652	2100245	2-2	B	15684
653	2504834	2-2	B	15684
654	2517289	2-2	B	15684
656	2611002	3-2	B	15684
657	2615016	3-2	B	15684
658	2601147	3-2	B	15684
659	2607031	3-2	B	15684
660	2607325	3-2	B	15684
661	2511810	3-2	B	15684
662	2520656	3-2	B	15684
663	2516850	3-2	B	15684
664	2608434	3-2	B	15684
665	2621407	3-2	B	15684
666	2602375	3-2	B	15684
667	2201178	3-2	B	15684
668	2401636	3-2	B	15684
669	2402314	3-2	B	15684
670	2605152	3-2	B	15684
671	2600653	3-2	B	15684
672	2606775	3-2	B	15684
673	2603383	3-2	B	15684
674	2620509	3-2	B	15684
101	2502616	CALIB	B	15685
102	25064	CALIB	B	15685
103	25123	CALIB	B	15685
104	25163	CALIB	B	15685
154	1612146	2-2	B	15685
155	1605629	1-3	B	15685
156	2620628	3-2	B	15685
157	1407712	1-3	B	15685
158	2104416	2-2	B	15685
159	1104478	1-3	B	15685
160	1503329	1-3	B	15685
161	1105055	2-2	B	15685
162	1203626	3-2	B	15685
163	1402762	1-3	B	15685
164	1601036	1-3	B	15685
165	1600616	2-2	B	15685
166	2606243	3-2	B	15685
167	2620316	3-2	B	15685
168	2402249	3-2	B	15685
169	2204525	3-2	B	15685
170	2604034	3-2	B	15685
171	2616455	3-2	B	15685
172	2618408	3-2	B	15685
173	2401672	3-2	B	15685
174	2617555	3-2	B	15685

175	2611332	3-2	B	15685
176	2605134	3-2	B	15685
177	2615429	3-2	B	15685
178	2615236	3-2	B	15685
179	2613514	3-2	B	15685
180	2202058	3-2	B	15685
181	2202132	3-2	B	15685
182	2305229	3-2	B	15685
183	2520519	3-2	B	15685
184	2517419	3-2	B	15685
185	2511508	3-2	B	15685
186	2300885	3-2	B	15685
187	2102317	3-2	B	15685
188	2518804	3-2	B	15685
189	2517354	3-2	B	15685
190	2303644	3-2	B	15685
191	2100667	3-2	B	15685
192	2102804	3-2	B	15685
193	2513753	3-2	B	15685
194	2301619	3-2	B	15685
195	2102150	3-2	B	15685
196	2518720	3-2	B	15685
197	2502440	3-2	B	15685
198	2303166	3-2	B	15685
199	2200309	3-2	B	15685
200	2200648	3-2	B	15685
201	2200721	3-2	B	15685
202	2402305	3-2	B	15685
203	2600258	3-2	B	15685
204	2306356	3-2	B	15685
205	2602853	3-2	B	15685
206	2617077	3-2	B	15685
207	2618004	3-2	B	15685
208	2621636	3-2	B	15685
209	2605125	3-2	B	15685
210	2617537	3-2	B	15685
211	2601064	3-2	B	15685
212	2620269	3-2	B	15685
213	2622368	3-2	B	15685
214	2406236	3-2	B	15685
215	2405605	3-2	B	15685
216	2400572	3-2	B	15685
217	2404155	3-2	B	15685
218	2404247	3-2	B	15685
219	2401158	3-2	B	15685
220	2201629	3-2	B	15685
221	2104167	3-2	B	15685
222	2103408	3-2	B	15685
223	2103058	3-2	B	15685
224	2305568	3-2	B	15685
225	2306026	3-2	B	15685
226	2303029	3-2	B	15685
227	2305752	3-2	B	15685
228	2304037	3-2	B	15685
229	2302700	3-2	B	15685
230	2701348	3-2	B	15685

231	2700165	3-2	B	15685
232	2507418	3-2	B	15685
233	2505723	3-2	B	15685
234	2507344	3-2	B	15685
235	2501359	3-2	B	15685
236	2502477	3-2	B	15685
237	2510572	3-2	B	15685
238	2515310	3-2	B	15685
239	2511378	3-2	B	15685
240	2511562	3-2	B	15685
241	2511737	3-2	B	15685
242	2506428	3-2	B	15685
243	2507133	3-2	B	15685
244	2511306	3-2	B	15685
245	2615079	3-2	B	15685
246	2620334	3-2	B	15685
247	2614778	3-2	B	15685
248	2602348	3-2	B	15685
249	2616832	3-2	B	15685
250	2618417	3-2	B	15685
251	2616805	3-2	B	15685
252	2605620	3-2	B	15685
253	2613467	3-2	B	15685
254	2600047	3-2	B	15685
255	2622579	3-2	B	15685
256	2606546	3-2	B	15685
257	2517473	3-2	B	15685
258	2512543	3-2	B	15685
259	2515255	3-2	B	15685
260	2518068	3-2	B	15685
261	2500039	3-2	B	15685
262	2511746	3-2	B	15685
263	2513423	3-2	B	15685
264	1107127	3-2	B	15685
265	1608552	3-2	B	15685
266	1402625	3-2	B	15685
267	1208785	3-2	B	15685
268	1203507	3-2	B	15685
269	1200480	3-2	B	15685
270	1203139	3-2	B	15685
271	1208179	3-2	B	15685
272	1401846	3-2	B	15685
273	1304202	3-2	B	15685
274	1107118	3-2	B	15685
275	1101308	3-2	B	15685
276	1104709	3-2	B	15685
277	1101876	3-2	B	15685
278	1100529	3-2	B	15685
279	1306667	3-2	B	15685
280	1304835	3-2	B	15685
281	1304725	3-2	B	15685
282	1611376	3-2	B	15685
283	1607618	3-2	B	15685
284	1412763	3-2	B	15685
285	1401056	3-2	B	15685
286	1402129	3-2	B	15685

287	1205063	3-2	B	15685
288	1200683	3-2	B	15685
289	1200720	3-2	B	15685
290	1200436	3-2	B	15685
291	1201022	3-2	B	15685
292	1105515	3-2	B	15685
293	1100235	3-2	B	15685
294	1103113	3-2	B	15685
295	1100684	3-2	B	15685
296	1101638	3-2	B	15685
297	1103755	3-2	B	15685
298	1107668	3-2	B	15685
299	1204660	3-2	B	15685
300	1405584	3-2	B	15685
301	1405254	3-2	B	15685
302	1403018	3-2	B	15685
303	1406428	3-2	B	15685
304	1401644	3-2	B	15685
305	1405263	3-2	B	15685
306	1412175	3-2	B	15685
307	1607012	3-2	B	15685
308	1613127	3-2	B	15685
309	1614566	3-2	B	15685
310	1605252	3-2	B	15685
311	1614034	3-2	B	15685
312	1310427	3-2	B	15685
313	1311022	3-2	B	15685
314	1303688	3-2	B	15685
315	1312570	3-2	B	15685
316	1310106	3-2	B	15685
317	1312240	3-2	B	15685
318	1310610	3-2	B	15685
319	1511258	3-2	B	15685
320	1500258	3-2	B	15685
321	1505538	3-2	B	15685
322	1504824	3-2	B	15685
323	1514412	3-2	B	15685
324	1504319	3-2	B	15685
601	2302378	3-2	B	15685
602	2100759	3-2	B	15685
603	2517363	3-2	B	15685
604	2516777	3-2	B	15685
605	2517704	3-2	B	15685
606	2511350	3-2	B	15685
607	2512754	3-2	B	15685
608	2517244	3-2	B	15685
609	2608755	3-2	B	15685
610	2605455	3-2	B	15685
611	2622433	3-2	B	15685
612	2622478	3-2	B	15685
613	2607471	3-2	B	15685
614	2611157	3-2	B	15685
615	2614640	3-2	B	15685
616	2610240	3-2	B	15685
617	2101758	3-2	B	15685
618	2515513	3-2	B	15685

619	2701274	3-2	B	15685
624	1104780	CALIB	B	15685
625	1613834	CALIB	B	15685
626	15124	CALIB	B	15685
627	1512019	CALIB	B	15685
628	1613659	CALIB	B	15685
629	15064	CALIB	B	15685
630	1103425	CALIB	B	15685
631	1412359	CALIB	B	15685
632	1300545	CALIB	B	15685
633	1501827	CALIB	B	15685
634	25161	CALIB	B	15685
635	25122	CALIB	B	15685
636	2303222	CALIB	B	15685
637	2103140	CALIB	B	15685
638	2500452	CALIB	B	15685
639	25063	CALIB	B	15685
640	2700466	CALIB	B	15685
641	2701624	CALIB	B	15685
642	2402626	CALIB	B	15685
643	2100153	CALIB	B	15685
644	25001	CALIB	B	15685
645	25004	CALIB	B	15685
646	15004	CALIB	B	15685
647	15061	CALIB	B	15685
648	15002	CALIB	B	15685
649	15122	CALIB	B	15685
652	1102470	2-2	B	15685
653	1104525	2-2	B	15685
654	1106586	2-2	B	15685
655	1106137	2-2	B	15685
656	1103672	2-2	B	15685
657	1305787	2-2	B	15685
658	1311334	2-2	B	15685
659	1302579	2-2	B	15685
660	1210125	2-2	B	15685
661	1210226	2-2	B	15685
662	1208657	2-2	B	15685
663	1303248	2-2	B	15685
664	1504667	2-2	B	15685
665	1507619	2-2	B	15685
666	1504658	2-2	B	15685
667	1200344	3-6	B	15685
668	1204542	3-6	B	15685
669	1410646	3-6	B	15685
670	1404448	3-6	B	15685
671	1602181	2-2	B	15685
672	1607479	2-2	B	15685
673	1602676	2-2	B	15685
674	1608083	2-2	B	15685
700	5001	CALIB	S	15686
707	5004	CALIB	S	15686
701	5061	CALIB	S	15686
705	5062	CALIB	S	15686
710	5121	CALIB	S	15686

708	5122	CALIB	S	15686
712	5273	CALIB	S	15686
703	5274	CALIB	S	15686
702	5431	CALIB	S	15686
713	5432	CALIB	S	15686
697	100500	CALIB	S	15686
690	100683	3-1	S	15686
622	100821	1-1	S	15686
706	101334	CALIB	S	15686
691	102609	3-1	S	15686
488	103846	2-3	S	15686
481	104046	2-3	S	15686
485	104414	2-3	S	15686
484	104468	2-3	S	15686
487	104477	2-3	S	15686
482	104708	2-3	S	15686
486	105210	2-3	S	15686
644	105624	3-2	S	15686
645	106089	3-2	S	15686
774	106614	2-3	S	15686
770	200343	1-1	S	15686
476	200408	2-3	S	15686
673	201342	3-1	S	15686
106	201460	1-1	S	15686
504	201746	1-1	S	15686
115	202478	3-1	S	15686
641	202525	3-2	S	15686
775	202635	2-3	S	15686
672	203652	3-1	S	15686
433	204202	2-3	S	15686
406	205154	1-1	S	15686
109	205677	3-2	S	15686
664	207428	3-2	S	15686
431	210106	2-3	S	15686
616	211224	1-1	S	15686
432	211462	2-3	S	15686
472	212277	2-3	S	15686
434	212719	2-3	S	15686
492	213736	2-3	S	15686
435	214486	2-3	S	15686
477	214578	2-3	S	15686
469	214660	2-3	S	15686
470	214726	2-3	S	15686
496	215357	2-3	S	15686
474	215559	2-3	S	15686
494	215678	2-3	S	15686
495	215707	2-3	S	15686
498	215760	2-3	S	15686
493	216338	2-3	S	15686
764	216356	2-3	S	15686
473	216448	2-3	S	15686
471	216513	2-3	S	15686
475	216686	2-3	S	15686
751	217061	2-3	S	15686
507	301340	1-1	S	15686
104	301450	1-1	S	15686

698	301754	CALIB	S	15686
684	302203	3-1	S	15686
768	302578	1-1	S	15686
683	302845	3-1	S	15686
704	307748	CALIB	S	15686
116	308168	3-1	S	15686
426	310655	2-3	S	15686
112	311003	3-2	S	15686
464	311700	2-3	S	15686
756	312083	2-3	S	15686
465	312487	2-3	S	15686
466	312516	2-3	S	15686
462	313275	2-3	S	15686
468	313423	2-3	S	15686
461	313506	2-3	S	15686
430	313533	2-3	S	15686
501	314054	2-3	S	15686
463	314303	2-3	S	15686
642	314384	3-2	S	15686
427	314476	2-3	S	15686
460	314734	2-3	S	15686
467	314788	2-3	S	15686
429	315026	2-3	S	15686
459	315035	2-3	S	15686
643	315127	3-2	S	15686
749	315310	2-3	S	15686
458	315504	2-3	S	15686
428	316126	2-3	S	15686
671	400083	3-1	S	15686
709	401863	CALIB	S	15686
105	402072	1-1	S	15686
767	404355	1-1	S	15686
114	407067	3-1	S	15686
670	407702	3-1	S	15686
421	408084	2-3	S	15686
497	408562	2-3	S	15686
422	408645	2-3	S	15686
640	408755	3-2	S	15686
449	410084	2-3	S	15686
108	410185	3-2	S	15686
457	410387	2-3	S	15686
455	410764	2-3	S	15686
448	411010	2-3	S	15686
762	411056	2-3	S	15686
454	411222	2-3	S	15686
425	411507	2-3	S	15686
752	411534	2-3	S	15686
451	411617	2-3	S	15686
423	412358	2-3	S	15686
424	412515	2-3	S	15686
456	412616	2-3	S	15686
639	412652	3-2	S	15686
453	412753	2-3	S	15686
452	413045	2-3	S	15686
450	413303	2-3	S	15686
696	414466	CALIB	S	15686

609	500082	1-1	S	15686
674	500385	3-1	S	15686
103	500809	1-1	S	15686
613	501128	1-1	S	15686
614	501779	1-1	S	15686
615	501265	1-1	S	15686
675	501808	3-1	S	15686
666	502200	3-1	S	15686
769	502228	1-1	S	15686
505	502347	3-1	S	15686
677	502585	3-1	S	15686
678	503622	3-1	S	15686
401	504107	1-1	S	15686
668	504363	3-1	S	15686
404	504502	1-1	S	15686
679	504556	3-1	S	15686
649	504648	1-1	S	15686
658	505362	3-1	S	15686
113	505804	3-1	S	15686
667	506206	3-1	S	15686
659	506388	3-1	S	15686
676	506453	3-1	S	15686
660	507039	3-1	S	15686
610	507333	1-1	S	15686
611	507782	1-1	S	15686
680	508451	3-1	S	15686
682	508516	3-1	S	15686
669	508617	3-1	S	15686
681	508671	3-1	S	15686
118	510002	3-1	S	15686
661	510139	3-1	S	15686
699	511165	CALIB	S	15686
632	511625	3-2	S	15686
442	512072	2-3	S	15686
418	515574	2-3	S	15686
440	515823	2-3	S	15686
630	516133	3-2	S	15686
633	517269	3-2	S	15686
629	518333	3-2	S	15686
778	518387	2-3	S	15686
653	523779	3-2	S	15686
650	524302	3-2	S	15686
755	524623	2-3	S	15686
419	525806	2-3	S	15686
651	526336	3-2	S	15686
711	527674	CALIB	S	15686
773	527703	2-3	S	15686
443	528004	2-3	S	15686
441	528058	2-3	S	15686
763	528325	2-3	S	15686
445	530114	2-3	S	15686
110	530132	3-2	S	15686
414	530224	2-3	S	15686
444	530563	2-3	S	15686
417	530811	2-3	S	15686
415	531048	2-3	S	15686

446	531342	2-3	S	15686
416	531407	2-3	S	15686
503	531654	2-3	S	15686
652	531728	3-2	S	15686
757	531737	2-3	S	15686
617	532120	3-2	S	15686
111	532213	3-2	S	15686
776	532763	2-3	S	15686
502	533423	2-3	S	15686
447	534256	2-3	S	15686
420	534808	2-3	S	15686
758	535154	2-3	S	15686
771	535466	2-3	S	15686
631	536272	3-2	S	15686
777	536622	2-3	S	15686
627	537510	3-2	S	15686
688	600430	3-1	S	15686
604	600577	1-1	S	15686
692	600633	3-1	S	15686
619	601504	1-1	S	15686
657	601558	3-2	S	15686
694	602108	3-1	S	15686
409	602209	1-1	S	15686
689	602878	3-1	S	15686
603	603289	1-1	S	15686
665	603327	1-1	S	15686
101	603381	1-1	S	15686
601	603464	1-1	S	15686
686	603684	3-1	S	15686
687	604472	3-1	S	15686
602	604519	1-1	S	15686
403	604555	1-1	S	15686
695	604876	3-1	S	15686
618	605269	1-1	S	15686
626	605572	1-1	S	15686
624	606378	1-1	S	15686
625	606461	1-1	S	15686
637	606681	1-1	S	15686
655	606874	3-2	S	15686
608	607184	1-1	S	15686
405	607258	3-1	S	15686
656	607561	3-2	S	15686
620	608165	1-1	S	15686
623	608313	1-1	S	15686
693	608349	3-1	S	15686
634	608753	3-2	S	15686
745	610239	2-3	S	15686
662	610275	3-2	S	15686
754	610607	2-3	S	15686
746	610818	2-3	S	15686
635	613676	3-2	S	15686
759	614648	2-3	S	15686
646	615216	3-2	S	15686
747	615409	2-3	S	15686
742	615739	2-3	S	15686
663	617865	3-2	S	15686

761	618516	2-3	S	15686
648	618543	3-2	S	15686
407	618561	3-2	S	15686
750	622532	2-3	S	15686
647	622889	3-2	S	15686
439	623659	2-3	S	15686
766	623724	2-3	S	15686
765	623860	2-3	S	15686
410	624153	2-3	S	15686
760	624382	2-3	S	15686
741	624465	2-3	S	15686
638	624824	3-2	S	15686
500	625152	2-3	S	15686
412	625161	2-3	S	15686
438	626068	2-3	S	15686
743	626528	2-3	S	15686
744	626573	2-3	S	15686
654	627076	3-2	S	15686
753	628315	2-3	S	15686
411	628324	2-3	S	15686
413	628544	2-3	S	15686
499	630553	2-3	S	15686
636	630680	3-2	S	15686
748	631800	2-3	S	15686
628	637069	3-2	S	15686
621	700219	1-1	S	15686
478	700530	2-3	S	15686
685	701153	3-1	S	15686
479	701209	2-3	S	15686
506	702069	1-1	S	15686
508	702161	3-1	S	15686
489	702805	2-3	S	15686
480	703454	2-3	S	15686
483	704325	2-3	S	15686
402	704628	2-3	S	15686
436	704664	2-3	S	15686
437	705048	2-3	S	15686
772	705084	2-3	S	15686
408	800117	1-1	S	15686
490	800227	3-1	S	15686
491	801482	2-3	S	15686
101	1604253	2-2	B	15687
102	1408765	2-2	B	15687
103	1203662	2-2	B	15687
108	1512477	2-2	B	15687
109	1305439	2-2	B	15687
324	1101830	2-2	B	15687
601	2202278	3-2	B	15687
602	2200805	3-2	B	15687
603	2401048	3-2	B	15687
604	2607563	3-2	B	15687
605	1607416	3-2	B	15687
606	1607075	3-2	B	15687
607	1615502	3-2	B	15687
608	1514365	3-2	B	15687

609	1513339	3-2	B	15687
610	1310187	3-2	B	15687
611	1310472	3-2	B	15687
612	1303872	3-2	B	15687
613	1105102	3-2	B	15687
614	1103012	3-2	B	15687
615	1103460	3-2	B	15687
616	1402542	3-2	B	15687
617	1410316	3-2	B	15687
618	1207520	3-2	B	15687
619	1203709	3-2	B	15687
620	1511469	3-2	B	15687
621	1401828	3-2	B	15687
622	1100767	3-2	B	15687
623	2202518	3-2	B	15687
641	2516281	3-2	B	15687
642	2603044	3-2	B	15687
643	2514128	3-2	B	15687
644	2515585	3-2	B	15687
645	2621223	2-2	B	15687
646	2516503	3-2	B	15687
647	2516319	3-2	B	15687
648	1402660	2-2	B	15687
649	1505363	2-2	B	15687
650	1407748	2-2	B	15687
651	1412846	2-2	B	15687
652	1404668	2-2	B	15687
653	1401882	3-6	B	15687
654	1601164	3-6	B	15687
655	1613457	3-6	B	15687
656	1603483	3-6	B	15687
657	1104800	3-6	B	15687
658	1305724	3-6	B	15687
659	1308564	3-6	B	15687
660	1103315	3-6	B	15687
661	1101059	3-6	B	15687
662	1103443	3-6	B	15687
663	1306117	3-6	B	15687
664	1512486	3-6	B	15687
665	1513265	3-6	B	15687
666	1507545	3-6	B	15687
667	1208078	1-3	B	15687
668	1401166	1-3	B	15687
669	1604318	1-3	B	15687
670	1200665	1-3	B	15687
671	1407187	1-3	B	15687
672	1605876	1-3	B	15687
673	1311738	1-3	B	15687
674	1306584	1-3	B	15687

Appendix D

Results from ANL-E Destructive Evaluations

Results from ANL-E Destructive Evaluations

Extensive chemical and physical measurements were performed on 17 LWBR rods. These measurements were subject to the following pre-defined error requirements and specifications.

Analysis	% Relative Bias	% Relative Standard Deviation
U-isotopic (U-233 + U-235)(%abundance)	0.05 (or 0.01 g/U-total per segment)[a]	0.08 (or 0.01 g/U-total per segment)[a]
U-total (g/segment)	0.15	0.15
Cs-137 (atoms/segment)	0.5	1.25
Ce-144 (atoms/segment)	2.0	2.0
Zr-95 (atoms/segment)	2.5[b]	4.0[b]
Rod Weight (g)[c]	0.1	0.10
Rod Length (in)	0.001	0.010
Segment Weight (g)[c]	0.001 if wt <286 g, otherwise 0.01 g	0.005
Cladding Segment Length (in)	0.001	0.005
Fuel Segment Length (in)	0.005	0.015
Cladding Segment Boundary Location (in)	0.010 total	
Fuel Segment Boundary Location (in)	0.005	0.015

a: The larger of the two shall apply.
b: Waived after two years out of the reactor (10/84), for low burn-up, or low concentration segments.
c: Weights are given as mass in air relative to 8.0 g/cm^3 density standard weights.
d: Not including the average fuel shear-plane displacement, which will be corrected for.

Dissolution/Sample Preparation/Sampling

The physical measurements performed on the fuel rods were weight, length, and temperature of the rod surface. The rods were then sheared into pre-defined lengths (segments) and collected in aluminum buckets. The shearing also served to pulverize the ceramic fuel material, aiding sample dissolution. The segments (and bucket) were then dissolved in one of two high pressure, high temperature dissolver systems. The dissolution was carried out using a 4 hour dissolution in Thorex (13.6 M HNO_3, 0.06 M HF) followed by a dilute nitric acid rinse, then a 3 hour secondary dissolution in a Thorex-0.06 M Al^{+3} solution, followed by a reflux rinse (hot rinse) and cold rinse with dilute nitric acid. Operating conditions for both dissolutions were 195°C and 120 psig. A sample of the second dissolution was obtained to measure the completeness of the dissolution scheme. Both dissolutions and all rinses were then combined in a blend tank and mixed prior to further sampling. Gases emitted during dissolution were collected and analyzed for Kr and Xe.

In all, three sets of samples were obtained from each segment. The first set (two samples) was taken from the secondary dissolution prior to blending to assess the completeness of the dissolution scheme. The second set (four samples) was then taken from the blended (both dissolutions and all rinses) tank contents. The third set (four samples) was taken after the addition of a known amount of U-238 spike (NBS Standard Sample 950a). Half of the samples were analyzed, the other half was placed in archive. Batch carry over or cross contamination was controlled and monitored by analyzing a blank (a full dissolution scheme with no segment material) between each rod and all segments were analyzed in order of increasing U content.

Implicit in all measurements is that dissolution is complete and fuel in solution is quantitatively transferred to the blend tank.

Uranium analysis

Total uranium and uranium isotopic (U-233, U-234, U-235, U-236, U-238) analyses were perform by thermal ionization mass spectrometry. Due to the interference of Th-232, U-232 was determined by alpha spectrometry.

Rod B – 2606481: The uncertainties for uranium results for segments B-03, B-04 and B-05 may be slightly more than reported due to losses in dissolution (order of 0.01%-0.02%).

Kr/Xe Analysis

Fission gases (Kr and Xe) collected from the fuel rod plenum and during dissolution were determined by gas mass spectrometry on a "best effort" basis. Gases released during shearing was estimated by using the in line radiation monitor in the cell ventilation system. The plenum (rod void volume) contained between 0.01% and 0.15%, and about 0.17% to 0.58% of the gas was released during shearing. The rest (>99%) was released during dissolution.

Rod B – 2606481: The total gram weight given in column entitled "gas released in dissolution" is incorrect. The total reflects the 0.0037 contribution of the plenum gases.

Rod C – 2513854: The Kr and Xe values for C-04 were estimated using fission gas data from C-03 and C-05 and an assumed correlation with Cs-137 over the three segments.

Cs-137, Ce-144, Nb-95 Analysis

The fission products Cs-137, Ce-144, and Nb-95 were determined by gamma spectrometry (high purity germanium detector with associated automated multi-channel analyzer/data management system) on weighed aliquots of the samples obtained prior to spiking the blend tank with 950a. Cs-137 and Ce-144 were determined on a sample aliquot by direct counting. Zr-95 was obtained after processing the sample aliquot through a cleanup procedure to reduce interferences. The losses of Zr-95 were accounted for by using before and after values of the Ce-144. Error requirements for Zr-95 measurements made after 10/84 were waived, due to the short half life (64.02 days).

Rod "B" 2606481 (PFB 3-6 E31)

	B-00	B-01	B-02	B-03	B-04	B-05	B-06	B-07	B-08
Segment length (in)	1.10E+01	1.10E+01	1.81E+01	1.75E+01	1.75E+01	1.75E+01	1.46E+01	9.43E+00	1.63E+00
Total length (in)									1.18E+02
U-232 (wt%)[1]	0.00E+00	1.13E-02	2.83E-02	1.09E-01	1.47E-01	1.15E-01	3.50E-02	1.84E-02	
Error (+/-)[1]	0.00E+00	4.00E-04	9.00E-04	3.40E-03	4.60E-03	3.60E-03	1.10E-03	6.00E-04	
U-232 (g)[8]	0.00E+00	3.23E-05	3.54E-03	1.25E-02	1.65E-02	1.28E-02	3.36E-03	9.38E-05	
Error (+/-)[9]	NA	1.14E-06	1.12E-04	3.89E-04	5.16E-04	4.01E-04	1.05E-04	3.06E-06	
Segment Total									4.88E-02
Error (+/-)[12]									7.77E-04
U-233 (wt%)[1]	1.00E+02	9.92E+01	9.37E+01	8.78E+01	8.56E+01	8.71E+01	9.22E+01	9.86E+01	
Error (+/-)[1]	0.00E+00	2.10E-02	4.80E-03	5.50E-03	6.10E-03	5.60E-03	5.00E-03	1.59E-02	
U-233 (g)[8]	4.00E-05	2.83E-01	1.17E+01	1.01E+01	9.61E+00	9.71E+00	8.84E+00	5.03E-01	
Error (+/-)[9]	1.00E-05	1.33E-04	3.29E-03	2.90E-03	2.71E-03	2.76E-03	2.43E-03	1.69E-04	
Segment Total									5.07E+01
Error (+/-)[12]									6.33E-03
U-234 (wt%)[1]	0.00E+00	7.16E-01	5.33E+00	9.98E+00	1.16E+01	1.06E+01	6.60E+00	1.29E+00	
Error (+/-)[1]	0.00E+00	6.00E-04	7.00E-04	9.00E-04	1.10E-03	1.00E-03	7.00E-04	6.00E-04	
U-234 (g)[8]	0.00E+00	2.05E-03	6.65E-01	1.14E+00	1.31E+00	1.18E+00	6.33E-01	6.59E-03	
Error (+/-)[9]	NA	1.92E-06	2.03E-04	3.37E-04	3.77E-04	3.46E-04	1.84E-04	3.62E-06	
Segment Total									4.94E+00
Error (+/-)[12]									6.71E-04
U-235 (wt%)[1]	0.00E+00	1.25E-02	6.38E-01	1.65E+00	2.09E+00	1.76E+00	8.21E-01	3.68E-02	
Error (+/-)[1]	0.00E+00	1.49E-02	3.50E-03	3.60E-03	3.70E-03	3.60E-03	3.70E-03	1.13E-02	
U-235 (g)[8]	0.00E+00	3.57E-05	7.98E-02	1.89E-01	2.35E-01	1.97E-01	7.87E-02	1.88E-04	
Error (+/-)[9]	NA	4.25E-05	4.38E-04	4.16E-04	4.20E-04	4.05E-04	3.55E-04	5.76E-05	
Segment Total									7.79E-01

Rod "B" 2606481 (PFB 3-6 E31)

	B-00	B-01	B-02	B-03	B-04	B-05	B-06	B-07	B-08
Error (+/-)[12]									9.15E-04
U-236 (wt%)[1]	0.00E+00	4.00E-04	8.10E-02	1.73E-01	2.32E-01	1.90E-01	9.81E-02	6.00E-04	
Error (+/-)[1]	0.00E+00	2.00E-04	1.00E-04	1.00E-04	1.00E-04	1.00E-04	1.00E-04	2.00E-04	
U-236 (g)[8]	0.00E+00	1.14E-06	1.01E-02	1.98E-02	2.60E-02	2.12E-02	9.41E-03	3.06E-06	
Error (+/-)[9]	NA	5.71E-07	1.28E-05	1.27E-05	1.33E-05	1.26E-05	9.92E-06	1.02E-06	
Segment Total									8.65E-02
Error (+/-)[12]									2.76E-05
U-238 (wt%)[1]	0.00E+00	2.98E-02	2.75E-01	2.70E-01	2.67E-01	2.76E-01	2.88E-01	1.46E-02	
Error (+/-)[1]	0.00E+00	1.50E-02	3.50E-03	3.60E-03	3.80E-03	3.70E-03	3.70E-03	1.14E-02	
U-238 (g)[8]	0.00E+00	8.51E-05	3.44E-02	3.09E-02	3.00E-02	3.08E-02	2.76E-02	7.44E-05	
Error (+/-)[9]	NA	4.28E-05	4.37E-04	4.12E-04	4.27E-04	4.13E-04	3.55E-04	5.81E-05	
Segment Total									1.54E-01
Error (+/-)[12]									9.19E-04
Total U[2]	4.00E-05	2.86E-01	1.25E+01	1.15E+01	1.12E+01	1.12E+01	9.59E+00	5.10E-01	
Error (+/-)[2]	1.00E-05	1.20E-04	3.45E-03	3.22E-03	3.06E-03	3.09E-03	2.59E-03	1.50E-04	
Kr-82 (mol%)[3]	2.00E-01	2.00E-01	2.00E-01	2.00E-01	2.00E-01	2.00E-01	2.00E-01	2.00E-01	
Error (+/-)[3]	2.00E-01	2.00E-01	2.00E-01	2.00E-01	2.00E-01	2.00E-01	2.00E-01	2.00E-01	
Kr-82 (g)[10]	1.15E-06	0.00E+00	1.85E-04	3.27E-04	4.13E-04	3.38E-04	1.63E-04	8.80E-06	
Error (+/-)[9]	1.15E-06	NA	1.85E-04	3.28E-04	4.15E-04	3.39E-04	1.64E-04	1.08E-05	
Segment Total									1.44E-03
Error (+/-)[12]									6.75E-04
Kr-83 (mol%)[3]	1.54E+01	1.54E+01	1.54E+01	1.54E+01	1.54E+01	1.54E+01	1.54E+01	1.54E+01	
Error (+/-)[3]	1.00E-01	1.00E-01	1.00E-01	1.00E-01	1.00E-01	1.00E-01	1.00E-01	1.00E-01	
Kr-83 (g)[10]	8.94E-05	0.00E+00	1.44E-02	2.55E-02	3.22E-02	2.64E-02	1.27E-02	6.86E-04	

Rod "B" 2606481 (PFB 3-6 E31)

	B-00	B-01	B-02	B-03	B-04	B-05	B-06	B-07	B-08
Error (+/-)[9]	5.80E-07	NA	1.03E-03	2.47E-03	2.47E-03	1.50E-03	1.34E-03	4.85E-04	
Segment Total									1.12E-01
Error (+/-)[12]									4.19E-03
Kr-84 (mol%)[3]	3.01E+01	3.01E+01	3.01E+01	3.01E+01	3.01E+01	3.01E+01	3.01E+01	3.01E+01	
Error (+/-)[3]	3.00E-01	3.00E-01	3.00E-01	3.00E-01	3.00E-01	3.00E-01	3.00E-01	3.00E-01	
Kr-84 (g)[10]	1.77E-04	0.00E+00	2.85E-02	5.04E-02	6.37E-02	5.22E-02	2.51E-02	1.36E-03	
Error (+/-)[9]	1.76E-06	NA	2.04E-03	4.90E-03	4.92E-03	3.00E-03	2.66E-03	9.60E-04	
Segment Total									2.21E-01
Error (+/-)[12]									8.33E-03
Kr-85 (mol%)[3]	6.20E+00	6.20E+00	6.20E+00	6.20E+00	6.20E+00	6.20E+00	6.20E+00	6.20E+00	
Error (+/-)[3]	1.00E-01	1.00E-01	1.00E-01	1.00E-01	1.00E-01	1.00E-01	1.00E-01	1.00E-01	
Kr-85 (g)[10]	3.69E-05	0.00E+00	5.93E-03	1.05E-02	1.33E-02	1.09E-02	5.24E-03	2.83E-04	
Error (+/-)[9]	5.94E-07	NA	4.32E-04	1.03E-03	1.04E-03	6.41E-04	5.59E-04	2.00E-04	
Segment Total									4.62E-02
Error (+/-)[12]									1.76E-03
Kr-86 (mol%)[3]	4.82E+01	4.82E+01	4.82E+01	4.82E+01	4.82E+01	4.82E+01	4.82E+01	4.82E+01	
Error (+/-)[3]	3.00E-01	3.00E-01	3.00E-01	3.00E-01	3.00E-01	3.00E-01	3.00E-01	3.00E-01	
Kr-86 (g)[10]	2.90E-04	0.00E+00	4.67E-02	8.26E-02	1.04E-01	8.55E-02	4.12E-02	2.22E-03	
Error (+/-)[9]	1.80E-06	NA	3.33E-03	8.01E-03	8.02E-03	4.87E-03	4.36E-03	1.57E-03	
Segment Total									3.63E-01
Error (+/-)[12]									1.36E-02
Rod Total									7.44E-01
Error (+/-)[12]									1.66E-02
Shear Gas (g)[4]	0.00E+00	0.00E+00	1.20E-03	3.00E-03	3.90E-03	3.70E-03	2.00E-03	2.00E-04	
Error (+/-)[4]	NA	NA	2.00E-04	6.00E-04	8.00E-04	8.00E-04	4.00E-04	0.00E+00	

Rod "B" 2606481 (PFB 3-6 E31)

	B-00	B-01	B-02	B-03	B-04	B-05	B-06	B-07	B-08
Diss+Pl Kr (mol)[3]	7.00E-06	0.00E+00	1.13E-03	1.99E-03	2.52E-03	2.06E-03	9.91E-04	5.30E-05	
Error (+/-)[3]	0.00E+00	NA	8.00E-05	1.93E-04	1.93E-04	1.17E-04	1.05E-04	3.80E-05	
Diss+Pl Kr+Xe (g)[3]	3.70E-03	0.00E+00	6.69E-01	1.23E+00	1.54E+00	1.30E+00	5.81E-01	1.53E-02	
Error (+/-)[3]	2.00E-04	NA	4.08E-02	5.44E-02	5.47E-02	5.64E-02	1.68E-02	8.60E-03	
Total Kr (mol)	7.00E-06	0.00E+00	1.13E-03	1.99E-03	2.52E-03	2.07E-03	9.94E-04	5.37E-05	
Error (+/-)[9]	0.00E+00	NA	8.00E-05	1.93E-04	1.93E-04	1.17E-04	1.05E-04	3.80E-05	
Xe-128 (mol)[3]	1.00E-01	1.00E-01	1.00E-01	1.00E-01	1.00E-01	1.00E-01	1.00E-01	1.00E-01	
Error (+/-)[3]	0.00E+00	0.00E+00	0.00E+00	0.00E+00	0.00E+00	0.00E+00	0.00E+00	0.00E+00	
Xe-128 (g)[10]	2.94E-06	0.00E+00	5.48E-04	1.01E-03	1.26E-03	1.08E-03	4.75E-04	1.04E-05	
Error (+/-)[3]	1.28E-07	NA	3.82E-05	4.92E-05	4.95E-05	5.27E-05	1.34E-05	1.02E-05	
SegmentTotal									4.39E-03
Error (+/1)[12]									9.70E-05
Xe-130 (mol)[3]	1.00E-01	1.00E-01	1.00E-01	1.00E-01	1.00E-01	1.00E-01	1.00E-01	1.00E-01	
Error (+/-)[3]	0.00E+00	0.00E+00	0.00E+00	0.00E+00	0.00E+00	0.00E+00	0.00E+00	0.00E+00	
Xe-130 (g)[10]	2.99E-06	0.00E+00	5.56E-04	1.03E-03	1.28E-03	1.10E-03	4.82E-04	1.05E-05	
Error (+/-)[3]	1.30E-07	NA	3.88E-05	5.00E-05	5.03E-05	5.35E-05	1.36E-05	1.04E-05	
SegmentTotal									4.46E-03
Error (+/1)[12]									9.85E-05
Xe-131 (mol)[3]	1.19E+01	1.19E+01	1.19E+01	1.19E+01	1.19E+01	1.19E+01	1.19E+01	1.19E+01	
Error (+/-)[3]	1.00E-01	1.00E-01	1.00E-01	1.00E-01	1.00E-01	1.00E-01	1.00E-01	1.00E-01	
Xe-131 (g)[10]	3.58E-04	0.00E+00	6.67E-02	1.23E-01	1.54E-01	1.31E-01	5.78E-02	1.26E-03	
Error (+/-)[3]	1.59E-05	NA	4.69E-03	6.09E-03	6.17E-03	6.51E-03	1.71E-03	1.25E-03	

Rod "B" 2606481 (PFB 3-6 E31)

	B-00	B-01	B-02	B-03	B-04	B-05	B-06	B-07	B-08
SegmentTotal									5.35E-01
Error (+/1)[12]									1.20E-02
Xe-132 (mol)[3]	2.23E+01	2.23E+01	2.23E+01	2.23E+01	2.23E+01	2.23E+01	2.23E+01	2.23E+01	
Error (+/-)[3]	2.00E-01	2.00E-01	2.00E-01	2.00E-01	2.00E-01	2.00E-01	2.00E-01	2.00E-01	
Xe-132 (g)[10]	6.77E-04	0.00E+00	1.26E-01	2.33E-01	2.90E-01	2.48E-01	1.09E-01	2.38E-03	
Error (+/-)[3]	3.00E-05	NA	8.87E-03	1.15E-02	1.17E-02	1.23E-02	3.24E-03	2.35E-03	
SegmentTotal									1.01E+00
Error (+/1)[12]									2.27E-02
Xe-134 (mol)[3]	2.54E+01	2.54E+01	2.54E+01	2.54E+01	2.54E+01	2.54E+01	2.54E+01	2.54E+01	
Error (+/-)[3]	3.00E-01	3.00E-01	3.00E-01	3.00E-01	3.00E-01	3.00E-01	3.00E-01	3.00E-01	
Xe-134 (g)[10]	7.82E-04	0.00E+00	1.46E-01	2.69E-01	3.36E-01	2.87E-01	1.26E-01	2.76E-03	
Error (+/-)[3]	3.52E-05	NA	1.03E-02	1.35E-02	1.38E-02	1.44E-02	3.87E-03	2.72E-03	
SegmentTotal									1.17E+00
Error (+/1)[12]									2.66E-02
Xe-136 (mol)[3]	4.01E+01	4.01E+01	4.01E+01	4.01E+01	4.01E+01	4.01E+01	4.01E+01	4.01E+01	
Error (+/-)[3]	2.00E-01	2.00E-01	2.00E-01	2.00E-01	2.00E-01	2.00E-01	2.00E-01	2.00E-01	
Xe-136 (g)[10]	1.25E-03	0.00E+00	2.33E-01	4.32E-01	5.38E-01	4.59E-01	2.02E-01	4.42E-03	
Error (+/-)[3]	5.49E-05	NA	1.63E-02	2.11E-02	2.13E-02	2.26E-02	5.81E-03	4.36E-03	
SegmentTotal									1.87E+00
Error (+/1)[12]									4.16E-02
Rod total									4.59E+00
Error (+/-)[12]									5.56E-02

Rod "B" 2606481 (PFB 3-6 E31)

	B-00	B-01	B-02	B-03	B-04	B-05	B-06	B-07	B-08
Shear Gas (g)[4]	0.00E+00	0.00E+00	1.20E-03	3.00E-03	3.90E-03	3.70E-03	2.00E-03	2.00E-04	
Error (+/-)[4]	0.00E+00	0.00E+00	2.00E-04	6.00E-04	8.00E-04	8.00E-04	4.00E-04	0.00E+00	
Diss+Pl Xe (mol)[3]	2.30E-05	0.00E+00	4.28E-03	7.90E-03	9.85E-03	8.41E-03	3.70E-03	8.00E-05	
Error (+/-)[3]	1.00E-06	0.00E+00	2.99E-04	3.85E-04	3.87E-04	4.12E-04	1.05E-04	8.00E-05	
Diss+Pl Kr+Xe (g)[3]	3.70E-03	0.00E+00	6.69E-01	1.23E+00	1.54E+00	1.30E+00	5.81E-01	1.53E-02	
Error (+/-)[3]	2.00E-04	0.00E+00	4.08E-02	5.44E-02	5.47E-02	5.64E-02	1.68E-02	8.60E-03	
Total Xe (mol)	2.30E-05	0.00E+00	4.28E-03	7.92E-03	9.87E-03	8.43E-03	3.71E-03	8.10E-05	
Error (+/-)[9]	1.00E-06	0.00E+00	2.99E-04	3.85E-04	3.87E-04	4.12E-04	1.05E-04	8.00E-05	
Values corrected to 1/1/84 (page 181, Final Report for the LWBR Proof of Breeding Analytical Support Project									
Cs-137 (atoms)[5]	NA	2.74E+18	6.62E+20	1.38E+21	1.66E+21	1.46E+21	6.83E+20	8.40E+18	
Error (+/-)[4]	NA	1.18E+16	2.75E+18	5.93E+18	7.13E+18	6.27E+18	2.93E+18	3.61E+16	
Cs-137 (g)[11]	NA	6.24E-04	1.51E-01	3.14E-01	3.78E-01	3.32E-01	1.55E-01	1.91E-03	
Error (+/-)[9]	NA	2.68E-06	6.25E-04	1.35E-03	1.62E-03	1.43E-03	6.66E-04	8.21E-06	
Total									1.33E+00
Error (+/-)[12]									2.70E-03
Ce-144 (atoms)[5]	NA	3.50E+17	4.26E+19	7.01E+19	8.07E+19	6.61E+19	2.56E+19	4.04E+17	
Error (+/-)[4]	NA	2.56E+15	3.17E+17	5.55E+17	6.53E+17	5.36E+17	2.29E+17	3.20E+15	
Ce-144 (g)[11]	NA	8.35E-05	1.02E-02	1.68E-02	1.93E-02	1.58E-02	6.12E-03	9.65E-05	
Error (+/-)[9]	NA	6.12E-07	7.57E-05	1.33E-04	1.56E-04	1.28E-04	5.47E-05	7.65E-07	
Total									6.83E-02
Error (+/-)[12]									2.59E-04
Zr-95 (atoms)[5]	NA	3.88E+15	3.51E+17	5.34E+17	5.88E+17	3.49E+17	6.31E+16	7.16E+14	

Rod "B" 2606481 (PFB 3-6 E31)

	B-00	B-01	B-02	B-03	B-04	B-05	B-06	B-07	B-08
Error (+/-)[4]	NA	7.97E+13	4.25E+15	1.10E+16	9.71E+15	7.65E+15	2.37E+15	2.54E+13	
Zr-95 (g)[11]	NA	6.12E-07	5.53E-05	8.41E-05	9.27E-05	5.50E-05	9.94E-06	1.13E-07	
Error (+/-)[9]	NA	1.26E-08	6.70E-07	1.73E-06	1.53E-06	1.21E-06	3.73E-07	4.00E-09	
Total									2.98E-04
Error (+/-)[12]									2.72E-06

References

1. ANL Destructive Chemical Assay of 33-Rod LWBR EOL Sample - Rod B, 2606481, page 7
2. ANL Destructive Chemical Assay of 33-Rod LWBR EOL Sample - Rod B, 2606481, page 8
3. ANL Destructive Chemical Assay of 33-Rod LWBR EOL Sample - Rod B, 2606481, page 10
4. ANL Destructive Chemical Assay of 33-Rod LWBR EOL Sample - Rod B, 2606481, page 11
5. ANL Destructive Chemical Assay of 33-Rod LWBR EOL Sample - Rod B, 2606481, page 12
6. ANL Destructive Chemical Assay of 33-Rod LWBR EOL Sample - Rod B, 2606481, page 13
7. ANL Destructive Chemical Assay of 33-Rod LWBR EOL Sample - Rod B, 2606481, page 14
8. (abundance of the specified isotope)(total weight of uranium)

   1.00E+02
9. Error Propagation = ((+/-x/x)2+(+/-y/y)2)1/2(xy)
10. (mole%)(number moles gas recovered)(molec wt)

    1.00E+02
11. (number of atoms per segment)(atomic weight)

    6.02E+23
12. Error Propagation = (SUM(+/-I)1/2

Rod "C" 2513854 (PFB 3-6 F73)

	C-00	C-01	C-02	C-03	C-04	C-05	C-06	C-07	C-08
Segment length (in)	1.11E+01	7.99E+00	1.80E+01	1.75E+01	1.75E+01	1.75E+01	1.45E+01	1.14E+01	2.65E+00
Total length (in)									1.18E+02
U-232 (wt%)[1]	0.00E+00	1.01E-02	2.08E-02	8.41E-02	1.14E-01	8.69E-02	2.49E-02	1.42E-02	
Error (+/-)[1]	0.00E+00	3.00E-04	6.00E-04	2.60E-03	3.50E-03	2.70E-03	8.00E-04	4.00E-04	
U-232 (g)[8]	0.00E+00	2.19E-05	2.65E-03	9.86E-03	1.31E-02	1.01E-02	2.49E-03	6.40E-05	
Error (+/-)[9]	NA	6.51E-07	7.65E-05	3.05E-04	4.03E-04	3.12E-04	7.99E-05	1.80E-06	
Segment Total									3.83E-02
Error (+/-)[12]									6.04E-04
U-233 (wt%)[1]	1.00E+02	9.93E+01	9.45E+01	8.97E+01	8.79E+01	8.94E+01	9.38E+01	9.90E+01	
Error (+/-)[1]	0.00E+00	3.45E-02	4.70E-03	5.20E-03	5.90E-03	5.50E-03	6.40E-03	1.88E-02	
U-233 (g)[8]	1.60E-04	2.15E-01	1.20E+01	1.05E+01	1.01E+01	1.03E+01	9.38E+00	4.46E-01	
Error (+/-)[9]	2.00E-05	4.04E-04	3.20E-03	3.18E-03	2.88E-03	2.87E-03	2.68E-03	1.54E-04	
Segment Total									5.31E+01
Error (+/-)[12]									6.65E-03
U-234 (wt%)[1]	0.00E+00	6.31E-01	4.59E+00	8.55E+00	9.91E+00	8.81E+00	5.19E+00	9.90E-01	
Error (+/-)[1]	0.00E+00	1.10E-03	1.00E-03	1.10E-03	1.20E-03	1.20E-03	1.10E-03	1.10E-03	
U-234 (g)[8]	0.00E+00	1.37E-03	5.84E-01	1.00E+00	1.14E+00	1.02E+00	5.19E-01	4.47E-03	
Error (+/-)[9]	NA	3.47E-06	1.99E-04	3.24E-04	3.44E-04	3.09E-04	1.81E-04	5.13E-06	
Segment Total									4.27E+00
Error (+/-)[12]									6.25E-04
U-235 (wt%)[1]	0.00E+00	3.25E-02	5.21E-01	1.29E+00	1.62E+00	1.33E+00	5.91E-01	2.31E-02	
Error (+/-)[1]	0.00E+00	2.49E-02	3.40E-03	3.60E-03	4.00E-03	3.80E-03	4.80E-03	1.36E-02	
U-235 (g)[8]	0.00E+00	7.03E-05	6.64E-02	1.52E-01	1.87E-01	1.54E-01	5.91E-02	1.04E-04	
Error (+/-)[9]	NA	5.39E-05	4.34E-04	4.24E-04	4.64E-04	4.42E-04	4.80E-04	6.13E-05	
Segment									6.18E-01

Rod "C" 2513854 (PFB 3-6 F73)

	C-00	C-01	C-02	C-03	C-04	C-05	C-06	C-07	C-08
Total									
Error (+/-)[12]									1.01E-03
U-236 (wt%)[1]	0.00E+00	2.00E-04	7.44E-02	1.34E-01	1.70E-01	1.40E-01	8.04E-02	5.00E-04	
Error (+/-)[1]	0.00E+00	2.00E-04	2.00E-04	2.00E-04	2.00E-04	2.00E-04	2.00E-04	2.00E-04	
U-236 (g)[8]	0.00E+00	4.33E-07	9.48E-03	1.57E-02	1.96E-02	1.62E-02	8.03E-03	2.26E-06	
Error (+/-)[9]	NA	4.33E-07	2.56E-05	2.39E-05	2.37E-05	2.36E-05	2.01E-05	9.02E-07	
Segment Total									6.90E-02
Error (+/-)[12]									5.24E-05
U-238 (wt%)[1]	0.00E+00	3.14E-02	2.69E-01	2.66E-01	2.64E-01	2.69E-01	2.74E-01	2.04E-02	
Error (+/-)[1]	0.00E+00	2.42E-02	3.30E-03	3.50E-03	3.90E-03	3.70E-03	4.60E-03	1.32E-02	
U-238 (g)[8]	0.00E+00	6.80E-05	3.42E-02	3.11E-02	3.04E-02	3.11E-02	2.74E-02	9.20E-05	
Error (+/-)[9]	NA	5.24E-05	4.21E-04	4.10E-04	4.49E-04	4.28E-04	4.60E-04	5.95E-05	
Segment Total									1.54E-01
Error (+/-)[12]									9.74E-04
Total U[2]	1.60E-04	2.16E-01	1.27E+01	1.17E+01	1.15E+01	1.16E+01	9.99E+00	4.51E-01	
Error (+/-)[2]	2.00E-05	4.00E-04	3.32E-03	3.48E-03	3.18E-03	3.13E-03	2.77E-03	1.30E-04	
Kr-82 (mol%)[3]	1.00E-01	1.00E-01	1.00E-01	1.00E-01	1.00E-01	1.00E-01	1.00E-01	1.00E-01	
Error (+/-)[3]	1.00E-01	1.00E-01	1.00E-01	1.00E-01	1.00E-01	1.00E-01	1.00E-01	1.00E-01	
Kr-82 (g)[10]	3.28E-07	0.00E+00	7.72E-05	1.55E-04	1.86E-04	1.61E-04	6.90E-05	0.00E+00	
Error (+/-)[9]	3.28E-07	NA	7.77E-05	1.57E-04	1.88E-04	1.62E-04	6.95E-05	NA	
Segment Total									6.49E-04
Error (+/-)[12]									3.12E-04
Kr-83 (mol%)[3]	1.56E+01	1.56E+01	1.56E+01	1.56E+01	1.56E+01	1.56E+01	1.56E+01	1.56E+01	
Error (+/-)[3]	1.00E-01	1.00E-01	1.00E-01	1.00E-01	1.00E-01	1.00E-01	1.00E-01	1.00E-01	

Rod "C" 2513854 (PFB 3-6 F73)

	C-00	C-01	C-02	C-03	C-04	C-05	C-06	C-07	C-08
Kr-83 (g)[10]	5.17E-05	0.00E+00	1.22E-02	2.45E-02	2.94E-02	2.54E-02	1.09E-02	0.00E+00	
Error (+/-)[9]	3.32E-07	NA	1.44E-03	3.50E-03	4.51E-03	2.82E-03	1.28E-03	NA	
Segment Total									1.03E-01
Error (+/-)[12]									6.65E-03
Kr-84 (mol%)[3]	2.99E+01	2.99E+01	2.99E+01	2.99E+01	2.99E+01	2.99E+01	2.99E+01	2.99E+01	
Error (+/-)[3]	2.00E-01	2.00E-01	2.00E-01	2.00E-01	2.00E-01	2.00E-01	2.00E-01	2.00E-01	
Kr-84 (g)[10]	1.00E-04	0.00E+00	2.37E-02	4.76E-02	5.70E-02	4.94E-02	2.11E-02	0.00E+00	
Error (+/-)[9]	6.71E-07	NA	2.79E-03	6.78E-03	8.74E-03	5.48E-03	2.49E-03	NA	
Segment Total									1.99E-01
Error (+/-)[12]									1.29E-02
Kr-85 (mol%)[3]	6.00E+00	6.00E+00	6.00E+00	6.00E+00	6.00E+00	6.00E+00	6.00E+00	6.00E+00	
Error (+/-)[3]	1.00E-01	1.00E-01	1.00E-01	1.00E-01	1.00E-01	1.00E-01	1.00E-01	1.00E-01	
Kr-85 (g)[10]	2.04E-05	0.00E+00	4.80E-03	9.66E-03	1.16E-02	1.00E-02	4.29E-03	0.00E+00	
Error (+/-)[9]	3.40E-07	NA	5.71E-04	1.39E-03	1.78E-03	1.12E-03	5.09E-04	NA	
Segment Total									4.04E-02
Error (+/-)[12]									2.64E-03
Kr-86 (mol%)[3]	4.85E+01	4.85E+01	4.85E+01	4.85E+01	4.85E+01	4.85E+01	4.85E+01	4.85E+01	
Error (+/-)[3]	2.00E-01	2.00E-01	2.00E-01	2.00E-01	2.00E-01	2.00E-01	2.00E-01	2.00E-01	
Kr-86 (g)[10]	1.67E-04	0.00E+00	3.93E-02	7.90E-02	9.47E-02	8.20E-02	3.51E-02	0.00E+00	
Error (+/-)[9]	6.87E-07	NA	4.63E-03	1.13E-02	1.45E-02	9.09E-03	4.13E-03	NA	
Segment Total									3.30E-01
Error (+/-)[12]									2.14E-02
Rod Total									6.73E-01
Error (+/-)[12]									2.60E-02

Rod "C" 2513854 (PFB 3-6 F73)

	C-00	C-01	C-02	C-03	C-04	C-05	C-06	C-07	C-08
[redacted]									
Shear Gas (g)[4]	0.00E+00	0.00E+00	1.00E-03	3.40E-03	4.30E-03	3.70E-03	1.20E-03	2.00E-04	
Error (+/-)[4]	0.00E+00	0.00E+00	2.00E-04	6.00E-04	9.00E-04	8.00E-04	2.00E-04	0.00E+00	
Diss+Pl Kr (mol)[3]	4.00E-06	0.00E+00	9.41E-04	1.89E-03	2.27E-03	1.96E-03	8.41E-04	0.00E+00	
Error (+/-)[3]	0.00E+00	0.00E+00	1.11E-04	2.70E-04	3.48E-04	2.18E-04	9.90E-05	0.00E+00	
Diss+Pl Kr+Xe (g)[3]	1.70E-03	0.00E+00	5.77E-01	1.18E+00	1.40E+00	1.20E+00	5.69E-01	0.00E+00	
Error (+/-)[3]	0.00E+00	0.00E+00	5.28E-02	7.61E-02	1.07E-01	7.55E-02	4.72E-02	0.00E+00	
Total Kr (mol)	4.00E-06	0.00E+00	9.43E-04	1.90E-03	2.27E-03	1.97E-03	8.43E-04	2.95E-07	
Error (+/-)[9]	0.00E+00	NA	1.11E-04	2.70E-04	3.48E-04	2.18E-04	9.90E-05	NA	
[redacted]									
Xe-128 (mol)[3]	1.00E-01	1.00E-01	1.00E-01	1.00E-01	1.00E-01	1.00E-01	1.00E-01	1.00E-01	
Error (+/-)[3]	1.00E-01	1.00E-01	1.00E-01	1.00E-01	1.00E-01	1.00E-01	1.00E-01	1.00E-01	
Xe-128 (g)[10]	1.53E-06	0.00E+00	4.75E-04	9.70E-04	1.15E-03	9.93E-04	4.76E-04	0.00E+00	
Error (+/-)[3]	1.53E-06	NA	4.78E-04	9.73E-04	1.16E-03	9.95E-04	4.78E-04	NA	
SegmentTotal									4.07E-03
Error (+/1)[12]									1.93E-03
Xe-130 (mol)[3]	1.00E-01	1.00E-01	1.00E-01	1.00E-01	1.00E-01	1.00E-01	1.00E-01	1.00E-01	
Error (+/-)[3]	1.00E-01	1.00E-01	1.00E-01	1.00E-01	1.00E-01	1.00E-01	1.00E-01	1.00E-01	
Xe-130 (g)[10]	1.56E-06	0.00E+00	4.82E-04	9.86E-04	1.17E-03	1.01E-03	4.83E-04	0.00E+00	
Error (+/-)[3]	1.56E-06	NA	4.85E-04	9.88E-04	1.18E-03	1.01E-03	4.85E-04	NA	
SegmentTotal									4.13E-03
Error (+/1)[12]									1.96E-03
Xe-131 (mol)[3]	1.24E+01	1.24E+01	1.24E+01	1.24E+01	1.24E+01	1.24E+01	1.24E+01	1.24E+01	
Error (+/-)[3]	1.00E-01	1.00E-01	1.00E-01	1.00E-01	1.00E-01	1.00E-01	1.00E-01	1.00E-01	
Xe-131 (g)[10]	1.95E-04	0.00E+00	6.03E-02	1.23E-01	1.46E-01	1.26E-01	6.04E-02	2.12E-05	

Rod "C" 2513854 (PFB 3-6 F73)

	C-00	C-01	C-02	C-03	C-04	C-05	C-06	C-07	C-08
Error (+/-)[3]	1.57E-06	NA	6.30E-03	8.82E-03	1.25E-02	8.91E-03	5.64E-03	1.71E-07	
SegmentTotal									5.16E-01
Error (+/1)[12]									1.96E-02
Xe-132 (mol)[3]	2.26E+01	2.26E+01	2.26E+01	2.26E+01	2.26E+01	2.26E+01	2.26E+01	2.26E+01	
Error (+/-)[3]	1.00E-01	1.00E-01	1.00E-01	1.00E-01	1.00E-01	1.00E-01	1.00E-01	1.00E-01	
Xe-132 (g)[10]	3.58E-04	0.00E+00	1.11E-01	2.26E-01	2.69E-01	2.31E-01	1.11E-01	3.89E-05	
Error (+/-)[3]	1.58E-06	NA	1.15E-02	1.61E-02	2.29E-02	1.63E-02	1.03E-02	1.72E-07	
SegmentTotal									9.48E-01
Error (+/1)[12]									3.59E-02
Xe-134 (mol)[3]	2.59E+01	2.59E+01	2.59E+01	2.59E+01	2.59E+01	2.59E+01	2.59E+01	2.59E+01	
Error (+/-)[3]	2.00E-01	2.00E-01	2.00E-01	2.00E-01	2.00E-01	2.00E-01	2.00E-01	2.00E-01	
Xe-134 (g)[10]	4.16E-04	0.00E+00	1.29E-01	2.63E-01	3.13E-01	2.69E-01	1.29E-01	4.52E-05	
Error (+/-)[3]	3.21E-06	NA	1.35E-02	1.88E-02	2.67E-02	1.90E-02	1.20E-02	3.49E-07	
SegmentTotal									1.10E+00
Error (+/1)[12]									4.19E-02
Xe-136 (mol)[3]	3.90E+01	3.90E+01	3.90E+01	3.90E+01	3.90E+01	3.90E+01	3.90E+01	3.90E+01	
Error (+/-)[3]	1.00E-01	1.00E-01	1.00E-01	1.00E-01	1.00E-01	1.00E-01	1.00E-01	1.00E-01	
Xe-136 (g)[10]	6.36E-04	0.00E+00	1.97E-01	4.02E-01	4.78E-01	4.11E-01	1.97E-01	6.91E-05	
Error (+/-)[3]	1.63E-06	NA	2.05E-02	2.86E-02	4.06E-02	2.89E-02	1.83E-02	1.77E-07	
SegmentTotal									1.69E+00
Error (+/1)[12]									6.38E-02
Rod total									4.26E+00
Error (+/-)[12]									8.66E-02

Rod "C" 2513854 (PFB 3-6 F73)

	C-00	C-01	C-02	C-03	C-04	C-05	C-06	C-07	C-08
Shear Gas (g)[4]	0.00E+00	0.00E+00	1.00E-03	3.40E-03	4.30E-03	3.70E-03	1.20E-03	2.00E-04	
Error (+/-)[4]	0.00E+00	0.00E+00	2.00E-04	6.00E-04	9.00E-04	8.00E-04	2.00E-04	0.00E+00	
Diss+Pl Xe (mol)[3]	1.20E-05	0.00E+00	3.71E-03	7.57E-03	9.00E-03	7.74E-03	3.71E-03	0.00E+00	
Error (+/-)[3]	0.00E+00	0.00E+00	3.87E-04	5.40E-04	7.66E-04	5.45E-04	3.46E-04	0.00E+00	
Diss+Pl Kr+Xe (g)[3]	1.70E-03	0.00E+00	5.77E-01	1.18E+00	1.40E+00	1.20E+00	5.69E-01	0.00E+00	
Error (+/-)[3]	0.00E+00	0.00E+00	5.28E-02	7.61E-02	1.07E-01	7.55E-02	4.72E-02	0.00E+00	
Total Xe (mol)	1.20E-05	0.00E+00	3.71E-03	7.59E-03	9.02E-03	7.76E-03	3.72E-03	1.30E-06	
Error (+/-)[9]	0.00E+00	NA	3.87E-04	5.40E-04	7.66E-04	5.45E-04	3.46E-04	0.00E+00	
Values corrected to 1/1/84 (page 181, Final Report for the LWBR Proof of Breeding Analytical Support Project									
Cs-137 (atoms)[5]	NA	1.88E+18	5.37E+20	1.16E+21	1.38E+21	1.20E+21	5.06E+20	5.84E+18	
Error (+/-)[4]	NA	6.12E+15	1.49E+18	3.22E+18	3.80E+18	3.32E+18	1.39E+18	1.70E+16	
Cs-137 (g)[11]	NA	4.28E-04	1.22E-01	2.63E-01	3.15E-01	2.72E-01	1.15E-01	1.33E-03	
Error (+/-)[9]	NA	1.39E-06	3.39E-04	7.32E-04	8.64E-04	7.55E-04	3.16E-04	3.86E-06	
Total									1.09E+00
Error (+/-)[12]									1.44E-03
Ce-144 (atoms)[5]	NA	2.35E+17	3.49E+19	6.02E+19	6.95E+19	5.58E+19	1.96E+19	2.91E+17	
Error (+/-)[4]	NA	1.37E+15	1.97E+17	3.57E+17	4.04E+17	3.31E+17	1.16E+17	1.72E+15	
Ce-144 (g)[11]	NA	5.61E-05	8.35E-03	1.44E-02	1.66E-02	1.33E-02	4.68E-03	6.94E-05	
Error (+/-)[9]	NA	3.27E-07	4.71E-05	8.53E-05	9.65E-05	7.91E-05	2.77E-05	4.11E-07	
Total									5.75E-02
Error (+/-)[12]									1.61E-04
Zr-95 (atoms)[5]	NA	2.62E+15	2.87E+17	4.68E+17	5.04E+17	3.04E+17	5.37E+16	5.90E+14	
Error (+/-)[4]	NA	4.04E+13	4.55E+15	8.56E+15	1.02E+16	6.06E+15	1.48E+15	1.81E+13	
Zr-95 (g)[11]	NA	4.12E-07	4.52E-05	7.38E-05	7.94E-05	4.80E-05	8.46E-06	9.30E-08	

Rod "C" 2513854 (PFB 3-6 F73)

[redacted]

	C-00	C-01	C-02	C-03	C-04	C-05	C-06	C-07	C-08
Error (+/-)[9]	NA	6.37E-09	7.17E-07	1.35E-06	1.61E-06	9.55E-07	2.33E-07	2.85E-09	
Total									2.55E-04
Error (+/-)[12]									2.43E-06

[redacted]

References

1. ANL Destructive Chemical Assay of 33-Rod LWBR EOL Sample - Rod C, 2513854, page 6
2. ANL Destructive Chemical Assay of 33-Rod LWBR EOL Sample - Rod C, 2513854, page 7
3. ANL Destructive Chemical Assay of 33-Rod LWBR EOL Sample - Rod C, 2513854, page 9
4. ANL Destructive Chemical Assay of 33-Rod LWBR EOL Sample - Rod C, 2513854, page 10
5. ANL Destructive Chemical Assay of 33-Rod LWBR EOL Sample - Rod C, 2513854, page 11
6. ANL Destructive Chemical Assay of 33-Rod LWBR EOL Sample - Rod C, 2513854, page 12
7. ANL Destructive Chemical Assay of 33-Rod LWBR EOL Sample - Rod C, 2513854, page 13
8. (abundance of the specified isotope)(total weight of uranium)

   1.00E+02
9. Error Propagation = ((+/-x/x)2+(+/-y/y)2)1/2(xy)
10. (mole%)(number moles gas recovered)(molec wt)

    1.00E+02
11. (number of atoms per segment)(atomic weight)

    6.02E+23
12. Error Propagation = (SUM(+/-I)1/2

Rod "D" 2502102 (PFB 3-6 H1)

	D-00	D-01	D-02	D-03	D-04	D-05	D-06	D-07	D-08
Segment length (in)	1.12E+01	8.06E+00	1.78E+01	1.75E+01	1.75E+01	1.75E+01	1.45E+01	1.14E+01	2.63E+00
Total length (in)									1.18E+02
U-232 (wt%)[1]	0.00E+00	4.90E-03	5.80E-03	2.38E-02	3.36E-02	2.39E-02	6.50E-03	6.20E-03	
Error (+/-)[1]	0.00E+00	2.00E-04	2.00E-04	7.00E-04	1.00E-03	7.00E-04	2.00E-04	2.00E-04	
U-232 (g)[8]	0.00E+00	5.36E-06	7.52E-04	2.92E-03	4.06E-03	2.93E-03	6.77E-04	1.31E-05	
Error (+/-)[9]	NA	2.19E-07	2.59E-05	8.60E-05	1.21E-04	8.57E-05	2.08E-05	4.22E-07	
Segment Total									1.14E-02
Error (+/-)[12]									1.75E-04
U-233 (wt%)[1]	1.00E+02	9.96E+01	9.63E+01	9.39E+01	9.30E+01	9.39E+01	9.61E+01	9.95E+01	
Error (+/-)[1]	0.00E+00	1.21E-01	5.60E-03	5.80E-03	5.60E-03	6.00E-03	6.20E-03	4.00E-02	
U-233 (g)[8]	4.00E-05	1.09E-01	1.25E+01	1.15E+01	1.12E+01	1.15E+01	1.00E+01	2.10E-01	
Error (+/-)[9]	1.00E-05	1.99E-04	3.33E-03	3.31E-03	3.16E-03	3.29E-03	2.80E-03	1.38E-04	
Segment Total									5.71E+01
Error (+/-)[12]									7.12E-03
U-234 (wt%)[1]	0.00E+00	3.18E-01	2.71E+00	4.80E+00	5.61E+00	4.83E+00	2.87E+00	4.67E-01	
Error (+/-)[1]	0.00E+00	8.00E-04	6.00E-04	7.00E-04	7.00E-04	7.00E-04	7.00E-04	7.00E-04	
U-234 (g)[8]	0.00E+00	3.47E-04	3.51E-01	5.90E-01	6.79E-01	5.91E-01	2.98E-01	9.84E-04	
Error (+/-)[9]	NA	9.96E-07	1.20E-04	1.86E-04	2.05E-04	1.86E-04	1.09E-04	1.56E-06	
Segment Total									2.51E+00
Error (+/-)[12]									3.71E-04
U-235 (wt%)[1]	0.00E+00	4.20E-03	1.86E-01	4.55E-01	5.87E-01	4.55E-01	2.06E-01	6.10E-03	
Error (+/-)[1]	0.00E+00	8.58E-02	4.80E-03	5.00E-03	4.80E-03	5.10E-03	5.20E-03	2.85E-02	
U-235 (g)[8]	0.00E+00	4.59E-06	2.41E-02	5.60E-02	7.10E-02	5.57E-02	2.14E-02	1.29E-05	
Error (+/-)[9]	NA	9.38E-05	6.22E-04	6.15E-04	5.81E-04	6.25E-04	5.41E-04	6.01E-05	
Segment Total									2.28E-01

Rod "D" 2502102 (PFB 3-6 H1)

	D-00	D-01	D-02	D-03	D-04	D-05	D-06	D-07	D-08
Error (+/-)[12]									1.34E-03
U-236 (wt%)[1]	0.00E+00	3.00E-04	1.62E-02	2.66E-02	3.36E-02	2.66E-02	1.64E-02	0.00E+00	
Error (+/-)[1]	0.00E+00	3.00E-04	2.00E-04	2.00E-04	2.00E-04	2.00E-04	2.00E-04	3.00E-04	
U-236 (g)[8]	0.00E+00	3.28E-07	2.10E-03	3.27E-03	4.06E-03	3.26E-03	1.71E-03	0.00E+00	
Error (+/-)[9]	NA	3.28E-07	2.59E-05	2.46E-05	2.42E-05	2.45E-05	2.08E-05	NA	
Segment Total									1.44E-02
Error (+/-)[12]									5.38E-05
U-238 (wt%)[1]	0.00E+00	7.01E-02	7.58E-01	7.61E-01	7.64E-01	7.64E-01	7.61E-01	3.70E-02	
Error (+/-)[1]	0.00E+00	8.58E-02	3.10E-03	3.50E-03	3.30E-03	3.70E-03	3.70E-03	2.83E-02	
U-238 (g)[8]	0.00E+00	7.66E-05	9.82E-02	9.35E-02	9.24E-02	9.36E-02	7.92E-02	7.80E-05	
Error (+/-)[9]	NA	9.38E-05	4.03E-04	4.31E-04	4.00E-04	4.54E-04	3.86E-04	5.97E-05	
Segment Total									4.57E-01
Error (+/-)[12]									9.35E-04
Total U[2]	4.20E-04	1.09E-01	1.30E+01	1.23E+01	1.21E+01	1.22E+01	1.04E+01	2.11E-01	
Error (+/-)[2]	2.00E-05	1.50E-04	3.37E-03	3.44E-03	3.32E-03	3.42E-03	2.83E-03	1.10E-04	
Kr-82 (mol%)[3]	0.00E+00	0.00E+00	0.00E+00	0.00E+00	0.00E+00	0.00E+00	0.00E+00	0.00E+00	
Error (+/-)[3]	0.00E+00	0.00E+00	0.00E+00	0.00E+00	0.00E+00	0.00E+00	0.00E+00	0.00E+00	
Kr-82 (g)[10]	0.00E+00	0.00E+00	0.00E+00	0.00E+00	0.00E+00	0.00E+00	0.00E+00	0.00E+00	
Error (+/-)[9]	NA	NA	NA	NA	NA	NA	NA	NA	
Segment Total									0.00E+00
Error (+/-)[12]									NA
Kr-83 (mol%)[3]	1.64E+01	1.64E+01	1.64E+01	1.64E+01	1.64E+01	1.64E+01	1.64E+01	1.64E+01	
Error (+/-)[3]	1.00E-01	1.00E-01	1.00E-01	1.00E-01	1.00E-01	1.00E-01	1.00E-01	1.00E-01	
Kr-83 (g)[10]	0.00E+00	0.00E+00	6.06E-03	1.20E-02	1.69E-02	1.35E-02	5.48E-03	2.47E-06	

Rod "D" 2502102 (PFB 3-6 H1)

	D-00	D-01	D-02	D-03	D-04	D-05	D-06	D-07	D-08
Error (+/-)[9]	NA	0.00E+00	1.51E-03	1.80E-03	1.40E-03	1.35E-03	1.09E-03	2.47E-06	
Segment Total									5.39E-02
Error (+/-)[12]									3.24E-03
Kr-84 (mol%)[3]	2.91E+01	2.91E+01	2.91E+01	2.91E+01	2.91E+01	2.91E+01	2.91E+01	2.91E+01	
Error (+/-)[3]	2.00E-01	2.00E-01	2.00E-01	2.00E-01	2.00E-01	2.00E-01	2.00E-01	2.00E-01	
Kr-84 (g)[10]	0.00E+00	0.00E+00	1.09E-02	2.15E-02	3.03E-02	2.43E-02	9.83E-03	4.44E-06	
Error (+/-)[9]	NA	NA	2.71E-03	3.23E-03	2.52E-03	2.42E-03	1.95E-03	4.44E-06	
Segment Total									9.68E-02
Error (+/-)[12]									5.82E-03
Kr-85 (mol%)[3]	6.10E+00	6.10E+00	6.10E+00	6.10E+00	6.10E+00	6.10E+00	6.10E+00	6.10E+00	
Error (+/-)[3]	1.00E-01	1.00E-01	1.00E-01	1.00E-01	1.00E-01	1.00E-01	1.00E-01	1.00E-01	
Kr-85 (g)[10]	0.00E+00	0.00E+00	2.31E-03	4.57E-03	6.42E-03	5.15E-03	2.09E-03	9.42E-07	
Error (+/-)[9]	NA	NA	5.76E-04	6.88E-04	5.44E-04	5.20E-04	4.16E-04	9.42E-07	
Segment Total									2.05E-02
Error (+/-)[12]									1.24E-03
Kr-86 (mol%)[3]	4.85E+01	4.85E+01	4.85E+01	4.85E+01	4.85E+01	4.85E+01	4.85E+01	4.85E+01	
Error (+/-)[3]	3.00E-01	3.00E-01	3.00E-01	3.00E-01	3.00E-01	3.00E-01	3.00E-01	3.00E-01	
Kr-86 (g)[10]	0.00E+00	0.00E+00	1.86E-02	3.68E-02	5.17E-02	4.14E-02	1.68E-02	7.58E-06	
Error (+/-)[9]	NA	NA	4.63E-03	5.50E-03	4.30E-03	4.13E-03	3.33E-03	7.58E-06	
Segment Total									1.65E-01
Error (+/-)[12]									9.92E-03
Rod Total									3.36E-01
Error (+/-)[12]									1.20E-02
Shear Gas (g)[4]	0.00E+00	0.00E+00	4.00E-04	1.50E-03	2.40E-03	1.70E-03	4.00E-04	1.00E-04	
Error (+/-)[4]	0.00E+00	1.00E-04	3.00E-04	3.00E-04	5.00E-04	3.00E-04	3.00E-04	1.00E-04	

Rod "D" 2502102 (PFB 3-6 H1)

	D-00	D-01	D-02	D-03	D-04	D-05	D-06	D-07	D-08
Xe-132 (mol) [3]	2.23E+01	2.23E+01	2.23E+01	2.23E+01	2.23E+01	2.23E+01	2.23E+01	2.23E+01	
Error (+/-) [3]	1.00E-01	1.00E-01	1.00E-01	1.00E-01	1.00E-01	1.00E-01	1.00E-01	1.00E-01	
Xe-132 (g) [10]	5.88E-05	0.00E+00	4.59E-02	1.12E-01	1.34E-01	1.05E-01	4.11E-02	1.85E-05	
Error (+/-) [3]	2.64E-07	NA	6.56E-03	1.17E-02	9.11E-03	8.75E-03	4.74E-03	1.85E-05	
SegmentTotal									4.38E-01
Error (+/1) [12]									1.90E-02
Xe-134 (mol) [3]	2.73E+01	2.73E+01	2.73E+01	2.73E+01	2.73E+01	2.73E+01	2.73E+01	2.73E+01	
Error (+/-) [3]	1.00E-01	1.00E-01	1.00E-01	1.00E-01	1.00E-01	1.00E-01	1.00E-01	1.00E-01	
Xe-134 (g) [10]	7.31E-05	0.00E+00	5.71E-02	1.39E-01	1.66E-01	1.31E-01	5.11E-02	2.30E-05	
Error (+/-) [3]	2.68E-07	NA	8.15E-03	1.45E-02	1.13E-02	1.09E-02	5.89E-03	2.30E-05	
SegmentTotal									5.44E-01
Error (+/1) [12]									2.36E-02
Xe-136 (mol) [3]	3.65E+01	3.65E+01	3.65E+01	3.65E+01	3.65E+01	3.65E+01	3.65E+01	3.65E+01	
Error (+/-) [3]	1.00E-01	1.00E-01	1.00E-01	1.00E-01	1.00E-01	1.00E-01	1.00E-01	1.00E-01	
Xe-136 (g) [10]	9.92E-05	0.00E+00	7.75E-02	1.88E-01	2.26E-01	1.78E-01	6.93E-02	3.13E-05	
Error (+/-) [3]	2.72E-07	NA	1.11E-02	1.97E-02	1.53E-02	1.47E-02	7.99E-03	3.13E-05	
SegmentTotal									7.38E-01
Error (+/1) [12]									3.20E-02
Rod total									1.99E+00
Error (+/-) [12]									4.56E-02
Shear Gas (g) [4]	0.00E+00	0.00E+00	4.00E-04	1.50E-03	2.40E-03	1.70E-03	4.00E-04	1.00E-04	
Error (+/-) [4]	0.00E+00	1.00E-04	3.00E-04	3.00E-04	5.00E-04	3.00E-04	3.00E-04	1.00E-04	
Diss+Pl Xe (mol) [3]	2.00E-06	0.00E+00	1.56E-03	3.78E-03	4.53E-03	3.57E-03	1.39E-03	0.00E+00	
Error (+/-) [3]	0.00E+00	0.00E+00	2.23E-04	3.96E-04	3.09E-04	2.97E-04	1.61E-04	0.00E+00	
Diss+Pl Kr+Xe (g) [3]	3.00E-04	0.00E+00	2.47E-01	5.82E-01	7.13E-01	5.63E-01	2.21E-01	0.00E+00	

Rod "D" 2502102 (PFB 3-6 H1)

	D-00	D-01	D-02	D-03	D-04	D-05	D-06	D-07	D-08
Error (+/-)[3]	0.00E+00	0.00E+00	3.13E-02	5.43E-02	4.24E-02	4.08E-02	2.26E-02	0.00E+00	
Total Xe (mol)	2.00E-06	0.00E+00	1.56E-03	3.79E-03	4.55E-03	3.58E-03	1.40E-03	6.30E-07	
Error (+/-)[9]	0.00E+00	0.00E+00	2.23E-04	3.96E-04	3.09E-04	2.97E-04	1.61E-04	6.30E-07	
Values corrected to 1/1/84 (page 181, Final Report for the LWBR Proof of Breeding Analytical Support Project									
Cs-137 (atoms)[5]	NA	5.39E+17	2.66E+20	6.00E+20	7.33E+20	6.04E+20	2.35E+20	1.39E+18	
Error (+/-)[4]	NA	2.15E+15	9.13E+17	2.06E+18	2.58E+18	2.06E+18	8.06E+17	5.07E+15	
Cs-137 (g)[11]	NA	1.23E-04	6.04E-02	1.36E-01	1.67E-01	1.37E-01	5.33E-02	3.16E-04	
Error (+/-)[9]	NA	4.89E-07	2.08E-04	4.68E-04	5.86E-04	4.68E-04	1.83E-04	1.15E-06	
Total									5.55E-01
Error (+/-)[12]									9.27E-04
Ce-144 (atoms)[5]	NA	6.63E+16	1.74E+19	3.23E+19	3.86E+19	2.87E+19	9.43E+18	7.48E+16	
Error (+/-)[4]	NA	3.98E+14	1.01E+17	1.94E+17	2.31E+17	1.72E+17	5.66E+16	4.74E+14	
Ce-144 (g)[11]	NA	1.58E-05	4.16E-03	7.72E-03	9.23E-03	6.87E-03	2.25E-03	1.79E-05	
Error (+/-)[9]	NA	9.51E-08	2.41E-05	4.64E-05	5.52E-05	4.11E-05	1.35E-05	1.13E-07	
Total									3.03E-02
Error (+/-)[12]									8.75E-05
Zr-95 (atoms)[5]	NA	6.76E+14	1.48E+17	2.60E+17	2.99E+17	1.60E+17	2.84E+16	1.83E+14	
Error (+/-)[4]	NA	1.08E+13	1.88E+15	3.48E+15	4.69E+15	3.16E+15	9.56E+14	8.83E+12	
Zr-95 (g)[11]	NA	1.06E-07	2.34E-05	4.10E-05	4.71E-05	2.52E-05	4.47E-06	2.89E-08	
Error (+/-)[9]	NA	1.70E-09	2.96E-07	5.48E-07	7.39E-07	4.98E-07	1.51E-07	1.39E-09	
Total									1.41E-04
Error (+/-)[12]									1.10E-06

Rod "D" 2502102 (PFB 3-6 H1)

	D-00	D-01	D-02	D-03	D-04	D-05	D-06	D-07	D-08

References

1. ANL Destructive Chemical Assay of 33-Rod LWBR EOL Sample - Rod D, 2502102, page 6
2. ANL Destructive Chemical Assay of 33-Rod LWBR EOL Sample - Rod D, 2502102, page 7
3. ANL Destructive Chemical Assay of 33-Rod LWBR EOL Sample - Rod D, 2502102, page 9
4. ANL Destructive Chemical Assay of 33-Rod LWBR EOL Sample - Rod D, 2502102, page 10
5. ANL Destructive Chemical Assay of 33-Rod LWBR EOL Sample - Rod D, 2502102, page 11
6. ANL Destructive Chemical Assay of 33-Rod LWBR EOL Sample - Rod D, 2502102, page 12
7. ANL Destructive Chemical Assay of 33-Rod LWBR EOL Sample - Rod D, 2502102, page 13
8. (abundance of the specified isotope)(total weight of uranium)

   1.00E+02
9. Error Propagation = ((+/-x/x)2+(+/-y/y)2)1/2(xy)
10. (mole%)(number moles gas recovered)(molec wt)

    1.00E+02
11. (number of atoms per segment)(atomic weight)

    6.02E+23
12. Error Propagation = (SUM(+/-I)1/2

Rod "E" 2102187 (PFB 3-6 B62)

	E-00	E-01	E-02	E-03	E-04	E-05	E-06	E-07	E-08
Segment length (in)	1.13E+01	8.49E+00	1.41E+01	1.40E+01	1.41E+01	1.75E+01	1.75E+01	1.84E+01	2.63E+00
Total length (in)									1.18E+02
U-232 (wt%)[1]	0.00E+00	1.16E-02	2.45E-02	9.26E-02	1.45E-01	2.07E-01	1.46E-01	4.52E-02	
Error (+/-)[1]	0.00E+00	4.00E-04	8.00E-04	2.90E-03	4.50E-03	6.40E-03	4.50E-03	1.40E-03	
U-232 (g)[8]	0.00E+00	2.99E-05	1.61E-03	6.22E-03	9.98E-03	1.12E-02	6.27E-03	6.49E-04	
Error (+/-)[9]	NA	1.03E-06	5.26E-05	1.95E-04	3.10E-04	3.47E-04	1.93E-04	2.01E-05	
Segment Total									3.60E-02
Error (+/-)[12]									5.43E-04
U-233 (wt%)[1]	1.00E+02	9.92E+01	9.46E+01	9.01E+01	8.77E+01	9.09E+01	9.31E+01	9.76E+01	
Error (+/-)[1]	0.00E+00	2.37E-02	7.60E-03	7.60E-03	8.20E-03	7.90E-03	8.50E-03	1.01E-02	
U-233 (g)[8]	4.00E-05	2.55E-01	6.23E+00	6.06E+00	6.05E+00	4.93E+00	4.00E+00	1.40E+00	
Error (+/-)[9]	1.00E-05	1.16E-04	1.71E-03	1.67E-03	1.72E-03	1.20E-03	9.92E-04	3.98E-04	
Segment Total									2.89E+01
Error (+/-)[12]									3.35E-03
U-234 (wt%)[1]	0.00E+00	7.10E-01	4.61E+00	8.26E+00	1.01E+01	7.75E+00	5.99E+00	2.25E+00	
Error (+/-)[1]	0.00E+00	4.00E-04	6.00E-04	9.00E-04	1.20E-03	8.00E-04	7.00E-04	4.00E-04	
U-234 (g)[8]	0.00E+00	1.33E-03	3.04E-01	5.55E-01	6.98E-01	4.20E-01	2.57E-01	3.24E-02	
Error (+/-)[9]	NA	1.25E-06	8.91E-05	1.57E-04	2.05E-04	1.05E-04	6.65E-05	1.03E-05	
Segment Total									2.27E+00
Error (+/-)[12]									3.00E-04
U-235 (wt%)[1]	0.00E+00	1.34E-02	4.52E-01	1.18E+00	1.67E+00	1.11E+00	6.94E-01	1.18E-01	
Error (+/-)[1]	0.00E+00	1.69E-02	5.70E-03	5.80E-03	5.70E-03	4.20E-03	5.60E-03	7.20E-03	
U-235 (g)[8]	0.00E+00	3.45E-05	2.97E-02	7.92E-02	1.15E-01	6.01E-02	2.98E-02	1.69E-03	
Error (+/-)[9]	NA	4.35E-05	3.75E-04	3.90E-04	3.94E-04	2.28E-04	2.40E-04	1.03E-04	
Segment Total									3.16E-01

Rod "D" 2502102 (PFB 3-6 H1)

	D-00	D-01	D-02	D-03	D-04	D-05	D-06	D-07	D-08
Diss+Pl Kr (mol)[3]	0.00E+00	0.00E+00	4.45E-04	8.80E-04	1.24E-03	9.91E-04	4.02E-04	0.00E+00	
Error (+/-)[3]	0.00E+00	0.00E+00	1.11E-04	1.32E-04	1.03E-04	9.90E-05	8.00E-05	0.00E+00	
Diss+Pl Kr+Xe (g)[3]	3.00E-04	0.00E+00	2.47E-01	5.82E-01	7.13E-01	5.63E-01	2.21E-01	0.00E+00	
Error (+/-)[3]	0.00E+00	0.00E+00	3.13E-02	5.43E-02	4.24E-02	4.08E-02	2.26E-02	0.00E+00	
Total Kr (mol)	0.00E+00	0.00E+00	4.46E-04	8.82E-04	1.24E-03	9.94E-04	4.03E-04	1.82E-07	
Error (+/-)[9]	0.00E+00	1.82E-07	1.11E-04	1.32E-04	1.03E-04	9.90E-05	8.00E-05	1.82E-07	
Xe-128 (mol)[3]	0.00E+00	0.00E+00	0.00E+00	0.00E+00	0.00E+00	0.00E+00	0.00E+00	0.00E+00	
Error (+/-)[3]	0.00E+00	0.00E+00	0.00E+00	0.00E+00	0.00E+00	0.00E+00	0.00E+00	0.00E+00	
Xe-128 (g)[10]	0.00E+00	0.00E+00	0.00E+00	0.00E+00	0.00E+00	0.00E+00	0.00E+00	0.00E+00	
Error (+/-)[3]	NA	NA	NA	NA	NA	NA	NA	NA	
SegmentTotal									0.00E+00
Error (+/1)[12]									NA
Xe-130 (mol)[3]	0.00E+00	0.00E+00	0.00E+00	0.00E+00	0.00E+00	0.00E+00	0.00E+00	0.00E+00	
Error (+/-)[3]	0.00E+00	0.00E+00	0.00E+00	0.00E+00	0.00E+00	0.00E+00	0.00E+00	0.00E+00	
Xe-130 (g)[10]	0.00E+00	0.00E+00	0.00E+00	0.00E+00	0.00E+00	0.00E+00	0.00E+00	0.00E+00	
Error (+/-)[3]	NA	NA	NA	NA	NA	NA	NA	NA	
SegmentTotal									0.00E+00
Error (+/1)[12]									NA
Xe-131 (mol)[3]	1.39E+01	1.39E+01	1.39E+01	1.39E+01	1.39E+01	1.39E+01	1.39E+01	1.39E+01	
Error (+/-)[3]	1.00E-01	1.00E-01	1.00E-01	1.00E-01	1.00E-01	1.00E-01	1.00E-01	1.00E-01	
Xe-131 (g)[10]	3.64E-05	0.00E+00	2.84E-02	6.90E-02	8.27E-02	6.51E-02	2.54E-02	1.15E-05	
Error (+/-)[3]	2.62E-07	NA	4.06E-03	7.22E-03	5.65E-03	5.42E-03	2.94E-03	1.15E-05	
SegmentTotal									2.71E-01
Error (+/1)[12]									1.18E-02

Rod "E" 2102187 (PFB 3-6 B62)

	E-00	E-01	E-02	E-03	E-04	E-05	E-06	E-07	E-08
Error (+/-)[12]									7.56E-04
U-236 (wt%)[1]	0.00E+00	3.00E-04	4.54E-02	9.81E-02	1.51E-01	6.97E-02	3.39E-02	2.70E-03	
Error (+/-)[1]	0.00E+00	1.00E-04	1.00E-04	1.00E-04	1.00E-04	1.00E-04	1.00E-04	1.00E-04	
U-236 (g)[8]	0.00E+00	7.72E-07	2.99E-03	6.59E-03	1.04E-02	3.78E-03	1.46E-03	3.88E-05	
Error (+/-)[9]	NA	2.57E-07	6.63E-06	6.94E-06	7.44E-06	5.49E-06	4.31E-06	1.44E-06	
Segment Total									2.53E-02
Error (+/-)[12]									1.41E-05
U-238 (wt%)[1]	0.00E+00	3.32E-02	2.52E-01	2.28E-01	2.12E-01	3.50E-03	3.70E-03	9.90E-03	
Error (+/-)[1]	0.00E+00	1.69E-02	5.60E-03	5.50E-03	5.80E-03	4.10E-03	5.50E-03	7.20E-03	
U-238 (g)[8]	0.00E+00	8.55E-05	1.66E-02	1.53E-02	1.46E-02	1.90E-04	1.59E-04	1.42E-04	
Error (+/-)[9]	NA	4.35E-05	3.69E-04	3.69E-04	4.00E-04	2.22E-04	2.36E-04	1.03E-04	
Segment Total									4.72E-02
Error (+/-)[12]									7.42E-04
Total U[2]	8.00E-04	2.57E-01	6.58E+00	6.72E+00	6.89E+00	5.43E+00	4.29E+00	1.44E+00	
Error (+/-)[2]	2.00E-05	1.00E-04	1.73E-03	1.76E-03	1.85E-03	1.23E-03	9.90E-04	3.80E-04	
Kr-82 (mol%)[3]	1.00E-01	1.00E-01	1.00E-01	1.00E-01	1.00E-01	1.00E-01	1.00E-01	1.00E-01	
Error (+/-)[3]	1.00E-01	1.00E-01	1.00E-01	1.00E-01	1.00E-01	1.00E-01	1.00E-01	1.00E-01	
Kr-82 (g)[10]	8.19E-08	0.00E+00	4.84E-05	9.82E-05	1.33E-04	8.03E-05	4.21E-05	6.08E-06	
Error (+/-)[9]	8.19E-08	0.00E+00	5.02E-05	9.90E-05	1.34E-04	8.08E-05	4.26E-05	6.79E-06	
Segment Total									4.09E-04
Error (+/-)[12]									1.97E-04
Kr-83 (mol%)[3]	1.56E+01	1.56E+01	1.56E+01	1.56E+01	1.56E+01	1.56E+01	1.56E+01	1.56E+01	
Error (+/-)[3]	2.00E-01	2.00E-01	2.00E-01	2.00E-01	2.00E-01	2.00E-01	2.00E-01	2.00E-01	
Kr-83 (g)[10]	1.29E-05	0.00E+00	7.64E-03	1.55E-02	2.11E-02	1.27E-02	6.65E-03	9.59E-04	

Rod "E" 2102187 (PFB 3-6 B62)

	E-00	E-01	E-02	E-03	E-04	E-05	E-06	E-07	E-08
Error (+/-)[9]	1.66E-07	0.00E+00	2.08E-03	2.03E-03	2.11E-03	1.42E-03	1.01E-03	4.79E-04	
Segment Total									6.45E-02
Error (+/-)[12]									4.02E-03
Kr-84 (mol%)[3]	2.97E+01	2.97E+01	2.97E+01	2.97E+01	2.97E+01	2.97E+01	2.97E+01	2.97E+01	
Error (+/-)[3]	3.00E-01	3.00E-01	3.00E-01	3.00E-01	3.00E-01	3.00E-01	3.00E-01	3.00E-01	
Kr-84 (g)[10]	2.49E-05	0.00E+00	1.47E-02	2.99E-02	4.06E-02	2.44E-02	1.28E-02	1.85E-03	
Error (+/-)[9]	2.52E-07	0.00E+00	4.02E-03	3.90E-03	4.06E-03	2.73E-03	1.95E-03	9.22E-04	
Segment Total									1.24E-01
Error (+/-)[12]									7.74E-03
Kr-85 (mol%)[3]	6.10E+00	6.10E+00	6.10E+00	6.10E+00	6.10E+00	6.10E+00	6.10E+00	6.10E+00	
Error (+/-)[3]	2.00E-01	2.00E-01	2.00E-01	2.00E-01	2.00E-01	2.00E-01	2.00E-01	2.00E-01	
Kr-85 (g)[10]	5.18E-06	0.00E+00	3.06E-03	6.21E-03	8.43E-03	5.08E-03	2.66E-03	3.84E-04	
Error (+/-)[9]	1.70E-07	0.00E+00	8.40E-04	8.33E-04	8.83E-04	5.89E-04	4.13E-04	1.92E-04	
Segment Total									2.58E-02
Error (+/-)[12]									1.65E-03
Kr-86 (mol%)[3]	4.86E+01	4.86E+01	4.86E+01	4.86E+01	4.86E+01	4.86E+01	4.86E+01	4.86E+01	
Error (+/-)[3]	3.00E-01	3.00E-01	3.00E-01	3.00E-01	3.00E-01	3.00E-01	3.00E-01	3.00E-01	
Kr-86 (g)[10]	4.18E-05	0.00E+00	2.47E-02	5.01E-02	6.80E-02	4.09E-02	2.15E-02	3.10E-03	
Error (+/-)[9]	2.58E-07	#REF!	6.72E-03	6.52E-03	6.78E-03	4.56E-03	3.26E-03	1.54E-03	
Segment Total									2.08E-01
Error (+/-)[12]									1.29E-02
Rod Total									4.23E-01
Error (+/-)[12]									1.57E-02
Shear Gas (g)[4]	0.00E+00	0.00E+00	4.00E-04	1.60E-03	2.30E-03	1.50E-03	6.00E-04	1.00E-04	
Error (+/-)[4]	0.00E+00	1.00E-04	1.00E-04	3.00E-04	5.00E-04	3.00E-04	1.00E-04	1.00E-04	

Rod "E" 2102187 (PFB 3-6 B62)

	E-00	E-01	E-02	E-03	E-04	E-05	E-06	E-07	E-08
Diss+Pl Kr (mol)[3]	1.00E-06	0.00E+00	5.90E-04	1.20E-03	1.62E-03	9.78E-04	5.13E-04	7.40E-05	
Error (+/-)[3]	0.00E+00	0.00E+00	1.61E-04	1.56E-04	1.62E-04	1.09E-04	7.80E-05	3.70E-05	
Diss+Pl Kr+Xe (g)[3]	5.00E-04	0.00E+00	3.24E-01	6.74E-01	9.37E-01	5.64E-01	3.10E-01	4.10E-02	
Error (+/-)[3]	0.00E+00	0.00E+00	3.19E-02	2.48E-02	3.22E-02	2.38E-02	2.89E-02	1.11E-02	
Total Kr (mol)	1.00E-06	0.00E+00	5.91E-04	1.20E-03	1.63E-03	9.81E-04	5.14E-04	7.42E-05	
Error (+/-)[9]	0.00E+00	1.82E-07	1.61E-04	1.56E-04	1.62E-04	1.09E-04	7.80E-05	3.70E-05	
Xe-128 (mol)[3]	1.00E-01	1.00E-01	1.00E-01	1.00E-01	1.00E-01	1.00E-01	1.00E-01	1.00E-01	
Error (+/-)[3]	1.00E-01	1.00E-01	1.00E-01	1.00E-01	1.00E-01	1.00E-01	1.00E-01	1.00E-01	
Xe-128 (g)[10]	3.84E-07	0.00E+00	2.61E-04	5.47E-04	7.63E-04	4.60E-04	2.55E-04	3.32E-05	
Error (+/-)[3]	3.84E-07	NA	2.63E-04	5.47E-04	7.64E-04	4.60E-04	2.56E-04	3.47E-05	
SegmentTotal									2.32E-03
Error (+/1)[12]									1.11E-03
Xe-130 (mol)[3]	1.00E-01	1.00E-01	1.00E-01	1.00E-01	1.00E-01	1.00E-01	1.00E-01	1.00E-01	
Error (+/-)[3]	1.00E-01	1.00E-01	1.00E-01	1.00E-01	1.00E-01	1.00E-01	1.00E-01	1.00E-01	
Xe-130 (g)[10]	3.90E-07	0.00E+00	2.65E-04	5.55E-04	7.75E-04	4.67E-04	2.59E-04	3.37E-05	
Error (+/-)[3]	3.90E-07	NA	2.67E-04	5.56E-04	7.76E-04	4.67E-04	2.60E-04	3.53E-05	
SegmentTotal									2.36E-03
Error (+/1)[12]									1.13E-03
Xe-131 (mol)[3]	1.21E+01	1.21E+01	1.21E+01	1.21E+01	1.21E+01	1.21E+01	1.21E+01	1.21E+01	
Error (+/-)[3]	1.00E-01	1.00E-01	1.00E-01	1.00E-01	1.00E-01	1.00E-01	1.00E-01	1.00E-01	
Xe-131 (g)[10]	4.75E-05	0.00E+00	3.23E-02	6.77E-02	9.45E-02	5.69E-02	3.15E-02	4.11E-03	
Error (+/-)[3]	3.93E-07	NA	3.42E-03	2.53E-03	3.53E-03	2.62E-03	3.32E-03	1.25E-03	

Rod "E" 2102187 (PFB 3-6 B62)

	E-00	E-01	E-02	E-03	E-04	E-05	E-06	E-07	E-08
SegmentTotal									2.87E-01
Error (+/1)[12]									7.07E-03
Xe-132 (mol)[3]	2.19E+01	2.19E+01	2.19E+01	2.19E+01	2.19E+01	2.19E+01	2.19E+01	2.19E+01	
Error (+/-)[3]	1.00E-01	1.00E-01	1.00E-01	1.00E-01	1.00E-01	1.00E-01	1.00E-01	1.00E-01	
Xe-132 (g)[10]	8.67E-05	0.00E+00	5.90E-02	1.23E-01	1.72E-01	1.04E-01	5.75E-02	7.50E-03	
Error (+/-)[3]	3.96E-07	NA	6.22E-03	4.54E-03	6.32E-03	4.73E-03	6.04E-03	2.28E-03	
SegmentTotal									5.24E-01
Error (+/1)[12]									1.28E-02
Xe-134 (mol)[3]	2.54E+01	2.54E+01	2.54E+01	2.54E+01	2.54E+01	2.54E+01	2.54E+01	2.54E+01	
Error (+/-)[3]	2.00E-01	2.00E-01	2.00E-01	2.00E-01	2.00E-01	2.00E-01	2.00E-01	2.00E-01	
Xe-134 (g)[10]	1.02E-04	0.00E+00	6.94E-02	1.45E-01	2.03E-01	1.22E-01	6.77E-02	8.83E-03	
Error (+/-)[3]	8.03E-07	NA	7.33E-03	5.43E-03	7.55E-03	5.63E-03	7.13E-03	2.69E-03	
SegmentTotal									6.17E-01
Error (+/1)[12]									1.52E-02
Xe-136 (mol)[3]	4.04E+01	4.04E+01	4.04E+01	4.04E+01	4.04E+01	4.04E+01	4.04E+01	4.04E+01	
Error (+/-)[3]	2.00E-01	2.00E-01	2.00E-01	2.00E-01	2.00E-01	2.00E-01	2.00E-01	2.00E-01	
Xe-136 (g)[10]	1.65E-04	0.00E+00	1.12E-01	2.35E-01	3.28E-01	1.97E-01	1.09E-01	1.43E-02	
Error (+/-)[3]	8.15E-07	NA	1.18E-02	8.64E-03	1.20E-02	9.00E-03	1.15E-02	4.34E-03	
SegmentTotal									9.96E-01
Error (+/1)[12]									2.43E-02
Rod total									2.43E+00
Error (+/-)[12]									3.22E-02

Rod "E" 2102187 (PFB 3-6 B62)

	E-00	E-01	E-02	E-03	E-04	E-05	E-06	E-07	E-08
Shear Gas (g)[4]	0.00E+00	0.00E+00	4.00E-04	1.60E-03	2.30E-03	1.50E-03	6.00E-04	1.00E-04	
Error (+/-)[4]	0.00E+00	1.00E-04	1.00E-04	3.00E-04	5.00E-04	3.00E-04	1.00E-04	1.00E-04	
Diss+Pl Xe (mol)[3]	3.00E-06	0.00E+00	2.04E-03	4.27E-03	5.95E-03	3.59E-03	1.99E-03	2.59E-04	
Error (+/-)[3]	0.00E+00	0.00E+00	2.15E-04	1.56E-04	2.17E-04	1.63E-04	2.09E-04	7.90E-05	
Diss+Pl Kr+Xe (g)[3]	5.00E-04	0.00E+00	3.24E-01	6.74E-01	9.37E-01	5.64E-01	3.10E-01	4.10E-02	
Error (+/-)[3]	0.00E+00	0.00E+00	3.19E-02	2.48E-02	3.22E-02	2.38E-02	2.89E-02	1.11E-02	
Total Xe (mol)	3.00E-06	0.00E+00	2.04E-03	4.28E-03	5.97E-03	3.59E-03	1.99E-03	2.60E-04	
Error (+/-)[9]	0.00E+00	6.30E-07	2.15E-04	1.56E-04	2.17E-04	1.63E-04	2.09E-04	7.90E-05	
Values corrected to 1/1/84 (page 181, Final Report for the LWBR Proof of Breeding Analytical Support Project									
Cs-137 (atoms)[5]	NA	2.47E+18	3.05E+20	6.73E+20	8.89E+20	5.26E+20	3.18E+20	4.01E+19	
Error (+/-)[4]	NA	9.06E+15	1.06E+18	2.40E+18	3.07E+18	1.93E+18	1.16E+18	1.38E+17	
Cs-137 (g)[11]	NA	5.61E-04	6.94E-02	1.53E-01	2.02E-01	1.19E-01	7.22E-02	9.10E-03	
Error (+/-)[9]	NA	2.06E-06	2.40E-04	5.45E-04	6.99E-04	4.38E-04	2.65E-04	3.14E-05	
Total									6.26E-01
Error (+/-)[12]									1.05E-03
Ce-144 (atoms)[5]	NA	3.18E+17	2.14E+19	3.77E+19	4.66E+19	3.84E+19	2.03E+19	2.18E+18	
Error (+/-)[4]	NA	2.33E+15	1.55E+17	2.80E+17	3.45E+17	2.85E+17	1.50E+17	1.61E+16	
Ce-144 (g)[11]	NA	7.61E-05	5.10E-03	9.01E-03	1.11E-02	9.17E-03	4.84E-03	5.20E-04	
Error (+/-)[9]	NA	5.57E-07	3.70E-05	6.68E-05	8.25E-05	6.80E-05	3.58E-05	3.85E-06	
Total									3.99E-02
Error (+/-)[12]									1.36E-04
Zr-95 (atoms)[5]	NA	3.40E+15	1.80E+17	2.96E+17	3.52E+17	4.63E+17	1.73E+17	5.17E+15	

Rod "E" 2102187 (PFB 3-6 B62)

[redacted]

	E-00	E-01	E-02	E-03	E-04	E-05	E-06	E-07	E-08
Error (+/-)[4]	NA	4.42E+13	2.46E+15	5.85E+15	9.75E+15	6.64E+15	2.54E+15	1.46E+14	
Zr-95 (g)[11]	NA	5.36E-07	2.84E-05	4.67E-05	5.55E-05	7.29E-05	2.73E-05	8.15E-07	
Error (+/-)[9]	NA	6.97E-09	3.88E-07	9.22E-07	1.54E-06	1.05E-06	4.00E-07	2.29E-08	
Total									2.32E-04
Error (+/-)[12]									2.15E-06

[redacted]

References

1. ANL Destructive Chemical Assay of 33-Rod LWBR EOL Sample - Rod E, 2102187, page 6
2. ANL Destructive Chemical Assay of 33-Rod LWBR EOL Sample - Rod E, 2102187, page 7
3. ANL Destructive Chemical Assay of 33-Rod LWBR EOL Sample - Rod E, 2102187, page 10
4. ANL Destructive Chemical Assay of 33-Rod LWBR EOL Sample - Rod E, 2102187, page 11
5. ANL Destructive Chemical Assay of 33-Rod LWBR EOL Sample - Rod E, 2102187, page 12
6. ANL Destructive Chemical Assay of 33-Rod LWBR EOL Sample - Rod E, 2102187, page 13
7. ANL Destructive Chemical Assay of 33-Rod LWBR EOL Sample - Rod E, 2102187, page 14
8. (abundance of the specified isotope)(total weight of uranium)

    1.00E+02
9. Error Propagation = ((+/-x/x)2+(+/-y/y)2)1/2(xy)
10. (mole%)(number moles gas recovered)(molec wt)

    1.00E+02
11. (number of atoms per segment)(atomic weight)

    6.02E+23
12. Error Propagation = (SUM(+/-I)1/2
13. Nb-95 values for segments 5 and 6 corrected per LWBR EOL Sample - Rod E, 2102187, page 14

Rod "F" 2400408 (PFB 3-6 C13)

	F-00	F-01	F-02	F-03	F-04	F-05	F-06	F-07	F-08	F-09
Segment length (in)	1.13E+01	1.16E+01	1.40E+01	1.40E+01	1.40E+01	1.42E+01	1.40E+01	1.05E+01	1.29E+01	1.64E+00
Total length (in)										1.18E+02
U-232 (wt%)[1]	0.00E+00	9.20E-03	1.34E-02	5.28E-02	8.58E-02	9.07E-02	1.46E-01	7.66E-02	2.31E-02	
Error (+/-)[1]	0.00E+00	3.00E-04	4.00E-04	1.60E-03	2.70E-03	2.80E-03	4.50E-03	2.40E-03	7.00E-04	
U-232 (g)[8]	0.00E+00	1.94E-05	1.04E-03	4.08E-03	6.63E-03	6.92E-03	4.49E-03	1.17E-03	1.44E-04	
Error (+/-)[9]	NA	6.32E-07	3.09E-05	1.24E-04	2.09E-04	2.14E-04	1.38E-04	3.66E-05	4.38E-06	
Segment Total										2.45E-02
Error (+/-)[12]										3.55E-04
U-233 (wt%)[1]	1.00E+02	9.94E+01	9.57E+01	9.26E+01	9.07E+01	8.99E+01	9.46E+01	9.65E+01	9.87E+01	
Error (+/-)[1]	0.00E+00	3.69E-02	5.50E-03	6.70E-03	7.30E-03	6.80E-03	8.30E-03	1.05E-02	1.19E-02	
U-233 (g)[8]	4.00E-05	2.09E-01	7.40E+00	7.15E+00	7.01E+00	6.86E+00	2.90E+00	1.47E+00	6.17E-01	
Error (+/-)[9]	1.00E-05	1.34E-04	2.16E-03	2.19E-03	2.26E-03	2.14E-03	8.17E-04	4.72E-04	1.93E-04	
Segment Total										3.36E+01
Error (+/-)[12]										4.48E-03
U-234 (wt%)[1]	0.00E+00	4.95E-01	3.61E+00	6.29E+00	7.81E+00	8.40E+00	4.74E+00	3.19E+00	1.22E+00	
Error (+/-)[1]	0.00E+00	4.00E-04	4.00E-04	7.00E-04	9.00E-04	9.00E-04	6.00E-04	5.00E-04	4.00E-04	
U-234 (g)[8]	0.00E+00	1.04E-03	2.79E-01	4.86E-01	6.04E-01	6.41E-01	1.45E-01	4.86E-02	7.63E-03	
Error (+/-)[9]	NA	1.00E-06	8.56E-05	1.54E-04	2.01E-04	2.06E-04	4.30E-05	1.65E-05	3.33E-06	
Segment Total										2.21E+00
Error (+/-)[12]										3.41E-04
U-235 (wt%)[1]	0.00E+00	1.53E-02	3.24E-01	7.70E-01	1.10E+00	1.23E+00	4.60E-01	2.13E-01	3.45E-02	
Error (+/-)[1]	0.00E+00	2.67E-02	4.20E-03	5.00E-03	5.40E-03	5.00E-03	5.40E-03	7.60E-03	8.70E-03	
U-235 (g)[8]	0.00E+00	3.22E-05	2.50E-02	5.94E-02	8.53E-02	9.36E-02	1.41E-02	3.25E-03	2.16E-04	
Error (+/-)[9]	NA	5.62E-05	3.25E-04	3.86E-04	4.18E-04	3.83E-04	1.66E-04	1.16E-04	5.44E-05	
Segment Total										2.81E-01
Error (+/-)[12]										7.89E-04
U-236 (wt%)[1]	0.00E+00	2.00E-04	3.91E-02	6.30E-02	8.82E-02	1.00E-01	1.67E-02	5.40E-03	5.00E-04	
Error (+/-)[1]	0.00E+00	1.00E-04	0.00E+00	0.00E+00	0.00E+00	0.00E+00	0.00E+00	0.00E+00	1.00E-04	

Rod "F" 2400408 (PFB 3-6 C13)

	F-00	F-01	F-02	F-03	F-04	F-05	F-06	F-07	F-08	F-09
U-236 (g)[8]	0.00E+00	4.21E-07	3.02E-03	4.86E-03	6.82E-03	7.64E-03	5.12E-04	8.23E-05	3.13E-06	
Error (+/-)[9]	NA	2.11E-07	8.64E-07	1.45E-06	2.13E-06	2.31E-06	1.37E-07	2.48E-08	6.25E-07	
Segment Total										2.29E-02
Error (+/-)[12]										3.63E-06
U-238 (wt%)[1]	0.00E+00	4.95E-02	2.64E-01	2.52E-01	2.44E-01	2.47E-01	4.40E-03	7.10E-03	1.77E-02	
Error (+/-)[1]	0.00E+00	2.58E-02	3.90E-03	4.80E-03	5.20E-03	4.80E-03	5.20E-03	7.30E-03	8.30E-03	
U-238 (g)[8]	0.00E+00	1.04E-04	2.04E-02	1.95E-02	1.89E-02	1.88E-02	1.35E-04	1.08E-04	1.11E-04	
Error (+/-)[9]	NA	5.43E-05	3.01E-04	3.71E-04	4.02E-04	3.66E-04	1.59E-04	1.11E-04	5.19E-05	
Segment Total										7.80E-02
Error (+/-)[12]										7.53E-04
Total U[2]	6.00E-05	2.11E-01	7.72E+00	7.72E+00	7.73E+00	7.63E+00	3.07E+00	1.52E+00	6.25E-01	
Error (+/-)[2]	1.00E-05	1.10E-04	2.21E-03	2.30E-03	2.41E-03	2.31E-03	8.20E-04	4.60E-04	1.80E-04	
Kr-82 (mol%)[3]	0.00E+00	0.00E+00	0.00E+00	0.00E+00	0.00E+00	0.00E+00	0.00E+00	0.00E+00	0.00E+00	
Error (+/-)[3]	0.00E+00	0.00E+00	0.00E+00	0.00E+00	0.00E+00	0.00E+00	0.00E+00	0.00E+00	0.00E+00	
Kr-82 (g)[10]	0.00E+00	0.00E+00	0.00E+00	0.00E+00	0.00E+00	0.00E+00	0.00E+00	0.00E+00	0.00E+00	
Error (+/-)[9]	NA	NA	NA	NA	NA	NA	NA	NA	NA	
Segment Total										0.00E+00
Error (+/-)[12]										NA
Kr-83 (mol%)[3]	1.59E+01	1.59E+01	1.59E+01	1.59E+01	1.59E+01	1.59E+01	1.59E+01	1.59E+01	1.59E+01	
Error (+/-)[3]	2.00E-01	2.00E-01	2.00E-01	2.00E-01	2.00E-01	2.00E-01	2.00E-01	2.00E-01	2.00E-01	
Kr-83 (g)[10]	1.32E-05	0.00E+00	5.65E-03	1.09E-02	1.43E-02	1.79E-02	3.75E-03	1.36E-03	6.46E-04	
Error (+/-)[9]	1.66E-07	NA	6.50E-04	1.10E-03	1.44E-03	1.44E-03	3.46E-04	3.97E-04	6.46E-04	
Segment Total										5.45E-02
Error (+/-)[12]										2.54E-03
Kr-84 (mol%)[3]	2.93E+01	2.93E+01	2.93E+01	2.93E+01	2.93E+01	2.93E+01	2.93E+01	2.93E+01	2.93E+01	
Error (+/-)[3]	2.00E-01	2.00E-01	2.00E-01	2.00E-01	2.00E-01	2.00E-01	2.00E-01	2.00E-01	2.00E-01	
Kr-84 (g)[10]	2.46E-05	0.00E+00	1.05E-02	2.03E-02	2.67E-02	3.33E-02	6.99E-03	2.53E-03	1.20E-03	
Error (+/-)[9]	1.68E-07	NA	1.21E-03	2.05E-03	2.66E-03	2.67E-03	6.41E-04	7.39E-04	1.20E-03	

Rod "F" 2400408 (PFB 3-6 C13)

	F-00	F-01	F-02	F-03	F-04	F-05	F-06	F-07	F-08	F-09
Segment Total										1.02E-01
Error (+/-)[12]										4.72E-03
Kr-85 (mol%)[3]	6.00E+00	6.00E+00	6.00E+00	6.00E+00	6.00E+00	6.00E+00	6.00E+00	6.00E+00	6.00E+00	
Error (+/-)[3]	1.00E-01	1.00E-01	1.00E-01	1.00E-01	1.00E-01	1.00E-01	1.00E-01	1.00E-01	1.00E-01	
Kr-85 (g)[10]	5.09E-06	0.00E+00	2.18E-03	4.22E-03	5.53E-03	6.90E-03	1.45E-03	5.25E-04	2.50E-04	
Error (+/-)[9]	8.49E-08	NA	2.52E-04	4.29E-04	5.58E-04	5.62E-04	1.35E-04	1.53E-04	2.50E-04	
Segment Total										2.11E-02
Error (+/-)[12]										9.89E-04
Kr-86 (mol%)[3]	4.88E+01	4.88E+01	4.88E+01	4.88E+01	4.88E+01	4.88E+01	4.88E+01	4.88E+01	4.88E+01	
Error (+/-)[3]	2.00E-01	2.00E-01	2.00E-01	2.00E-01	2.00E-01	2.00E-01	2.00E-01	2.00E-01	2.00E-01	
Kr-86 (g)[10]	4.19E-05	0.00E+00	1.80E-02	3.47E-02	4.55E-02	5.68E-02	1.19E-02	4.32E-03	2.05E-03	
Error (+/-)[9]	1.72E-07	NA	2.06E-03	3.48E-03	4.53E-03	4.53E-03	1.09E-03	1.26E-03	2.05E-03	
Segment Total										1.73E-01
Error (+/-)[12]										8.03E-03
Rod Total										3.50E-01
Error (+/-)[12]										9.70E-03
Shear Gas (g)[4]	0.00E+00	0.00E+00	2.00E-04	9.00E-04	1.40E-03	1.70E-03	2.00E-04	0.00E+00	0.00E+00	
Error (+/-)[4]	0.00E+00	0.00E+00	0.00E+00	2.00E-04	3.00E-04	3.00E-04	0.00E+00	0.00E+00	0.00E+00	
Diss+Pl Kr (mol)[3]	1.00E-06	0.00E+00	4.28E-04	8.26E-04	1.08E-03	1.35E-03	2.84E-04	1.03E-04	4.90E-05	
Error (+/-)[3]	0.00E+00	0.00E+00	4.90E-05	8.30E-05	1.08E-04	1.08E-04	2.60E-05	3.00E-05	4.90E-05	
Diss+Pl Kr+Xe (g)[3]	5.00E-04	0.00E+00	2.43E-01	5.24E-01	6.73E-01	8.19E-01	1.76E-01	5.47E-02	1.43E-02	
Error (+/-)[3]	0.00E+00	0.00E+00	8.50E-03	4.49E-02	4.46E-02	3.75E-02	1.18E-02	1.05E-02	1.10E-02	
Total Kr (mol)	1.00E-06	0.00E+00	4.28E-04	8.27E-04	1.09E-03	1.35E-03	2.84E-04	1.03E-04	4.90E-05	
Error (+/-)[9]	0.00E+00	NA	4.90E-05	8.30E-05	1.08E-04	1.08E-04	2.60E-05	3.01E-05	4.90E-05	
Xe-128 (mol)[3]	0.00E+00	0.00E+00	0.00E+00	0.00E+00	0.00E+00	0.00E+00	0.00E+00	0.00E+00	0.00E+00	
Error (+/-)[3]	0.00E+00	0.00E+00	0.00E+00	0.00E+00	0.00E+00	0.00E+00	0.00E+00	0.00E+00	0.00E+00	
Xe-128 (g)[10]	0.00E+00	0.00E+00	0.00E+00	0.00E+00	0.00E+00	0.00E+00	0.00E+00	0.00E+00	0.00E+00	
Error (+/-)[3]	NA	NA	NA	NA	NA	NA	NA	NA	NA	

Rod "F" 2400408 (PFB 3-6 C13)

	F-00	F-01	F-02	F-03	F-04	F-05	F-06	F-07	F-08	F-09
SegmentTotal										0.00E+00
Error (+/1)[12]										NA
Xe-130 (mol)[3]	0.00E+00	0.00E+00	0.00E+00	0.00E+00	0.00E+00	0.00E+00	0.00E+00	0.00E+00	0.00E+00	
Error (+/-)[3]	0.00E+00	0.00E+00	0.00E+00	0.00E+00	0.00E+00	0.00E+00	0.00E+00	0.00E+00	0.00E+00	
Xe-130 (g)[10]	0.00E+00	0.00E+00	0.00E+00	0.00E+00	0.00E+00	0.00E+00	0.00E+00	0.00E+00	0.00E+00	
Error (+/-)[3]	NA	NA	NA	NA	NA	NA	NA	NA	NA	
SegmentTotal										0.00E+00
Error (+/1)[12]										NA
Xe-131 (mol)[3]	1.29E+01	1.29E+01	1.29E+01	1.29E+01	1.29E+01	1.29E+01	1.29E+01	1.29E+01	1.29E+01	
Error (+/-)[3]	1.00E-01	1.00E-01	1.00E-01	1.00E-01	1.00E-01	1.00E-01	1.00E-01	1.00E-01	1.00E-01	
Xe-131 (g)[10]	5.07E-05	0.00E+00	2.60E-02	5.73E-02	7.33E-02	8.88E-02	1.91E-02	5.78E-03	1.28E-03	
Error (+/-)[3]	3.93E-07	NA	9.50E-04	5.59E-03	5.52E-03	4.61E-03	1.46E-03	1.29E-03	1.28E-03	
SegmentTotal										2.72E-01
Error (+/1)[12]										9.45E-03
Xe-132 (mol)[3]	2.21E+01	2.21E+01	2.21E+01	2.21E+01	2.21E+01	2.21E+01	2.21E+01	2.21E+01	2.21E+01	
Error (+/-)[3]	2.00E-01	2.00E-01	2.00E-01	2.00E-01	2.00E-01	2.00E-01	2.00E-01	2.00E-01	2.00E-01	
Xe-132 (g)[10]	8.75E-05	0.00E+00	4.48E-02	9.88E-02	1.27E-01	1.53E-01	3.30E-02	9.97E-03	2.22E-03	
Error (+/-)[3]	7.91E-07	NA	1.65E-03	9.66E-03	9.54E-03	7.99E-03	2.52E-03	2.22E-03	2.22E-03	
SegmentTotal										4.69E-01
Error (+/1)[12]										1.63E-02
Xe-134 (mol)[3]	2.62E+01	2.62E+01	2.62E+01	2.62E+01	2.62E+01	2.62E+01	2.62E+01	2.62E+01	2.62E+01	
Error (+/-)[3]	1.00E-01	1.00E-01	1.00E-01	1.00E-01	1.00E-01	1.00E-01	1.00E-01	1.00E-01	1.00E-01	
Xe-134 (g)[10]	1.05E-04	0.00E+00	5.40E-02	1.19E-01	1.52E-01	1.84E-01	3.97E-02	1.20E-02	2.67E-03	
Error (+/-)[3]	4.02E-07	NA	1.94E-03	1.16E-02	1.14E-02	9.50E-03	3.02E-03	2.67E-03	2.67E-03	
SegmentTotal										5.64E-01
Error (+/1)[12]										1.95E-02
Xe-136 (mol)[3]	3.88E+01	3.88E+01	3.88E+01	3.88E+01	3.88E+01	3.88E+01	3.88E+01	3.88E+01	3.88E+01	
Error (+/-)[3]	2.00E-01	2.00E-01	2.00E-01	2.00E-01	2.00E-01	2.00E-01	2.00E-01	2.00E-01	2.00E-01	

Rod "F" 2400408 (PFB 3-6 C13)

	F-00	F-01	F-02	F-03	F-04	F-05	F-06	F-07	F-08	F-09
Xe-136 (g)[10]	1.58E-04	0.00E+00	8.11E-02	1.79E-01	2.29E-01	2.77E-01	5.97E-02	1.80E-02	4.01E-03	
Error (+/-)[3]	8.15E-07	NA	2.93E-03	1.74E-02	1.72E-02	1.43E-02	4.55E-03	4.02E-03	4.01E-03	
SegmentTotal										8.48E-01
Error (+/1)[12]										2.94E-02
Rod total										2.15E+00
Error (+/-)[12]										4.00E-02
Shear Gas (g)[4]	0.00E+00	0.00E+00	2.00E-04	9.00E-04	1.40E-03	1.70E-03	2.00E-04	0.00E+00	0.00E+00	
Error (+/-)[4]	0.00E+00	0.00E+00	0.00E+00	2.00E-04	3.00E-04	3.00E-04	0.00E+00	0.00E+00	0.00E+00	
Diss+Pl Xe (mol)[3]	3.00E-06	0.00E+00	1.54E-03	3.39E-03	4.33E-03	5.25E-03	1.13E-03	3.42E-04	7.60E-05	
Error (+/-)[3]	0.00E+00	0.00E+00	5.50E-05	3.30E-04	3.25E-04	2.70E-04	8.60E-05	7.60E-05	7.60E-05	
Diss+Pl Kr+Xe (g)[3]	5.00E-04	0.00E+00	2.43E-01	5.24E-01	6.73E-01	8.19E-01	1.76E-01	5.47E-02	1.43E-02	
Error (+/-)[3]	0.00E+00	0.00E+00	8.50E-03	4.49E-02	4.46E-02	3.75E-02	1.18E-02	1.05E-02	1.10E-02	
Total Xe (mol)	3.00E-06	0.00E+00	1.54E-03	3.39E-03	4.34E-03	5.26E-03	1.13E-03	3.42E-04	7.60E-05	
Error (+/-)[9]	0.00E+00	0.00E+00	5.50E-05	3.30E-04	3.25E-04	2.70E-04	8.60E-05	7.62E-05	7.60E-05	
Values corrected to 1/1/84 (page 181, Final Report for the LWBR Proof of Breeding Analytical Support Project										
Cs-137 (atoms)[5]	NA	1.50E+18	2.37E+20	5.27E+20	7.00E+20	7.70E+20	1.75E+20	5.87E+19	9.68E+18	
Error (+/-)[4]	NA	5.08E+15	8.03E+17	1.78E+18	2.29E+18	2.43E+18	5.90E+17	1.92E+17	3.05E+16	
Cs-137 (g)[11]	NA	3.41E-04	5.40E-02	1.20E-01	1.59E-01	1.75E-01	3.97E-02	1.33E-02	2.20E-03	
Error (+/-)[9]	NA	1.15E-06	1.83E-04	4.05E-04	5.20E-04	5.52E-04	1.34E-04	4.37E-05	6.94E-06	
Total										5.63E-01
Error (+/-)[12]										8.90E-04
Ce-144 (atoms)[5]	NA	1.97E+17	1.68E+19	2.98E+19	3.71E+19	3.97E+19	1.20E+19	3.49E+18	5.02E+17	
Error (+/-)[4]	NA	1.37E+15	1.17E+17	2.15E+17	2.63E+17	2.76E+17	8.51E+16	2.40E+16	3.50E+15	
Ce-144 (g)[11]	NA	4.70E-05	4.02E-03	7.12E-03	8.87E-03	9.48E-03	2.87E-03	8.33E-04	1.20E-04	
Error (+/-)[9]	NA	3.27E-07	2.80E-05	5.13E-05	6.29E-05	6.60E-05	2.03E-05	5.73E-06	8.36E-07	
Total										3.34E-02
Error (+/-)[12]										1.10E-04

Rod "F" 2400408 (PFB 3-6 C13)

	F-00	F-01	F-02	F-03	F-04	F-05	F-06	F-07	F-08	F-09
Zr-95 (atoms)[5]	NA	2.00E+15	1.42E+17	2.52E+17	2.80E+17	2.89E+17	6.94E+16	1.11E+16	1.07E+15	
Error (+/-)[4]	NA	3.98E+13	2.00E+15	7.29E+15	9.03E+15	9.33E+15	2.85E+15	3.03E+14	4.91E+13	
Zr-95 (g)[11]	NA	3.15E-07	2.24E-05	3.98E-05	4.40E-05	4.56E-05	1.09E-05	1.75E-06	1.69E-07	
Error (+/-)[9]	NA	6.27E-09	3.15E-07	1.15E-06	1.42E-06	1.47E-06	4.49E-07	4.78E-08	7.74E-09	
Total										1.65E-04
Error (+/-)[12]										2.41E-06

References

1. ANL Destructive Chemical Assay of 33-Rod LWBR EOL Sample - Rod F, 2400408, page 6
2. ANL Destructive Chemical Assay of 33-Rod LWBR EOL Sample - Rod F, 2400408, page 7
3. ANL Destructive Chemical Assay of 33-Rod LWBR EOL Sample - Rod F, 2400408, page 10
4. ANL Destructive Chemical Assay of 33-Rod LWBR EOL Sample - Rod F, 2400408, page 11
5. ANL Destructive Chemical Assay of 33-Rod LWBR EOL Sample - Rod F, 2400408, page 12
6. ANL Destructive Chemical Assay of 33-Rod LWBR EOL Sample - Rod F, 2400408, page 13
7. ANL Destructive Chemical Assay of 33-Rod LWBR EOL Sample - Rod F, 2400408, page 14
8. (abundance of the specified isotope)(total weight of uranium)

   1.00E+02

9. Error Propagation = ((+/-x/x)2+(+/-y/y)2)1/2(xy)
10. (mole%)(number moles gas recovered)(molec wt) F, 2400408

    1.00E+02

11. (number of atoms per segment)(atomic weight)

    6.02E+23

12. Error Propagation = (SUM(+/-I)1/2

Rod "G" 2300711 (PFB 3-6 D29)

	G-00	G-01	G-02	G-03	G-04	G-05	G-06	G-07	G-08
Segment length (in)	1.12E+01	8.37E+00	1.80E+01	1.75E+01	1.75E+01	1.76E+01	1.05E+01	1.49E+01	2.64E+00
Total length (in)									1.18E+02
U-232 (wt%)[1]	0.00E+00	1.34E-02	2.81E-02	1.07E-01	1.40E-01	1.13E-01	1.21E-01	3.59E-02	
Error (+/-)[1]	0.00E+00	4.00E-04	9.00E-04	3.30E-03	4.30E-03	3.50E-03	3.80E-03	1.10E-03	
U-232 (g)[8]	0.00E+00	3.69E-05	3.54E-03	1.24E-02	1.58E-02	1.26E-02	2.50E-03	3.53E-04	
Error (+/-)[9]	NA	1.10E-06	1.13E-04	3.80E-04	4.85E-04	3.89E-04	7.86E-05	1.08E-05	
Segment Total									4.72E-02
Error (+/-)[12]									7.42E-04
U-233 (wt%)[1]	1.00E+02	9.92E+01	9.37E+01	8.80E+01	8.58E+01	8.69E+01	9.50E+01	9.81E+01	
Error (+/-)[1]	0.00E+00	1.54E-02	4.10E-03	5.00E-03	5.30E-03	5.00E-03	1.03E-02	8.30E-03	
U-233 (g)[8]	4.00E-05	2.73E-01	1.18E+01	1.01E+01	9.67E+00	9.66E+00	1.96E+00	9.64E-01	
Error (+/-)[9]	1.00E-05	1.08E-04	2.97E-03	2.56E-03	2.37E-03	2.55E-03	5.12E-04	2.22E-04	
Segment Total									4.45E+01
Error (+/-)[12]									5.27E-03
U-234 (wt%)[1]	0.00E+00	7.75E-01	5.27E+00	9.83E+00	1.15E+01	1.07E+01	4.49E+00	1.74E+00	
Error (+/-)[1]	0.00E+00	5.00E-04	6.00E-04	9.00E-04	1.00E-03	9.00E-04	8.00E-04	5.00E-04	
U-234 (g)[8]	0.00E+00	2.14E-03	6.64E-01	1.13E+00	1.30E+00	1.19E+00	9.28E-02	1.71E-02	
Error (+/-)[9]	NA	1.58E-06	1.81E-04	2.97E-04	3.28E-04	3.24E-04	2.75E-05	6.12E-06	
Segment Total									4.40E+00
Error (+/-)[12]									5.78E-04
U-235 (wt%)[1]	0.00E+00	1.38E-02	6.28E-01	1.61E+00	2.07E+00	1.82E+00	4.12E-01	7.41E-02	
Error (+/-)[1]	0.00E+00	1.09E-02	3.00E-03	3.10E-03	3.00E-03	3.10E-03	7.10E-03	5.90E-03	
U-235 (g)[8]	0.00E+00	3.81E-05	7.91E-02	1.86E-01	2.33E-01	2.02E-01	8.52E-03	7.28E-04	
Error (+/-)[9]	NA	3.01E-05	3.79E-04	3.60E-04	3.43E-04	3.49E-04	1.47E-04	5.79E-05	
Segment Total									7.10E-01

Rod "G" 2300711 (PFB 3-6 D29)

	G-00	G-01	G-02	G-03	G-04	G-05	G-06	G-07	G-08
Error (+/-)[12]									7.33E-04
U-236 (wt%)[1]	0.00E+00	1.00E-04	7.74E-02	1.65E-01	2.24E-01	1.93E-01	1.48E-02	1.30E-03	
Error (+/-)[1]	0.00E+00	1.00E-04	1.00E-04	1.00E-04	1.00E-04	1.00E-04	1.00E-04	1.00E-04	
U-236 (g)[8]	0.00E+00	2.76E-07	9.75E-03	1.90E-02	2.53E-02	2.14E-02	3.06E-04	1.28E-05	
Error (+/-)[9]	NA	2.76E-07	1.28E-05	1.24E-05	1.28E-05	1.24E-05	2.07E-06	9.82E-07	
Segment Total									7.58E-02
Error (+/-)[12]									2.53E-05
U-238 (wt%)[1]	0.00E+00	3.03E-02	2.67E-01	2.61E-01	2.59E-01	2.69E-01	5.40E-03	1.01E-02	
Error (+/-)[1]	0.00E+00	1.10E-02	3.00E-03	3.20E-03	3.10E-03	3.20E-03	7.30E-03	6.00E-03	
U-238 (g)[8]	0.00E+00	8.35E-05	3.36E-02	3.01E-02	2.92E-02	2.99E-02	1.12E-04	9.92E-05	
Error (+/-)[9]	NA	3.03E-05	3.78E-04	3.69E-04	3.50E-04	3.56E-04	1.51E-04	5.89E-05	
Segment Total									1.23E-01
Error (+/-)[12]									7.45E-04
Total U[2]	1.10E-04	2.76E-01	1.26E+01	1.15E+01	1.13E+01	1.11E+01	2.07E+00	9.82E-01	
Error (+/-)[2]	1.00E-05	1.00E-04	3.12E-03	2.83E-03	2.67E-03	2.87E-03	4.90E-04	2.10E-04	
Kr-82 (mol%)[3]	1.00E-01	1.00E-01	1.00E-01	1.00E-01	1.00E-01	1.00E-01	1.00E-01	1.00E-01	
Error (+/-)[3]	0.00E+00	0.00E+00	0.00E+00	0.00E+00	0.00E+00	0.00E+00	0.00E+00	0.00E+00	
Kr-82 (g)[10]	4.10E-07	0.00E+00	1.00E-04	1.73E-04	2.16E-04	1.89E-04	1.49E-05	4.65E-06	
Error (+/-)[9]	4.10E-11	NA	1.81E-05	1.80E-05	2.05E-05	2.02E-05	2.94E-06	4.52E-06	
Segment Total									6.98E-04
Error (+/-)[12]									3.89E-05
Kr-83 (mol%)[3]	1.56E+01	1.56E+01	1.56E+01	1.56E+01	1.56E+01	1.56E+01	1.56E+01	1.56E+01	
Error (+/-)[3]	1.00E-01	1.00E-01	1.00E-01	1.00E-01	1.00E-01	1.00E-01	1.00E-01	1.00E-01	
Kr-83 (g)[10]	6.47E-05	0.00E+00	1.58E-02	2.73E-02	3.42E-02	2.98E-02	2.35E-03	7.35E-04	

Rod "G" 2300711 (PFB 3-6 D29)

	G-00	G-01	G-02	G-03	G-04	G-05	G-06	G-07	G-08
Error (+/-)[9]	4.15E-07	NA	2.87E-03	2.86E-03	3.25E-03	3.21E-03	4.66E-04	7.24E-04	
Segment Total									1.10E-01
Error (+/-)[12]									6.17E-03
Kr-84 (mol%)[3]	2.99E+01	2.99E+01	2.99E+01	2.99E+01	2.99E+01	2.99E+01	2.99E+01	2.99E+01	
Error (+/-)[3]	2.00E-01	2.00E-01	2.00E-01	2.00E-01	2.00E-01	2.00E-01	2.00E-01	2.00E-01	
Kr-84 (g)[10]	1.25E-04	0.00E+00	3.07E-02	5.30E-02	6.63E-02	5.78E-02	4.55E-03	1.43E-03	
Error (+/-)[9]	8.39E-07	NA	5.57E-03	5.56E-03	6.31E-03	6.24E-03	9.04E-04	1.41E-03	
Segment Total									2.14E-01
Error (+/-)[12]									1.20E-02
Kr-85 (mol%)[3]	5.90E+00	5.90E+00	5.90E+00	5.90E+00	5.90E+00	5.90E+00	5.90E+00	5.90E+00	
Error (+/-)[3]	1.00E-01	1.00E-01	1.00E-01	1.00E-01	1.00E-01	1.00E-01	1.00E-01	1.00E-01	
Kr-85 (g)[10]	2.50E-05	0.00E+00	6.13E-03	1.06E-02	1.32E-02	1.15E-02	9.09E-04	2.85E-04	
Error (+/-)[9]	4.25E-07	NA	1.12E-03	1.12E-03	1.28E-03	1.26E-03	1.81E-04	2.81E-04	
Segment Total									4.27E-02
Error (+/-)[12]									2.42E-03
Kr-86 (mol%)[3]	4.87E+01	4.87E+01	4.87E+01	4.87E+01	4.87E+01	4.87E+01	4.87E+01	4.87E+01	
Error (+/-)[3]	2.00E-01	2.00E-01	2.00E-01	2.00E-01	2.00E-01	2.00E-01	2.00E-01	2.00E-01	
Kr-86 (g)[10]	2.09E-04	0.00E+00	5.12E-02	8.83E-02	1.11E-01	9.64E-02	7.59E-03	2.38E-03	
Error (+/-)[9]	8.59E-07	NA	9.29E-03	9.25E-03	1.05E-02	1.04E-02	1.51E-03	2.34E-03	
Segment Total									3.57E-01
Error (+/-)[12]									2.00E-02
Rod Total									7.24E-01
Error (+/-)[12]									2.42E-02
Shear Gas (g)[4]	0.00E+00	0.00E+00	1.80E-03	4.70E-03	6.20E-03	5.80E-03	3.00E-04	4.00E-04	
Error (+/-)[4]	0.00E+00	3.00E-04	4.00E-04	9.00E-04	1.20E-03	1.20E-03	3.00E-04	3.00E-04	

Rod "G" 2300711 (PFB 3-6 D29)

	G-00	G-01	G-02	G-03	G-04	G-05	G-06	G-07	G-08
Diss+Pl Kr (mol)[3]	5.00E-06	0.00E+00	1.22E-03	2.10E-03	2.63E-03	2.29E-03	1.81E-04	5.60E-05	
Error (+/-)[3]	0.00E+00	0.00E+00	2.22E-04	2.21E-04	2.51E-04	2.48E-04	3.60E-05	5.60E-05	
Diss+Pl Kr+Xe (g)[3]	3.00E-03	0.00E+00	6.54E-01	1.29E+00	1.49E+00	1.36E+00	1.22E-01	2.75E-02	
Error (+/-)[3]	1.00E-04	0.00E+00	5.54E-02	1.50E-01	1.70E-01	1.68E-01	1.97E-02	1.23E-02	
Total Kr (mol)	5.00E-06	0.00E+00	1.22E-03	2.11E-03	2.64E-03	2.30E-03	1.81E-04	5.68E-05	
Error (+/-)[9]	5.00E-10	1.01E-09	2.22E-04	2.21E-04	2.51E-04	2.48E-04	3.60E-05	5.60E-05	
Xe-128 (mol)[3]	1.00E-01	1.00E-01	1.00E-01	1.00E-01	1.00E-01	1.00E-01	1.00E-01	1.00E-01	
Error (+/-)[3]	0.00E+00	0.00E+00	0.00E+00	0.00E+00	0.00E+00	0.00E+00	0.00E+00	0.00E+00	
Xe-128 (g)[10]	2.43E-06	0.00E+00	5.26E-04	1.07E-03	1.21E-03	1.12E-03	1.02E-04	2.19E-05	
Error (+/-)[3]	1.28E-07	NA	4.96E-05	1.42E-04	1.60E-04	1.59E-04	1.85E-05	1.07E-05	
SegmentTotal									4.04E-03
Error (+/1)[12]									2.72E-04
Xe-130 (mol)[3]	1.00E-01	1.00E-01	1.00E-01	1.00E-01	1.00E-01	1.00E-01	1.00E-01	1.00E-01	
Error (+/-)[3]	0.00E+00	0.00E+00	0.00E+00	0.00E+00	0.00E+00	0.00E+00	0.00E+00	0.00E+00	
Xe-130 (g)[10]	2.47E-06	0.00E+00	5.34E-04	1.08E-03	1.23E-03	1.13E-03	1.04E-04	2.23E-05	
Error (+/-)[3]	1.30E-07	NA	5.04E-05	1.44E-04	1.63E-04	1.61E-04	1.88E-05	1.09E-05	
SegmentTotal									4.10E-03
Error (+/1)[12]									2.76E-04
Xe-131 (mol)[3]	1.17E+01	1.17E+01	1.17E+01	1.17E+01	1.17E+01	1.17E+01	1.17E+01	1.17E+01	
Error (+/-)[3]	1.00E-01	1.00E-01	1.00E-01	1.00E-01	1.00E-01	1.00E-01	1.00E-01	1.00E-01	
Xe-131 (g)[10]	2.91E-04	0.00E+00	6.30E-02	1.28E-01	1.45E-01	1.34E-01	1.22E-02	2.63E-03	
Error (+/-)[3]	1.55E-05	NA	5.97E-03	1.70E-02	1.92E-02	1.90E-02	2.22E-03	1.29E-03	
SegmentTotal									4.84E-01
Error (+/1)[12]									3.26E-02

Rod "G" 2300711 (PFB 3-6 D29)

	G-00	G-01	G-02	G-03	G-04	G-05	G-06	G-07	G-08
Xe-132 (mol)[3]	2.24E+01	2.24E+01	2.24E+01	2.24E+01	2.24E+01	2.24E+01	2.24E+01	2.24E+01	
Error (+/-)[3]	1.00E-01	1.00E-01	1.00E-01	1.00E-01	1.00E-01	1.00E-01	1.00E-01	1.00E-01	
Xe-132 (g)[10]	5.61E-04	0.00E+00	1.22E-01	2.46E-01	2.79E-01	2.58E-01	2.36E-02	5.07E-03	
Error (+/-)[3]	2.97E-05	NA	1.15E-02	3.28E-02	3.70E-02	3.67E-02	4.29E-03	2.48E-03	
SegmentTotal									9.33E-01
Error (+/1)[12]									6.28E-02
Xe-134 (mol)[3]	2.54E+01	2.54E+01	2.54E+01	2.54E+01	2.54E+01	2.54E+01	2.54E+01	2.54E+01	
Error (+/-)[3]	1.00E-01	1.00E-01	1.00E-01	1.00E-01	1.00E-01	1.00E-01	1.00E-01	1.00E-01	
Xe-134 (g)[10]	6.46E-04	0.00E+00	1.40E-01	2.84E-01	3.21E-01	2.97E-01	2.71E-02	5.83E-03	
Error (+/-)[3]	3.41E-05	NA	1.32E-02	3.77E-02	4.26E-02	4.22E-02	4.93E-03	2.86E-03	
SegmentTotal									1.07E+00
Error (+/1)[12]									7.23E-02
Xe-136 (mol)[3]	4.03E+01	4.03E+01	4.03E+01	4.03E+01	4.03E+01	4.03E+01	4.03E+01	4.03E+01	
Error (+/-)[3]	1.00E-01	1.00E-01	1.00E-01	1.00E-01	1.00E-01	1.00E-01	1.00E-01	1.00E-01	
Xe-136 (g)[10]	1.04E-03	0.00E+00	2.25E-01	4.57E-01	5.17E-01	4.77E-01	4.37E-02	9.39E-03	
Error (+/-)[3]	5.48E-05	NA	2.13E-02	6.07E-02	6.87E-02	6.79E-02	7.94E-03	4.60E-03	
SegmentTotal									1.73E+00
Error (+/1)[12]									1.16E-01
Rod total									4.23E+00
Error (+/-)[12]									1.54E-01
Shear Gas (g)[4]	0.00E+00	0.00E+00	1.80E-03	4.70E-03	6.20E-03	5.80E-03	3.00E-04	4.00E-04	
Error (+/-)[4]	0.00E+00	3.00E-04	4.00E-04	9.00E-04	1.20E-03	1.20E-03	3.00E-04	3.00E-04	
Diss+Pl Xe (mol)[3]	1.90E-05	0.00E+00	4.10E-03	8.31E-03	9.40E-03	8.68E-03	7.96E-04	1.69E-04	
Error (+/-)[3]	1.00E-06	0.00E+00	3.88E-04	1.11E-03	1.25E-03	1.24E-03	1.45E-04	8.40E-05	
Diss+Pl Kr+Xe (g)[3]	3.00E-03	0.00E+00	6.54E-01	1.29E+00	1.49E+00	1.36E+00	1.22E-01	2.75E-02	

Rod "G" 2300711 (PFB 3-6 D29)

	G-00	G-01	G-02	G-03	G-04	G-05	G-06	G-07	G-08
Error (+/-)[3]	1.00E-04	0.00E+00	5.54E-02	1.50E-01	1.70E-01	1.68E-01	1.97E-02	1.23E-02	
Total Xe (mol)	1.90E-05	0.00E+00	4.11E-03	8.34E-03	9.44E-03	8.72E-03	7.98E-04	1.71E-04	
Error (+/-)[9]	1.00E-06	3.39E-09	3.88E-04	1.11E-03	1.25E-03	1.24E-03	1.45E-04	8.40E-05	
Values corrected to 1/1/84 (page 181, Final Report for the LWBR Proof of Breeding Analytical Support Project									
Cs-137 (atoms)[5]	NA	2.84E+18	6.55E+20	1.37E+21	1.65E+21	1.49E+21	1.11E+20	2.12E+19	
Error (+/-)[4]	NA	9.85E+15	1.91E+18	3.99E+18	4.82E+18	4.55E+18	3.74E+17	6.20E+16	
Cs-137 (g)[11]	NA	6.46E-04	1.49E-01	3.11E-01	3.75E-01	3.39E-01	2.53E-02	4.82E-03	
Error (+/-)[9]	NA	2.24E-06	4.34E-04	9.08E-04	1.09E-03	1.03E-03	8.51E-05	1.41E-05	
Total									1.20E+00
Error (+/-)[12]									1.81E-03
Ce-144 (atoms)[5]	NA	3.58E+17	4.18E+19	6.86E+19	7.99E+19	6.52E+19	6.48E+18	1.09E+18	
Error (+/-)[4]	NA	2.10E+15	2.39E+17	3.92E+17	4.57E+17	3.82E+17	4.02E+16	6.25E+15	
Ce-144 (g)[11]	NA	8.55E-05	9.98E-03	1.64E-02	1.91E-02	1.56E-02	1.55E-03	2.61E-04	
Error (+/-)[9]	NA	5.03E-07	5.70E-05	9.37E-05	1.09E-04	9.14E-05	9.60E-06	1.49E-06	
Total									6.29E-02
Error (+/-)[12]									1.80E-04
Zr-95 (atoms)[5]	NA	3.81E+15	3.52E+17	5.41E+17	5.76E+17	3.57E+17	2.09E+16	2.53E+15	
Error (+/-)[4]	NA	9.73E+13	9.35E+15	1.75E+16	1.59E+16	1.49E+16	8.65E+14	1.54E+14	
Zr-95 (g)[11]	NA	6.00E-07	5.55E-05	8.52E-05	9.07E-05	5.62E-05	3.29E-06	3.98E-07	
Error (+/-)[9]	NA	1.53E-08	1.47E-06	2.76E-06	2.51E-06	2.34E-06	1.36E-07	2.42E-08	
Total									2.92E-04
Error (+/-)[12]									4.65E-06

Rod "G" 2300711 (PFB 3-6 D29)

[redacted]									
	G-00	G-01	G-02	G-03	G-04	G-05	G-06	G-07	G-08

References

1. ANL Destructive Chemical Assay of 33-Rod LWBR EOL Sample - Rod G, 2300711, page 6
2. ANL Destructive Chemical Assay of 33-Rod LWBR EOL Sample - Rod G, 2300711, page 7
3. ANL Destructive Chemical Assay of 33-Rod LWBR EOL Sample - Rod G, 2300711, page 10
4. ANL Destructive Chemical Assay of 33-Rod LWBR EOL Sample - Rod G, 2300711, page 11
5. ANL Destructive Chemical Assay of 33-Rod LWBR EOL Sample - Rod G, 2300711, page 12
6. ANL Destructive Chemical Assay of 33-Rod LWBR EOL Sample - Rod G, 2300711, page 13
7. ANL Destructive Chemical Assay of 33-Rod LWBR EOL Sample - Rod G, 2300711, page 14
8. (abundance of the specified isotope)(total weight of uranium)

   1.00E+02
9. Error Propagation = ((+/-x/x)2+(+/-y/y)2)1/2(xy)
10. (mole%)(number moles gas recovered)(molec wt)

    1.00E+02
11. (number of atoms per segment)(atomic weight)

    6.02E+23
12. Error Propagation = (SUM(+/-I)1/2

Rod "H" 3211456 (R 4-3 B1)

	H-00	H-01	H-02	H-03	H-04	H-05	H-06	H-07	H-08	H-09	H-10	H-11	H-12	H-13	H-14	H-15	H-16
Segment length (in)	6.26E+00	6.43E+00	6.99E+00	6.95E+00	6.99E+00	6.99E+00	6.96E+00	6.98E+00	6.97E+00	6.98E+00	6.95E+00	7.01E+00	6.96E+00	6.98E+00	7.00E+00	6.05E+00	1.71E+00
Total length (in)																	1.11E+02
U-232 (wt%)[1]	0.00E+00	3.10E-03	1.84E-02	4.32E-02	6.91E-02	9.58E-02	1.13E-01	1.26E-01	1.29E-01	1.27E-01	1.20E-01	1.01E-01	7.94E-02	4.94E-02	2.11E-02	4.20E-03	
Error (+/-)[1]	0.00E+00	1.00E-04	6.00E-04	1.30E-03	2.10E-03	3.00E-03	3.50E-03	3.90E-03	4.00E-03	3.90E-03	3.70E-03	3.10E-03	2.50E-03	1.50E-03	7.00E-04	1.00E-04	
U-232 (g)[8]	0.00E+00	5.21E-06	1.34E-04	6.77E-04	1.63E-03	3.02E-03	4.03E-03	4.89E-03	5.10E-03	4.92E-03	4.52E-03	3.44E-03	2.16E-03	9.37E-04	2.04E-04	1.10E-05	
Error (+/-)[9]	NA	1.68E-07	4.36E-06	2.04E-05	4.95E-05	9.44E-05	1.25E-04	1.52E-04	1.58E-04	1.52E-04	1.40E-04	1.06E-04	6.79E-05	2.85E-05	6.78E-06	2.63E-07	
Segment Total																	3.57E-02
Error (+/-)[12]																	3.67E-04
U-233 (wt%)[1]	1.00E+02	9.97E+01	9.90E+01	9.80E+01	9.69E+01	9.56E+01	9.48E+01	9.42E+01	9.40E+01	9.42E+01	9.43E+01	9.51E+01	9.62E+01	9.75E+01	9.88E+01	9.95E+01	
Error (+/-)[1]	0.00E+00	4.12E-02	1.22E-02	8.30E-03	7.00E-03	7.20E-03	7.80E-03	8.10E-03	7.90E-03	8.10E-03	7.70E-03	8.40E-03	8.90E-03	8.90E-03	8.70E-03	2.56E-02	
U-233 (g)[8]	4.00E-05	1.68E-01	7.19E-01	1.54E+00	2.28E+00	3.01E+00	3.39E+00	3.66E+00	3.71E+00	3.66E+00	3.56E+00	3.24E+00	2.61E+00	1.85E+00	9.56E-01	2.61E-01	
Error (+/-)[9]	1.00E-05	1.13E-04	1.90E-04	3.49E-04	5.39E-04	5.99E-04	7.11E-04	7.91E-04	2.85E-03	7.82E-04	7.48E-04	7.07E-04	5.82E-04	4.70E-04	2.06E-04	1.20E-04	
Segment Total																	3.46E+01
Error (+/-)[12]																	3.51E-03
U-234 (wt%)[1]	0.00E+00	2.61E-01	8.94E-01	1.87E+00	2.85E+00	3.97E+00	4.63E+00	5.09E+00	5.26E+00	5.11E+00	5.00E+00	4.40E+00	3.45E+00	2.32E+00	1.18E+00	3.85E-01	
Error (+/-)[1]	0.00E+00	6.00E-04	6.00E-04	6.00E-04	6.00E-04	7.00E-04	7.00E-04	8.00E-04	8.00E-04	8.00E-04	7.00E-04	7.00E-04	7.00E-04	6.00E-04	6.00E-04	6.00E-04	
U-234 (g)[8]	0.00E+00	4.39E-04	6.49E-03	2.94E-02	6.71E-02	1.25E-01	1.66E-01	1.98E-01	2.08E-01	1.99E-01	1.89E-01	1.50E-01	9.36E-02	4.40E-02	1.15E-02	1.01E-03	
Error (+/-)[9]	NA	1.04E-06	4.61E-06	1.13E-05	2.07E-05	3.19E-05	4.06E-05	5.00E-05	1.62E-04	4.98E-05	4.50E-05	3.83E-05	2.69E-05	1.54E-05	6.23E-06	1.62E-06	
Segment Total																	1.49E+00
Error (+/-)[12]																	1.97E-04

Rod "H" 3211456 (R 4-3 B1)

	H-00	H-01	H-02	H-03	H-04	H-05	H-06	H-07	H-08	H-09	H-10	H-11	H-12	H-13	H-14	H-15	H-16
U-235 (wt%)[1]	0.00E+00	3.90E-03	1.85E-02	7.66E-02	1.78E-01	3.34E-01	4.58E-01	5.44E-01	5.74E-01	5.44E-01	5.11E-01	3.99E-01	2.49E-01	1.15E-01	3.04E-02	2.56E-02	
Error (+/-)[1]	0.00E+00	3.05E-02	9.20E-03	6.30E-03	5.20E-03	5.20E-03	5.60E-03	5.70E-03	5.50E-03	5.70E-03	5.40E-03	6.20E-03	6.60E-03	6.70E-03	6.60E-03	1.90E-02	
U-235 (g)[8]	0.00E+00	6.56E-06	1.34E-04	1.20E-03	4.20E-03	1.05E-02	1.64E-02	2.11E-02	2.27E-02	2.12E-02	1.93E-02	1.36E-02	6.77E-03	2.18E-03	2.94E-04	6.72E-05	
Error (+/-)[9]	NA	5.13E-05	6.68E-05	9.87E-05	1.23E-04	1.64E-04	2.01E-04	2.22E-04	2.18E-04	2.22E-04	2.04E-04	2.11E-04	1.79E-04	1.27E-04	6.39E-05	4.99E-05	
Segment Total																	1.40E-01
Error (+/-)[12]																	6.21E-04
U-236 (wt%)[1]	0.00E+00	1.40E-03	3.00E-04	1.20E-03	4.20E-03	1.00E-02	1.59E-02	2.14E-02	2.29E-02	2.12E-02	1.93E-02	1.30E-02	6.50E-03	2.50E-03	6.00E-04	4.00E-04	
Error (+/-)[1]	0.00E+00	2.00E-04	2.00E-04	2.00E-04	1.00E-04	1.00E-04	1.00E-04	1.00E-04	1.00E-04	1.00E-04	1.00E-04	1.00E-04	1.00E-04	1.00E-04	2.00E-04	2.00E-04	
U-236 (g)[8]	0.00E+00	2.35E-06	2.18E-06	1.88E-05	9.90E-05	3.15E-04	5.69E-04	8.32E-04	9.05E-04	8.25E-04	7.28E-04	4.43E-04	1.77E-04	4.74E-05	5.81E-06	1.05E-06	
Error (+/-)[9]	NA	3.36E-07	1.45E-06	3.13E-06	2.36E-06	3.15E-06	3.58E-06	3.89E-06	4.01E-06	3.89E-06	3.78E-06	3.41E-06	2.72E-06	1.90E-06	1.94E-06	5.25E-07	
Segment Total																	4.97E-03
Error (+/-)[12]																	1.13E-05
U-238 (wt%)[1]	0.00E+00	7.44E-02	2.40E-02	8.60E-03	6.50E-03	5.30E-03	4.50E-03	4.80E-03	3.90E-03	4.70E-03	4.80E-03	4.80E-03	6.10E-03	8.80E-03	1.36E-02	5.90E-02	
Error (+/-)[1]	0.00E+00	2.78E-02	8.20E-03	5.50E-03	4.50E-03	4.50E-03	4.90E-03	5.00E-03	4.80E-03	5.00E-03	4.80E-03	5.40E-03	5.90E-03	6.00E-03	5.80E-03	1.73E-02	
U-238 (g)[8]	0.00E+00	1.25E-04	1.74E-04	1.35E-04	1.53E-04	1.67E-04	1.61E-04	1.87E-04	1.54E-04	1.83E-04	1.81E-04	1.64E-04	1.66E-04	1.67E-04	1.32E-04	1.55E-04	
Error (+/-)[9]	NA	4.68E-05	5.95E-05	8.62E-05	1.06E-04	1.42E-04	1.75E-04	1.94E-04	1.90E-04	1.94E-04	1.81E-04	1.84E-04	1.60E-04	1.14E-04	5.62E-05	4.54E-05	
Segment Total																	2.40E-03
Error (+/-)[12]																	5.45E-04
Total U[2]	5.00E-05	1.68E-01	7.26E-01	1.57E+00	2.36E+00	3.15E+00	3.58E+00	3.89E+00	3.95E+00	3.89E+00	3.77E+00	3.41E+00	2.72E+00	1.90E+00	9.68E-01	2.62E-01	
Error (+/-)[2]	1.00E-05	9.00E-05	1.70E-04	3.30E-04	5.30E-04	5.80E-04	6.90E-04	7.70E-04	3.01E-03	7.60E-04	7.30E-04	6.80E-04	5.50E-04	4.50E-04	1.90E-04	1.00E-04	

Rod "H" 3211456 (R 4-3 B1)

	H-00	H-01	H-02	H-03	H-04	H-05	H-06	H-07	H-08	H-09	H-10	H-11	H-12	H-13	H-14	H-15	H-16
Kr-82 (mol%)[3]	0.00E+00	0.00E+00	0.00E+00	0.00E+00	0.00E+00	0.00E+00	0.00E+00	0.00E+00	0.00E+00	0.00E+00	0.00E+00	0.00E+00	0.00E+00	0.00E+00	0.00E+00	0.00E+00	
Error (+/-)[3]	0.00E+00	0.00E+00	0.00E+00	0.00E+00	0.00E+00	0.00E+00	0.00E+00	0.00E+00	0.00E+00	0.00E+00	0.00E+00	0.00E+00	0.00E+00	0.00E+00	0.00E+00	0.00E+00	
Kr-82 (g)[10]	0.00E+00	0.00E+00	0.00E+00	0.00E+00	0.00E+00	0.00E+00	0.00E+00	0.00E+00	0.00E+00	0.00E+00	0.00E+00	0.00E+00	0.00E+00	0.00E+00	0.00E+00	0.00E+00	
Error (+/-)[9]	NA	NA	NA	NA	NA	NA	NA	NA	NA	NA	NA	NA	NA	NA	NA	NA	
Segment Total																	0.00E+00
Error (+/-)[12]																	NA
Kr-83 (mol%)[3]	1.56E+01	1.56E+01	1.56E+01	1.56E+01	1.56E+01	1.56E+01	1.56E+01	1.56E+01	1.56E+01	1.56E+01	1.56E+01	1.56E+01	1.56E+01	1.56E+01	1.56E+01	1.56E+01	
Error (+/-)[3]	2.00E-01	2.00E-01	2.00E-01	2.00E-01	2.00E-01	2.00E-01	2.00E-01	2.00E-01	2.00E-01	2.00E-01	2.00E-01	2.00E-01	2.00E-01	2.00E-01	2.00E-01	2.00E-01	
Kr-83 (g)[10]	0.00E+00	0.00E+00	0.00E+00	1.10E-03	1.81E-03	3.24E-03	3.72E-03	5.82E-03	6.43E-03	6.35E-03	5.07E-03	5.14E-03	3.64E-03	1.36E-03	3.10E-04	0.00E+00	
Error (+/-)[9]	NA	NA	NA	3.63E-04	4.68E-04	6.48E-04	5.32E-04	8.05E-04	1.48E-03	7.03E-04	7.40E-04	7.40E-04	1.22E-03	2.46E-04	1.55E-04	NA	
Segment Total																	4.40E-02
Error (+/-)[12]																	2.65E-03
Kr-84 (mol%)[3]	2.93E+01	2.93E+01	2.93E+01	2.93E+01	2.93E+01	2.93E+01	2.93E+01	2.93E+01	2.93E+01	2.93E+01	2.93E+01	2.93E+01	2.93E+01	2.93E+01	2.93E+01	2.93E+01	
Error (+/-)[3]	3.00E-01	3.00E-01	3.00E-01	3.00E-01	3.00E-01	3.00E-01	3.00E-01	3.00E-01	3.00E-01	3.00E-01	3.00E-01	3.00E-01	3.00E-01	3.00E-01	3.00E-01	3.00E-01	
Kr-84 (g)[10]	0.00E+00	0.00E+00	0.00E+00	2.09E-03	3.44E-03	6.16E-03	7.07E-03	1.11E-02	1.22E-02	1.21E-02	9.63E-03	9.78E-03	6.91E-03	2.59E-03	5.90E-04	0.00E+00	
Error (+/-)[9]	NA	NA	NA	6.90E-04	8.88E-04	1.23E-03	1.01E-03	1.53E-03	2.81E-03	1.33E-03	1.40E-03	1.40E-03	2.31E-03	4.68E-04	2.95E-04	NA	
Segment Total																	8.36E-02
Error (+/-)[12]																	5.04E-03
Kr-85 (mol%)[3]	6.10E+00	6.10E+00	6.10E+00	6.10E+00	6.10E+00	6.10E+00	6.10E+00	6.10E+00	6.10E+00	6.10E+00	6.10E+00	6.10E+00	6.10E+00	6.10E+00	6.10E+00	6.10E+00	

Rod "H" 3211456 (R 4-3 B1)

	H-00	H-01	H-02	H-03	H-04	H-05	H-06	H-07	H-08	H-09	H-10	H-11	H-12	H-13	H-14	H-15	H-16
Error (+/-)[3]	2.00E-01	2.00E-01	2.00E-01	2.00E-01	2.00E-01	2.00E-01	2.00E-01	2.00E-01	2.00E-01	2.00E-01	2.00E-01	2.00E-01	2.00E-01	2.00E-01	2.00E-01	2.00E-01	
Kr-85 (g)[10]	0.00E+00	0.00E+00	0.00E+00	4.40E-04	7.25E-04	1.30E-03	1.49E-03	2.33E-03	2.57E-03	2.54E-03	2.03E-03	2.06E-03	1.46E-03	5.45E-04	1.24E-04	0.00E+00	
Error (+/-)[9]	NA	NA	NA	1.46E-04	1.89E-04	2.62E-04	2.18E-04	3.30E-04	5.96E-04	2.92E-04	3.03E-04	3.03E-04	4.89E-04	1.00E-04	6.23E-05	NA	
Segment Total																	1.76E-02
Error (+/-)[12]																	1.08E-03
Kr-86 (mol%)[3]	4.92E+01	4.92E+01	4.92E+01	4.92E+01	4.92E+01	4.92E+01	4.92E+01	4.92E+01	4.92E+01	4.92E+01	4.92E+01	4.92E+01	4.92E+01	4.92E+01	4.92E+01	4.92E+01	
Error (+/-)[3]	3.00E-01	3.00E-01	3.00E-01	3.00E-01	3.00E-01	3.00E-01	3.00E-01	3.00E-01	3.00E-01	3.00E-01	3.00E-01	3.00E-01	3.00E-01	3.00E-01	3.00E-01	3.00E-01	
Kr-86 (g)[10]	0.00E+00	0.00E+00	0.00E+00	3.59E-03	5.92E-03	1.06E-02	1.22E-02	1.90E-02	2.10E-02	2.08E-02	1.66E-02	1.68E-02	1.19E-02	4.45E-03	1.01E-03	0.00E+00	
Error (+/-)[9]	NA	NA	NA	1.19E-03	1.53E-03	2.11E-03	1.73E-03	2.62E-03	4.82E-03	2.29E-03	2.41E-03	2.41E-03	3.97E-03	8.04E-04	5.07E-04	NA	
Segment Total																	1.44E-01
Error (+/-)[12]																	8.65E-03
Rod Total																	2.89E-01
Error (+/-)[12]																	1.04E-02
Shear Gas (g)[4]	0.00E+00	0.00E+00	0.00E+00	0.00E+00	0.00E+00	2.00E-04	3.00E-04	6.00E-04	6.00E-04	6.00E-04	4.00E-04	3.00E-04	1.00E-04	1.00E-04	0.00E+00	0.00E+00	
Error (+/-)[4]	0.00E+00	0.00E+00	0.00E+00	0.00E+00	0.00E+00	0.00E+00	1.00E-04	1.00E-04	1.00E-04	1.00E-04	1.00E-04	1.00E-04	0.00E+00	0.00E+00	0.00E+00	0.00E+00	
Diss+Pl Kr (mol)[3]	0.00E+00	0.00E+00	0.00E+00	8.50E-05	1.40E-04	2.50E-04	2.87E-04	4.49E-04	4.96E-04	4.90E-04	3.91E-04	3.97E-04	2.81E-04	1.05E-04	2.40E-05	0.00E+00	
Error (+/-)[3]	0.00E+00	0.00E+00	0.00E+00	2.80E-05	3.60E-05	5.00E-05	4.10E-05	6.20E-05	1.14E-04	5.40E-05	5.70E-05	5.70E-05	9.40E-05	1.90E-05	1.20E-05	0.00E+00	
Diss+Pl Kr+Xe (g)[3]	1.00E-04	0.00E+00	0.00E+00	4.76E-02	7.30E-02	1.42E-01	1.73E-01	2.47E-01	2.88E-01	2.97E-01	2.32E-01	1.78E-01	1.24E-01	5.10E-02	1.41E-02	0.00E+00	
Error (+/-)[3]	0.00E+00	0.00E+00	0.00E+00	6.80E-03	7.00E-03	1.41E-02	1.69E-02	3.42E-02	3.72E-02	2.96E-02	1.37E-02	1.60E-02	1.49E-02	6.00E-03	4.20E-03	0.00E+00	
Total Kr (mol)	0.00E+00	0.00E+00	0.00E+00	8.50E-05	1.40E-04	2.50E-04	2.87E-04	4.50E-04	4.97E-04	4.91E-04	3.92E-04	3.98E-04	2.81E-04	1.05E-04	2.40E-05	0.00E+00	
Error (+/-)[9]	0.00E+00	0.00E+00	0.00E+00	2.80E-05	3.61E-05	5.00E-05	4.10E-05	6.20E-05	1.14E-04	5.40E-05	5.70E-05	5.70E-05	9.40E-05	1.90E-05	1.20E-05	0.00E+00	

Rod "H" 3211456 (R 4-3 B1)

	H-00	H-01	H-02	H-03	H-04	H-05	H-06	H-07	H-08	H-09	H-10	H-11	H-12	H-13	H-14	H-15	H-16
Xe-128 (mol)[3]	0.00E+00	0.00E+00	0.00E+00	0.00E+00	0.00E+00	0.00E+00	0.00E+00	0.00E+00	0.00E+00	0.00E+00	0.00E+00	0.00E+00	0.00E+00	0.00E+00	0.00E+00	0.00E+00	
Error (+/-)[3]	0.00E+00	0.00E+00	0.00E+00	0.00E+00	0.00E+00	0.00E+00	0.00E+00	0.00E+00	0.00E+00	0.00E+00	0.00E+00	0.00E+00	0.00E+00	0.00E+00	0.00E+00	0.00E+00	
Xe-128 (g)[10]	0.00E+00	0.00E+00	0.00E+00	0.00E+00	0.00E+00	0.00E+00	0.00E+00	0.00E+00	0.00E+00	0.00E+00	0.00E+00	0.00E+00	0.00E+00	0.00E+00	0.00E+00	0.00E+00	
Error (+/-)[3]	NA	NA	NA	NA	NA	NA	NA	NA	NA	NA	NA	NA	NA	NA	NA	NA	
SegmentTotal																	0.00E+00
Error (+/1)[12]																	NA
Xe-130 (mol)[3]	0.00E+00	0.00E+00	0.00E+00	0.00E+00	0.00E+00	0.00E+00	0.00E+00	0.00E+00	0.00E+00	0.00E+00	0.00E+00	0.00E+00	0.00E+00	0.00E+00	0.00E+00	0.00E+00	
Error (+/-)[3]	0.00E+00	0.00E+00	0.00E+00	0.00E+00	0.00E+00	0.00E+00	0.00E+00	0.00E+00	0.00E+00	0.00E+00	0.00E+00	0.00E+00	0.00E+00	0.00E+00	0.00E+00	0.00E+00	
Xe-130 (g)[10]	0.00E+00	0.00E+00	0.00E+00	0.00E+00	0.00E+00	0.00E+00	0.00E+00	0.00E+00	0.00E+00	0.00E+00	0.00E+00	0.00E+00	0.00E+00	0.00E+00	0.00E+00	0.00E+00	
Error (+/-)[3]	NA	NA	NA	NA	NA	NA	NA	NA	NA	NA	NA	NA	NA	NA	NA	NA	
SegmentTotal																	0.00E+00
Error (+/1)[12]																	NA
Xe-131 (mol)[3]	1.27E+01	1.27E+01	1.27E+01	1.27E+01	1.27E+01	1.27E+01	1.27E+01	1.27E+01	1.27E+01	1.27E+01	1.27E+01	1.27E+01	1.27E+01	1.27E+01	1.27E+01	1.27E+01	
Error (+/-)[3]	1.00E-01	1.00E-01	1.00E-01	1.00E-01	1.00E-01	1.00E-01	1.00E-01	1.00E-01	1.00E-01	1.00E-01	1.00E-01	1.00E-01	1.00E-01	1.00E-01	1.00E-01	1.00E-01	
Xe-131 (g)[10]	1.66E-05	0.00E+00	0.00E+00	5.00E-03	7.56E-03	1.50E-02	1.84E-02	2.60E-02	3.05E-02	3.17E-02	2.47E-02	1.79E-02	1.25E-02	5.23E-03	1.50E-03	0.00E+00	
Error (+/-)[3]	1.31E-07	#DIV/0!	#DIV/0!	7.84E-04	7.87E-04	1.67E-03	2.05E-03	3.60E-03	4.45E-03	3.63E-03	1.59E-03	1.88E-03	1.57E-03	7.16E-04	4.99E-04	NA	
SegmentTotal																	1.96E-01
Error (+/1)[12]																	7.96E-03
Xe-132 (mol)[3]	2.12E+01	2.12E+01	2.12E+01	2.12E+01	2.12E+01	2.12E+01	2.12E+01	2.12E+01	2.12E+01	2.12E+01	2.12E+01	2.12E+01	2.12E+01	2.12E+01	2.12E+01	2.12E+01	

Rod "H" 3211456 (R 4-3 B1)

	H-00	H-01	H-02	H-03	H-04	H-05	H-06	H-07	H-08	H-09	H-10	H-11	H-12	H-13	H-14	H-15	H-16
Error (+/-)[3]	2.00E-01	2.00E-01	2.00E-01	2.00E-01	2.00E-01	2.00E-01	2.00E-01	2.00E-01	2.00E-01	2.00E-01	2.00E-01	2.00E-01	2.00E-01	2.00E-01	2.00E-01	2.00E-01	
Xe-132 (g)[10]	2.80E-05	0.00E+00	0.00E+00	8.42E-03	1.27E-02	2.52E-02	3.10E-02	4.37E-02	5.13E-02	5.34E-02	4.15E-02	3.01E-02	2.10E-02	8.80E-03	2.52E-03	0.00E+00	
Error (+/-)[3]	2.64E-07	#DIV/0!	#DIV/0!	1.32E-03	1.33E-03	2.81E-03	3.45E-03	6.05E-03	7.48E-03	6.12E-03	2.69E-03	3.17E-03	2.64E-03	1.21E-03	8.39E-04	NA	
SegmentTotal																	3.30E-01
Error (+/1)[12]																	1.34E-02
Xe-134 (mol)[3]	2.61E+01	2.61E+01	2.61E+01	2.61E+01	2.61E+01	2.61E+01	2.61E+01	2.61E+01	2.61E+01	2.61E+01	2.61E+01	2.61E+01	2.61E+01	2.61E+01	2.61E+01	2.61E+01	
Error (+/-)[3]	2.00E-01	2.00E-01	2.00E-01	2.00E-01	2.00E-01	2.00E-01	2.00E-01	2.00E-01	2.00E-01	2.00E-01	2.00E-01	2.00E-01	2.00E-01	2.00E-01	2.00E-01	2.00E-01	
Xe-134 (g)[10]	3.49E-05	0.00E+00	0.00E+00	1.05E-02	1.59E-02	3.15E-02	3.87E-02	5.46E-02	6.41E-02	6.67E-02	5.18E-02	3.77E-02	2.62E-02	1.10E-02	3.15E-03	0.00E+00	
Error (+/-)[3]	2.68E-07	#DIV/0!	#DIV/0!	1.65E-03	1.66E-03	3.50E-03	4.31E-03	7.56E-03	9.34E-03	7.64E-03	3.34E-03	3.96E-03	3.29E-03	1.51E-03	1.05E-03	NA	
SegmentTotal																	4.12E-01
Error (+/1)[12]																	1.67E-02
Xe-136 (mol)[3]	4.01E+01	4.01E+01	4.01E+01	4.01E+01	4.01E+01	4.01E+01	4.01E+01	4.01E+01	4.01E+01	4.01E+01	4.01E+01	4.01E+01	4.01E+01	4.01E+01	4.01E+01	4.01E+01	
Error (+/-)[3]	3.00E-01	3.00E-01	3.00E-01	3.00E-01	3.00E-01	3.00E-01	3.00E-01	3.00E-01	3.00E-01	3.00E-01	3.00E-01	3.00E-01	3.00E-01	3.00E-01	3.00E-01	3.00E-01	
Xe-136 (g)[10]	5.45E-05	0.00E+00	0.00E+00	1.64E-02	2.48E-02	4.91E-02	6.04E-02	8.51E-02	1.00E-01	1.04E-01	8.09E-02	5.87E-02	4.09E-02	1.71E-02	4.90E-03	0.00E+00	
Error (+/-)[3]	4.08E-07	#DIV/0!	#DIV/0!	2.57E-03	2.58E-03	5.46E-03	6.72E-03	1.18E-02	1.46E-02	1.19E-02	5.21E-03	6.17E-03	5.13E-03	2.35E-03	1.64E-03	NA	
SegmentTotal																	6.42E-01
Error (+/1)[12]																	2.61E-02
Rod total																	1.58E+00
Error (+/-)[12]																	3.47E-02
Shear Gas (g)[4]	0.00E+00	0.00E+00	0.00E+00	0.00E+00	0.00E+00	2.00E-04	3.00E-04	6.00E-04	6.00E-04	6.00E-04	4.00E-04	3.00E-04	1.00E-04	1.00E-04	0.00E+00	0.00E+00	
Error (+/-)[4]	0.00E+00	0.00E+00	0.00E+00	0.00E+00	0.00E+00	0.00E+00	1.00E-04	1.00E-04	1.00E-04	1.00E-04	1.00E-04	1.00E-04	0.00E+00	0.00E+00	0.00E+00	0.00E+00	

Rod "H" 3211456 (R 4-3 B1)

	H-00	H-01	H-02	H-03	H-04	H-05	H-06	H-07	H-08	H-09	H-10	H-11	H-12	H-13	H-14	H-15	H-16
Diss+Pl Xe (mol)[3]	1.00E-06	0.00E+00	0.00E+00	3.01E-04	4.55E-04	8.99E-04	1.11E-03	1.56E-03	1.83E-03	1.91E-03	1.48E-03	1.08E-03	7.49E-04	3.14E-04	9.00E-05	0.00E+00	
Error (+/-)[3]	0.00E+00	0.00E+00	0.00E+00	4.70E-05	4.70E-05	1.00E-04	1.23E-04	2.16E-04	2.67E-04	2.18E-04	9.50E-05	1.13E-04	9.40E-05	4.30E-05	3.00E-05	0.00E+00	
Diss+Pl Kr+Xe (g)[3]	1.00E-04	0.00E+00	0.00E+00	4.76E-02	7.30E-02	1.42E-01	1.73E-01	2.47E-01	2.88E-01	2.97E-01	2.32E-01	1.78E-01	1.24E-01	5.10E-02	1.41E-02	0.00E+00	
Error (+/-)[3]	0.00E+00	0.00E+00	0.00E+00	6.80E-03	7.00E-03	1.41E-02	1.69E-02	3.42E-02	3.72E-02	2.96E-02	1.37E-02	1.60E-02	1.49E-02	6.00E-03	4.20E-03	0.00E+00	
Total Xe (mol)	1.00E-06	0.00E+00	0.00E+00	3.01E-04	4.55E-04	9.00E-04	1.11E-03	1.56E-03	1.83E-03	1.91E-03	1.48E-03	1.08E-03	7.50E-04	3.15E-04	9.00E-05	0.00E+00	
Error (+/-)[9]	0.00E+00	0.00E+00	0.00E+00	4.71E-05	4.72E-05	1.00E-04	1.23E-04	2.16E-04	2.67E-04	2.18E-04	9.50E-05	1.13E-04	9.40E-05	4.30E-05	3.00E-05	0.00E+00	
Values corrected to 1/1/84 (page 181, Final Report for the LWBR Proof of Breeding Analytical Support Project																	
Cs-137 (atoms)[5]	NA	6.75E+17	8.62E+18	3.59E+19	8.00E+19	1.48E+20	1.96E+20	2.35E+20	2.48E+20	2.36E+20	2.27E+20	1.79E+20	1.11E+20	5.27E+19	1.45E+19	1.44E+18	
Error (+/-)[4]	NA	2.32E+15	2.95E+16	1.23E+17	2.74E+17	4.16E+17	6.72E+17	8.05E+17	7.31E+17	8.08E+17	7.79E+17	5.94E+17	3.56E+17	1.75E+17	4.81E+16	4.60E+15	
Cs-137 (g)[11]	NA	1.54E-04	1.96E-03	8.15E-03	1.82E-02	3.37E-02	4.46E-02	5.34E-02	5.63E-02	5.36E-02	5.16E-02	4.08E-02	2.52E-02	1.20E-02	3.30E-03	3.27E-04	
Error (+/-)[9]	NA	5.26E-07	6.71E-06	2.79E-05	6.23E-05	9.45E-05	1.53E-04	1.83E-04	1.66E-04	1.84E-04	1.77E-04	1.35E-04	8.09E-05	3.97E-05	1.09E-05	1.05E-06	
Total																	4.03E-01
Error (+/-)[12]																	4.35E-04
Ce-144 (atoms)[5]	NA	8.91E+16	9.91E+17	3.65E+18	7.19E+18	1.22E+19	1.50E+19	1.76E+19	1.86E+19	1.76E+19	1.64E+19	1.21E+19	7.06E+18	3.16E+18	8.21E+17	7.55E+16	
Error (+/-)[4]	NA	5.16E+14	5.74E+15	2.11E+16	4.16E+16	6.43E+16	8.69E+16	1.02E+17	9.14E+16	1.02E+17	9.51E+16	6.99E+16	4.09E+16	1.88E+16	5.03E+15	4.37E+14	
Ce-144 (g)[11]	NA	2.13E-05	2.37E-04	8.71E-04	1.72E-03	2.91E-03	3.59E-03	4.20E-03	4.43E-03	4.22E-03	3.92E-03	2.88E-03	1.69E-03	7.55E-04	1.96E-04	1.80E-05	
Error (+/-)[9]	NA	1.23E-07	1.37E-06	5.04E-06	9.95E-06	1.54E-05	2.08E-05	2.43E-05	2.18E-05	2.44E-05	2.27E-05	1.67E-05	9.78E-06	4.49E-06	1.20E-06	1.04E-07	
Total																	3.17E-02
Error (+/-)[12]																	5.80E-05

Rod "H" 3211456 (R 4-3 B1)

	H-00	H-01	H-02	H-03	H-04	H-05	H-06	H-07	H-08	H-09	H-10	H-11	H-12	H-13	H-14	H-15	H-16
Zr-95 (atoms)[5]	NA	1.02E+15	9.49E+15	3.42E+16	6.76E+16	1.09E+17	1.32E+17	1.48E+17	1.55E+17	1.42E+17	1.21E+17	7.00E+16	3.01E+16	1.09E+16	1.97E+15	1.87E+14	
Error (+/-)[4]	NA	4.80E+13	1.36E+14	6.64E+14	1.40E+15	1.71E+15	1.89E+15	2.77E+15	2.71E+15	2.95E+15	2.59E+15	1.72E+15	8.23E+14	5.45E+14	7.88E+13	2.75E+13	
Zr-95 (g)[11]	NA	1.61E-07	1.50E-06	5.39E-06	1.07E-05	1.72E-05	2.08E-05	2.34E-05	2.43E-05	2.24E-05	1.91E-05	1.10E-05	4.74E-06	1.71E-06	3.11E-07	2.94E-08	
Error (+/-)[9]	NA	7.57E-09	2.14E-08	1.05E-07	2.21E-07	2.70E-07	2.98E-07	4.37E-07	4.27E-07	4.64E-07	4.09E-07	2.71E-07	1.30E-07	8.58E-08	1.24E-08	4.33E-09	
Total																	1.63E-04
Error (+/-)[12]																	1.04E-06

References

1. ANL Destructive Chemical Assay of 33-Rod LWBR EOL Sample - Rod H, 3211456, page 7
2. ANL Destructive Chemical Assay of 33-Rod LWBR EOL Sample - Rod H, 3211456, page 8
3. ANL Destructive Chemical Assay of 33-Rod LWBR EOL Sample - Rod H, 3211456, page 11
4. ANL Destructive Chemical Assay of 33-Rod LWBR EOL Sample - Rod H, 3211456, page 12
5. ANL Destructive Chemical Assay of 33-Rod LWBR EOL Sample - Rod H, 3211456, page 13
6. ANL Destructive Chemical Assay of 33-Rod LWBR EOL Sample - Rod H, 3211456, page 14
7. ANL Destructive Chemical Assay of 33-Rod LWBR EOL Sample - Rod H, 3211456, page 15
8. (abundance of the specified isotope)(total weight of uranium)

   1.00E+02
9. Error Propagation = ((+/-x/x)2+(+/-y/y)2)1/2(xy)
10. (mole%)(number moles gas recovered)(molec wt)

    1.00E+02
11. (number of atoms per segment)(atomic weight)

    6.02E+23
12. Error Propagation = (SUM(+/-I)1/2

Rod "I" 1605519 (SB1-3 E56)

	I-00	I-01	I-02	I-03	I-04	I-05	I-06	I-07	I-08	I-09
Segment length (in)	1.10E+01	1.12E+01	1.43E+01	1.41E+01	1.41E+01	1.41E+01	1.41E+01	1.42E+01	9.41E+00	1.65E+00
Total length (in)										1.18E+02
U-232 (wt%)[1]	0.00E+00	1.58E-02	3.58E-02	1.23E-01	1.85E-01	1.95E-01	1.58E-01	6.00E-02	2.75E-02	
Error (+/-)[1]	0.00E+00	5.00E-04	1.10E-03	3.80E-03	5.70E-03	6.00E-03	4.90E-03	1.90E-03	9.00E-04	
U-232 (g)[8]	0.00E+00	6.68E-05	3.33E-03	1.16E-02	1.81E-02	1.89E-02	1.48E-02	5.36E-03	2.15E-04	
Error (+/-)[9]	NA	2.11E-06	1.02E-04	3.61E-04	5.56E-04	5.83E-04	4.60E-04	1.70E-04	7.03E-06	
Segment Total										7.24E-02
Error (+/-)[12]										1.02E-03
U-233 (wt%)[1]	1.00E+02	9.91E+01	9.40E+01	8.90E+01	8.60E+01	8.55E+01	8.69E+01	9.15E+01	9.82E+01	
Error (+/-)[1]	0.00E+00	1.46E-02	6.20E-03	6.30E-03	6.90E-03	6.80E-03	6.90E-03	5.20E-03	8.00E-03	
U-233 (g)[8]	4.00E-05	4.19E-01	8.74E+00	8.45E+00	8.38E+00	8.31E+00	8.17E+00	8.18E+00	7.67E-01	
Error (+/-)[9]	1.00E-05	1.34E-04	2.30E-03	2.23E-03	2.16E-03	2.23E-03	2.11E-03	1.92E-03	1.87E-04	
Segment Total										5.14E+01
Error (+/-)[12]										5.30E-03
U-234 (wt%)[1]	0.00E+00	8.87E-01	5.12E+00	9.08E+00	1.13E+01	1.17E+01	1.07E+01	7.15E+00	1.73E+00	
Error (+/-)[1]	0.00E+00	2.10E-03	1.90E-03	1.90E-03	1.90E-03	1.90E-03	1.90E-03	1.90E-03	2.10E-03	
U-234 (g)[8]	0.00E+00	3.75E-03	4.76E-01	8.62E-01	1.10E+00	1.14E+00	1.00E+00	6.39E-01	1.35E-02	
Error (+/-)[9]	NA	8.94E-06	2.14E-04	2.84E-04	3.27E-04	3.45E-04	3.04E-04	2.23E-04	1.67E-05	
Segment Total										5.23E+00
Error (+/-)[12]										7.04E-04
U-235 (wt%)[1]	0.00E+00	1.87E-02	5.59E-01	1.48E+00	2.14E+00	2.26E+00	1.90E+00	9.49E-01	6.72E-02	
Error (+/-)[1]	0.00E+00	1.03E-02	4.40E-03	4.00E-03	3.70E-03	3.40E-03	4.10E-03	3.50E-03	5.60E-03	
U-235 (g)[8]	0.00E+00	7.90E-05	5.19E-02	1.40E-01	2.09E-01	2.19E-01	1.79E-01	8.47E-02	5.25E-04	
Error (+/-)[9]	NA	4.35E-05	4.09E-04	3.81E-04	3.64E-04	3.35E-04	3.88E-04	3.13E-04	4.38E-05	
Segment Total										8.84E-01
Error (+/-)[12]										9.00E-04
U-236 (wt%)[1]	0.00E+00	0.00E+00	3.70E-02	1.12E-01	1.96E-01	2.14E-01	1.63E-01	6.49E-02	1.10E-03	
Error (+/-)[1]	0.00E+00	2.00E-04	2.00E-04	2.00E-04	2.00E-04	2.00E-04	2.00E-04	2.00E-04	2.00E-04	
U-236 (g)[8]	0.00E+00	0.00E+00	3.44E-03	1.07E-02	1.91E-02	2.08E-02	1.53E-02	5.80E-03	8.59E-06	

Rod "I" 1605519 (SB1-3 E56)

	I-00	I-01	I-02	I-03	I-04	I-05	I-06	I-07	I-08	I-09
Error (+/-)[9]	NA	NA	1.86E-05	1.92E-05	2.01E-05	2.02E-05	1.92E-05	1.79E-05	1.56E-06	
Segment Total										7.52E-02
Error (+/-)[12]										4.70E-05
U-238 (wt%)[1]	0.00E+00	1.80E-02	2.33E-01	2.08E-01	1.91E-01	1.91E-01	2.04E-01	2.34E-01	8.70E-03	
Error (+/-)[1]	0.00E+00	1.03E-02	4.30E-03	4.00E-03	3.70E-03	3.40E-03	4.20E-03	3.50E-03	5.50E-03	
U-238 (g)[8]	0.00E+00	7.60E-05	2.17E-02	1.97E-02	1.86E-02	1.86E-02	1.91E-02	2.09E-02	6.80E-05	
Error (+/-)[9]	NA	4.35E-05	4.00E-04	3.80E-04	3.61E-04	3.31E-04	3.95E-04	3.13E-04	4.30E-05	
Segment Total										1.19E-01
Error (+/-)[12]										8.95E-04
Total U[2]	1.10E-04	4.22E-01	9.29E+00	9.49E+00	9.75E+00	9.72E+00	9.40E+00	8.93E+00	7.81E-01	
Error (+/-)[2]	1.00E-05	1.20E-04	2.37E-03	2.41E-03	2.39E-03	2.49E-03	2.31E-03	2.03E-03	1.80E-04	
Kr-82 (mol%)[3]	2.00E-01	2.00E-01	2.00E-01	2.00E-01	2.00E-01	2.00E-01	2.00E-01	2.00E-01	2.00E-01	
Error (+/-)[3]	1.00E-01	1.00E-01	1.00E-01	1.00E-01	1.00E-01	1.00E-01	1.00E-01	1.00E-01	1.00E-01	
Kr-82 (g)[10]	9.83E-07	0.00E+00	1.37E-04	2.64E-04	4.58E-04	3.51E-04	3.74E-04	1.92E-04	1.08E-07	
Error (+/-)[9]	4.91E-07	NA	7.04E-05	1.34E-04	2.34E-04	1.80E-04	1.91E-04	1.03E-04	4.91E-05	
Segment Total										1.78E-03
Error (+/-)[12]										3.96E-04
Kr-83 (mol%)[3]	1.54E+01	1.54E+01	1.54E+01	1.54E+01	1.54E+01	1.54E+01	1.54E+01	1.54E+01	1.54E+01	
Error (+/-)[3]	1.00E-01	1.00E-01	1.00E-01	1.00E-01	1.00E-01	1.00E-01	1.00E-01	1.00E-01	1.00E-01	
Kr-83 (g)[10]	7.66E-05	0.00E+00	1.07E-02	2.06E-02	3.57E-02	2.73E-02	2.92E-02	1.50E-02	8.38E-06	
Error (+/-)[9]	4.97E-07	NA	1.33E-03	1.87E-03	3.70E-03	3.04E-03	2.98E-03	2.85E-03	3.83E-03	
Segment Total										1.39E-01
Error (+/-)[12]										6.72E-03
Kr-84 (mol%)[3]	3.02E+01	3.02E+01	3.02E+01	3.02E+01	3.02E+01	3.02E+01	3.02E+01	3.02E+01	3.02E+01	
Error (+/-)[3]	2.00E-01	2.00E-01	2.00E-01	2.00E-01	2.00E-01	2.00E-01	2.00E-01	2.00E-01	2.00E-01	
Kr-84 (g)[10]	1.52E-04	0.00E+00	2.11E-02	4.08E-02	7.09E-02	5.43E-02	5.79E-02	2.97E-02	1.66E-05	
Error (+/-)[9]	1.01E-06	NA	2.64E-03	3.71E-03	7.34E-03	6.04E-03	5.92E-03	5.65E-03	7.60E-03	
Segment Total										2.75E-01
Error (+/-)[12]										1.33E-02

Rod "I" 1605519 (SB1-3 E56)

	I-00	I-01	I-02	I-03	I-04	I-05	I-06	I-07	I-08	I-09
Kr-85 (mol%)[3]	5.80E+00	5.80E+00	5.80E+00	5.80E+00	5.80E+00	5.80E+00	5.80E+00	5.80E+00	5.80E+00	
Error (+/-)[3]	1.00E-01	1.00E-01	1.00E-01	1.00E-01	1.00E-01	1.00E-01	1.00E-01	1.00E-01	1.00E-01	
Kr-85 (g)[10]	2.95E-05	0.00E+00	4.11E-03	7.94E-03	1.38E-02	1.05E-02	1.13E-02	5.77E-03	3.23E-06	
Error (+/-)[9]	5.09E-07	NA	5.17E-04	7.32E-04	1.44E-03	1.19E-03	1.16E-03	1.10E-03	1.48E-03	
Segment Total										5.34E-02
Error (+/-)[12]										2.62E-03
Kr-86 (mol%)[3]	4.86E+01	4.86E+01	4.86E+01	4.86E+01	4.86E+01	4.86E+01	4.86E+01	4.86E+01	4.86E+01	
Error (+/-)[3]	2.00E-01	2.00E-01	2.00E-01	2.00E-01	2.00E-01	2.00E-01	2.00E-01	2.00E-01	2.00E-01	
Kr-86 (g)[10]	2.51E-04	0.00E+00	3.48E-02	6.73E-02	1.17E-01	8.94E-02	9.54E-02	4.90E-02	2.74E-05	
Error (+/-)[9]	1.03E-06	NA	4.34E-03	6.10E-03	1.21E-02	9.94E-03	9.74E-03	9.31E-03	1.25E-02	
Segment Total										4.53E-01
Error (+/-)[12]										2.20E-02
Rod Total										9.22E-01
Error (+/-)[12]										2.67E-02
Shear Gas (g)[4]	0.00E+00	0.00E+00	9.00E-04	2.30E-03	3.30E-03	3.30E-03	3.00E-03	2.10E-03	4.00E-04	
Error (+/-)[4]	0.00E+00	3.00E-04	3.00E-04	5.00E-04	7.00E-04	7.00E-04	6.00E-04	4.00E-04	3.00E-04	
Diss+Pl Kr (mol)[3]	6.00E-06	0.00E+00	8.33E-04	1.61E-03	2.79E-03	2.14E-03	2.28E-03	1.17E-03	0.00E+00	
Error (+/-)[3]	0.00E+00	0.00E+00	1.04E-04	1.46E-04	2.89E-04	2.38E-04	2.33E-04	2.23E-04	0.00E+00	
Diss+Pl Kr+Xe (g)[3]	3.30E-03	0.00E+00	5.39E-01	9.87E-01	1.66E+00	1.46E+00	1.26E+00	7.12E-01	0.00E+00	
Error (+/-)[3]	2.00E-04	0.00E+00	2.28E-02	6.66E-02	1.32E-01	1.29E-01	1.27E-01	6.27E-02	0.00E+00	
Total Kr (mol)	6.00E-06	0.00E+00	8.34E-04	1.61E-03	2.80E-03	2.14E-03	2.29E-03	1.17E-03	6.57E-07	
Error (+/-)[9]	0.00E+00	0.00E+00	1.04E-04	1.46E-04	2.89E-04	2.38E-04	2.33E-04	2.23E-04	3.00E-04	
Xe-128 (mol)[3]	1.00E-01	1.00E-01	1.00E-01	1.00E-01	1.00E-01	1.00E-01	1.00E-01	1.00E-01	1.00E-01	
Error (+/-)[3]	0.00E+00	0.00E+00	0.00E+00	0.00E+00	0.00E+00	0.00E+00	0.00E+00	0.00E+00	0.00E+00	
Xe-128 (g)[10]	2.69E-06	0.00E+00	4.47E-04	8.12E-04	1.36E-03	1.22E-03	1.01E-03	5.86E-04	3.28E-07	
Error (+/-)[3]	1.28E-07	NA	2.00E-05	6.23E-05	1.23E-04	1.22E-04	1.19E-04	5.69E-05	9.84E-11	
SegmentTotal										5.44E-03
Error (+/1)[12]										2.27E-04
Xe-130 (mol)[3]	1.00E-01	1.00E-01	1.00E-01	1.00E-01	1.00E-01	1.00E-01	1.00E-01	1.00E-01	1.00E-01	

Rod "I" 1605519 (SB1-3 E56)

	I-00	I-01	I-02	I-03	I-04	I-05	I-06	I-07	I-08	I-09
Error (+/-)[3]	0.00E+00	0.00E+00	0.00E+00	0.00E+00	0.00E+00	0.00E+00	0.00E+00	0.00E+00	0.00E+00	
Xe-130 (g)[10]	2.73E-06	0.00E+00	4.54E-04	8.25E-04	1.38E-03	1.24E-03	1.03E-03	5.95E-04	3.33E-07	
Error (+/-)[3]	1.30E-07	NA	2.03E-05	6.33E-05	1.25E-04	1.23E-04	1.21E-04	5.78E-05	9.99E-11	
SegmentTotal										5.52E-03
Error (+/1)[12]										2.31E-04
Xe-131 (mol)[3]	1.14E+01	1.14E+01	1.14E+01	1.14E+01	1.14E+01	1.14E+01	1.14E+01	1.14E+01	1.14E+01	
Error (+/-)[3]	1.00E-01	1.00E-01	1.00E-01	1.00E-01	1.00E-01	1.00E-01	1.00E-01	1.00E-01	1.00E-01	
Xe-131 (g)[10]	3.13E-04	0.00E+00	5.22E-02	9.48E-02	1.58E-01	1.42E-01	1.18E-01	6.83E-02	3.83E-05	
Error (+/-)[3]	1.52E-05	NA	2.37E-03	7.32E-03	1.44E-02	1.42E-02	1.39E-02	6.67E-03	3.36E-07	
SegmentTotal										6.34E-01
Error (+/1)[12]										2.66E-02
Xe-132 (mol)[3]	2.27E+01	2.27E+01	2.27E+01	2.27E+01	2.27E+01	2.27E+01	2.27E+01	2.27E+01	2.27E+01	
Error (+/-)[3]	1.00E-01	1.00E-01	1.00E-01	1.00E-01	1.00E-01	1.00E-01	1.00E-01	1.00E-01	1.00E-01	
Xe-132 (g)[10]	6.29E-04	0.00E+00	1.05E-01	1.90E-01	3.18E-01	2.85E-01	2.37E-01	1.37E-01	7.68E-05	
Error (+/-)[3]	3.01E-05	NA	4.69E-03	1.46E-02	2.89E-02	2.85E-02	2.79E-02	1.33E-02	3.39E-07	
SegmentTotal										1.27E+00
Error (+/1)[12]										5.33E-02
Xe-134 (mol)[3]	2.58E+01	2.58E+01	2.58E+01	2.58E+01	2.58E+01	2.58E+01	2.58E+01	2.58E+01	2.58E+01	
Error (+/-)[3]	1.00E-01	1.00E-01	1.00E-01	1.00E-01	1.00E-01	1.00E-01	1.00E-01	1.00E-01	1.00E-01	
Xe-134 (g)[10]	7.25E-04	0.00E+00	1.21E-01	2.19E-01	3.67E-01	3.29E-01	2.74E-01	1.58E-01	8.86E-05	
Error (+/-)[3]	3.47E-05	NA	5.41E-03	1.68E-02	3.33E-02	3.28E-02	3.22E-02	1.54E-02	3.44E-07	
SegmentTotal										1.47E+00
Error (+/1)[12]										6.14E-02
Xe-136 (mol)[3]	4.00E+01	4.00E+01	4.00E+01	4.00E+01	4.00E+01	4.00E+01	4.00E+01	4.00E+01	4.00E+01	
Error (+/-)[3]	1.00E-01	1.00E-01	1.00E-01	1.00E-01	1.00E-01	1.00E-01	1.00E-01	1.00E-01	1.00E-01	
Xe-136 (g)[10]	1.14E-03	0.00E+00	1.90E-01	3.45E-01	5.77E-01	5.18E-01	4.31E-01	2.49E-01	1.39E-04	
Error (+/-)[3]	5.44E-05	NA	8.49E-03	2.65E-02	5.24E-02	5.17E-02	5.06E-02	2.42E-02	3.51E-07	
SegmentTotal										2.31E+00
Error (+/1)[12]										9.66E-02
Rod total										5.70E+00

Rod "I" 1605519 (SB1-3 E56)

	I-00	I-01	I-02	I-03	I-04	I-05	I-06	I-07	I-08	I-09
Error (+/-)[12]										1.29E-01
Shear Gas (g)[4]	0.00E+00	0.00E+00	9.00E-04	2.30E-03	3.30E-03	3.30E-03	3.00E-03	2.10E-03	4.00E-04	
Error (+/-)[4]	0.00E+00	3.00E-04	3.00E-04	5.00E-04	7.00E-04	7.00E-04	6.00E-04	4.00E-04	3.00E-04	
Diss+Pl Xe (mol)[3]	2.10E-05	0.00E+00	3.49E-03	6.34E-03	1.06E-02	9.50E-03	7.91E-03	4.57E-03	0.00E+00	
Error (+/-)[3]	1.00E-06	0.00E+00	1.56E-04	4.87E-04	9.63E-04	9.50E-04	9.31E-04	4.45E-04	0.00E+00	
Diss+Pl Kr+Xe (g)[3]	3.30E-03	0.00E+00	5.39E-01	9.87E-01	1.66E+00	1.46E+00	1.26E+00	7.12E-01	0.00E+00	
Error (+/-)[3]	2.00E-04	0.00E+00	2.28E-02	6.66E-02	1.32E-01	1.29E-01	1.27E-01	6.27E-02	0.00E+00	
Total Xe (mol)	2.10E-05	0.00E+00	3.50E-03	6.35E-03	1.06E-02	9.52E-03	7.93E-03	4.58E-03	2.56E-06	
Error (+/-)[9]	1.00E-06	0.00E+00	1.56E-04	4.87E-04	9.63E-04	9.50E-04	9.31E-04	4.45E-04	7.69E-10	
Values corrected to 1/1/84 (page 181, Final Report for the LWBR Proof of Breeding Analytical Support Project										
Cs-137 (atoms)[5]	ND	4.71E+18	4.82E+20	1.04E+21	1.39E+21	1.45E+21	1.26E+21	7.26E+20	1.62E+19	
Error (+/-)[4]	NA	2.09E+16	2.13E+18	4.58E+18	6.13E+18	6.14E+18	5.33E+18	3.21E+18	6.90E+16	
Cs-137 (g)[11]	NA	1.07E-03	1.10E-01	2.35E-01	3.16E-01	3.28E-01	2.85E-01	1.65E-01	3.67E-03	
Error (+/-)[9]	NA	4.76E-06	4.84E-04	1.04E-03	1.39E-03	1.39E-03	1.21E-03	7.30E-04	1.57E-05	
Total										1.44E+00
Error (+/-)[12]										2.68E-03
Ce-144 (atoms)[5]	ND	5.96E+17	3.26E+19	5.51E+19	6.80E+19	7.14E+19	5.57E+19	2.72E+19	7.65E+17	
Error (+/-)[4]	NA	3.77E+15	2.20E+17	3.81E+17	4.59E+17	4.60E+17	3.67E+17	1.88E+17	4.84E+15	
Ce-144 (g)[11]	NA	1.42E-04	7.79E-03	1.32E-02	1.63E-02	1.71E-02	1.33E-02	6.50E-03	1.83E-04	
Error (+/-)[9]	NA	9.00E-07	5.26E-05	9.11E-05	1.10E-04	1.10E-04	8.76E-05	4.49E-05	1.16E-06	
Total										7.44E-02
Error (+/-)[12]										2.12E-04
Zr-95 (atoms)[5]	ND	6.52E+15	2.64E+17	4.44E+17	5.28E+17	5.37E+17	2.66E+17	7.16E+16	1.45E+15	
Error (+/-)[4]	NA	1.37E+14	1.02E+16	1.91E+16	1.99E+16	2.68E+16	1.63E+16	8.72E+15	1.02E+14	
Zr-95 (g)[11]	NA	1.03E-06	4.16E-05	7.00E-05	8.32E-05	8.46E-05	4.19E-05	1.13E-05	2.28E-07	
Error (+/-)[9]	NA	2.16E-08	1.61E-06	3.01E-06	3.14E-06	4.22E-06	2.56E-06	1.37E-06	1.61E-08	
Total										3.34E-04
Error (+/-)[12]										6.91E-06

Rod "I" 1605519 (SB1-3 E56)

	I-00	I-01	I-02	I-03	I-04	I-05	I-06	I-07	I-08	I-09

References

1. ANL Destructive Chemical Assay of 33-Rod LWBR EOL Sample - Rod I, 1605519, page 6
2. ANL Destructive Chemical Assay of 33-Rod LWBR EOL Sample - Rod I, 1605519, page 7
3. ANL Destructive Chemical Assay of 33-Rod LWBR EOL Sample - Rod I, 1605519, page 10
4. ANL Destructive Chemical Assay of 33-Rod LWBR EOL Sample - Rod I, 1605519, page 11
5. ANL Destructive Chemical Assay of 33-Rod LWBR EOL Sample - Rod I, 1605519, page 12
6. ANL Destructive Chemical Assay of 33-Rod LWBR EOL Sample - Rod I, 1605519, page 13
7. ANL Destructive Chemical Assay of 33-Rod LWBR EOL Sample - Rod I, 1605519, page 14
8. (abundance of the specified isotope)(total weight of uranium)

   1.00E+02

9. Error Propagation = ((+/-x/x)2+(+/-y/y)2)1/2(xy)
10. (mole%)(number moles gas recovered)(molec wt)

    1.00E+02

11. (number of atoms per segment)(atomic weight)

    6.02E+23

12. Error Propagation = (SUM(+/-I)1/2

Rod "J" 1200830 (SB1-3 A49)

	J-00	J-01	J-02	J-03	J-04	J-05	J-06	J-07	J-08	J-09
Segment length (in)	1.13E+01	1.14E+01	1.42E+01	1.40E+01	1.41E+01	1.39E+01	1.05E+01	1.40E+01	1.30E+01	1.62E+00
Total length (in)										1.18E+02
U-232 (wt%)[1]	0.00E+00	1.76E-02	5.64E-02	1.69E-01	2.36E-01	2.70E-01	2.54E-01	1.75E-01	5.84E-02	
Error (+/-)[1]	0.00E+00	5.00E-04	1.70E-03	5.20E-03	7.30E-03	8.40E-03	7.90E-03	5.40E-03	1.80E-03	
U-232 (g)[8]	0.00E+00	9.75E-05	3.72E-03	1.27E-02	1.94E-02	1.84E-02	1.20E-02	8.08E-03	9.38E-04	
Error (+/-)[9]	NA	2.77E-06	1.12E-04	3.92E-04	6.00E-04	5.72E-04	3.72E-04	2.50E-04	2.89E-05	
Segment Total										7.53E-02
Error (+/-)[12]										1.03E-03
U-233 (wt%)[1]	1.00E+02	9.87E+01	9.27E+01	8.69E+01	8.38E+01	8.63E+01	8.78E+01	9.17E+01	9.71E+01	
Error (+/-)[1]	0.00E+00	1.19E-02	9.10E-03	9.00E-03	9.30E-03	1.07E-02	9.40E-03	6.70E-03	8.80E-03	
U-233 (g)[8]	4.00E-05	5.47E-01	6.12E+00	6.55E+00	6.88E+00	5.87E+00	4.13E+00	4.25E+00	1.56E+00	
Error (+/-)[9]	1.00E-05	1.53E-04	1.80E-03	4.82E-03	2.10E-03	1.82E-03	1.09E-03	9.16E-04	5.52E-04	
Segment Total										3.59E+01
Error (+/-)[12]										6.05E-03
U-234 (wt%)[1]	0.00E+00	1.18E+00	6.24E+00	1.07E+01	1.29E+01	1.11E+01	9.97E+00	7.06E+00	2.70E+00	
Error (+/-)[1]	0.00E+00	8.00E-04	1.00E-03	1.50E-03	1.70E-03	1.70E-03	1.30E-03	8.00E-04	8.00E-04	
U-234 (g)[8]	0.00E+00	6.56E-03	4.12E-01	8.05E-01	1.06E+00	7.53E-01	4.69E-01	3.27E-01	4.34E-02	
Error (+/-)[9]	NA	4.73E-06	1.32E-04	5.98E-04	3.32E-04	2.43E-04	1.29E-04	7.60E-05	1.96E-05	
Segment Total										3.87E+00
Error (+/-)[12]										7.53E-04
U-235 (wt%)[1]	0.00E+00	3.75E-02	7.44E-01	1.94E+00	2.67E+00	2.17E+00	1.81E+00	9.83E-01	1.66E-01	
Error (+/-)[1]	0.00E+00	9.30E-03	7.50E-03	6.90E-03	6.30E-03	6.90E-03	5.70E-03	4.30E-03	7.00E-03	
U-235 (g)[8]	0.00E+00	2.08E-04	4.91E-02	1.46E-01	2.19E-01	1.48E-01	8.50E-02	4.55E-02	2.66E-03	
Error (+/-)[9]	NA	5.15E-05	4.95E-04	5.31E-04	5.21E-04	4.71E-04	2.69E-04	1.99E-04	1.12E-04	
Segment Total										6.96E-01
Error (+/-)[12]										1.07E-03
U-236 (wt%)[1]	0.00E+00	1.20E-03	4.57E-02	1.75E-01	3.01E-01	2.14E-01	1.55E-01	5.97E-02	4.10E-03	
Error (+/-)[1]	0.00E+00	1.00E-04	1.00E-04	1.00E-04	1.00E-04	1.00E-04	1.00E-04	1.00E-04	1.00E-04	
U-236 (g)[8]	0.00E+00	6.64E-06	3.02E-03	1.32E-02	2.47E-02	1.45E-02	7.31E-03	2.77E-03	6.59E-05	

Rod "J" 1200830 (SB1-3 A49)

	J-00	J-01	J-02	J-03	J-04	J-05	J-06	J-07	J-08	J-09
Error (+/-)[9]	NA	5.54E-07	6.65E-06	1.22E-05	1.08E-05	7.96E-06	5.03E-06	4.67E-06	1.61E-06	
Segment Total										6.55E-02
Error (+/-)[12]										2.06E-05
U-238 (wt%)[1]	0.00E+00	2.63E-02	2.00E-01	1.55E-01	1.32E-01	3.00E-03	2.10E-03	1.90E-03	4.30E-03	
Error (+/-)[1]	0.00E+00	7.60E-03	6.00E-03	5.50E-03	5.10E-03	5.60E-03	4.30E-03	2.40E-03	5.40E-03	
U-238 (g)[8]	0.00E+00	1.46E-04	1.32E-02	1.17E-02	1.09E-02	2.04E-04	9.88E-05	8.80E-05	6.91E-05	
Error (+/-)[9]	NA	4.21E-05	3.96E-04	4.14E-04	4.19E-04	3.81E-04	2.02E-04	1.11E-04	8.68E-05	
Segment Total										3.64E-02
Error (+/-)[12]										8.44E-04
Total U[2]	1.50E-04	5.54E-01	6.60E+00	7.53E+00	8.21E+00	6.80E+00	4.71E+00	4.63E+00	1.61E+00	
Error (+/-)[2]	8.00E-05	1.40E-04	1.83E-03	5.49E-03	2.34E-03	1.93E-03	1.14E-03	9.40E-04	5.50E-04	
Kr-82 (mol%)[3]	2.00E-01	2.00E-01	2.00E-01	2.00E-01	2.00E-01	2.00E-01	2.00E-01	2.00E-01	2.00E-01	
Error (+/-)[3]	1.00E-01	1.00E-01	1.00E-01	1.00E-01	1.00E-01	1.00E-01	1.00E-01	1.00E-01	1.00E-01	
Kr-82 (g)[10]	4.91E-07	0.00E+00	1.18E-04	2.90E-04	3.95E-04	2.37E-04	1.43E-04	1.46E-04	2.70E-05	
Error (+/-)[9]	2.46E-07	NA	7.08E-05	1.52E-04	2.02E-04	1.21E-04	7.41E-05	7.53E-05	1.49E-05	
Segment Total										1.36E-03
Error (+/-)[12]										3.08E-04
Kr-83 (mol%)[3]	1.47E+01	1.47E+01	1.47E+01	1.47E+01	1.47E+01	1.47E+01	1.47E+01	1.47E+01	1.47E+01	
Error (+/-)[3]	1.00E-01	1.00E-01	1.00E-01	1.00E-01	1.00E-01	1.00E-01	1.00E-01	1.00E-01	1.00E-01	
Kr-83 (g)[10]	3.66E-05	0.00E+00	8.77E-03	2.15E-02	2.94E-02	1.76E-02	1.06E-02	1.09E-02	2.01E-03	
Error (+/-)[9]	2.49E-07	NA	2.91E-03	3.48E-03	2.94E-03	1.95E-03	1.51E-03	1.35E-03	4.76E-04	
Segment Total										1.01E-01
Error (+/-)[12]										6.12E-03
Kr-84 (mol%)[3]	3.06E+01	3.06E+01	3.06E+01	3.06E+01	3.06E+01	3.06E+01	3.06E+01	3.06E+01	3.06E+01	
Error (+/-)[3]	1.00E-01	1.00E-01	1.00E-01	1.00E-01	1.00E-01	1.00E-01	1.00E-01	1.00E-01	1.00E-01	
Kr-84 (g)[10]	7.70E-05	0.00E+00	1.85E-02	4.54E-02	6.20E-02	3.71E-02	2.23E-02	2.29E-02	4.23E-03	
Error (+/-)[9]	2.52E-07	NA	6.14E-03	7.32E-03	6.19E-03	4.11E-03	3.18E-03	2.85E-03	1.00E-03	
Segment Total										2.13E-01
Error (+/-)[12]										1.29E-02

Rod "J" 1200830 (SB1-3 A49)

	J-00	J-01	J-02	J-03	J-04	J-05	J-06	J-07	J-08	J-09
Kr-85 (mol%)[3]	6.00E+00	6.00E+00	6.00E+00	6.00E+00	6.00E+00	6.00E+00	6.00E+00	6.00E+00	6.00E+00	
Error (+/-)[3]	1.00E-01	1.00E-01	1.00E-01	1.00E-01	1.00E-01	1.00E-01	1.00E-01	1.00E-01	1.00E-01	
Kr-85 (g)[10]	1.53E-05	0.00E+00	3.67E-03	9.01E-03	1.23E-02	7.36E-03	4.43E-03	4.55E-03	8.39E-04	
Error (+/-)[9]	2.55E-07	NA	1.22E-03	1.46E-03	1.24E-03	8.24E-04	6.36E-04	5.71E-04	1.99E-04	
Segment Total										4.22E-02
Error (+/-)[12]										2.57E-03
Kr-86 (mol%)[3]	4.86E+01	4.86E+01	4.86E+01	4.86E+01	4.86E+01	4.86E+01	4.86E+01	4.86E+01	4.86E+01	
Error (+/-)[3]	2.00E-01	4.86E+01	4.86E+01	4.86E+01	4.86E+01	4.86E+01	4.86E+01	4.86E+01	4.86E+01	
Kr-86 (g)[10]	1.25E-04	0.00E+00	3.00E-02	7.38E-02	1.01E-01	6.04E-02	3.63E-02	3.73E-02	6.87E-03	
Error (+/-)[9]	5.15E-07	NA	3.17E-02	7.48E-02	1.01E-01	6.07E-02	3.67E-02	3.75E-02	7.06E-03	
Segment Total										3.46E-01
Error (+/-)[12]										1.53E-01
Rod Total										7.03E-01
Error (+/-)[12]										1.53E-01
Shear Gas (g)[4]	0.00E+00	0.00E+00	1.00E-03	2.90E-03	4.10E-03	3.70E-03	2.40E-03	1.40E-03	3.00E-04	
Error (+/-)[4]	0.00E+00	3.00E-04	3.00E-04	6.00E-04	8.00E-04	7.00E-04	5.00E-04	3.00E-04	3.00E-04	
Diss+Pl Kr (mol)[3]	3.00E-06	0.00E+00	7.18E-04	1.76E-03	2.41E-03	1.44E-03	8.66E-04	8.90E-04	1.64E-04	
Error (+/-)[3]	0.00E+00	0.00E+00	2.39E-04	2.85E-04	2.41E-04	1.60E-04	1.24E-04	1.11E-04	3.90E-05	
Diss+Pl Kr+Xe (g)[3]	1.60E-03	9.90E-03	4.63E-01	1.07E+00	1.40E+00	9.82E-01	4.89E-01	5.09E-01	8.10E-02	
Error (+/-)[3]	0.00E+00	9.90E-03	8.29E-02	1.73E-01	1.15E-01	1.44E-01	5.09E-02	3.14E-02	1.10E-02	
Total Kr (mol)	3.00E-06	0.00E+00	7.20E-04	1.77E-03	2.41E-03	1.45E-03	8.70E-04	8.92E-04	1.65E-04	
Error (+/-)[9]	0.00E+00	9.90E-03	2.39E-04	2.85E-04	2.41E-04	1.60E-04	1.24E-04	1.11E-04	3.90E-05	
Xe-128 (mol)[3]	1.00E-01	1.00E-01	1.00E-01	1.00E-01	1.00E-01	1.00E-01	1.00E-01	1.00E-01	1.00E-01	
Error (+/-)[3]	0.00E+00	0.00E+00	0.00E+00	0.00E+00	0.00E+00	0.00E+00	0.00E+00	0.00E+00	0.00E+00	
Xe-128 (g)[10]	1.28E-06	9.46E-06	3.83E-04	8.79E-04	1.14E-03	8.21E-04	3.97E-04	4.14E-04	6.42E-05	
Error (+/-)[3]	0.00E+00	9.47E-06	7.65E-05	1.41E-04	1.05E-04	1.36E-04	4.75E-05	2.85E-05	9.98E-06	
SegmentTotal										4.11E-03
Error (+/1)[12]										2.43E-04

Rod "J" 1200830 (SB1-3 A49)

	J-00	J-01	J-02	J-03	J-04	J-05	J-06	J-07	J-08	J-09
Xe-130 (mol)[3]	2.00E-01	2.00E-01	2.00E-01	2.00E-01	2.00E-01	2.00E-01	2.00E-01	2.00E-01	2.00E-01	
Error (+/-)[3]	0.00E+00	0.00E+00	0.00E+00	0.00E+00	0.00E+00	0.00E+00	0.00E+00	0.00E+00	0.00E+00	
Xe-130 (g)[10]	2.60E-06	1.92E-05	7.79E-04	1.78E-03	2.32E-03	1.67E-03	8.07E-04	8.40E-04	1.30E-04	
Error (+/-)[3]	0.00E+00	1.92E-05	1.55E-04	2.87E-04	2.14E-04	2.77E-04	9.64E-05	5.79E-05	2.03E-05	
SegmentTotal										8.35E-03
Error (+/1)[12]										4.93E-04
Xe-131 (mol)[3]	1.06E+01	1.06E+01	1.06E+01	1.06E+01	1.06E+01	1.06E+01	1.06E+01	1.06E+01	1.06E+01	
Error (+/-)[3]	1.00E-01	1.00E-01	1.00E-01	1.00E-01	1.00E-01	1.00E-01	1.00E-01	1.00E-01	1.00E-01	
Xe-131 (g)[10]	1.39E-04	1.03E-03	4.16E-02	9.53E-02	1.24E-01	8.91E-02	4.31E-02	4.49E-02	6.96E-03	
Error (+/-)[3]	1.31E-06	1.03E-03	8.31E-03	1.54E-02	1.15E-02	1.48E-02	5.16E-03	3.12E-03	1.08E-03	
SegmentTotal										4.46E-01
Error (+/1)[12]										2.64E-02
Xe-132 (mol)[3]	2.23E+01	2.23E+01	2.23E+01	2.23E+01	2.23E+01	2.23E+01	2.23E+01	2.23E+01	2.23E+01	
Error (+/-)[3]	1.00E-01	1.00E-01	1.00E-01	1.00E-01	1.00E-01	1.00E-01	1.00E-01	1.00E-01	1.00E-01	
Xe-132 (g)[10]	2.94E-04	2.18E-03	8.81E-02	2.02E-01	2.63E-01	1.89E-01	9.14E-02	9.52E-02	1.48E-02	
Error (+/-)[3]	1.32E-06	2.18E-03	1.76E-02	3.25E-02	2.43E-02	3.14E-02	1.09E-02	6.57E-03	2.30E-03	
SegmentTotal										9.46E-01
Error (+/1)[12]										5.58E-02
Xe-134 (mol)[3]	2.47E+01	2.47E+01	2.47E+01	2.47E+01	2.47E+01	2.47E+01	2.47E+01	2.47E+01	2.47E+01	
Error (+/-)[3]	1.00E-01	1.00E-01	1.00E-01	1.00E-01	1.00E-01	1.00E-01	1.00E-01	1.00E-01	1.00E-01	
Xe-134 (g)[10]	3.31E-04	2.45E-03	9.91E-02	2.27E-01	2.95E-01	2.12E-01	1.03E-01	1.07E-01	1.66E-02	
Error (+/-)[3]	1.34E-06	2.45E-03	1.98E-02	3.66E-02	2.73E-02	3.53E-02	1.23E-02	7.39E-03	2.58E-03	
SegmentTotal										1.06E+00
Error (+/1)[12]										6.27E-02
Xe-136 (mol)[3]	4.21E+01	4.21E+01	4.21E+01	4.21E+01	4.21E+01	4.21E+01	4.21E+01	4.21E+01	4.21E+01	
Error (+/-)[3]	1.00E-01	1.00E-01	1.00E-01	1.00E-01	1.00E-01	1.00E-01	1.00E-01	1.00E-01	1.00E-01	
Xe-136 (g)[10]	5.72E-04	4.23E-03	1.71E-01	3.93E-01	5.11E-01	3.67E-01	1.78E-01	1.85E-01	2.87E-02	
Error (+/-)[3]	1.36E-06	4.23E-03	3.42E-02	6.33E-02	4.72E-02	6.10E-02	2.12E-02	1.28E-02	4.46E-03	
SegmentTotal										1.84E+00
Error (+/1)[12]										1.09E-01

Rod "J" 1200830 (SB1-3 A49)

	J-00	J-01	J-02	J-03	J-04	J-05	J-06	J-07	J-08	J-09
Rod total										4.31E+00
Error (+/-)[12]										1.40E-01
Shear Gas (g)[4]	0.00E+00	0.00E+00	1.00E-03	2.90E-03	4.10E-03	3.70E-03	2.40E-03	1.40E-03	3.00E-04	
Error (+/-)[4]	0.00E+00	3.00E-04	3.00E-04	6.00E-04	8.00E-04	7.00E-04	5.00E-04	3.00E-04	3.00E-04	
Diss+Pl Xe (mol)[3]	1.00E-05	7.40E-05	2.99E-03	6.85E-03	8.91E-03	6.40E-03	3.09E-03	3.23E-03	5.00E-04	
Error (+/-)[3]	0.00E+00	7.40E-05	5.98E-04	1.11E-03	8.24E-04	1.07E-03	3.71E-04	2.23E-04	7.80E-05	
Diss+Pl Kr+Xe (g)[3]	1.60E-03	9.90E-03	4.63E-01	1.07E+00	1.40E+00	9.82E-01	4.89E-01	5.09E-01	8.10E-02	
Error (+/-)[3]	0.00E+00	9.90E-03	8.29E-02	1.73E-01	1.15E-01	1.44E-01	5.09E-02	3.14E-02	1.10E-02	
Total Xe (mol)	1.00E-05	7.40E-05	3.00E-03	6.87E-03	8.93E-03	6.42E-03	3.11E-03	3.23E-03	5.02E-04	
Error (+/-)[9]	0.00E+00	7.40E-05	5.98E-04	1.11E-03	8.24E-04	1.07E-03	3.71E-04	2.23E-04	7.80E-05	
Values corrected to 1/1/84 (page 181, Final Report for the LWBR Proof of Breeding Analytical Support Project										
Cs-137 (atoms)[5]	NA	7.96E+18	4.79E+20	1.06E+21	1.43E+21	9.50E+20	5.73E+20	3.92E+20	5.20E+19	
Error (+/-)[4]	NA	3.03E+16	1.76E+18	3.37E+18	5.12E+18	3.42E+18	2.06E+18	1.40E+18	1.87E+17	
Cs-137 (g)[11]	NA	1.81E-03	1.09E-01	2.40E-01	3.26E-01	2.16E-01	1.30E-01	8.92E-02	1.18E-02	
Error (+/-)[9]	NA	6.88E-06	4.00E-04	7.66E-04	1.16E-03	7.78E-04	4.69E-04	3.18E-04	4.25E-05	
Total										1.12E+00
Error (+/-)[12]										1.74E-03
Ce-144 (atoms)[5]	NA	9.50E+17	3.27E+19	5.90E+19	7.59E+19	6.45E+19	3.72E+19	2.27E+19	2.66E+18	
Error (+/-)[4]	NA	6.84E+15	2.39E+17	3.85E+17	5.46E+17	4.65E+17	2.68E+17	1.63E+17	1.91E+16	
Ce-144 (g)[11]	NA	2.27E-04	7.82E-03	1.41E-02	1.81E-02	1.54E-02	8.88E-03	5.42E-03	6.35E-04	
Error (+/-)[9]	NA	1.63E-06	5.72E-05	9.20E-05	1.30E-04	1.11E-04	6.39E-05	3.89E-05	4.57E-06	
Total										7.06E-02
Error (+/-)[12]										2.16E-04
Zr-95 (atoms)[5]	NA	9.40E+15	3.03E+17	4.67E+17	5.85E+17	4.98E+17	2.23E+17	8.83E+16	6.39E+15	
Error (+/-)[4]	NA	1.97E+14	1.02E+16	2.05E+16	2.90E+16	1.44E+16	1.09E+16	6.72E+15	4.76E+14	
Zr-95 (g)[11]	NA	1.48E-06	4.77E-05	7.36E-05	9.22E-05	7.85E-05	3.51E-05	1.39E-05	1.01E-06	
Error (+/-)[9]	NA	3.10E-08	1.61E-06	3.23E-06	4.56E-06	2.27E-06	1.72E-06	1.06E-06	7.51E-08	
Total										3.43E-04

Rod "J" 1200830 (SB1-3 A49)

[redacted]

	J-00	J-01	J-02	J-03	J-04	J-05	J-06	J-07	J-08	J-09
Error (+/-)[12]										6.56E-06

[redacted]

References

1. ANL Destructive Chemical Assay of 33-Rod LWBR EOL Sample - Rod J, 1200830, page 6
2. ANL Destructive Chemical Assay of 33-Rod LWBR EOL Sample - Rod J, 1200830, page 7
3. ANL Destructive Chemical Assay of 33-Rod LWBR EOL Sample - Rod J, 1200830, page 10
4. ANL Destructive Chemical Assay of 33-Rod LWBR EOL Sample - Rod J, 1200830, page 11
5. ANL Destructive Chemical Assay of 33-Rod LWBR EOL Sample - Rod J, 1200830, page 12
6. ANL Destructive Chemical Assay of 33-Rod LWBR EOL Sample - Rod J, 1200830, page 13
7. ANL Destructive Chemical Assay of 33-Rod LWBR EOL Sample - Rod J, 1200830, page 14
8. (abundance of the specified isotope)(total weight of uranium)

   1.00E+02
9. Error Propagation = ((+/-x/x)2+(+/-y/y)2)1/2(xy)
10. (mole%)(number moles gas recovered)(molec wt)

    1.00E+02
11. (number of atoms per segment)(atomic weight)

    6.02E+23
12. Error Propagation = (SUM(+/-I)1/2

Rod "K" 1302864 (SB1-3 D24)

	K-00	K-01	K-02	K-03	K-04	K-05	K-06	K-07	K-08	K-09
Segment length (in)	1.14E+01	8.31E+00	1.42E+01	1.40E+01	1.40E+01	1.40E+01	1.41E+01	1.04E+01	1.50E+01	2.64E+00
Total length (in)										1.18E+02
U-232 (wt%)[1]	0.00E+00	1.28E-02	2.91E-02	1.05E-01	1.59E-01	1.68E-01	1.33E-01	1.37E-01	4.44E-02	
Error (+/-)[1]	0.00E+00	4.00E-04	9.00E-04	3.20E-03	4.90E-03	5.20E-03	4.10E-03	4.30E-03	1.40E-03	
U-232 (g)[8]	0.00E+00	5.85E-05	2.73E-03	9.94E-03	1.54E-02	1.61E-02	1.23E-02	3.54E-03	5.81E-04	
Error (+/-)[9]	NA	1.83E-06	8.44E-05	3.03E-04	4.74E-04	5.00E-04	3.79E-04	1.11E-04	1.83E-05	
Segment Total										6.07E-02
Error (+/-)[12]										8.55E-04
U-233 (wt%)[1]	1.00E+02	9.84E+01	9.44E+01	8.99E+01	8.74E+01	8.67E+01	8.76E+01	9.46E+01	9.79E+01	
Error (+/-)[1]	0.00E+00	1.38E-02	5.50E-03	6.40E-03	6.30E-03	7.00E-03	6.40E-03	1.05E-02	1.26E-02	
U-233 (g)[8]	4.00E-05	4.49E-01	8.85E+00	8.52E+00	8.46E+00	8.33E+00	8.10E+00	2.44E+00	1.28E+00	
Error (+/-)[9]	1.00E-05	1.43E-04	2.38E-03	2.38E-03	2.16E-03	2.29E-03	2.21E-03	7.77E-04	3.89E-04	
Segment Total										4.64E+01
Error (+/-)[12]										5.19E-03
U-234 (wt%)[1]	0.00E+00	1.44E+00	4.73E+00	8.33E+00	1.02E+01	1.08E+01	1.01E+01	4.73E+00	1.95E+00	
Error (+/-)[1]	0.00E+00	7.00E-04	7.00E-04	9.00E-04	1.00E-03	1.20E-03	1.10E-03	8.00E-04	7.00E-04	
U-234 (g)[8]	0.00E+00	6.57E-03	4.44E-01	7.89E-01	9.91E-01	1.04E+00	9.35E-01	1.22E-01	2.55E-02	
Error (+/-)[9]	NA	3.70E-06	1.34E-04	2.30E-04	2.61E-04	2.96E-04	2.66E-04	4.19E-05	1.15E-05	
Segment Total										4.35E+00
Error (+/-)[12]										5.47E-04
U-235 (wt%)[1]	0.00E+00	8.48E-02	5.40E-01	1.33E+00	1.87E+00	2.01E+00	1.80E+00	4.87E-01	9.75E-02	
Error (+/-)[1]	0.00E+00	1.00E-02	4.10E-03	4.50E-03	3.70E-03	4.30E-03	4.20E-03	7.30E-03	9.20E-03	
U-235 (g)[8]	0.00E+00	3.87E-04	5.06E-02	1.26E-01	1.81E-01	1.93E-01	1.67E-01	1.26E-02	1.28E-03	
Error (+/-)[9]	NA	4.57E-05	3.85E-04	4.28E-04	3.61E-04	4.17E-04	3.91E-04	1.88E-04	1.20E-04	
Segment Total										7.31E-01
Error (+/-)[12]										9.16E-04
U-236 (wt%)[1]	0.00E+00	1.31E-02	6.01E-02	1.19E-01	1.79E-01	1.99E-01	1.71E-01	1.82E-02	1.60E-03	
Error (+/-)[1]	0.00E+00	1.00E-04	1.00E-04	1.00E-04	1.00E-04	1.00E-04	1.00E-04	1.00E-04	1.00E-04	
U-236 (g)[8]	0.00E+00	5.99E-05	5.64E-03	1.13E-02	1.73E-02	1.91E-02	1.58E-02	4.70E-04	2.09E-05	

Rod "K" 1302864 (SB1-3 D24)

	K-00	K-01	K-02	K-03	K-04	K-05	K-06	K-07	K-08	K-09
Error (+/-)[9]	NA	4.57E-07	9.50E-06	9.95E-06	1.06E-05	1.08E-05	1.01E-05	2.58E-06	1.31E-06	
Segment Total										6.96E-02
Error (+/-)[12]										2.30E-05
U-238 (wt%)[1]	0.00E+00	8.11E-02	2.35E-01	2.11E-01	1.94E-01	1.97E-01	2.07E-01	4.10E-03	1.04E-02	
Error (+/-)[1]	0.00E+00	9.80E-03	3.90E-03	4.40E-03	3.60E-03	4.20E-03	4.10E-03	7.20E-03	8.90E-03	
U-238 (g)[8]	0.00E+00	3.71E-04	2.20E-02	2.00E-02	1.88E-02	1.89E-02	1.92E-02	1.06E-04	1.36E-04	
Error (+/-)[9]	NA	4.48E-05	3.66E-04	4.17E-04	3.49E-04	4.04E-04	3.79E-04	1.86E-04	1.16E-04	
Segment Total										9.95E-02
Error (+/-)[12]										8.87E-04
Total U[2]	2.36E-03	4.57E-01	9.38E+00	9.47E+00	9.68E+00	9.62E+00	9.25E+00	2.58E+00	1.31E+00	
Error (+/-)[2]	2.00E-05	1.30E-04	2.46E-03	2.56E-03	2.37E-03	2.53E-03	2.43E-03	7.70E-04	3.60E-04	
Kr-82 (mol%)[3]	2.00E-01	2.00E-01	2.00E-01	2.00E-01	2.00E-01	2.00E-01	2.00E-01	2.00E-01	2.00E-01	
Error (+/-)[3]	1.00E-01	1.00E-01	1.00E-01	1.00E-01	1.00E-01	1.00E-01	1.00E-01	1.00E-01	1.00E-01	
Kr-82 (g)[10]	4.91E-07	1.89E-07	1.21E-04	2.66E-04	3.38E-04	3.91E-04	3.81E-04	4.57E-05	1.38E-05	
Error (+/-)[9]	2.46E-07	NA	6.25E-05	1.35E-04	1.72E-04	1.99E-04	1.94E-04	2.46E-05	7.42E-06	
Segment Total										1.56E-03
Error (+/-)[12]										3.60E-04
Kr-83 (mol%)[3]	1.56E+01	1.56E+01	1.56E+01	1.56E+01	1.56E+01	1.56E+01	1.56E+01	1.56E+01	1.56E+01	
Error (+/-)[3]	1.00E-01	1.00E-01	1.00E-01	1.00E-01	1.00E-01	1.00E-01	1.00E-01	1.00E-01	1.00E-01	
Kr-83 (g)[10]	3.88E-05	1.49E-05	9.57E-03	2.10E-02	2.67E-02	3.09E-02	3.01E-02	3.61E-03	1.09E-03	
Error (+/-)[9]	2.49E-07	NA	1.19E-03	1.97E-03	2.49E-03	2.94E-03	2.87E-03	7.25E-04	2.20E-04	
Segment Total										1.23E-01
Error (+/-)[12]										5.38E-03
Kr-84 (mol%)[3]	2.98E+01	2.98E+01	2.98E+01	2.98E+01	2.98E+01	2.98E+01	2.98E+01	2.98E+01	2.98E+01	
Error (+/-)[3]	1.00E-01	1.00E-01	1.00E-01	1.00E-01	1.00E-01	1.00E-01	1.00E-01	1.00E-01	1.00E-01	
Kr-84 (g)[10]	7.50E-05	2.88E-05	1.85E-02	4.06E-02	5.16E-02	5.96E-02	5.82E-02	6.98E-03	2.10E-03	
Error (+/-)[9]	2.52E-07	NA	2.30E-03	3.80E-03	4.80E-03	5.68E-03	5.53E-03	1.40E-03	4.26E-04	
Segment Total										2.38E-01
Error (+/-)[12]										1.04E-02

Rod "K" 1302864 (SB1-3 D24)

	K-00	K-01	K-02	K-03	K-04	K-05	K-06	K-07	K-08	K-09
Kr-85 (mol%)[3]	5.80E+00	5.80E+00	5.80E+00	5.80E+00	5.80E+00	5.80E+00	5.80E+00	5.80E+00	5.80E+00	
Error (+/-)[3]	1.00E-01	1.00E-01	1.00E-01	1.00E-01	1.00E-01	1.00E-01	1.00E-01	1.00E-01	1.00E-01	
Kr-85 (g)[10]	1.48E-05	5.67E-06	3.64E-03	7.99E-03	1.02E-02	1.17E-02	1.15E-02	1.38E-03	4.14E-04	
Error (+/-)[9]	2.55E-07	NA	4.57E-04	7.61E-04	9.62E-04	1.14E-03	1.11E-03	2.77E-04	8.41E-05	
Segment Total										4.68E-02
Error (+/-)[12]										2.08E-03
Kr-86 (mol%)[3]	4.86E+01	4.86E+01	4.86E+01	4.86E+01	4.86E+01	4.86E+01	4.86E+01	4.86E+01	4.86E+01	
Error (+/-)[3]	1.00E-01	1.00E-01	1.00E-01	1.00E-01	1.00E-01	1.00E-01	1.00E-01	1.00E-01	1.00E-01	
Kr-86 (g)[10]	1.25E-04	4.81E-05	3.09E-02	6.77E-02	8.61E-02	9.96E-02	9.72E-02	1.17E-02	3.51E-03	
Error (+/-)[9]	2.58E-07	NA	3.84E-03	6.35E-03	8.02E-03	9.48E-03	9.23E-03	2.34E-03	7.11E-04	
Segment Total										3.97E-01
Error (+/-)[12]										1.73E-02
Rod Total										8.06E-01
Error (+/-)[12]										2.10E-02
Shear Gas (g)[4]	0.00E+00	6.00E-04	5.00E-04	1.70E-03	2.40E-03	2.00E-03	1.80E-03	1.00E-04	0.00E+00	
Error (+/-)[4]	0.00E+00	3.00E-04	3.00E-04	3.00E-04	5.00E-04	4.00E-04	4.00E-04	3.00E-04	3.00E-04	
Diss+Pl Kr (mol)[3]	3.00E-06	0.00E+00	7.39E-04	1.62E-03	2.06E-03	2.38E-03	2.33E-03	2.79E-04	8.40E-05	
Error (+/-)[3]	0.00E+00	0.00E+00	9.20E-05	1.52E-04	1.92E-04	2.27E-04	2.21E-04	5.60E-05	1.70E-05	
Diss+Pl Kr+Xe (g)[3]	1.80E-03	0.00E+00	3.85E-01	9.12E-01	1.14E+00	1.42E+00	1.31E+00	1.36E-01	3.72E-02	
Error (+/-)[3]	1.00E-04	0.00E+00	3.20E-02	5.58E-02	1.30E-01	7.86E-02	1.50E-01	1.57E-02	7.60E-03	
Total Kr (mol)	3.00E-06	1.15E-06	7.40E-04	1.62E-03	2.06E-03	2.39E-03	2.33E-03	2.79E-04	8.40E-05	
Error (+/-)[9]	3.00E-10	3.46E-10	9.20E-05	1.52E-04	1.92E-04	2.27E-04	2.21E-04	5.60E-05	1.70E-05	
Xe-128 (mol)[3]	1.00E-01	1.00E-01	1.00E-01	1.00E-01	1.00E-01	1.00E-01	1.00E-01	1.00E-01	1.00E-01	
Error (+/-)[3]	0.00E+00	0.00E+00	0.00E+00	0.00E+00	0.00E+00	0.00E+00	0.00E+00	0.00E+00	0.00E+00	
Xe-128 (g)[10]	1.41E-06	4.79E-07	3.07E-04	7.39E-04	9.21E-04	1.16E-03	1.06E-03	1.07E-04	2.87E-05	
Error (+/-)[3]	1.28E-07	1.44E-10	2.95E-05	5.18E-05	1.23E-04	7.25E-05	1.42E-04	1.43E-05	7.17E-06	
SegmentTotal										4.33E-03
Error (+/1)[12]										2.10E-04

Rod "K" 1302864 (SB1-3 D24)

	K-00	K-01	K-02	K-03	K-04	K-05	K-06	K-07	K-08	K-09
Xe-130 (mol)[3]	2.00E-01	2.00E-01	2.00E-01	2.00E-01	2.00E-01	2.00E-01	2.00E-01	2.00E-01	2.00E-01	
Error (+/-)[3]	0.00E+00	0.00E+00	0.00E+00	0.00E+00	0.00E+00	0.00E+00	0.00E+00	0.00E+00	0.00E+00	
Xe-130 (g)[10]	2.86E-06	9.72E-07	6.24E-04	1.50E-03	1.87E-03	2.36E-03	2.16E-03	2.18E-04	5.82E-05	
Error (+/-)[3]	2.60E-07	2.92E-10	6.00E-05	1.05E-04	2.49E-04	1.47E-04	2.88E-04	2.91E-05	1.46E-05	
SegmentTotal										8.80E-03
Error (+/1)[12]										4.27E-04
Xe-131 (mol)[3]	1.18E+01	1.18E+01	1.18E+01	1.18E+01	1.18E+01	1.18E+01	1.18E+01	1.18E+01	1.18E+01	
Error (+/-)[3]	1.00E-01	1.00E-01	1.00E-01	1.00E-01	1.00E-01	1.00E-01	1.00E-01	1.00E-01	1.00E-01	
Xe-131 (g)[10]	1.70E-04	5.78E-05	3.71E-02	8.92E-02	1.11E-01	1.40E-01	1.28E-01	1.29E-02	3.46E-03	
Error (+/-)[3]	1.55E-05	4.90E-07	3.58E-03	6.30E-03	1.48E-02	8.84E-03	1.71E-02	1.73E-03	8.67E-04	
SegmentTotal										5.23E-01
Error (+/1)[12]										2.55E-02
Xe-132 (mol)[3]	2.27E+01	2.27E+01	2.27E+01	2.27E+01	2.27E+01	2.27E+01	2.27E+01	2.27E+01	2.27E+01	
Error (+/-)[3]	1.00E-01	1.00E-01	1.00E-01	1.00E-01	1.00E-01	1.00E-01	1.00E-01	1.00E-01	1.00E-01	
Xe-132 (g)[10]	3.29E-04	1.12E-04	7.20E-02	1.73E-01	2.16E-01	2.72E-01	2.49E-01	2.51E-02	6.71E-03	
Error (+/-)[3]	3.00E-05	4.95E-07	6.92E-03	1.22E-02	2.87E-02	1.70E-02	3.32E-02	3.36E-03	1.68E-03	
SegmentTotal										1.01E+00
Error (+/1)[12]										4.92E-02
Xe-134 (mol)[3]	2.58E+01	2.58E+01	2.58E+01	2.58E+01	2.58E+01	2.58E+01	2.58E+01	2.58E+01	2.58E+01	
Error (+/-)[3]	1.00E-01	1.00E-01	1.00E-01	1.00E-01	1.00E-01	1.00E-01	1.00E-01	1.00E-01	1.00E-01	
Xe-134 (g)[10]	3.80E-04	1.29E-04	8.30E-02	2.00E-01	2.49E-01	3.14E-01	2.87E-01	2.89E-02	7.74E-03	
Error (+/-)[3]	3.46E-05	5.03E-07	7.99E-03	1.40E-02	3.31E-02	1.96E-02	3.83E-02	3.87E-03	1.94E-03	
SegmentTotal										1.17E+00
Error (+/1)[12]										5.68E-02
Xe-136 (mol)[3]	3.94E+01	3.94E+01	3.94E+01	3.94E+01	3.94E+01	3.94E+01	3.94E+01	3.94E+01	3.94E+01	
Error (+/-)[3]	1.00E-01	1.00E-01	1.00E-01	1.00E-01	1.00E-01	1.00E-01	1.00E-01	1.00E-01	1.00E-01	
Xe-136 (g)[10]	5.89E-04	2.00E-04	1.29E-01	3.09E-01	3.85E-01	4.87E-01	4.45E-01	4.49E-02	1.20E-02	
Error (+/-)[3]	5.36E-05	5.12E-07	1.24E-02	2.17E-02	5.13E-02	3.04E-02	5.93E-02	6.00E-03	3.00E-03	
SegmentTotal										1.81E+00
Error (+/1)[12]										8.80E-02

Rod "K" 1302864 (SB1-3 D24)

	K-00	K-01	K-02	K-03	K-04	K-05	K-06	K-07	K-08	K-09
Rod total										4.53E+00
Error (+/-)[12]										1.18E-01
Shear Gas (g)[4]	0.00E+00	6.00E-04	5.00E-04	1.70E-03	2.40E-03	2.00E-03	1.80E-03	1.00E-04	0.00E+00	
Error (+/-)[4]	0.00E+00	3.00E-04	3.00E-04	3.00E-04	5.00E-04	4.00E-04	4.00E-04	3.00E-04	3.00E-04	
Diss+Pl Xe (mol)[3]	1.10E-05	0.00E+00	2.40E-03	5.77E-03	7.18E-03	9.07E-03	8.30E-03	8.37E-04	2.24E-04	
Error (+/-)[3]	1.00E-06	0.00E+00	2.31E-04	4.05E-04	9.58E-04	5.67E-04	1.11E-03	1.12E-04	5.60E-05	
Diss+Pl Kr+Xe (g)[3]	1.80E-03	0.00E+00	3.85E-01	9.12E-01	1.14E+00	1.42E+00	1.31E+00	1.36E-01	3.72E-02	
Error (+/-)[3]	1.00E-04	0.00E+00	3.20E-02	5.58E-02	1.30E-01	7.86E-02	1.50E-01	1.57E-02	7.60E-03	
Total Xe (mol)	1.10E-05	3.74E-06	2.40E-03	5.78E-03	7.20E-03	9.09E-03	8.32E-03	8.38E-04	2.24E-04	
Error (+/-)[9]	1.00E-06	1.12E-09	2.31E-04	4.05E-04	9.58E-04	5.67E-04	1.11E-03	1.12E-04	5.61E-05	
Values corrected to 1/1/84 (page 181, Final Report for the LWBR Proof of Breeding Analytical Support Project										
Cs-137 (atoms)[5]	NA	6.28E+18	4.22E+20	9.12E+20	1.21E+21	1.28E+21	1.14E+21	1.39E+20	2.99E+19	
Error (+/-)[4]	NA	2.20E+16	1.42E+18	2.97E+18	3.93E+18	4.17E+18	3.72E+18	4.73E+17	1.01E+17	
Cs-137 (g)[11]	NA	1.43E-03	9.60E-02	2.07E-01	2.75E-01	2.91E-01	2.60E-01	3.17E-02	6.79E-03	
Error (+/-)[9]	NA	5.01E-06	3.23E-04	6.74E-04	8.94E-04	9.47E-04	8.44E-04	1.07E-04	2.28E-05	
Total										1.17E+00
Error (+/-)[12]										1.73E-03
Ce-144 (atoms)[5]	NA	6.74E+17	2.91E+19	4.98E+19	6.12E+19	6.47E+19	5.08E+19	8.10E+18	1.51E+18	
Error (+/-)[4]	NA	3.83E+15	1.69E+17	2.82E+17	3.47E+17	3.66E+17	2.87E+17	5.05E+16	9.39E+15	
Ce-144 (g)[11]	NA	1.61E-04	6.95E-03	1.19E-02	1.46E-02	1.55E-02	1.21E-02	1.93E-03	3.61E-04	
Error (+/-)[9]	NA	9.14E-07	4.04E-05	6.73E-05	8.28E-05	8.74E-05	6.86E-05	1.21E-05	2.24E-06	
Total										6.35E-02
Error (+/-)[12]										1.60E-04
Zr-95 (atoms)[5]	NA	6.75E+15	2.54E+17	4.15E+17	4.28E+17	4.43E+17	2.51E+17	2.94E+16	3.66E+15	
Error (+/-)[4]	NA	1.49E+14	7.08E+15	1.68E+16	2.66E+16	2.36E+16	2.04E+16	3.44E+15	4.78E+14	
Zr-95 (g)[11]	NA	1.06E-06	4.01E-05	6.53E-05	6.75E-05	6.98E-05	3.95E-05	4.64E-06	5.77E-07	
Error (+/-)[9]	NA	2.35E-08	1.11E-06	2.64E-06	4.19E-06	3.71E-06	3.22E-06	5.42E-07	7.54E-08	
Total										2.89E-04

Rod "K" 1302864 (SB1-3 D24)

[redacted]										
	K-00	K-01	K-02	K-03	K-04	K-05	K-06	K-07	K-08	K-09
Error (+/-)[12]										7.09E-06
[redacted]										

References

1. ANL Destructive Chemical Assay of 33-Rod LWBR EOL Sample - Rod K, 1302864, page 6
2. ANL Destructive Chemical Assay of 33-Rod LWBR EOL Sample - Rod K, 1302864, page 7
3. ANL Destructive Chemical Assay of 33-Rod LWBR EOL Sample - Rod K, 1302864, page 10
4. ANL Destructive Chemical Assay of 33-Rod LWBR EOL Sample - Rod K, 1302864, page 11
5. ANL Destructive Chemical Assay of 33-Rod LWBR EOL Sample - Rod K, 1302864, page 12
6. ANL Destructive Chemical Assay of 33-Rod LWBR EOL Sample - Rod K, 1302864, page 13
7. ANL Destructive Chemical Assay of 33-Rod LWBR EOL Sample - Rod K, 1302864, page 14
8. (abundance of the specified isotope)(total weight of uranium)

   1.00E+02
9. Error Propagation = ((+/-x/x)2+(+/-y/y)2)1/2(xy)
10. (mole%)(number moles gas recovered)(molec wt)

    1.00E+02
11. (number of atoms per segment)(atomic weight)

    6.02E+23
12. Error Propagation = (SUM(+/-I)1/2

Rod "L" 1400544 (SB1-3 C3)

	L-00	L-01	L-02	L-03	L-04	L-05	L-06	L-07	L-08	L-09
Segment length (in)	1.12E+01	1.10E+01	1.44E+01	1.42E+01	1.42E+01	1.43E+01	1.39E+01	1.05E+01	1.29E+01	1.64E+00
Total length (in)										1.18E+02
U-232 (wt%)[1]	0.00E+00	1.43E-02	3.36E-02	1.19E-01	1.77E-01	1.85E-01	2.23E-01	1.33E-01	4.56E-02	
Error (+/-)[1]	0.00E+00	4.00E-04	1.00E-03	3.70E-03	5.50E-03	5.70E-03	6.90E-03	4.10E-03	1.40E-03	
U-232 (g)[8]	0.00E+00	5.33E-05	2.77E-03	1.03E-02	1.60E-02	1.65E-02	1.16E-02	3.57E-03	5.79E-04	
Error (+/-)[9]	NA	1.49E-06	8.23E-05	3.21E-04	4.96E-04	5.09E-04	3.59E-04	1.10E-04	1.78E-05	
Segment Total										6.14E-02
Error (+/-)[12]										8.70E-04
U-233 (wt%)[1]	1.00E+02	9.91E+01	9.45E+01	8.99E+01	8.72E+01	8.62E+01	9.13E+01	9.42E+01	9.77E+01	
Error (+/-)[1]	0.00E+00	1.65E-02	7.20E-03	6.90E-03	7.80E-03	7.80E-03	8.30E-03	7.40E-03	8.50E-03	
U-233 (g)[8]	4.00E-05	3.70E-01	7.78E+00	7.79E+00	7.87E+00	7.70E+00	4.74E+00	2.53E+00	1.24E+00	
Error (+/-)[9]	1.00E-05	1.43E-04	2.40E-03	2.34E-03	2.47E-03	2.40E-03	1.25E-03	7.43E-04	3.40E-04	
Segment Total										4.00E+01
Error (+/-)[12]										5.04E-03
U-234 (wt%)[1]	0.00E+00	8.09E-01	4.73E+00	8.42E+00	1.04E+01	1.11E+01	7.35E+00	5.05E+00	2.15E+00	
Error (+/-)[1]	0.00E+00	1.00E-03	1.00E-03	1.20E-03	1.40E-03	1.40E-03	1.10E-03	1.00E-03	1.00E-03	
U-234 (g)[8]	0.00E+00	3.02E-03	3.89E-01	7.29E-01	9.36E-01	9.92E-01	3.82E-01	1.36E-01	2.73E-02	
Error (+/-)[9]	NA	3.88E-06	1.43E-04	2.36E-04	3.09E-04	3.21E-04	1.11E-04	4.69E-05	1.45E-05	
Segment Total										3.59E+00
Error (+/-)[12]										5.38E-04
U-235 (wt%)[1]	0.00E+00	1.68E-02	4.77E-01	1.31E+00	1.88E+00	2.13E+00	1.10E+00	5.51E-01	1.13E-01	
Error (+/-)[1]	0.00E+00	1.18E-02	5.50E-03	4.80E-03	5.00E-03	5.00E-03	4.30E-03	4.80E-03	6.20E-03	
U-235 (g)[8]	0.00E+00	6.27E-05	3.93E-02	1.14E-01	1.70E-01	1.90E-01	5.71E-02	1.48E-02	1.43E-03	
Error (+/-)[9]	NA	4.40E-05	4.53E-04	4.17E-04	4.54E-04	4.50E-04	2.24E-04	1.29E-04	7.87E-05	
Segment Total										5.86E-01
Error (+/-)[12]										9.29E-04
U-236 (wt%)[1]	0.00E+00	2.00E-04	2.50E-02	8.77E-02	1.54E-01	1.87E-01	6.46E-02	2.18E-02	2.10E-03	
Error (+/-)[1]	0.00E+00	1.00E-04	1.00E-04	1.00E-04	1.00E-04	1.00E-04	1.00E-04	1.00E-04	1.00E-04	
U-236 (g)[8]	0.00E+00	7.46E-07	2.06E-03	7.60E-03	1.39E-02	1.67E-02	3.36E-03	5.86E-04	2.67E-05	

Rod "L" 1400544 (SB1-3 C3)

	L-00	L-01	L-02	L-03	L-04	L-05	L-06	L-07	L-08	L-09
Error (+/-)[9]	NA	3.73E-07	8.26E-06	8.94E-06	9.95E-06	1.02E-05	5.26E-06	2.69E-06	1.27E-06	
Segment Total										4.42E-02
Error (+/-)[12]										1.97E-05
U-238 (wt%)[1]	0.00E+00	3.36E-02	2.45E-01	2.10E-01	1.90E-01	1.90E-01	1.90E-03	2.70E-03	6.90E-03	
Error (+/-)[1]	0.00E+00	1.16E-02	5.10E-03	4.40E-03	4.70E-03	4.70E-03	3.80E-03	4.40E-03	5.90E-03	
U-238 (g)[8]	0.00E+00	1.25E-04	2.02E-02	1.82E-02	1.72E-02	1.70E-02	9.87E-05	7.26E-05	8.76E-05	
Error (+/-)[9]	NA	4.33E-05	4.20E-04	3.81E-04	4.24E-04	4.20E-04	1.97E-04	1.18E-04	7.49E-05	
Segment Total										7.30E-02
Error (+/-)[12]										8.59E-04
Total U[2]	3.60E-04	3.73E-01	8.23E+00	8.66E+00	9.02E+00	8.93E+00	5.20E+00	2.69E+00	1.27E+00	
Error (+/-)[2]	2.00E-05	1.30E-04	2.46E-03	2.52E-03	2.72E-03	2.66E-03	1.29E-03	7.60E-04	3.30E-04	
Kr-82 (mol%)[3]	1.00E-01	1.00E-01	1.00E-01	1.00E-01	1.00E-01	1.00E-01	1.00E-01	1.00E-01	1.00E-01	
Error (+/-)[3]	1.00E-01	1.00E-01	1.00E-01	1.00E-01	1.00E-01	1.00E-01	1.00E-01	1.00E-01	1.00E-01	
Kr-82 (g)[10]	3.28E-07	0.00E+00	5.75E-05	1.34E-04	1.72E-04	1.52E-04	7.06E-05	2.49E-05	6.35E-06	
Error (+/-)[9]	3.28E-07	NA	5.80E-05	1.35E-04	1.72E-04	1.53E-04	7.13E-05	2.54E-05	6.76E-06	
Segment Total										6.17E-04
Error (+/-)[12]										2.84E-04
Kr-83 (mol%)[3]	1.52E+01	1.52E+01	1.52E+01	1.52E+01	1.52E+01	1.52E+01	1.52E+01	1.52E+01	1.52E+01	
Error (+/-)[3]	2.00E-01	2.00E-01	2.00E-01	2.00E-01	2.00E-01	2.00E-01	2.00E-01	2.00E-01	2.00E-01	
Kr-83 (g)[10]	5.04E-05	0.00E+00	8.84E-03	2.06E-02	2.64E-02	2.34E-02	1.09E-02	3.83E-03	9.78E-04	
Error (+/-)[9]	6.63E-07	NA	1.19E-03	2.36E-03	2.42E-03	3.34E-03	1.46E-03	7.70E-04	3.53E-04	
Segment Total										9.49E-02
Error (+/-)[12]										5.18E-03
Kr-84 (mol%)[3]	3.01E+01	3.01E+01	3.01E+01	3.01E+01	3.01E+01	3.01E+01	3.01E+01	3.01E+01	3.01E+01	
Error (+/-)[3]	2.00E-01	2.00E-01	2.00E-01	2.00E-01	2.00E-01	2.00E-01	2.00E-01	2.00E-01	2.00E-01	
Kr-84 (g)[10]	1.01E-04	0.00E+00	1.77E-02	4.12E-02	5.30E-02	4.68E-02	2.18E-02	7.67E-03	1.96E-03	
Error (+/-)[9]	6.71E-07	NA	2.38E-03	4.71E-03	4.81E-03	6.68E-03	2.91E-03	1.54E-03	7.07E-04	
Segment Total										1.90E-01
Error (+/-)[12]										1.03E-02

Rod "L" 1400544 (SB1-3 C3)

	L-00	L-01	L-02	L-03	L-04	L-05	L-06	L-07	L-08	L-09
Kr-85 (mol%)[3]	5.40E+00	5.40E+00	5.40E+00	5.40E+00	5.40E+00	5.40E+00	5.40E+00	5.40E+00	5.40E+00	
Error (+/-)[3]	2.00E-01	2.00E-01	2.00E-01	2.00E-01	2.00E-01	2.00E-01	2.00E-01	2.00E-01	2.00E-01	
Kr-85 (g)[10]	1.83E-05	0.00E+00	3.22E-03	7.48E-03	9.61E-03	8.50E-03	3.95E-03	1.39E-03	3.56E-04	
Error (+/-)[9]	6.79E-07	NA	4.47E-04	8.97E-04	9.41E-04	1.25E-03	5.47E-04	2.84E-04	1.29E-04	
Segment Total										3.45E-02
Error (+/-)[12]										1.96E-03
Kr-86 (mol%)[3]	4.92E+01	4.92E+01	4.92E+01	4.92E+01	4.92E+01	4.92E+01	4.92E+01	4.92E+01	4.92E+01	
Error (+/-)[3]	3.00E-01	3.00E-01	3.00E-01	3.00E-01	3.00E-01	3.00E-01	3.00E-01	3.00E-01	3.00E-01	
Kr-86 (g)[10]	1.69E-04	0.00E+00	2.97E-02	6.90E-02	8.86E-02	7.84E-02	3.64E-02	1.28E-02	3.28E-03	
Error (+/-)[9]	1.03E-06	NA	3.98E-03	7.87E-03	8.05E-03	1.12E-02	4.87E-03	2.58E-03	1.18E-03	
Segment Total										3.18E-01
Error (+/-)[12]										1.73E-02
Rod Total										6.39E-01
Error (+/-)[12]										2.09E-02
Shear Gas (g)[4]	0.00E+00	0.00E+00	4.00E-04	1.50E-03	2.20E-03	2.50E-03	7.00E-04	3.00E-04	3.00E-04	
Error (+/-)[4]	0.00E+00	3.00E-04	3.00E-04	3.00E-04	4.00E-04	5.00E-04	3.00E-04	3.00E-04	3.00E-04	
Diss+Pl Kr (mol)[3]	4.00E-06	0.00E+00	7.01E-04	1.63E-03	2.09E-03	1.85E-03	8.61E-04	3.03E-04	7.70E-05	
Error (+/-)[3]	0.00E+00	0.00E+00	9.40E-05	1.86E-04	1.90E-04	2.64E-04	1.15E-04	6.10E-05	2.80E-05	
Diss+Pl Kr+Xe (g)[3]	2.20E-03	0.00E+00	4.11E-01	9.51E-01	1.20E+00	1.03E+00	4.97E-01	1.72E-01	3.98E-02	
Error (+/-)[3]	1.00E-04	0.00E+00	3.24E-02	6.45E-02	1.29E-01	9.15E-02	4.73E-02	1.71E-02	6.40E-03	
Total Kr (mol)	4.00E-06	0.00E+00	7.02E-04	1.63E-03	2.10E-03	1.85E-03	8.62E-04	3.04E-04	7.76E-05	
Error (+/-)[9]	4.00E-10	0.00E+00	9.40E-05	1.86E-04	1.90E-04	2.64E-04	1.15E-04	6.10E-05	2.80E-05	
Xe-128 (mol)[3]	1.00E-01	1.00E-01	1.00E-01	1.00E-01	1.00E-01	1.00E-01	1.00E-01	1.00E-01	1.00E-01	
Error (+/-)[3]	0.00E+00	0.00E+00	0.00E+00	0.00E+00	0.00E+00	0.00E+00	0.00E+00	0.00E+00	0.00E+00	
Xe-128 (g)[10]	1.66E-06	0.00E+00	3.35E-04	7.75E-04	9.75E-04	8.30E-04	4.05E-04	1.40E-04	3.20E-05	
Error (+/-)[3]	1.28E-07	NA	2.99E-05	5.95E-05	1.22E-04	8.45E-05	4.41E-05	1.55E-05	5.63E-06	
SegmentTotal										3.49E-03
Error (+/1)[12]										1.69E-04
Xe-130 (mol)[3]	1.00E-01	1.00E-01	1.00E-01	1.00E-01	1.00E-01	1.00E-01	1.00E-01	1.00E-01	1.00E-01	

Rod "L" 1400544 (SB1-3 C3)

	L-00	L-01	L-02	L-03	L-04	L-05	L-06	L-07	L-08	L-09
Error (+/-)[3]	0.00E+00	0.00E+00	0.00E+00	0.00E+00	0.00E+00	0.00E+00	0.00E+00	0.00E+00	0.00E+00	
Xe-130 (g)[10]	1.69E-06	0.00E+00	3.41E-04	7.87E-04	9.91E-04	8.43E-04	4.11E-04	1.42E-04	3.25E-05	
Error (+/-)[3]	1.30E-07	NA	3.04E-05	6.04E-05	1.24E-04	8.59E-05	4.48E-05	1.57E-05	5.72E-06	
SegmentTotal										3.55E-03
Error (+/1)[12]										1.72E-04
Xe-131 (mol)[3]	1.11E+01	1.11E+01	1.11E+01	1.11E+01	1.11E+01	1.11E+01	1.11E+01	1.11E+01	1.11E+01	
Error (+/-)[3]	1.00E-01	1.00E-01	1.00E-01	1.00E-01	1.00E-01	1.00E-01	1.00E-01	1.00E-01	1.00E-01	
Xe-131 (g)[10]	1.89E-04	0.00E+00	3.81E-02	8.81E-02	1.11E-01	9.43E-02	4.60E-02	1.59E-02	3.63E-03	
Error (+/-)[3]	1.46E-05	NA	3.42E-03	6.80E-03	1.39E-02	9.64E-03	5.03E-03	1.76E-03	6.40E-04	
SegmentTotal										3.97E-01
Error (+/1)[12]										1.93E-02
Xe-132 (mol)[3]	2.26E+01	2.26E+01	2.26E+01	2.26E+01	2.26E+01	2.26E+01	2.26E+01	2.26E+01	2.26E+01	
Error (+/-)[3]	1.00E-01	1.00E-01	1.00E-01	1.00E-01	1.00E-01	1.00E-01	1.00E-01	1.00E-01	1.00E-01	
Xe-132 (g)[10]	3.88E-04	0.00E+00	7.81E-02	1.81E-01	2.27E-01	1.93E-01	9.43E-02	3.26E-02	7.45E-03	
Error (+/-)[3]	2.99E-05	NA	6.98E-03	1.39E-02	2.84E-02	1.97E-02	1.03E-02	3.61E-03	1.31E-03	
SegmentTotal										8.14E-01
Error (+/1)[12]										3.94E-02
Xe-134 (mol)[3]	2.56E+01	2.56E+01	2.56E+01	2.56E+01	2.56E+01	2.56E+01	2.56E+01	2.56E+01	2.56E+01	
Error (+/-)[3]	2.00E-01	2.00E-01	2.00E-01	2.00E-01	2.00E-01	2.00E-01	2.00E-01	2.00E-01	2.00E-01	
Xe-134 (g)[10]	4.46E-04	0.00E+00	8.99E-02	2.08E-01	2.61E-01	2.23E-01	1.08E-01	3.75E-02	8.57E-03	
Error (+/-)[3]	3.45E-05	NA	8.05E-03	1.60E-02	3.27E-02	2.27E-02	1.19E-02	4.16E-03	1.51E-03	
SegmentTotal										9.36E-01
Error (+/1)[12]										4.54E-02
Xe-136 (mol)[3]	4.07E+01	4.07E+01	4.07E+01	4.07E+01	4.07E+01	4.07E+01	4.07E+01	4.07E+01	4.07E+01	
Error (+/-)[3]	2.00E-01	2.00E-01	2.00E-01	2.00E-01	2.00E-01	2.00E-01	2.00E-01	2.00E-01	2.00E-01	
Xe-136 (g)[10]	7.19E-04	0.00E+00	1.45E-01	3.35E-01	4.22E-01	3.59E-01	1.75E-01	6.05E-02	1.38E-02	
Error (+/-)[3]	5.54E-05	NA	1.30E-02	2.58E-02	5.26E-02	3.66E-02	1.91E-02	6.70E-03	2.43E-03	
SegmentTotal										1.51E+00
Error (+/1)[12]										7.32E-02
Rod total										3.67E+00

Rod "L" 1400544 (SB1-3 C3)

	L-00	L-01	L-02	L-03	L-04	L-05	L-06	L-07	L-08	L-09
Error (+/-)[12]										9.67E-02
Shear Gas (g)[4]	0.00E+00	0.00E+00	4.00E-04	1.50E-03	2.20E-03	2.50E-03	7.00E-04	3.00E-04	3.00E-04	
Error (+/-)[4]	0.00E+00	3.00E-04	3.00E-04	3.00E-04	4.00E-04	5.00E-04	3.00E-04	3.00E-04	3.00E-04	
Diss+Pl Xe (mol)[3]	1.30E-05	0.00E+00	2.62E-03	6.05E-03	7.61E-03	6.48E-03	3.16E-03	1.09E-03	2.48E-04	
Error (+/-)[3]	1.00E-06	0.00E+00	2.34E-04	4.65E-04	9.51E-04	6.61E-04	3.45E-04	1.21E-04	4.40E-05	
Diss+Pl Kr+Xe (g)[3]	2.20E-03	0.00E+00	4.11E-01	9.51E-01	1.20E+00	1.03E+00	4.97E-01	1.72E-01	3.98E-02	
Error (+/-)[3]	1.00E-04	0.00E+00	3.24E-02	6.45E-02	1.29E-01	9.15E-02	4.73E-02	1.71E-02	6.40E-03	
Total Xe (mol)	1.30E-05	0.00E+00	2.62E-03	6.06E-03	7.62E-03	6.49E-03	3.16E-03	1.09E-03	2.50E-04	
Error (+/-)[9]	1.00E-06	0.00E+00	2.34E-04	4.65E-04	9.51E-04	6.61E-04	3.45E-04	1.21E-04	4.40E-05	

Values corrected to 1/1/84 (page 181, Final Report for the LWBR Proof of Breeding Analytical Support Project

	L-00	L-01	L-02	L-03	L-04	L-05	L-06	L-07	L-08	L-09
Cs-137 (atoms)[5]	NA	3.81E+18	3.93E+20	8.71E+20	1.17E+21	1.27E+21	4.45E+20	1.56E+20	3.21E+19	
Error (+/-)[4]	NA	1.20E+16	1.13E+18	2.50E+18	3.35E+18	3.64E+18	1.28E+18	4.53E+17	9.20E+16	
Cs-137 (g)[11]	NA	8.66E-04	8.92E-02	1.98E-01	2.65E-01	2.88E-01	1.01E-01	3.54E-02	7.29E-03	
Error (+/-)[9]	NA	2.73E-06	2.56E-04	5.68E-04	7.61E-04	8.26E-04	2.90E-04	1.03E-04	2.09E-05	
Total										9.85E-01
Error (+/-)[12]										1.32E-03
Ce-144 (atoms)[5]	NA	4.91E+17	2.75E+19	4.86E+19	6.07E+19	6.49E+19	2.90E+19	8.75E+18	1.62E+18	
Error (+/-)[4]	NA	3.63E+15	2.03E+17	3.59E+17	4.49E+17	4.79E+17	2.14E+17	6.48E+16	1.19E+16	
Ce-144 (g)[11]	NA	1.17E-04	6.56E-03	1.16E-02	1.45E-02	1.55E-02	6.92E-03	2.09E-03	3.86E-04	
Error (+/-)[9]	NA	8.67E-07	4.84E-05	8.57E-05	1.07E-04	1.15E-04	5.11E-05	1.55E-05	2.85E-06	
Total										5.77E-02
Error (+/-)[12]										1.93E-04
Zr-95 (atoms)[5]	NA	5.39E+15	2.46E+17	3.73E+17	5.47E+17	4.19E+17	1.77E+17	2.77E+16	4.32E+15	
Error (+/-)[4]	NA	1.61E+14	9.00E+15	1.90E+16	4.11E+16	4.66E+16	1.53E+16	3.82E+15	7.09E+14	
Zr-95 (g)[11]	NA	8.49E-07	3.87E-05	5.88E-05	8.62E-05	6.61E-05	2.78E-05	4.37E-06	6.80E-07	
Error (+/-)[9]	NA	2.54E-08	1.42E-06	3.00E-06	6.47E-06	7.34E-06	2.41E-06	6.02E-07	1.12E-07	
Total										2.84E-04
Error (+/-)[12]										1.06E-05

Rod "L" 1400544 (SB1-3 C3)

	L-00	L-01	L-02	L-03	L-04	L-05	L-06	L-07	L-08	L-09

References

1. ANL Destructive Chemical Assay of 33-Rod LWBR EOL Sample - Rod L, 1400544, page 6
2. ANL Destructive Chemical Assay of 33-Rod LWBR EOL Sample - Rod L, 1400544, page 7
3. ANL Destructive Chemical Assay of 33-Rod LWBR EOL Sample - Rod L, 1400544, page 10
4. ANL Destructive Chemical Assay of 33-Rod LWBR EOL Sample - Rod L, 1400544, page 11
5. ANL Destructive Chemical Assay of 33-Rod LWBR EOL Sample - Rod L, 1400544, page 12
6. ANL Destructive Chemical Assay of 33-Rod LWBR EOL Sample - Rod L, 1400544, page 13
7. ANL Destructive Chemical Assay of 33-Rod LWBR EOL Sample - Rod L, 1400544, page 14
8. (abundance of the specified isotope)(total weight of uranium)

   1.00E+02
9. Error Propagation = ((+/-x/x)2+(+/-y/y)2)1/2(xy)
10. (mole%)(number moles gas recovered)(molec wt)

    1.00E+02
11. (number of atoms per segment)(atomic weight)

    6.02E+23
12. Error Propagation = (SUM(+/-I)1/2

Rod "W" 2514716 Calibration

	W-00	W-01	W-02	W-03	W-04	W-05
Segment length (in)	3.70E+00	1.75E+01	1.75E+01	1.75E+01	1.75E+01	6.85E+00
Total length (in)						8.05E+01
U-232 (wt%)[1]		7.30E-04	6.10E-04	5.80E-04	7.40E-04	
Error (+/-)[1]		2.00E-05	2.00E-05	2.00E-05	2.00E-05	
U-232 (g)[8]		2.34E-05	1.02E-05	9.72E-06	2.37E-05	
Error (+/-)[9]		6.41E-07	3.35E-07	3.35E-07	6.40E-07	
Segment Total						6.70E-05
Error (+/-)[12]						1.02E-06
U-233 (wt%)[1]		9.83E+01	9.77E+01	9.77E+01	9.83E+01	
Error (+/-)[1]		6.10E-03	2.74E-02	9.40E-03	6.30E-03	
U-233 (g)[8]		3.15E+00	1.64E+00	1.64E+00	3.15E+00	
Error (+/-)[9]		8.49E-04	1.14E-03	4.67E-04	8.50E-04	
Segment Total						9.57E+00
Error (+/-)[12]						1.72E-03
U-234 (wt%)[1]		1.31E+00	1.16E+00	1.16E+00	1.31E+00	
Error (+/-)[1]		2.00E-04	5.00E-04	2.00E-04	2.00E-04	
U-234 (g)[8]		4.19E-02	1.94E-02	1.94E-02	4.18E-02	
Error (+/-)[9]		1.27E-05	1.50E-05	6.19E-06	1.27E-05	
Segment Total						1.23E-01
Error (+/-)[12]						2.42E-05
U-235 (wt%)[1]		7.61E-02	8.52E-02	8.46E-02	7.63E-02	
Error (+/-)[1]		4.40E-03	1.98E-02	6.80E-03	4.50E-03	
U-235 (g)[8]		2.44E-03	1.43E-03	1.42E-03	2.44E-03	
Error (+/-)[9]		1.41E-04	3.32E-04	1.14E-04	1.44E-04	
Segment Total						7.73E-03
Error (+/-)[12]						4.04E-04

Rod "W" 2514716 Calibration

	W-00	W-01	W-02	W-03	W-04	W-05
U-236 (wt%)[1]		1.90E-02	1.26E-02	1.27E-02	1.92E-02	
Error (+/-)[1]		1.00E-04	1.00E-04	1.00E-04	1.00E-04	
U-236 (g)[8]		6.09E-04	2.11E-04	2.13E-04	6.15E-04	
Error (+/-)[9]		3.21E-06	1.68E-06	1.68E-06	3.21E-06	
Segment Total						1.65E-03
Error (+/-)[12]						5.12E-06
U-238 (wt%)[1]		2.63E-01	1.02E+00	1.02E+00	2.64E-01	
Error (+/-)[1]		4.40E-03	1.97E-02	6.70E-03	4.50E-03	
U-238 (g)[8]		8.44E-03	1.71E-02	1.71E-02	8.44E-03	
Error (+/-)[9]		1.41E-04	3.30E-04	1.12E-04	1.44E-04	
Segment Total						5.11E-02
Error (+/-)[12]						4.03E-04
Total U[2]		3.20E+00	1.67E+00	1.68E+00	3.20E+00	
Error (+/-)[2]		8.40E-04	1.07E-03	4.50E-04	8.40E-04	
Kr-82 (mol%)[3]						
Error (+/-)[3]						
Kr-82 (g)[10]						
Error (+/-)[9]						
Segment Total						
Error (+/-)[12]						
Kr-83 (mol%)[3]						
Error (+/-)[3]						
Kr-83 (g)[10]						
Error (+/-)[9]						
Segment Total						

Rod "W" 2514716 Calibration

	W-00	W-01	W-02	W-03	W-04	W-05
Error (+/-)[12]						
Kr-84 (mol%)[3]						
Error (+/-)[3]						
Kr-84 (g)[10]						
Error (+/-)[9]						
Segment Total						
Error (+/-)[12]						
Kr-85 (mol%)[3]						
Error (+/-)[3]						
Kr-85 (g)[10]						
Error (+/-)[9]						
Segment Total						
Error (+/-)[12]						
Kr-86 (mol%)[3]						
Error (+/-)[3]						
Kr-86 (g)[10]						
Error (+/-)[9]						
Segment Total						
Error (+/-)[12]						
Rod Total						
Error (+/-)[12]						
Shear Gas (g)[4]						
Error (+/-)[4]						
Diss+Pl Kr (mol)[3]						
Error (+/-)[3]						
Diss+Pl Kr+Xe (g)[3]						

Rod "W" 2514716 Calibration

	W-00	W-01	W-02	W-03	W-04	W-05
Error (+/-)[3]						
Total Kr (mol)						
Error (+/-)[9]						
Xe-128 (mol)[3]						
Error (+/-)[3]						
Xe-128 (g)[10]						
Error (+/-)[3]						
SegmentTotal						
Error (+/1)[12]						
Xe-130 (mol)[3]						
Error (+/-)[3]						
Xe-130 (g)[10]						
Error (+/-)[3]						
SegmentTotal						
Error (+/1)[12]						
Xe-131 (mol)[3]						
Error (+/-)[3]						
Xe-131 (g)[10]						
Error (+/-)[3]						
SegmentTotal						
Error (+/1)[12]						
Xe-132 (mol)[3]						
Error (+/-)[3]						
Xe-132 (g)[10]						
Error (+/-)[3]						
SegmentTotal						

Rod "W" 2514716 Calibration

	W-00	W-01	W-02	W-03	W-04	W-05
Error (+/1)[12]						
Xe-134 (mol)[3]						
Error (+/-)[3]						
Xe-134 (g)[10]						
Error (+/-)[3]						
SegmentTotal						
Error (+/1)[12]						
Xe-136 (mol)[3]						
Error (+/-)[3]						
Xe-136 (g)[10]						
Error (+/-)[3]						
SegmentTotal						
Error (+/1)[12]						
Rod total						
Error (+/-)[12]						
Shear Gas (g)[4]						
Error (+/-)[4]						
Diss+Pl Xe (mol)[3]						
Error (+/-)[3]						
Diss+Pl Kr+Xe (g)[3]						
Error (+/-)[3]						
Total Xe (mol)						
Error (+/-)[9]						
Values corrected to 1/1/84 (page 181, Final Report for the LWBR Proof of Breeding Analytical Support Project						

Rod "W" 2514716 Calibration

	W-00	W-01	W-02	W-03	W-04	W-05
Cs-137 (atoms)[5]						
Error (+/-)[4]						
Cs-137 (g)[11]						
Error (+/-)[9]						
Total						
Error (+/-)[12]						
Ce-144 (atoms)[5]						
Error (+/-)[4]						
Ce-144 (g)[11]						
Error (+/-)[9]						
Total						
Error (+/-)[12]						
Zr-95 (atoms)[5]						
Error (+/-)[4]						
Zr-95 (g)[11]						
Error (+/-)[9]						
Total						
Error (+/-)[12]						

Rod "M" 0504042 (S1-1, 5L29)

	M-00	M-01	M-02	M-03	M-04	M-05	M-06	M-07
Segment length (in)	1.01E+01	1.01E+01	2.14E+01	2.12E+01	2.12E+01	2.13E+01	9.57E+00	2.02E+00
Total length (in)								1.17E+02
U-232 (wt%)[1]	0.00E+00	4.20E-02	7.01E-02	1.42E-01	1.35E-01	4.37E-02	2.53E-02	
Error (+/-)[1]	0.00E+00	1.30E-03	2.20E-03	4.40E-03	4.20E-03	1.40E-03	8.00E-04	
U-232 (g)[8]	0.00E+00	1.44E-04	4.37E-03	8.20E-03	8.11E-03	3.10E-03	5.01E-05	
Error (+/-)[9]	NA	4.46E-06	1.37E-04	2.55E-04	2.53E-04	9.93E-05	1.58E-06	
Segment Total								2.40E-02
Error (+/-)[12]								3.97E-04
U-233 (wt%)[1]	1.00E+02	9.71E+01	8.75E+01	8.27E+01	8.41E+01	9.16E+01	9.81E+01	
Error (+/-)[1]	0.00E+00	1.04E-02	6.10E-03	6.80E-03	6.60E-03	3.80E-03	1.83E-02	
U-233 (g)[8]	4.00E-05	3.33E-01	5.45E+00	4.79E+00	5.07E+00	6.50E+00	1.94E-01	
Error (+/-)[9]	1.00E-05	1.03E-04	1.39E-03	1.33E-03	1.37E-03	1.57E-03	7.77E-05	
Segment Total								2.23E+01
Error (+/-)[12]								2.84E-03
U-234 (wt%)[1]	0.00E+00	2.71E+00	1.03E+01	1.39E+01	1.28E+01	7.06E+00	1.76E+00	
Error (+/-)[1]	0.00E+00	2.10E-03	1.90E-03	2.10E-03	1.80E-03	1.90E-03	2.20E-03	
U-234 (g)[8]	0.00E+00	9.30E-03	6.44E-01	8.04E-01	7.74E-01	5.01E-01	3.48E-03	
Error (+/-)[9]	NA	7.70E-06	1.98E-04	2.45E-04	2.28E-04	1.80E-04	4.52E-06	
Segment Total								2.74E+00
Error (+/-)[12]								4.28E-04
U-235 (wt%)[1]	0.00E+00	1.52E-01	1.61E+00	2.63E+00	2.38E+00	9.20E-01	6.05E-02	
Error (+/-)[1]	0.00E+00	7.30E-03	4.40E-03	4.60E-03	4.40E-03	2.30E-03	1.30E-02	
U-235 (g)[8]	0.00E+00	5.20E-04	1.00E-01	1.52E-01	1.43E-01	6.52E-02	1.20E-04	
Error (+/-)[9]	NA	2.51E-05	2.75E-04	2.69E-04	2.68E-04	1.64E-04	2.57E-05	
Segment Total								4.62E-01
Error (+/-)[12]								4.98E-04

Rod "M" 0504042 (S1-1, 5L29)

	M-00	M-01	M-02	M-03	M-04	M-05	M-06	M-07
U-236 (wt%)[1]	0.00E+00	3.50E-03	1.25E-01	2.60E-01	2.21E-01	5.75E-02	1.10E-03	
Error (+/-)[1]	0.00E+00	1.00E-04	1.00E-04	1.00E-04	1.00E-04	1.00E-04	2.00E-04	
U-236 (g)[8]	0.00E+00	1.20E-05	7.78E-03	1.50E-02	1.33E-02	4.08E-03	2.18E-06	
Error (+/-)[9]	NA	3.43E-07	6.52E-06	7.02E-06	6.94E-06	7.16E-06	3.96E-07	
Segment Total								4.02E-02
Error (+/-)[12]								1.38E-05
U-238 (wt%)[1]	0.00E+00	1.29E-02	3.38E-01	3.40E-01	3.26E-01	3.06E-01	1.77E-02	
Error (+/-)[1]	0.00E+00	7.40E-03	4.50E-03	4.70E-03	4.50E-03	2.40E-03	1.31E-02	
U-238 (g)[8]	0.00E+00	4.43E-05	2.10E-02	1.97E-02	1.96E-02	2.17E-02	3.50E-05	
Error (+/-)[9]	NA	2.54E-05	2.80E-04	2.72E-04	2.71E-04	1.70E-04	2.59E-05	
Segment Total								8.21E-02
Error (+/-)[12]								5.06E-04
Total U[2]	7.00E-05	3.43E-01	6.23E+00	5.79E+00	6.03E+00	7.09E+00	1.98E-01	
Error (+/-)[2]	1.00E-05	1.00E-04	1.53E-03	1.53E-03	1.56E-03	1.69E-03	7.00E-05	
Kr-82 (mol%)[3]	2.00E-01	2.00E-01	2.00E-01	2.00E-01	2.00E-01	2.00E-01	2.00E-01	
Error (+/-)[3]	0.00E+00	0.00E+00	0.00E+00	0.00E+00	0.00E+00	0.00E+00	0.00E+00	
Kr-82 (g)[10]	8.19E-07	0.00E+00	2.52E-04	2.98E-04	2.59E-04	1.72E-04	0.00E+00	
Error (+/-)[9]	8.19E-11	NA	2.18E-05	3.18E-05	3.11E-05	2.02E-05	NA	
Segment Total								9.81E-04
Error (+/-)[12]								5.35E-05
Kr-83 (mol%)[3]	1.49E+01	1.49E+01	1.49E+01	1.49E+01	1.49E+01	1.49E+01	1.49E+01	
Error (+/-)[3]	1.00E-01	1.00E-01	1.00E-01	1.00E-01	1.00E-01	1.00E-01	1.00E-01	
Kr-83 (g)[10]	6.18E-05	0.00E+00	1.90E-02	2.25E-02	1.95E-02	1.29E-02	0.00E+00	
Error (+/-)[9]	4.15E-07	NA	1.65E-03	2.40E-03	2.35E-03	1.52E-03	NA	
Segment Total								7.40E-02
Error (+/-)[12]								4.04E-03

Rod "M" 0504042 (S1-1, 5L29)

	M-00	M-01	M-02	M-03	M-04	M-05	M-06	M-07
Kr-84 (mol%)[3]	3.08E+01	3.08E+01	3.08E+01	3.08E+01	3.08E+01	3.08E+01	3.08E+01	
Error (+/-)[3]	1.00E-01	1.00E-01	1.00E-01	1.00E-01	1.00E-01	1.00E-01	1.00E-01	
Kr-84 (g)[10]	1.29E-04	0.00E+00	3.98E-02	4.70E-02	4.09E-02	2.71E-02	0.00E+00	
Error (+/-)[9]	4.20E-07	NA	3.44E-03	5.02E-03	4.91E-03	3.18E-03	NA	
Segment Total								1.55E-01
Error (+/-)[12]								8.44E-03
Kr-85 (mol%)[3]	5.70E+00	5.70E+00	5.70E+00	5.70E+00	5.70E+00	5.70E+00	5.70E+00	
Error (+/-)[3]	1.00E-01	1.00E-01	1.00E-01	1.00E-01	1.00E-01	1.00E-01	1.00E-01	
Kr-85 (g)[10]	2.42E-05	0.00E+00	7.44E-03	8.80E-03	7.65E-03	5.07E-03	0.00E+00	
Error (+/-)[9]	4.25E-07	NA	6.57E-04	9.52E-04	9.29E-04	6.02E-04	NA	
Segment Total								2.90E-02
Error (+/-)[12]								1.60E-03
Kr-86 (mol%)[3]	4.85E+01	4.85E+01	4.85E+01	4.85E+01	4.85E+01	4.85E+01	4.85E+01	
Error (+/-)[3]	1.00E-01	1.00E-01	1.00E-01	1.00E-01	1.00E-01	1.00E-01	1.00E-01	
Kr-86 (g)[10]	2.08E-04	0.00E+00	6.41E-02	7.57E-02	6.59E-02	4.36E-02	0.00E+00	
Error (+/-)[9]	4.30E-07	NA	5.54E-03	8.09E-03	7.92E-03	5.13E-03	NA	
Segment Total								2.50E-01
Error (+/-)[12]								1.36E-02
Rod Total								5.08E-01
Error (+/-)[12]								1.66E-02
Shear Gas (g)[4]	0.00E+00	1.00E-04	3.10E-03	7.10E-03	6.00E-03	2.00E-03	0.00E+00	
Error (+/-)[4]	0.00E+00	3.00E-04	6.00E-04	1.40E-03	1.20E-03	4.00E-04	3.00E-04	
Diss+Pl Kr (mol)[3]	5.00E-06	0.00E+00	1.53E-03	1.81E-03	1.57E-03	1.04E-03	0.00E+00	
Error (+/-)[3]	0.00E+00	0.00E+00	1.33E-04	1.94E-04	1.90E-04	1.23E-04	0.00E+00	
Diss+Pl Kr+Xe (g)[3]	2.90E-03	1.12E-02	9.44E-01	1.11E+00	9.64E-01	6.41E-01	9.00E-03	
Error (+/-)[3]	1.00E-04	1.12E-02	5.49E-02	8.81E-02	6.60E-02	4.25E-02	9.00E-03	
Total Kr (mol)	5.00E-06	0.00E+00	1.54E-03	1.82E-03	1.58E-03	1.05E-03	0.00E+00	
Error (+/-)[9]	5.00E-10	3.54E-06	1.33E-04	1.94E-04	1.90E-04	1.23E-04	0.00E+00	

Rod "M" 0504042 (S1-1, 5L29)

	M-00	M-01	M-02	M-03	M-04	M-05	M-06	M-07
Xe-128 (mol)[3]	1.00E-01	1.00E-01	1.00E-01	1.00E-01	1.00E-01	1.00E-01	1.00E-01	
Error (+/-)[3]	0.00E+00	0.00E+00	0.00E+00	0.00E+00	0.00E+00	0.00E+00	0.00E+00	
Xe-128 (g)[10]	2.43E-06	1.07E-05	7.78E-04	9.13E-04	7.97E-04	5.28E-04	8.57E-06	
Error (+/-)[3]	1.28E-07	1.06E-05	5.12E-05	8.25E-05	6.09E-05	3.93E-05	8.57E-06	
SegmentTotal								3.04E-03
Error (+/1)[12]								1.22E-04
Xe-130 (mol)[3]	1.00E-01	1.00E-01	1.00E-01	1.00E-01	1.00E-01	1.00E-01	1.00E-01	
Error (+/-)[3]	0.00E+00	0.00E+00	0.00E+00	0.00E+00	0.00E+00	0.00E+00	0.00E+00	
Xe-130 (g)[10]	2.47E-06	1.09E-05	7.90E-04	9.27E-04	8.09E-04	5.36E-04	8.70E-06	
Error (+/-)[3]	1.30E-07	1.08E-05	5.20E-05	8.38E-05	6.18E-05	3.99E-05	8.70E-06	
SegmentTotal								3.09E-03
Error (+/1)[12]								1.24E-04
Xe-131 (mol)[3]	1.07E+01	1.07E+01	1.07E+01	1.07E+01	1.07E+01	1.07E+01	1.07E+01	
Error (+/-)[3]	1.00E-01	1.00E-01	1.00E-01	1.00E-01	1.00E-01	1.00E-01	1.00E-01	
Xe-131 (g)[10]	2.66E-04	1.17E-03	8.52E-02	1.00E-01	8.72E-02	5.78E-02	9.38E-04	
Error (+/-)[3]	1.42E-05	1.16E-03	5.66E-03	9.08E-03	6.72E-03	4.33E-03	9.39E-04	
SegmentTotal								3.33E-01
Error (+/1)[12]								1.34E-02
Xe-132 (mol)[3]	2.36E+01	2.36E+01	2.36E+01	2.36E+01	2.36E+01	2.36E+01	2.36E+01	
Error (+/-)[3]	1.00E-01	1.00E-01	1.00E-01	1.00E-01	1.00E-01	1.00E-01	1.00E-01	
Xe-132 (g)[10]	5.91E-04	2.61E-03	1.89E-01	2.22E-01	1.94E-01	1.28E-01	2.09E-03	
Error (+/-)[3]	3.12E-05	2.58E-03	1.25E-02	2.01E-02	1.48E-02	9.57E-03	2.09E-03	
SegmentTotal								7.39E-01
Error (+/1)[12]								2.97E-02
Xe-134 (mol)[3]	2.57E+01	2.57E+01	2.57E+01	2.57E+01	2.57E+01	2.57E+01	2.57E+01	
Error (+/-)[3]	1.00E-01	1.00E-01	1.00E-01	1.00E-01	1.00E-01	1.00E-01	1.00E-01	
Xe-134 (g)[10]	6.54E-04	2.88E-03	2.09E-01	2.46E-01	2.14E-01	1.42E-01	2.31E-03	

Rod "M" 0504042 (S1-1, 5L29)

	M-00	M-01	M-02	M-03	M-04	M-05	M-06	M-07
Error (+/-)[3]	3.45E-05	2.86E-03	1.38E-02	2.22E-02	1.64E-02	1.06E-02	2.31E-03	
SegmentTotal								8.17E-01
Error (+/1)[12]								3.28E-02
Xe-136 (mol)[3]	3.98E+01	3.98E+01	3.98E+01	3.98E+01	3.98E+01	3.98E+01	3.98E+01	
Error (+/-)[3]	1.00E-01	3.98E+01	3.98E+01	3.98E+01	3.98E+01	3.98E+01	3.98E+01	
Xe-136 (g)[10]	1.03E-03	4.53E-03	3.29E-01	3.86E-01	3.37E-01	2.23E-01	3.62E-03	
Error (+/-)[3]	5.42E-05	6.38E-03	3.30E-01	3.88E-01	3.38E-01	2.24E-01	5.13E-03	
SegmentTotal								1.28E+00
Error (+/1)[12]								6.51E-01
Rod total								3.18E+00
Error (+/-)[12]								6.52E-01
Shear Gas (g)[4]	0.00E+00	1.00E-04	3.10E-03	7.10E-03	6.00E-03	2.00E-03	0.00E+00	
Error (+/-)[4]	0.00E+00	3.00E-04	6.00E-04	1.40E-03	1.20E-03	4.00E-04	3.00E-04	
Diss+Pl Xe (mol)[3]	1.90E-05	8.30E-05	6.07E-03	7.09E-03	6.19E-03	4.12E-03	6.70E-05	
Error (+/-)[3]	1.00E-06	8.30E-05	4.00E-04	6.45E-04	4.76E-04	3.07E-04	6.70E-05	
Diss+Pl Kr+Xe (g)[3]	2.90E-03	1.12E-02	9.44E-01	1.11E+00	9.64E-01	6.41E-01	9.00E-03	
Error (+/-)[3]	1.00E-04	1.12E-02	5.49E-02	8.81E-02	6.60E-02	4.25E-02	9.00E-03	
Total Xe (mol)	1.90E-05	8.37E-05	6.08E-03	7.14E-03	6.23E-03	4.13E-03	6.70E-05	
Error (+/-)[9]	1.00E-06	8.30E-05	4.00E-04	6.45E-04	4.76E-04	3.07E-04	6.70E-05	
Values corrected to 1/1/84 (page 181, Final Report for the LWBR Proof of Breeding Analytical Support Project								
Cs-137 (atoms)[5]	ND	1.08E+19	7.99E+20	1.06E+21	1.00E+21	5.61E+20	3.99E+18	
Error (+/-)[4]	NA	5.65E+16	3.51E+18	5.39E+18	5.12E+18	2.94E+18	2.24E+16	
Cs-137 (g)[11]	NA	2.45E-03	1.82E-01	2.40E-01	2.28E-01	1.27E-01	9.08E-04	
Error (+/-)[9]	NA	1.28E-05	7.97E-04	1.22E-03	1.16E-03	6.69E-04	5.09E-06	
Total								7.80E-01
Error (+/-)[12]								1.98E-03

Rod "M" 0504042 (S1-1, 5L29)

	M-00	M-01	M-02	M-03	M-04	M-05	M-06	M-07
Ce-144 (atoms)[5]	ND	3.36E+17	2.02E+19	3.92E+19	5.25E+19	4.58E+19	6.22E+17	
Error (+/-)[4]	NA	2.61E+15	1.39E+17	2.91E+17	4.04E+17	3.52E+17	4.84E+15	
Ce-144 (g)[11]	NA	8.02E-05	4.84E-03	9.36E-03	1.25E-02	1.09E-02	1.49E-04	
Error (+/-)[9]	NA	6.24E-07	3.31E-05	6.95E-05	9.65E-05	8.41E-05	1.16E-06	
Total								3.79E-02
Error (+/-)[12]								1.49E-04
Zr-95 (atoms)[5]	ND	ND	ND	2.62E+17	4.65E+17	4.00E+17	8.29E+15	
Error (+/-)[4]	NA	NA	NA	2.90E+16	5.60E+16	2.90E+16	4.77E+14	
Zr-95 (g)[11]	NA	NA	NA	4.13E-05	7.33E-05	6.30E-05	1.31E-06	
Error (+/-)[9]	NA	NA	NA	4.57E-06	8.82E-06	4.56E-06	7.52E-08	
Total								1.79E-04
Error (+/-)[12]								1.09E-05

References

1. ANL Destructive Chemical Assay of 33-Rod LWBR EOL Sample - Rod M, 0504042, page 7
2. ANL Destructive Chemical Assay of 33-Rod LWBR EOL Sample - Rod M, 0504042, page 8
3. ANL Destructive Chemical Assay of 33-Rod LWBR EOL Sample - Rod M, 0504042, page 11
4. ANL Destructive Chemical Assay of 33-Rod LWBR EOL Sample - Rod M, 0504042, page 12
5. ANL Destructive Chemical Assay of 33-Rod LWBR EOL Sample - Rod M, 0504042, page 13
6. ANL Destructive Chemical Assay of 33-Rod LWBR EOL Sample - Rod M, 0504042, page 14
7. ANL Destructive Chemical Assay of 33-Rod LWBR EOL Sample - Rod M, 0504042, page 15

8. (abundance of the specified isotope)(total weight of uranium)

   1.00E+02

9. Error Propagation = ((+/-x/x)2+(+/-y/y)2)1/2(xy)
10. (mole%)(number moles gas recovered)(molec wt)

    1.00E+02

11. (number of atoms per segment)(atomic weight)

    6.02E+23

12. Error Propagation = (SUM(+/-I)1/2

Rod "N" 0507057 (S1-1, 5C10)

	N-00	N-01	N-02	N-03	N-04	N-05	N-06	N-07
Segment length (in)	1.02E+01	1.01E+01	2.14E+01	2.12E+01	2.12E+01	2.12E+01	9.64E+00	2.07E+00
Total length (in)								1.17E+02
U-232 (wt%)[1]	0.00E+00	4.00E-02	5.50E-02	1.18E-01	1.23E-01	4.13E-02	2.61E-02	
Error (+/-)[1]	0.00E+00	1.20E-03	1.70E-03	3.70E-03	3.80E-03	1.30E-03	8.00E-04	
U-232 (g)[8]	0.00E+00	1.30E-04	3.97E-03	7.75E-03	7.99E-03	3.05E-03	4.97E-05	
Error (+/-)[9]	NA	3.90E-06	1.23E-04	2.43E-04	2.47E-04	9.61E-05	1.52E-06	
Segment Total								2.29E-02
Error (+/-)[12]								3.80E-04
U-233 (wt%)[1]	1.00E+02	9.73E+01	9.10E+01	8.63E+01	8.60E+01	9.23E+01	9.82E+01	
Error (+/-)[1]	0.00E+00	1.29E-02	4.90E-03	5.90E-03	5.00E-03	6.20E-03	2.15E-02	
U-233 (g)[8]	4.00E-05	3.17E-01	6.57E+00	5.66E+00	5.59E+00	6.82E+00	1.87E-01	
Error (+/-)[9]	1.00E-05	9.71E-05	1.49E-03	1.35E-03	1.31E-03	1.71E-03	1.06E-04	
Segment Total								2.52E+01
Error (+/-)[12]								2.95E-03
U-234 (wt%)[1]	0.00E+00	2.49E+00	7.54E+00	1.11E+01	1.14E+01	6.49E+00	1.67E+00	
Error (+/-)[1]	0.00E+00	9.00E-04	9.00E-04	1.20E-03	1.10E-03	9.00E-04	9.00E-04	
U-234 (g)[8]	0.00E+00	8.09E-03	5.44E-01	7.32E-01	7.39E-01	4.80E-01	3.18E-03	
Error (+/-)[9]	NA	3.69E-06	1.36E-04	1.85E-04	1.82E-04	1.33E-04	2.39E-06	
Segment Total								2.51E+00
Error (+/-)[12]								3.22E-04
U-235 (wt%)[1]	0.00E+00	1.30E-01	1.06E+00	2.00E+00	2.06E+00	8.39E-01	5.48E-02	
Error (+/-)[1]	0.00E+00	9.40E-03	3.60E-03	4.00E-03	3.10E-03	4.60E-03	1.55E-02	
U-235 (g)[8]	0.00E+00	4.22E-04	7.65E-02	1.31E-01	1.34E-01	6.20E-02	1.04E-04	
Error (+/-)[9]	NA	3.06E-05	2.60E-04	2.64E-04	2.04E-04	3.40E-04	2.95E-05	
Segment Total								4.05E-01
Error (+/-)[12]								5.45E-04

Rod "N" 0507057 (S1-1, 5C10)

	N-00	N-01	N-02	N-03	N-04	N-05	N-06	N-07
U-236 (wt%)[1]	0.00E+00	2.60E-03	6.63E-02	1.62E-01	1.71E-01	4.95E-02	9.00E-04	
Error (+/-)[1]	0.00E+00	1.00E-04	1.00E-04	1.00E-04	1.00E-04	1.00E-04	1.00E-04	
U-236 (g)[8]	0.00E+00	8.46E-06	4.79E-03	1.06E-02	1.11E-02	3.66E-03	1.71E-06	
Error (+/-)[9]	NA	3.25E-07	7.29E-06	7.00E-06	6.98E-06	7.45E-06	1.91E-07	
Segment Total								3.02E-02
Error (+/-)[12]								1.44E-05
U-238 (wt%)[1]	0.00E+00	1.04E-02	2.98E-01	3.03E-01	3.01E-01	2.95E-01	2.12E-02	
Error (+/-)[1]	0.00E+00	9.30E-03	3.50E-03	3.90E-03	2.90E-03	4.50E-03	1.55E-02	
U-238 (g)[8]	0.00E+00	3.38E-05	2.15E-02	1.99E-02	1.96E-02	2.18E-02	4.04E-05	
Error (+/-)[9]	NA	3.03E-05	2.53E-04	2.56E-04	1.89E-04	3.33E-04	2.95E-05	
Segment Total								8.29E-02
Error (+/-)[12]								5.27E-04
Total U[2]	9.00E-05	3.25E-01	7.22E+00	6.56E+00	6.51E+00	7.39E+00	1.91E-01	
Error (+/-)[2]	1.00E-05	9.00E-05	1.59E-03	1.50E-03	1.47E-03	1.78E-03	1.00E-04	
Kr-82 (mol%)[3]	2.00E-01	2.00E-01	2.00E-01	2.00E-01	2.00E-01	2.00E-01	2.00E-01	
Error (+/-)[3]	0.00E+00	0.00E+00	0.00E+00	0.00E+00	0.00E+00	0.00E+00	0.00E+00	
Kr-82 (g)[10]	4.91E-07	0.00E+00	2.06E-04	2.16E-04	2.75E-04	1.63E-04	1.11E-07	
Error (+/-)[9]	4.91E-11	NA	2.42E-05	2.98E-05	3.05E-05	1.92E-05	3.33E-11	
Segment Total								8.61E-04
Error (+/-)[12]								5.27E-05
Kr-83 (mol%)[3]	1.57E+01	1.57E+01	1.57E+01	1.57E+01	1.57E+01	1.57E+01	1.57E+01	
Error (+/-)[3]	2.00E-01	2.00E-01	2.00E-01	2.00E-01	2.00E-01	2.00E-01	2.00E-01	
Kr-83 (g)[10]	3.91E-05	0.00E+00	1.64E-02	1.71E-02	2.18E-02	1.30E-02	8.83E-06	
Error (+/-)[9]	4.98E-07	NA	1.94E-03	2.38E-03	2.44E-03	1.53E-03	1.12E-07	
Segment Total								6.84E-02
Error (+/-)[12]								4.21E-03
Kr-84 (mol%)[3]	2.99E+01	2.99E+01	2.99E+01	2.99E+01	2.99E+01	2.99E+01	2.99E+01	

Rod "N" 0507057 (S1-1, 5C10)

	N-00	N-01	N-02	N-03	N-04	N-05	N-06	N-07
Error (+/-)[3]	1.00E-01	1.00E-01	1.00E-01	1.00E-01	1.00E-01	1.00E-01	1.00E-01	
Kr-84 (g)[10]	7.53E-05	0.00E+00	3.16E-02	3.30E-02	4.21E-02	2.50E-02	1.70E-05	
Error (+/-)[9]	2.52E-07	NA	3.71E-03	4.57E-03	4.67E-03	2.94E-03	5.71E-08	
Segment Total								1.32E-01
Error (+/-)[12]								8.07E-03
Kr-85 (mol%)[3]	5.70E+00	5.70E+00	5.70E+00	5.70E+00	5.70E+00	5.70E+00	5.70E+00	
Error (+/-)[3]	1.00E-01	1.00E-01	1.00E-01	1.00E-01	1.00E-01	1.00E-01	1.00E-01	
Kr-85 (g)[10]	1.45E-05	0.00E+00	6.10E-03	6.38E-03	8.12E-03	4.82E-03	3.28E-06	
Error (+/-)[9]	2.55E-07	NA	7.24E-04	8.88E-04	9.11E-04	5.73E-04	5.76E-08	
Segment Total								2.54E-02
Error (+/-)[12]								1.57E-03
Kr-86 (mol%)[3]	4.85E+01	4.85E+01	4.85E+01	4.85E+01	4.85E+01	4.85E+01	4.85E+01	
Error (+/-)[3]	1.00E-01	1.00E-01	1.00E-01	1.00E-01	1.00E-01	1.00E-01	1.00E-01	
Kr-86 (g)[10]	1.25E-04	0.00E+00	5.25E-02	5.49E-02	6.99E-02	4.15E-02	2.83E-05	
Error (+/-)[9]	2.58E-07	NA	6.17E-03	7.58E-03	7.75E-03	4.88E-03	5.89E-08	
Segment Total								2.19E-01
Error (+/-)[12]								1.34E-02
Rod Total								4.45E-01
Error (+/-)[12]								1.63E-02
Shear Gas (g)[4]	0.00E+00	0.00E+00	1.60E-03	4.10E-03	5.00E-03	2.00E-03	4.00E-04	
Error (+/-)[4]	0.00E+00	3.00E-04	3.00E-04	8.00E-04	1.00E-03	4.00E-04	3.00E-04	
Diss+Pl Kr (mol)[3]	3.00E-06	0.00E+00	1.26E-03	1.31E-03	1.67E-03	9.93E-04	0.00E+00	
Error (+/-)[3]	0.00E+00	0.00E+00	1.48E-04	1.82E-04	1.86E-04	1.17E-04	0.00E+00	
Diss+Pl Kr+Xe (g)[3]	1.60E-03	1.64E-02	7.52E-01	7.46E-01	9.71E-01	5.86E-01	0.00E+00	
Error (+/-)[3]	1.00E-04	1.64E-02	4.17E-02	9.89E-02	8.45E-02	4.81E-02	0.00E+00	
Total Kr (mol)	3.00E-06	0.00E+00	1.26E-03	1.32E-03	1.68E-03	9.96E-04	6.78E-07	
Error (+/-)[9]	3.00E-10	0.00E+00	1.48E-04	1.82E-04	1.86E-04	1.17E-04	2.03E-10	

Rod "N" 0507057 (S1-1, 5C10)

	N-00	N-01	N-02	N-03	N-04	N-05	N-06	N-07
Xe-128 (mol)[3]	1.00E-01	1.00E-01	1.00E-01	1.00E-01	1.00E-01	1.00E-01	1.00E-01	
Error (+/-)[3]	0.00E+00	0.00E+00	0.00E+00	0.00E+00	0.00E+00	0.00E+00	0.00E+00	
Xe-128 (g)[10]	1.28E-06	1.56E-05	6.16E-04	6.08E-04	7.95E-04	4.80E-04	3.26E-07	
Error (+/-)[3]	1.28E-10	1.56E-05	3.79E-05	9.31E-05	7.90E-05	4.48E-05	9.79E-11	
SegmentTotal								2.52E-03
Error (+/1)[12]								1.36E-04
Xe-130 (mol)[3]	1.00E-01	1.00E-01	1.00E-01	1.00E-01	1.00E-01	1.00E-01	1.00E-01	
Error (+/-)[3]	0.00E+00	0.00E+00	0.00E+00	0.00E+00	0.00E+00	0.00E+00	0.00E+00	
Xe-130 (g)[10]	1.30E-06	1.58E-05	6.26E-04	6.18E-04	8.07E-04	4.87E-04	3.32E-07	
Error (+/-)[3]	1.30E-10	1.59E-05	3.85E-05	9.46E-05	8.03E-05	4.55E-05	9.95E-11	
SegmentTotal								2.56E-03
Error (+/1)[12]								1.39E-04
Xe-131 (mol)[3]	1.18E+01	1.18E+01	1.18E+01	1.18E+01	1.18E+01	1.18E+01	1.18E+01	
Error (+/-)[3]	1.00E-01	1.00E-01	1.00E-01	1.00E-01	1.00E-01	1.00E-01	1.00E-01	
Xe-131 (g)[10]	1.54E-04	1.88E-03	7.44E-02	7.35E-02	9.60E-02	5.79E-02	3.94E-05	
Error (+/-)[3]	1.31E-06	1.89E-03	4.62E-03	1.13E-02	9.58E-03	5.43E-03	3.34E-07	
SegmentTotal								3.04E-01
Error (+/1)[12]								1.65E-02
Xe-132 (mol)[3]	2.40E+01	2.40E+01	2.40E+01	2.40E+01	2.40E+01	2.40E+01	2.40E+01	
Error (+/-)[3]	1.00E-01	1.00E-01	1.00E-01	1.00E-01	1.00E-01	1.00E-01	1.00E-01	
Xe-132 (g)[10]	3.17E-04	3.86E-03	1.53E-01	1.51E-01	1.97E-01	1.19E-01	8.08E-05	
Error (+/-)[3]	1.32E-06	3.86E-03	9.39E-03	2.31E-02	1.96E-02	1.11E-02	3.38E-07	
SegmentTotal								6.23E-01
Error (+/1)[12]								3.38E-02
Xe-134 (mol)[3]	2.66E+01	2.66E+01	2.66E+01	2.66E+01	2.66E+01	2.66E+01	2.66E+01	
Error (+/-)[3]	1.00E-01	1.00E-01	1.00E-01	1.00E-01	1.00E-01	1.00E-01	1.00E-01	
Xe-134 (g)[10]	3.56E-04	4.35E-03	1.72E-01	1.69E-01	2.21E-01	1.34E-01	9.09E-05	

Rod "N" 0507057 (S1-1, 5C10)

	N-00	N-01	N-02	N-03	N-04	N-05	N-06	N-07
Error (+/-)[3]	1.34E-06	4.35E-03	1.06E-02	2.59E-02	2.20E-02	1.25E-02	3.43E-07	
SegmentTotal								7.01E-01
Error (+/1)[12]								3.80E-02
Xe-136 (mol)[3]	3.75E+01	3.75E+01	3.75E+01	3.75E+01	3.75E+01	3.75E+01	3.75E+01	
Error (+/-)[3]	2.00E-01	2.00E-01	2.00E-01	2.00E-01	2.00E-01	2.00E-01	2.00E-01	
Xe-136 (g)[10]	5.10E-04	6.22E-03	2.46E-01	2.42E-01	3.17E-01	1.91E-01	1.30E-04	
Error (+/-)[3]	2.72E-06	6.22E-03	1.51E-02	3.71E-02	3.15E-02	1.79E-02	6.95E-07	
SegmentTotal								1.00E+00
Error (+/1)[12]								5.44E-02
Rod total								2.64E+00
Error (+/-)[12]								7.63E-02
Shear Gas (g)[4]	0.00E+00	0.00E+00	1.60E-03	4.10E-03	5.00E-03	2.00E-03	4.00E-04	
Error (+/-)[4]	0.00E+00	3.00E-04	3.00E-04	8.00E-04	1.00E-03	4.00E-04	3.00E-04	
Diss+Pl Xe (mol)[3]	1.00E-05	1.22E-04	4.81E-03	4.73E-03	6.18E-03	3.74E-03	0.00E+00	
Error (+/-)[3]	0.00E+00	1.22E-04	2.96E-04	7.28E-04	6.18E-04	3.50E-04	0.00E+00	
Diss+Pl Kr+Xe (g)[3]	1.60E-03	1.64E-02	7.52E-01	7.46E-01	9.71E-01	5.86E-01	0.00E+00	
Error (+/-)[3]	1.00E-04	1.64E-02	4.17E-02	9.89E-02	8.45E-02	4.81E-02	0.00E+00	
Total Xe (mol)	1.00E-05	1.22E-04	4.82E-03	4.76E-03	6.21E-03	3.75E-03	2.55E-06	
Error (+/-)[9]	1.00E-09	1.22E-04	2.96E-04	7.28E-04	6.18E-04	3.50E-04	7.66E-10	
Values corrected to 1/1/84 (page 181, Final Report for the LWBR Proof of Breeding Analytical Support Project								
Cs-137 (atoms)[5]	NA	9.35E+18	5.92E+20	8.92E+20	9.13E+20	5.16E+20	3.68E+18	
Error (+/-)[4]	NA	2.73E+16	1.63E+18	2.47E+18	2.64E+18	1.56E+18	1.31E+16	
Cs-137 (g)[11]	NA	2.13E-03	1.35E-01	2.03E-01	2.07E-01	1.17E-01	8.37E-04	
Error (+/-)[9]	NA	6.21E-06	3.71E-04	5.61E-04	6.00E-04	3.54E-04	2.98E-06	
Total								6.65E-01

Rod "N" 0507057 (S1-1, 5C10)

	N-00	N-01	N-02	N-03	N-04	N-05	N-06	N-07
Error (+/-)[12]								9.68E-04
Ce-144 (atoms)[5]	NA	2.92E+17	1.63E+19	3.52E+19	4.84E+19	4.23E+19	5.77E+17	
Error (+/-)[4]	NA	2.00E+15	1.11E+17	2.39E+17	3.38E+17	2.87E+17	3.86E+15	
Ce-144 (g)[11]	NA	6.98E-05	3.89E-03	8.40E-03	1.16E-02	1.01E-02	1.38E-04	
Error (+/-)[9]	NA	4.79E-07	2.64E-05	5.70E-05	8.08E-05	6.85E-05	9.23E-07	
Total								3.42E-02
Error (+/-)[12]								1.23E-04
Zr-95 (atoms)[5]	NA	ND	ND	2.05E+17	3.96E+17	4.27E+17	8.44E+15	
Error (+/-)[4]	NA	NA	NA	3.69E+16	5.30E+16	3.28E+16	4.62E+14	
Zr-95 (g)[11]	NA	NA	NA	3.23E-05	6.23E-05	6.73E-05	1.33E-06	
Error (+/-)[9]	NA	NA	NA	5.82E-06	8.36E-06	5.17E-06	7.28E-08	
Total								1.63E-04
Error (+/-)[12]								1.14E-05

References

1. ANL Destructive Chemical Assay of 33-Rod LWBR EOL Sample - Rod N, 0507057, page 7
2. ANL Destructive Chemical Assay of 33-Rod LWBR EOL Sample - Rod N, 0507057, page 8
3. ANL Destructive Chemical Assay of 33-Rod LWBR EOL Sample - Rod N, 0507057, page 11
4. ANL Destructive Chemical Assay of 33-Rod LWBR EOL Sample - Rod N, 0507057, page 12
5. ANL Destructive Chemical Assay of 33-Rod LWBR EOL Sample - Rod N, 0507057, page 13
6. ANL Destructive Chemical Assay of 33-Rod LWBR EOL Sample - Rod N, 0507057, page 14
7. ANL Destructive Chemical Assay of 33-Rod LWBR EOL Sample - Rod N, 0507057, page 15
8. (abundance of the specified isotope)(total weight of uranium)

   1.00E+02
9. Error Propagation = ((+/-x/x)2+(+/-y/y)2)1/2(xy)
10. (mole%)(number moles gas recovered)(molec wt)

    1.00E+02
11. (number of atoms per segment)(atomic weight)

    6.02E+23
12. Error Propagation = (SUM(+/-I)1/2

Rod "O" 0201562 (S1-1, 2P39)

	O-00	O-01	O-02	O-03	O-04	O-05	O-06	O-07
Segment length (in)	1.15E+01	1.79E+01	1.76E+01	1.74E+01	2.13E+01	2.12E+01	8.92E+00	1.04E+00
Total length (in)								1.17E+02
U-232 (wt%)[1]	0.00E+00	9.26E-02	2.16E-01	2.78E-01	1.65E-01	5.60E-02	2.55E-02	
Error (+/-)[1]	0.00E+00	2.90E-03	6.70E-03	8.60E-03	5.10E-03	1.70E-03	8.00E-04	
U-232 (g)[8]	0.00E+00	8.70E-04	4.18E-03	5.92E-03	7.94E-03	3.15E-03	5.12E-05	
Error (+/-)[9]	NA	2.72E-05	1.30E-04	1.83E-04	2.46E-04	9.55E-05	1.61E-06	
Segment Total								2.21E-02
Error (+/-)[12]								3.47E-04
U-233 (wt%)[1]	1.00E+02	9.45E+01	8.81E+01	8.60E+01	8.09E+01	8.98E+01	9.80E+01	
Error (+/-)[1]	0.00E+00	6.30E-03	9.60E-03	9.00E-03	6.80E-03	7.00E-03	1.97E-02	
U-233 (g)[8]	4.00E-05	8.88E-01	1.70E+00	1.83E+00	3.91E+00	5.05E+00	1.97E-01	
Error (+/-)[9]	1.00E-05	2.25E-04	5.44E-04	2.43E-03	1.03E-03	1.40E-03	8.78E-05	
Segment Total								1.36E+01
Error (+/-)[12]								3.04E-03
U-234 (wt%)[1]	0.00E+00	4.84E+00	9.83E+00	1.13E+01	1.52E+01	8.48E+00	1.87E+00	
Error (+/-)[1]	0.00E+00	1.00E-03	1.50E-03	1.50E-03	1.70E-03	1.20E-03	1.20E-03	
U-234 (g)[8]	0.00E+00	4.55E-02	1.90E-01	2.40E-01	7.33E-01	4.76E-01	3.75E-03	
Error (+/-)[9]	NA	1.46E-05	6.39E-05	3.19E-04	2.01E-04	1.44E-04	2.84E-06	
Segment Total								1.69E+00
Error (+/-)[12]								4.09E-04
U-235 (wt%)[1]	0.00E+00	5.02E-01	1.70E+00	2.15E+00	3.01E+00	1.17E+00	6.65E-02	
Error (+/-)[1]	0.00E+00	4.20E-03	6.00E-03	4.00E-03	4.50E-03	5.30E-03	1.42E-02	
U-235 (g)[8]	0.00E+00	4.72E-03	3.29E-02	4.57E-02	1.45E-01	6.55E-02	1.34E-04	
Error (+/-)[9]	NA	3.95E-05	1.16E-04	1.04E-04	2.20E-04	2.98E-04	2.85E-05	
Segment Total								2.94E-01
Error (+/-)[12]								4.05E-04

Rod "O" 0201562 (S1-1, 2P39)

	O-00	O-01	O-02	O-03	O-04	O-05	O-06	O-07
U-236 (wt%)[1]	0.00E+00	2.37E-02	1.47E-01	2.16E-01	3.27E-01	7.30E-02	1.10E-03	
Error (+/-)[1]	0.00E+00	1.00E-04	1.00E-04	1.00E-04	1.00E-04	1.00E-04	1.00E-04	
U-236 (g)[8]	0.00E+00	2.23E-04	2.84E-03	4.59E-03	1.58E-02	4.10E-03	2.21E-06	
Error (+/-)[9]	NA	9.41E-07	2.11E-06	6.43E-06	6.24E-06	5.72E-06	2.01E-07	
Segment Total								2.75E-02
Error (+/-)[12]								1.09E-05
U-238 (wt%)[1]	0.00E+00	5.90E-03	4.50E-03	6.50E-03	4.29E-01	4.12E-01	2.06E-02	
Error (+/-)[1]	0.00E+00	4.20E-03	6.00E-03	4.00E-03	4.60E-03	5.30E-03	1.42E-02	
U-238 (g)[8]	0.00E+00	5.54E-05	8.70E-05	1.38E-04	2.07E-02	2.31E-02	4.14E-05	
Error (+/-)[9]	NA	3.95E-05	1.16E-04	8.50E-05	2.22E-04	2.98E-04	2.85E-05	
Segment Total								4.42E-02
Error (+/-)[12]								4.01E-04
Total U[2]	1.50E-04	9.40E-01	1.93E+00	2.13E+00	4.83E+00	5.62E+00	2.01E-01	
Error (+/-)[2]	1.00E-05	2.30E-04	5.80E-04	2.81E-03	1.21E-03	1.50E-03	8.00E-05	
Kr-82 (mol%)[3]	2.00E-01	2.00E-01	2.00E-01	2.00E-01	2.00E-01	2.00E-01	2.00E-01	
Error (+/-)[3]	0.00E+00	0.00E+00	0.00E+00	0.00E+00	0.00E+00	0.00E+00	0.00E+00	
Kr-82 (g)[10]	3.28E-07	1.72E-05	5.80E-05	7.93E-05	3.29E-04	1.68E-04	0.00E+00	
Error (+/-)[9]	3.28E-11	2.13E-06	7.04E-06	1.97E-05	4.80E-05	1.97E-05	NA	
Segment Total								6.52E-04
Error (+/-)[12]								5.60E-05
Kr-83 (mol%)[3]	1.52E+01	1.52E+01	1.52E+01	1.52E+01	1.52E+01	1.52E+01	1.52E+01	
Error (+/-)[3]	1.00E-01	1.00E-01	1.00E-01	1.00E-01	1.00E-01	1.00E-01	1.00E-01	
Kr-83 (g)[10]	2.52E-05	1.33E-03	4.47E-03	6.10E-03	2.53E-02	1.30E-02	0.00E+00	
Error (+/-)[9]	1.66E-07	1.64E-04	5.43E-04	1.51E-03	3.70E-03	1.51E-03	NA	
Segment Total								5.02E-02
Error (+/-)[12]								4.31E-03
Kr-84 (mol%)[3]	3.04E+01	3.04E+01	3.04E+01	3.04E+01	3.04E+01	3.04E+01	3.04E+01	

Rod "O" 0201562 (S1-1, 2P39)

	O-00	O-01	O-02	O-03	O-04	O-05	O-06	O-07
Error (+/-)[3]	1.00E-01	1.00E-01	1.00E-01	1.00E-01	1.00E-01	1.00E-01	1.00E-01	
Kr-84 (g)[10]	5.10E-05	2.68E-03	9.04E-03	1.23E-02	5.12E-02	2.62E-02	0.00E+00	
Error (+/-)[9]	1.68E-07	3.32E-04	1.10E-03	3.06E-03	7.48E-03	3.06E-03	NA	
Segment Total								1.02E-01
Error (+/-)[12]								8.72E-03
Kr-85 (mol%)[3]	5.70E+00	5.70E+00	5.70E+00	5.70E+00	5.70E+00	5.70E+00	5.70E+00	
Error (+/-)[3]	1.00E-01	1.00E-01	1.00E-01	1.00E-01	1.00E-01	1.00E-01	1.00E-01	
Kr-85 (g)[10]	9.68E-06	5.09E-04	1.71E-03	2.34E-03	9.72E-03	4.98E-03	0.00E+00	
Error (+/-)[9]	1.70E-07	6.36E-05	2.10E-04	5.82E-04	1.43E-03	5.87E-04	NA	
Segment Total								1.93E-02
Error (+/-)[12]								1.67E-03
Kr-86 (mol%)[3]	4.87E+01	4.87E+01	4.87E+01	4.87E+01	4.87E+01	4.87E+01	4.87E+01	
Error (+/-)[3]	2.00E-01	2.00E-01	2.00E-01	2.00E-01	2.00E-01	2.00E-01	2.00E-01	
Kr-86 (g)[10]	8.37E-05	4.40E-03	1.48E-02	2.02E-02	8.40E-02	4.30E-02	0.00E+00	
Error (+/-)[9]	3.44E-07	5.44E-04	1.80E-03	5.02E-03	1.23E-02	5.02E-03	NA	
Segment Total								1.67E-01
Error (+/-)[12]								1.43E-02
Rod Total								3.38E-01
Error (+/-)[12]								1.74E-02
Shear Gas (g)[4]	0.00E+00	1.00E-04	8.00E-04	1.30E-03	1.11E-02	2.60E-03	2.00E-04	
Error (+/-)[4]	0.00E+00	3.00E-04	3.00E-04	3.00E-04	2.20E-03	5.00E-04	3.00E-04	
Diss+Pl Kr (mol)[3]	2.00E-06	1.05E-04	3.53E-04	4.82E-04	1.99E-03	1.02E-03	0.00E+00	
Error (+/-)[3]	0.00E+00	1.30E-05	4.30E-05	1.20E-04	2.93E-04	1.20E-04	0.00E+00	
Diss+Pl Kr+Xe (g)[3]	1.30E-03	6.35E-02	2.12E-01	3.32E-01	1.27E+00	5.96E-01	1.46E-02	
Error (+/-)[3]	1.00E-04	5.40E-03	1.98E-02	4.17E-02	1.59E-01	4.96E-02	1.46E-02	
Total Kr (mol)	2.00E-06	1.05E-04	3.54E-04	4.84E-04	2.01E-03	1.03E-03	0.00E+00	
Error (+/-)[9]	2.00E-10	1.30E-05	4.30E-05	1.20E-04	2.93E-04	1.20E-04	5.26E-06	

Rod "O" 0201562 (S1-1, 2P39)

	O-00	O-01	O-02	O-03	O-04	O-05	O-06	O-07
Xe-128 (mol)[3]	1.00E-01	1.00E-01	1.00E-01	1.00E-01	1.00E-01	1.00E-01	1.00E-01	
Error (+/-)[3]	0.00E+00	0.00E+00	0.00E+00	0.00E+00	0.00E+00	0.00E+00	0.00E+00	
Xe-128 (g)[10]	1.02E-06	5.21E-05	1.74E-04	3.06E-04	1.06E-03	4.87E-04	1.41E-05	
Error (+/-)[3]	1.02E-10	4.99E-06	1.85E-05	3.85E-05	1.50E-04	4.62E-05	1.39E-05	
SegmentTotal								2.09E-03
Error (+/1)[12]								1.63E-04
Xe-130 (mol)[3]	2.00E-01	2.00E-01	2.00E-01	2.00E-01	2.00E-01	2.00E-01	2.00E-01	
Error (+/-)[3]	0.00E+00	0.00E+00	0.00E+00	0.00E+00	0.00E+00	0.00E+00	0.00E+00	
Xe-130 (g)[10]	2.08E-06	1.06E-04	3.53E-04	6.22E-04	2.15E-03	9.90E-04	2.87E-05	
Error (+/-)[3]	2.08E-10	1.01E-05	3.77E-05	7.82E-05	3.04E-04	9.38E-05	2.83E-05	
SegmentTotal								4.25E-03
Error (+/1)[12]								3.31E-04
Xe-131 (mol)[3]	1.09E+01	1.09E+01	1.09E+01	1.09E+01	1.09E+01	1.09E+01	1.09E+01	
Error (+/-)[3]	1.00E-01	1.00E-01	1.00E-01	1.00E-01	1.00E-01	1.00E-01	1.00E-01	
Xe-131 (g)[10]	1.14E-04	5.82E-03	1.94E-02	3.42E-02	1.18E-01	5.44E-02	1.58E-03	
Error (+/-)[3]	1.05E-06	5.59E-04	2.08E-03	4.31E-03	1.67E-02	5.18E-03	1.56E-03	
SegmentTotal								2.33E-01
Error (+/1)[12]								1.82E-02
Xe-132 (mol)[3]	2.29E+01	2.29E+01	2.29E+01	2.29E+01	2.29E+01	2.29E+01	2.29E+01	
Error (+/-)[3]	1.00E-01	1.00E-01	1.00E-01	1.00E-01	1.00E-01	1.00E-01	1.00E-01	
Xe-132 (g)[10]	2.42E-04	1.23E-02	4.10E-02	7.24E-02	2.50E-01	1.15E-01	3.34E-03	
Error (+/-)[3]	1.06E-06	1.18E-03	4.38E-03	9.10E-03	3.54E-02	1.09E-02	3.29E-03	
SegmentTotal								4.94E-01
Error (+/1)[12]								3.86E-02
Xe-134 (mol)[3]	2.50E+01	2.50E+01	2.50E+01	2.50E+01	2.50E+01	2.50E+01	2.50E+01	
Error (+/-)[3]	1.00E-01	1.00E-01	1.00E-01	1.00E-01	1.00E-01	1.00E-01	1.00E-01	
Xe-134 (g)[10]	2.68E-04	1.36E-02	4.55E-02	8.02E-02	2.77E-01	1.28E-01	3.70E-03	

Rod "O" 0201562 (S1-1, 2P39)

	O-00	O-01	O-02	O-03	O-04	O-05	O-06	O-07
Error (+/-)[3]	1.07E-06	1.31E-03	4.86E-03	1.01E-02	3.92E-02	1.21E-02	3.65E-03	
SegmentTotal								5.48E-01
Error (+/1)[12]								4.27E-02
Xe-136 (mol)[3]	4.10E+01	4.10E+01	4.10E+01	4.10E+01	4.10E+01	4.10E+01	4.10E+01	
Error (+/-)[3]	1.00E-01	1.00E-01	1.00E-01	1.00E-01	1.00E-01	1.00E-01	1.00E-01	
Xe-136 (g)[10]	4.46E-04	2.27E-02	7.57E-02	1.33E-01	4.61E-01	2.12E-01	6.16E-03	
Error (+/-)[3]	1.09E-06	2.17E-03	8.08E-03	1.68E-02	6.53E-02	2.01E-02	6.07E-03	
SegmentTotal								9.12E-01
Error (+/1)[12]								7.11E-02
Rod total								2.19E+00
Error (+/-)[12]								9.33E-02
Shear Gas (g)[4]	0.00E+00	1.00E-04	8.00E-04	1.30E-03	1.11E-02	2.60E-03	2.00E-04	
Error (+/-)[4]	0.00E+00	3.00E-04	3.00E-04	3.00E-04	2.20E-03	5.00E-04	3.00E-04	
Diss+Pl Xe (mol)[3]	8.00E-06	4.07E-04	1.35E-03	2.39E-03	8.20E-03	3.79E-03	1.09E-04	
Error (+/-)[3]	0.00E+00	3.90E-05	1.45E-04	3.01E-04	1.17E-03	3.61E-04	1.09E-04	
Diss+Pl Kr+Xe (g)[3]	1.30E-03	6.35E-02	2.12E-01	3.32E-01	1.27E+00	5.96E-01	1.46E-02	
Error (+/-)[3]	1.00E-04	5.40E-03	1.98E-02	4.17E-02	1.59E-01	4.96E-02	1.46E-02	
Total Xe (mol)	8.00E-06	4.08E-04	1.36E-03	2.40E-03	8.27E-03	3.81E-03	1.10E-04	
Error (+/-)[9]	8.00E-10	3.90E-05	1.45E-04	3.01E-04	1.17E-03	3.61E-04	1.09E-04	
Values corrected to 1/1/84 (page 181, Final Report for the LWBR Proof of Breeding Analytical Support Project								
Cs-137 (atoms)[5]	ND	5.29E+19	2.31E+20	3.04E+20	1.02E+21	5.80E+20	4.31E+18	
Error (+/-)[4]	NA	1.45E+17	6.32E+17	9.72E+17	2.72E+18	1.70E+18	1.50E+16	
Cs-137 (g)[11]	NA	1.20E-02	5.24E-02	6.90E-02	2.32E-01	1.32E-01	9.80E-04	
Error (+/-)[9]	NA	3.28E-05	1.44E-04	2.21E-04	6.18E-04	3.87E-04	3.41E-06	
Total								4.98E-01

Rod "O" 0201562 (S1-1, 2P39)

	O-00	O-01	O-02	O-03	O-04	O-05	O-06	O-07
Error (+/-)[12]								7.76E-04
Ce-144 (atoms)[5]	ND	1.89E+18	1.03E+19	1.85E+19	5.21E+19	4.68E+19	6.75E+17	
Error (+/-)[4]	NA	1.34E+16	7.50E+16	1.33E+17	3.69E+17	3.23E+17	4.71E+15	
Ce-144 (g)[11]	NA	4.52E-04	2.46E-03	4.41E-03	1.25E-02	1.12E-02	1.61E-04	
Error (+/-)[9]	NA	3.21E-06	1.79E-05	3.18E-05	8.81E-05	7.72E-05	1.12E-06	
Total								3.11E-02
Error (+/-)[12]								1.23E-04
Zr-95 (atoms)[5]	ND	ND	6.13E+16	1.41E+17	4.63E+17	4.37E+17	9.17E+15	
Error (+/-)[4]	NA	NA	1.42E+16	2.30E+16	9.46E+16	3.69E+16	2.59E+14	
Zr-95 (g)[11]	NA	NA	9.65E-06	2.22E-05	7.29E-05	6.88E-05	1.45E-06	
Error (+/-)[9]	NA	NA	2.23E-06	3.62E-06	1.49E-05	5.82E-06	4.08E-08	
Total								1.75E-04
Error (+/-)[12]								1.66E-05

References

1. ANL Destructive Chemical Assay of 33-Rod LWBR EOL Sample - Rod O, 0201562, page 7
2. ANL Destructive Chemical Assay of 33-Rod LWBR EOL Sample - Rod O, 0201562, page 8
3. ANL Destructive Chemical Assay of 33-Rod LWBR EOL Sample - Rod O, 0201562, page 11
4. ANL Destructive Chemical Assay of 33-Rod LWBR EOL Sample - Rod O, 0201562, page 12
5. ANL Destructive Chemical Assay of 33-Rod LWBR EOL Sample - Rod O, 0201562, page 13
6. ANL Destructive Chemical Assay of 33-Rod LWBR EOL Sample - Rod O, 0201562, page 14
7. ANL Destructive Chemical Assay of 33-Rod LWBR EOL Sample - Rod O, 0201562, page 15
8. (abundance of the specified isotope)(total weight of uranium)

   1.00E+02
9. Error Propagation = ((+/-x/x)2+(+/-y/y)2)1/2(xy)
10. (mole%)(number moles gas recovered)(molec wt)

    1.00E+02
11. (number of atoms per segment)(atomic weight)

    6.02E+23
12. Error Propagation = (SUM(+/-I)1/2

Rod "P" 0307602 (S1-1, 3N63)

	P-00	P-01	P-02	P-03	P-04	P-05	P-06	P-07
Segment length (in)	1.04E+01	1.76E+01	2.05E+01	2.14E+01	1.77E+01	1.77E+01	9.66E+00	2.05E+00
Total length (in)								1.17E+02
U-232 (wt%)[1]	0.00E+00	9.35E-02	2.33E-01	1.62E-01	1.27E-01	3.99E-02	2.27E-02	
Error (+/-)[1]	0.00E+00	2.90E-03	7.20E-03	5.00E-03	3.90E-03	1.20E-03	7.00E-04	
U-232 (g)[8]	0.00E+00	8.24E-04	5.09E-03	7.92E-03	5.61E-03	2.02E-03	4.31E-05	
Error (+/-)[9]	NA	2.56E-05	1.57E-04	2.45E-04	1.73E-04	6.07E-05	1.33E-06	
Segment Total								2.15E-02
Error (+/-)[12]								3.44E-04
U-233 (wt%)[1]	1.00E+02	9.50E+01	8.95E+01	8.07E+01	8.46E+01	9.17E+01	9.82E+01	
Error (+/-)[1]	0.00E+00	7.00E-03	9.40E-03	7.30E-03	7.70E-03	7.10E-03	2.02E-02	
U-233 (g)[8]	4.00E-05	8.37E-01	1.95E+00	3.95E+00	3.74E+00	4.64E+00	1.86E-01	
Error (+/-)[9]	1.00E-05	1.64E-04	5.17E-04	9.34E-04	9.04E-04	1.11E-03	7.03E-05	
Segment Total								1.53E+01
Error (+/-)[12]								1.79E-03
U-234 (wt%)[1]	0.00E+00	4.44E+00	8.79E+00	1.52E+01	1.24E+01	6.93E+00	1.69E+00	
Error (+/-)[1]	0.00E+00	1.40E-03	1.60E-03	2.00E-03	1.80E-03	1.50E-03	1.50E-03	
U-234 (g)[8]	0.00E+00	3.91E-02	1.92E-01	7.46E-01	5.50E-01	3.51E-01	3.22E-03	
Error (+/-)[9]	NA	1.42E-05	5.82E-05	1.90E-04	1.47E-04	1.10E-04	3.02E-06	
Segment Total								1.88E+00
Error (+/-)[12]								2.71E-04
U-235 (wt%)[1]	0.00E+00	4.29E-01	1.41E+00	3.17E+00	2.29E+00	9.21E-01	5.92E-02	
Error (+/-)[1]	0.00E+00	4.60E-03	5.20E-03	5.00E-03	5.50E-03	5.20E-03	1.45E-02	
U-235 (g)[8]	0.00E+00	3.78E-03	3.09E-02	1.55E-01	1.01E-01	4.66E-02	1.12E-04	
Error (+/-)[9]	NA	4.05E-05	1.14E-04	2.47E-04	2.44E-04	2.63E-04	2.75E-05	
Segment Total								3.37E-01
Error (+/-)[12]								4.53E-04
U-236 (wt%)[1]	0.00E+00	1.81E-02	1.05E-01	3.86E-01	2.34E-01	7.92E-02	1.20E-03	

Rod "P" 0307602 (S1-1, 3N63)

	P-00	P-01	P-02	P-03	P-04	P-05	P-06	P-07
Error (+/-)[1]	0.00E+00	2.00E-04	2.00E-04	2.00E-04	2.00E-04	2.00E-04	2.00E-04	
U-236 (g)[8]	0.00E+00	1.59E-04	2.30E-03	1.89E-02	1.04E-02	4.01E-03	2.28E-06	
Error (+/-)[9]	NA	1.76E-06	4.40E-06	1.06E-05	9.15E-06	1.02E-05	3.80E-07	
Segment Total								3.57E-02
Error (+/-)[12]								1.80E-05
U-238 (wt%)[1]	0.00E+00	9.20E-03	5.70E-03	3.69E-01	3.50E-01	3.37E-01	2.87E-02	
Error (+/-)[1]	0.00E+00	4.70E-03	5.30E-03	5.10E-03	5.60E-03	5.30E-03	1.45E-02	
U-238 (g)[8]	0.00E+00	8.11E-05	1.25E-04	1.81E-02	1.55E-02	1.70E-02	5.45E-05	
Error (+/-)[9]	NA	4.14E-05	1.16E-04	2.50E-04	2.48E-04	2.68E-04	2.75E-05	
Segment Total								5.08E-02
Error (+/-)[12]								4.60E-04
Total U[2]	2.90E-04	8.81E-01	2.18E+00	4.89E+00	4.42E+00	5.06E+00	1.90E-01	
Error (+/-)[2]	1.00E-05	1.60E-04	5.30E-04	1.07E-03	9.90E-04	1.14E-03	6.00E-05	
Kr-82 (mol%)[3]	2.00E-01	2.00E-01	2.00E-01	2.00E-01	2.00E-01	2.00E-01	2.00E-01	
Error (+/-)[3]	0.00E+00	0.00E+00	0.00E+00	0.00E+00	0.00E+00	0.00E+00	0.00E+00	
Kr-82 (g)[10]	3.28E-07	2.05E-05	8.26E-05	2.95E-04	2.13E-04	1.25E-04	6.55E-06	
Error (+/-)[9]	0.00E+00	3.11E-06	8.85E-06	2.83E-05	2.90E-05	2.08E-05	6.55E-06	
Segment Total								7.42E-04
Error (+/-)[12]								4.70E-05
Kr-83 (mol%)[3]	1.51E+01	1.51E+01	1.51E+01	1.51E+01	1.51E+01	1.51E+01	1.51E+01	
Error (+/-)[3]	1.00E-01	1.00E-01	1.00E-01	1.00E-01	1.00E-01	1.00E-01	1.00E-01	
Kr-83 (g)[10]	2.50E-05	1.57E-03	6.31E-03	2.25E-02	1.63E-02	9.54E-03	5.01E-04	
Error (+/-)[9]	1.66E-07	2.38E-04	6.77E-04	2.17E-03	2.22E-03	1.59E-03	5.01E-04	
Segment Total								5.67E-02
Error (+/-)[12]								3.60E-03
Kr-84 (mol%)[3]	3.05E+01	3.05E+01	3.05E+01	3.05E+01	3.05E+01	3.05E+01	3.05E+01	
Error (+/-)[3]	1.00E-01	1.00E-01	1.00E-01	1.00E-01	1.00E-01	1.00E-01	1.00E-01	

Rod "P" 0307602 (S1-1, 3N63)

	P-00	P-01	P-02	P-03	P-04	P-05	P-06	P-07
Kr-84 (g)[10]	5.12E-05	3.20E-03	1.29E-02	4.60E-02	3.33E-02	1.95E-02	1.02E-03	
Error (+/-)[9]	1.68E-07	4.86E-04	1.38E-03	4.43E-03	4.53E-03	3.25E-03	1.02E-03	
Segment Total								1.16E-01
Error (+/-)[12]								7.34E-03
Kr-85 (mol%)[3]	5.70E+00	5.70E+00	5.70E+00	5.70E+00	5.70E+00	5.70E+00	5.70E+00	
Error (+/-)[3]	1.00E-01	1.00E-01	1.00E-01	1.00E-01	1.00E-01	1.00E-01	1.00E-01	
Kr-85 (g)[10]	9.68E-06	6.06E-04	2.44E-03	8.70E-03	6.30E-03	3.69E-03	1.94E-04	
Error (+/-)[9]	1.70E-07	9.26E-05	2.65E-04	8.51E-04	8.64E-04	6.18E-04	1.94E-04	
Segment Total								2.19E-02
Error (+/-)[12]								1.40E-03
Kr-86 (mol%)[3]	4.85E+01	4.85E+01	4.85E+01	4.85E+01	4.85E+01	4.85E+01	4.85E+01	
Error (+/-)[3]	1.00E-01	1.00E-01	1.00E-01	1.00E-01	1.00E-01	1.00E-01	1.00E-01	
Kr-86 (g)[10]	8.33E-05	5.22E-03	2.10E-02	7.49E-02	5.42E-02	3.17E-02	1.67E-03	
Error (+/-)[9]	1.72E-07	7.92E-04	2.25E-03	7.21E-03	7.38E-03	5.29E-03	1.67E-03	
Segment Total								1.89E-01
Error (+/-)[12]								1.20E-02
Rod Total								3.84E-01
Error (+/-)[12]								1.46E-02
Shear Gas (g)[4]	0.00E+00	1.00E-04	7.00E-04	7.80E-03	3.60E-03	1.20E-03	0.00E+00	
Error (+/-)[4]	0.00E+00	3.00E-04	3.00E-04	1.60E-03	7.00E-04	3.00E-04	3.00E-04	
Diss+Pl Kr (mol)[3]	2.00E-06	1.25E-04	5.03E-04	1.79E-03	1.30E-03	7.60E-04	4.00E-05	
Error (+/-)[3]	0.00E+00	1.90E-05	5.40E-05	1.73E-04	1.77E-04	1.27E-04	4.00E-05	
Diss+Pl Kr+Xe (g)[3]	1.20E-03	6.94E-02	3.00E-01	1.08E+00	8.13E-01	4.81E-01	1.06E-02	
Error (+/-)[3]	0.00E+00	8.50E-03	2.46E-02	7.87E-02	7.27E-02	4.39E-02	8.00E-03	
Total Kr (mol)	2.00E-06	1.25E-04	5.04E-04	1.80E-03	1.30E-03	7.62E-04	4.00E-05	
Error (+/-)[9]	0.00E+00	1.90E-05	5.40E-05	1.73E-04	1.77E-04	1.27E-04	4.00E-05	
Xe-128 (mol)[3]	1.00E-01	1.00E-01	1.00E-01	1.00E-01	1.00E-01	1.00E-01	1.00E-01	
Error (+/-)[3]	0.00E+00	0.00E+00	0.00E+00	0.00E+00	0.00E+00	0.00E+00	0.00E+00	

Rod "P" 0307602 (S1-1, 3N63)

	P-00	P-01	P-02	P-03	P-04	P-05	P-06	P-07
Xe-128 (g)[10]	1.02E-06	5.61E-05	2.46E-04	8.90E-04	6.73E-04	3.98E-04	6.91E-06	
Error (+/-)[3]	0.00E+00	8.06E-06	2.30E-05	7.37E-05	6.78E-05	4.05E-05	6.91E-06	
SegmentTotal								2.27E-03
Error (+/1)[12]								1.11E-04
Xe-130 (mol)[3]	2.00E-01	2.00E-01	2.00E-01	2.00E-01	2.00E-01	2.00E-01	2.00E-01	
Error (+/-)[3]	0.00E+00	0.00E+00	0.00E+00	0.00E+00	0.00E+00	0.00E+00	0.00E+00	
Xe-130 (g)[10]	2.08E-06	1.14E-04	4.99E-04	1.81E-03	1.37E-03	8.08E-04	1.40E-05	
Error (+/-)[3]	0.00E+00	1.64E-05	4.68E-05	1.50E-04	1.38E-04	8.24E-05	1.40E-05	
SegmentTotal								4.61E-03
Error (+/1)[12]								2.25E-04
Xe-131 (mol)[3]	1.08E+01	1.08E+01	1.08E+01	1.08E+01	1.08E+01	1.08E+01	1.08E+01	
Error (+/-)[3]	1.00E-01	1.00E-01	1.00E-01	1.00E-01	1.00E-01	1.00E-01	1.00E-01	
Xe-131 (g)[10]	1.13E-04	6.20E-03	2.72E-02	9.84E-02	7.44E-02	4.40E-02	7.63E-04	
Error (+/-)[3]	1.05E-06	8.93E-04	2.56E-03	8.20E-03	7.52E-03	4.50E-03	7.64E-04	
SegmentTotal								2.51E-01
Error (+/1)[12]								1.23E-02
Xe-132 (mol)[3]	2.31E+01	2.31E+01	2.31E+01	2.31E+01	2.31E+01	2.31E+01	2.31E+01	
Error (+/-)[3]	1.00E-01	1.00E-01	1.00E-01	1.00E-01	1.00E-01	1.00E-01	1.00E-01	
Xe-132 (g)[10]	2.44E-04	1.34E-02	5.85E-02	2.12E-01	1.60E-01	9.48E-02	1.65E-03	
Error (+/-)[3]	1.06E-06	1.92E-03	5.49E-03	1.76E-02	1.62E-02	9.67E-03	1.65E-03	
SegmentTotal								5.41E-01
Error (+/1)[12]								2.65E-02
Xe-134 (mol)[3]	2.54E+01	2.54E+01	2.54E+01	2.54E+01	2.54E+01	2.54E+01	2.54E+01	
Error (+/-)[3]	2.00E-01	2.00E-01	2.00E-01	2.00E-01	2.00E-01	2.00E-01	2.00E-01	
Xe-134 (g)[10]	2.72E-04	1.49E-02	6.53E-02	2.37E-01	1.79E-01	1.06E-01	1.84E-03	
Error (+/-)[3]	2.14E-06	2.15E-03	6.14E-03	1.97E-02	1.81E-02	1.08E-02	1.84E-03	
SegmentTotal								6.04E-01
Error (+/1)[12]								2.96E-02

Rod "P" 0307602 (S1-1, 3N63)

	P-00	P-01	P-02	P-03	P-04	P-05	P-06	P-07
Xe-136 (mol)[3]	4.05E+01	4.05E+01	4.05E+01	4.05E+01	4.05E+01	4.05E+01	4.05E+01	
Error (+/-)[3]	2.00E-01	2.00E-01	2.00E-01	2.00E-01	2.00E-01	2.00E-01	2.00E-01	
Xe-136 (g)[10]	4.40E-04	2.41E-02	1.06E-01	3.83E-01	2.90E-01	1.71E-01	2.97E-03	
Error (+/-)[3]	2.17E-06	3.47E-03	9.92E-03	3.18E-02	2.92E-02	1.75E-02	2.97E-03	
SegmentTotal								9.77E-01
Error (+/1)[12]								4.78E-02
Rod total								2.38E+00
Error (+/-)[12]								6.34E-02
Shear Gas (g)[4]	0.00E+00	1.00E-04	7.00E-04	7.80E-03	3.60E-03	1.20E-03	0.00E+00	
Error (+/-)[4]	0.00E+00	3.00E-04	3.00E-04	1.60E-03	7.00E-04	3.00E-04	3.00E-04	
Diss+Pl Xe (mol)[3]	8.00E-06	4.38E-04	1.92E-03	6.91E-03	5.24E-03	3.10E-03	5.40E-05	
Error (+/-)[3]	0.00E+00	6.30E-05	1.80E-04	5.76E-04	5.30E-04	3.17E-04	5.40E-05	
Diss+Pl Kr+Xe (g)[3]	1.20E-03	6.94E-02	3.00E-01	1.08E+00	8.13E-01	4.81E-01	1.06E-02	
Error (+/-)[3]	0.00E+00	8.50E-03	2.46E-02	7.87E-02	7.27E-02	4.39E-02	8.00E-03	
Total Xe (mol)	8.00E-06	4.39E-04	1.92E-03	6.96E-03	5.26E-03	3.11E-03	5.40E-05	
Error (+/-)[9]	0.00E+00	6.30E-05	1.80E-04	5.76E-04	5.30E-04	3.17E-04	5.40E-05	
Values corrected to 1/1/84 (page 181, Final Report for the LWBR Proof of Breeding Analytical Support Project								
Cs-137 (atoms)[5]	ND	4.50E+19	2.28E+20	1.03E+21	7.09E+20	3.89E+20	3.71E+18	
Error (+/-)[4]	NA	1.27E+17	6.34E+17	2.84E+18	2.02E+18	1.21E+18	1.32E+16	
Cs-137 (g)[11]	NA	1.02E-02	5.18E-02	2.33E-01	1.61E-01	8.84E-02	8.42E-04	
Error (+/-)[9]	NA	2.89E-05	1.44E-04	6.46E-04	4.59E-04	2.74E-04	2.99E-06	
Total								5.45E-01
Error (+/-)[12]								8.51E-04
Ce-144 (atoms)[5]	ND	1.63E+18	1.09E+19	4.23E+19	4.14E+19	3.42E+19	5.92E+17	
Error (+/-)[4]	NA	1.34E+16	8.86E+16	3.45E+17	3.38E+17	2.75E+17	4.86E+15	
Ce-144 (g)[11]	NA	3.90E-04	2.59E-03	1.01E-02	9.88E-03	8.16E-03	1.41E-04	

Rod "P" 0307602 (S1-1, 3N63)

	P-00	P-01	P-02	P-03	P-04	P-05	P-06	P-07
Error (+/-)[9]	NA	3.19E-06	2.12E-05	8.24E-05	8.08E-05	6.56E-05	1.16E-06	
Total								3.13E-02
Error (+/-)[12]								1.34E-04
Zr-95 (atoms)[5]	ND	ND	8.16E+16	2.23E+17	3.57E+17	2.98E+17	8.56E+15	
Error (+/-)[4]	NA	NA	1.90E+16	6.99E+16	5.21E+16	2.26E+16	3.23E+14	
Zr-95 (g)[11]	NA	NA	1.29E-05	3.52E-05	5.63E-05	4.70E-05	1.35E-06	
Error (+/-)[9]	NA	NA	3.00E-06	1.10E-05	8.20E-06	3.56E-06	5.08E-08	
Total								1.53E-04
Error (+/-)[12]								1.45E-05

References

1. ANL Destructive Chemical Assay of 33-Rod LWBR EOL Sample - Rod P, 0307602, page 6
2. ANL Destructive Chemical Assay of 33-Rod LWBR EOL Sample - Rod P, 0307602, page 7
3. ANL Destructive Chemical Assay of 33-Rod LWBR EOL Sample - Rod P, 0307602, page 10
4. ANL Destructive Chemical Assay of 33-Rod LWBR EOL Sample - Rod P, 0307602, page 11
5. ANL Destructive Chemical Assay of 33-Rod LWBR EOL Sample - Rod P, 0307602, page 12
6. ANL Destructive Chemical Assay of 33-Rod LWBR EOL Sample - Rod P, 0307602, page 13
7. ANL Destructive Chemical Assay of 33-Rod LWBR EOL Sample - Rod P, 0307602, page 14
8. (abundance of the specified isotope)(total weight of uranium)

9. Error Propagation = ((+/-x/x)2+(+/-y/y)2)1/2(xy)
10. (mole%)(number moles gas recovered)(molec wt)

11. (number of atoms per segment)(atomic weight) 1.00E+02

12. Error Propagation = (SUM(+/-I)1/2 6.02E+23

Rod "Q" 0401744 (S1-1, 4M49)

	Q-00	Q-01	Q-02	Q-03	Q-04	Q-05	Q-06	Q-07
Segment length (in)	1.13E+01	2.49E+01	1.79E+01	1.77E+01	1.77E+01	1.77E+01	8.82E+00	1.02E+00
Total length (in)								1.17E+02
U-232 (wt%)[1]	0.00E+00	1.46E-01	1.37E-01	1.67E-01	1.31E-01	4.15E-02	2.48E-02	
Error (+/-)[1]	0.00E+00	4.50E-03	4.20E-03	5.20E-03	4.00E-03	1.30E-03	8.00E-04	
U-232 (g)[8]	0.00E+00	2.17E-03	5.75E-03	7.07E-03	5.88E-03	2.11E-03	4.56E-05	
Error (+/-)[9]	NA	6.70E-05	1.76E-04	2.20E-04	1.80E-04	6.61E-05	1.47E-06	
Segment Total								2.30E-02
Error (+/-)[12]								3.47E-04
U-233 (wt%)[1]	1.00E+02	9.39E+01	8.29E+01	8.22E+01	8.53E+01	9.22E+01	9.81E+01	
Error (+/-)[1]	0.00E+00	7.80E-03	8.40E-03	8.30E-03	7.50E-03	7.20E-03	2.27E-02	
U-233 (g)[8]	4.00E-05	1.40E+00	3.48E+00	3.47E+00	3.84E+00	4.69E+00	1.81E-01	
Error (+/-)[9]	1.00E-05	3.84E-04	1.11E-03	1.11E-03	1.17E-03	1.42E-03	8.89E-05	
Segment Total								1.71E+01
Error (+/-)[12]								2.45E-03
U-234 (wt%)[1]	0.00E+00	5.29E+00	1.37E+01	1.41E+01	1.19E+01	6.59E+00	1.77E+00	
Error (+/-)[1]	0.00E+00	1.00E-03	1.90E-03	1.90E-03	1.50E-03	1.00E-03	1.10E-03	
U-234 (g)[8]	0.00E+00	7.88E-02	5.75E-01	5.97E-01	5.35E-01	3.35E-01	3.25E-03	
Error (+/-)[9]	NA	2.55E-05	1.91E-04	1.98E-04	1.70E-04	1.11E-04	2.47E-06	
Segment Total								2.12E+00
Error (+/-)[12]								3.43E-04
U-235 (wt%)[1]	0.00E+00	6.08E-01	2.63E+00	2.76E+00	2.11E+00	7.90E-01	6.05E-02	
Error (+/-)[1]	0.00E+00	5.00E-03	6.40E-03	5.90E-03	5.50E-03	5.50E-03	1.64E-02	
U-235 (g)[8]	0.00E+00	9.06E-03	1.10E-01	1.17E-01	9.48E-02	4.02E-02	1.11E-04	
Error (+/-)[9]	NA	7.45E-05	2.71E-04	2.52E-04	2.49E-04	2.80E-04	3.02E-05	
Segment Total								3.71E-01
Error (+/-)[12]								5.32E-04
U-236 (wt%)[1]	0.00E+00	3.01E-02	2.46E-01	2.74E-01	1.72E-01	3.75E-02	1.20E-03	

Rod "Q" 0401744 (S1-1, 4M49)

	Q-00	Q-01	Q-02	Q-03	Q-04	Q-05	Q-06	Q-07
Error (+/-)[1]	0.00E+00	1.00E-04	1.00E-04	1.00E-04	1.00E-04	1.00E-04	1.00E-04	
U-236 (g)[8]	0.00E+00	4.48E-04	1.03E-02	1.16E-02	7.74E-03	1.91E-03	2.21E-06	
Error (+/-)[9]	NA	1.49E-06	5.24E-06	5.49E-06	5.03E-06	5.12E-06	1.84E-07	
Segment Total								3.20E-02
Error (+/-)[12]								1.06E-05
U-238 (wt%)[1]	0.00E+00	4.40E-03	4.26E-01	4.08E-01	3.94E-01	3.86E-01	1.66E-02	
Error (+/-)[1]	0.00E+00	4.80E-03	6.30E-03	5.90E-03	5.30E-03	5.30E-03	1.62E-02	
U-238 (g)[8]	0.00E+00	6.55E-05	1.79E-02	1.72E-02	1.78E-02	1.96E-02	3.05E-05	
Error (+/-)[9]	NA	7.14E-05	2.65E-04	2.49E-04	2.39E-04	2.70E-04	2.98E-05	
Segment Total								7.26E-02
Error (+/-)[12]								5.17E-04
Total U[2]	8.00E-05	1.49E+00	4.20E+00	4.22E+00	4.50E+00	5.08E+00	1.84E-01	
Error (+/-)[2]	1.00E-05	3.90E-04	1.27E-03	1.28E-03	1.31E-03	1.49E-03	8.00E-05	
Kr-82 (mol%)[3]	2.00E-01	2.00E-01	2.00E-01	2.00E-01	2.00E-01	2.00E-01	2.00E-01	
Error (+/-)[3]	0.00E+00	0.00E+00	0.00E+00	0.00E+00	0.00E+00	0.00E+00	0.00E+00	
Kr-82 (g)[10]	1.31E-06	2.99E-05	2.33E-04	2.57E-04	1.93E-04	1.13E-04	0.00E+00	
Error (+/-)[9]	2.62E-10	4.91E-06	1.23E-05	3.06E-05	3.03E-05	2.05E-05	NA	
Segment Total								8.27E-04
Error (+/-)[12]								4.95E-05
Kr-83 (mol%)[3]	1.52E+01	1.52E+01	1.52E+01	1.52E+01	1.52E+01	1.52E+01	1.52E+01	
Error (+/-)[3]	2.00E-01	2.00E-01	2.00E-01	2.00E-01	2.00E-01	2.00E-01	2.00E-01	
Kr-83 (g)[10]	1.01E-04	2.30E-03	1.79E-02	1.98E-02	1.48E-02	8.71E-03	0.00E+00	
Error (+/-)[9]	1.33E-06	3.79E-04	9.74E-04	2.37E-03	2.34E-03	1.58E-03	NA	
Segment Total								6.36E-02
Error (+/-)[12]								3.83E-03
Kr-84 (mol%)[3]	3.06E+01	3.06E+01	3.06E+01	3.06E+01	3.06E+01	3.06E+01	3.06E+01	
Error (+/-)[3]	2.00E-01	2.00E-01	2.00E-01	2.00E-01	2.00E-01	2.00E-01	2.00E-01	

Rod "Q" 0401744 (S1-1, 4M49)

	Q-00	Q-01	Q-02	Q-03	Q-04	Q-05	Q-06	Q-07
Kr-84 (g)[10]	2.05E-04	4.68E-03	3.65E-02	4.03E-02	3.02E-02	1.77E-02	0.00E+00	
Error (+/-)[9]	1.34E-06	7.71E-04	1.94E-03	4.81E-03	4.75E-03	3.21E-03	NA	
Segment Total								1.30E-01
Error (+/-)[12]								7.77E-03
Kr-85 (mol%)[3]	5.70E+00	5.70E+00	5.70E+00	5.70E+00	5.70E+00	5.70E+00	5.70E+00	
Error (+/-)[3]	1.00E-01	1.00E-01	1.00E-01	1.00E-01	1.00E-01	1.00E-01	1.00E-01	
Kr-85 (g)[10]	3.87E-05	8.83E-04	6.88E-03	7.60E-03	5.69E-03	3.34E-03	0.00E+00	
Error (+/-)[9]	6.79E-07	1.46E-04	3.83E-04	9.15E-04	9.01E-04	6.08E-04	NA	
Segment Total								2.44E-02
Error (+/-)[12]								1.48E-03
Kr-86 (mol%)[3]	4.83E+01	4.83E+01	4.83E+01	4.83E+01	4.83E+01	4.83E+01	4.83E+01	
Error (+/-)[3]	2.00E-01	2.00E-01	2.00E-01	2.00E-01	2.00E-01	2.00E-01	2.00E-01	
Kr-86 (g)[10]	3.32E-04	7.57E-03	5.89E-02	6.52E-02	4.88E-02	2.87E-02	0.00E+00	
Error (+/-)[9]	1.38E-06	1.25E-03	3.12E-03	7.76E-03	7.68E-03	5.19E-03	NA	
Segment Total								2.09E-01
Error (+/-)[12]								1.25E-02
Rod Total								4.28E-01
Error (+/-)[12]								1.53E-02
Shear Gas (g)[4]	0.00E+00	2.00E-04	5.30E-03	7.20E-03	4.20E-03	1.20E-03	0.00E+00	
Error (+/-)[4]	0.00E+00	3.00E-04	1.10E-03	1.40E-03	8.00E-04	3.00E-04	3.00E-04	
Diss+Pl Kr (mol)[3]	8.00E-06	1.82E-04	1.41E-03	1.56E-03	1.17E-03	6.89E-04	0.00E+00	
Error (+/-)[3]	0.00E+00	3.00E-05	7.50E-05	1.87E-04	1.85E-04	1.25E-04	0.00E+00	
Diss+Pl Kr+Xe (g)[3]	4.60E-03	1.05E-01	8.72E-01	9.61E-01	7.27E-01	4.20E-01	0.00E+00	
Error (+/-)[3]	2.00E-04	1.65E-02	4.62E-02	8.52E-02	6.80E-02	3.53E-02	0.00E+00	
Total Kr (mol)	8.00E-06	1.82E-04	1.42E-03	1.57E-03	1.18E-03	6.91E-04	0.00E+00	
Error (+/-)[9]	1.60E-09	3.00E-05	7.50E-05	1.87E-04	1.85E-04	1.25E-04	0.00E+00	
Xe-128 (mol)[3]	1.00E-01	1.00E-01	1.00E-01	1.00E-01	1.00E-01	1.00E-01	1.00E-01	
Error (+/-)[3]	0.00E+00	0.00E+00	0.00E+00	0.00E+00	0.00E+00	0.00E+00	0.00E+00	

Rod "Q" 0401744 (S1-1, 4M49)

	Q-00	Q-01	Q-02	Q-03	Q-04	Q-05	Q-06	Q-07
Xe-128 (g)[10]	3.84E-06	8.57E-05	7.21E-04	7.95E-04	6.02E-04	3.45E-04	0.00E+00	
Error (+/-)[3]	1.28E-07	1.56E-05	3.80E-05	7.97E-05	6.29E-05	3.20E-05	NA	
SegmentTotal								2.55E-03
Error (+/1)[12]								1.14E-04
Xe-130 (mol)[3]	2.00E-01	2.00E-01	2.00E-01	2.00E-01	2.00E-01	2.00E-01	2.00E-01	
Error (+/-)[3]	0.00E+00	0.00E+00	0.00E+00	0.00E+00	0.00E+00	0.00E+00	0.00E+00	
Xe-130 (g)[10]	7.79E-06	1.74E-04	1.46E-03	1.62E-03	1.22E-03	7.02E-04	0.00E+00	
Error (+/-)[3]	2.60E-07	3.17E-05	7.72E-05	1.62E-04	1.28E-04	6.50E-05	NA	
SegmentTotal								5.19E-03
Error (+/1)[12]								2.32E-04
Xe-131 (mol)[3]	1.09E+01	1.09E+01	1.09E+01	1.09E+01	1.09E+01	1.09E+01	1.09E+01	
Error (+/-)[3]	1.00E-01	1.00E-01	1.00E-01	1.00E-01	1.00E-01	1.00E-01	1.00E-01	
Xe-131 (g)[10]	4.28E-04	9.56E-03	8.04E-02	8.87E-02	6.71E-02	3.85E-02	0.00E+00	
Error (+/-)[3]	1.48E-05	1.74E-03	4.30E-03	8.93E-03	7.05E-03	3.58E-03	NA	
SegmentTotal								2.85E-01
Error (+/1)[12]								1.28E-02
Xe-132 (mol)[3]	2.33E+01	2.33E+01	2.33E+01	2.33E+01	2.33E+01	2.33E+01	2.33E+01	
Error (+/-)[3]	1.00E-01	1.00E-01	1.00E-01	1.00E-01	1.00E-01	1.00E-01	1.00E-01	
Xe-132 (g)[10]	9.22E-04	2.06E-02	1.73E-01	1.91E-01	1.45E-01	8.30E-02	0.00E+00	
Error (+/-)[3]	3.10E-05	3.75E-03	9.16E-03	1.92E-02	1.51E-02	7.69E-03	NA	
SegmentTotal								6.13E-01
Error (+/1)[12]								2.75E-02
Xe-134 (mol)[3]	2.54E+01	2.54E+01	2.54E+01	2.54E+01	2.54E+01	2.54E+01	2.54E+01	
Error (+/-)[3]	1.00E-01	1.00E-01	1.00E-01	1.00E-01	1.00E-01	1.00E-01	1.00E-01	
Xe-134 (g)[10]	1.02E-03	2.28E-02	1.92E-01	2.12E-01	1.60E-01	9.19E-02	0.00E+00	
Error (+/-)[3]	3.42E-05	4.15E-03	1.01E-02	2.12E-02	1.67E-02	8.51E-03	NA	
SegmentTotal								6.79E-01
Error (+/1)[12]								3.04E-02

Rod "Q" 0401744 (S1-1, 4M49)

	Q-00	Q-01	Q-02	Q-03	Q-04	Q-05	Q-06	Q-07
Xe-136 (mol)[3]	4.02E+01	4.02E+01	4.02E+01	4.02E+01	4.02E+01	4.02E+01	4.02E+01	
Error (+/-)[3]	2.00E-01	2.00E-01	2.00E-01	2.00E-01	2.00E-01	2.00E-01	2.00E-01	
Xe-136 (g)[10]	1.64E-03	3.66E-02	3.08E-01	3.40E-01	2.57E-01	1.48E-01	0.00E+00	
Error (+/-)[3]	5.52E-05	6.67E-03	1.63E-02	3.41E-02	2.69E-02	1.37E-02	NA	
SegmentTotal								1.09E+00
Error (+/1)[12]								4.88E-02
Rod total								2.68E+00
Error (+/-)[12]								6.50E-02
Shear Gas (g)[4]	0.00E+00	2.00E-04	5.30E-03	7.20E-03	4.20E-03	1.20E-03	0.00E+00	
Error (+/-)[4]	0.00E+00	3.00E-04	1.10E-03	1.40E-03	8.00E-04	3.00E-04	3.00E-04	
Diss+Pl Xe (mol)[3]	3.00E-05	6.69E-04	5.60E-03	6.17E-03	4.68E-03	2.69E-03	0.00E+00	
Error (+/-)[3]	1.00E-06	1.22E-04	2.97E-04	6.23E-04	4.92E-04	2.50E-04	0.00E+00	
Diss+Pl Kr+Xe (g)[3]	4.60E-03	1.05E-01	8.72E-01	9.61E-01	7.27E-01	4.20E-01	0.00E+00	
Error (+/-)[3]	2.00E-04	1.65E-02	4.62E-02	8.52E-02	6.80E-02	3.53E-02	0.00E+00	
Total Xe (mol)	3.00E-05	6.70E-04	5.63E-03	6.22E-03	4.71E-03	2.70E-03	0.00E+00	
Error (+/-)[9]	1.00E-06	1.22E-04	2.97E-04	6.23E-04	4.92E-04	2.50E-04	0.00E+00	
Values corrected to 1/1/84 (page 181, Final Report for the LWBR Proof of Breeding Analytical Support Project								
Cs-137 (atoms)[5]	ND	9.01E+19	7.64E+20	8.00E+20	6.86E+20	3.71E+20	3.73E+18	
Error (+/-)[4]	NA	2.36E+17	2.07E+18	2.17E+18	1.85E+18	1.11E+18	1.28E+16	
Cs-137 (g)[11]	NA	2.05E-02	1.74E-01	1.82E-01	1.56E-01	8.44E-02	8.48E-04	
Error (+/-)[9]	NA	5.37E-05	4.70E-04	4.93E-04	4.21E-04	2.51E-04	2.91E-06	
Total								6.17E-01
Error (+/-)[12]								8.41E-04
Ce-144 (atoms)[5]	ND	3.49E+18	2.41E+19	3.50E+19	3.99E+19	3.23E+19	5.85E+17	
Error (+/-)[4]	NA	2.30E+16	1.68E+17	2.59E+17	2.71E+17	2.19E+17	3.99E+15	
Ce-144 (g)[11]	NA	8.35E-04	5.76E-03	8.36E-03	9.54E-03	7.72E-03	1.40E-04	
Error (+/-)[9]	NA	5.49E-06	4.02E-05	6.18E-05	6.47E-05	5.23E-05	9.52E-07	

Rod "Q" 0401744 (S1-1, 4M49)

[redacted]								
	Q-00	Q-01	Q-02	Q-03	Q-04	Q-05	Q-06	Q-07
Total								3.24E-02
Error (+/-)[12]								1.11E-04
Zr-95 (atoms)[5]	ND	ND	1.60E+17	2.17E+17	2.88E+17	3.46E+17	8.30E+15	
Error (+/-)[4]	NA	NA	4.61E+16	6.21E+16	6.70E+16	3.49E+16	7.28E+14	
Zr-95 (g)[11]	NA	NA	2.53E-05	3.42E-05	4.54E-05	5.44E-05	1.31E-06	
Error (+/-)[9]	NA	NA	7.27E-06	9.78E-06	1.06E-05	5.50E-06	1.15E-07	
Total								1.61E-04
Error (+/-)[12]								1.70E-05
[redacted]								

References

1. ANL Destructive Chemical Assay of 33-Rod LWBR EOL Sample - Rod Q, 0401744, page 6
2. ANL Destructive Chemical Assay of 33-Rod LWBR EOL Sample - Rod Q, 0401744 , page 7
3. ANL Destructive Chemical Assay of 33-Rod LWBR EOL Sample - Rod Q, 0401744, page 10
4. ANL Destructive Chemical Assay of 33-Rod LWBR EOL Sample - Rod Q, 0401744, page 11
5. ANL Destructive Chemical Assay of 33-Rod LWBR EOL Sample - Rod Q, 0401744, page 12
6. ANL Destructive Chemical Assay of 33-Rod LWBR EOL Sample - Rod Q, 0401744, page 13
7. ANL Destructive Chemical Assay of 33-Rod LWBR EOL Sample - Rod Q, 0401744, page 14
8. (abundance of the specified isotope)(total weight of uranium)

   1.00E+02
9. Error Propagation = ((+/-x/x)2+(+/-y/y)2)1/2(xy)
10. (mole%)(number moles gas recovered)(molec wt)

    1.00E+02
11. (number of atoms per segment)(atomic weight)

    6.02E+23
12. Error Propagation = (SUM(+/-I)1/2

Rod "R" 3110505 (R4-3 E3)

	R-00	R-01	R-02	R-03	R-04	R-05	R-06	R-07	R-08	R-09	R-10	R-11	R-12	R-13	R-14	R-15	R-16
Segment length (in)	6.18E+00	3.28E+00	7.00E+00	7.00E+00	7.00E+00	7.00E+00	7.00E+00	7.00E+00	6.99E+00	7.02E+00	6.98E+00	7.02E+00	7.00E+00	7.00E+00	7.00E+00	7.02E+00	3.73E+00
Total length (in)																	1.11E+02
U-232 (wt%)[1]	0.00E+00	1.90E-03	8.20E-03	2.12E-02	3.61E-02	5.22E-02	6.42E-02	7.21E-02	7.63E-02	7.40E-02	7.07E-02	6.06E-02	4.63E-02	2.95E-02	1.38E-02	3.50E-03	
Error (+/-)[1]	0.00E+00	1.00E-04	3.00E-04	7.00E-04	1.10E-03	1.60E-03	2.00E-03	2.20E-03	2.40E-03	2.30E-03	2.20E-03	1.90E-03	1.40E-03	9.00E-04	4.00E-04	1.00E-04	
U-232 (g)[8]	0.00E+00	9.69E-07	3.11E-05	2.01E-04	5.41E-04	1.09E-03	1.58E-03	1.89E-03	2.12E-03	1.98E-03	1.84E-03	1.42E-03	8.53E-04	3.80E-04	8.97E-05	6.34E-06	
Error (+/-)[9]	NA	5.10E-08	1.14E-06	6.63E-06	1.65E-05	3.35E-05	4.92E-05	5.78E-05	6.65E-05	6.16E-05	5.73E-05	4.45E-05	2.58E-05	1.16E-05	2.60E-06	1.81E-07	
Segment Total																	1.40E-02
Error (+/-)[12]																	1.47E-04
U-233 (wt%)[1]	1.00E+02	9.97E+01	9.94E+01	9.88E+01	9.80E+01	9.72E+01	9.66E+01	9.63E+01	9.61E+01	9.63E+01	9.63E+01	9.68E+01	9.75E+01	9.83E+01	9.91E+01	9.97E+01	
Error (+/-)[1]	0.00E+00	1.24E-01	1.68E-02	8.50E-03	8.00E-03	7.50E-03	7.40E-03	7.90E-03	9.10E-03	8.20E-03	7.50E-03	8.50E-03	7.90E-03	9.40E-03	1.00E-02	3.49E-02	
U-233 (g)[8]	4.00E-05	5.09E-02	3.77E-01	9.35E-01	1.47E+00	2.03E+00	2.38E+00	2.53E+00	2.66E+00	2.58E+00	2.51E+00	2.27E+00	1.80E+00	1.27E+00	6.44E-01	1.81E-01	
Error (+/-)[9]	1.00E-05	9.42E-05	1.10E-04	2.22E-04	3.63E-04	5.29E-04	5.25E-04	5.69E-04	6.47E-04	6.00E-04	5.65E-04	5.32E-04	4.62E-04	3.19E-04	1.53E-04	1.02E-04	
Segment Total																	2.37E+01
Error (+/-)[12]																	1.68E-03
U-234 (wt%)[1]	0.00E+00	1.42E-01	5.05E-01	1.17E+00	1.84E+00	2.61E+00	3.12E+00	3.35E+00	3.57E+00	3.40E+00	3.35E+00	2.96E+00	2.30E+00	1.61E+00	8.27E-01	2.54E-01	
Error (+/-)[1]	0.00E+00	3.00E-03	3.00E-04	3.00E-04	3.00E-04	4.00E-04	4.00E-04	4.00E-04	5.00E-04	4.00E-04	4.00E-04	4.00E-04	3.00E-04	3.00E-04	3.00E-04	3.00E-04	
U-234 (g)[8]	0.00E+00	7.26E-05	1.91E-03	1.11E-02	2.76E-02	5.46E-02	7.69E-02	8.80E-02	9.91E-02	9.10E-02	8.72E-02	6.95E-02	4.24E-02	2.07E-02	5.37E-03	4.60E-04	
Error (+/-)[9]	NA	1.53E-06	1.22E-06	3.76E-06	7.86E-06	1.59E-05	1.87E-05	2.12E-05	2.61E-05	2.24E-05	2.12E-05	1.78E-05	1.17E-05	6.18E-06	2.27E-06	5.80E-07	
Segment Total																	6.76E-01
Error (+/-)[12]																	5.71E-05
U-235 (wt%)[1]	0.00E+00	2.90E-03	6.70E-03	3.11E-02	7.51E-02	1.48E-01	2.14E-01	2.52E-01	2.78E-01	2.56E-01	2.43E-01	1.90E-01	1.23E-01	5.69E-02	1.69E-02	1.40E-02	

Rod "R" 3110505 (R4-3 E3)

	R-00	R-01	R-02	R-03	R-04	R-05	R-06	R-07	R-08	R-09	R-10	R-11	R-12	R-13	R-14	R-15	R-16
Error (+/-)[1]	0.00E+00	8.82E-02	1.20E-02	6.20E-03	5.80E-03	5.50E-03	5.30E-03	5.60E-03	6.60E-03	5.90E-03	5.40E-03	6.10E-03	5.70E-03	6.80E-03	7.20E-03	2.49E-02	
U-235 (g)[8]	0.00E+00	1.48E-06	2.54E-05	2.94E-04	1.12E-03	3.10E-03	5.26E-03	6.62E-03	7.72E-03	6.86E-03	6.33E-03	4.46E-03	2.26E-03	7.33E-04	1.10E-04	2.54E-05	
Error (+/-)[9]	NA	4.50E-05	4.55E-05	5.87E-05	8.69E-05	1.15E-04	1.30E-04	1.47E-04	1.83E-04	1.58E-04	1.41E-04	1.43E-04	1.05E-04	8.75E-05	4.68E-05	4.51E-05	
Segment Total																	4.49E-02
Error (+/-)[12]																	4.34E-04
U-236 (wt%)[1]	0.00E+00	1.00E-04	2.00E-04	3.00E-04	1.00E-03	2.50E-03	4.70E-03	5.80E-03	7.10E-03	6.40E-03	5.90E-03	4.00E-03	1.90E-03	8.00E-04	1.00E-04	2.00E-04	
Error (+/-)[1]	0.00E+00	2.00E-04	1.00E-04	1.00E-04	1.00E-04	1.00E-04	1.00E-04	1.00E-04	1.00E-04	1.00E-04	1.00E-04	1.00E-04	1.00E-04	1.00E-04	1.00E-04	1.00E-04	
U-236 (g)[8]	0.00E+00	5.10E-08	7.58E-07	2.84E-06	1.50E-05	5.23E-05	1.16E-04	1.52E-04	1.97E-04	1.71E-04	1.54E-04	9.38E-05	3.50E-05	1.03E-05	6.50E-07	3.62E-07	
Error (+/-)[9]	NA	1.02E-07	3.79E-07	9.46E-07	1.50E-06	2.09E-06	2.46E-06	2.63E-06	2.77E-06	2.68E-06	2.61E-06	2.34E-06	1.84E-06	1.29E-06	6.50E-07	1.81E-07	
Segment Total																	1.00E-03
Error (+/-)[12]																	7.30E-06
U-238 (wt%)[1]	0.00E+00	1.46E-01	3.12E-02	1.16E-02	6.90E-03	4.80E-03	4.80E-03	4.40E-03	3.90E-03	4.50E-03	4.60E-03	5.00E-03	5.80E-03	9.10E-03	1.72E-02	5.69E-02	
Error (+/-)[1]	0.00E+00	8.75E-02	1.18E-02	6.00E-03	5.60E-03	5.30E-03	5.10E-03	5.40E-03	6.40E-03	5.70E-03	5.20E-03	6.00E-03	5.50E-03	6.60E-03	7.00E-03	2.47E-02	
U-238 (g)[8]	0.00E+00	7.46E-05	1.18E-04	1.10E-04	1.03E-04	1.01E-04	1.18E-04	1.16E-04	1.08E-04	1.20E-04	1.20E-04	1.17E-04	1.07E-04	1.17E-04	1.12E-04	1.03E-04	
Error (+/-)[9]	NA	4.46E-05	4.47E-05	5.68E-05	8.39E-05	1.11E-04	1.26E-04	1.42E-04	1.77E-04	1.53E-04	1.36E-04	1.41E-04	1.01E-04	8.50E-05	4.55E-05	4.48E-05	
Segment Total																	1.64E-03
Error (+/-)[12]																	4.21E-04
Total U[2]	3.00E-05	5.10E-02	3.79E-01	9.46E-01	1.50E+00	2.09E+00	2.46E+00	2.63E+00	2.77E+00	2.68E+00	2.61E+00	2.34E+00	1.84E+00	1.29E+00	6.50E-01	1.81E-01	
Error (+/-)[2]	1.00E-05	7.00E-05	9.00E-05	2.10E-04	3.50E-04	5.20E-04	5.10E-04	5.50E-04	6.20E-04	5.80E-04	5.50E-04	5.10E-04	4.50E-04	3.00E-04	1.40E-04	8.00E-05	
Kr-82 (mol%)[3]																	
Error (+/-)[3]																	
Kr-82 (g)[10]	0.00E+00	0.00E+00	0.00E+00	0.00E+00	0.00E+00	0.00E+00	0.00E+00	0.00E+00	0.00E+00	0.00E+00	0.00E+00	0.00E+00	0.00E+00	0.00E+00	0.00E+00	0.00E+00	

Rod "R" 3110505 (R4-3 E3)

	R-00	R-01	R-02	R-03	R-04	R-05	R-06	R-07	R-08	R-09	R-10	R-11	R-12	R-13	R-14	R-15	R-16
Error (+/-)[9]	NA	NA	NA	NA	NA	NA	NA	NA	NA	NA	NA	NA	NA	NA	NA	NA	
Segment Total																	0.00E+00
Error (+/-)[12]																	NA
Kr-83 (mol%)[3]																	
Error (+/-)[3]																	
Kr-83 (g)[10]	0.00E+00	0.00E+00	0.00E+00	0.00E+00	0.00E+00	0.00E+00	0.00E+00	0.00E+00	0.00E+00	0.00E+00	0.00E+00	0.00E+00	0.00E+00	0.00E+00	0.00E+00	0.00E+00	
Error (+/-)[9]	NA	NA	NA	NA	NA	NA	NA	NA	NA	NA	NA	NA	NA	NA	NA	NA	
Segment Total																	0.00E+00
Error (+/-)[12]																	#VALUE!
Kr-84 (mol%)[3]																	
Error (+/-)[3]																	
Kr-84 (g)[10]	0.00E+00	0.00E+00	0.00E+00	0.00E+00	0.00E+00	0.00E+00	0.00E+00	0.00E+00	0.00E+00	0.00E+00	0.00E+00	0.00E+00	0.00E+00	0.00E+00	0.00E+00	0.00E+00	
Error (+/-)[9]	NA	NA	NA	NA	NA	NA	NA	NA	NA	NA	NA	NA	NA	NA	NA	NA	
Segment Total																	0.00E+00
Error (+/-)[12]																	NA
Kr-85 (mol%)[3]																	
Error (+/-)[3]																	
Kr-85 (g)[10]	0.00E+00	0.00E+00	0.00E+00	0.00E+00	0.00E+00	0.00E+00	0.00E+00	0.00E+00	0.00E+00	0.00E+00	0.00E+00	0.00E+00	0.00E+00	0.00E+00	0.00E+00	0.00E+00	
Error (+/-)[9]	NA	NA	NA	NA	NA	NA	NA	NA	NA	NA	NA	NA	NA	NA	NA	NA	
Segment Total																	0.00E+00
Error (+/-)[12]																	NA
Kr-86 (mol%)[3]																	

Rod "R" 3110505 (R4-3 E3)

	R-00	R-01	R-02	R-03	R-04	R-05	R-06	R-07	R-08	R-09	R-10	R-11	R-12	R-13	R-14	R-15	R-16
Error (+/-)[3]																	
Kr-86 (g)[10]	0.00E+00	0.00E+00	0.00E+00	0.00E+00	0.00E+00	0.00E+00	0.00E+00	0.00E+00	0.00E+00	0.00E+00	0.00E+00	0.00E+00	0.00E+00	0.00E+00	0.00E+00	0.00E+00	
Error (+/-)[9]	NA	NA	NA	NA	NA	NA	NA	NA	NA	NA	NA	NA	NA	NA	NA	NA	
Segment Total																	0.00E+00
Error (+/-)[12]																	NA
Rod Total																	0.00E+00
Error (+/-)[12]																	NA
Shear Gas (g)[4]																	
Error (+/-)[4]																	
Diss+Pl Kr (mol)[3]																	
Error (+/-)[3]																	
Diss+Pl Kr+Xe (g)[3]																	
Error (+/-)[3]																	
Total Kr (mol)																	
Error (+/-)[9]																	
Xe-128 (mol)[3]																	
Error (+/-)[3]																	
Xe-128 (g)[10]	0.00E+00	0.00E+00	0.00E+00	0.00E+00	0.00E+00	0.00E+00	0.00E+00	0.00E+00	0.00E+00	0.00E+00	0.00E+00	0.00E+00	0.00E+00	0.00E+00	0.00E+00	0.00E+00	
Error (+/-)[3]	NA	NA	NA	NA	NA	NA	NA	NA	NA	NA	NA	NA	NA	NA	NA	NA	
SegmentTotal																	0.00E+00
Error (+/1)[12]																	NA
Xe-130 (mol)[3]																	
Error (+/-)[3]																	

Rod "R" 3110505 (R4-3 E3)

	R-00	R-01	R-02	R-03	R-04	R-05	R-06	R-07	R-08	R-09	R-10	R-11	R-12	R-13	R-14	R-15	R-16
Xe-130 (g)[10]	0.00E+00	0.00E+00	0.00E+00	0.00E+00	0.00E+00	0.00E+00	0.00E+00	0.00E+00	0.00E+00	0.00E+00	0.00E+00	0.00E+00	0.00E+00	0.00E+00	0.00E+00	0.00E+00	
Error (+/-)[3]	NA	NA	NA	NA	NA	NA	NA	NA	NA	NA	NA	NA	NA	NA	NA	NA	
SegmentTotal																	0.00E+00
Error (+/1)[12]																	NA
Xe-131 (mol)[3]																	
Error (+/-)[3]																	
Xe-131 (g)[10]	0.00E+00	0.00E+00	0.00E+00	0.00E+00	0.00E+00	0.00E+00	0.00E+00	0.00E+00	0.00E+00	0.00E+00	0.00E+00	0.00E+00	0.00E+00	0.00E+00	0.00E+00	0.00E+00	
Error (+/-)[3]	NA	NA	NA	NA	NA	NA	NA	NA	NA	NA	NA	NA	NA	NA	NA	NA	
SegmentTotal																	0.00E+00
Error (+/1)[12]																	NA
Xe-132 (mol)[3]																	
Error (+/-)[3]																	
Xe-132 (g)[10]	0.00E+00	0.00E+00	0.00E+00	0.00E+00	0.00E+00	0.00E+00	0.00E+00	0.00E+00	0.00E+00	0.00E+00	0.00E+00	0.00E+00	0.00E+00	0.00E+00	0.00E+00	0.00E+00	
Error (+/-)[3]	NA	NA	NA	NA	NA	NA	NA	NA	NA	NA	NA	NA	NA	NA	NA	NA	
SegmentTotal																	0.00E+00
Error (+/1)[12]																	NA
Xe-134 (mol)[3]																	
Error (+/-)[3]																	
Xe-134 (g)[10]	0.00E+00	0.00E+00	0.00E+00	0.00E+00	0.00E+00	0.00E+00	0.00E+00	0.00E+00	0.00E+00	0.00E+00	0.00E+00	0.00E+00	0.00E+00	0.00E+00	0.00E+00	0.00E+00	
Error (+/-)[3]	NA	NA	NA	NA	NA	NA	NA	NA	NA	NA	NA	NA	NA	NA	NA	NA	
SegmentTotal																	0.00E+00
Error (+/1)[12]																	NA

Rod "R" 3110505 (R4-3 E3)

	R-00	R-01	R-02	R-03	R-04	R-05	R-06	R-07	R-08	R-09	R-10	R-11	R-12	R-13	R-14	R-15	R-16
Xe-136 (mol)[3]																	
Error (+/-)[3]																	
Xe-136 (g)[10]	0.00E+00	0.00E+00	0.00E+00	0.00E+00	0.00E+00	0.00E+00	0.00E+00	0.00E+00	0.00E+00	0.00E+00	0.00E+00	0.00E+00	0.00E+00	0.00E+00	0.00E+00	0.00E+00	
Error (+/-)[3]	NA	NA	NA	NA	NA	NA	NA	NA	NA	NA	NA	NA	NA	NA	NA	NA	
SegmentTotal																	0.00E+00
Error (+/1)[12]																	NA
Rod total																	0.00E+00
Error (+/-)[12]																	NA
Shear Gas (g)[4]																	
Error (+/-)[4]																	
Diss+Pl Xe (mol)[3]																	
Error (+/-)[3]																	
Diss+Pl Kr+Xe (g)[3]																	
Error (+/-)[3]																	
Total Xe (mol)																	
Error (+/-)[9]																	
Values corrected to 1/1/84 (page 181, Final Report for the LWBR Proof of Breeding Analytical Support Project																	
Cs-137 (atoms)[5]	ND	1.35E+17	2.63E+18	1.38E+19	3.28E+19	6.42E+19	8.95E+19	1.02E+20	1.15E+20	1.05E+20	1.02E+20	8.09E+19	4.91E+19	2.47E+19	6.84E+18	7.07E+17	
Error (+/-)[4]	NA	5.06E+14	7.30E+15	3.81E+16	9.05E+16	1.70E+17	2.49E+17	2.83E+17	3.20E+17	2.77E+17	2.83E+17	2.26E+17	1.37E+17	6.16E+16	1.70E+16	1.76E+15	
Cs-137 (g)[11]	NA	3.08E-05	5.98E-04	3.13E-03	7.44E-03	1.46E-02	2.03E-02	2.31E-02	2.61E-02	2.39E-02	2.31E-02	1.84E-02	1.12E-02	5.61E-03	1.55E-03	1.61E-04	
Error (+/-)[9]	NA	1.15E-07	1.66E-06	8.67E-06	2.06E-05	3.85E-05	5.66E-05	6.42E-05	7.27E-05	6.31E-05	6.44E-05	5.13E-05	3.10E-05	1.40E-05	3.87E-06	4.01E-07	
Total																	1.79E-01
Error (+/-)[12]																	1.63E-04

Rod "R" 3110505 (R4-3 E3)

	R-00	R-01	R-02	R-03	R-04	R-05	R-06	R-07	R-08	R-09	R-10	R-11	R-12	R-13	R-14	R-15	R-16
Ce-144 (atoms)[5]	ND	1.79E+16	3.17E+17	1.47E+18	3.14E+18	5.59E+18	7.31E+18	8.13E+18	9.17E+18	8.36E+18	7.78E+18	5.90E+18	3.38E+18	1.58E+18	4.18E+17	4.09E+16	
Error (+/-)[4]	NA	1.96E+14	2.43E+15	1.12E+16	2.35E+16	4.19E+16	5.69E+16	6.33E+16	6.87E+16	6.39E+16	5.94E+16	4.60E+16	2.63E+16	1.23E+16	3.25E+15	3.18E+14	
Ce-144 (g)[11]	NA	4.28E-06	7.58E-05	3.51E-04	7.50E-04	1.34E-03	1.75E-03	1.94E-03	2.19E-03	2.00E-03	1.86E-03	1.41E-03	8.06E-04	3.77E-04	9.98E-05	9.77E-06	
Error (+/-)[9]	NA	4.69E-08	5.79E-07	2.68E-06	5.62E-06	1.00E-05	1.36E-05	1.51E-05	1.64E-05	1.53E-05	1.42E-05	1.10E-05	6.28E-06	2.93E-06	7.77E-07	7.61E-08	
Total																	1.50E-02
Error (+/-)[12]																	3.78E-05
Zr-95 (atoms)[5]	ND	ND	4.37E+15	1.60E+16	2.91E+16	5.90E+16	7.51E+16	8.78E+16	9.05E+16	7.20E+16	4.75E+16	4.74E+16	2.12E+16	ND	2.10E+15	8.82E+14	
Error (+/-)[4]	NA	NA	4.35E+14	1.06E+15	3.19E+15	5.38E+15	6.06E+15	7.47E+15	9.85E+15	8.15E+15	7.05E+15	6.78E+15	3.22E+15	NA	5.83E+14	2.21E+14	
Zr-95 (g)[11]	NA	NA	6.89E-07	2.53E-06	4.58E-06	9.29E-06	1.18E-05	1.38E-05	1.43E-05	1.13E-05	7.49E-06	7.47E-06	3.34E-06	NA	3.31E-07	1.39E-07	
Error (+/-)[9]	NA	NA	6.85E-08	1.67E-07	5.03E-07	8.47E-07	9.55E-07	1.18E-06	1.55E-06	1.28E-06	1.11E-06	1.07E-06	5.07E-07	NA	9.18E-08	3.48E-08	
Total																	8.71E-05
Error (+/-)[12]																	3.16E-06

References

1. ANL Destructive Chemical Assay of 33-Rod LWBR EOL Sample - Rod R, 3110505, page 7
2. ANL Destructive Chemical Assay of 33-Rod LWBR EOL Sample - Rod R, 3110505, page 8
3. ANL Destructive Chemical Assay of 33-Rod LWBR EOL Sample - Rod R, 3110505, page 11
4. ANL Destructive Chemical Assay of 33-Rod LWBR EOL Sample - Rod R, 3110505, page 12
5. ANL Destructive Chemical Assay of 33-Rod LWBR EOL Sample - Rod R, 3110505, page 13
6. ANL Destructive Chemical Assay of 33-Rod LWBR EOL Sample - Rod R, 3110505, page 14
7. ANL Destructive Chemical Assay of 33-Rod LWBR EOL Sample - Rod R, 3110505, page 15
8. (abundance of the specified isotope)(total weight of uranium)

   1.00E+02

Rod "R" 3110505 (R4-3 E3)

	R-00	R-01	R-02	R-03	R-04	R-05	R-06	R-07	R-08	R-09	R-10	R-11	R-12	R-13	R-14	R-15	R-16

9. Error Propagation = ((+/-x/x)2+(+/-y/y)2)1/2(xy)

10. (mole%)(number moles gas recovered)(molec wt)

    1.00E+02

11. (number of atoms per segment)(atomic weight)

    6.02E+23

12. Error Propagation = (SUM(+/-I)1/2